Université
de Toulouse

THÈSE

En vue de l'obtention du

DOCTORAT DE L'UNIVERSITÉ DE TOULOUSE

Délivré par l'Université Toulouse III - Paul Sabatier
Discipline ou spécialité : Chimie

Présentée et soutenue par *Céline ROUGEOT*
Le *3 décembre 2012*

Titre :

Deracemisation of active compound precursors by physical treatments

---

JURY
Pr. N. de Viguerie, Université Paul Sabatier Toulouse III, *President*
Pr. G. Gouhier, Université de Rouen, *Reviewer*
Pr. P. Cintas, Facultad de Ciencias – University of Extremadura, *Reviewer*
Pr. M. Mazzotti, ETH-Zentrum, Zurich, *Reviewer*
Pr. R. M. Kellogg, Syncom, Groningen, *Examinator*
Pr. F. Guillen, Université Paul Sabatier Toulouse III, *Examinator*
Pr. G. Coquerel, Université de Rouen, *Supervisor*
Dr. J.-C. Plaquevent, Université Paul Sabatier Toulouse III, *Supervisor*

Ecole doctorale : SCIENCES DE LA MATIÈRE - Toulouse
Unités de recherche : LSPCMIB - UMR 5068 - Université Paul Sabatier Toulouse III
Laboratoire SMS - EA3233 - Université de Rouen
Directeurs de thèse : Dr. Jean-Christophe PLAQUEVENT
Pr. Gérard COQUEREL

CONFIDENTIAL

THÈSE

En vue de l'obtention du

DOCTORAT DE L'UNIVERSITÉ DE TOULOUSE

Délivré par l'Université Toulouse III - Paul Sabatier
Discipline ou spécialité : Chimie

Présentée et soutenue par *Céline ROUGEOT*
Le *3 décembre 2012*

Titre :

Deracemisation of active compound precursors by physical treatments

---

JURY
Pr. N. de Viguerie, Université Paul Sabatier Toulouse III, *President*
Pr. G. Gouhier, Université de Rouen, *Reviewer*
Pr. P. Cintas, Facultad de Ciencias - UEX, *Reviewer*
Pr. M. Mazzotti, ETH-Zentrum, Zurich, *Reviewer*
Pr. R. M. Kellogg, Syncom, Groningen, *Examinator*
Pr. F. Guillen, Université Paul Sabatier Toulouse III, *Examinator*
Pr. G. Coquerel, Université de Rouen, *Supervisor*
Dr. J.-C. Plaquevent, Université Paul Sabatier Toulouse III, *Supervisor*

Ecole doctorale : SCIENCES DE LA MATIÈRE - Toulouse
Unités de recherche : LSPCMIB - UMR 5068 - Université Paul Sabatier Toulouse III
Laboratoire SMS - EA3233 - Université de Rouen
Directeurs de thèse : Dr. Jean-Christophe PLAQUEVENT
Pr. Gérard COQUEREL

CONFIDENTIAL

“La perfection n'existe pas. Ce monde est imparfait, vous le constatez tous les jours. Et c'est pour ça qu'il est intéressant d'y vivre” - Hiromu Arakawa

“Les merveilleuses découvertes de la chimie sont surpassées peut-être par la confiserie. Jadis toute drogue avait un goût particulier ; aujourd'hui, c'est le contraire.” - Alexandre Pothey

Acknowledgments

First of all, I would like to thank my two supervisors, Dr. Jean-Christophe Plaquevent and Prof. Gérard Coquerel, for giving me the opportunity to achieve a so rewarding thesis, giving me the possibility to progress in the field of organic chemistry and to discover a new facet of chemistry: crystallization.

I would also like to especially thank Professor Frédéric Guillen, present in Toulouse and in Rouen, for the valuable assistance he has given me throughout these four years, especially during the writing of the manuscript. I also want to congratulate him for his nomination as professor at the Université Paul Sabatier of Toulouse.

I would like to thank the members of the board, Prof. Nancy De Viguerie, Prof. Géraldine Gouhier, Prof. Pedro Cintas, Prof. Richard Kellogg and Prof. Marco Mazzotti. The discussion during the defence was very fruitful for me.

During my thesis, I had the chance to spend three months at Groningen in The Netherlands, in a laboratory of Syncom BV. I would like to thank again Professor Richard Kellogg which gave me this opportunity and Wolter ten Hoeve for his warm welcome. I would like also to thank Maarten van der Meijden for his good mood and thanks whom I had great time in Syncom, en feliciteer hem voor zijn doctoraat!

I would like to thank the European Community for the IntEnant program for having financed my thesis, and which gave me the opportunity to build a very important scientific network and also to travel in Europe.

Je tiens également à remercier tous les membres du laboratoire SPCMIB de Toulouse et plus particulièrement ceux du deuxième étage : Christiane André-Barress, Stéphanie Ballereau, Cécile Bauboin-Dehoux, Florence Bedos-Belval, Yves Genisson, Frédéric Guillen, Marie-Rose Mazières et Jean-Christophe Plaquevent, ainsi qu'Anne-Marie Arroyo, Nathalie Gouardière (Vive le stade Toulousain !!) et Michel Baltas, le directeur du laboratoire.

Je remercie tous les membres du laboratoire SMS, et plus particulièrement les permanents de l'équipe cristallogenèse, Yohan Cartigny, Nicolas Couvrat (Pika), le petit (!) nouveau Gabin Gbabode, Samuel Petit (on se reverra sur les pistes de ski) et Morgane Sanselme pour leurs conseils et leurs disponibilités.

Je remercie mes collègues de bureau, passés : Audrey (c'est calme le bureau maintenant!), Guillaume (G2, Dora est toujours là pour nous faire penser à toi), Olivier (grâce à qui je ne verrai plus les blaireaux de la même façon), Sarah (j'espère que tu résisteras au froid canadien), et présents : Morgane (very demotivational power !), Grace (courage pour ta thèse) et Damien (est-ce parce que tu es entouré de filles que certain mots incongrus sortent de ta bouche de temps en temps ??)

Je remercie les collègues du bureau d'à côté : Anais (la chaudière), Silvia (je n'ai jamais vu quelqu'un aussi heureux de recevoir des chaussettes en cadeau !), Florian, Guillaume (G1, l'homme fort du labo), les petits : Clément, Florent, Julien et Simon (plus que 1 an et demi !!) ainsi que Steven.

Je tiens à remercier également Françoise, Ghislaine et Annick, pour les nombreux moments passés à papoter et, les organiciens, Agathe, Fabien, Philip et Thomas, pour ne pas m'avoir laissé seule petite organicienne dans ce monde de crist ! Merci aussi à Amélie et Delphine de supporter tant bien que mal toutes nos discussions boulot !

Je remercie maintenant mes oncles, tantes, cousin et cousines pour tous les bons moments passés ensemble. J'espère que notre famille sera toujours aussi unie.

Papi et Mamie, merci pour votre soutien tout au long de ces années. J'ai parfois l'impression que la voiture sent encore le rôti de veau aux oignons!

Grand-Papa et Grand-Maman, j'espère que de là ou vous êtes, vous êtes fiers de vos petits enfants.

Je remercie mes parents, sans qui je n'aurais jamais pu arriver là ou je suis aujourd'hui. J'espère réussir ma vie aussi bien que vous avez réussi la vôtre.

Je remercie enfin mon frère, Pti Juju, grâce à qui je n'ai jamais été seule. Avoir un frère jumeau, c'est vraiment formidable.

Contents

Contents

Contents ***15***

General Introduction ***25***

Chapter 1: **Chirality and separation of enantiomers** **29**

I - Chirality ***31***
- ***1. Definition*** ***31***
- ***2. History*** ***31***
- ***3. Nomenclature of chiral compounds*** ***33***
- ***4. Chirality around us*** ***34***
  - a. The biological homochirality 34
  - b. Chirality in the pharmaceutical industry 34

II - Thermodynamics of chiral molecules ***36***
- ***1. Thermodynamics*** ***36***
- ***2. Binary diagrams of racemic mixtures*** ***36***
- ***3. Ternary diagrams of racemic mixtures*** ***38***

III - How to detect a conglomerate? ***40***
- ***1. Comparison of spectroscopic data*** ***40***
- ***2. Second Harmonic Generation*** ***41***
- ***3. Structural resolution*** ***42***

IV - Access to pure enantiomers ***42***
- ***1. Non enantioselective synthesis from the chiral pool*** ***44***
- ***2. Asymmetric synthesis from an achiral substrate*** ***44***
- ***3. Resolution of racemic mixtures*** ***44***
- ***4. Analysis methods*** ***47***
  - a. Chiral HPLC 47
  - b. Polarimetry 47

V - Purification by crystallisation ***48***
- ***1. Pasteurian resolution*** ***48***
- ***2. Preferential crystallisation*** ***49***
  - a. Definition and history 49
  - b. General scheme of preferential crystallisation 50
  - c. Seeded isothermal preferential crystallisation 50
  - d. Auto-seeded polythermic programmed preferential crystallization 51
  - e. Auto-seeded preferential crystallisation induced by solvent evaporation 51
  - f. Second-order asymmetric transformation 51
  - g. Comparison between preferential crystallisation methods 52

3. Inclusion complexes ***52***
a. Crystal-lattice inclusion complexes 53
b. Inclusion complex in a host molecule 56

VI - Spontaneous symmetry breaking ***59***
1. History ***60***
2. Theory of the mother crystal ***60***
3. Reassessment of the theory of the mother crystal ***61***
4. Benefits of grinding ***62***
5. Total symmetry breaking of organic compounds ***63***
a. Formation of Schiff bases: an efficient tool for the preparation of pure enantiomers of amino-acid derivatives 64
b. Naproxen 66
c. Racemisation thanks to a chemical equilibrium 67
d. Combination of grinding, racemisation and controlled cooling 68
6. Deracemisation mechanisms: the current hypotheses ***69***
a. Introduction 69
b. Cairns-Smith's experiment 72
c. Model based on Ostwald ripening 72
d. Models based on clusters 74
f. Discussion 75
g. Conclusion 78

VII - Conclusion ***78***

Chapter 2: **Synthesis of monosubstituted β-cyclodextrins for chiral separation** **79**
I - Introduction ***81***

II - Synthesis of mono-substituted cyclodextrins: state of the art ***81***
1. Cyclodextrins ***81***
a. History 81
b. Structure and nomenclature 83
c. Reactivity 85
2. Synthesis of monosubstituted cyclodextrins ***86***
a. Monosubstitution at the 2-position of cyclodextrins 86
b. Monosubstitution at the 3-position of cyclodextrins 87
c. Monosubstitution at the 6-position of cyclodextrins 88
3. Inclusion complexes ***89***
a. In industries 89
b. Complexes formation 90
c. Characterisation of complexes 91
4. Cyclodextrins and chiral recognition ***92***
a. Chiral recognition in the solid state 92
b. Permethylated β-cyclodextrins/(±)p-fluorophenylethanol complexes 94

III - Synthesis of monosubstituted β-cyclodextrins ***94***

  1. 6-O-p-toluenesulfonyl-β-cyclodextrin β-CDOTs ***94***
    a. Synthesis of 6-O-p-toluenesulfonyl-β-cyclodextrin 94
    b. 2 dimensions NMR analysis 97
  2. Synthesis of 6-deoxy-6-azido-β-cyclodextrin and its derivatives ***98***
    a. Synthesis of 6-deoxy-6-azido-β-cyclodextrin β-CDN$_3$ 98
    b. Synthesis of 6-deoxy-6-amino-β-cyclodextrin CDNH$_2$ 100
    c. Synthesis of 6-deoxy-1,2,3-triazole-β-cyclodextrin derivatives 100
  3. Synthesis of diamino-β-cyclodextrins ***102***
    a. Synthesis of 6-deoxy-(2-aminoethylamino)-β-cyclodextrin 102
    b. Synthesis of 6-deoxy-(aminoalkylamino)-β-cyclodextrin 102
    c. Synthesis of 6-deoxy-6-benzylamino-β-cyclodextrin 103
  4. Synthesis of acid derivatives ***103***
    a. Synthesis of aliphatic amino acid derivatives 103
    b. Synthesis of the L-phenylalanine derivative 105
    c. Synthesis of polyacid derivatives 105

IV - Study of the crystallisation of monosubstituted β-cyclodextrins and of inclusion complexes ***106***

  1. Crystallisation of monosubstituted β-cyclodextrins ***106***
    a. β-CDN$_3$ 107
    b. β-CDNH$_2$ 108
    c. β-CDNH(CH$_2$)$_6$NH$_2$ 110
  2. Inclusion complexes ***110***
    a. Native β-cyclodextrin and 1-(p-toluenesulfonyl)imidazole 110
    b. β-CDNH$_2$ and ibuprofen 112

V- Conclusion ***114***

Chapter 3: **Stochastic chiral symmetry breaking of a conglomerate forming system; study of a series of triazoyl ketone** **117**

I - Introduction ***120***

II - Synthesis of the triazolyl ketones ***122***

  1. Synthesis of 1-(4-chlorophenyl)-4,4-dimethyl-2-(1H-1,2,4-triazol-1-yl) pentan-3-one ClTAK ***122***
  2. Synthesis of the triazoyl ketone derivatives ***124***

III. Characterisation of the solid phases ***126***

  1. Solubility data ***126***
  2. Thermal anaylses ***127***
  3. X ray powder diffraction (XRPD) ***128***
  4. Conclusion ***128***

IV- Structural studies 129
1. *Structural resolution of 1-(4-chlorophenyl)-4,4-dimethyl-2-(1H-1,2,4-triazol-1-yl)pentan-3-one ClTAK* *129*
    a. Crystallisation from racemic mixture 129
    b. Crystallisation from pure enantiomer 130
    c. Structure 130
2. *Structural resolution of 4,4-dimethyl-1-phenyl-2-(1H-1,2,4-triazol-1-yl)pentan-3-one HTAK* *132*
    a. Crystallisation from pure enantiomer 132
    b. Structure 132
3. *Structural resolution of 4,4-dimethyl-1-(p-toluyl)-2-(1H-1,2,4-triazol-1-yl)pentan-3-one MeTAK* *134*
    a. Crystallisation from racemic mixture 134
    b. Structure 135
4. *Structural resolution of 1-(4-bromophenyl)-4,4-dimethyl-2-(1H-1,2,4-triazol-1-yl)pentan-3-one BrTAK* *136*
    a. Crystallisation from racemic mixture 136
    b. Crystallisation from pure enantiomer 137
    c. Structure 137
5. *Case of 1-(4-tert-butylphenyl)-4,4-dimethyl-2-(1H-1,2,4-triazol-1-yl) pentan-3-one tBuTAK* *138*
6. *Comparison between the different crystal packings* *139*
    a. Comparison between ClTAK, MeTAK and BrTAK 139
    b. Comparision between the crystal packings of HTAK and ClTAK 143
    c. Comparision between the crystal packings of 2F-4ClTAK and MeTAK 145
7. *Conclusion* *146*

V - Viedma ripening on TAK derivatives 146
1. *Deracemisation of 1-(4-chlorophenyl)-4,4-dimethyl-2-(1H-1,2,4-triazol-1-yl) pentan-3-one ClTAK* *146*
    a. Experimental conditions 147
    b. Results 148
2. *Deracemisation of 4,4-dimethyl-1-phenyl-2-(1H-1,2,4-triazol-1-yl)pentan-3-one HTAK* *150*
    a. Experimental conditions 150
    b. Results 151
3. *Deracemisation of 4,4-dimethyl-1-(p-toluyl)-2-(1H-1,2,4-triazol-1-yl) pentan-3-one MeTAK* *151*
    a. Experimental conditions 151
    b. Results 152
4. *Deracemisation of 1-(4-bromophenyl)-4,4-dimethyl-2-(1H-1,2,4-triazol-1-yl) pentan-3-one BrTAK* *153*
    a. Experimental conditions 153
    b. Results 154
5. *Comparison between kinetics* *155*

VI - Evolution of the crystal size distribution ... ***157***

1. 1-(4-chlorophenyl)-4,4-dimethyl-2-(1H-1,2,4-triazol-1-yl)pentan-3-one ClTAK ... ***157***
  a. Starting material ... 157
  b. Evolution of the CSD ... 158

2. Evolution of the CSD for the other TAK derivatives ... ***160***
  a. 4,4-dimethyl-1-phenyl-2-(1H-1,2,4-triazol-1-yl)pentan-3-one HTAK ... 160
  b. 4,4-dimethyl-1-(p-toluyl)-2-(1H-1,2,4-triazol-1-yl)pentan-3-one MeTAK ... 161
  c.1-(4-bromophenyl)-4,4-dimethyl-2-(1H-1,2,4-triazol-1-yl)pentan-3-one BrTAK ... 162

3. Comparisons between the sizes of particles ... ***164***

VII – Deracemisation by using ultrasounds ... ***165***

1. Deracemisation in an ultrasonic bath ... ***165***

2. Deracemisation in controlled conditions: use of an ultrasonic probe ... ***166***
  a. Experimental results ... 166
  b. Comparison between glass beads and ultrasounds: a different mechanism? ... 169

3. Conclusion ... ***171***

VIII – Conclusion ... ***172***

Chapter 4: **Synthesis of pure enantiomer of Prasugrel by deracemisation** ... **175**

I - Introduction ... ***177***

1. Enzymatic dynamic kinetic resolution of amino acid derivatives ... ***177***

2. Clopidogrel and Prasugrel ... ***180***

II - First synthetic route: synthesis of 2-amino-1-cyclopropyl-2-(2-fluorophenyl)ethanone ... ***183***

1. Synthesis of 2-amino-1-cyclopropyl-2-(2-fluorophenyl)ethanone ... ***184***

2. Screening of conglomerate ... ***189***

III - Alternative synthetic route ... ***191***

1. Synthesis of 2-fluorophenylglycinamide ... ***191***

2. Screening of conglomerates ... ***191***

IV - Deracemisations ... ***193***

1. Determination of the solubility of the imine ... ***193***
  a. Solubility in acetonitrile ... 193
  b. Solubility in tertbutylmethylether ... 194
  c. Solubilities in other solvents ... 194

2. Optimisation of the experimental conditions ... ***195***

V - Study and characterisation of the different solid phases of the 2-(benzylideneamino)-2-(2-fluorophenyl)acetamide ... ***196***

1. Study of the conglomerate ... ***197***
  a. Resolution of the structure ... 197
  b. Thermal analysis ... 200

2. Study of the unknown phase **200**
a. X Ray diffraction analyses 200
b. Thermal analyses 201
3. Study of the monohydrate **202**
a. Resolution of the structure 202
b. Relative stability in solution 205
c. Thermal analyses 206
4. Comparisons between structures **208**
VI - Conclusion 211

General Conclusion 213

Résumé en français 217
Introduction Générale **219**
I - La chiralité et la séparation d'énantiomères 220
1. Généralités **220**
2. La déracémisation **221**
a. La découverte de la déracémisation 221
b. Le mûrissement de Viedma 222
3. Mécanisme **222**
a. L'expérience de Cairns-Smith 222
b. Le mûrissement d'Ostwald 223
c. Modèle basé sur la réincorporation de clusters 224
d. Discussion 224
II - Synthèse de β-cyclodextrines monofonctionnalisées 225
1. Introduction **225**
2. Synthèse de β-cyclodextrines monosubstituées **225**
3. Etude de la cristallisation des β-cyclodextrines monosubstituées et des complexes d'inclusion **227**
a. Cristallisation des β-cyclodextrines monosubstituées : influence de l'eau 227
b. Etude du complexe β-CDNH$_2$/ibuprofène 227
4. Conclusion **228**
III - Déracémisation d'une famille de conglomérats 228
1. Introduction **228**
2. Etude structurale **229**
3. Le mûrissement de Viedma **231**
a. ClTAK 231
b. ClTAK, MeTAK, BrTAK et HTAK 232
5. Déracémisation par les ultrasons **233**
6. Mécanisme **234**
IV - Synthèse de l'énantiomère pur du Prasugrel 235

1. Synthèse de la 2-amino-1-cyclopropyl-2-(2-fluorophényl)éthanone ... ***236***

a. Rétrosynthèse ... 236

b. Synthèse ... 236

1. Synthèse de la (2-fluorophényl)glycinamide ... ***237***

a. Synthèse ... 237

b. Recherche de conglomérats ... 238

2. Déracémisation ... ***238***

Conclusion générale ... ***239***

Experimental Part ... *241*

I - Generality ... ***243***

II - Synthesis of monosubstituted β-cyclodextrins for chiral separation ... ***245***

III - Stochastic chiral symmetry breaking of a conglomerate forming system; study of a series of triazoyl ketone ... ***256***

IV - Synthesis of pure enantiomer of Prasugrel by deracemisation ... ***265***

Appendix: Crystallographic Data ... 275

I - ClTAK ... ***277***

II - HTAK ... ***281***

III - MeTAK ... ***285***

IV - BrTAK ... ***288***

V – Imine monohydrate 52a ... ***292***

VI – Dimer 46 ... ***296***

Bibliography ... *301*

General Introduction

Even if the chirality and its consequences on the human body has been known for more than one century, the pharmaceutical industries have begun to be concerned about the different effects of the two enantiomers of active pharmaceutical ingredients only since the late eighties. The access to pure enantiomers has since become a considerable scientific and economical issue. In 2008, the European Community has launched a scientific program, called IntEnant, bringing together 13 academic groups and pharmaceutical industries working on different and complementary methods to obtain pure enantiomers. The SPCMIB laboratory of the University of Toulouse and the SMS laboratory of the University of Rouen, the two laboratories in which I worked during my PhD, were partners of this program. The main skills of these laboratory, respectively organic chemistry and purification by crystallisation, were combined to make a contribution to the access of pure enantiomers.

Among all the methods to have access to pure enantiomers, the resolutions by crystallisation, such as pasteurian resolution, are generally productive processes but can not be applied to all the compounds. In order to increase the scope of this method, new chiral selectors must be synthesized. Cyclodextrins are chiral molecules known to form different inclusion complexes with the two enantiomers of a compound. Unfortunately the difference between the diastereomeric complexes is generally too small to lead to a chiral discrimination in the solid state. Therefore it is necessary to enhance this difference. From this perspective, a small library of monosubstituted β-cyclodextrins with an acidic or basic hook was synthesised and the study of the formation of diastereomeric complexes between these modified β-cyclodextrins and a chiral guest was initiated.

Another resolution method, called deracemisation or total symmetry breaking, was recently designed. Deracemisation is a powerful resolution method since the targeted pure enantiomer can be obtained with 100% yield in one step from its racemic suspension. Unfortunately, the limitations inherent in this process are significant: only compounds crystallising as conglomerates and racemisable in the same conditions can be candidate.

The proportion of products crystallising as conglomerate is poor (≈5%) and such crystallisation are currently unpredictable. However, some families of organic compounds exhibit a higher tendency to crystallise as conglomerate. In this manuscript, two new families of compounds exhibiting this behaviour will be presented. One of these families is used in intermediate steps of the synthesis of the pure enantiomer of active pharmaceutical ingredients.

Moreover the deracemisation mechanism, leading the entire conversion of a racemic suspension into pure enantiomer, remains an open question. Many studies were carried out and the broad outline of the mechanism is known. The study presented in chapter 3 will provide some clarifications.

In addition a new method of deracemisation, with a higher efficiency, will be presented.

Chapter 1: Chirality and separation of enantiomers

I - Chirality

1. *Definition*

The word “chiral” was first introduced by Lord Kelvin, Professor of Natural Philosophy at the University of Glasgow, in 1884: *“I call any geometrical figure, or group of points, chiral, and say that it has chirality, if its image in a plane mirror, ideally realized, cannot be brought to coincide with itself.”* [1] The term “chiral” is derived from the greek “cheir” which means “hand” (Figure I - 1).

A molecule and its image in a mirror are called “enantiomers” and are said “chiral” whereas the term “achiral” is used for molecules which can be superimposed with their mirror image.

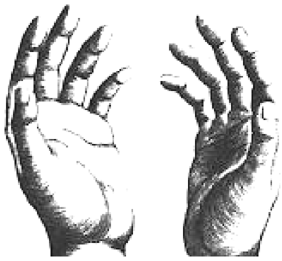

Figure I - 1. The right hand and the left hand are image of each other in a mirror but are not superimposed.

Chiral molecules have the particular ability to interact with the polarised light: one of the two enantiomers rotates the plan of the polarized light to the right (or clockwise) whereas the other enantiomer rotates the plan of the polarized light to the left (or counter clockwise);

Because chiral molecules are image of each other in a mirror, they have the same physical properties (melting point, solubility…) and the same reactivity towards achiral molecules. But the two enantiomers can have a different behaviour with chiral molecules (See paragraph I.3).

2. *History*[2]

Even if the word “chiral” was first introduced in 1884, the phenomenon was observed for the first time by René-Just Haüy, a French mineralogist, in 1801.[3] By comparing crystals of quartz, he noticed that there were two kinds of crystals, image of each other through a mirror, that he called “*plagièdre droit*” and “*plagièdre gauche*” (Figure I - 2).

---

[1] Lord Kelvin; *Baltimore Lectures on Molecular Dynamics and the Wave Theory of Light* **1884**.

[2] A. Collet, J. Crassous, J. P. Dutasta, L. Guy; *Molécules chirales : stéréochimie et propriétés*, EDP Sciences, CNRS editions: Les Ulis; Paris, **2006**.

[3] R. J. Hauy; *Traité de minéralogie*: *Paris*, **1801**.

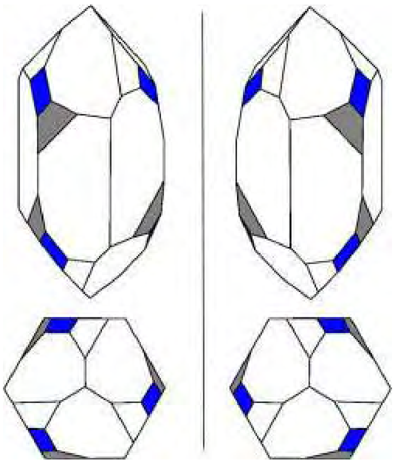

Figure I - 2. Morphology of enantiomorphous crystals of quartz.

In 1815, Jean-Baptiste Biot observed that molecules such as sucrose, tartaric acid and camphor are able to rotate the polarised light clockwise or counter clockwise at the solid state (crystal), at the liquid state or in solution.[4] He assumed that this ability was directly correlated to the molecular properties.

But the first major discovery in the field of chirality was made by Louis Pasteur in 1848. In 1820 Kestner, an industrial researcher, synthesized a compound having exactly the same composition than the tartaric acid[5] but which did not rotate the polarized light,[6] contrary to the tartaric acid prepared from wine. Joseph Louis Gay-Lussac suggested naming this compound "*racemic acid*" (from the Latin *"racemus"* meaning "grapes"). In 1848, Kestner gave this racemic acid to Pasteur. He crystallised the sodium ammonium tartrate tetrahydrate and was disappointed when he realized that the salt did not rotate the polarised light. By looking more closely to the crystals he noticed that the sample was not composed of one but of two kinds of crystals with a symmetrical shape.[7,8] He separated manually the two families of crystals then he checked their ability to rotate the polarised light. He noticed that the two kinds of crystals had an optical rotation with exactly the same intensity but with opposite signs.[9] He deduced that these crystals were composed by two kinds of molecules, also image of each other in a mirror. Thus, just 26-year old, Louis Pasteur established the bases of the chirality in chemistry.

In 1866, Desiré Gernez, a student of Pasteur, crystallized a pure enantiomer of sodium ammonium tartrate tetrahydrate by seeding a racemic supersaturated solution with enantiopure crystals.[10] He discovered the basic principle of preferential crystallization but he did not experiment further on the subject.

---

[4] J. B. Biot; *Bull. Soc. Philomatique,* **1815**, 190-192.

[5] J. L. Gay-Lussac; *Schweigger's journal,* **1828**, *48*, 381.

[6] J. B. Biot; *Annal. Chim.Phys. I,I,* **1838**, 69, 22.

[7] L. Pasteur; *C. R. Acad. Sci. Paris,* **1848**, *26*, 535-538.

[8] L. Pasteur; *C. R. Acad. Sci. Paris,* **1849**, *28*, 477-478.

[9] L. Pasteur; *Annal. Chim.Phys.,* **1848**, *24*, 442-459.

About ten years later, the next step in establishing the bases of stereochemistry was simultaneously taken by Jacobus Henricus van't Hoff and Joseph Achille Le Bel.[11,12] They proposed that the chirality was due to a spatial arrangement around a tetrahedral carbon. If a carbon is linked to four different substituents, the tetrahedron will be irregular and therefore become a chiral centre.

3. Nomenclature of chiral compounds

To describe the chirality of an enantiomer, several nomenclatures can be used, each based on a different particularity of compound:

- An enantiomer can be labelled (+) when it rotates the plan of the polarized light to the right, and (-) when it rotates the plan of the polarized light to the left. The (+) and (-) compounds have also been termed d- and l-, respectively for dextrorotatory and levorotatory.
- The terms of *R* (*rectus*) and *S* (*sinister*), introduced by Cahn, Ingold and Prelog, describe the configuration of the asymmetric carbon.[13]

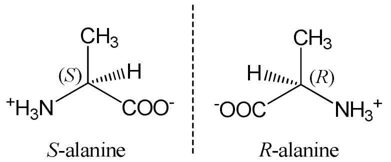

Figure I - 3. Chemical structures of *S*- and *R*-alanine.

- Amino acids and sugars can be labelled *D*- or *L*-, depending on whether the substituent with the highest priority is to the right or to the left in the Fisher projection of the molecule.

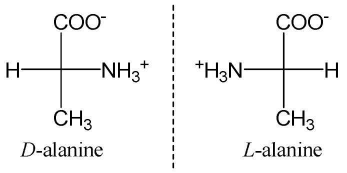

Figure I - 4. Fisher projection of *L*- and *D*-alanine.

---

[10] D. Gernez; *C. R. Acad. Sci. Paris,,* **1866**, 63, 843.

[11] J.H. van't Hoff; *Bul.l Soc. Chim. Fr.,* **1875**, 23, 295.

[12] J. A. Le Bel; *Bul.l Soc. Chim. Fr.,* **1874**, 22, 337.

[13] R. S. Cahn, C. Ingold, V. Prelog; *Angew. Chem. Int. Ed. Engl.,* **1966**, 5, 385-415.

4. Chirality around us

a. The biological homochirality

The human body as well as the other living systems is made of many chiral molecules. Indeed, all the chiral proteinogenic amino acids are *L* and sugars building blocks of DNA and RNA are *D*. Therefore the human body can be considered as a chiral entity; the two enantiomers of a compound thus have a different biological activity. For example, the smell of two enantiomers can be different. (Figure I - 5)[14,15,16]

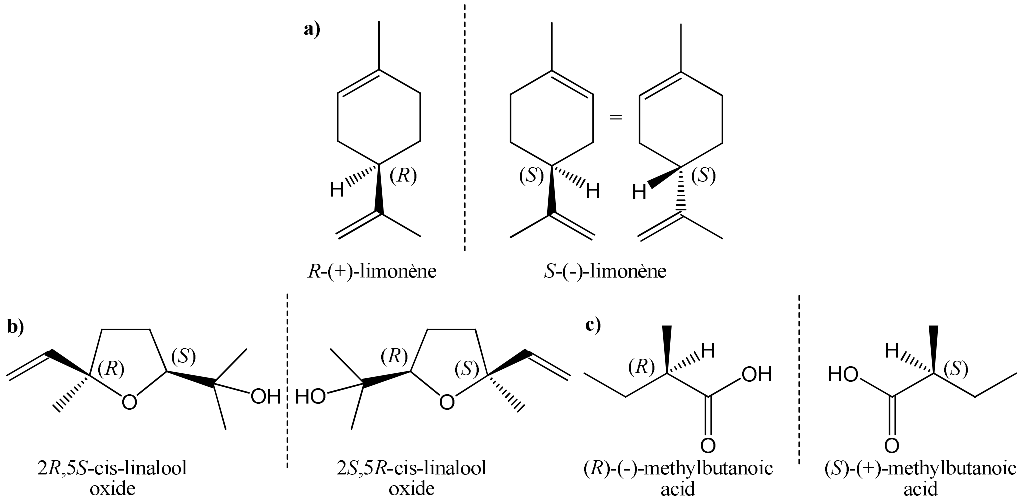

Figure I - 5. Odours of the two enantiomers of a) Limonene: fresh citrus, orange-like/harsh, turpentine-like, lemon note,[17] b) cis-linalool oxide: earthy/sweet, floral, creamy,[15] c) 2-methylbutanoic acid: cheesy, sweaty/fruity, sweet.[16]

b. Chirality in the pharmaceutical industry

The fact that the two enantiomers are seen as two different molecules by the human body is also valid for API (Active Pharmaceutical Ingredient). Their difference in behaviour can be insignificant or lead to disastrous consequences. For example, in the case of the:

- Cocaine, the two enantiomers have similar effects.
- Adrenaline, the *S* enantiomer is less active than the *R* enantiomer.
- Ibuprofen, only the *S* enantiomer is active.
- Thyroxin, the levothyroxin is used to treat the hypothyroidism, when the dextrothyroxin is used against the hypercholesterolemia.[18]
- In other cases, one the two enantiomers can reduce the effect of the other enantiomer.

---

[14] L. Friedman, J.G. Miller; *Science*, **1971**, 172, 1044-1046.

[15] D. Wang, K. Ando, K. Morita, K. Kubota, A. Kobayashi; *Biosci. Biotechnol. Biochem.* **1994**, 58 (11), 2050-2053.

[16] M. H. Boelens, H. Boelens, L. J. van Gemert, *P. & F.*, **1993**, 18(6), 1-15.

[17] L. Friedman, J.G. Miller; *Science*, **1971,** 172, 1044-1046.

[18] C. Bommer, E. Werle, I. Walter-Sack, C. Keller, F. Gehlen, C. Wanner, M. Nauck, W. März, H. Wieland, J. Bommer; *J. Am. Chem. Nephrol.*, **2005**, 16, 2789-2795.

One of the most infamous examples is the thalidomide. While the *R* enantiomer is a sedative drug, the *S* enantiomer is a teratogen compound.[19] In the years 1950 and 1960, the effect of the *S* enantiomer was not known and the racemic thalidomide was typically used to cure morning sickness during pregnancy. The dramatic consequences were that more than 10,000 children in 46 countries were born with deformities such as phocomelia.

Even if the importance of the different behaviour between the two enantiomers of a drug was known for a long time, the interest for the use of pure enantiomer in pharmaceutical industry dates from a few decades. Until then, the scientists thought that the distomer was not used by the organism and eliminated without more complications. But in 1984, Everhardus Jacobus Ariëns compared the non-active enantiomer (i.e. the distomer) to an impurity.[20] An impurity of 50%! He spoke about a "*highly sophisticated scientific nonsense*". Since that day, the interest for enantiopur drugs has grown more and more until 2001 when no more drug were sold as a racemic mixture. (Figure I - 6)[21]

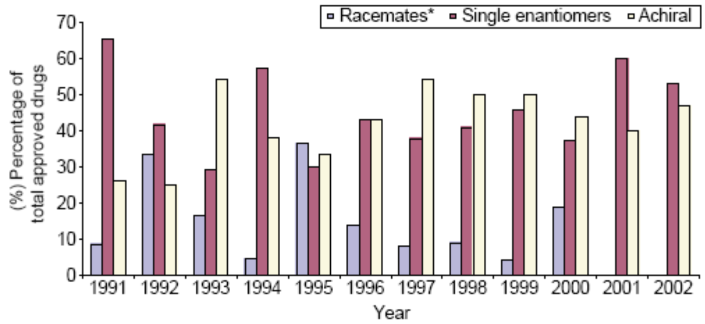

Figure I - 6. Annual distribution of FDA-approved drugs according to chirality in the period 1991-2002. * Including diastereomeric mixtures.

The need for pure enantiomers has become a major issue in the pharmaceutical industry for two main reasons. The first and the more important one is that the distomer can be toxic. Nobody wants the disaster of the thalidomide to happen again. The second reason is an economical reason; even if the distomer is not dangerous, its cost of production is not insignificant. The sooner it can be removed during the synthesis, the lower the cost, for the industry and for the customer. The sale of an enantiopure drug, initially available as a racemic mixture, also allows extending the term of the patent.

Currently enantiopure drugs are obtained by:[21]

- Synthesis from the chiral pool, i.e. from easily available chiral molecules (45%).
- Enantioselective synthesis (9%).

---

[19] B. K. Patel, A. J. Hutt; *Chirality in Drug Design and Development* **2004,** Chap. 5, I. K. Reddy, R. Mehvar, Eds, New-York, Marcel Dekker Inc.

[20] E. J. Arien; *Eur. J. Clin. Pharmacol.,* **1984**, 26, 663-668.

[21] H. Caner, E. Groner, L. Levy; *Discovery Drug Today*, **2004**, 9(3), 105-110.

- Resolution of the racemic mixture, mainly from the crystallisation of diastereomeric salts (46%).

Details about these methods will be given in paragraphs IV and V.

II - Thermodynamics of chiral molecules

1. Thermodynamics

A system is in equilibrium when it is in thermal, chemical and mechanical equilibrium. That means that for a system of n components, the intensive parameters, i.e. the temperature T (thermal equilibrium), the pressure P (mechanical equilibrium) and the chemical potentials μ_i (chemical equilibrium for the component i), are the same in all phases.

In a system of n independent components, with φ phases in equilibriums, there are n + 2 intensive parameters which are related to φ equations. The variance v defined by the Gibb's rules (Equation I - 1) corresponds to the number of intensive variables which can be varied independently without changing the equilibrium between all the phases.

$$\mathrm{v} = n + 2 - \varphi$$ **Equation I - 1**

In some case, the variance can decrease when the intensive parameters are linked together. For example, the two enantiomers have the same chemical potential then the Gibbs-Scott phase rule[22] must be applied. (Equation I - 2)

$$\mathrm{v} = n + \frac{n'}{2} + 2 - \varphi - \frac{\varphi'}{2}$$ **Equation I - 2**

2. Binary diagrams of racemic mixtures

There are many possibilities for a racemic mixture to form condensed phases. [23] To simplify, if we assume the absence of partial solid solutions and solid-solid transitions, three possibilities exist. (Figure I - 7)

---

[22] R. L. Scott; *J. Chem. Soc., Faraday Trans. 2*, **1977**, 73, 356-360.

[23] G. Coquerel; *Enantiomer*, **2000**, 5, 481-498.

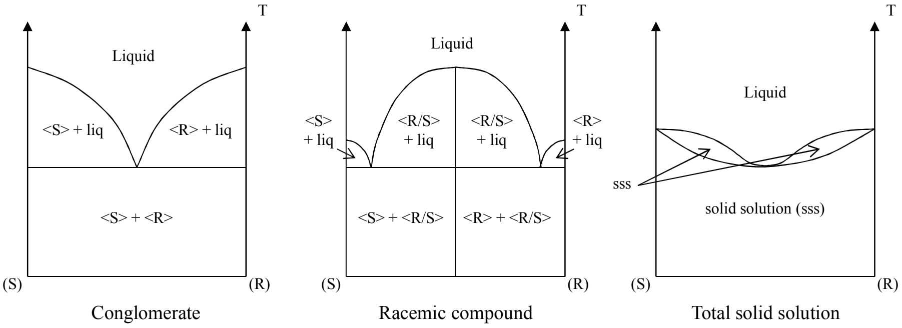

Figure I - 7. Binary phase diagrams of an enantiomer pair in absence of partial solid solution and solid/solid transition.

- Conglomerate (5-10% of the pair of enantiomers):[24] the two enantiomers crystallise separately, as in a physical mixture. The binary diagram of a conglomerate is an eutectic and it is symmetric because of the properties of the enantiomers. Below the eutectic temperature (T_E), the solid phase is composed of crystals of pure enantiomer whatever the composition of the mixture and there is a full chiral discrimination in the solid state.
- Racemic compound (90-95% of the pair of enantiomers): there is a defined compound formed by a stoichiometric mixture of the two enantiomers. In the solid state there is a mixture of the racemic crystals and crystals of the pure enantiomer (*R* or *S*, depending on the composition of the system). This compound exhibits a congruent melting which can be higher (as it is the case in the example) or lower than the pure enantiomer melting.
- Total solid solution (<1%): crystals are composed of the two enantiomers randomly distributed inside the structure. Each crystal is representative of the composition of the system, whatever its composition. The chiral discrimination is almost impossible in this case; only few cases of preferential enrichment were described in the literature.[25]

Unfortunately these three cases are not the only one to exist and mixtures of them are frequently observed.

Figure I - 8 represents a partial solid solution, a mixed situation between a conglomerate (the right diagram) and a complete solid solution (the left diagram). A part of the molecules of one enantiomer is substituted by the other enantiomer preventing the total discrimination at the solid state.

---

[24] R.A. Sheldon; *Chirotechnology : industrial synthesis of optically active compounds*; Marcel Dekker: New York, **1993**.

[25] R. Tamura, D. Fujimoto, Z. Lepp, K. Misaki, H. Miura, H. Takahashi, T. Ushio, T. Nakai, K. Hirotsu*; J. Am. Chem. Soc.*, **2002,** 124(44), 13139-13153.

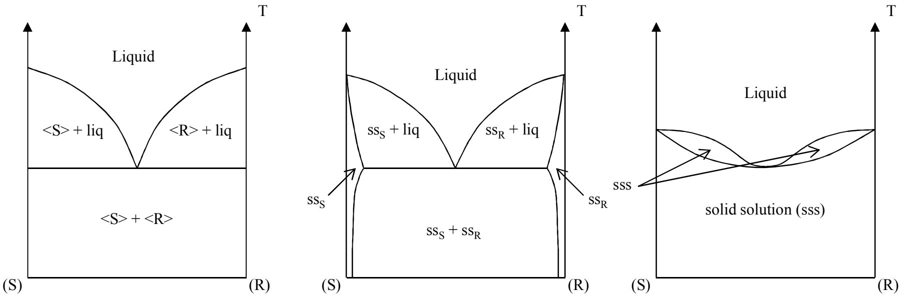

Conglomerate

Partial solid solution

Total solid solution

Figure I - 8. Evolution of the discrimination at the solid state.

Of course, many other possibilities can be encountered, as mixed situations between a conglomerate and a racemic compound, or polymorphic transition both for pure enantiomer and racemic compound. However, these cases require dedicated studies and will not be described in this manuscript.

3. Ternary diagrams of racemic mixtures

Unfortunately, it is almost impossible to work up to the melting with organic molecules. Indeed, melting is often concomitant to degradation of the product. To prevent it, most of crystallisations are carried out in an achiral solvent, therefore a third component have to be added, transforming binary diagrams into ternary diagrams. Figure I - 9 depicts isothermic ternary phase diagrams of a conglomerate, a racemic compound and a complete solid solution, in the case where the solvent is liquid and the two enantiomers are solid at the considered temperature. Of course many other and more complicated cases are possible but they are not described in this manuscript.[23]

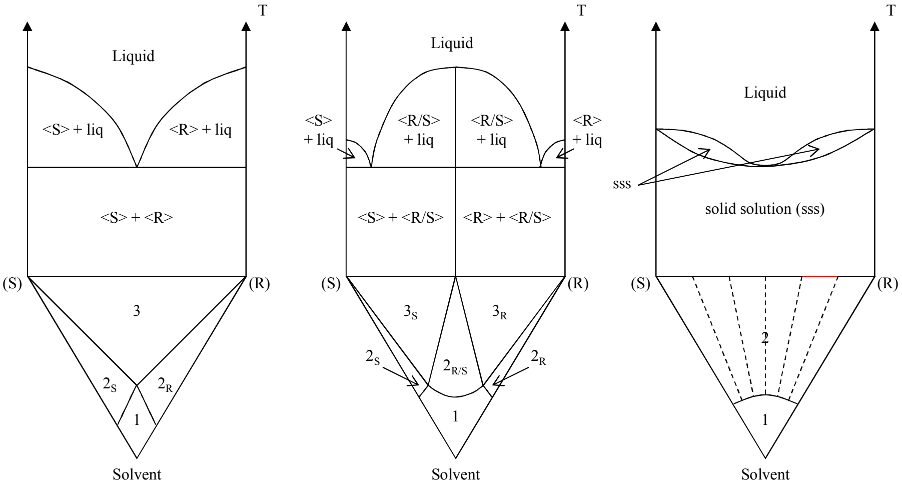

Conglomerate

Racemic compound

Total solid solution

Figure I - 9. Ternary phase diagrams of a conglomerate (left), a racemic compound (middle) and a complete solid solution (right) in absence of partial solid solution and solid/solid transition.

- The isotherm associated with a conglomerate is divided into four domains. The monophasic domain 1 is composed by an undersaturated liquid phase and is located at the solvent apex of the triangle. Two symmetrical domains exist in which a solid phase composed by crystals of a pure enantiomer (the enantiomer *R* in the domain 2_R and the enantiomer *S* in the domain 2_S) is in equilibrium with a saturated liquid. The fourth domain is a three phase domain in which a polysaturated solution is in equilibrium with the two solid phases.
- The isotherm associated with a racemic compound is divided into six domains. The domains 1, 2_R and 2_S are the same as in the ternary diagram of the conglomerate (respectively a liquid phase, pure crystals of *R* in equilibrium with a saturated liquid, and pure crystals of *S* in equilibrium with a saturated liquid). The racemic compound is present in three domains: $2_{R/S}$, 3_R and 3_S. $2_{R/S}$ is a biphasic domain composed by the racemic compound in equilibrium with a saturated liquid. 3_R and 3_S are three phase domains in which the racemic compound is in equilibrium with crystals of a pure enantiomer (the enantiomer *R* in 3_R and the enantiomer *S* in 3_S) and a polysaturated solution. The locations of the 3_R and 3_S domains are the key data for the enantiomeric separation from a racemic compound.
- The isotherm associated with a complete solid solution exhibits only two domains. The monophasic domain 1 is composed by a liquid phase and is located at the solvent apex of the triangle. The domain 2 is a biphasic domain: the solid phase is in equilibrium with a saturated liquid. The composition of both phases in equilibrium is linked by tie lines represented by dashed lines in the diagram.

The solvent can also modify the ternary diagram by stabilising a phase or ensuring the existence of news phases, as, for example, a stable conglomerate.

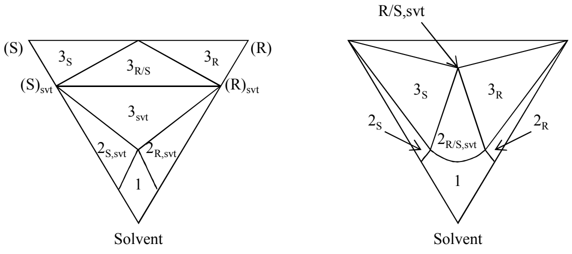

Solvated conglomerate   Solvated racemic compound

Figure I - 10. Possible ternary phase diagrams when solvated solid phases exist

Figure I - 10 depicts two cases in which the solvent modifies the crystallisation of the enantiomers by the presence of a solvated phase.

- In the left diagram, the solvated phase crystallise as a conglomerate while the asolvated phase crystallises as a racemic compound. Domains 1, $2_{S,\mathrm{svt}}$, $2_{R,\mathrm{svt}}$ and 3_{svt} correspond to the typical diagram of a conglomerate in which the conglomerate is a solvate; the chiral discrimination is possible in this solvent. The asolvated phases are only present in the domains 3_S, 3_R and $3_{R/S}$.

- In the right diagram, the existence of a solvated racemic compound (*R*/*S*,svt) prevent the formation of the conglomerate between asolvated solids. In the three phases domain 3, asolvated *R* and *S* are in equilibrium with the solvated racemic compound.

The separation of the two enantiomers is made easier when the compound crystallise as a conglomerate. Unfortunately, as seen previously, conglomerates are not prevalent in Nature and the prediction of the crystallisation of a compound as a conglomerate remains an open question. Therefore it is very important to detect the conglomerate.

III - How to detect a conglomerate?

1. Comparison of spectroscopic data

As said previously, a racemic molecule crystallising as a conglomerate has the particular property to be a physical mixture of single crystals of pure enantiomers. Indeed, all the solid phases in a conglomerate (the pure *S* or *R* crystals and the mixture of these two solids) exhibit the mirror image crystal packing whereas the crystal packing of the solid phases in the case of a racemic compound (the pure *S* or *R* enantiomers and the racemic compound) are different. As a consequence, the spectroscopic data (X-Ray diffraction, InfraRed or Raman spectroscopy and solid state NMR) of the racemic mixture and of the pure enantiomer are exactly the same in the case of a conglomerate (anomalous scattering is not considered here), whereas they are different in the case of a racemic compound. Comparison of spectroscopic data can prove the existence of a conglomerate.

However, in the case of a total solid solution, there is only one single phase, so only one crystal packing. Spectroscopic data of a mixture of any composition of a total solid solution are almost the same (few weak differences are possible due to the substitution of one enantiomer by the other one) but should not be confused with a conglomerate.[26] Nevertheless, complete solid solutions are unusual (less than 1%) and can be differentiated from conglomerate by using other analyses.

---

[26] B. Chion, J. Lajzerowicz, D. Bordeaux, A. Collet, J. Jacques; *J. Phys. Chem.*, **1978**, 82, 2682-2688.

2. Second Harmonic Generation

Another problem concerning the use of spectroscopic data is the need to have access to the pure enantiomer. A new method to detect conglomerates, from racemic samples, has been designed in the laboratory: the SHG (Second Harmonic Generation). It is a nonlinear optic technique, in which photons interacting in a non centro symmetric material are combined to form new photons with twice energies (i.e. double frequence) of the initial photons. A powder sample is irradiated with a LASER (wave length λ) and the signal generated by the sample (diffused light) is analysed. (Figure I - 11) If the product crystallises in a non-centrosymmetric space group, a part of the signal generated will have a wave length divided by two (i.e. a double frequency),[27] when the signal generated by a centrosymmetric space group is the same as that of the incident wave.[28] All the conglomerates crystallise in a non centrosymmetric space group since in a centrosymmetric space group, the presence of an inversion centre induce the presence of the two enantiomers in the crystal packing.

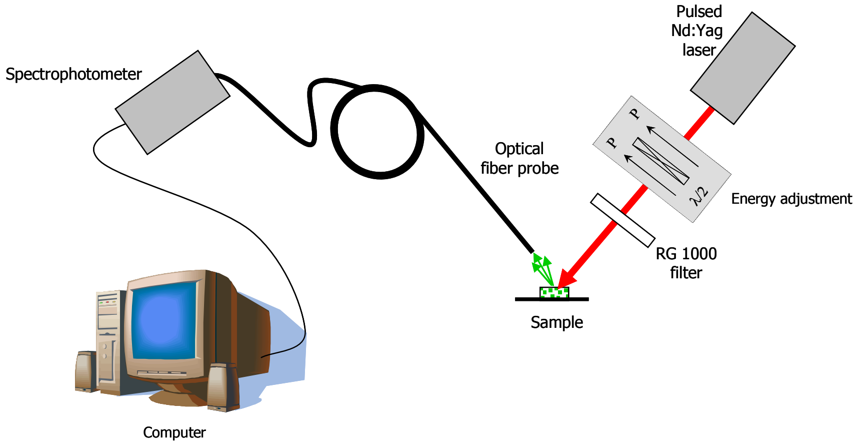

Figure I - 11. Second harmonic generation set-up.

Unfortunately, a positive signal in SHG (i.e. a wave length divided by two) is not a proof that the sample is a conglomerate. Indeed: (i) some racemic compound crystallise in a non centrosymmetric space group with Z'=2 (i.e. the two enantiomers are combined in the asymmetric unit), (ii) a racemic compound can crystallise in a non centrosymmetric but non chiral space group (e.g. Pca2, Pna2, Pc, Cc…). These cases remain in minor proportion, so the SHG remains a fast and accurate analysis to do a pre-screening of conglomerates. Additional spectroscopic data can be used to remove false positive.

---

[27] S. K. Kurtz, T. T. Perry; *J. Appl. Phys.*, **1968**, 39, 3798-3813.

[28] A. Galland, V. Dupray, B. Berton, S. Morin-Grognet, M. Sanselme, H. Atmani, G. Coquerel; *Cryst. Growth Des.*, **2009**, 9, 2713-2718.

3. Structural resolution

The best method to know if the molecule crystallises as a conglomerate remains the X Ray diffraction on single crystal. Indeed, this method gives us, among other things, the space group of the crystal and the asymmetric unit, removing all the ambiguity.

IV - Access to pure enantiomers

Since chirality was discovered, and especially since it is known that the two enantiomers have a different behaviour toward another chiral system (such as molecules of the human body), researchers try to find methods to have access to pure enantiomers. Methods mainly used are summarised in Figure I - 12.[24] A short description of these methods is given in the following paragraphs.

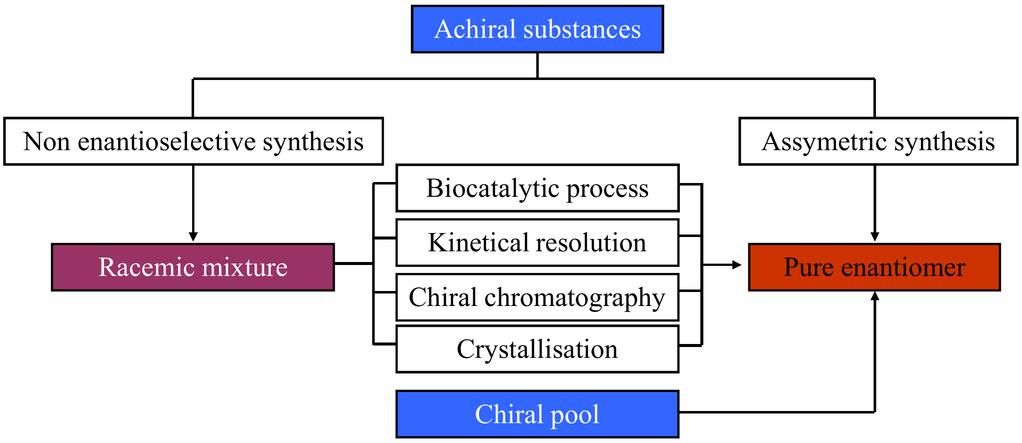
Achiral substances
Non enantioselective synthesis
Assymetric synthesis
Racemic mixture
Biocatalytic process
Kinetical resolution
Chiral chromatography
Crystallisation
Pure enantiomer
Chiral pool

Figure I - 12. Different routes to access to pure enantiomer

The choice of the method depends on the enantiopure intermediate to obtain during the synthesis of the final compound, i.e. depends on its physico-chemical behaviour (solubility, stability…) and on the ratio time to reach pure enantiomer/cost of the method. A typical industrial decision tree for the resolution of a racemic mixture is presented below:

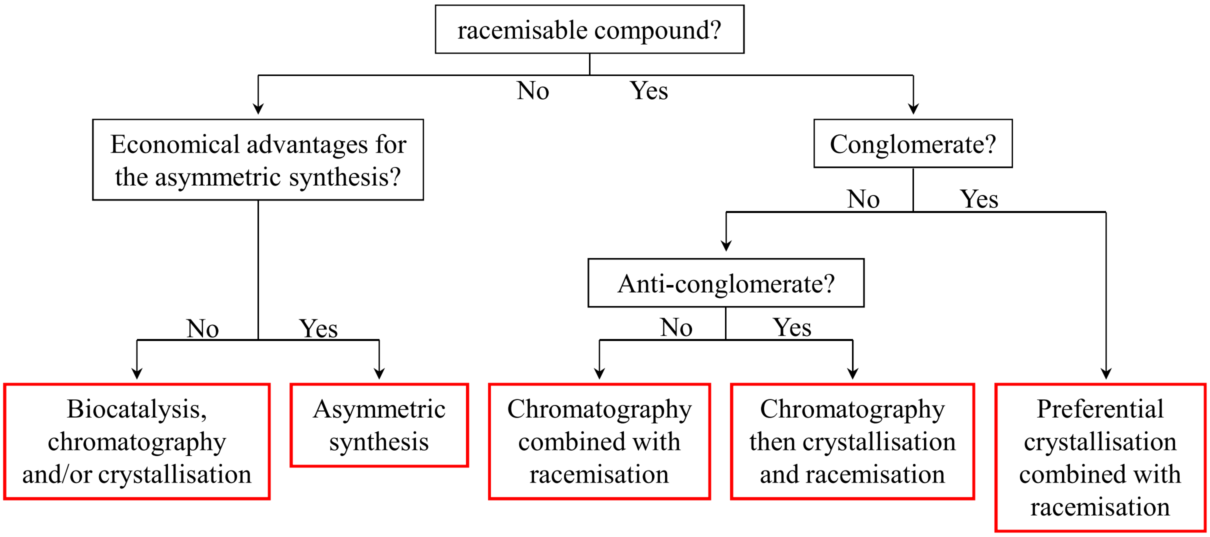
racemisable compound?
No
Yes
Economical advantages for the asymmetric synthesis?
Conglomerate?
No
Yes
Anti-conglomerate?
No
Yes
No
Yes
Biocatalysis, chromatography and/or crystallisation
Asymmetric synthesis
Chromatography combined with racemisation
Chromatography then crystallisation and racemisation
Preferential crystallisation combined with racemisation

Figure I - 13. Decision tree for an industrial compound to resolve.

In order to improve the research on enantiomeric substances, the European Community has launched a project called IntEnant[29,30] (acronym for "Integrated synthesis and purification of Enantiomers", Figure I - 14), a part of the seventh Framework Program (or FP7). This project lasted 3 years, from June 2008 to June 2011. IntEnant brought together 13 institutions, both academic groups (as the University of Rouen and the University of Paul Sabatier of Toulouse) and pharmaceutical companies, in 11 geographical locations in 6 countries (France, Germany, Italy, Sweden, Switzerland and United Kingdom). IntEnant aimed at designing new methods to obtain pure enantiomers or to improve the existing ones, or even to combine different methods by ensuring communication between the different groups. Several work packages were formed, bringing together the different specialities of each group such as crystallisation, organic synthesis, chromatography, biocatalytic processes, computer simulation…

Figure I - 14. Logo of IntEnant.

---

[29] H.-J. Federsel; *Org. Proc. Res. Dev.*, **2012**, 16, 260-261.
[30] IntEnant website: http://www.intenant.eu/

1. Non enantioselective synthesis from the chiral pool

Chiral compounds can be prepared from the chiral pool, i.e. from chiral molecules readily available and inexpensive. Most of these molecules come from natural product, like amino-acids, saccharides or alkaloids. The chirality already exists in the starting material and classical organic synthesis can be performed to achieve the production of the target compound.

2. Asymmetric synthesis from an achiral substrate

When a chiral molecule cannot be synthesised from the chiral pool, the chiral centre can be created during steps of the synthesis from a prochiral precursor. The final chirality of the chiral centre can be controlled by the use of:[31]

- Chiral reagent:[32] chiral molecule used during the synthesis but not present on the product, such as a chiral reducing agent to perform a reduction.
- Chiral auxiliary:[33] temporary chiral compound added during a step of the synthesis of the API. This temporary chiral centre drives the selectivity of the second chiral centre during its formation. It is a step of diastereoselective synthesis.
- Chiral catalyst:[32,34] chiral compound involved in the formation of a chiral transition state from the prochiral precursor. Once the product is formed, the catalyst goes back into the reaction mixture without modification then can be used again. This method is mainly used at the industrial scale, because the amount of catalyst can be small and/or it can be recycled, therefore reducing the cost of the synthesis.[31]

3. Resolution of racemic mixtures

When the synthesis of a single enantiomer is difficult to design (low yield, expensive catalyst or chiral auxiliary…), the synthesis of the racemic mixture, following by the resolution of the two enantiomers, can be the best option. Techniques mainly used to separate the two enantiomers are described below:

---

[31] A. N. Collins, G. N. Sheldrake, J. Crosby; *Chirality in industry: the commercial manufacture and applications of optically active compounds*; Wiley: Chichester, **1992**.

[32] E. J. Corey, S. Shibata, R. K. Baksi; *J. Org. Chem.*, **1988**, 53, 2861-2863.

[33] H. E. Ensley, C. A. Parnell, E. J. Corey; *J. Org. Chem.*, **1978**, 43, 1610-1612.

[34] H. Takaya, K. Mashima, K. Koyano, M. Yagi, H. Kumobayashi, T. Taketomi, S. Akutagawa, R. Noyori; *J. Org. Chem.*, **1986**, 51, 629-635.

- Chiral chromatography:[35] mixture of enantiomer is eluted through a chiral stationary phase by a mobile phase. The chiral stationary phase is typically constituted by chiral molecule (like cyclodextrins, chiral amino acids…) grafted on silica. The two enantiomers have a different behaviour towards the stationary phase, therefore they have different retention time and they can be separated. A variant used at the industrial scale is the Simulated Moving Bed Chromatography (SMB chromatography).[36] The SMB chromatography process employs several connected chiral columns. These are switched periodically against the fluid flow, which simulates a counter-current of liquid and solid phases, ensuring a continuous separation of the compounds, as illustrated in the Figure I - 15. The performance is often superior compared to a classical use of (chiral) columns.

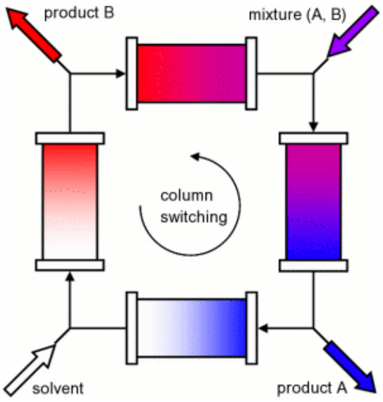

Figure I - 15. General principle of SMB chromatography.

Unfortunately, chromatographic methods are very expensive to set up because of the cost of columns, and a large amount of solvent is used. However, when the chromatographic method is well designed for a compound, it can be a very attractive way to obtain pure enantiomer, especially if the solvent can be recycled.

- Kinetic resolution: this method plays with the kinetic of reaction of the two enantiomers. Indeed, in a chiral environment, one of the two enantiomers will react quickly than the other one. The final mixture is composed by the unreacted enantiomer and the product of the reaction, easier to separate than a racemic mixture. The chiral environment can be due to an enzyme (see the next paragraph)[37] or a chiral catalyst.[38] However, the maximal yield is 50%.

---

[35] T.E. Beesley, R. P. W. Scott; *Chiral chromatography*; J. Wiley: Chichester, England; New York, **1998**.

[36] G. Subramanian; *Chiral Separation Techniques: A Pratical Approach*, Wiley-VCH ed., **2006**.

[37] A. Abate, E. Brenna, A. Constantini, C. Fuganti, F. G. Gatti, L. Malpezzi, S. Serra; *J. Org. Chem.*, **2006**, 71, 5228-5240.

[38] S. E. Schaus, B. D. Brandes, J. F. Larrow, M. Tokunaga, K. B. Hansen, A. E. Gould, M. E. Furrow, E. N. Jacobsen; *J. Am. Chem. Soc.*, **2002**, 1307-1315.

- Dynamic Kinetic Resolution DKR:[39] technique combining kinetic resolution and racemisation of the substrate in solution. As illustrated in the Figure I - 16, the kinetic of racemisation must be very fast compared to the kinetic of the reaction of the target compound (*S*)-B, ensuring a continuous supply in compound (*S*)-A

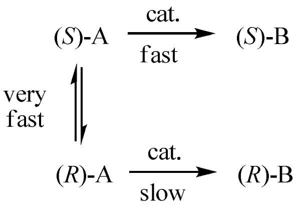
(S)-A
cat.
fast
(S)-B
very fast
(R)-A
cat.
slow
(R)-B

Figure I - 16. General principle of DKR.

For example, a reaction with a Grignard reagent can be catalyzed by chiral nickel complexes of β-aminoalkylphosphines with good yield and enantiomeric excess. (Figure I - 17)

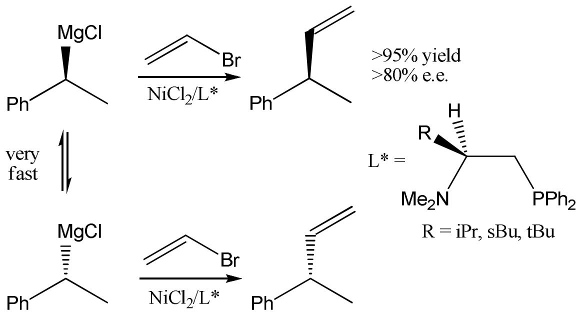
MgCl
Ph
Br
NiCl2/L*
Ph
>95% yield
>80% e.e.
very fast
L* =
H
R
Me2N
PPh2
R = iPr, sBu, tBu
MgCl
Ph
Br
NiCl2/L*
Ph

Figure I - 17. DKR applied to a Grignard reaction.

- Biocatalysis: kinetic resolution ensured by an enzyme or a microorganism, like yeasts.[40] Biocatalysis DKR can also be performed, as illustrated in Figure I - 18: the two enantiomers of the N-benzoylphenylalanine can be prepared in 100% yield and 99% e.e. from the racemic 2-phenyloxazolin-5-one. A porcine pancreatic lipase was used to synthesise the *S* enantiomer whereas a lipase from *Aspergillus niger* was used to prepare the *R* enantiomer.[39]

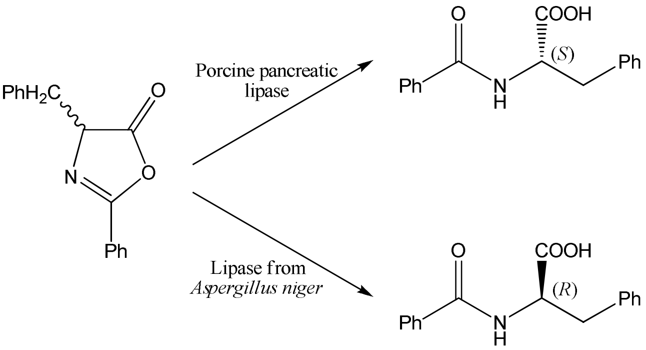
PhH2C
O
N
O
Ph
Porcine pancreatic lipase
Lipase from Aspergillus niger
O
COOH
(S)
Ph
N
H
Ph
O
COOH
(R)
Ph
N
H
Ph

Figure I - 18. Enzyme catalysed reactions.

---

[39] R. S. Ward; *Tetrahedron: Asymmetry*, **1995**, 6, 1475-1490.

[40] K. Leijondahl, L. Borén, R. Braun, J.-E. Bäckvall; *J. Org. Chem.*, **2009**, 75, 1988-1993.

Unfortunately, this process is limited by its moderate productivity (especially by the volume productivity) and by the difficulty to find the best enzyme or microorganism, but also by the experimental conditions. Most of them are efficient around 37°C and in an aqueous environment whereas organic solvents are often necessary to solubilise reagents and to promote synthesis. However, new enzymes and microorganisms can be designed by genetic manipulations in order to improve their performances.

- Crystallisation: many resolution methods based on a crystallisation step have been designed. A brief overview of the separation techniques by crystallization is presented in the paragraph V.

4. Analysis methods

To know if the asymmetric synthesis or the resolution of the two enantiomers have been efficient, it is necessary to have methods to determine the enantiomeric composition of the final product.

a. Chiral HPLC

The chiral HPLC (High Performance Liquid Chromatography) is very similar to the chiral chromatography described above, but it is designed for an analytical use. It is not necessary to know the concentration of the analytical sample because the two enantiomers have the same behaviour towards a detector as UV detector or a symmetric behaviour towards detectors as a micropolarimetre or a circular dichroism detector. The peak areas are directly proportional to the relative percentage of the two enantiomers. Unfortunately, HPLC analyses are not instantaneous (10-30 minutes). HPLC cannot be used on-line to know the composition of the reaction mixture, but is a convenient method to analyse final products.

b. Polarimetry

The measurement of the optical rotation was at the origin of the discovery of the chirality (see paragraph I.2) and it is still used to determine the enantiomeric excess of a sample. As said previously, the two enantiomers have the same specific optical rotation (α_0) but with opposite signs. α_0 is dependant on the temperature, on the wavelength of the polarized light and on the solvent. The optical rotation of the sample depends on the number of each molecule encountered by the light, therefore depends on the concentration of the sample and on the length of the measurement cell (Equation I - 3). The optical rotation can be related to the enantiomeric excess thanks to a small modification of the Equation I - 3 (Equation I - 4). The polarimetry method has several inconvenients: the need to know the exact concentration of the sample and to perform a calibration, but also to have chemically pure samples. Indeed, if sample are contaminated by another chiral compound, the optical rotation will not only due to the target molecule. But the result is instantaneous and can be used to follow the evolution of the enantiomeric excess during an experiment.

$$\alpha = \alpha_0.\ell.(C_+ - C_-)$$

Equation I - 3

$$\alpha = \alpha_0.\ell \frac{e.e.}{C_{tot}}$$

Equation I - 4

V - Purification by crystallisation

The purification by crystallisation is one of the oldest methods to purify a product and still one of the most widely used. Crystallisation is used both for chemical and enantiomeric purification of molecules. Three kinds of purifications by crystallisations are described in the following paragraphs; their efficiency is directly linked to the properties of the molecule.

1. Pasteurian resolution

This method, the oldest one, was designed by Louis Pasteur in 1853 and is based on the symmetry breaking between the two enantiomers. The principle of this method is to transform an enantiomer pair into a diastereomeric pair by adding a pure chiral agent to a solution of a racemic mixture in an achiral solvent. Contrary to enantiomeric compounds, diastereomeric compounds are not mirror images and therefore have different physico-chemical properties,[41] such as the difference of solubility, make it possible the separation of the two diastereomers. Then the pure enantiomer is separated from the chiral agent. Thus, Louis Pasteur added a chiral base to the racemic mixture of tartaric acid in order the form the two diastereomeric salts. Then he separated the two diastereoisomers by crystallisation, by using their difference in solubility.

However, for this method to be interesting economically, the chiral agent must be cheap and easily available in large amount with a good enantiomeric purity, and/or be easily recycled.

---

[41] J. Jacques, A. Collet, S. H. Wilen; *Enantiomers, racemates, and resolutions* **1981**, New York, Wiley.

Therefore, most of chiral agents come from the chiral pool. Another limitation is the need to have a strong enough acidic or basic function on the pair of enantiomers to form the diastereomeric salt. Often, several diastereomeric salts must be formed in order to find the best combination, i.e. the best difference in solubility, the best yield and the easiest separation of the pure enantiomer and of the chiral agent.

2. Preferential crystallisation[42]

a. Definition and history

Preferential crystallisation (hereafter PC) is a stereoselective crystallisation making possible the separation of the two enantiomers. From a racemic or nearly racemic supersaturated solution, and thanks to a careful management of the system, only one enantiomer crystallises. Historically, the first preferential crystallisation was carried out in 1866 by a Pasteur's student, Desiré Gernez.[10] He described to Pasteur the strange behaviour of a saturated solution of sodium ammonium tartrate tetrahydrate:

- A saturated solution of pure enantiomer seeded by small crystals of the other enantiomer does not give new crystals.
- A saturated solution of racemic mixture seeded by small crystals of the one of the two enantiomers gives bigger crystals of the same enantiomer.

In 1882, Jungfleish[43] emphasized the importance of the supersaturation on the success of the preferential crystallisation. In 1914, Werner described the first resolution of enantiomeric compounds: complexes of potassium cobalt trioxalate[44] and in 1934, the resolution of the histidine mono chlorohydrate [45] was carried out. But it is only in 1959 that the proof of the large scale resolution was made by performing the resolution of the (1*R*,2*R*)-chloramphenicol.[46] Since the second part of the 20th century, with the publications of Secor[47] then Jacques and collaborators,[48] the preferential crystallisation has become a widely used method to obtain pure enantiomers.

---

[42] G. Levilain, G. Coquerel; *Crystengcomm*, **2010**, 12(7), 1983-1992.

[43] M. E. Jungfleisch; *J. Pharm. Chim.,* **1882**, 5, 346-357.

[44] A. Werner; *Chem. Ber.,* **1914**, 47, 2171-2182.

[45] R. Duschinsky; *Chem. Ind.,* **1934**, 53, 10-20.

[46] G. Amiard; *Experientia,* **1959**, 15, 1-7.

[47] R. M. Secor; *Chem. Rev.* **1963**, 63, 297-309.

[48] A. Collet, M. J. Brienne, J. Jacques*; Chem. Rev.,* **1980**, 80, 215-230.

b. General scheme of preferential crystallisation

Typically, preferential crystallisation is a cyclic process, alternating the crystallisation of the two enantiomers (Figure I - 19).

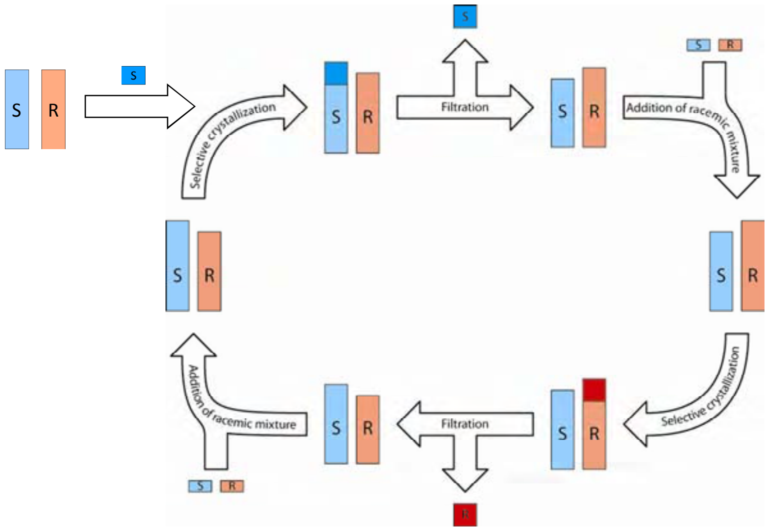
S
R
S
Selective crystallization
S
R
S
Filtration
S
R
S R
Addition of racemic mixture
S
R
S
R
Selective crystallization
S
R
R
Filtration
S
R
Addition of racemic mixture
S R

Figure I - 19. Basic description of preferential crystallization.

Starting from a slightly enriched mixture (typically 10% e.e.) in one enantiomer (e.g. the *S* enantiomer), this enantiomer is selectively crystallised. The solid is collected by filtration (or centrifugation) then racemic mixture, corresponding to the mass of pure enantiomer harvested, is added to the mother liquor in order to reach a mixture having exactly the mirror image composition than the starting mother liquor (i.e. a mixture slightly enriched in the *R* enantiomer). Then the *R* enantiomer is selectively crystallised. By adding racemic mixture, the mother liquor gets back to the initial situation and the *S* enantiomer is crystallised again. As the preferential crystallisation is a cyclic process and as the mother liquor is recycled, yields of this kind of resolution can be very good, and the two enantiomers are recovered. Several methods of preferential crystallisation were performed and are described below.

c. Seeded isothermal preferential crystallisation

Seeded isothermal preferential crystallisation (SIPC) is the oldest method of preferential crystallisation. A saturated liquid enriched with one enantiomer (e.g. the enantiomer *R*) at the temperature T_{homo} is cooled down to T_F in order to induce a sufficient supersaturation then seeds of pure crystals of *R* are added. Ideally, only the crystallisation of the *R* enantiomer takes place then the solid and the suspension are separated. The mother liquor, containing thus an excess of the *S* enantiomer, is heated to T_{homo} then racemic mixture is added to have a system with the exact opposite composition as the initial one. The mother liquor, enriched with the S enantiomer, is cooled down to T_F and seeds of pure crystals of *S* are added. The solid (ideally only the *S* enantiomer) and the liquid (containing an excess of the *R* enantiomer) are separated. The system is came back to the initial composition by adding racemic mixture to the mother liquor and by heating it to T_{homo}. The crystallisation of the *R* enantiomer can be performed again.

d. Auto-seeded polythermic programmed preferential crystallization

Auto-seeded polythermic programmed preferential crystallization (AS3PC), [49] developed by the SMS laboratory, is similar to the SIPC mode but the initial system is composed of a saturated solution in equilibrium with crystals of a pure enantiomer (e.g. the enantiomer *R*). The crystallisation of the *R* enantiomer is ensured by a controlled cooling, thanks to a temperature ramp from T_i to T_f. In the ideal case, only the *R* enantiomer crystallises. The solid and the liquid are separated, before the crystallisation of the *S* enantiomer. Then, racemic solid is added and the system is heated to Ti to obtain a system with the exact opposite composition of the initial one; a saturated solution in equilibrium with crystals of the *S* enantiomer.

e. Auto-seeded preferential crystallisation induced by solvent evaporation

Auto-seeded preferential crystallisation induced by solvent evaporation (ASPreCISE)[50] is a new method of preferential crystallisation, developed by the SMS laboratory. The principle of this method is the same than in the AS3PC mode (i.e. a cyclic process with a saturated solution in equilibrium with crystals of a pure enantiomer as initial composition) but the supersaturation is generated and controlled by solvent evaporation and not by cooling.

f. Second-order asymmetric transformation

Second-Order Asymmetric Transformation (SOAT) combines preferential crystallisation and *in-situ* racemisation.[51,52,24] It is the ultimate version of the preferential crystallisation since starting from a racemic mixture, a single enantiomer can be quantitatively harvested in a single step. The initial system is composed by a saturated solution in equilibrium with crystals of a pure enantiomer at T_i. All along the controlled cooling, from T_i to T_f, crystals of pure enantiomer are in equilibrium with a racemic mixture. The *in-situ* racemisation erodes the chiral imbalance, making more difficult the crystallisation of the counter enantiomer.

---

[49] WO9508522, **1995**.

[50] WO2011/07330.

[51] US4417070 **1983**.

[52] S. N. Black, L. J. Williams, R. J. Davey, F. Moffat, R. V. H. Jones, D. M. McEwan, D. E. Sadler; T*etrahedron*, **1989**, 45, 2677-2682.

Therefore it is possible to decrease more the temperature or to evaporate a larger volume of solvent than in the case of AS3PC or ASPreCISE, increasing the yield.

g. Comparison between preferential crystallisation methods

Usually, ASP3C mode gives better results than SIPC mode.[53,54] The initial composition of the system is the major difference, seeding being not necessary in the AS3PC mode. Furthermore, the larger amount of solid in suspension in AS3PC mode compared with the seeds in SIPC mode, combined with the controlled cooling in AS3PC (in opposition with the initial supersaturation in SIPC), ensures a better yield and a better enantiomeric excess to the AS3PC mode. The slow cooling in presence of many crystals of pure enantiomer favours the crystal growth; the enantiopurity is increased and the filterability is improved.

ASPreCISE is a recent technique, mainly used for thermally sensitive molecules and molecules with poor variation of solubility versus temperature. Only few examples are described in the literature, so it is difficult to compare its efficiency with the other ones. The main restriction of this method is the use a solvent easy to evaporate. But, if an appropriate solvent is found, the yield should be increased compare to the AS3PC mode; a solvent evaporation generally ensures a higher difference of solubility (and so, a higher theoretically harvested mass) than a cooling.

Theoretically, the SOAT mode have non negligible advantages (e.g. yield > 50% in one step). However, it is not often used, mainly because the target compound must crystallise as a conglomerate and be quickly racemised in solution under the same operating conditions.

3. Inclusion complexes

Formation of inclusion complexes is another way to have access to pure enantiomers by using the properties of diastereoisomers. As in the Pasteurian resolution, a chiral agent is added to the racemic mixture to break the symmetry, by the formation of diastereoisomeric entities. The main difference with the Pasteurian resolution is the nature of the chiral agent, and, consequently, the nature of the interactions with the two enantiomers. The formation of the diastereoisomeric entities is not ensured by salt formation but by formation of inclusion complexes thanks to weak interactions (hydrogen bond, van der Waals interactions…). In the

---

[53] L. Courvoisier, E. Ndzié, M. N. Petit, U. Hedtmann, U. Sprengard,, G. Coquerel; *Chem. Lett.,* **2001**, 30, 364-365.

[54] L. Courvoisier, L. Mignot, M.N. Petit, G. Coquerel; *Org. Process Res. Dev.*, **2003**, 7, 1007-1016.

case of the inclusions complexes, two types of inclusions can be encountered, depending on the chiral agent used:

- Crystal-lattice inclusion: chiral cavities of a crystal lattice play the role of chiral host.
- Molecular inclusion: the host molecule is a chiral molecule.

These two types of inclusions are described in the following paragraphs.

a. Crystal-lattice inclusion complexes

As said previously, the symmetry breaking is ensured by the existence of chiral cavities inside the crystal packing. The chirality of these cavities is due to the chirality of the host molecule, or to the particular geometry (and so, to the specific interactions) of the cavity, even if the host molecule is achiral. Of course, it is necessary that the cavity and the guest molecule are compatible in terms of size and selectivity to have stable complex and an efficient resolution. (Figure I - 20)

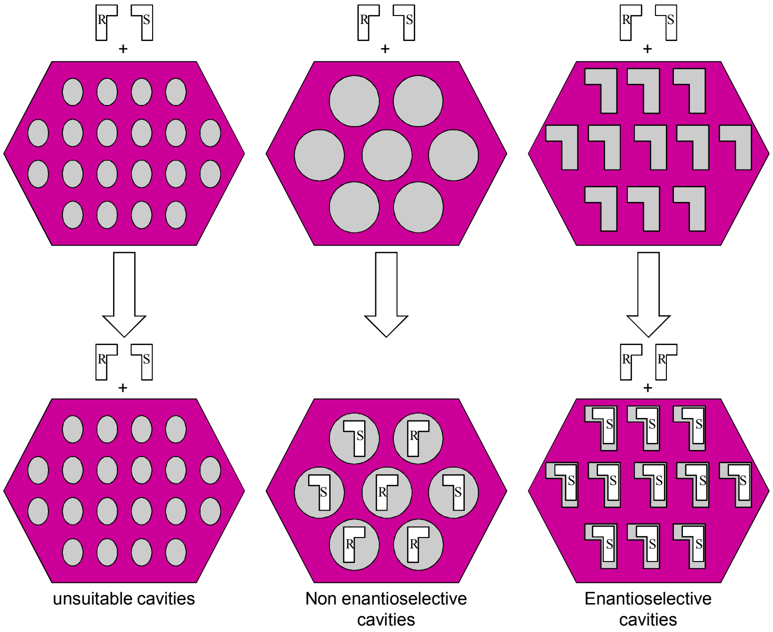

Figure I - 20. General scheme of resolution by inclusion in a crystal lattice.

Chiral cavities can be directly present inside the crystal lattice of the host molecule but sometimes, chiral cavities are created only when the host and guest molecule crystallise together. Few examples of structural inclusion complexes are described below.

- Urea: it was the first case depicted in the literature.[55] Although achiral, (Figure I - 21) this molecule is able to crystallize in the enantiomorphous space groups $P6_122/P6_522$ when appropriate molecules are present. The result is the formation of a conglomerate, and the two enantiomers can be separated by using the classical method like preferential crystallisation.[56] Thus, by using inclusion complexes with urea, Schlenk performed the separation of the two enantiomers of the 2-chlorooctane, with a final enantiomeric excess of 95.6%.[55]

---

[55] W. Schlenk; *Analyst* **1952**, 77, 870; Justus Liebigs; *Ann. Chem*., **1973**, 1145; 1156; 1179; 1195.

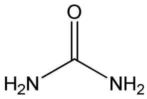

Figure I - 21. Chemical formula of urea.

- Tri-*o*-thymotide (TOT): this tricyclic lactone (Figure I - 22) exhibits a conformational chirality with a fast racemisation in solution. Like the urea, the TOT is able to form inclusion complexes with many different guests,[56,57] (for example, the 2-bromobutane) and it crystallise in chiral space groups only in the presence of chiral molecules to give enantiomorphous crystals.

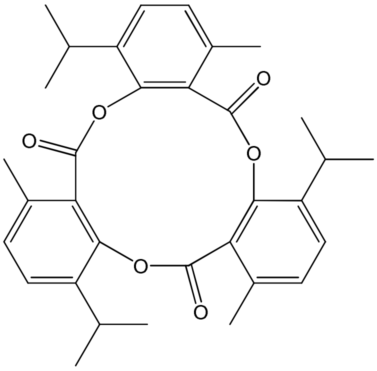

Figure I - 22. Chemical formula of the Tri-*o*-thymotide.

- Sterically hindered polyols: these molecules (Figure I - 23), derived from the BINOL (2,2'-dihydroxy-1,1'-binaphthyle) or the TADDOLs (α,α,α',α'-tetraaryl-1,3-dioxolane-4,5-diméthanol), were studied mainly by the team of Fumio Toda. [58,59,60]

---

[56] R. Arad-Yellin, B. S. Green, M. Knossow, G. Tsoucaris; *Inclusion Compounds III,* **1984**, Academic Press, London, chap. 9, 278-284.

[57] H. M. Powell; *Nature,* **1952**, 170, 155-155.

[58] F. Toda; *Aust. J. Chem.,* **2001**, 54, 573-582.

[59] Z. Urbanczyk-Lipkowska, F. Toda; *Separations and reactions in organic supramolecular chemistry,* **2004**, J. Wiley & Sons: New York, Chapter 1.

[60] F. Toda; *Enantiomer Separation: Fundamental and Practical Methods,* **2004**, Kluwer Academic Publisher: Dordrecht, Chapter 1, 1-47.

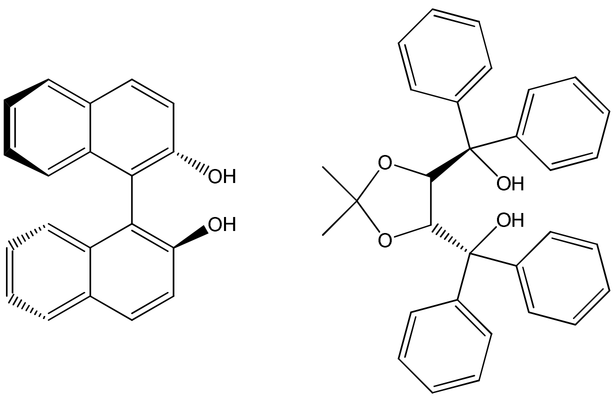

Figure I - 23. Chemical structure of BINOL (left) and TADDOL (right).

In addition to the geometry of the cavity, the steric effect (aromatic groups) of this kind of molecules prevents the formation of intermolecular hydrogen bonds between two TADDOLs. However a small guest molecule is able to form H-bonds with two TADDOL units, bridging them (Figure I - 24), as it was demonstrated in the case of (*R,R*)-(-)-trans-2,3-bis(hydroxydiphénylméthyl)-1,4-dioxaspiro[4.4]nonane (tBHDN) and methyl 3-hydroxybutanoate.[61]

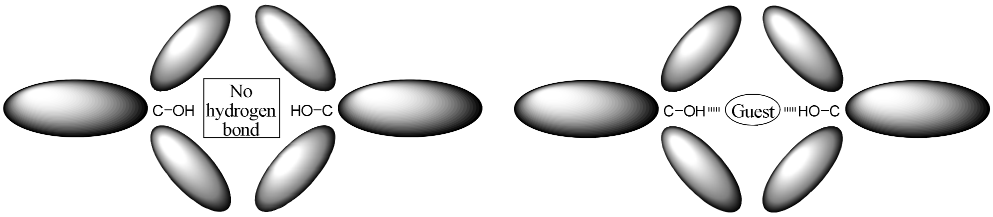

Figure I - 24. Schematical representation of the formation hydrogen bonds in the presence of a guest molecule.

- (2*R*,3*R*)-(*O,O'*)-dibenzoyltartric acid (DBTA) : this chiral molecule was often used for the pasteurian resolution, but, in 1994, Hamato and collaborators studied the system formed by the DBTA and the racemic trans-bicyclo[2.2.1]heptane-2,3-diamine.[62] They observed that instead of salt, a structural inclusion was formed. The possibility to form complexes with the DBTA was confirmed by different authors and the existence of a hydrophobic cavity was highlighted.[63,64]

---

[61] F. Toda, A. Sato, L. R. Nassimbeni, M. L. Niven; *J. Chem. Soc. Perkin Trans. 2,* **1991**, 1971-1975.

[62] K. Hatano, T. Takeda, R. Saito; *J. Chem. Soc., Perkin Trans. 2*, **1994**, 579-584.

[63] B. Szczepanska, M. Gdaniec, U. Rychlewska; *J. Incl. Phen. Mol. Recogn. Chem.*, **1995**, *22*, 211-219.

[64] K. Nemak, M. Acs, Z. M. Jaszay, D. Kozma, E. Fogassy; *Tetrahedron,* **1996**, 52(5), 1637-1642.

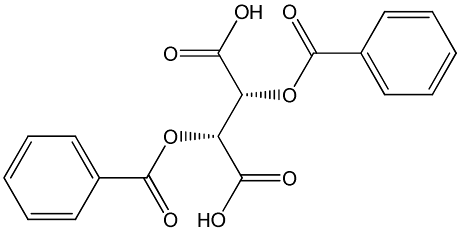

Figure I - 25. Chemical formula of the (2*R*,3*R*)-DBTA.

- Biliary acids: these natural molecules, like the cholic acid, are produced by the liver of mammals. A chiral channel exists inside the crystal lattice[65] therefore they can also be used to form inclusion complexes.[66] The chiral recognition is ensured buy a combination of van der Waals interactions and steric effects. For example, Bertolasi *et al.* described the resolution of cyclic ketone with e.e. > 65%.

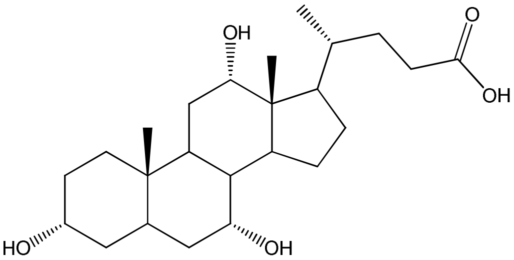

Figure I - 26. Chemical formula of the cholic acid.

b. Inclusion complex in a host molecule

Contrary to the previous case, the cavity is not formed by the crystal lattice but by the molecule itself. The interactions involving the complex formation between the host entity and the guest molecule are the same in the two cases, but real diastereoisomeric complexes are formed in the case of molecular inclusion. (Figure I - 27) Consequently, this kind of complexes exists in the solvated state and the chiral discrimination is possible in solution.

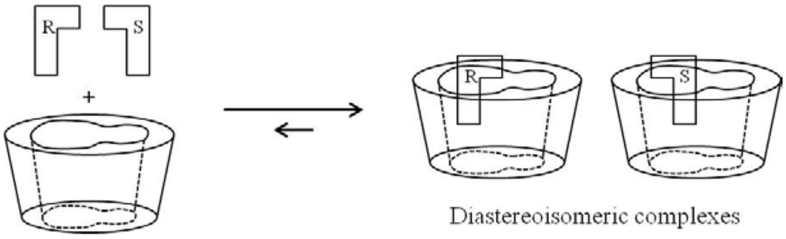

Figure I - 27. General principle of inclusion complexes.

---

[65] O. Bortolini, G. Fantin, M. Fogagnolo; *Chirality*, **2005**, 17, 121-130.

[66] V. Bertolasi, O. Bortolini, M. Fogagnolo, G. Fantin, P. Pedrini; *Tetrahedron: Asymm*etry, **2001**, 12, 1479–1483.

It is necessary for the host molecule to have a chiral cavity. These molecules are often depicted in the literature, for example, for the preparation of stationary phases for HPLC. Four examples of host molecules are described below.

- Crown ethers: heterocycles which the main unit is the ethylene oxide (-CH_2-CH_2-O-). They are named following their total number of atoms *x* and of oxygen *y* to give x-crown-y or x-C-y. (Figure I - 28a) Basic crown ethers are achiral but they can be functionalised in order to make them chiral. (Figure I - 28b) They are mainly used for the separation of enantiomers by chromatography[67] (there are grafted on the stationary phase) and there are few examples of resolution by crystallisation.[68]

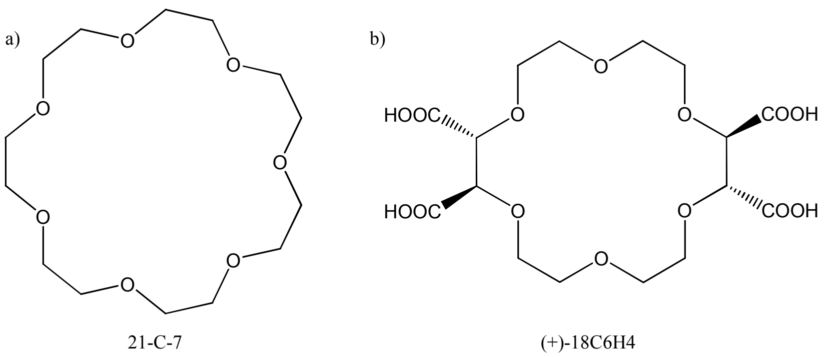

Figure I - 28. Chemical formula of a) 21-C-7 and b) (+)-18-C-6 tetracarboxylic acid.

- Cucurbiturils: achiral macrocyclic molecules made of glycoluril monomers (=$C_4H_2N_4O_2$=).[69] Their name is derived from the resemblance with a pumpkin, of the family of the cucurbitaceae. Cucurbiturils are commonly written as cucurbit[n]uril (CB[n], or CBn) where *n* is the number of glycoluril units. (Figure I - 29) Until now, these molecules were mainly used for the complexation of cations.[70] But recently, the first example of cucurbituril used for chiral recognition in solution was depicted.[71] By complexing the CB6 with two different guest molecules, a chiral agent then the two enantiomers of the compound of interest (2-methylbutylamine), Rekharsky *et al.* highlighted the different behaviour of the two enantiomers, ensuring a final enantiomeric excess of 95%.

---

[67] L. R. Sousa, G. D. Y. Sogah , D. H. Hofmann, D. J. Cram; *J. Am. Chem. Soc.*, **1978**, 100, 4569-4576.
[68] H. Nagata, H. Nishi, M. Kamigauchi, T. Ishida; *Chem. Pharm. Bull.,* **2006,** 54(4), 452-457.
[69] W. A. Freeman, W. L. Mock, N. Y. Shin; *J. Am. Chem. Soc.*, **1981**, 103, 7367-7368.
[70] D. Whang, J. Heo, J. H. Park, K. Kim; *Angew. Chem. Int. Ed.,* **1998**, 37(1-2), 78-80.
[71] V. M. Rekharsky, H. Yamamura, C. Inoue, M. Kawai, I. Osaka, R. Arakawa, K. Shiba, A. Sato, Y. Ho Ko, N. Selvapalam, K. Kim, Y. Inoue; *J. Am. Chem. Soc.,* **2006***,* 128, 14871-14880.

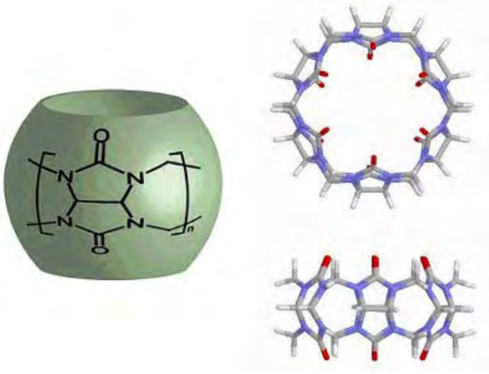

Figure I - 29. Schematic representation with chemical formula of CBn (left) and structure of CB6 (right).

- Calixarenes: macrocycles made of phenolic units. The word calixarene is derived from the greek "calix", meaning vase, and from the word "arene" used to refer to the aromatic groups. Calixarenes are commonly written as calix[n]arene where n is the number of phenolic units. (Figure I - 30) These molecules are achiral but they can be chemically modified to make them chiral.[72] Most of examples of chiral recognition were made in solution,[73,74] but few discriminations at the solid state were depicted in the literature.[75,76,77]

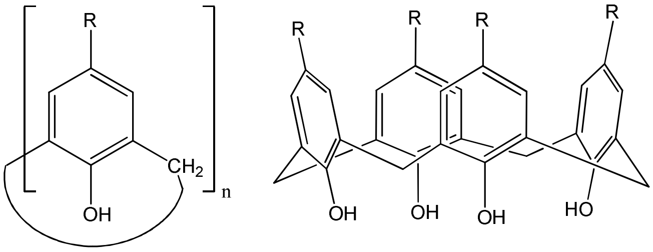

Figure I - 30. Chemical formula of calix[n]arene (left) and calix[4]arene (right).

- Cyclodextrins: cyclic oligosaccharides linked by α-1→4-glycosidic bonds. The more popular cyclodextrins are α-, β- and γ-cyclodextrins, respectively made of six, seven and eight glycosidic units.[78] (Figure I - 31) Cyclodextrins are able to form complexes with many different molecules. Contrary to the previous compounds, cyclodextrins are chiral. Complexes made from cyclodextrins with a racemic mixture are thus diastereoisomers. This interesting property explains why many researchers are working on this subject.[79,80] Additional details are given in the chapter II.

---

[72] Z. Asfari, V. Böhmer, J. Harrowfield, J. Vicens; *Calixarenes*, **2001**, Kluwer Academic Publishers: Dordrecht, Holland.

[73] U. Darbost, M.-N. Rager, S. Petit, I. Jabin, O. Reinaud; *J. Am. Chem. Soc.,* **2005***,* 127, 8517-8525.

[74] L. Mutihac, J. H. Lee, J. S. Kim, J. Vicens; *Chem. Soc. Rev*., **2011**, 40, 2777-2796.

[75] E. Weber, J. Ahrendt, A, Lohner, P. J. Reddy, K. K. Chacko; *J. Incl. Phenom*., **1993**, 15, 231-245.

[76] J. L. Atwood, S. J. Dalgarno, M. J. Hardie, C. L. Raston; *Chem. Commun*., **2005**, 337-339.

[77] P. R. Martinez-Alanis, I. Castillo; *Tetrahedron Lett*., **2005**, 46, 8845-8848.

[78] W. Saenger; *Angew. Chem., Int. Ed. Eng.*, **1980**, 19, 344-362.

[79] A. Grandeury, E. Condamine, L. Hilfert, G. Gouhier, S. Petit, G. Coquerel; *J. Phys. Chem. B*, **2007**, 111, 7017-7026.

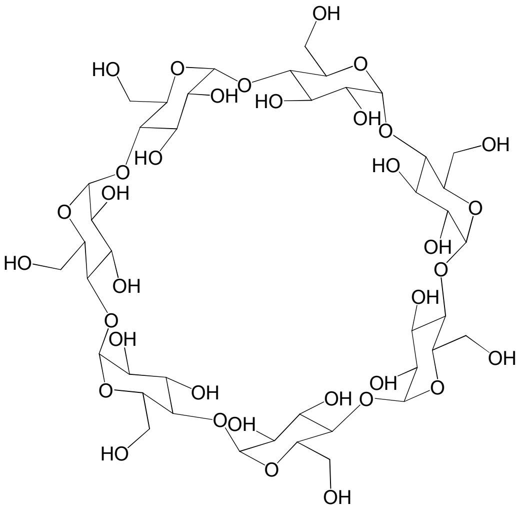

Figure I - 31. Chemical formula of β-cyclodextrin.

VI - Spontaneous symmetry breaking

The preferential crystallisation methods previously described are based on the alternate crystallisation of the two enantiomers of a conglomerate. Thus, for a molecule, both pure *R* and *S* are harvested even if only one is the target compound, engendering a maximum of 50% yield. Sometimes, the non-desired enantiomer can be racemised and then used again to reach, theoretically, 100% yield. Unfortunately, the number of additional steps increases the time and the cost of the production of the pure target enantiomer.

Recently a new crystallisation process called deracemisation, combining *in-situ* racemisation and grinding (and preferential crystallisation) was designed. Contrary to classical preferential crystallisation, a racemising agent is added to the system in order to racemise the counter enantiomer during the crystallisation of the target one (e.g. the enantiomer *R*). Thus, pure crystals of *S* are "transformed" into pure crystals of *R*. This method, also called "spontaneous symmetry breaking", allows to obtain only one enantiomer with a very good optical purity (>99%) and with a maximal yield, theoretically close to 100%.

The first observations of the benefit of the grinding during the resolution by preferential crystallisation combined with *in-situ* racemisation were made by Viedma in 2005.[81]

The discovery of this process, as well as the last improvements, is described in the following paragraphs. Hypothesis about the mechanism involved during the set-up will be also discussed.

---

[80] Y. Amharar, A. Grandeury, M. Sanselme, S. Petit, G. Coquerel; *J. Phys. Chem.*, **2012**, 116(20), 6027-6040.

[81] C. Viedma; *Phys. Rev. Lett.*, **2005**, 94, 065504.

1. History

The first observations of the spontaneous symmetry breaking were made by Frank in 1953.[82] He suggested that an enantiomer was able to catalyse its own synthesis, suppressing that of its mirror image, with a nonlinear amplification of a small initial enantiomeric excess.

Almost twenty years later, the spontaneous symmetry breaking of the 1,1'-binaphthyl was reported by Richard E. Pincock and Keith R. Wilson.[83] One of the polymorphic form of the 1,1'-binaphthyl is a conglomerate and its racemisation (i.e. the rotation around the single bond) is very fast at 150°C. Pincock and Wilson managed to do the resolution of the crystalline material from the melt by inducing the crystallisation at 150°C by touching the sample with dry ice. They also noticed that the use of seeds of pure enantiomer improved the final enantiomeric excess. Indeed, without seeds, "*it is apparent that obtaining binaphthyl with an optical purity above 90 percent by this method would be a very exceptional event (observable about one in 150 tries)*".

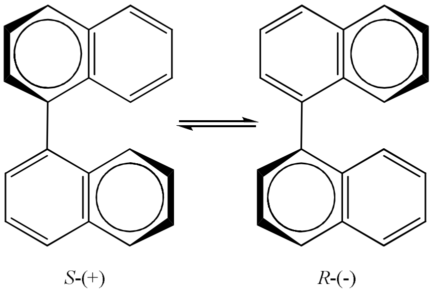

Figure I - 32. *S*-(+)- and *R*-(-)-1,1'-binaphthyl.

2. Theory of the mother crystal

In 1990, Kondepudi *et al.* confirmed the observations made by Kipping and Pope almost one century before, about the particular crystallisation of the sodium chlorate $NaClO_3$.[84,85] This inorganic compound, though achiral, crystallise as two enantiomeric chiral crystals, *D* and *L*, in the cubic space group $P2_13$. Kipping and Pope noticed that, during the crystallisation of $NaClO_3$ by evaporation of a saturated solution, without seeding, the difference between the number of *D* and *L* crystals was due to statistical fluctuations (from 17 different crystallisations, 525 *L*-crystals and 475 *D*-crystals were harvested), whereas seeds ensure a greater final enantiomeric excess. Kondepudi *et al.* also depicted for the first time the particular contribution of the stirring for the chiral symmetry breaking. They compared crystals obtained after evaporation of the solvent (water) with and without magnetic bar in the absence of seed. Crystals harvested from the experiment with stirring were smaller and more numerous than the ones obtained without stirring. Moreover, every try gave an enantiomeric excess greater than 99% under stirring whereas the enantiomeric excess obtained without stirring was close to 0%. To explain these observations, they put forward the hypothesis that secondary nuclei were quickly produced from a primary nucleus, called "mother crystal", thanks to the stirrer. These new nucleus grew up then gave in turn new secondary nucleus, thus propagating the chirality of the mother crystal. Kondepudi et al. spoke about a "*chirally autocatalytic*" process. They also highlighted that secondary nucleation was not sufficient to explain the final enantiomeric excess. Indeed, during the time of the experiment, nucleus of the opposite enantiomer had time to appear, grow and form secondary nucleus. The proliferation of the first crystal of a particular chirality must be linked to a suppression of the nucleation of the opposite handedness. They explained this suppression of nucleation by the very weak supersaturation. Indeed, supersaturation was ensured by a slow evaporation of the solvent (around 25mL of water were evaporated in 4-5 days), so, when the first nucleus appeared, and with the contribution of the secondary nucleus, the rate of primary nucleation became very close to zero. Therefore, only crystals of the same handedness than the first nuclei grow during the experiment. The chirality of the first nucleus, and then of the final crystals, is stochastic.

---

[82] F. C. Frank; *Biochem. Biophys. Acta*, **1953**, 11, 459-463.
[83] R. E. Pincock, K. R. Wilson; *J. Am. Chem. Soc.*, **1971**, 93(5), 1291-1292.
[84] F. S. Kipping, W. J. Pope; *J. Chem. Soc. Trans.*, **1898**, 73, 606-617.
[85] D. K. Kondepudi, R. J. Kaufman, N. Singh; *Science*, **1990**, 250, 975-976.

Few years later, two new studies of Kondepudi et al., [86,87] and another one of Martin et al.,[88] confirmed the important role of the stirring during the chiral symmetry breaking process, and particularly the role of the stirring rate. At the end of the century, they offered another proof by improving the resolution of the 1,1'-binaphthyl thanks to stirring.[89]

3. Reassessment of the theory of the mother crystal

The theory of the "mother crystal" was called into question by Viedma in 2004.[90] Indeed, he performed the total chiral symmetry breaking of the sodium chlorate from a high supersaturated solution, i.e. with a very high primary nucleation rate. Immediately after he began to stir a highly supersaturated solution ($\beta>1.5$ with 60°C of supercooling), the solution

---

[86] D.K. Kondepudi, K. L. Bullock, J. A. Digits, J. K. Hall, J. M. Miller; *J. Am. Chem. Soc.*, **1993**, 115, 10211-10216.

[87] D. K. Kondepudi, K. L. Bullock, J. A. Digits, P. D. Yarborough; *J. Am. Chem. Soc.*, **1995**, 117, 401-404.

[88] B. Martin, A. Tharrington, X.-I. Wu; *Phys. Rev. Lett.*, **1996**, 77(13), 2826-2829.

[89] D. K. Kondepudi, J. Laudadio, K. Asakura; *J. Am. Chem. Soc.*, **1999**, 121, 1448-1451.

[90] C. Viedma; *J. Crystal Growth*, **2004**, 261, 118-121.

became milky, meaning the formation of many crystals. In spite of this catastrophic primary nucleation (the two enantiomers crystallised), and after 2 days of growth, 100% of the crystals were of the same handedness. Viedma concluded that "*the results of our experiment suggest that the current explanation for chiral symmetry breaking via nucleation of a single "mother crystal" may explain some cases but not all, and as such, the mechanism to explain the chiral symmetry breaking in crystallisation remains as an open question.*"

These observations were confirmed the year after, when he performed the complete chiral symmetry breaking of the sodium chlorate from a suspension of racemic material.[81] In this case, it was clear that the theory of the "mother crystal" was not valid and he proposed a new model of "complete chiral purity induced by nonlinear autocatalysis and recycling". This theory will be detailed in the paragraph VI-6.

4. Benefits of grinding

In the same publication,[81] Viedma described the effect of stirring combined with the addition of 3mm diameter glass beads. The result was a significant increase of the kinetics, i.e. a significant decrease of the time to reach a complete resolution of sodium chlorate, depending on the number of glass balls and on the stirring rate (Figure I - 33).[81] Indeed, glass beads have an abrasive effect, enhancing the effect of the stirring and then enhancing the rate of secondary nucleation.

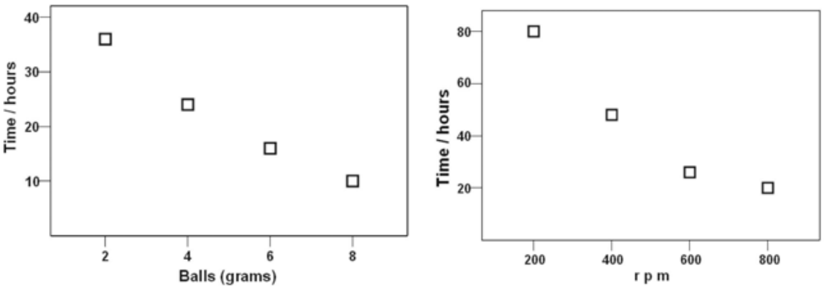

Figure I - 33. Solutions with initial symmetric mixtures of *L* and *D* crystals of $NaClO_3$ and glass beads show total symmetry breaking and chiral crystal purity. The data show the necessary time to achieve chiral purity depending on: a) the number of balls in the system (600rpm) and b) the speed of agitation of the system (4g of balls).

The discovery of benefits of the abrasive grinding for the obtaining of pure enantiomers was the major advance in the field of total symmetry breaking. Since 2005 and the publication of Viedma, the number of publications on the subject increases, as well as for the understanding of the mechanism than for the production of pure enantiomers.

5. Total symmetry breaking of organic compounds

In 2006, Crustats *et al.*[91] following by Donna G. Blackmond[92] in 2007 speculated that this crystallisation process might be extended to intrinsically chiral molecules which can be very quickly racemised when a racemising agent is present. Moreover, such a chiral molecule should crystallise as a conglomerate to imitate the enantiomeric chiral crystals of the $NaClO_3$. (Figure I - 34)

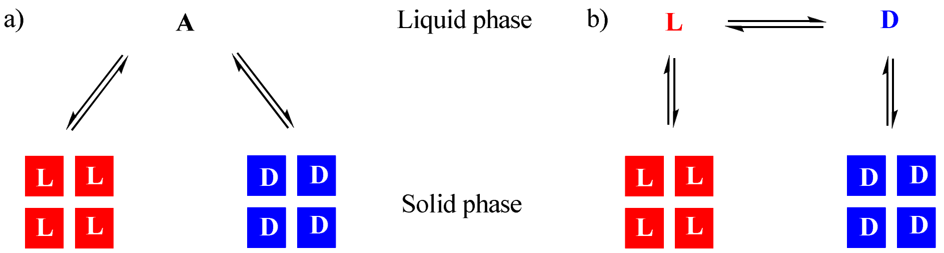

Figure I - 34. Illustration of solid-liquid equilibrium for systems forming chiral solids. a) achiral material in equilibrium with chiral crystals, b) chiral compound crystallising as a conglomerate.

The first try was made jointly between the Blackmond research group and a Dutch consortium, composed by two chemical companies, Syncom and DSM, and the Radboud University of Nijmegen. They studied the behaviour of an amino-acid derivative, the *N*-(2-methyl-benzylidene)-phenylglycine-amide, known to crystallise as a conglomerate. This kind of molecule can be easily racemised in solution in the presence of a catalytic amount of an organic base such as DBU (1,8-diazabicyclo[5.4.0]undec-ène). (Figure I - 35)[93] They performed the complete deracemisation of the solid phase within approximately 30 days.[94,95] They also introduced for the first time the term of "*chiral amnesia*".

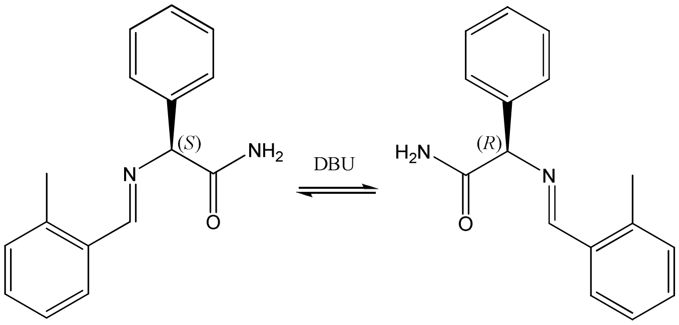

Figure I - 35. Chemical formula of N-(2-methyl-benzylidene)-phenylglycine-amide.

---

[91] J. Crusats, S. Vientemillas-Verdaguer, J. M. Ribó; *Chem. Eur. J.*, **2006**, 12, 7776-7781.

[92] D. G. Blackmond; *Chem. Eur. J.*, **2007**, 13, 3291-3295.

[93] R. M. Kellogg, B. Kaptein, T. R. Vries; *Top. Curr. Chem.*, **2007**, 269, 159-197.

[94] W. L. Noorduin, T. Izumi, A. Millemaggi, M. Leeman, H. Meekes, W. J. P. Van Enckevort, R. M. Kellogg, B. Kaptein, E. Vlieg, D. G. Blackmond; *J. Am. Chem. Soc.*, **2008**, 130, 1158-1159.

[95] W. L. Noorduin, H. Meekes, W. J. P. van Enckevort, A. Millemaggi, M. Leeman, B. Kaptein,R. M. Kellogg, E. Vlieg; *Angew. Chem. Int. Ed.*, **2008**, 47, 6445-6447.

However they noticed that the result of the experiment was not random because only the *R* enantiomer was harvested. They did more than 100 experiments though, carried out in different laboratories. They suspected a contamination by a chiral impurity of the natural origin. This hypothesis was validated one year later by the addition of an enantiopure compound (*R* or *S*-phenylglycine).[94] In 2009, it has been demonstrated that the use of enantiopure amino-acid allows to predict and then to choose the final chirality of the solid phase.[96]

a. Formation of Schiff bases: an efficient tool for the preparation of pure enantiomers of amino-acid derivatives

Since this success, the total deracemisation of many other amino-acid derivatives were performed. The need of chiral amino acids is always a major issue for the pharmaceutical industries because they often are building blocks for the synthesis of new drugs. Unfortunately, amino acids crystallising as a conglomerate, and easily racemisable, are very uncommon. However, most of them can be modified into Schiff base. Schiff bases are compounds with aryl- or an alkylimine derived from an aldehyde and a primary amine. Amino acids can be converted into Schiff base (Figure I - 36) and a screening of aldehyde is performed in order to find a compound crystallising as a conglomerate.

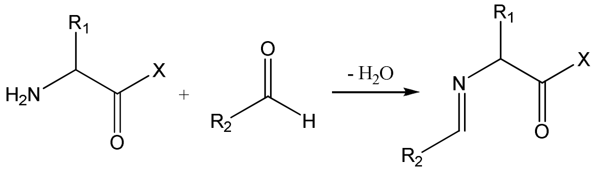

Figure I - 36. Synthesis of Schiff base from amino acids.

The great advantage of the Schiff bases derivate from amino-acid is that they are easily racemisable: the hydrogen α to the imine is labile and an organic base like DBU is able to remove it. (See Figure I - 35) The second great advantage is that the synthesis of this kind of compound is reversible. Indeed, Schiff bases are not stable in the presence of acid and water, and are hydrolysed into the starting materials. (Figure I - 37).

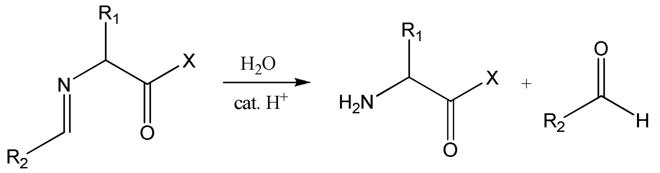

Figure I - 37. Hydrolysis of Schiff bases in the presence of acid.

---

[96] P. S. M. Cheung, L. A. Cuccia; *Chem. Commun.*, **2009**, 1337- 1338.

Thus, even if the target compound does not crystallise as a conglomerate, it can be reversibly converted into a racemisable imine; a screening of aldehydes is therefore carried out to find a conglomerate and then the resolution can be performed. This process has ensured the resolution of several amino acid derivatives.[97,98]

The deracemisation of the *N*-(4-chlorobenzylidene)phenylalanine (Figure I - 38a) also highlighted that epitaxy (Figure I - 38b) does not disturb the process, kinetic remaining exponential (Figure I - 39).[99]

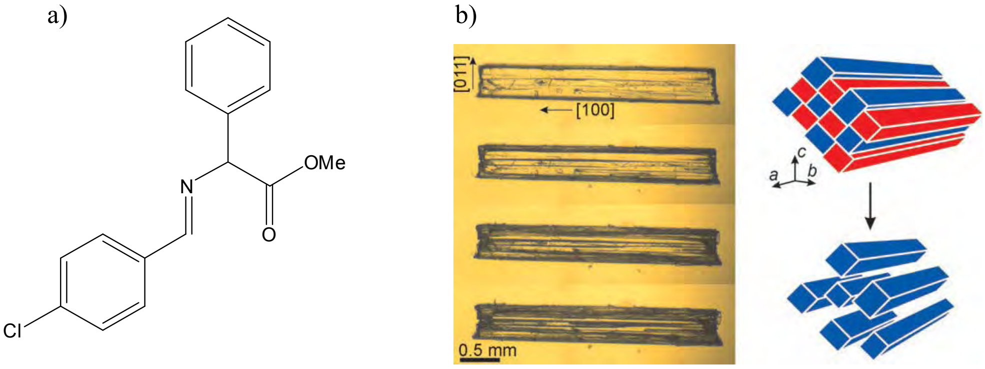
a)

b)

Figure I - 38. a) Chemical structure of the *N*-(4-cholorobenzylidene)phenylalanine, b) Partial dissolution of (RS)- *N*-(4-cholorobenzylidene)phenylalanine in a saturated solution of the S enantiomer (time interval between images: 10 minutes).[99]

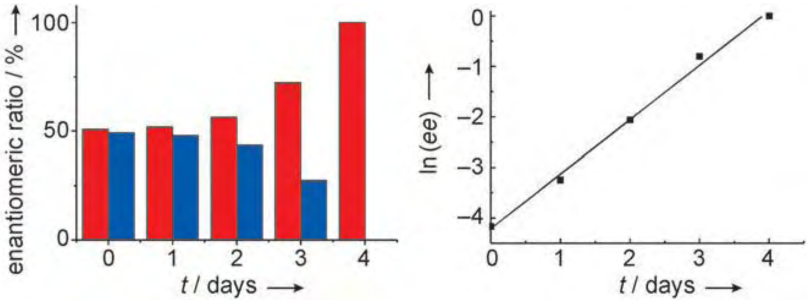

Figure I - 39. Typical change in the enantiomeric composition of the solid phase during grinding.[99]

In 2009, the Dutch group described the synthesis of the pure enantiomer of Clopidogrel (Plavix, Figure I - 40), [100] a platelet aggregation inhibitor used for the treatment of ischemic strokes, heart attacks, atherosclerosis and also for the prevention of thrombosis after

---

[97] W. L. Noorduin, P. van der Asdonk, H. Meekes, W. J. P. van Enckevort, B. Kaptein, M. Leeman, R. M. Kellogg, E. Vlieg; *Angew. Chem. Int. Ed.*, **2009**, 48(18), 3278-3280.

[98] M. Leeman, J. M. De Gooier, K. Boer, K. Zwaagstra, B. Kaptein, R. M. Kellogg; *Tetrahedron: Asymmetry,* **2010**, 21, 1191-1193.

[99] B. Kaptein, W. L. Noorduin, H. Meekes, W. J. P. van Enckevort, R. M. Kellogg, E. Vlieg; *Angew. Chem. Int. Ed.*, **2008**, 47(38), 7226-7229.

[100] M. W. van der Meijden, M. Leeman, E. Gelens, W. L. Noorduin, H. Meekes, W. J. P. van Enckevort, B. Kaptein, E. Vlieg, R. M. Kellogg; *Org. Process. Res. Dev.*, **2009**, 13, 1195-1198.

placement of intracoronary artery stents. Until that day, the pure (*S*)-Clopidogrel was prepared by pasteurian resolution.[101,102103]

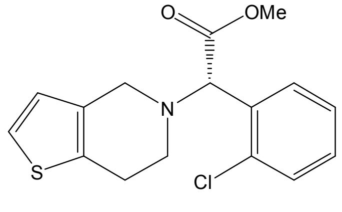

(*S*)-clopidogrel

Figure I - 40. Chemical formula of the (*S*)-Clopidogrel.

The Dutch consortium performed a new synthesis of the Clopidogrel, in which an intermediate is reversibly converted into an imine, the *N*-(*o*-chlorobenzylidene)phenylglycine-amide, and deracemised. Then, the benzaldehyde is removed by treatment of the imine with HCl.

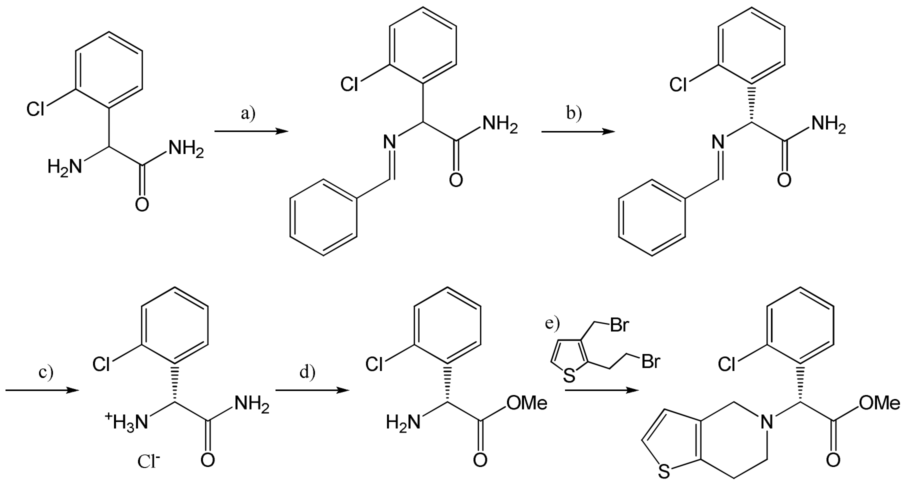

Figure I - 41. Synthesis of the (*S*)-Clopidogrel by deracemisation of the N-(*o*-chlorobenzylidene)phenylglycine-amide. a) benzaldehyde, Na_2SO_4, CH_2Cl_2; b)DBU, glass beads, acetonitrile; c) HCl/acetone; d) H_2SO_4/MeOH, e) acetonitrile.

b. Naproxen

The same year, the same Dutch group performed the synthesis of the (*S*)-Naproxen, a non-steroidal anti-inflammatory drug.[104] This molecule crystallises as a racemic compound but the methyl and ethyl ester derivatives crystallise as conglomerate and they can be easily racemised under basic conditions. Pure enantiomers of the ester derivative were thus obtained

---

[101] a) U.S. Patent 6,800,759, **2004**, b) U.S. Patent 6,737,411, **2004**. c) U.S. Patent 4,847,265, **1989** d) U.S. Patent 6,074,242, **2006**.

[102] L. Wang, J. Shen, Y. Tang, Y. Chen, W. Wang, Z. Cai, Z. Du; *Org. Process Res. Dev.,* **2007**, 11, 487-489.

[103] a) U.S. Patent 2004073057, **2004**, b) WO2006003671, **2006**, c) U.S. Patent 2007225320, **2007**.

[104] W. L. Noorduin, B. Kaptein, H. Meekes, W. J. P. Van Enckevort, R. M. Kellogg, E. Vlieg; Angew. *Chem. Int. Ed.,* **2009**, 48, 4581-4583.

by deracemisation by using NaOMe in methanol with grinding then the pure (*S*)-naproxen was synthesised.

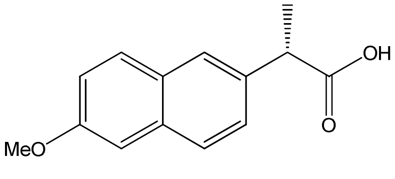

(*S*)-naproxen

Figure I - 42. Chemical structure of the (*S*)-naproxen.

c. Racemisation thanks to a chemical equilibrium

Sometimes, the racemisation of the target compound is not as easy as in the previous cases. In 2008, Viedma and Blackmond *et al.* reported the total resolution of aspartic acid.[105] Aspartic acid is one of only two proteinogenic amino acid which can crystallise directly as a conglomerate. Unfortunately, as all the natural amino acid, its racemisation is very slow on a laboratory time scale. But Yoshioka recently designed an efficient method for racemisation of amino acid by using a catalytic amount of aldehyde in an acidic media.[106] Therefore Viedma and Blackmond *et al.* performed the resolution of aspartic acid by using salicylaldehyde in acetic acid. (Figure I - 43)

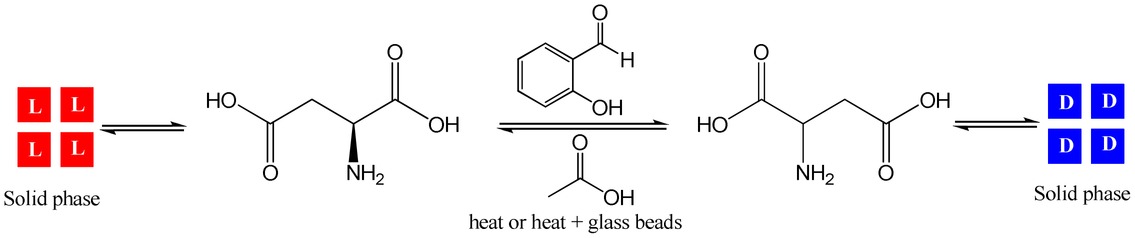

Figure I - 43. Aspartic acid solid phase in equilibrium with a solution under racemising conditions.

They also highlighted the benefit of grinding ensured by glass beads and the impact of the temperature on the kinetic of the process, as illustrated in the Figure I - 44.

---

[105] C. Viedma, J. E. Ortiz, T. De Torres, T.Izumi, D. G. Blackmond; *J. Am. Chem. Soc.*, **2008**, 130, 15274-15275.

[106] R. Yoshihoka; *Top. Curr. Chem.*, **2007**, 269, 83-132.

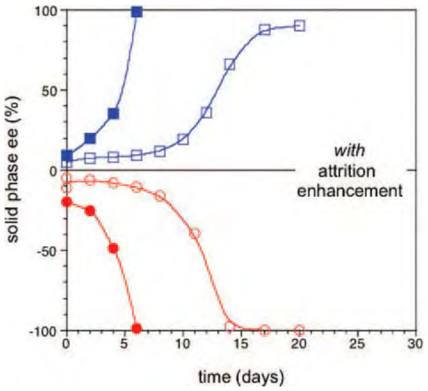

Figure I - 44. Evolution of solid-phase ee for D and L aspartic acid under racemizing conditions. Filled symbols: gradient heating to 160 °C. Open symbols: isothermal at 90 °C. Positive e.e. values are assigned to the naturally occurring L-asp.

More recently, Tsogoeva *et al.* described the enantioenrichment by symmetry breaking of an amino acid derivative using a reversible Mannich type reaction to racemise the chiral compound. The enrichment occurs via an iterative retro-aldol/aldol reaction in the presence of an achiral or racemic secondary amine catalyst. (Figure I - 45)[107] They performed deracemisation both with and without glass beads and they noticed that even if glass beads increased the kinetic, the benefit was weak.

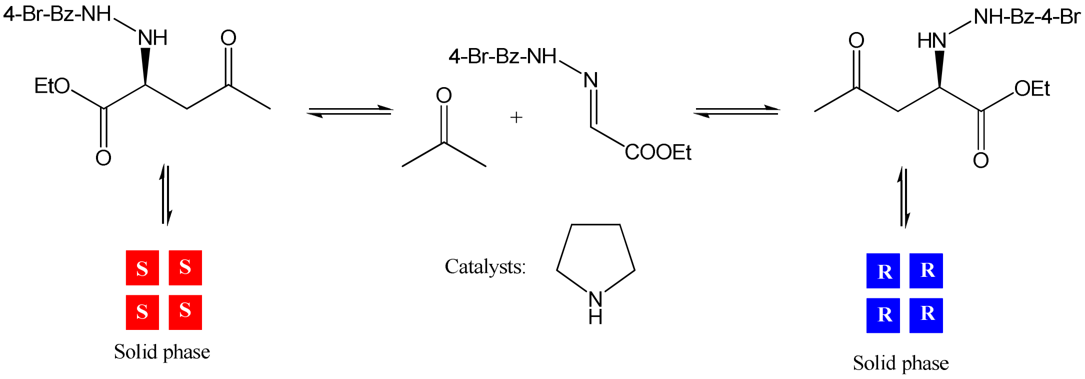

Figure I - 45. Deracemisation experiment with a Mannich type reaction at room temperature with an achiral secondary amine catalyst. 4-Br-Bz = 4-bromobenzoyl.

d. Combination of grinding, racemisation and controlled cooling

In 2009, we,[108] and the Dutch consortium[100,109] described a process mixing the Kondepudi's experiments (slow cooling rate, stirring and seeding) with the Viedma ripening (abrasive grinding ensured by glass beads). This new type of deracemisation can also be considered as a combination between the preferential crystallisation mode SOAT and Viedma's ripening. The

---

[107] S. B. Tsogoeva, S. Wei, M. Freund, M. Mauksch; *Angew. Chem. Int Ed.*, **2009**, 48(3), 590-594.

[108] G. Levilain, C. Rougeot, F. Guillen, J.-C. Plaquevent, G. Coquerel; *Tetrahedron: Asymmetry*, **2009**, 20, 2769-2771.

[109] M. Leeman, W. L. Noorduin, A. Millemaggi, E. Vlieg, H. Meekes, W. J. P. van Enckevort, B. Kaptein, R. M. Kellogg; *CrystEngComm,* **2010**, 12 (7), 2051-2053.

Dutch consortium applied this new process to their amino acid derivatives with a great success: the time of the reaction was significantly decreased and the enantiopurity still remains over 99.5%. We depicted the total resolution of a new kind of compound: a triazoylketone. (Figure I - 46).

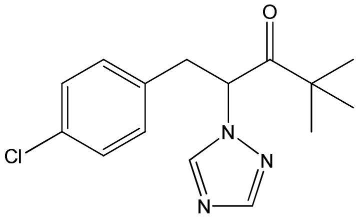

Figure I - 46. Chemical formula of the triazoylketone, 1-(4-chlorophenyl)-4,4'-dimethyl-2-(1H-1,2,4-triazol-1-yl)pentan-3-one.

The resolution of this compound by preferential crystallisation combined with *in-situ* racemisation was previously described by Black *et al.*[52] Nevertheless, the yield was low (20%) and a soft cooling profile (1°C.h^{-1}) was required to avoid the nucleation of the antipode. The addition of glass beads in the process ensured an increase of the yield (70%) without modifying the final enantiomeric excess and permitted to work with a rapid and deep cooling profile (15°C.h^{-1}): 2h were sufficient to reach the final state. (Figure I - 47)

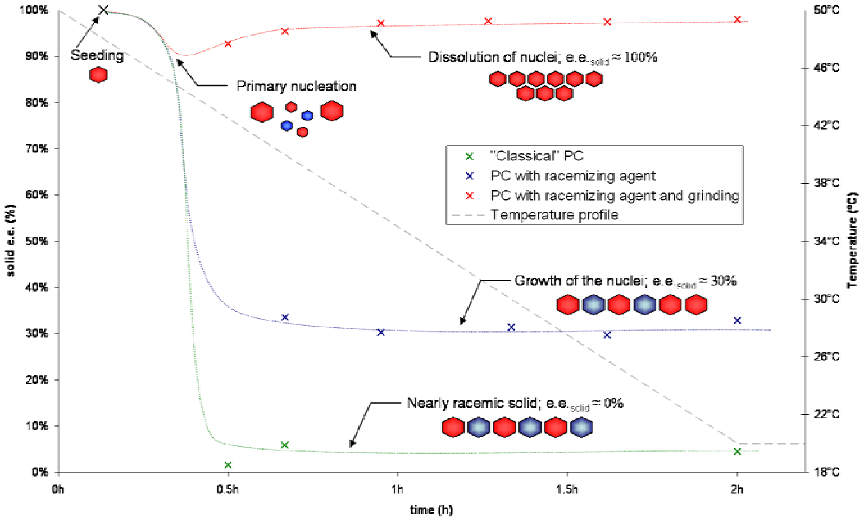

Figure I - 47. Evolution of the enantiomeric excess of the solid on fast cooling (the lines are a guide)

6. Deracemisation mechanisms: the current hypotheses

a. Introduction

The theory of the "mother" crystal was the first described to explain the spontaneous symmetry breaking phenomena (see paragraph VI.2.). This theory may be valid for processes starting from a relatively highly supersaturated solution, with or without seeding and/or abrasive grinding, but it can not be used to explain what happens in the cases of a racemic suspension in equilibrium with a saturated solution. Therefore, many research groups attempted to find another mechanism to explain why racemic suspensions in contact with a saturated solution and a racemising agent are able to evolve toward an enantiopure final state. Basic knowledge on crystallisation mechanism often named in these various explanations is described below:

- Primary nucleation: spontaneous nucleation from a saturated solution (dissolved molecules aggregate to from nucleus)
- Secondary nucleation: formation of nucleus from already existing crystals. When a crystal is submitted to shear stress or collisions (with another crystals, the wall of the reactor or the stirrer…) it is broken and small parts, called “daughter crystals”, are generated.[110] From a chiral point of view, daughter crystals have the same handedness than the mother crystal.[111]
- Gibbs-Thomson effect: in the middle of the 19th centrury, Gibbs noticed that small particles have a higher solubility than the large ones. This difference is a direct consequence of the minimization of the surface energy of the particles since the ratio surface area/volume is higher for small particles than for the large ones.
- Ostwald limit: due to the activation energy required to generate the first nucleus, a supersaturated solution spontaneously crystallizes only if the supersaturation exceeds a certain threshold. In 1897, Friedrich W. Ostwald defined the first concept of metastable zone. (Figure I - 48)[112,113] The biphasic domain (crystals in equilibrium with a saturated solution) is separated into two domains by the Ostwald limit. When the concentration is between the solubility line and the Ostwald limit (green domain), no primary nucleation spontaneously occurs and the supersaturated solution remains clear unless it is seeded. When the concentration of the solution is higher than the Ostwald limit (red domain), primary nucleus appears spontaneously from the clear supersaturated liquid. The location of the Ostwald limit depends of the supersaturation, of the increasing rate of the supersaturation (i.e. the cooling rate, the evaporation rate of the solvent…), the stirring rate, the stirring mode, the nature of the reactor…

---

[110] W. L. McCabe, J. C. Smith; *Unit operations of chemical engineering;* McGraw-Hill Book Co.: New York, **1956**

[111] D. K. Kondepudi, C. Sabanayagam; *Chem. Phy. Lett.*, **1994**, 217, 364-368.

[112] F. W. Ostwald; *Z. Phys. Chem.*, **1897**, 22, 289-330.

[113] F. W. Ostwald; *Z. Phys. Chem.*, **1900**, 34, 495-503.

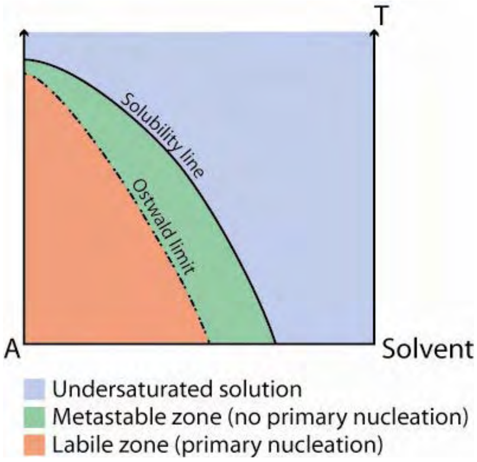
T
Solubility line
Ostwald limit
A
Solvent
Undersaturated solution
Metastable zone (no primary nucleation)
Labile zone (primary nucleation)

Figure I - 48. Ostwald limit representation in a binary diagram.

- Ostwald ripening: it a ubiquitous phenomenon in a stagnant solution. The larger crystals became larger at the expense of the small crystals, [114] which progressively disappear or denucleate. The Ostwald ripening is directly linked to the Gibbs-Thomson effect and the end state of such system is only one single crystal in equilibrium with a saturated solution. Figure I - 49 illustrates the Ostwald ripening.[115] Single crystals of $NaClO_3$ are in contact with a saturated solution. Smaller crystals progressively shrink and, after two months, and with only the diffusion process, only one large single crystal is present.

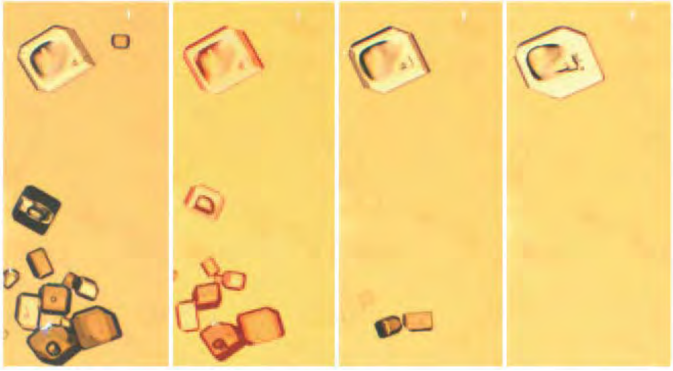

Figure I - 49. Polarized light microscope images showing the process of Ostwald ripening of $NaClO_3$ leading to a single chiral solid phase.

- Meyerhoffer double solubility rule: the solubility of a racemic conglomerate is roughly double than the solubility of pure enantiomers. Indeed, each enantiomer is in equilibrium with its own liquid phase (in an ideal mixture, each type of liquid phase exhibits its own vapour pressure, independent of the other). But in the case of an achiral compound crystallising as two enantiomeric chiral crystals (e.g. $NaClO_3$), the double solubility rule cannot be applied; crystals are in equilibrium with only one achiral molecule.

---

[114] W. Ostwald; Lehrbuch der Allgemeinen Chemie, Vol. 2, Part 1; Leipzig, Germany, **1896**.

[115] W. L. Noorduin, E. Vlieg, R. M. Kellogg, B. Kaptein; *Angew. Chem. Int. Ed.*, **2009**, 48, 9600-9606.

b. Cairns-Smith's experiment

Cairns- Smith performed an experiment using balls of two colours to explain how, from a racemic mixture (each enantiomer corresponding to one colour of the balls), it was possible to reach a pure chiral final state (i.e. only balls of one colour).[116] They put 100 balls in a box; 50 of one colour, 50 of the other one. At each step, they throw away at random half of the balls and duplicate those that remain. After some time, all of the balls in the box have the same colours, as it is illustrated in the Figure I - 50.

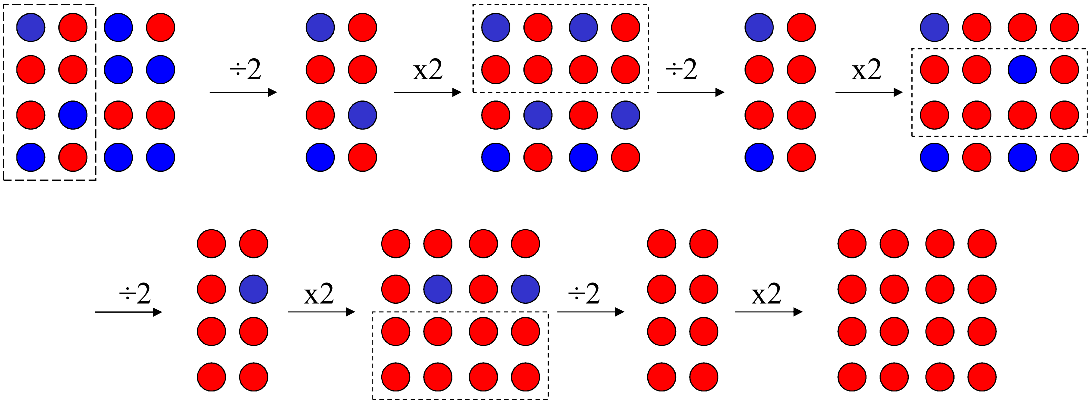

Figure I - 50. Cairns-Smith's experiment.

The Cairns-Smith's model is not representative of the deracemisation process because a ball of one colour keeps its colours all along the experiment without having the possibility to change, *i.e.* without having the possibility to be "racemised". But this model can give us an idea on the process which enables the random imbalance created from a racemic mixture.

c. Model based on Ostwald ripening

Another model described to explain the phenomena of total symmetry breaking from a suspension is based on the Ostwald ripening.[115,117] Indeed, besides the fact that only one single crystal is present at the end, Figure I - 49 exhibits that the final end state is only one handedness. The thermodynamic stable state is one enantiopure crystal, i.e. a result similar to the one of the deracemisation process.

Ostwald ripening also emphasize that smaller crystals progressively disappear until reaching the denucleation step. This phenomenon is absolutely necessary to reach the enantiopure final suspension both starting from a suspension or a clear warm solution. Indeed, even in the second case and with a very slow cooling rate, it is very difficult to assume that only one primary nucleus appears at the beginning and that no other is formed during the cooling process. Without the Ostwald ripening, since a crystal cannot disappear once it has formed, the chiral mixture present at the end is derived from the crystals independently nucleated. But the sole Ostwald ripening process takes a long time to reach the final state, typically months or even longer (See Figure I - 49), depending on the system volume, the solubility of the compound, its rate of racemisation and its surface energy. In a suspension, for an initial crystal size distribution (CSD) with a large number of small crystals, Ostwald ripening is relatively fast, but it rapidly decreases when crystals become bigger. A vigorous stirring and more the abrasive grinding ensured by glass beads decrease the crystal size distribution, speeding up the Ostwald ripening.

---

[116] A. G. Cairns-Smith; *Chemistry in Britain,* **1986**, 22, 559-561.

[117] J. H. E. Cartwright, O. Piro, I. Tuval; *Phys. Rev. Lett.*, **2007**, 165501.

In order to better understand how the Ostwald ripening and the abrasive grinding interact to produce a single chiral state with many small crystals, a computer model was developed.[118] A system composed by a saturated solution in equilibrium with the two CSDs of the enantiomers was subjected to a Monte Carlo simulation. This simulation considered the changes in the CSDs and the racemisation that took place in solution, with keeping constant the total number N of molecules. The flow diagram of the Monte Carlo simulation takes in account other parameters like the probability of an attrition event, P_{attr}, and the probability of an Ostwald event, P_{ost}.

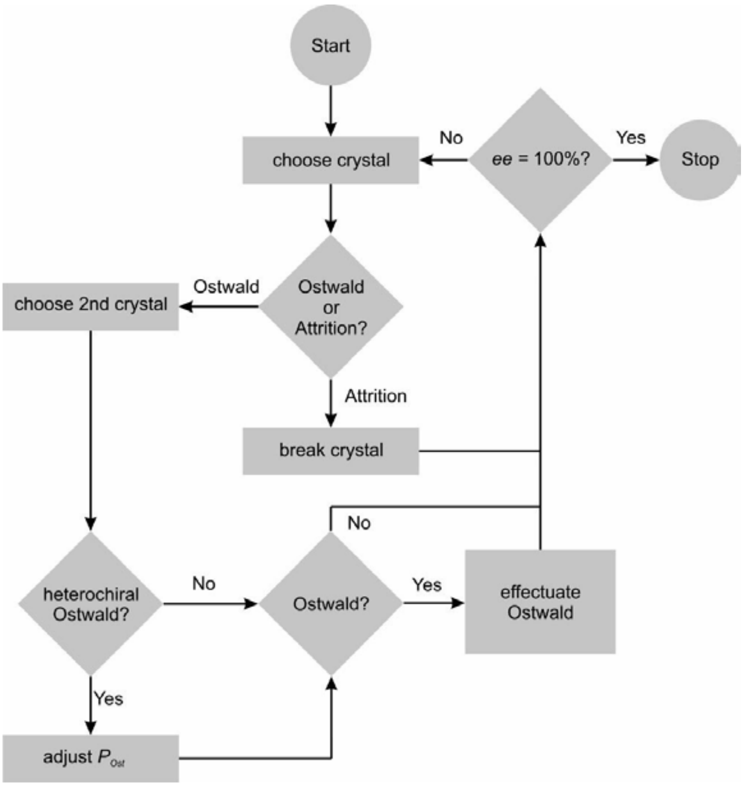

Figure I - 51. Flow diagram of the Monte Carlo simulation modelling the combined processes of Ostwald ripening and attrition.

---

[118] W. L. Noorduin, H. Meekes, A. A. C. Bode, W. J. P. Van Enckevort, B. Kaptein, R. M. Kellogg, E. Vielg; *Cryst. Growth Des.*, **2008**, 8(5), 1675-1681.

This simulation exhibits that the system always evolves into a single chiral end state and that once this state is reached, it persists, even if the stirring is stopped. The results also highlighted that the time to reach the final state depends on the attrition-ripening ratio (the more intense the attrition, the faster the process, until a threshold) and on the solution racemisation efficiency. This simulation exhibits that the initial enantiomeric excess is amplified exponentially, where the constant k depends on the attrition-ripening ratio and the racemisation efficiency. (Equation I – 5)

$$ee(t)=ee(t_0).\exp(kt) \qquad \textbf{Equation I - 5}$$

However, another behaviour was highlighted: when the racemisation in solution is instantaneous and even if enantiomeric excess is present at the beginning, deracemisation time decreases and the final handedness is stochastic.

To conclude, it had been demonstrated that Ostwald ripening is a non linear dynamical process able to drive symmetry breaking to the final enantiopure system with an exponential kinetic. Ostwald ripening thus plays a key role in the deracemisation process.

d. Models based on clusters

In 2004, Uwaha proposed a model based on a simple reaction-type that produces complete chiral symmetry breaking in crystallisation.[119] This model assumes that:

- The perpetual mixing of the solution and the abrasion of the crystals enable to describe the system by simple reaction-type equations. In classical crystallization, it impossible to do it because it requires a complex description of transport of the molecules and surface kinetics.
- A minimal size of cluster that possesses chirality exists in solution. These clusters are smaller than the critical size of nucleus. Clusters, as well as achiral molecules, can be incorporated to a chiral crystal to grow it.
- The decay of chiral units and crystals also occurs.

Uwaha used masses of five components (achiral molecules, the two kinds of chiral clusters and the two kind of chiral crystals of various sizes) to described the time evolution of the system. The Uwaha's model ensure a total symmetry breaking once a small symmetry breaking occurred by chance or by an external trigger (e.g. seeds). They assume that "*the existence of clusters is the origin of the autocatalysis and the perpetual disturbance of the system makes the decay processes efficient and assures the realization of complete chirality.*"

---

[119] M. Uwaha; *J. Phys. Soc. Jpn*, **2004**, 73(10), 2601-2603.

Grinding is thus the origin of many chiral clusters, the growth unit of chiral crystals, and their incorporation to the major crystal type accelerates the kinetic of crystallisation.

Crusats et al. linked the deracemisation process to a thermodynamic equilibrium which can only occur when the system is perturbed, by formation of chiral clusters.[91] The stable state of crystals in equilibrium with a saturated solution under perturbation (i.e. grinding) is only one solid state with 100% enantiomeric excess.

This model was also supported by McBride and Tully,[120] and then Saito and Hyuga[121] adapted it for the total symmetry breaking of intrinsically chiral molecules, emphasising that a back reaction (i.e. crystal and/or cluster decay) is essential to produce achiral components.

f. Discussion

In 2008, Uwaha and Katsuno compared these two models. For them, Ostwald ripening is not the essential mechanism which occurs under grinding, because the crystal size distribution must be almost steady during the grinding process.[119,122] To clarify the role of Ostwald ripening during deracemisation, Uwaha and Katsuno proposed a mathematical model based on an extended Becker-Döring model, in which clusters reaction and the grinding effect are implemented,[123] i.e. which described the change on cluster size distribution. They studied both achiral molecules and chiral molecules with a racemising agent. The results of their simulations were that Ostwald ripening, without grinding, can cause the chirality conversion only if the initial CSD is different for the two enantiomers. In the case of grinding and with a similar CSD for the two enantiomers, the total symmetry breaking occurs only with the crystallisation of chiral clusters, in addition to the usual monomers. Ostwald ripening does not have a key role in this mechanism.

In contrary, T. Izumi and D. G. Blackmond affirmed that "*invoking clusters of molecules to insure chiral identity of the species adding to growing crystals is therefore not required to rationalize the mechanism of the evolution of solid-phase homochirality in conglomerate systems of enantiomers.*"[124] They also highlighted that even in the case of a molecules crystallising as conglomerate, the Meyerhoffer double solubility rule is followed whereas Crusats et al. claimed the opposite.[125]

---

[120] J. M. McBride, J. C. Tully; *Nature*, **2008**, 452, 161-162.
[121] Y. Saito, H. Hyuga; *J. Phys. Soc. Jpn*, **2004,** 73, 33-35.
[122] M. Uwaha; *J. Phys. Soc. Jpn*, **2008**, 77, 083802.
[123] Y. Saito, H. Hyuga; *J. Phys. Soc. Jpn*, **2005**, 74, 535-537.
[124] T. Izumi, D. G. Blackmond; *Chem. Eur. J.*, **2009**, 15, 3065-3068.
[125] J. Crusats, S. Veintemillas-Verdaguer, J. M. Ribó; *Chem. Eur. J.*, **2007**, 13, 10303-10305.

As for McBride and Tully,[120] Ostwald ripening combined with a step of molecular recognition (i.e. clusters incorporation) is imperative to explain the autocatalytic properties of the deracemisation.

In 2010, the Dutch group in association with McBride and Tully proposed a mechanism combining Ostwald ripening and reincorporation of chiral clusters.[126] They have found experimental evidences for the existence of clusters. Thus, they conclude that four processes are necessary to explain the deracemisatioon of a racemic conglomerate: 1) racemisation in solution, 2) Ostwald ripening, 3) incorporation of chiral clusters and 4) attrition.

In 2011, two studies about a mathematical model describing the deracemisation process were carried out. Peter J. Skrdla modelled the deracemization process by an exponential equation describing the sigmoidal-shaped (or “S”-shaped) kinetic (Figure I - 52), but without removing uncertainty about the details.[127]

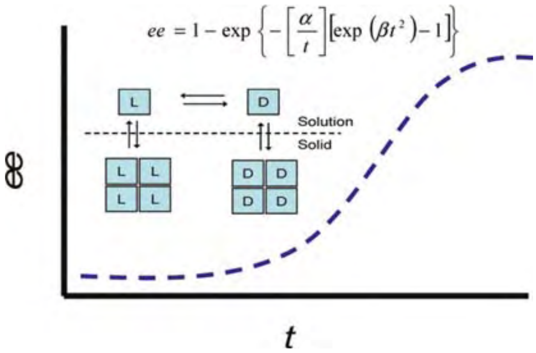

Figure I - 52. Exponential kinetic for deracemisation described by P. J. Skrdla.

The second study was performed by Iggland and Mazzotti.[128] They assumed a mechanism based on the propositions of several authors, including racemisation in solution, growth and dissolution due to a size-dependent solubility (i.e. Ostwald ripening), agglomeration (clusters) and attrition. Each of these propositions was modelled by mathematical equations:

- Growth and dissolution of particles subject to size-dependent solubility: Equation I - 6 gives the critical size x_c, beyond which a nuclei is stable and can grow, where k_a and k_v are volume shape factors, γ the surface tension, V_m the molar volume, R the universal gas constant, T the absolute temperature and S the supersaturation of the solution. c represents the concentration in the solution and c_∞, the bulk solubility, that is to say the solubility of an infinitely large particle.

---

[126] W. L. Noordiun, W. J. P. Van Enckevort, H. Meekes, B. Kaptein, R. M. Kellogg, J. C. Tully, J. M. McBride, E. Vlieg; *Angew. Chem. Int. Ed.*, **2010**, 49(45), 8435-8438.

[127] P. J. Skrdla; *Cryst. Growth Des.*, **2011**, 11, 1957-1965.

[128] M. Iggland, M. Mazzotti; *Cryst. Growth Des.*, **2011**, 11, 4611-4622.

$$x_c = \frac{2k_a \gamma V_m}{3k_v RT \ln S} = \frac{\alpha}{\ln S}$$

Equation I - 6

$$S = \frac{c}{c_\infty}$$

Equation I - 7

As the solubility of a crystalline material depends on its size, the concentration of a particle of size x, c*(x), can be obtained from the Equation I - 7, and then can be simplified to give the Equation I - 8:

$$S^*(x) = \frac{c^*(x)}{c_\infty} = \exp\left(\frac{\alpha}{x}\right) = 1 + \frac{\alpha}{x}$$

Equation I - 8

Thus the growth-rate expression can be written as follow:

$$G_i(x) = k_g\left(\frac{c_i}{c_\infty} - 1 - \frac{\alpha}{x}\right)$$

Equation I - 9

- Agglomeration: it can be described by using two different equations. In Equation I - 10, agglomeration is slowest for combination of two small particles while in Equation I - 11, agglomeration is slowest for combination of two large particles.

$$A_1(x_1, x_2) = \left(\frac{x_1 + x_2}{2}\right)^3 \frac{a_{1,2}}{1 + a_{1,1} X_{eq}(x_1, x_2)}$$

Equation I - 10

$$A_2(x_1, x_2) = a_{2,2}\left(\frac{x_1 + x_2}{2}\right)^3 \exp(-a_{2,1} X_{eq}(x_1, x_2))$$

Equation I - 11

$$X_{eq}(x_1, x_2) = \frac{(x_1 x_2)^2}{x_1^2 + x_2^2 - x_1 x_2}$$

Equation I - 12

- Attrition: in this model, the attrition is a U-shaped and is symmetric in volume-space, thus gives only two fragments, and is characterized by a single adjustable, integer parameter q (the larger the value of q, the larger the difference in size between the two resulting fragments)

$$g(x, \eta) = 3x^2(2q+1)\left(\frac{2}{\eta 3}\right)^{2q+1}\left(x3 - \frac{\eta 3}{2}\right)^{2q}$$

Equation I - 13

η and x represent the sizes of the original particle and of the formed fragment, respectively. The rate of the breakage by attrition of particles of size x is given by the following equation, where k and β are adjustable parameters and x_0 is a scaling factor:

$$b(x) = k_b\left(\frac{x}{x_0}\right)^\beta$$

Equation I - 14

- Racemisation: it is a first order reaction and the two enantiomers have the same constant of reaction so k_D=k_L=k_r.

The results of this modelling confirmed the necessity to have racemisation, growth and dissolution due to size dependent solubility and agglomeration to perform deracemisation. Moreover, kinetics obtained by the modelling are very similar to the experimental ones, whatever the initial conditions (CSD, initial e.e., racemisation rate...). However, they pointed out that attrition is not necessary to reach the complete chiral purity but it increased the deracemisation rate, and therefore the kinetics.

g. Conclusion

In spite of the numerous studies and computer simulations carried out on the deracemisation process, the mechanism is still under vigorous discussion. However, it seems to be clear that production of chiral clusters and small crystals by attrition is a key step. Clusters can be reincorporated to crystals of the same handedness or be dissolved and racemised. Small crystals can also be dissolved or grow (i.e. to be subjected to Ostwald ripening) by reincorporation of chiral clusters or chiral molecules, propagating the chirality of its "mother crystal". Moreover, all the researchers are to agree that deracemisation is a nonlinear autocatalytic process following an exponential kinetics.

However, this process remains a paradox in the chemistry world, as was pointed out by Viedma *et al.* in 2010: "*the key driving force for the evolution of solid-phase homochirality is solution racemisation – a process that conventionally erodes chiral discrimination.*"

VII - Conclusion

Since the discovery of the chirality and its vital role for living systems, many methods to give access to pure enantiomer were designed by researchers. In this chapter, an overview of these techniques, such as asymmetric synthesis, kinetic resolution of a racemic mixture, resolution by chromatography or by crystallisation, was depicted. Each method has its advantages and its drawbacks. The more effective method depends on the target compound and need to be adapted to give the best productivity.

The recent technique of chiral symmetry breaking by crystallisation was studied with great details. Even if this method is limited to conglomerates that can be quickly racemised in conditions compatible with its crystallisation, it remains a very promising technique because the yield and the final enantiomeric excess are very good. Moreover, no chiral auxiliary are necessary.

Chapter 2: Synthesis of monosubstituted β-cyclodextrins for chiral separation

I - Introduction

The separation of the enantiomers in the solid state is an important economical issue; in most of cases, less solvents and less expensive equipments are necessary than for the purification by chromatography for example. However, the separation in the solid state can not be applied to all the compounds. Therefore, the acess to new chiral auxiliaries is became a major issue in order to enlarge the range of enantiomers which can be separated by crystallisation.

Cyclodextrins are macrocyclic molecules able to form inclusion complexes with organic compounds and are also known in literature to be chiral selectors. This ability to discriminate enantiomers is widely used in chromatography but only few successes were poined out in the solid state, mainly because the difference between the complexes formed from the two enantiomers of a molecule is not sufficient to lead to a chiral separation.

In order to increase the chiral discrimination between the two enantiomers, monosubstituted β-cyclodextrins with a "hook" were synthesized. This hook, with an acidic or basic function, may create strong bonds with a basic or acidic guest, increasing the cohesion energy in the complex. This hook may also force the direction of the inclusion of the guest inside the cavity of the cyclodextrin, and therefore to induce a higher energy difference between the two enantiomers, making possible their separation.

In this chapter, the synthesis of a small library of monosubstituted β-cyclodextrins is described, as well as the study of a few complexes. But first, an overview on cyclodextrins, history, functionalisation, and formation of complexes, is given.

II - Synthesis of mono-substituted cyclodextrins: state of the art

1. Cyclodextrins

a. History

The earliest reference to cyclodextrins in the scientific literature was made in 1891 by Villiers.[129,130] They appeared as by-product of the fermentation of potato starch by *Bacillus amylobacter*. He noticed that two different crystalline forms existed, most probably due to two different molecules. However, he could not determine the exact composition of these molecules. He could only state that the empirical formula was a multiple of $C_{12}H_{20}O_{10}.3H_2O$.

---

[129] A. Villiers; *Comptes Rendus Hebdomadaires des Séances de l'Académie des Sciences*, **1891**, 112, 536-538.

[130] J. Szejtli; *Chem. Rev.*, **1998**, 98(5), 1743-1754.

Twelve years later, Schardinger,[131] who sought to isolate bacteria that cause food poisoning, published a report on the formation of crystalline compounds resulting from the digestion of starch by bacteria. These compounds appeared to be identical to those previously described by Villiers. Schardinger isolated a bacterium, which he named *Bacillus macerans*, which seems to be the cause of the formation of these crystalline compounds. He found that these products reacted differently with iodine: he called them α- and β-dextrins.

In the early '30s, Pringsheim and his group published several articles on cyclodextrins but most of them contained only speculations based on non-reproducible experiments and irrelevant analyses. However, they found that these dextrins were able to form complexes with many organic compounds.[132,133]

Shortly after, Freudenberg and his group discovered that the Schardinger's dextrins were made of maltose units, connected between them by α-1,4-glycosidic bonds.[134,135] In the late '30s, the γ-cyclodextrin was discovered and its structure was elucidated.[136]

In the early '50s, groups of French and Cramer studied the enzymatic production of cyclodextrins and characterised their chemical and physical properties.

In 1953, a first patent was filed on application of cyclodextrins in the pharmaceutical field, stabilizing the active ingredients in the human body. This patent paved the way for intensive researches on complexes made of cyclodextrins.

But, in the end of the '60s, cyclodextrins were suspected to be toxic, restricting their uses in pharmaceutical and food processing industries. It was only in the early '70s that further analyses showed that this toxicity was due to impurities complexed in cyclodextrins rather than cyclodextrins themselves.

Since these results, studies on cyclodextrins grew exponentially (Figure II - 1) as well as the quantities produced, resulting in lower cost (divided by 1000 in 30 years).

---

[131] F. Z. Schardinger; *Unters. Nahr. u. Genussm.*, **1903**, 6, 865-880.

[132] H. Pringsheim: *A Comprehensive Survey Of Starch Chemistry*, Ed. Chemical CatalogueCo, R. Walton, New York, **1928**.

[133] H. Pringsheim; *Chemistry of the Saccharides*, McGraw-Hill, New York, **1932**.

[134] P. Karrer, C. Nageli; *Helv. Chim. Acta* **1921**, 4, 169-173.

[135] A. Miekeley; *Ber. Dtsch. Chem. Ges.* **1932**, 65, 69.

[136] K. Freudenberg, G. Blomquist, L. Ewald, K. Soff; *Ber. Dtsch. Chem. Ges.* **1936**, *69*, 1258-1266.

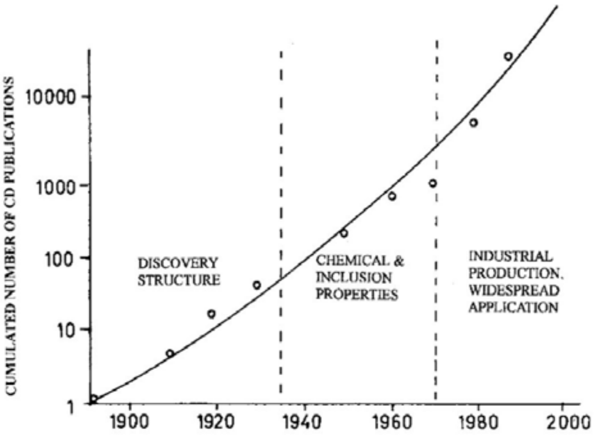

Figure II - 1. The three stages in development of CD technology. Erreur ! Signet non défini.

b. Structure and nomenclature

Cyclodextrins (or cyclohexa/hepta/octaamylose, cyclomaltohexa/hepta/octaose...) are cyclic oligosaccharides. There are considered as natural compounds since they are produced by the digesting of starch by bacteria.

Cyclodextrins are made of glucopyranose units connected between them by α-1,4-glycosidic bonds. Different size of cycles exists and the most commonly studied are made of six, seven and eight units, respectively named α-, β- and γ-cyclodextrins (Figure II - 2).

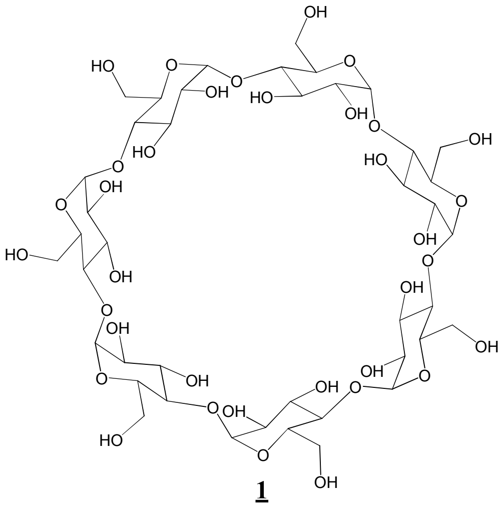

1

Figure II - 2. Chemical structure of β-cyclodextrin 1.

All glycosidic units adopt a chair-type conformation ($^4C_1$), all the alcohols being in the equatorial position (Figure II - 3).

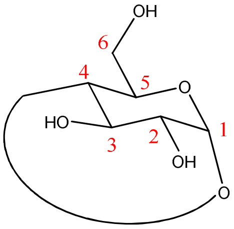

Figure II - 3. Chair-type conformation of the glucose units and numbering of carbons.

Consequently, all the alcohol groups are rejected outside the cyclodextrin. One of the most important properties of the cyclodextrins directly results of this conformation: cyclodextrins exhibit the shape of a truncated cone (Figure II - 4). The primary face (with the primary alcohols) is smaller than the secondary face (with the secondary alcohols) and the cavity is hydrophobic.

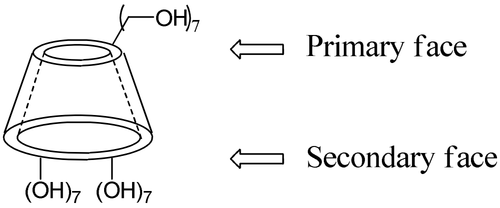

1

Figure II - 4. Schematic representation of the hydrophobic cavity of β-cyclodextrins.

The size of cavity depends on the number of glucose units as shown in Table II - 1.

	α-CD	β-CD (1)	γ-CD
Number of glucose units	6	7	8
Molecular weight (g.mol^{-1})	972.84	1134.98	1297.12
Internal diameter of cavity (Å)	5.7-13.7	7.8-15.3	9.5-16.9
Heigh of cavity (Å)	7.8	7.8	7.8
Volume of cavity (Å^3)	174	262	427

Table II - 1. Approximate dimensions of cavities of α-, β- et γ-cyclodextrins.

Native cyclodextrins are molecules exhibiting an axis of symmetry with an order equal to the number of units that composed them. For example, the β-cyclodextrins exhibits a C7 axis. Therefore, the ^{1}H RMN spectra is relatively simple (Figure II - 5). The importance of peak of water is due to the particular hygroscopicity of cyclodextrins. For example, the hydration rate of the commercial β-cyclodextrin is ≈14% and its entire cavity is filled with water molecules.

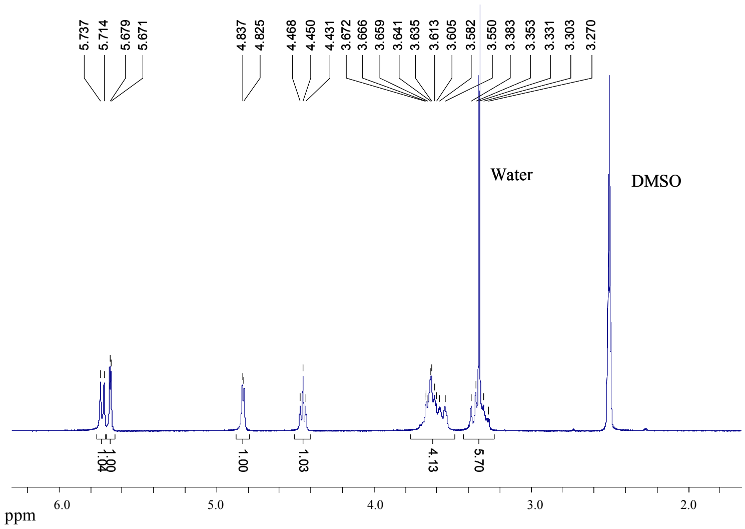

Figure II - 5. 1H NMR spectra of β-cyclodextrins in DMSO-d6.

c. Reactivity

The reactivity of cyclodextrins is mainly due to the alcohol groups. The functionalisation of these alcohols gives cyclodextrins with different properties. For example, the native cyclodextrins, which has only OH groups, are completely insoluble in organic solvents such as dichloromethane or ethyl acetate, whereas the permethylated cyclodextrins are soluble in most of them.

The totally modified cyclodextrins can be easily synthesized by using a large excess of reagent. Thus, the methyl-β-cyclodextrins (Me-β-CD) and the hydroxypropyl-β-cyclodextrins (HP-β-CD) are easily available. On the other hand, it is more difficult to modify only one of the twenty one alcohols of the molecules (in the case of the β-cyclodextrin). The secondary alcohols are less reactive than the primary ones; they are involved in hydrogen bonds between them and they rotation is restricted, whereas the rotation of the secondary alcohols is free. It is therefore possible to discriminate these two kinds of alcohols, but it is generally difficult to obtain a controlled functionalisation (Figure II - 6); the results are often a mixture of different polysubstituted cyclodextrins.

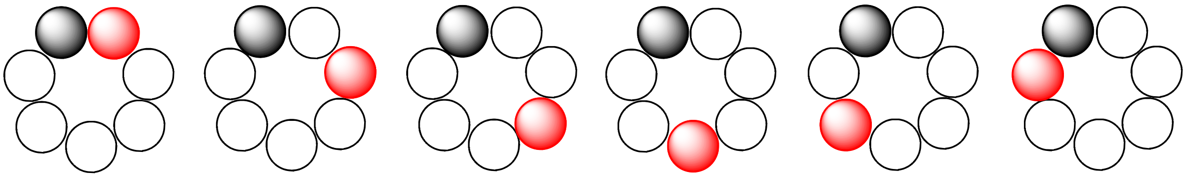

Figure II - 6. Possible positions of the substituents of a difunctionalised β-cyclodextrin.

Polysubstituted cyclodextrins (on the same kind of position, 2, 3 or 6) are generally difficult to purify. They are almost insoluble in conventional organic solvent. Classical purification by liquid-liquid extraction and chromatography on silica gel are therefore particularly complicated to carry out, eluents being generally composed of viscous solvents such as water or butanol.

And yet, it is essential to be able to purify and characterise the synthesized compounds, particularly for pharmaceutical and food industries. Therefore numerous studies were carried out to control the substitution of cyclodextrins.[129] Key steps are generally based on the different reactivity of the alcohols (the ratio of reagent can be optimised to obtain the desired compound) or on protection/deprotection reactions.

Methods exist to selectively functionalise several positions on one cyclodextrin but they are not described in this manuscript. Only the selective monosubstitution is studied in the following paragraph.[137]

2. Synthesis of monosubstituted cyclodextrins

a. Monosubstitution at the 2-position of cyclodextrins

One of the methods used to prepare monosubstituted cyclodextrin at the 2-position is the group transfer strategy (Figure II - 7 **I** and **II**). A complex is first formed then the functional group, commonly a tosyl group (coming from *m*-nitrophenyl tosylate)[138] is transferred preferentially at the 2-position due to the orientation of the reagent within the host molecule. Then nucleophilic substitutions can be carried out to have access to a large number of monosubstituted cyclodextrins.

The hydroxyl groups at the 2-position are also more acidic (due to the proximity of two oxygen atoms) than those at the 6-position. NaH under anhydrous conditions is able to selectively deprotonated the alcohol at the 2-position and therefore only this position is tosylated (Figure II - 7 **III**).[139]

If the substitution of the primary alcohols is favoured, they can be protected (e.g. by a silyl group) then the substitution of the 2-position can be performed. After a deprotection step, the desired compound is obtained (Figure II - 7 **IV, V** and **II**).[140]

However, the selectivity at the 2-position is generally not complete and an additional step of purification if necessary.

---

[137] A. R. Khan, P. Forgo, K. J. Stine, V. T. D'Souza; *Chem. Rev.*, **1998**, 98, 1977-1996.

[138] A. Ueno, R. Breslow; *Tetrahedron Lett.*, **1982**, 23, 3451-3454.

[139] D. Rong, V. T. D'Souza, *Tetrahedron Lett.*, **1990**, 31, 4275-4278.

[140] E. V. van Dienst, B. H. M. Snellink, I. Von Piekartz, M. H. B. Gansey, F. Venema, M. C. Feiters, R. J. M. Nolte, J. F. J. Engbersen, D. N. Reinhoudt, *J. Org. Chem.*, **1995**, 60, 6537-6545.

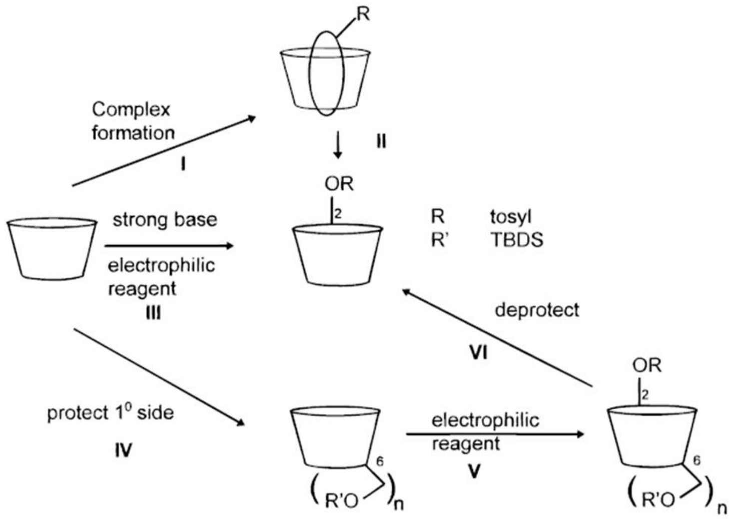

Figure II - 7. Strategies for modification at the 2-position of cyclodextrins. n = 6 for α-CD , n = 7 for β-CD and n = 8 for γ-CD.[137]

b. Monosubstitution at the 3-position of cyclodextrins

Direct substitution at the 3-position is a very complicated and difficult process because of the higher reactivity of the 2- and 6-hydroxyl groups. However, two reagents, the 2-naphtalenesulfonyl chloride and the 3-nitrobenzenesylfonyl chloride give a higher yield of the 3-substituted cyclodextrins.[141,142]

Most modifications at the 3-position are obtained by reaction of manno-mono-2,3-epoxycyclodextrin with a nucleophile as illustrated on Figure II - 8. This epoxycyclodextrin is obtained by elimination of the tosyl group at the 2-position by the hydroxyl group at the 3-position. In most of the cases, the ring opening with a nucleophile, such as ammoniac or hydroxylamine, leads to the formation of the monosubstituted cyclodextrin at the 3-position.[143,144,145,146] However, imidazole is an exception since it has been reported that it attacks both the 2- and the 3-position of the 2,3-epoxycyclodextrin.[147]

---

[141] K. Fujita, S. Nagamura, T. Imoto, T. Tahara, T. Koga; *J. Am. Chem. Soc.*, **1985**, 107, 3233-3235.

[142] K. Fujita, T. Tahara, Y. Egashira, T. Imoto, T. Koga; *Tetrahedron Lett.*, **1992**, 33, 5385-5388.

[143] M. Kojima, F. Toda, K. Hattori*; J. Chem. Soc., Perkin Trans 1*, **1981**, 1647-1651.

[144] T. Ikeda, R. Kojin, C. J. Yoon, H. Ikeda, M. Iijima, F. Toda; *J. Inclusion Phenom. Mol. Recognit. Chem.*, **1987**, 5, 93-98.

[145] K. Fujita, Y. Egashira, T. Imoto, T. Fujoka, K. Mihashi, K. Tahara, T. Koga; *Chem. Lett.*, **1989**, 429-432.

[146] A. M. Mortellaro, A. W. Czarnik; *Bioorg. Med. Chem. Lett.*, **1992**, 2, 1635-1638.

[147] D.-Q. Yuan, K. Ohta, K. Fujita; *J. Chem. Soc., Chem. Commun.*, **1996**, 821-822.

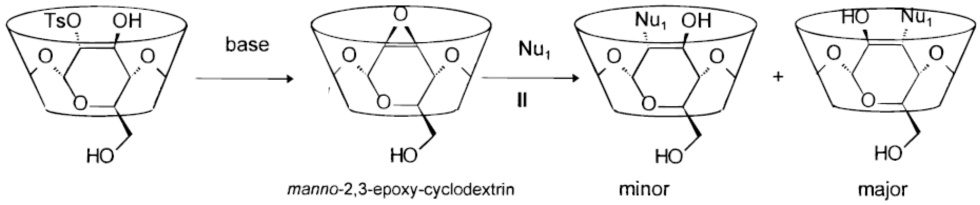

Figure II - 8. Reactions of mono-2-tosylcyclodextrin.[137]

c. Monosubstitution at the 6-position of cyclodextrins

The 6-position is the easiest to functionalise, primary alcohols being the most reactive. The most popular method to access to monomodified cyclodextrins is the nucleophilic substitutions, with various reagents, on the 6-O-*p*-toluenesulfonyl-β-cyclodextrine CDOTs **2** (Figure II - 9 and Figure II - 10 **I**). This compound is relatively easy to obtain with an acceptable purity (90-95%) without purification and with a quite satisfactory yield (50%).

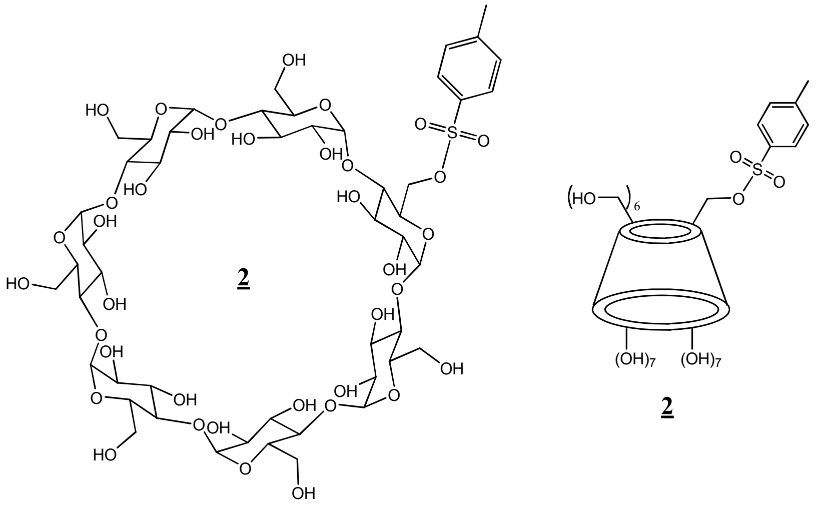

Figure II - 9. Chemical structure and schematic representation of 6-O-*p*-toluenesulfonyl-β-cyclodextrin CDOTs 2.

CDOTs is generally prepared from the native cyclodextrin and the *p*-toluenesulfonyl chloride TsCl. In order to prevent the polytosylation (tosylation is a non selective process because both primary and secondary alcohols can react, giving di- or tritosylated cyclodextrins), numerous studies were carried out to find the best conditions to obtain only the monosubstituted 6-O-*p*-toluenesulfonyl-β-cyclodextrin. Good results were obtained by using *p*-toluenesulfonyl chloride and native cyclodextrin in pyridine. Even if the work-up of the synthesis was complicated (formation of complexes with pyridinium which is difficult to remove), the direct monosubstitution of the 6-position is widely favoured. But as pyridine is not a user-friendly solvent, the method of choice to prepare the 6-O-*p*-toluenesulfonyl-β-cyclodextrin is a 1:1 ratio of native cyclodextrin and TsCl in aqueous alkaline medium for a short time. The product is obtained with a fairly good purity and repeated crystallisations or chromatography on a charcoal column can increase its purity.

Another important intermediate is the monoaldehydic cyclodextrin because they provide a route for further modifications. The monoaldehydic cyclodextrin can be obtained by oxidation of the CDOTs (Figure II - 10 **VI**) but it can also directly be obtained with a better yield (85-100%) from the native cyclodextrin by reaction with Dess-Martin periodinane (Figure II - 10 **IX**).

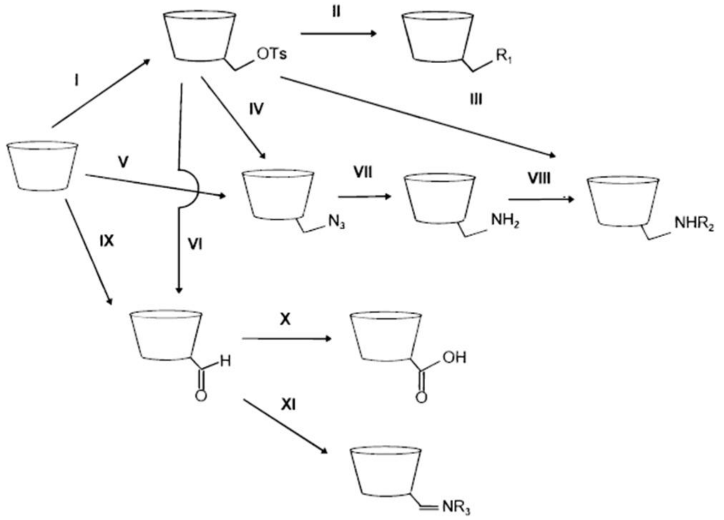

Figure II - 10. Overwiev of methods for monosubstitution at the 6-position of cyclodextrins. R_1 = -I, $-N_3$, -$SCOCH_3$, alkyl or polyalkyl amines, thioalkyl, R_2 = derivatives of β-D-glucose, β-D-galactose, α-D-mannose, β-D- and β-L-fructose, R_3 = -OH, -NHPh.[137]

The ether derivatives cannot be easily prepared from native cyclodextrins or by substitution of the tosyl group; alkoxide ions act as strong bases and not as nucleophiles. A multi-steps synthesis with protection/deprotection steps is necessary to obtain the desired compound.

3. Inclusion complexes

a. In industries

Thanks to their hydrophobic cavity, cyclodextrins are able to easily form inclusion complexes with organic molecules as guests. Moreover, large amounts of cyclodextrins are industrially produced and so they are often used for pharmaceutical and food industries. Indeed, the formation of inclusion complexes with cyclodextrins has a lot of advantages:[148]

- Increasing of the solubility of the guests in water. This property is probably the most widely used in pharmaceutical industry; formation of complexes increasing the bioavailability of API, making them more soluble in physiological environment.

---

[148] A.R. Hedges; *Chem. Rev.*, **1998**, 98(5), 2035-2044.

- Increasing of the chemical stability of the guest molecules (e.g. photosensitive compounds or compounds unstable in acidic media such as stomach).

- Modification of the reactivity. In most cases, the reactivity decreases, the guest being stabilised by the cavity. But in few cases, the cyclodextrins may act as an artificial enzyme, speeding up or modifying a reaction.

- Manipulation of volatile or liquid compounds or compounds having an unpleasant odour as powders.

- Gradual release of a compound (drug, flavour…)

Pharmaceutical industry	
Itraconazole	Increased solubility
Piroxicam/Brexin	Reduce irritation
Hydrocortisone	Increased solubility
garlic oil	Mask odour

Food industry	
peppermint-flavoured chewing gum	Flavour delivery
Acetic acid	Convert to a powder
lemon-flavoured sugar	Flavour stabilization
flavoured tea	Flavour stabilization
aloe-containing beverage	Mask bitterness

Cosmetics and Personal Care Items	
powdered hair bleach	Stability
Cold Cream	Increased solubility

Table II - 2. Examples of industrial use of cyclodextrins.[148]

b. Complexes formation

An important factor to obtain inclusion complexes is the structural compatibility between the guest molecule and the cavity of the host, ensuring the formation of a maximum of interactions. In the case of complexes with cyclodextrins, only hydrogen bonds and low energy interactions, such as van der Waals interactions, are brought into play. The presence of seven alcohols on one side of the cyclodextrins and fourteen alcohols on the other side (in the case of the β-cyclodextrin) leads to the existence of an important dipolar moment. Therefore electrostatic interactions (dipole/dipole) also contribute to the formation and the stabilisation of the complexes.

Furthermore, even if the cavity of cyclodextrins is hydrophobic, the entire cavity is filled of water molecules. These water molecules do not have the possibility to adopt the most stable configuration and can be considered as high-energy molecules. Thus, the inclusion of a hydrophobic molecule instead of water gives a complex with a lower energy and stabilises the system. This is one of the driving forces of the formation of complexes.

For example, a molecule such as toluene can be included in α- and β-cyclodextrins but not in γ-cyclodextrin. Naphthalene can form complexes with β- and γ-cyclodextrins while anthracene can be included only in γ-cyclodextrin, being to large to be included in the cavity of the smaller cyclodextrins. All this complexes exhibit a 1:1 stoichiometry but, different combinations of host and guest also exist.[80] For example, the salicylic acid forms 1:2 and 1:4 (host/guest) complexes with the γ-cyclodextrin.[149]

These complexes are generally prepared in water. The cyclodextrin is dissolved in water then the guest is added. After stirring, the complex may be recovered by precipitation or evaporation of the solvent. To help the formation of the complex, an increase of the temperature or an addition of solvent may be used to increase the solubility of the host. The cyclodextrin is also generally close to the saturation.

However, several different methods can be used:[148]

- Slurry method: cyclodextrin is suspended in water up to a 40-50% w/w concentration. This method can be used when the complex is less soluble in water than the cyclodextrin.
- Paste method: a minimum of water is used (20-30% w/w) then the host is added and the paste is mixed. This method is generally used in industry.
- Dry mixing method: no solvent are used. Cyclodextrin and the host molecule are mixed together. This method is efficient when the host is liquid.

c. Characterisation of complexes

Many techniques can be used to characterize the complexes. As all the techniques give different information, they are generally complementary. Separate analyses of host and guest are also necessary to fully characterise the complexes. The classical analyses in solution (NMR, mass spectrometry, IR and UV spectroscopies, fluorimetry…) and in the solid state (XRPD, IR and Raman spectroscopies, DSC/TGA-DSC, solid state NMR…) can be used.[150] X ray diffraction on single crystal and the 2D NMR are analyses given the most important details. Indeed, these methods allow having access to structural information. However, the analyses in solution and in the solid state may give contradictory information: in solution, the complex can be stabilised (or destabilised) by the interactions with the solvent.

---

[149] K. Higashi, Y. Tozuka, K. Moribe, K. Yamamoto; *J. Pharm. Sci.*, **2010**, 4192-4200.

[150] H.-J. Schneider, F. Hacket, V. Rüdiger; *Chem. Rev.*, **1998**, 1755-1785.

4. Cyclodextrins and chiral recognition

Besides their ability to form inclusion complexes, cyclodextrins are chiral and thus, they are able to discriminate the two enantiomers of a molecule.

This property for cyclodextrins to be a chiral selector is widely used in chromatography; cyclodextrins are grafted on the stationary phase, leading a different retention time for the two enantiomers which can be separated. Numerous researches were and are still carried out in order to improve the efficiency of the separation, particularly for gas chromatography and capillary electrophoresis.[151]

a. Chiral recognition in the solid state

However, except in the field of chromatography, only few studies were carried out on the ability of cyclodextrins to discriminate enantiomers. In the '80s, the first structures of complexes were resolved by Harata *et al.*[152,153] and Hamilton and Chen.[154] Harata *et al.* studied the system formed by the β-cyclodextrin and the flurbiprofene (Figure II - 11) by resolving the crystalline structures of the racemic and of the diastereomeric complexes. The structures of the two diastereomeric complexes were characterized by the existence of dimers of cyclodextrins, in which two guest molecules were included. The two enantiomers of the guest formed different interactions with the host. For example, the *R*-flurbiprofene crystallised as a monohydrate with the β-CD whereas the *S*-flurbiprofene crystallised as an anhydrate with the β-CD. However, these differences were not sufficient to induce a chiral discrimination; the resolution of the structure of the racemic complex revealed that the two enantiomers are present in the dimers.

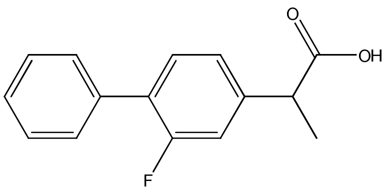

Figure II - 11. Chemical structure of the Flurbiprofene.

---

[151] W. Tang, S.-C. Ng; *J. Spe. Sci.*, **2008**, 31, 3246-3256.

[152] K. Harata; *Bull. Chem. Soc. Jpn,* **1982**, 55, 1367.

[153] K. Uekama, F. Hirayama, T. Imai, M. Otagiri, K. Harata; *Chem. Pharm. Bull.,* **1984**, 33, 1662.

[154] J. A. Hamilton, L. Chen; *J. Am. Chem. Soc.* **1988**, 110, 4379.

A similar study was carried out by Hamilton and Chen with the β-CD and the fenoprofene.[154] As for the previous case, the structures obtained from the racemic mixture and from the two enantiomers are isomorphous and are characterized by the formation of dimers. However, the geometry of inclusion is totally different for the two enantiomers (Figure II - 12). In a dimer, the two molecules of *S*-fenoprofene were in the same direction (head-to-tail) whereas the two molecules of *R*-fenoprofene faced each other (head-to-head).

Crystals obtained from the racemic mixture exhibited an enantiomeric excess over 50% (for the *S* enantiomer). This chiral discrimination was attributed to the different geometry of inclusion of the two enantiomers inside the cavity of the β-CD.

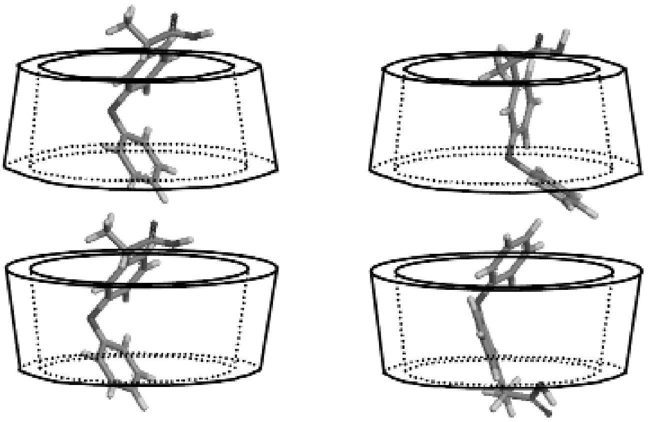

Figure II - 12. Schematic representation of the dimers formed with the *S*-fenoprofene (left) and with the *R*-fenoprofene (right) with the β-CD.

The chiral recognition induced by cyclodextrins can also be detected in solution by NMR.[150] Some NMR studies, and especially 2D NMR, showed the splitting peaks in two of the guest molecule,[155] proving that the two enantiomers interact differently with the cavity of the cyclodextrin. Computer simulations also demonstrated that the optimal configuration of the complex depends on the enantiomer: interactions between both enantiomers and the cyclodextrin are different leading to a different positioning inside the cavity and therefore different association constants.[156] Microcalorimetric analyses also demonstrated that the chiral recognition was possible with the native β-cyclodextrin.[157] However, these studies highlighted that the energy difference between the more and the less stable complexes was generally not sufficient to perform a chiral separation at the solid state.

---

[155] B. S. Jursic, P. K. Patel; *Tetrahedron*, **2005**, 61, 919-926.

[156] C.-J. Núñez-Agüero, C.-M. Escobar-Llanos, D. Díaz, C. Jaime, R. Garduño-Juárez; *Tetrahedron*, **2006**, 62, 4162-4172.

[157] M. Rekharsky, Y. Inoue; *J. Am. Chem. Soc.*, **2000**, 122, 4418-4435.

b. Permethylated β-cyclodextrins/(±)p-fluorophenylethanol complexes

Very recently, Amharar *et al.* described the unusual case of the permethylated β-cyclodextrins/(±)-*p*-fluorophenylethanol complexes, and the resulting separation of the two enantiomers.[80] This study follows the work carried out by Grandeury *et al.*, on the permethylated cyclodextrins/(±)-phenylethanol derivatives complexes.[158][159]

The study of the β-cyclodextrins/(±)-*p*-fluorophenylethanol/water system revealed that two different solid phases exist, with unusual features. On the one hand, a stable complete solid solution with two idependent complexes per asymmetric unit exibits a limited chiral recognition, and on the other hand, two metastable partial solid solutions with 1:2 host:guest stoichiometries behave as diastereomeric complexes. The structural study of these 1:2 complexes show that the chiral recognition is ensured both by the cavity of the cyclodextrin and by the crystal lattice; one of the guest molecule is included in the cavity while the second guest molecule do not have direct interaction with the cyclodextrins. It was the first time that such a hybrid mechanism of chiral recongnition was reported in the literature.

However, even if the separation of the two enantiomers is possible, successive recrystallisations are necessary to obtain a high enantiomeric excess, decreasing the yield of the separation: three recrystallisations must be carried out to obtain the *S*-1:2 (diastereomeric excess d.e.>98%) with 12.5% yield and eight recrystallisations must be carried out to obtain the *R*-1:2 (d.e.>95%) with ≈1% yield.

Therefore it is necessary to increase the discrimination between the two enantiomers. In this perspective, monosubstituted cyclodextrins with a hook were synthesized.

III - Synthesis of monosubstituted β-cyclodextrins

1. 6-O-p-toluenesulfonyl-β-cyclodextrin β-CDOTs

a. Synthesis of 6-O-p-toluenesulfonyl-β-cyclodextrin

The method widely used to synthesize the β-CDOTs involves TsCl (see paragraph II). However, different tosylate derivatives can also be used.

---

[158] A. Grandeury, S. Tisse, G. Gouhier, V. Peulon, S. Petit, G. Coquerel; *Chem. Eng. Technol.*, **2003**, 26, 354-358.

[159] A. Grandeury, S. Petit, G. Gouhier , V. Agasse, G. Coquerel; *Tetrahedron: Asymm.,* **2003**, 14, 2143-2152.

In 1998, Zhong *et al.* described the preparation of β-CDOTs from the *p*-toluenesulfonic anhydride Ts_2O.[160] Pure β-CDOTs was obtained with 61% yield without any purification step. However, tosic acid-free *p*-toluenesulfonic anhydride is difficult to prepare. The synthesis, described in the publication of Zhong *et al.*, was tested in the laboratory. The reaction between TsCl and TsOH in CH_2Cl_2 did not give Ts_2O; the reagents were recovered. Another synthesis was tested by using TsOH and $SOCl_2$. This time, the Ts_2O was observed in ^1H NMR but it was not pure; the solid harvested at the end of the synthesis was a mixture of Ts_2O and TsOH. As the purification was difficult, this route of synthesis was not pursued further.

In 2000, the same authors published a more efficient synthesis of β-CDOTs by using 1-(*p*-toluenesulfonyl)imidazole ImTs **3** (Figure II - 13).[161] The yield was lower (40% instead of 61%) but the selectivity was higher; multi-tosylation was not observed even with four equivalents of ImTs.

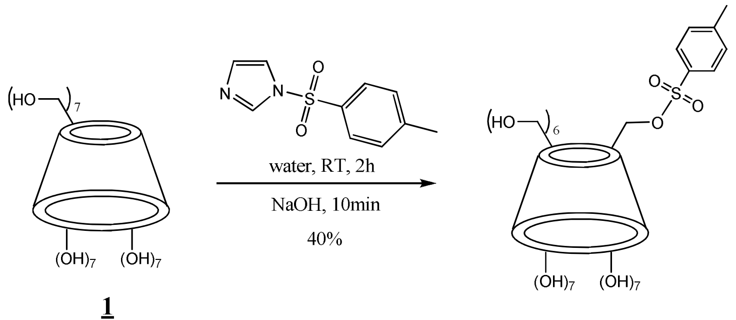

1

2

Figure II - 13. Synthesis of β-CDOTs 2 from native β-cyclodextrin and 1-(*p*-toluenesulfonyl)imidazole ImTs 3.

Actually, the purity of β-CDOTs obtained from *p*-toluenesulfonic anhydride Ts_2O was not perfect as described in the publication dated from 1998; a significant amount of native and disubstituted β-cyclodextrins were also synthesized.[161] Other advantages of ImTs are its stability (it is more resistant to hydrolysis at room temperature than TsCl and Ts_2O) and its solubility in water (ImTs exhibits a higher solubility than TsCl and Ts_2O). Moreover, ImTs is easy to synthesize and to purify.

The synthesis of β-CDOTs from ImTs was then tested in the laboratory. The synthesis of ImTs was carried out with success: pure ImTs was obtained with yields between 72% and 97% (Figure II - 14).

---

[160] N. Zhong, H.-S. Byun, R. Bittman; *Tetrahedron Lett.*, **1998**, 39, 2919-2920.

[161] H.-S. Byun, N. Zhong, R. Bittman; *Org. Synth.*, **2000**, 77, 225-227.

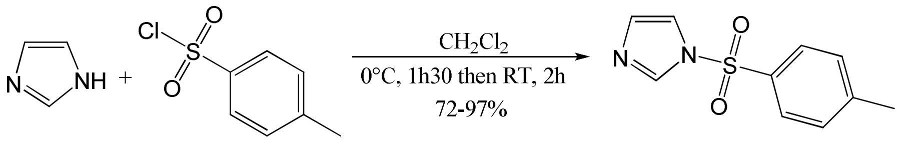

ImTs 3

Figure II - 14. Synthesis of 1-(*p*-toluenesulfonyl)imidazole ImTs 3.

The first synthesis of β-CDOTs from ImTs was carried out following the same procedure than the one descried the by Byun *et al.*,[161] but from 1.14g (1mmol) of native β-cyclodextrin instead of 40g. Unfortunately, the results were disappointing: even if the β-CDOTs was predominantly obtained, mass spectrometry and thin layer chromatography (hereafter TLC) revealed that significant amounts of native and disubstituted cyclodextrin β-CD(OTs)$_2$ were also formed. Different methods of purification were tested:

- Successive recrystallisations in hot water: the purity seemed to be slightly improved but to the detriment of the yield. Recrystallisation must be carefully carried out to avoid the hydrolysis of the tosylate.
- Recrystallisation in a 1/1 water/ethanol mixture: the purity was not significantly increased.
- Purification on silicagel by using mixtures of water and acetone (from 1/6 to 1/5) as eluent. A fraction enhanced in β-CDOTs was collected but with a very low yield (≈ 3%). Moreover, a large volume of solvents was necessary to perform this purification.

As the results were not satisfying with 1-(*p*-toluenesulfonyl)imidazole ImTs, synthesis of β-CDOTs from *p*-toluenesulfonyl chloride TsCl was tested (Figure II - 15). The experiment was carried out in water with sodium hydroxide. Unfortunately, but in accordance with the literature, the purity of the final product was worse than with ImTs.

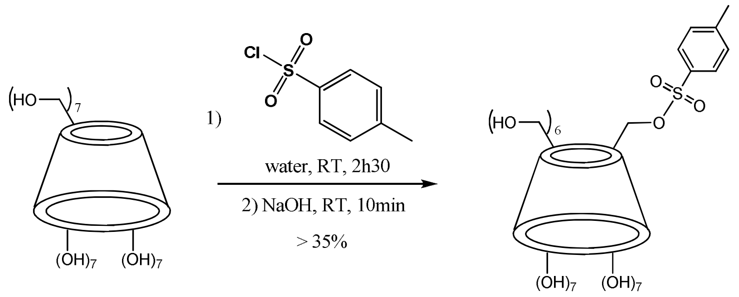

1 2

Figure II - 15. Synthesis of β-CDOTs 2 from native β-cyclodextrin and *p*-toluenesulfonyl chloride TsCl.

Therefore the synthesis of β-CDOTs was continued with ImTs and 10g of native β-CD were involved in the reaction. Surprisingly, the purity of the final product seemed to be better than previously and the yield was satisfying (47%). This product was then used without further purification in the next steps.

As the purity seemed to be increased when the amount of starting material increased, a synthesis on a larger scale was carried out. The same masses of reagents were used than those used by Byun *et al.*[161] Therefore, 40g of native β-CD were involved. Once again, the purity of the final product was increased compared to the previous synthesis and the yield was quite good (32%). Native β-CD and β-CD$(OTs)_2$ was almost no more visible on the mass spectrometry analyses. Of course, this analytical method is qualitative and not quantitative, but the comparison of spectra of different experiments carried out in the same conditions may give information on the relative purity of products.

The synthesis of β-CDOTs by using ImTs seems to be, at present, the best method to obtain satisfying purity and yield. This experiment was reproduced several times and the yield was increased up to 56%, without decreasing the purity.

b. 2 dimensions NMR analysis

After each synthesis, mass spectrometry analyses were carried out to determine if the monofunctionalisation was efficient or not, but did not give information about which alcohol was substituted. Therefore 2D NMR experiments were performed.

The HSQC (Heteronuclear Single Quantum Correlation) NMR analysis seemed to be the more relevant method to determine which kind of alcohol was substituted; direct correlations between carbon and attached hydrogen(s) are visible.

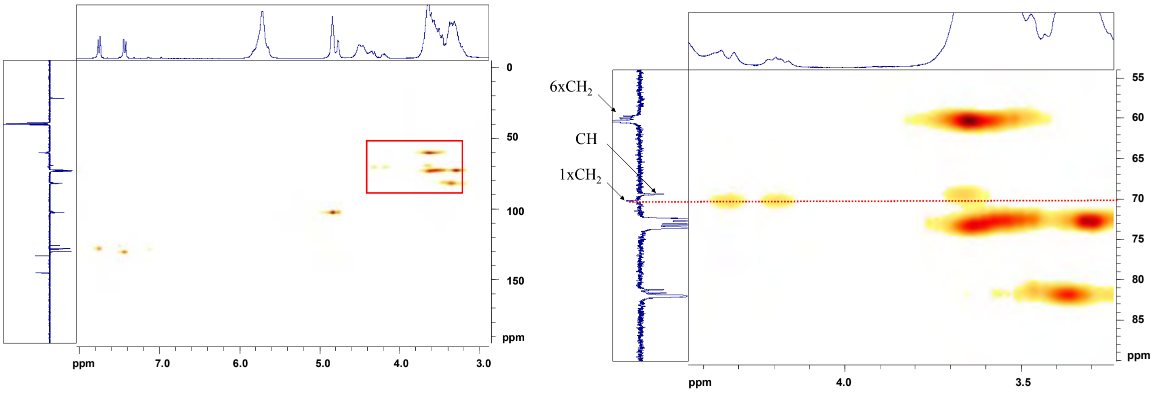

Figure II - 16. HSQC NMR of β-CDOTs (left) and magnification of the red square (right).

In this case, the ^{13}C NMR is a Jmod analysis, in which **C** and **CH$_2$** are on a side of the base line of the spectrum (here, to the left) and **CH** and **CH$_3$** are on the other side (to the right). On β-CDOTs, only two kinds of **CH$_2$** exist; those linked to the free primary alcohols and the one linked to the tosyl group. Therefore, it is easy to attribute the **CH$_2$** peaks, as drawn on the right spectrum of the Figure II - 16: six carbons give a signal at ≈60ppm while another single one is at ≈70ppm. Moreover, we can notice that the carbon at 70ppm is correlated to two different hydrogens, that is typical of diastereotopic hydrogens.

Combining mass spectrometry analysis and HSQC NMR analysis, it is clear that the monosubstitution occurred on a primary alcohol.

2. Synthesis of 6-deoxy-6-azido-β-cyclodextrin and its derivatives

a. Synthesis of 6-deoxy-6-azido-β-cyclodextrin β-CDN$_3$

The 6-deoxy-6-azido-β-cyclodextrin β-CDN$_3$ **4** can be easily synthesized from of β-CDOTs by nucleophilic substitution by using N_3^- as nucleophile (Figure II - 17).

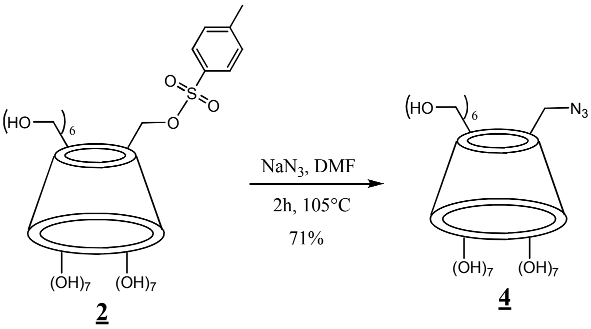

Figure II - 17. Synthesis of 6-deoxy-6-azido-β-cyclodextrin β-CDN$_3$ 4.

The synthesis and the purification were carried out according to the protocol described by Jicsinszky *et al.*[162] The nucleophilic substitution was a success, but not the purification. A purification by recrystallisation in a 10/1 acetone/water mixture was described but the product seemed to be almost insoluble in this mixture, even at high temperature. However, as this nucleophilic substitution is quantitative, the purity of the final product depends on the purity of the starting material. So, as the starting material was quite pure, the purity of β-CDN$_3$ was satisfying.

Actually, the main impurities were not native β-CD or polysubstituted CD, but were DMF, the solvent of the reaction, and a tosylate derivative: most probably TsONa. This impurity was encountered in all the syntheses of cyclodextrin derivatives by nucleophilic substitution (see the following paragraphs). TsONa seemed to give a stable complex with the substituted cyclodextrins, making its removal difficult. The presence of a tosylate derivative is clearly visible by ^{1}H NMR; peaks at $\delta \approx 7$ ppm cannot belong to the cyclodextrins **4** (Figure II - 18).

---

[162] L. Jicsinszky, R. Iványi; *Carbohyd. Polym.*, **2001**, 45, 139-145.

Integration of peak areas gave the proof that the amount of TsONa is thus absolutely not negligible.

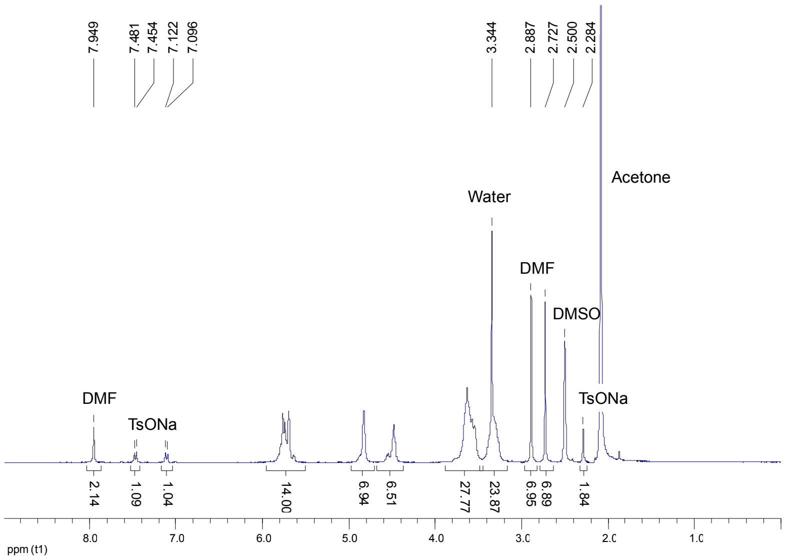

Figure II - 18. ^{1}H NMR of the crude β-CDN$_3$ in DMSO-d6.

To remove the DMF, the product was suspended in methanol and was stirred over night at RT. The solid was then analysed by ^{1}H NMR: as expected DMF almost disappeared but the amount of TsONa also significantly decreased (Figure II - 19). After an additional stirring in fresh methanol, peaks of DMF and TsONa were not detected.

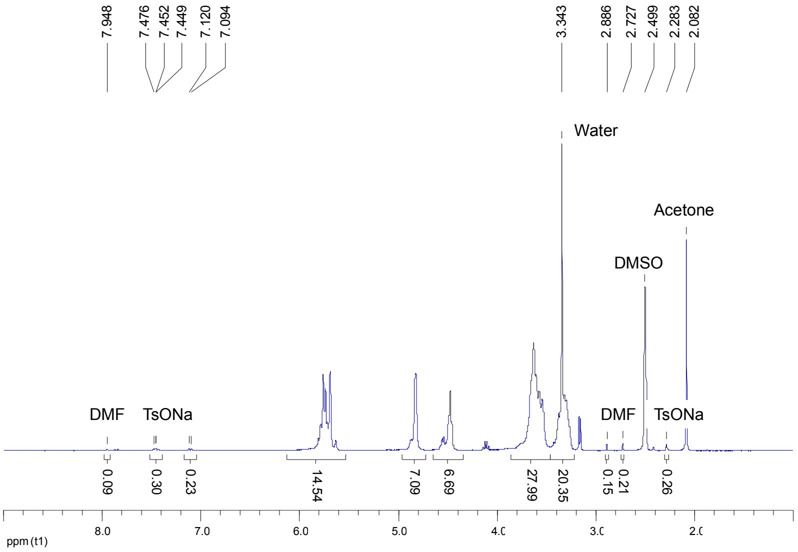

Figure II - 19. ^{1}H NMR of β-CDN$_3$ in DMSO-d6 after stirring one night in methanol.

b. Synthesis of 6-deoxy-6-amino-β-cyclodextrin CDNH$_2$

The 6-deoxy-6-amino-β-cyclodextrin β-CDNH$_2$ was synthesized by hydrolysis of β-CDN$_3$ by using triphenyl phosphine and water in DMF with a good yield (Figure II - 20).[163]

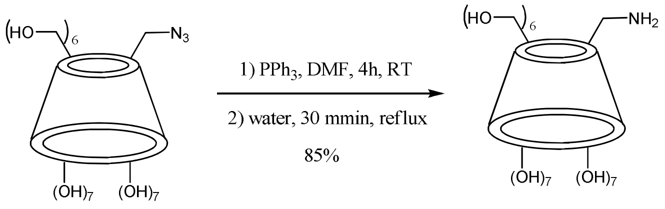

4 5

Figure II - 20. Synthesis of 6-deoxy-6-amino-β-cyclodextrin β-CDNH$_2$ 5.

β-CDNH$_2$ can be synthesized both from the crude and the purified β-CDN$_3$; the presence of TsONa did not disturb the reaction. However, it was still present at the end of the synthesis but it can be easily removed by using the same method as that used for β-CDN$_3$ (Figure II - 21).

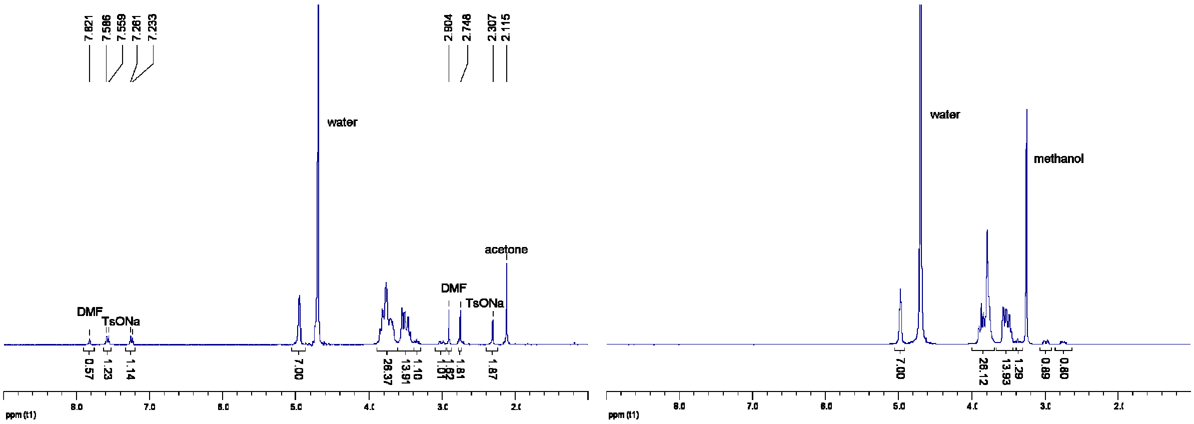

Figure II - 21. ^{1}H NMR of β-CDNH$_2$ in D$_2$O of the crude product (left) and after stirring twice in methanol (right).

c. Synthesis of 6-deoxy-1,2,3-triazole-β-cyclodextrin derivatives

The β-CDN$_3$ can also be involved in coupling reactions. The Huisgen [2+3] cycloaddition can be carried out with various alkyne precursors to give the 6-deoxy-1,2,3-triazole-β-cyclodextrin derivatives (Figure II - 22). This kind of reactions is named "Click-chemistry" and is widely used to graft cyclodextrins on silica to prepare the stationary phases of chiral chromatography columns.[164]

---

[163] I. W. Muderawan, T. T. Ong, T. C. Lee, D. J. Young, C. B. Chinga, S. C. Ng; *Tetrahedron Lett.*, **2005**, 46, 7905-7907.

[164] Z., Y. Jina, T. Lianga, Y. Liua, Q. Xua, X. Lianga, A. Lei; *J. Chromatogr. A*, **2009**, 1216, 257-263.

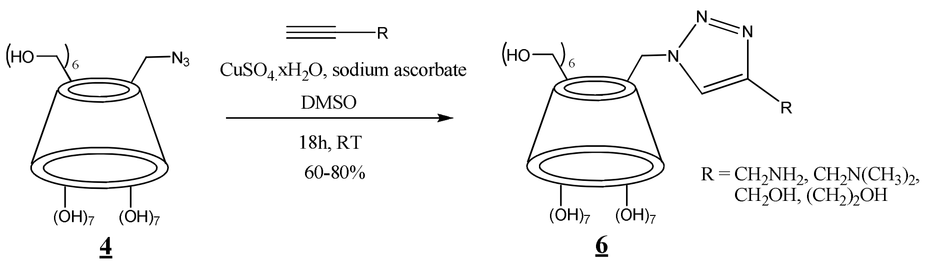

Figure II - 22. Synthesis of 6-deoxy-1,2,3-triazole-β-cyclodextrin derivatives.

Various functionalised cyclodextrins can be synthesized from β-CDN$_3$ by Click-chemistry. The first alkyne tested for this reaction was the propargyl alcohol. The reaction was carried out in DMSO, following the procedure of Mourer *et al.*; this solvent seemed to be more efficient in terms of yields than DMF.[165] Unfortunately, even if the desired product **6a** was synthesized (β-CDN$_3$ was not detected by the mass spectrometry analysis), the purification was difficult, and DMSO was particularly difficult to remove. Moreover, the crude product was green, due to the copper used as catalyst. But the purification described by Mourer *et al.* (chromatography on silicagel with water as eluent) was not efficient.

Therefore, a second experiment was made in DMF and with the propragyl amine in order to purify the product on an ion-exchange resin. An Amberlite IR-120 H$^+$ form was used and the copper-free 6-deoxy-(4-aminoethyl-1,2,3-triazole)-β-cyclodextrin **6b** was obtained with 37% yield. Another ion-exchange resin, the Dowex 50Wx 8H$^+$ form, gave similar results. Nevertheless, the purification was not very efficient and the yield significantly decreased when the purification was performed on a larger scale (≈1%). Chromatography with ion-exchange resin as stationary phase was also tested without success: the cyclodextrin was not retained enough in the column.

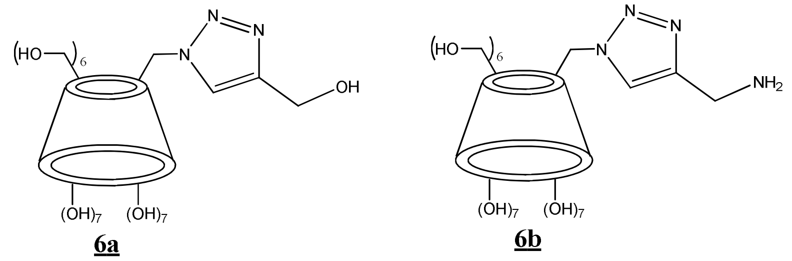

6a **6b**

Figure II - 23. Schematic representation of 6-deoxy-(4-hydroxymethyl-1,2,3-triazole)-β-cyclodextrin 6a and 6-deoxy-(4-aminomethyl-1,2,3-triazole)-β-cyclodextrin 6b.

---

[165] M. Mourer, F. Hapiot, S. Tilloy, E. Monflier, S. Menuel; *Eur. J. Org. Chem.*, **2008**, 5723-5730.

3. Synthesis of diamino-β-cyclodextrins

A small library of diamino-β-cyclodextrins was synthesized to have access to basic cyclodextrins with different length of "hook", in order to increase the possibility for a molecule to form a stable complex with one of this modified cyclodextrins (Figure II - 24).

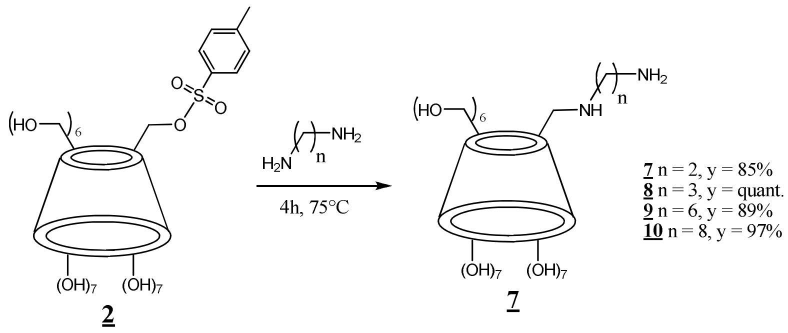

Figure II - 24. Synthesis of diamino-β-cyclodextrins.

a. Synthesis of 6-deoxy-(2-aminoethylamino)-β-cyclodextrin

The 6-deoxy-(2-aminoethylamino)-β-cyclodextrin **7** was easily synthesized from β-CDOTs by nucleophilic substitution with ethylenediamine as nucleophile. According to Liu *et al.*, ethylenediamine was used as solvent.[166] The ratio β-CDOTs/ethylenediamine can be decreased compare to the Liu's procedure, from 115 to 50 equivalents. However, it is difficult to use a lower ratio, the amount of diamine being not sufficient to dissolve β-CDOTs.

The position of the substituent was confirmed by HSQC, the two diastereotopic hydrogens linked on the functionalised secondary carbon are clearly visible.

As β-CDN_3 **4** and β-$CDNH_2$ **5**, the tosyl derivative gave a complex with **7**. Stirring in methanol were also able to purify the product.

b. Synthesis of 6-deoxy-(aminoalkylamino)-β-cyclodextrin

This monosubstituted cyclodextrins **8** et **9** were synthesized following the same procedure than **7** by using 1,3-diaminopropane and 1,6-diaminohexane as solvent, respectively.

The monosubstituted cyclodextrin **10** was synthesized by using *N*-methyl-2-pyrrolidone NMP as solvent with 4 equivalents of 1,8-diaminooctane (1,8-diaminooctane is a solid, and so can not be used as solvent).[167] The monosubstituted cyclodextrin **9** can also be carried out in NMP with 4 equivalents of 1,6-diaminohexane with similar results than with 1,6-diaminohexane only.

---

[166] Y.-Y. Liu, X.-D. Fan, L. Gao; *Macromol. Biosci.*, **2003**, 3, 715-719.

[167] J. S. Lock, B L. May, P. Clements, J. Tsanaktsidis, C. J. Easton, S. F. Lincoln; *J. Chem. Soc., Perkin Trans. 1*, **2001**, 3361–3364.

The substitution at the 6-position was confirmed by an HSQC NMR analysis and the tosylate derivative can be removed by stirring in methanol.

c. Synthesis of 6-deoxy-6-benzylamino-β-cyclodextrin

The 6-deoxy-6-benzylamine-β-cyclodextrin **11** was synthesized and purified following the same procedure than 7 by using benzylamine as solvent (50 equivalents).

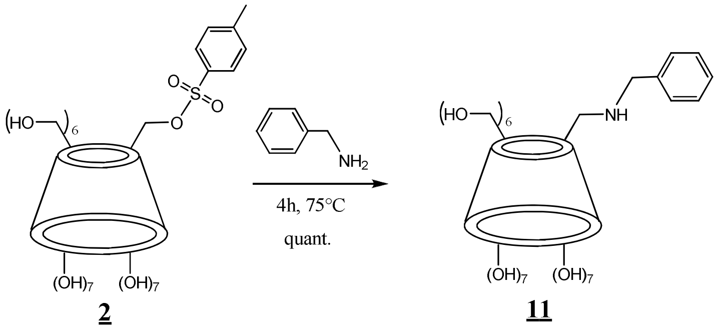

Figure II - 25. Synthesis of the 6-deoxy-benzylamino-β-cyclodextrin 11.

4. Synthesis of acid derivatives

A small library of amino acid derivatives was prepared to have access to cyclodextrins with an acidic hook. Aliphatic amino acids with different chain length were synthesized to increase the possibility to form a stable complex with a basic guest.

Polyacidic monosubstituted β-cyclodextrins were also prepared; the three acidic moieties may act as a polydentate complexing agent.

a. Synthesis of aliphatic amino acid derivatives

These derivatives were synthesized from the β-CDOTs. An organic base, such as triethyl amine (TEA) had to be added to make the nitrogen nucleophile. Indeed, amino acids exist as NH_3^+-CHR-COO^- form (and not as NH_2-CHR-COOH form). The nitrogen is therefore not nucleophile. The addition of a base is therefore necessary to form the nucleophile entity NH_2-CHR-COO^-.

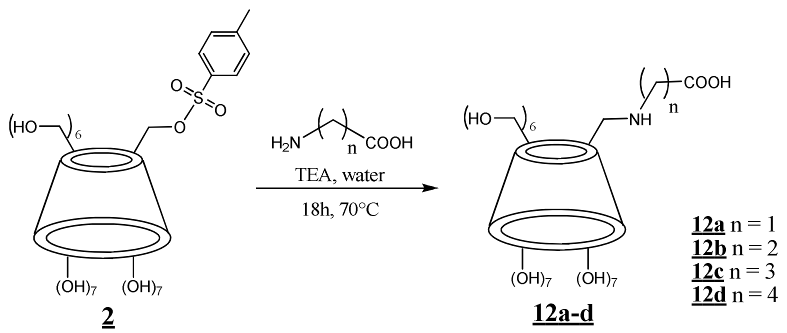

Figure II - 26. Synthesis of aliphatic amino acid derivatives.

First, reactions were carried out in NMP and DMF, but the substitution did not occur. Then water was used and the conversion was complete. However, some optimisations were necessary; when the amount of amino acid was too low, a significant amount of by-product appeared. On mass spectra, the peak corresponding to the mass of native cyclodextrin minus 18 (a water molecule) was visible. As this peak has never been observed before on the mass spectra of the other compounds (mass spectrometry analyses were carried out in the same conditions than the previous one), this peak corresponded to a by-product and not to a fragmentation of the native cyclodextrin. An excess of triethylamine was used compared to β-CDOTs, so alcohols may be deprotonated and an intramolecular substitution may occur. According to the literature,[168] the alcohol at the 3-position can be responsible of this substitution and the cyclodextrin **13a** was formed. However, the compound **13b**, resulting from the elimination of the tosylate, has also the same molecular mass. As the by-product had not been isolated, it was impossible to know which one was the by-product. To avoid the formation of **13a** and/or **13b**, 10 equivalents of amino acid had to be used.

Moreover, the final products were not pure; free amino acids are still present, as if they were complexed inside the cyclodextrins.

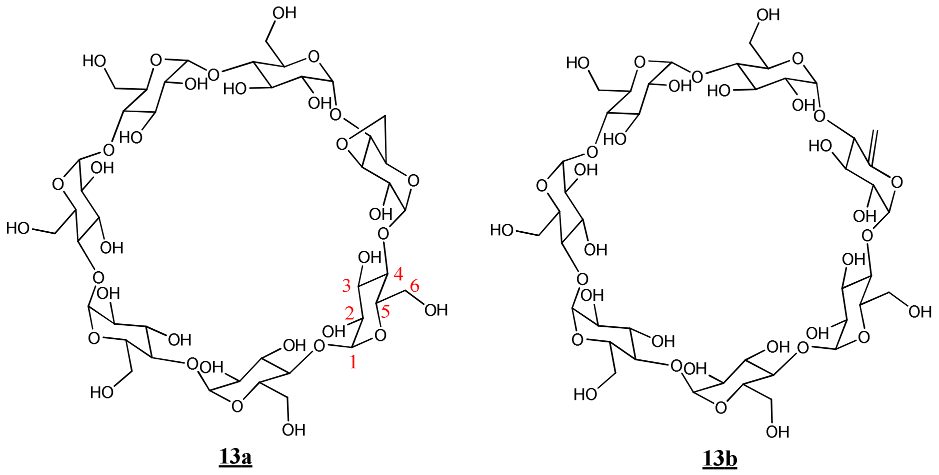

Figure II - 27. Chemical structure of the by-products 13a and 13b.

---

[168] J. A. Faiz, N. Spencer, Z. Pikramenou; *Org. Biomol. Chem.*, **2005**, 3, 4239-4245.

b. Synthesis of the L-phenylalanine derivative

The *L*-phenylalanine derivative was also synthesized to give the possibility to form π interactions between the host and the guest molecules. The same procedure as for the aliphatic amino acid derivatives was used.

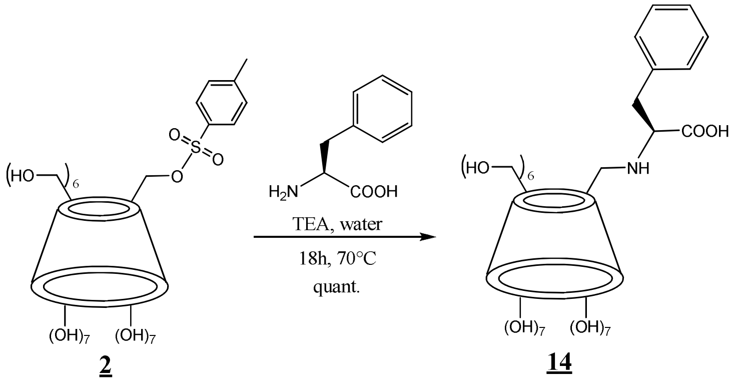
(HO—)6
O
S
O
O
H2N
COOH
TEA, water
18h, 70°C
quant.
(OH)7 (OH)7
2
(HO—)6
NH
COOH
(OH)7 (OH)7
14

Figure II - 28. Synthesis of the *L*-phenylalanine derivative.

c. Synthesis of polyacid derivatives

The amino-β-CD **5** and the diamino-β-CDs **7-10** can be modified by addition of chloroacetic acid to have access to poly acid cyclodextrins (Figure II - 29 and Figure II - 30). Pham *et al.* described the use of these compounds to combine the effect the EDTA (ethylenediaminetetraacetic acid), known to complex metallic ions, with the ability of cyclodextrin to be a chiral selector.[169]

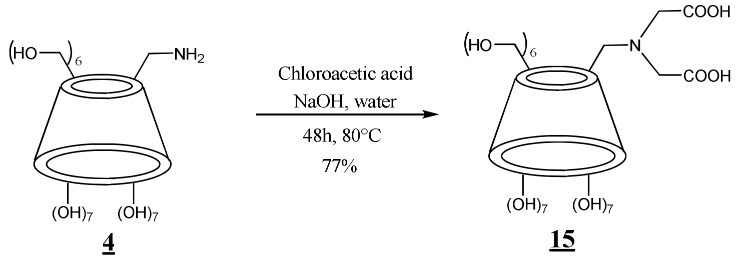
(HO—)6
NH2
Chloroacetic acid
NaOH, water
48h, 80°C
77%
(OH)7 (OH)7
4
(HO—)6
N
COOH
COOH
(OH)7 (OH)7
15

Figure II - 29. Synthesis of the amino-β-CD derivative.

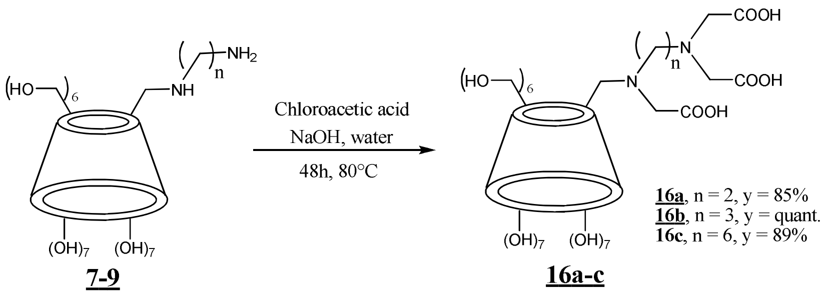
(HO—)6
NH2
n
NH
Chloroacetic acid
NaOH, water
48h, 80°C
(OH)7 (OH)7
7-9
(HO—)6
N
n
N
COOH
COOH
COOH
16a, n = 2, y = 85%
16b, n = 3, y = quant.
16c, n = 6, y = 89%
(OH)7 (OH)7
16a-c

Figure II - 30. Synthesis of the diamino-β-CD derivatives.

---

[169] D.-T. Pham, P. Clements, C. J. Easton, S. F. Lincoln; *Tetrahedron: Asymmetry*, **2008**, 19, 167-175.

IV - Study of the crystallisation of monosubstituted β-cyclodextrins and of inclusion complexes

1. Crystallisation of monosubstituted β-cyclodextrins

After purification by stirring overnight in methanol to remove the tosylate included in the cavity of the cyclodextrins, XRPD analyses were performed. Figure II - 31 exhibits the superimposition of β-CDN_3, β-$CDNH_2$ and β-$CDNH(CH_2)_nNH_2$.

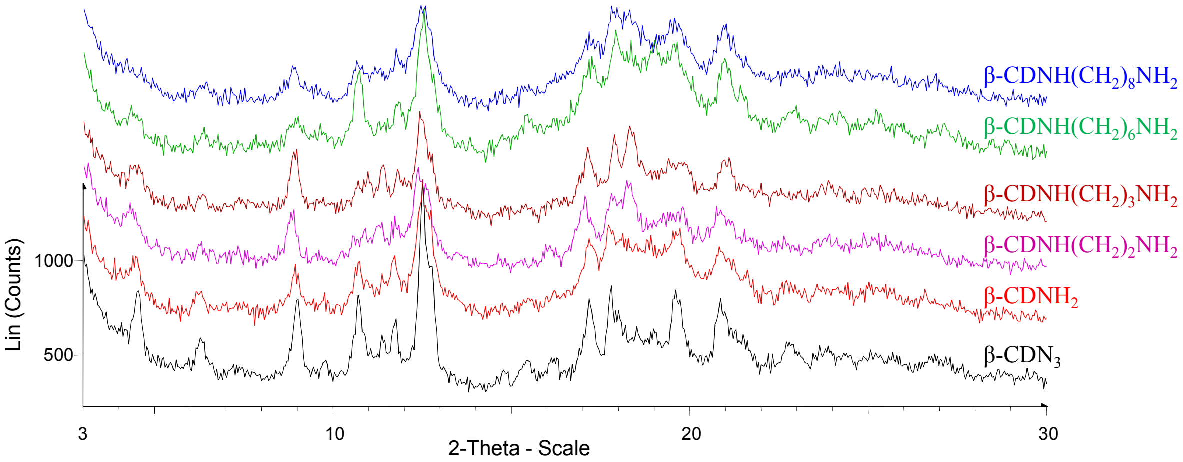

Figure II - 31. Superimposition of XRPD patterns of β-CDN_3, β-$CDNH_2$, and β-$CDNH(CH_2)_nNH_2$.

Each β-CD derivative exhibits a poor crystallinity. That can be explained by the purification work-up of these compounds: after stirring in methanol and filtration, powders are dried overnight in an oven at 50°C. This temperature may be sufficient to remove water to the crystal lattice and therefore to decrease its crystallinity.

The amino acid β-CD derivatives (**12a-d** and **14**) also exhibit a poor crystallinity and two of them (**12a** and **12d**) are amorphous.

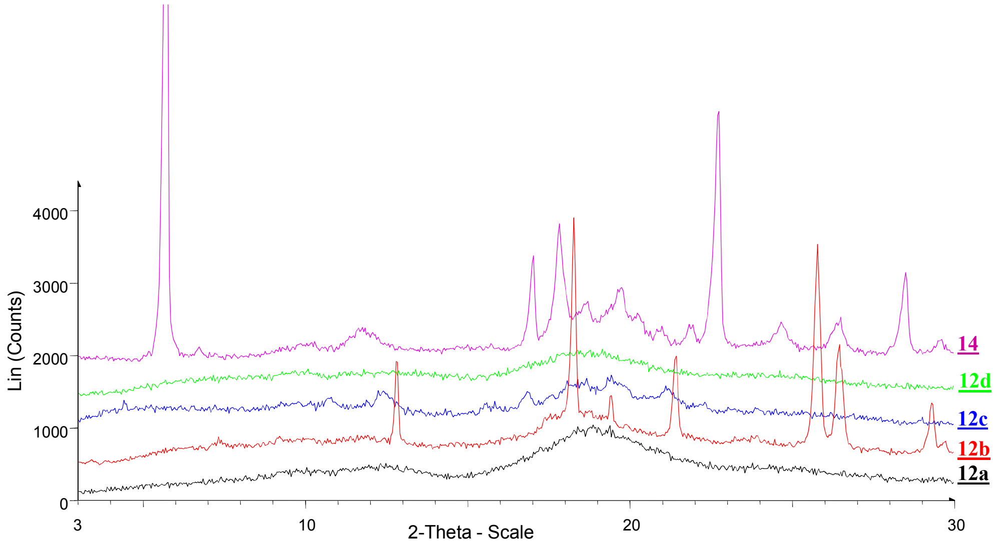

Figure II - 32. Superimposition of the XRPD patterns of the amino acid β-CD derivatives.

a. β-CDN₃

After purification, the β-CDN_3 exhibits a poor crystallinity that can be enhanced by recrystallisation in water from 40°C to room temperature (the red pattern of Figure II - 33). However, after maturation in water, a new phase appeared, probably due to the crystallisation of a hydrate with a different stoichiometry. When the temperature of the system is decreased to 10°C, a third phase appeared.

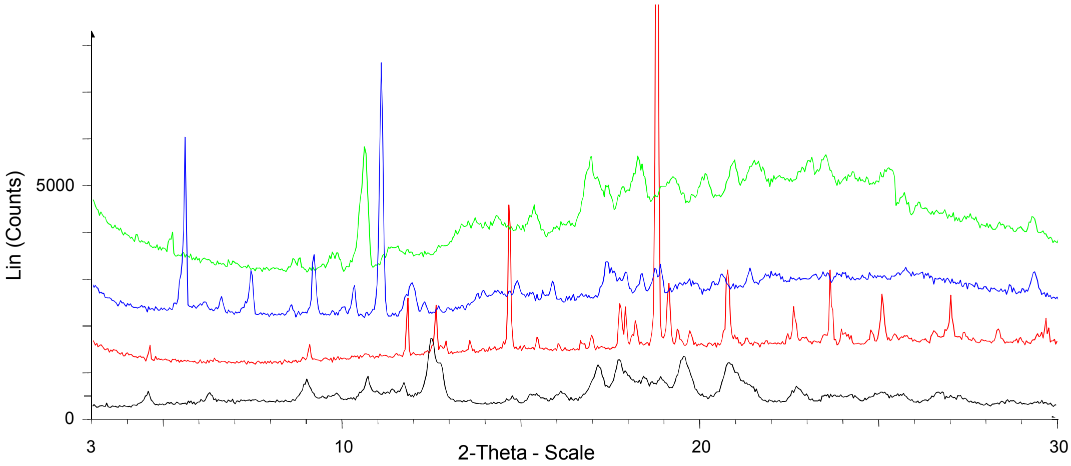

Figure II - 33. Superimposition of XRPD patterns of β-CDN_3 after purification (in black), after recrystallisation in water (from 40°C to RT, in red), after maturation (in blue) and after 72h at 10°C (in green).

The crystallisation of the β-CDN_3 seems be very sensitive to the temperature and to the presence of water. The existence of efflorescent hydrate was confirmed by microscopy; crystals of β-CDN_3 were obtained in water (Figure II - 34), but, after few minutes at room conditions, they became white, due to loss of water. Unfortunately, no single crystal with a sufficient quality was obtained. Furthermore, no structure of β-CDN_3 is register in the CSD (Cambridge Structural Database). A comparison between the phases obtained in the laboratory and the compounds described in the literature is therefore impossible.

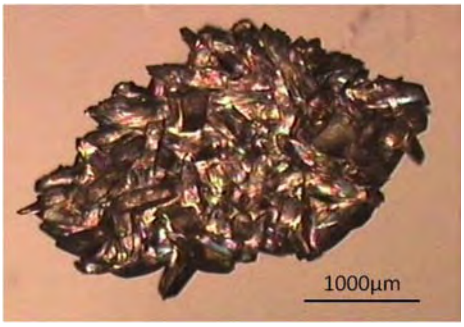

Figure II - 34. Crystals of β-CDN_3 in water.

b. β-CDNH$_2$

After purification, the β-CDNH$_2$ exhibits a poor crystallinity but it can be enhanced by recrystallisation in water from 40°C to room temperature as shown on Figure II - 35.

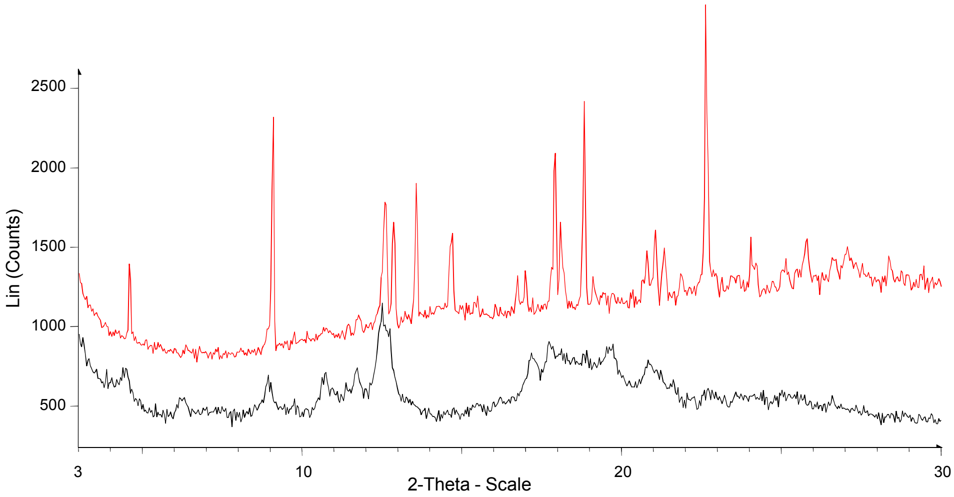

Figure II - 35. Superimposition of XRPD patterns of the β-CDNH$_2$ after purification (in black) and after recrystallisation in water from 40°C to RT (in red).

Cooling of a saturated solution of β-CDNH$_2$ in water led to the formation of crystals (Figure II - 36). Unfortunately, no single crystal was obtained. Moreover, these crystals were not stable in room conditions; as β-CDN$_3$, crystals became quickly white because of an efflorescent phase. Also in this case, no structure data are available on CSD and comparison with the literature was impossible.

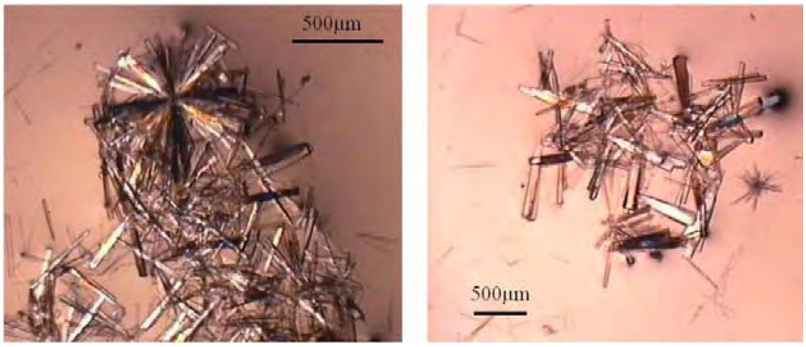

Figure II - 36. Crystals of β-CDNH$_2$ in water, from 50°C to 20°C for 5h then 20°C for 16h.

A TG-DSC analysis of the β-CDNH$_2$ obtained after purification was carried out. Only one phenomenon occurred between circa 50°C and 150°C, corresponding to dehydration. 10.11% of mass were lost, that correspond to the loss of seven molecules of water.

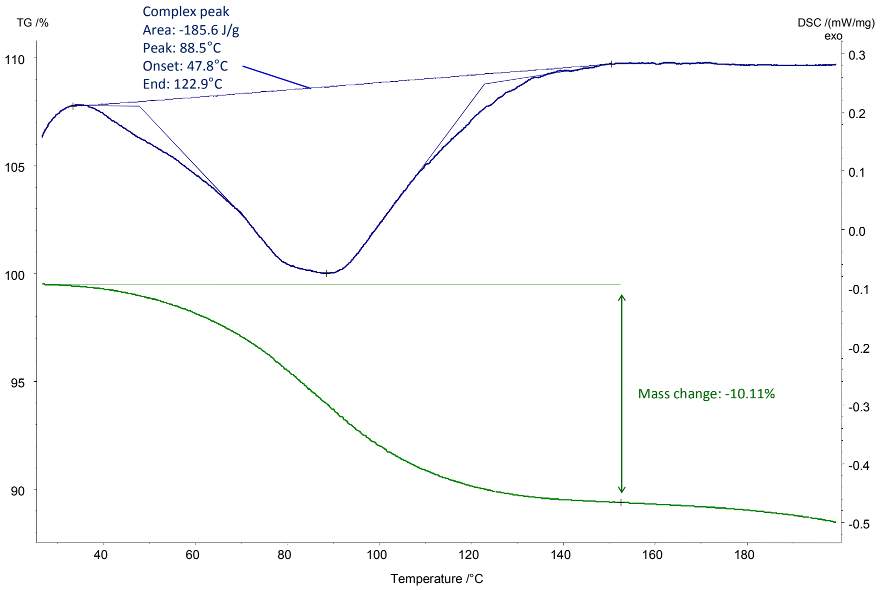

Figure II - 37. TGA-DSC analysis of β-CDNH$_2$. Heating rate: 5°C.min^{-1}.

A DVS (Dynamic Vapor Sorption) analysis was also carried out to study the behaviour of β-CDNH$_2$ toward the relative humidity. If stoichiometric hydrates exist, they can be detected by DVS, and their relative stability can be determined. Unfortunately, by looking at the result (Figure II - 38), no hydrate with a clear defined stoichiometry was detected; the percentage of water increased in the same time than the relative humidity increased without reaching a threshold. Moreover, the anhydrous β-CDNH$_2$ was hydrated as soon as the RH was different than zero.

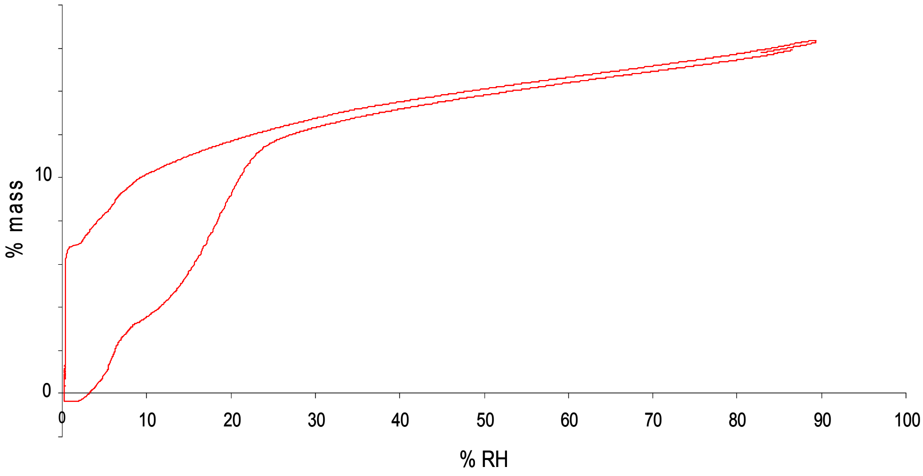

Figure II - 38. DVS analysis of the β-CDNH$_2$.

DVS analysis of the native β-cyclodextrins showed the same behaviour: hydration rate increased when the relative humidity was increasing; it was totally dependant of the moisture. If all the cyclodextrins behave similarly, it is not surprising that crystals obtained in water are not stable at room conditions.

c. *β-CDNH$(CH_2)_6NH_2$*

The β-CDNH$(CH_2)_6NH_2$ is the only one of the series of compounds described in this chapter for which the crystalline structure was available in the literature. Mentzafos *et al.* obtained suitable single crystals from recrystallisation in water and slow evaporation of the solvent (two months).[170] These crystals were not stable at room conditions. The structure resolution was therefore performed in a capillary with mother liquor. They found that β-CDNH$(CH_2)_6NH_2$ crystallised in the $P2_12_12_1$ space group with 9.68 molecules of water per molecules of β-CDNH$(CH_2)_6NH_2$. The corresponding crystal data are available under the reference code TEVCUS on the CSD database.

The calculated XRPD pattern corresponding to this crystal structure and the XRPD pattern of our β-CDNH$(CH_2)_6NH_2$ stored at room conditions were superimposed; as expected, they are totally different (Figure II - 39).

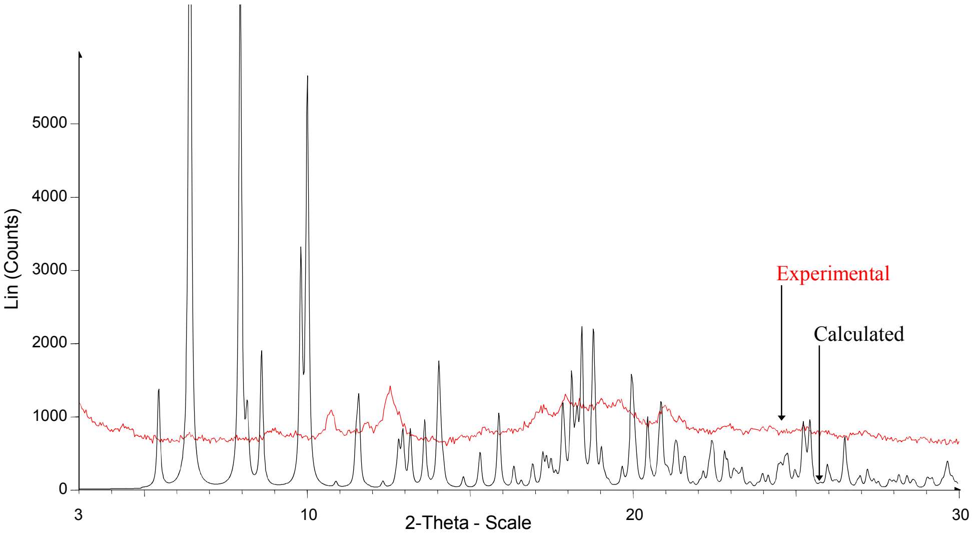

Figure II - 39. Superimposition of calculated (black) and experimental (red) XRPD pattern of β-CDNH$(CH_2)_6NH_2$.

2. Inclusion complexes

a. Native β-cyclodextrin and 1-(p-toluenesulfonyl)imidazole

First, the complex formed by the native β-CD and the 1-(*p*-toluenesulfonyl)imidazole ImTs was studied in order to understand the high selectivity of the substitution at the 6-position; ImTs may adopt a specific configuration inside the cavity to make possible only one substitution.

---

[170] D. Mentzafos, A. Terzis, A. W. Coleman, C. de Rango; *Carbohydr. Res.*, **1996**, 282, 125-135.

The complex was prepared in water: the native β-CD cyclodextrin was suspended in water then ImTs (1 equivalent) was added. The mixture was stirred for one day at room temperature when the solid was filtered, washed with acetone then dried at 40°C. ^{1}H NMR analysis of the powder confirmed the 1:1 stoichiometry (Figure II - 40).

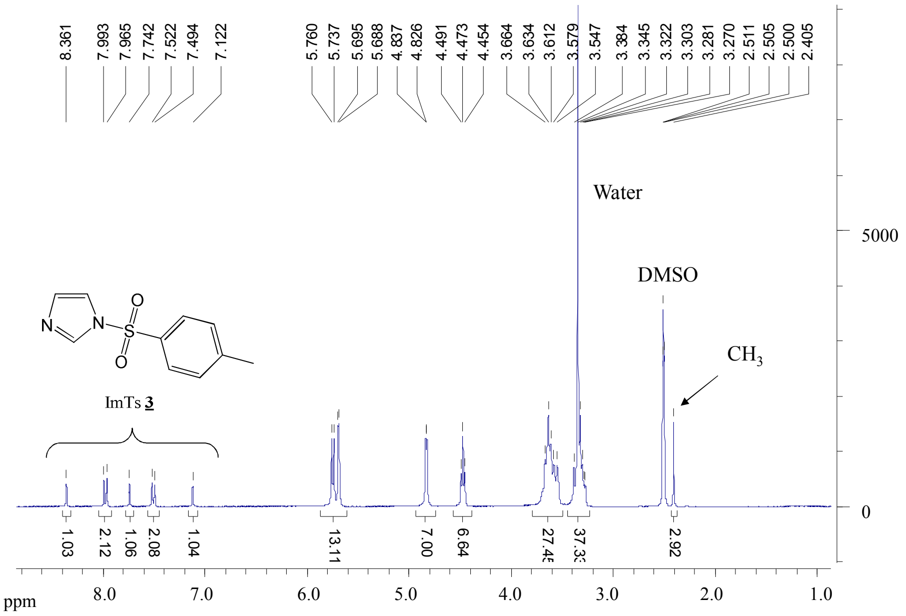

Figure II - 40. ^{1}H NMR of the complex between native β-CD and ImTs.

The XRPD pattern of this powder was compared to those of the native β-CD and of the ImTs; these three diffractograms were different; the existence of a new phase confirmed the formation of the complex (Figure II - 41).

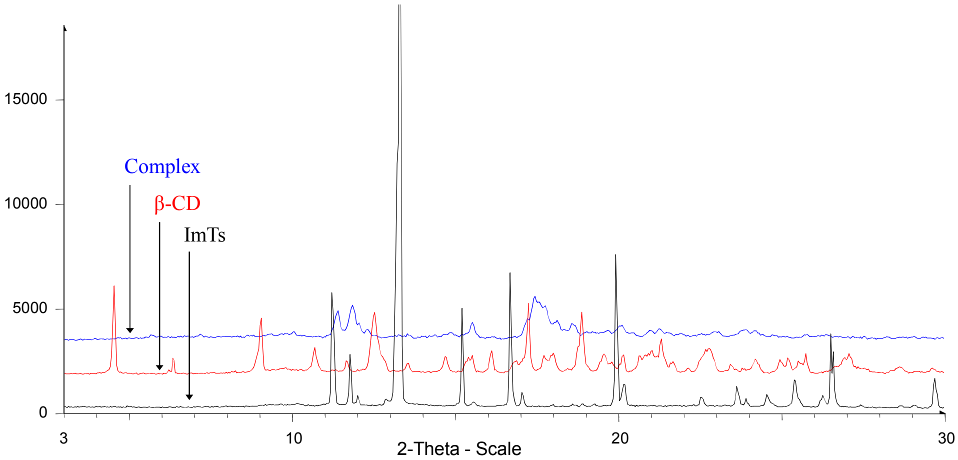

Figure II - 41. Superimposition of XRPD patterns of ImTs (in black), of the native β-CD (in red) and of the complex (in blue).

Crystallisation experiments were carried out in order to obtain single crystals. Unfortunately, no suitable crystals were obtained to perform the resolution of the structure.

b. β-CDNH₂ and ibuprofen

The complex formed between the native β-CD and ibuprofen was previously described by Núñez-Agüero *et al.*[156] They studied the energetic and conformational preferences involved in the formation of inclusion complexes, mainly by performing 2D NMR experiments and molecular mechanics simulations. However, the analysis revealed that a small energy difference (about 1kcal/mol) existed between the complexes formed by the two enantiomers. Therefore chiral separation of the two enantiomers was impossible by using the native β-CD.

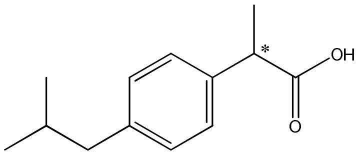

Figure II - 42. Chemical structure of ibuprofen.

In order to increase the energy interaction between the host and the guest, or to force a direction for the complexation, and therefore to induce a higher energy difference between the two enantiomers, a monosubtituted cyclodextrin with a “basic hook” was used.

A first test was performed by using the β-$CDNH_2$. β-$CDNH_2$ was dissolved in water then ibuprofen was added. As ibuprofen was not soluble in water, it tended to be included inside the hydrophobic cavity of the cyclodextrin to minimize the energy.

To see if a chiral discrimination was possible in these conditions, two equivalents of ibuprofen were used. After filtration, the mass of the harvested solid corresponded to one equivalent of ibuprofen, giving the proof that a 1:1 complex was formed. ^{1}H NMR confirmed the stoichiometry. Moreover, the “free” ibuprofen was racemic.

A recent study of Grandeury et al. described that the chiral recognition of the permethylated β-cyclodextrin/phenylethanol derivatives complexes progressively decreased with the duration of stirring.[159] Several experiments with different duration of stirring, between 10 minutes and 16 hours, were carried out but no enantiomeric excess was observed; if a chiral recognition exists, the energy difference between the two enantiomers is not sufficient to discriminate them in these conditions.

The complex was studied by X ray diffraction on powder. As expected, a new phase appeared, different from β-$CDNH_2$ and ibuprofen. However, as the other cyclodextrin derivatives, the crystallinity was poor.

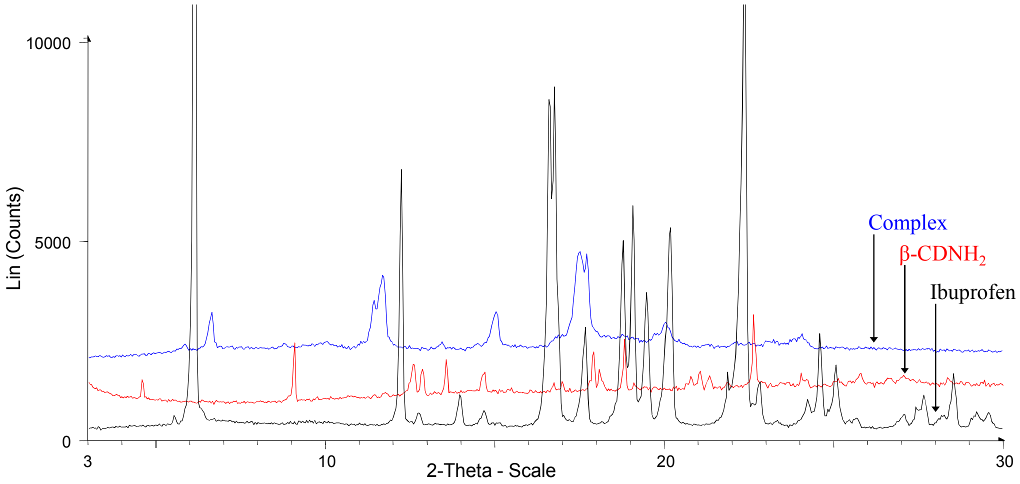

Figure II - 43. Superimposition of the XRPD patterns of ibuprofen (in black), β-CDNH$_2$ (in red) and the complex (in blue).

To determine if a chiral recognition exists at the solid state, crystallisation of single crystals was performed. Crystals were obtained in water, unfortunately, even after several experiments in different conditions, no crystal with a sufficient size and quality was obtained. The best results are shown on Figure II - 44, but these rather well-shaped particles were found to be not single crystals.

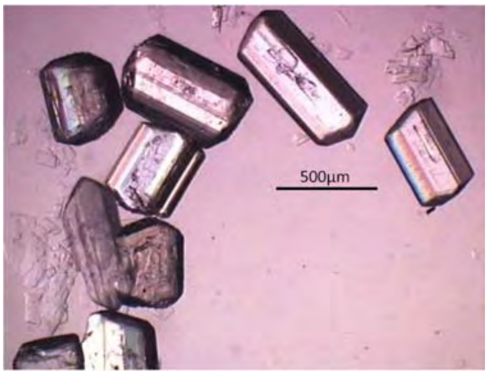

Figure II - 44. Crystals of β-CDNH$_2$/ibuprofen complex.

Moreover, these crystals are efflorescent. As the other cyclodextrins, different solvates may exist. The chiral separation is maybe possible with a solvate but of a different (nature) composition. The study of the liquid-solid quaternary phase diagram (*R*-ibuprofen/*S*-ibuprofen/β-CDNH$_2$/water) could give relevant information to perform a chiral separation, assuming that a chiral discrimination exist at the solid state for a solvate with a particular stoichiometry.

V- Conclusion

Monosubstituted cyclodextrins with various "hooks" were synthesized with success (Table II - 3) and with a quite good purity; the major impurity, tosylate derivatives, were easily removed. However, other impurities such as native β-cyclodextrin or disubstituted β-cyclodextrin are difficult to remove. Therefore it is very important to avoid the formation of these compounds during the step of synthesis of the monosubstituted β-CDOTs. The synthesis at the 40g scale of native β-cyclodextrin by using of 1-(*p*-toluenesulfonyl)imidazole gave the best results.

The sensitivity of cyclodextrins derivatives toward water was highlighted, more particularly by DVS analyses, and may explain why the crystallisation of cyclodextrins and their storage under room conditions are difficult.

Experiments gave the proof that formation of complexes between β-CDNH$_2$ and ibuprofen was possible but did show any chiral discrimination. Of course, further studies are necessary on this topic to determine if a chiral recognition exists at the solid state.

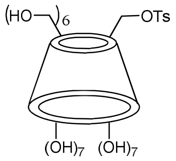 (HO—)6 OTs (OH)7 (OH)7	2 β-CDOTs	56%	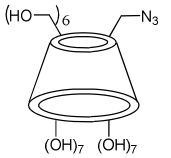 (HO—)6 N3 (OH)7 (OH)7	4 β-CDN$_3$	71%
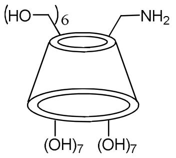 (HO—)6 NH2 (OH)7 (OH)7	5 β-CDNH$_2$	85%	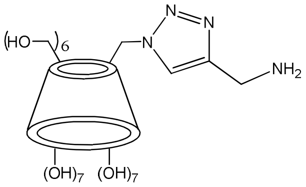 (HO—)6 N N N NH2 (OH)7 (OH)7	6b	92%
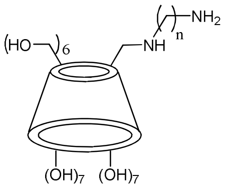 NH2 n (HO—)6 NH (OH)7 (OH)7	7 β-CDNH(CH$_2$)$_2$NH$_2$	82%	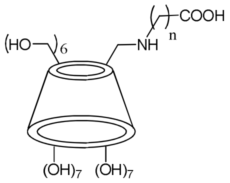 COOH n (HO—)6 NH (OH)7 (OH)7	12a β-CDNHCH$_2$COOH	Not pure*
	8 β-CDNH(CH$_2$)$_3$NH$_2$	93%		12b β-CDNH(CH$_2$)$_2$COOH	Not pure*
	9 β-CDNH(CH$_2$)$_6$NH$_2$	Quant.		12c β-CDNH(CH$_2$)$_3$COOH	Not pure*
	10 β-CDNH(CH$_2$)$_8$NH$_2$	97%		12d β-CDNH(CH$_2$)$_4$COOH	Not pure*
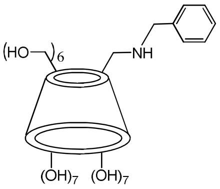 (HO—)6 NH (OH)7 (OH)7	11 β-CD benzylamine	Quant.	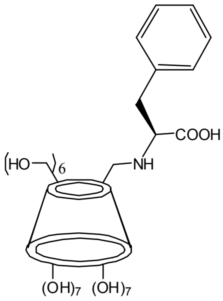 COOH (HO—)6 NH (OH)7 (OH)7	14 *L*-phenyl glycine β-CD	Not pure*
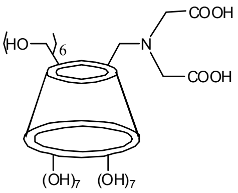 COOH (HO—)6 N COOH (OH)7 (OH)7	15	77%	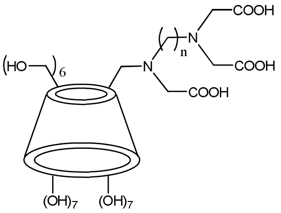 COOH n N COOH (HO—)6 N COOH (OH)7 (OH)7	16a	85%
				16b	Quant.
				16c	89%

Table II - 3. Summary table of monosubstituted β-cyclodextrins synthesized in this chapter. *The impurity is the amino acid used for the synthesis.

Chapter 3: Stochastic chiral symmetry breaking of a conglomerate forming system; study of a series of triazoyl ketone

In the previous chapter, mono-substituted β-cyclodextrins were synthesized in order to purify enantiomers thanks to the formation of complexes. In this part, pure enantiomers will be obtained by using a totally different method combining crystallisation and racemisation, called deracemisation, or total symmetry breaking.[115] The historical aspects of this discovery and related bibliographic data are developed in Chapter 1.

We decided to study the deracemisation of the 1-(4-chlorophenyl)-4,4-dimethyl-2-(1H-1,2,4-triazol-1-yl)pentan-3-one ClTAK **Cl-17** (Figure III - 1). The choice of this molecule resulted from the context of my PhD, which was a part of the European project IntEnant (see chapter 1). One of the partners of this project previously worked on this molecule and wished to perform additional studies on it. Therefore there was a need for the racemic mixture as well as to the pure enantiomers. As **Cl-17** meets the dual conditions required for the deracemisation process (crystallisation as a conglomerate and racemisation are compatible in the same medium[171]), pure enantiomers will be prepared by deracemisation, studying at the same time other aspects of this process such as the evolution of the crystal size distribution. Furthermore, except few exceptions, only amino acid derivatives were described in the literature (see Chapter 1). **Cl-17** and few other derivatives will thus be other examples of compounds possible to deracemise.

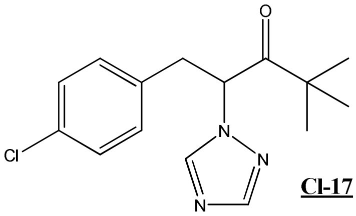

Cl-17 ClTAK

Figure III - 1. Chemical Structure of Cl-17.

In the last part of this chapter, a new deracemisation process will be described in which glass beads are replaced by ultrasounds. The efficiency of the two variants will be compared leading to new hypotheses on the mechanism of the deracemisation.

---

[171] S. N. Black, L. J. Williams, R. J. Davey, F. Moffat, R. V. H. Jones, D. M. McEwan, D. E. Sadler; *Tetrahedron*, **1989**, 45(9), 2677-2682.

I - Introduction

Paclobutrazol **18** (Figure III - 2) is a plant growth inhibitor.[52] The pure enantiomer was obtained by diastereoisomeric salt.[172] Unfortunately, the unwanted enantiomer was difficult to recycle and the final product was thus expensive.

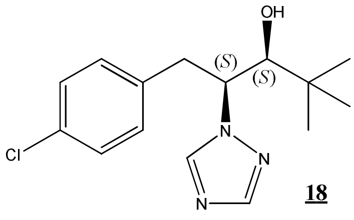

18

Figure III - 2. Chemical structure of Paclobutrazol.

Twenty years ago, Black *et al.* studied the 1-(4-chlorophenyl)-4,4-dimethyl-2-(1H-1,2,4-triazol-1-yl)pentan-3-one **Cl-17**, a precursor of Paclobutrazol. They noticed that **Cl-17** crystallised as a stable conglomerate, in the $P2_12_12_1$ space group, and thus that it was possible to obtain the target enantiomer by preferential crystallization. Then the ***S*-Cl-17** can be stereospecifically reduced to give only the (2*S*,3*S*)-paclobutrazol without further enantiopurification steps (Figure III - 3). Moreover, they noticed that **Cl-17** was easily racemisable: "*Addition of 1% w/w sodium hydroxide resulted in racemization which was too rapid to measure it. At much lower concentration of base (0.001%), the observed optical rotation fell to half its initial value in 30 minutes*."[171] The unwanted enantiomer can be recycled, increasing the overall yield and thus, decreasing the cost of the synthesis. As preferential crystallisation and racemisation can be carried out in the same experimental conditions (methanol/water mixtures), they combined them to perform a process named "crystallisation-induced asymmetric transformation" also called "second order asymmetric transformation" (SOAT, see Chapter I), increasing the productivity of the purification to 83% yield with 99% enantiomeric excess. Unfortunately, a slow cooling profile (1K.h^{-1}, from 30°C to 24.5°C) must be applied to prevent the heteronucleation of the counter enantiomer (mainly by epitaxy). Similar results were obtained when the cooling was replaced by a controlled evaporation of solvent or addition of water as anti-solvent.

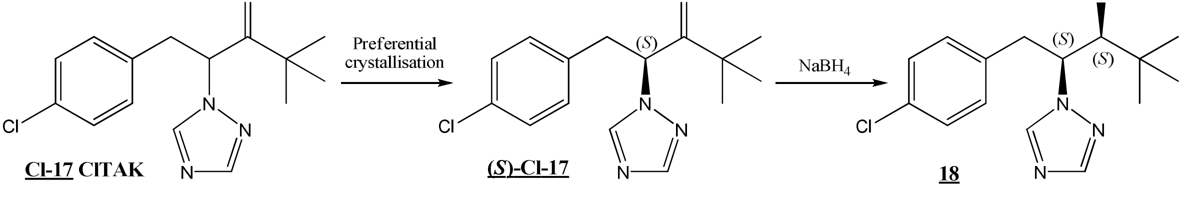

Figure III - 3. Synthesis of Paclobutrazol with a preferential crystallisation step.

---

[172] US4243405A1.

One of the first works for my PhD was to synthesize **Cl-17** to establish a collaboration between the SPCMIB laboratory at the University of Toulouse, in which I spent the first part of my PhD, and the SMS laboratory at the University of Rouen, in which I spent the second part of my PhD. After synthesis, **Cl-17** was provided to Guillaume Levilain, a student of the SMS laboratory. He worked on the design of the new process combining the experiments of Black *et al.* (that is to say cooling and *in-situ* racemisation) and the Viedma Ripening (deracemisation by using glass beads). The combination of all this conditions increased the productivity of the purification; the effect of glass beads makes it possible to apply a high cooling rate (15K.h^{-1}) from 50°c to 20°C, keeping the final enantiomeric excess at circa 99% (See Chapter I).[108]

In the literature, a compound with a very similar crystal structure was described: the 1-(2-fluoro-4-chlorophenyl)-4,4-dimethyl-2-(1H-1,2,4-triazol-1-yl)pentan-3-one **2F-4Cl-17**.[173] Both **Cl-17** and **2F-4Cl-17** crystallise in the $P2_12_12_1$ space group with very close cell parameters. Therefore we decided to synthezise a series of compounds to study the effect of the substitution of the aromatic group on the crystal packing (Figure III - 4). We wanted to know if a kind of pocket exists inside the crystal structure in which it was possible to put "almost everything" with similar size and/or similar kind of interactions without modifying the stereoselective packing. Then, the deracemisation of compounds crystallising as a conglomerate could be applied.

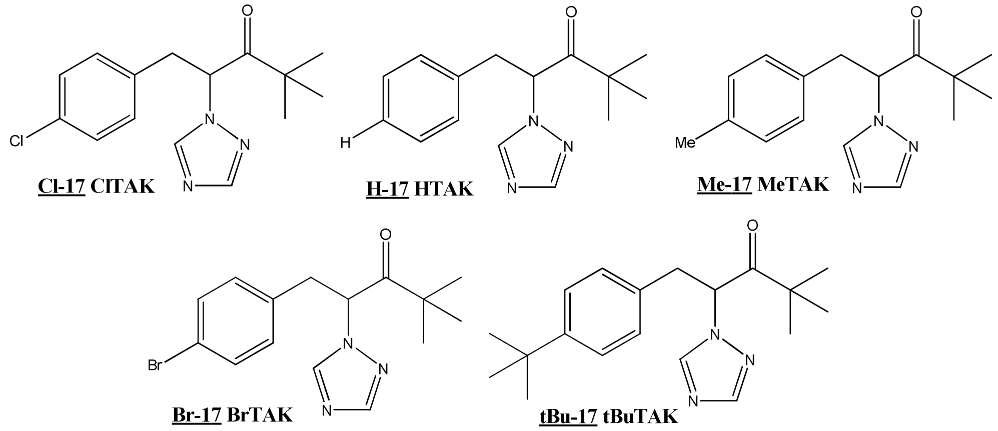

Cl-17 **ClTAK** H-17 **HTAK** Me-17 **MeTAK**

Br-17 **BrTAK** tBu-17 **tBuTAK**

Figure III - 4. Chemical structures of the five synthesised derivates of TAK.

---

[173] S. K. Branch, I. W. Nowell; *Acta Cryst.* , **1986**, *C42*, 440-442.

II - Synthesis of the triazolyl ketones

1. Synthesis of 1-(4-chlorophenyl)-4,4-dimethyl-2-(1H-1,2,4-triazol-1-yl) pentan-3-one ClTAK

The synthesis of ClTAK **Cl-17** was described in the patent concerning the preparation and the application of fungicidal compounds such as Paclobutrazol. In this patent, heterocyclic compounds containing an imidazole or a 1,2,4-triazole and a substituted aromatic cycle were studied (Figure III - 5).[172]

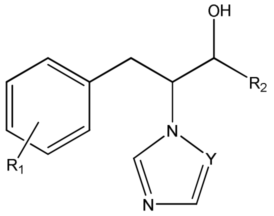

R1 = p-Cl, m-Cl, o-Cl, pBr, pMe, pOMe...
R2 = tBu, iPr
Y = C, N

Figure III - 5. Patented heterocyclic compounds.

The syntheses of only two compounds were described in the patent: the synthesis of **18** and therefore of **Cl-17** and the synthesis of the unsubstituted ketone **H-17**. Moreover, two different routes were published.

In the first route, only three steps were necessary to access to the final compound **18** (Figure III - 6). In the first step, the α-1,2,4-triazol-1-yl-pinacolone **19** was prepared by nucleophilic substitution from the bromopinacolone and the 1,2,4-triazole. Then another substitution with the *p*-chlorobenzylchloride gives the ClTAK **Cl-17**. Finally, the Paclobutrazol was obtained by reduction by using $NaBH_4$.

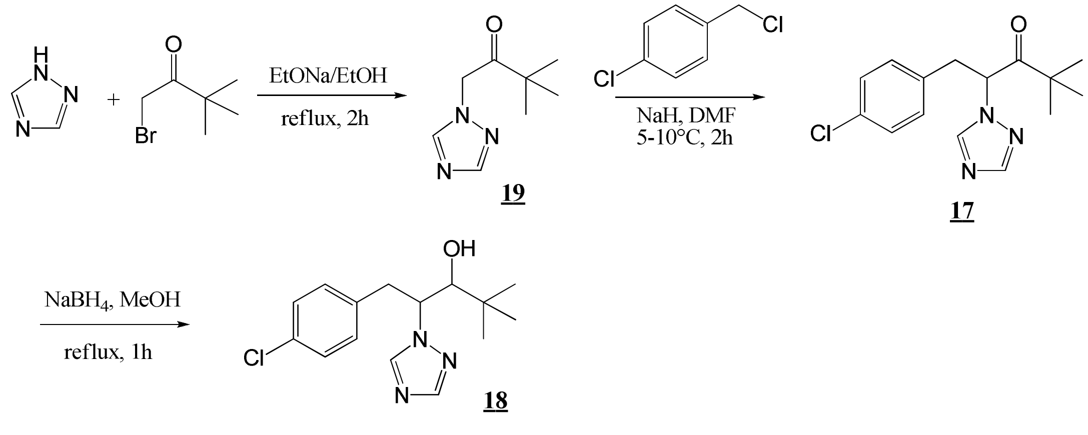

Figure III - 6. First synthetic route of Paclobutrazol.

In the second synthetic route, five steps were necessary to obtain the final product (Figure III - 7). First, an adolisation-crotonisation of the *p*-chlorobenzaldehyde with the pinacolone was carried out. The chalcone **20** was then reduced to give the hydrogenated compound **21**. The ketone was brominated in α position then a nucleophilic substitution with the 1,2,4-triazole gave the ClTAK **Cl-17**. The last step was a reduction by $NaBH_4$, as described in the first route.

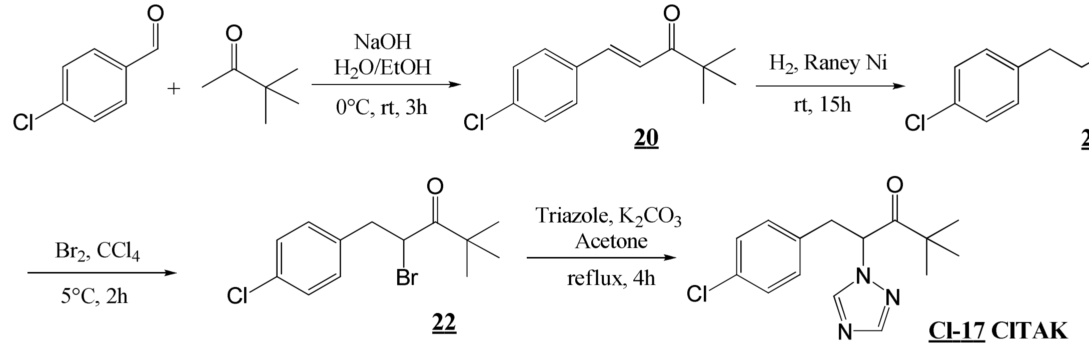

Figure III - 7. Second synthetic route of Paclobutrazol.

The second route is longer than the first one but reagents are cheaper; the starting material of the first route, the bromopinacolone, is an expensive product. It can be prepared by bromination of the pinacolone but it is difficult to control the number of substitutions and a significant amount of dibromopinacolone is formed. Its purification is quite difficult, making the compound expensive. Moreover, even after purification, a small amount of dibromopinacolone remains, giving by-products for the synthesis. On the contrary, reagents of the second route are cheaper and easy to find with a good purity.

In the patent, the experimental protocol is well described for these syntheses: stoechiometries of the reagents, volumes of solvent and reaction times are given as well as the purification steps. However, the yield and the analyses of intermediates and final products, such as ^{1}H NMR, ^{13}C NMR or mass spectrometry, are not given. Moreover, the synthesis of only two compounds, ClTAK **Cl-17** and the unsubstituted derivative HTAK **H-17** are depicted.

To perform the synthesis of **Cl-17**, we chose to follow the second route of the synthesis because all the reagents were available in the laboratory. A small modification of the protocol was made: the bromination step was carried out with tetrabutylammonium tribromide TBA.Br_3 in acetic acid instead of Br_2 in CCl_4 (Figure III - 8). The solvent is toxic and Br_2 is quite difficult to manipulate.

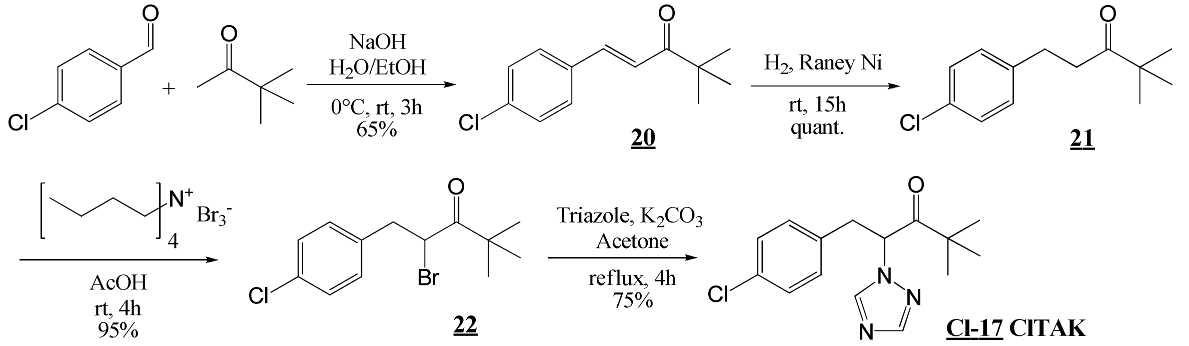

Figure III - 8. Synthetic route used in the laboratory.

The TBA.Br_3 can be easily synthesized from tetrabutylammonium TBA.Br (Figure III - 9).[174] TBA.Br instantaneously reacts with sodium bromate $NaBrO_3$ and hydrobromic acid HBr to give TBA.Br_3, an orange power. Purification by recrystallisation in a 1:1 CH_2Cl_2/Et_2O mixture gives pure orange crystals of TBA.Br_3. Moreover, this product can be recycled after the bromination step of the synthesis of compounds **Cl-17** by adding the right amount of sodium bromate and hydrobromic acid.

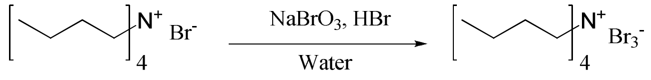

Figure III - 9. Synthesis of the tetrabutylammonium tribromide.

Some by-products are formed during this route of synthesis but a single purification at the final stage is sufficient to easily obtain pure compounds with an acceptable yield. In fact, two by-products were detected. During the hydrogenation step, a small percentage of Ar-Cl bonds were broken, giving at the end of the synthesis the dechlorinated compounds **H-17**. During the last step, the elimination of HBr can occur to give the intermediate **Cl-20**. These two by-products are very soluble in diisopropylether and/or methanol compared to the target compound, simple washings of the solid with these solvents are thus sufficient to purify it.

2. Synthesis of the triazoyl ketone derivatives

Four other TAK derivatives (Figure III - 4) were synthesized following the same procedure than the ClTAK, even if the work-up had to be modified in some cases (see experimental part).

The synthesis of the BrTAK **Br-17** was more complicated. Indeed, during the hydrogenation step, the proportion of debrominated product was significant. Of course, the presence of this by-product was not surprising, the Ar-Br bond being easier to break than the Ar-Cl bond under these experimental conditions. But this phenomenon seemed to be coupled with a decreasing of the efficiency of the catalyst; even by increasing the amount of hydrogen, the reaction was stopped before the total conversion, at circa 50%. When the crude product was hydrogenated again, with fresh Raney nickel, the conversation did not increase significantly when breakage of Ar-Br bond was substantial, giving a mixture of four compounds (Figure III - 10). Unfortunately, the purification by chromatography was complicated because all the compounds were similarly eluted.

---

[174] S. Kajigaeshi, T. Kakinami, T. Okamoto, S. Fujisaki; *Bull. Chem. Soc. Jpn.*, **1987**, 60, 1159-1160.

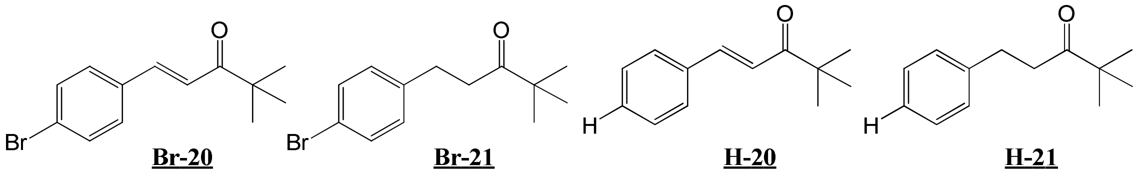

Br-20 **Br-21** **H-20** **H-21**

Figure III - 10. Molecules in the crude product after hydrogenation of Br-20.

The crude product was used without purification in the next step. Mixture of products was thus obtained. The presence of **Br-22** was confirmed by ^{1}H NMR and by mass spectrometry (characteristic peaks of a compounds having two bromines atoms and corresponding to the mass of **Br-22** were visible). The crude product was used in the final step then the desired compound **Br-17** was purified by crystallisation.

A different hydrogenation method was tested, using zinc and ammonium chloride in a mixture of methanol and water.[175] This method was described to be softer than the hydrogenation catalysed by Raney nickel but was not efficient in our case. As the final amount of **Br-17** (around 5g) was sufficient to study its behaviour in crystallisation and deracemization process, no alternative synthetic route was designed.

However, the first synthetic route described in the patent would have been beneficial since no reduction step is necessary.

---

[175] J.-P. Li, Y.-X. Zhang, Y. Ji; *J. Chin. Chem. Soc.*, **2008**, 55(2), 390-393.

III. Characterisation of the solid phases

1. Solubility data

Solubilities of the TAK derivatives were determined by using the gravimetric method in various methanol/water mixture. This mixture of solvents was the one used by Black *et al.* in 1989 for the preferential crystallisation of ClTAK in which both, crystallisation and racemisation, were compatible. The results are summarized in Table III - 1. The evolution of the solubilities of TAK derivatives depending on the ratio of methanol/water is represented in a ternary phase diagram (Figure III - 11).

Methanol/water w/w	0/100	45/55	47/53	50/50	60/40	65/35	75/25	80/20	90/10	100/0
ClTAK	0.0%	-		0.6%	-	-	4.1%*	**5.5%**	-	14.4%
HTAK	0.1%	4.0%	**4.7%**	7.4%	20.6%	-	-	-	-	68.3%
MeTAK	0.0%	-		1.5%	3.3%	**6.0%**	11.5%	15.2%	-	34.9%
BrTAK	-	-		0.5%	-	-	-	3.3%	**5.2%**	8.3%

Table III - 1. Solubilities of the racemic composition of TAK derivatives in various methanol/water mixtures. *The ratio of methanol and water was 76/24.

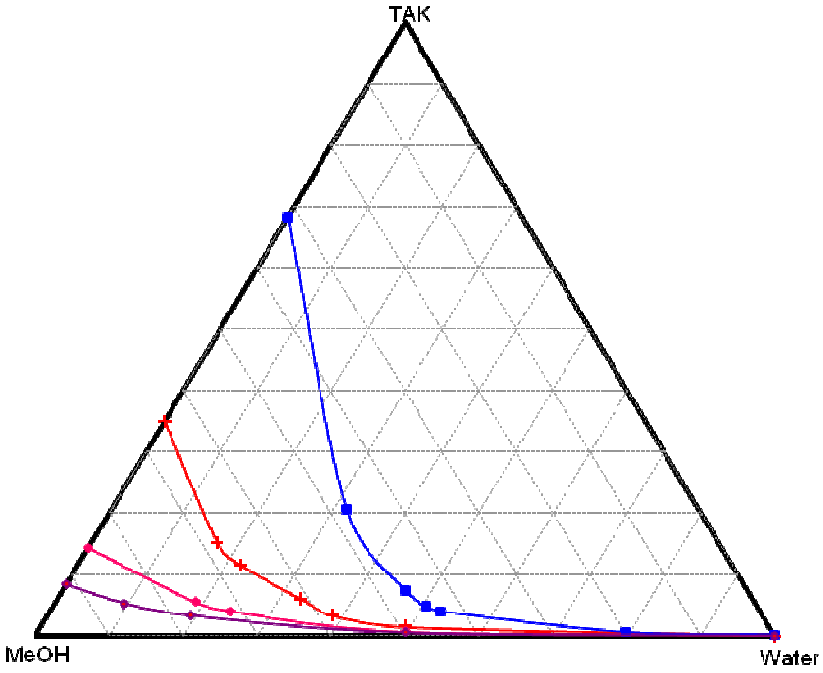

Figure III - 11. Evolution of the solubilities of the racemic composition of TAK derivatives in different ratios of methanol and water. ClTAK in pink, HTAK in blue, MeTAK in red and BrTAK in purple. Lines are given as a guide to the eye.

In the case of tBuTAK, demixions appear whatever the methanol/water system (Figure III - 12). The solubility of the tBuTAk was thus impossible to measure. In this condition, it seems to be difficult to perform deracemisation with this compound in this solvent.

Figure III - 12. Demixion of tBuTAK in a 65/35 methanol/water mixture.

2. Thermal anaylses

The melting points of the racemic composition of these derivatives were determined by differential scanning calorimetry (DSC) and are summarized below.

	ClTAK **Cl-17**	HTAK **H-17**	MeTAK **Me-17**	BrTAK **Br-17**	tBuTAK **tBu-17**
T_{melt} (°C)	126.1	71.2	104.1	139.3	47.3
M ($g.mol^{-1}$)	291.8	257.3	271.4	336.2	313.4

Table III - 2. Melting points of TAK derivatives by DSC analyses.

TAK derivatives with a high molecular mass had a higher melting point that was not surprising. Once again, the tBuTAK exhibited a different behaviour from the other derivatives; its melting point was much lower than the other one whereas its molecular mass was higher.

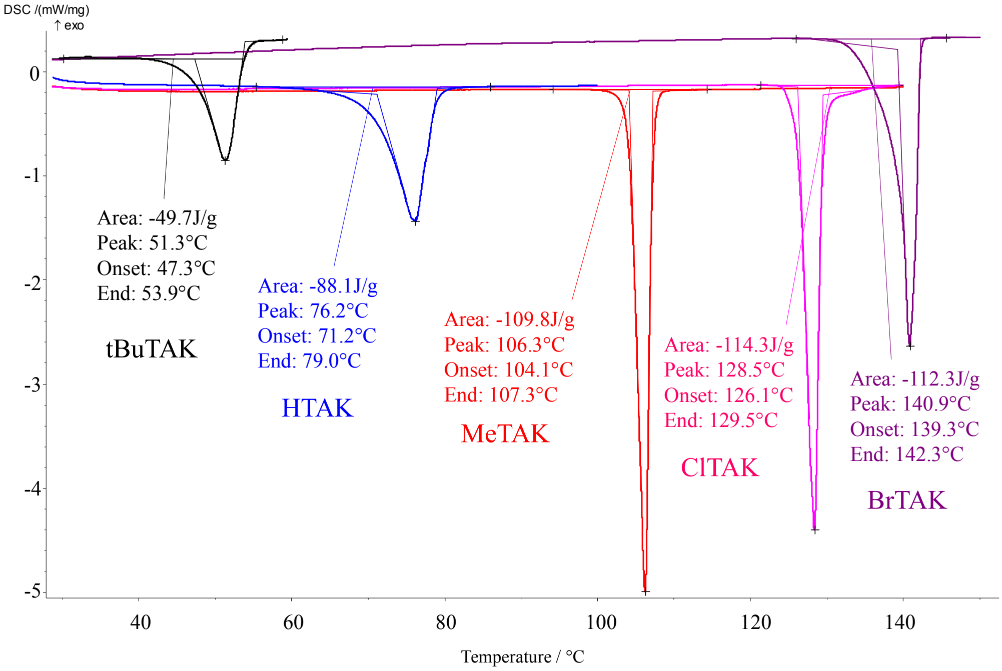

Figure III - 13. DCS analyses of the five racemic composition of TAK derivatives.

3. X ray powder diffraction (XRPD)

The five TAKs were analysed by X ray diffraction on powder and were compared. Figure III - 14 exhibits the superimposition of the five patterns.

XRPD patterns of ClTAK, MeTAK and BrTAK were very similar. This result suggested that these three TAKs were isomorphous. As ClTAK crystallised in the chiral space group $P2_12_12_1$, it was likely that MeTAK and BrTAK also crystallised in the $P2_12_12_1$ space group, corresponding to the conglomerate. Moreover, these compounds must be easily racemised in the same conditions as that used for ClTAK (the chiral centre should not be greatly affected by the nature of the substituent), thus MeTAK and BrTAK could probably be deracemised.

The XRPD patterns of HTAK and tBuTAK were different to the other ones. They must crystallise in a different crystal packing and so, it was impossible to predict if they crystallised as a conglomerate or not.

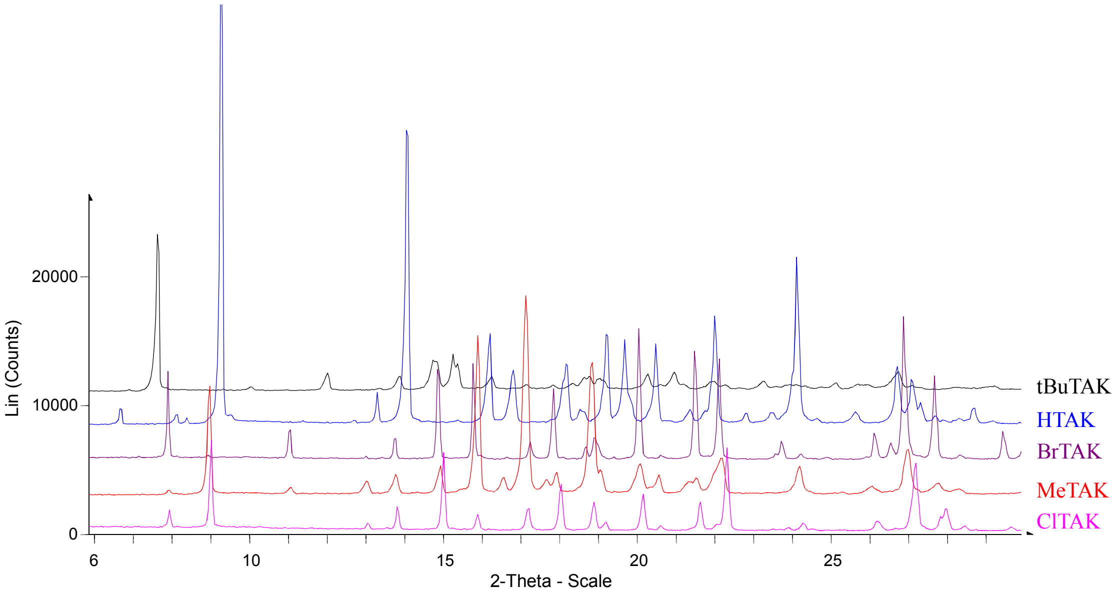

Figure III - 14. XRPD analyses of the five TAK derivatives.

4. Conclusion

Because of the high similarity between their XRPD patterns, MeTAK and BrTAK were likely to crystallise in the same space group than ClTAK: $P2_12_12_1$. Thus, they should be deracemisable. Of course, these hypotheses will be checked by using other methods such as resolution on single crystals (see paragraph IV) and by completing deracemisation (see paragraph V)

IV- Structural studies

1. Structural resolution of 1-(4-chlorophenyl)-4,4-dimethyl-2-(1H-1,2,4-triazol-1-yl)pentan-3-one ClTAK

The structure of ClTAK was already resolved by Black *et al.* in 1989.[176] The calculated diffractogram was compared to our experimental XRPD and they match perfectly.

However, for MeTAK and BrTAK, the tBu group exhibits a statistical disorder (see the following paragraphs). In the Black's resolution, this disorder was not mentioned. So, a new resolution of the structure was carried out to determine if this disorder was inexistent or simply not detected.

a. Crystallisation from racemic mixture

First, crystallisations were carried out from the racemic mixture of ClTAK. Unfortunately, whatever the system of crystallisation (solvents, temperature, supersaturation) rod particles appears and no single crystals were observed. This compound was known to crystallise with epitaxy, making difficult the formation of single crystals.

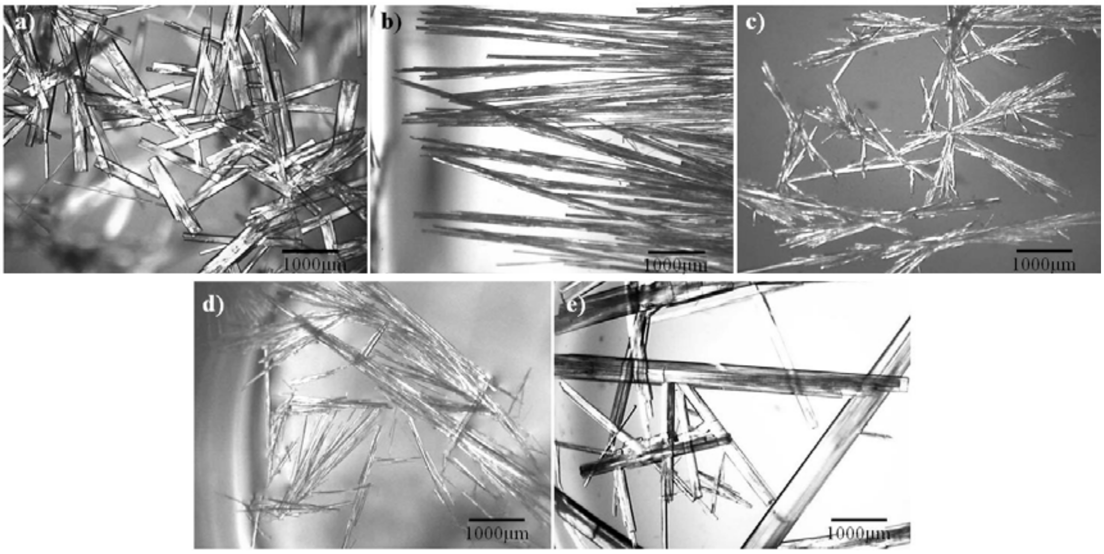

Figure III - 15. Crystals of ClTAK obtained from saturated solution in a) acetonitrile from 40°C to RT, b) ethanol at RT, c) MeOH at RT, d) MeOH/water 50/50 from 50°C to 20°C for 15h, e) MeOH/water 75/25 from 50°C to 20°C for 15h.

During the crystallisation experiments with a high initial surpersaturation, a layer of solid was formed, preventing the evaporation of solvent, decreasing the growth rate. After few days at room temperature (hereafter RT), the crystals were observed by optical microscopy. No single crystals were seen but large crystals with hourglass defects and hollow crystals were observed.[177]

---

[176] S. N. Black, L. J. Williams, R. J. Davey, F. Moffat, D. M. McEwan, D. E. Sadler, R. Docherty, D. J. Williams; *J. Phys. Chem.*, **1990**, 3223-3226.

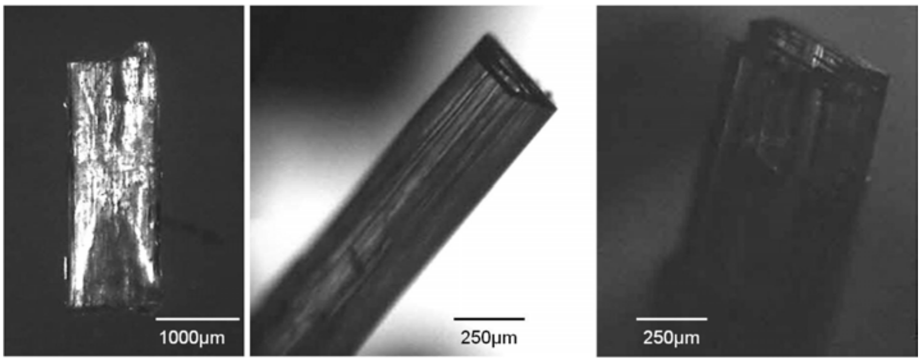

Figure III - 16. Crystal with macroscopic hourglass defects and hollow crystals.

b. Crystallisation from pure enantiomer

As ClTAK crystallised as a conglomerate, the racemic solid was just composed of crystals of the pure enantiomers. Crystallisation from pure enantiomer could prevent the epitaxial growth, making easier the formation of single crystals.

Suspensions of ClTAK in different systems of solvent were prepared at given temperatures (25°C or 35°C). The saturated liquid phase was taken, filtered then put at room temperature. After few days, crystals appeared. The results are summarized below. In a methanol/water mixture at 25°C, single crystals with sufficient size and quality were obtained.

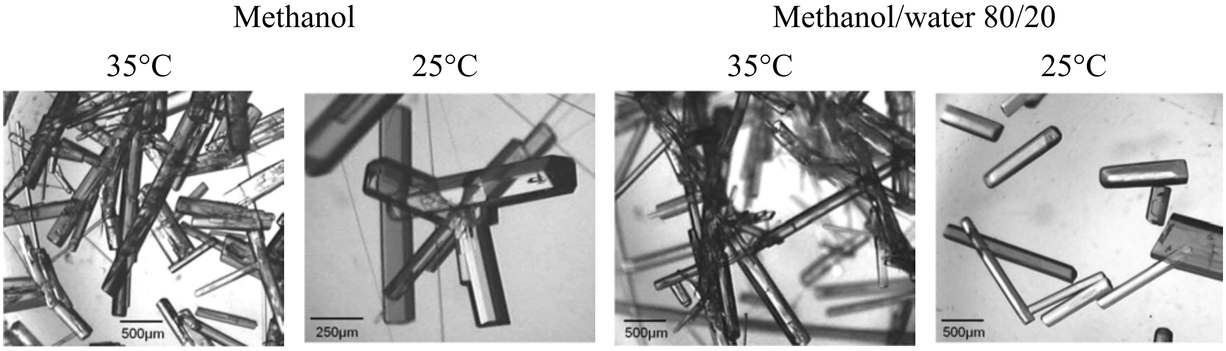
Methanol
Methanol/water 80/20
35°C
25°C
35°C
25°C

Figure III - 17. Crystals obtained from the pure enantiomer of ClTAK.

c. Structure

The resolution of the structure had been performed and the main crystal data are given in Table III - 3.

---

[177] C. Gervais, S. Beilles, P. Cardinael, S. Petit, G. Coquerel; *J. Phys. Chem. B*, **2002**, 106 (3), 646-652.

	Our data	Black's data[176]
Chemical Formula	$C_{15}H_{18}ClN_3O$	$C_{15}H_{18}ClN_3O$
Molecular Weight / *g.mol^{-1}*	291.77	291.77
Crystal System	Orthorhombic	Orthorhombic
Space group	$P2_12_12_1$	$P2_12_12_1$
Z , Z' (asymmetric units per unit cell)	4, 1	4,1
a / *Å*	5.8076(5)	5.799(1)
b / *Å*	19.661(2)	19.654(3)
c / *Å*	13.553(1)	13.552(2)
V / *Å^3*	1547.5(2)	1545
R factor (with I>2σI)	R1 = 0.0367 wR2 = 0.0871	R1 = 0.049 wR2 = 0.057
d_{calc} / *g.cm^{-3}*	1.252	1.25

Table III - 3. Crystal data of ClTAK

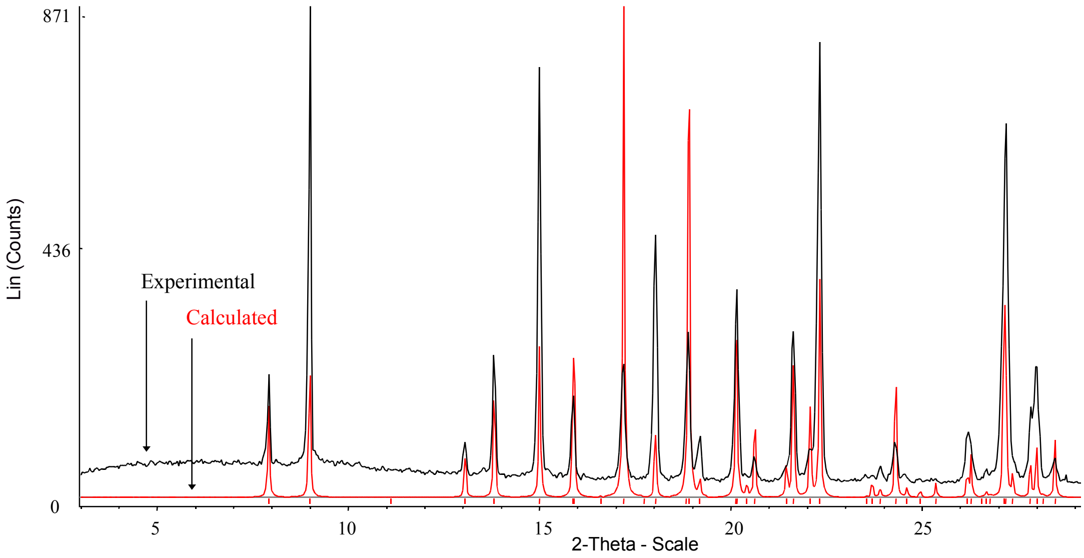

Figure III - 18. Superimposition of calculated (red) and experimental (black) XRPD patterns of ClTAK.

As expected, our results were very close to those obtained by Black *et al.* But, by looking closely the residual densities around the tertbutyl group, we noticed that two positions existed for this group. The tertbutyl extremity was split into two positions within statistical occupancy factors of 78% and 22% (Figure III - 19). Next pictures will be drawn with the most probable conformation.

When the structure was solved by taking into account the two positions of the tertbutyl group, the R1 value dropped down from 5.0% to 3.7%, and the residual electronic density from 0.306/-0.192$e^-.Å^{-3}$ to 0.123/-0.135 $e^-.Å^{-3}$. Indeed, the quite good R1 factor of 5.0% might have been sufficient; however the three highest residual electronic densities (~$0.3e^-.Å^{-3}$) were located between the atoms of carbon of the tertbutyl moiety and displayed a tertbutyl-like arrangement, so they were included in the structure solution as partial tertbutyl moiety, and led to the final R1 of 3.7%.

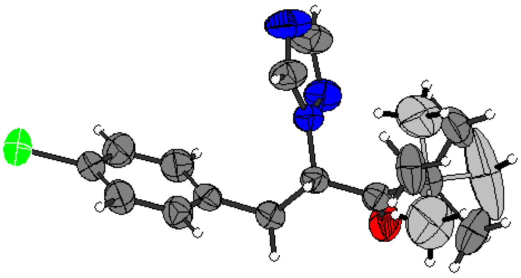

Figure III - 19. Asymmetric unit of ClTAK, in ellipsoid thermal representation (50% of probability). The two positions of the tBu are represented in grey (sof: 78%) and light grey (sof: 22%).

2. Structural resolution of 4,4-dimethyl-1-phenyl-2-(1H-1,2,4-triazol-1-yl)pentan-3-one HTAK

a. Crystallisation from pure enantiomer

First crystallisation experiments were carried out from the racemic mixture of HTAK but no single crystals were obtained; rod crystals appeared whatever the system of crystallisation but they were not suitable for structure resolution. Whereas when the crystallisations tests were performed from the pure enantiomer of HTAK, single crystals with a sufficient size and quality were easily obtained (Figure III - 20).

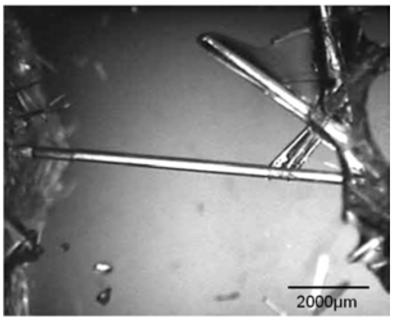

Figure III - 20. Single crystals of HTAK.

b. Structure

The resolution of a single crystal obtained from the pure enantiomer had been performed and the main crystal data are given in Table III - 4.

	HTAK
Chemical formula	$C_{15}H_{19}N_3O$
Molecular Weight / *g.mol^{-1}*	257.33
Crystal System	Monoclinic
Space group	$P2_1$ (n°4)
Z , Z' (asymmetric units per unit cell)	4, 2
a / *Å*	5.747(1)
b / *Å*	19.183(1)
c / *Å*	13.437(1)
β	96.561(1)
V / *Å^3*	1471.8(2)
R factor (with $I>2\sigma I$)	R1 = 0.0623 wR2 = 0.1142
d_{calc} / *g.cm^{-3}*	1.161

Table III - 4. Crystal data of HTAK.

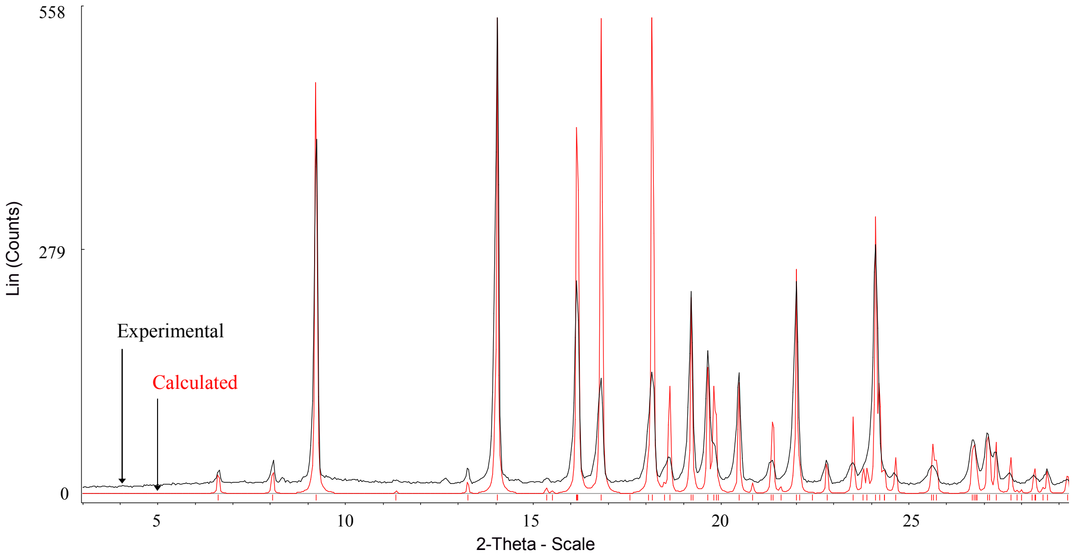

Figure III - 21. Superimposition of calculated (red) and experimental (black) XRPD patterns of HTAK.

HTAK crystallised in a chiral space group, $P2_1$. The asymmetric unit (Figure III - 22) was composed of two molecules and no disorder was observed with the tertbutyl group. In fact one molecule of the asymmetric unit differed to the other one mainly by the position of the tertbutyl group as shown on Figure III - 23, mimicking a 50/50 disorder.

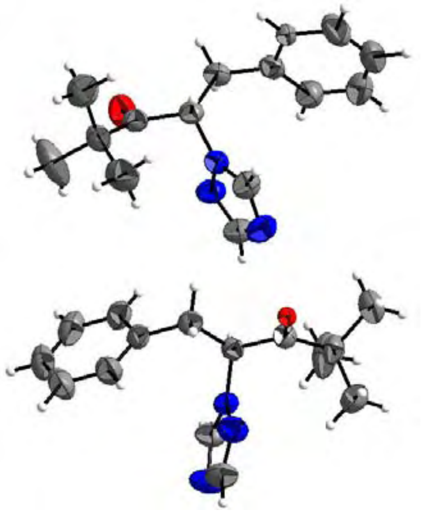

Figure III - 22. Asymmetric unit of HTAK, in ellipsoid thermal representation (50% of probability).

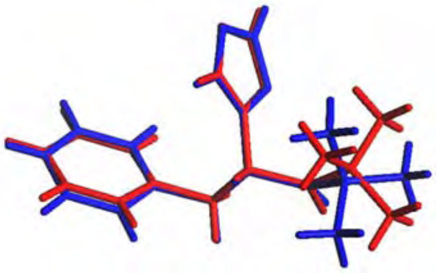

Figure III - 23. Superimposition of the two molecules of the asymmetric unit.

3. Structural resolution of 4,4-dimethyl-1-(p-toluyl)-2-(1H-1,2,4-triazol-1-yl)pentan-3-one MeTAK

a. Crystallisation from racemic mixture

Single crystals of the MeTAK were the easiest to obtain. Indeed, even if MeTAK crystallised as rod crystals in almost all the solvents used, this compound had the particularity to crystallise with a different morphology in acetonitrile. (Figure III - 24). Comparison between XRPD patterns confirmed that the same phase was present in each solvent (Figure III - 25), and therefore that only the morphology of crystals was different.

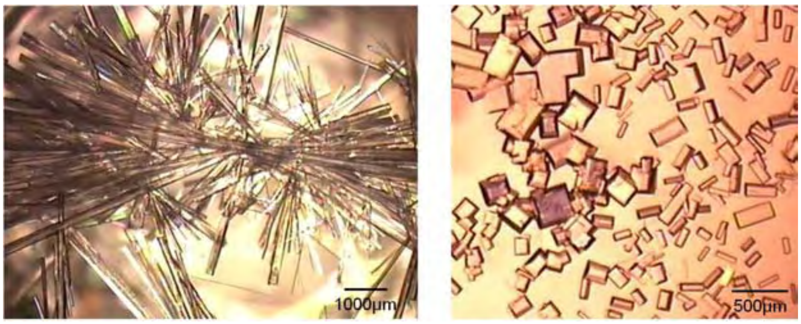

Figure III - 24. Crystals of MeTAK in MeOH/water 75/25 from 50°C to RT (left) and in acetonitrile from 50°C to RT (right).

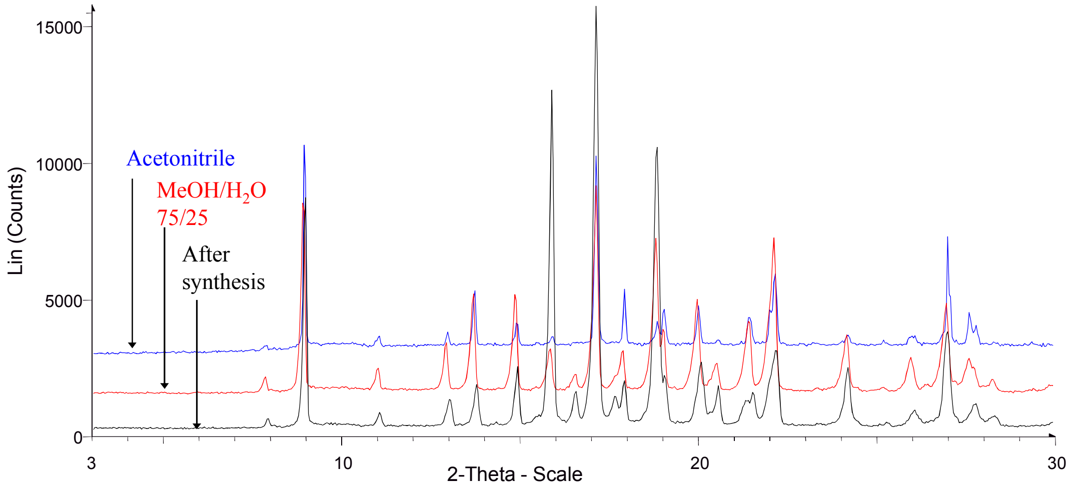

Figure III - 25. XRPD analyses of MeTAK in three different solvents.

During the crystallisation experiments in methanol/water mixture with a high supersaturation, crystals with hourglass defects and hollow crystals were observed.

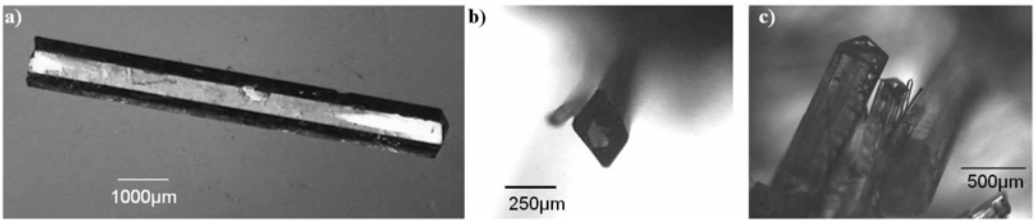

Figure III - 26. Crystal with hourglass defects and hollow crystals obtained from the racemic mixture in 8/2 methanol/water. a) from 30°C to RT, b) and c) slow evaporation of a saturated solution at RT.

b. Structure

In acetonitrile, single crystals with a sufficient size and quality were obtained. The resolution of the structure had been made. The main crystal data are given in Table III - 5.

	MeTAK
Chemical Formula	$C_{16}H_{21}N_3O$
Molecular Weight / *g.mol^{-1}*	271.36
Crystal System	Orthorhombic
Space group	$P2_12_12_1$
Z , Z' (asymmetric units per unit cell)	4, 1
a / *Å*	5.808(1)
b / *Å*	13.641(1)
c / *Å*	19.789(1)
V / *Å^3*	1567.9(2)
R factor (with I>2σI)	R1 = 0.0483 wR2 = 0.0938
d_{calc} / *g.cm^{-3}*	1.150

Table III - 5. Crystal data of MeTAK.

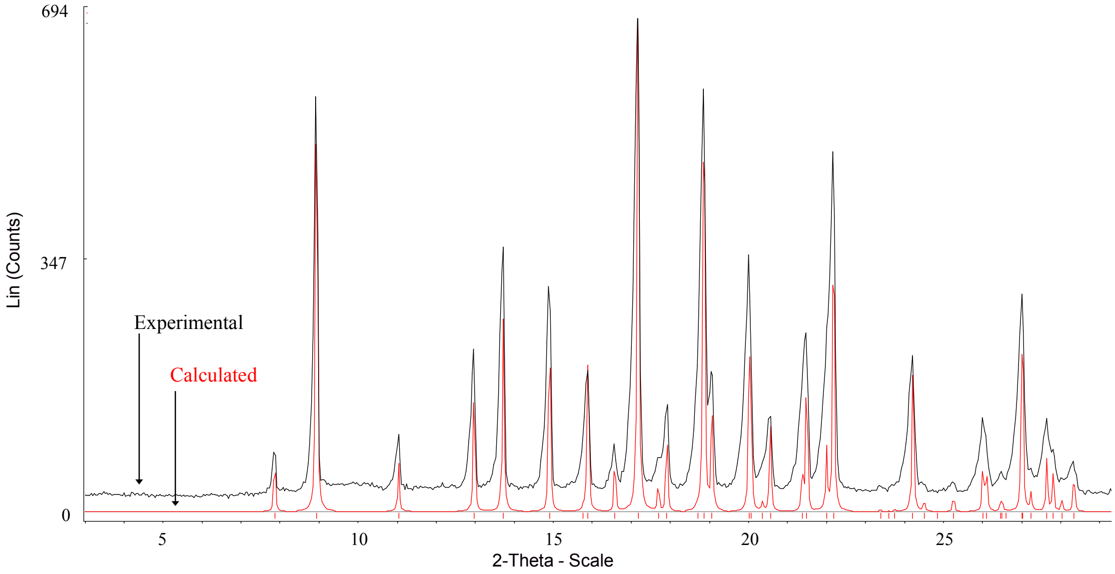

Figure III - 27. Superimposition of calculated (red) and experimental (black) XRPD patterns of MeTAK.

The structural data confirmed that XRPD patterns had predicted: MeTAK crystallised in the $P2_12_12_1$ space group with similar cell parameters than ClTAK. The asymmetric unit was also built from one molecule and the tertbutyl was split into two positions within statistical occupancy factors of 69% and 31%.

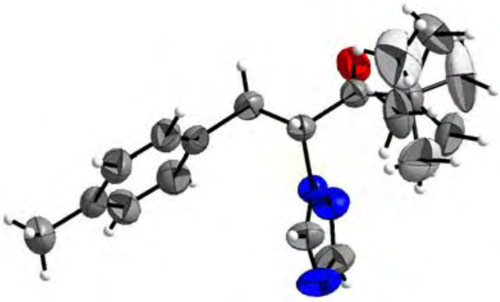

Figure III - 28. Asymmetric unit of MeTAK, in ellipsoid thermal representation (50% of probability). The two positions of the tertbuthyl are represented in grey (sof: 69%) and light grey (sof: 31%).

4. Structural resolution of 1-(4-bromophenyl)-4,4-dimethyl-2-(1H-1,2,4-triazol-1-yl)pentan-3-one BrTAK

a. Crystallisation from racemic mixture

As in the other cases, crystals obtained from the racemic mixture crystallised as needles and did not exhibit a sufficient quality to resolve the structure (Figure III - 29).

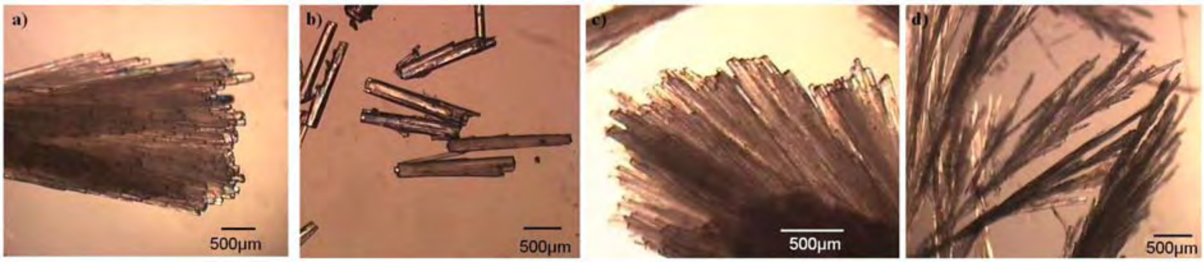

Figure III - 29. Crystals of BrTAK obtained in a) acetone from 40°C to RT for 4h, b) acetone form 40°C to RT, c) methanol from 40°C to RT, d) methanol/water 75/25 from 40°C to RT for 4h.

b. Crystallisation from pure enantiomer

Suspensions of BrTAK in methanol and methanol/water mixture were prepared at 25°C. The saturated liquid phase was taken, filtered then left at room temperature. After few days, crystals appeared (Figure III - 30).

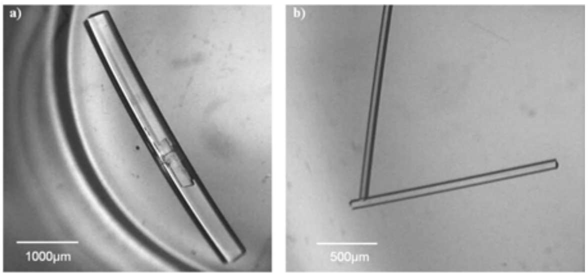

Figure III - 30. Crystals of BrTAK obtained from the pure enantiomer, from 25°C to RT in a) methanol b) methanol/water 80/20.

c. Structure

Single crystals with a sufficient size and quality were obtained in the methanol/water mixture. The resolution of the structure has been made. The main crystal data are given in Table III - 6.

	BrTAK
Chemical Formula	$C_{15}H_{18}BrN_3O$
Molecular Weight / *g.mol^{-1}*	336.23
Crystal System	Orthorhombic
Space Group	$P2_12_12_1$
Z , Z' (asymmetric units per unit cell)	4, 1
a / *Å*	5.7875(5)
b / *Å*	13.629(1)
c / *Å*	19.882(2)
V / *Å^3*	1568.3(2)
R factor (with I>2σI)	R1 = 0.0544 wR2 = 0.0913
d_{calc} / *g.cm^{-3}*	1.424

Table III - 6. Crystal data of BrTAK.

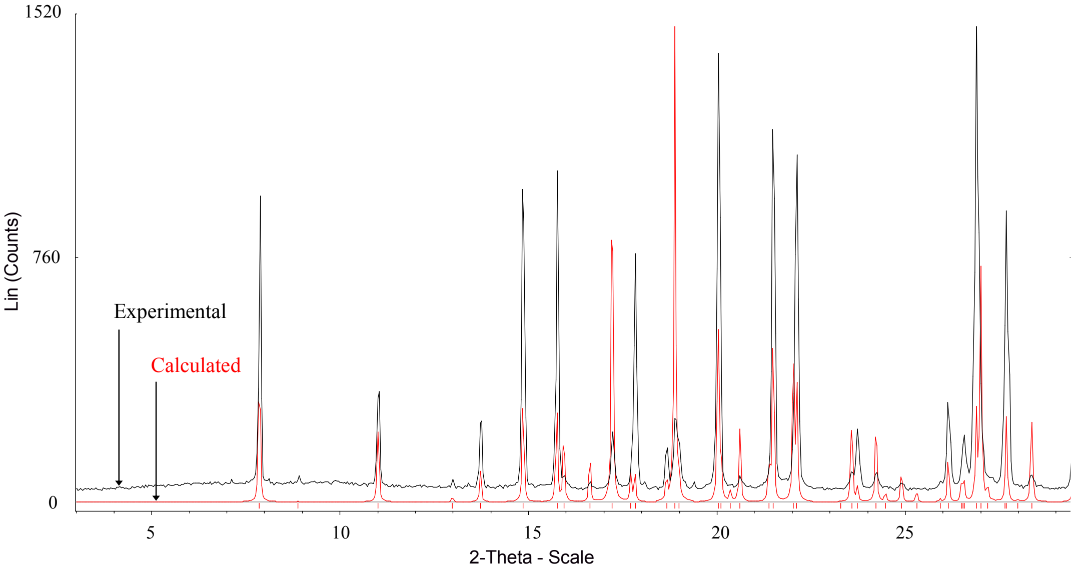

Figure III - 31. Superimposition of calculated (red) and experimental (black) XRPD patterns of BrTAK.

As for the MeTAK derivative, the structural data confirmed what XRPD patterns led to predict: BrTAK crystallised in the $P2_12_12_1$ space group with similar cell parameters as ClTAK and MeTAK. The asymmetric unit was also built from one molecule and the tertbutyl was split into two positions within statistical occupancy factors of 68% and 32%.

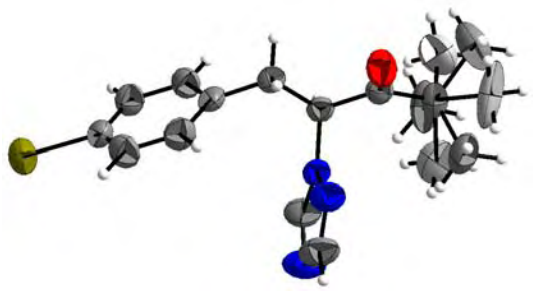

Figure III - 32. Asymmetric unit of BrTAK, in ellipsoid thermal representation (50% of probability). The two positions of the tertbuthyl are represented in grey (sof: 68%) and light grey (sof: 32%).

5. Case of 1-(4-tert-butylphenyl)-4,4-dimethyl-2-(1H-1,2,4-triazol-1-yl) pentan-3-one tBuTAK

Crystallisations of tBuTAK were tested in several solvents. In methanol/water mixtures, demixion appeared (Figure III - 12). In solvents such as CH_2Cl_2 or ethyl acetate, the evaporation of solvent led to the formation of an oil which became crystalline few days after. Therefore no single crystals were obtained.

Moreover, as this compound had no signal in SHG and as no solid-solid transitions are observed in DSC at low temperature (that is to say: no possibility to have a conglomerate at low temperature), attempts to obtain single crystals were stopped.

The difficulty to crystallise tBuTAK can be due to disorders of the two tertbutyl groups, instead of only one tertbutyl group, making its crystallisation more difficult.

6. Comparison between the different crystal packings

a. Comparison between ClTAK, MeTAK and BrTAK

In the previous paragraphs, we had already highlighted that ClTAK, MeTAK and BrTAK crystallise in the same space group. The crystallographic data were brought together in the following table; cell parameters of these three molecules were very close and confirmed the high similarity observed with the XRPD patterns.

	ClTAK	MeTAK	BrTAK
Chemical Formula	$C_{15}H_{18}ClN_3O$	$C_{16}H_{21}N_3O$	$C_{15}H_{18}BrN_3O$
Molecular Weight / *g.mol⁻¹*	291.77	271.36	336.23
Crystal System	Orthorhombic	Orthorhombic	Orthorhombic
Space group	$P2_12_12_1$	$P2_12_12_1$	$P2_12_12_1$
Z , Z' (asymmetric units per unit cell)	4, 1	4, 1	4, 1
a / *Å*	5.8076(5)	5.808(1)	5.7875(5)
b / *Å*	13.553(1)	13.641(1)	13.629(1)
c / *Å*	19.661(2)	19.789(1)	19.882(2)
V / $Å^3$	1547.5(2)	1567.9(2)	1568.3(2)
d_{calc} / $g.cm^{-3}$	1.252	1.150	1.424

Table III - 7. Cell parameters of ClTAK, MeTAK and BrTAK.

Then the crystal packing of the three TAK derivatives were compared.

First, we can observe that the asymmetric units are almost superimposable (Figure III - 33); the three structures are isomorphous.

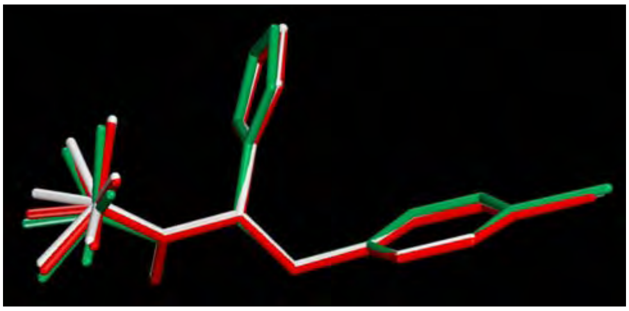

Figure III - 33. Superimposition of the asymmetric units. ClTAK in white, MeTAK in red and BrTAK in green.

Secondly, we can see that in each case, the aromatic rings are interacting with their adjacent equivalents along *b* axis by means of π interactions in T shape, generating infinite chains of molecules in [100] direction (Figure III - 34 and Figure III - 35). The angle between two consecutive aromatic rings involved into the interaction is circa 60°. The distance between two consecutive rings is 3.9Å. The cohesion between chains is ensured through Van der Waals interactions.

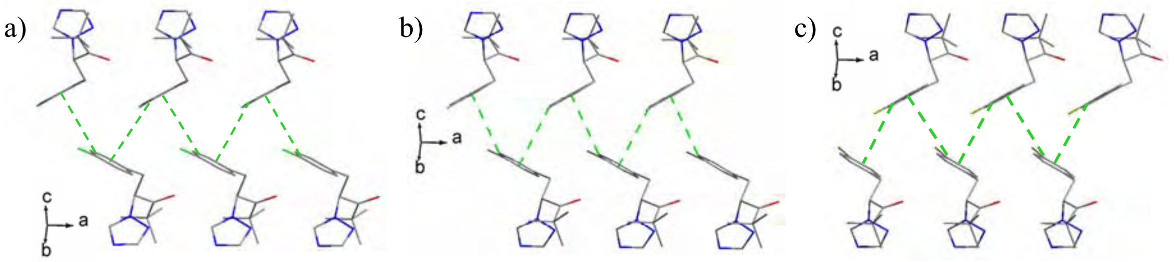

Figure III - 34. π stacking in T shape (dashed green lines). a) ClTAK, b) MeTAK, c) BrTAK.

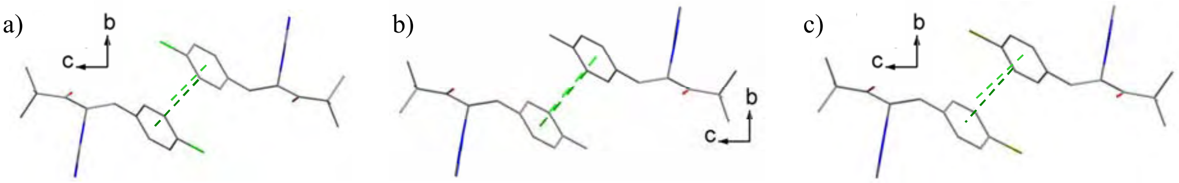

Figure III - 35. The interactions in T-shape generate double chains that are spreading along the [100] direction. a) ClTAK, b) MeTAK, c) BrTAK.

The chains are stacked along *c* and give rise to slices (blue and red).

However, we can notice that the representation of these three packing is not exactly identical; the cell edges are shifted from a compound to another. These shifts are only due to the choice of the origin during the resolution of the structure and not to a different packing. By translating the cell edges of MeTAK with a *c*/2 vector and the cell edges of BrTAK with a *b*/2+*c*/2, the origin of these crystal packings will be the same than for ClTAK.

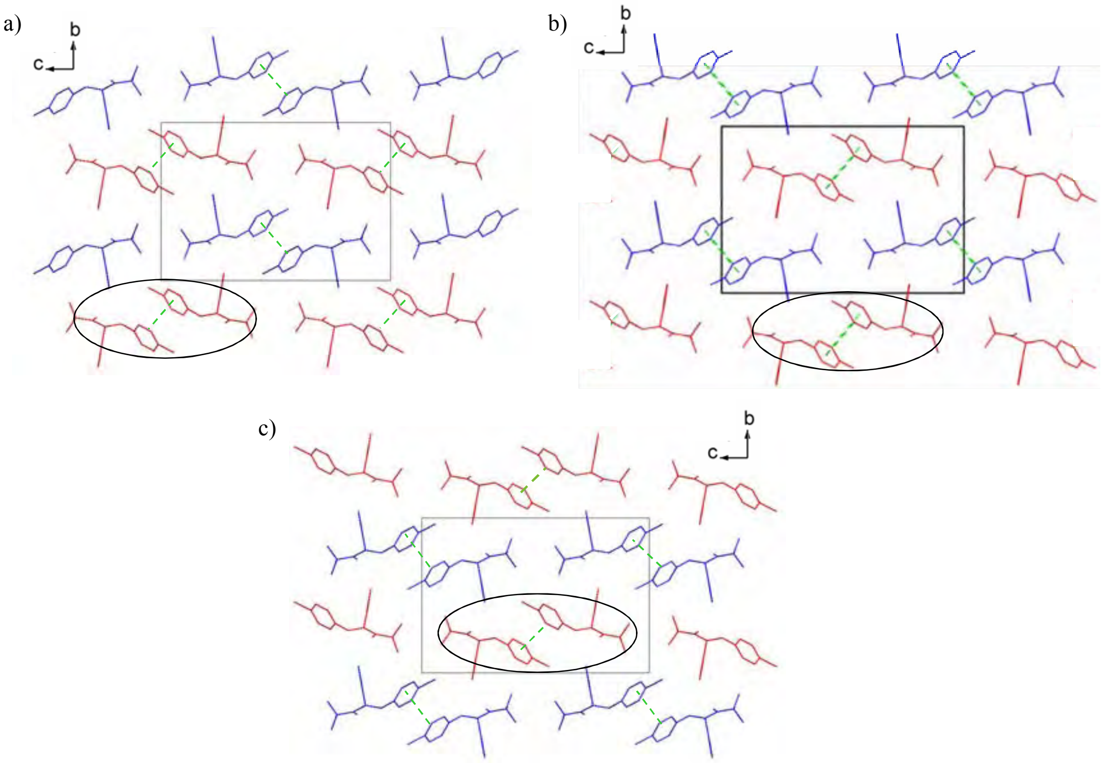

Figure III - 36. Projections along *a* axis. a) ClTAK, b) MeTAK, c) BrTAK. One chain is circled in black.

Figure III - 37 exhibits projections along *b* axis of the three TAK derivatives and Figure III - 38 exhibits projections along *c* axis. Infinite chains of molecules, created by π interactions in T shape, are clearly visible on these pictures (one chain in red, the other one in blue).

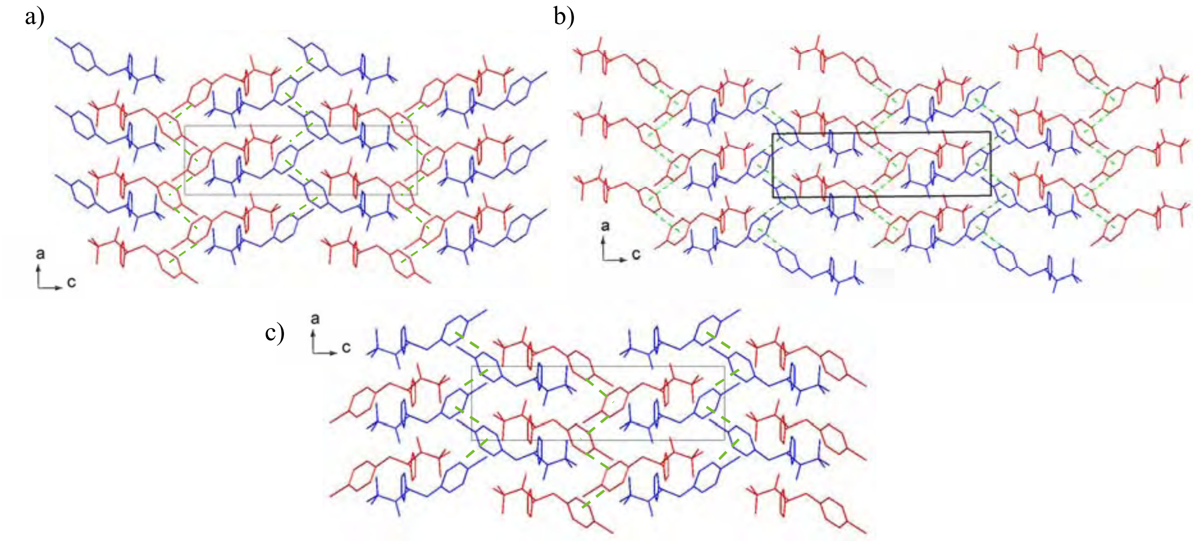

Figure III - 37. Projections along *b* axis. a) ClTAK, b) MeTAK, c) BrTAK.

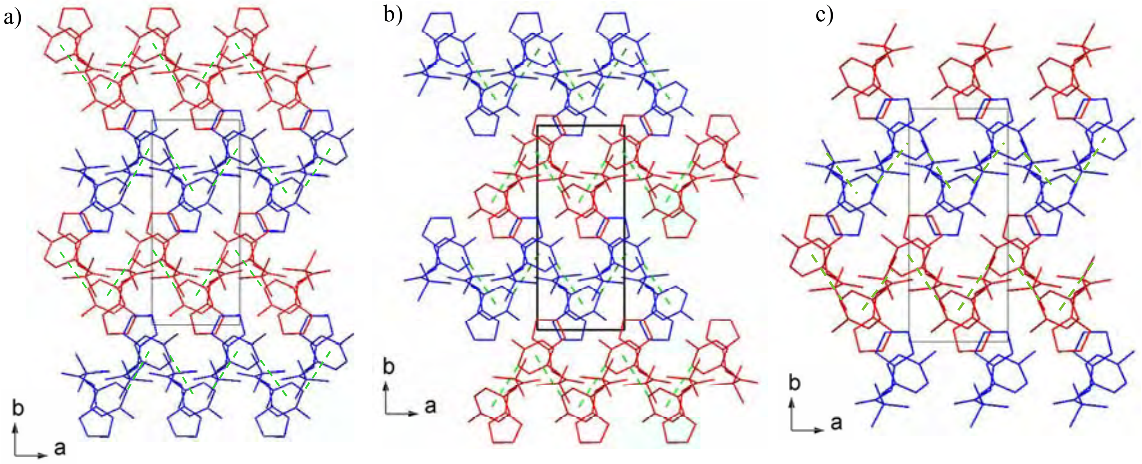

Figure III - 38. Projections along *c* axis. a) ClTAK, b) MeTAK, c) BrTAK.

Another common point between these compounds is the disorder induced by the tertbutyl group; in the three cases, two positions exist for this group with statistical occupancy factor of circa 70% and 30%. However, the structure resolution at room temperature did not give information about the nature of this disorder: is it a statistical disorder or a dynamical disorder? If it is a dynamical disorder, a decreasing of the temperature could stop the rotation of the tertbutyl group. If such phenomenon occurs, it should be visible by DSC analysis. DSC analyses of ClTAK, MeTAK and BrTAK were therefore carried out at low temperature (Figure III - 39); in each case, a slight endothermic phenomenon occurs at circa -30°C, which is probably due to the “freeze” of the tertbutyl group. The reversibility of this phenomenon (a slight exothermic phenomenon exists at circa -30°C when the temperature increased) confirmed this hypothesis.

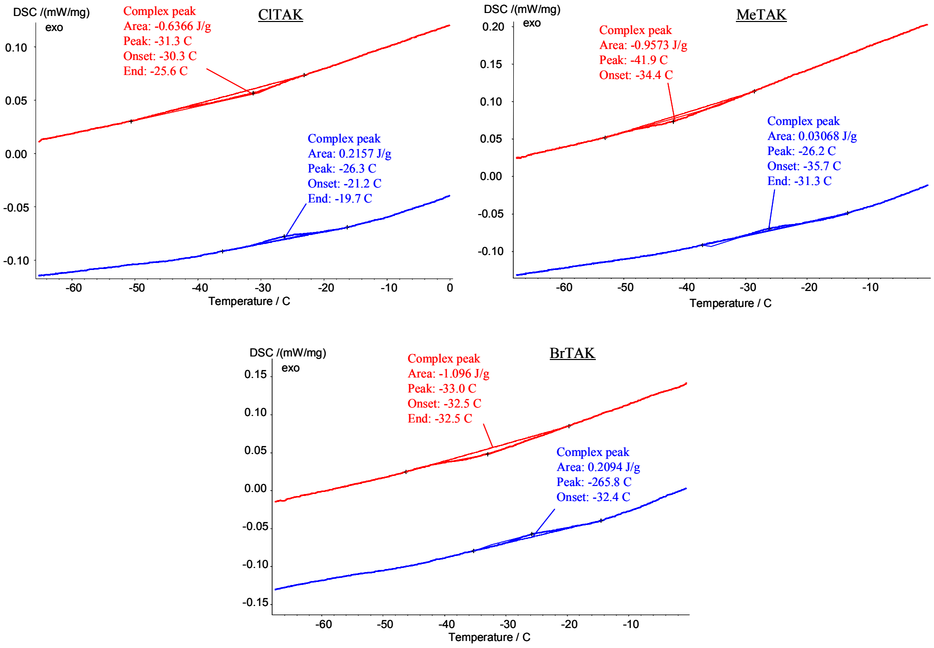

Figure III - 39. DSC analysis at low temperature of ClTAK, MeTAK and BrTAK. Heating rate: 5K.min^{-1}.

b. Comparision between the crystal packings of HTAK and ClTAK

HTAK crystallises in a different crystal packing than the other TAK derivatives since it crystallises in the monoclinic $P2_1$ space group and not in the orthorhombic $P2_12_12_1$ space group. Moreover, the asymmetric unit is composed of two molecules of HTAK. However, some similarities can be observed.

We demonstrated in the previous paragraph that the structures of ClTAK, MeTAK and BrTAK were isomorphous therefore similarities between HTAK and the other TAKs will be only described from ClTAK.

First, the crystal data are compared (Table III - 8). In the two cases, the unit cell is composed of four molecules and the cell parameters are very close. The parameters *b* and *c* are inverted but it is due to a convention; in the monoclinic system, the angle which is different from 90° is the β angle and the cell parameters *a*, *b* and *c* are given according to this angle.

	HTAK	**ClTAK**
Chemical Formula	$C_{15}H_{19}N_3O$	$C_{15}H_{18}ClN_3O$
Molecular Weight / g.mol^{-1}	257.33	291.77
Crystal System	Monoclinic	Orthorhombic
Space group	$P2_1$ (n°4)	$P2_12_12_1$
Z , Z’ (asymmetric units per unit cell)	4, 2	4, 1
a / Å	5.747(1)	5.8076(5)
b / Å	19.183(1)	13.553(1)
c / Å	13.437(1)	19.661(2)
β	96.561(1)	-
V / Å^3	1471.8(2)	1547.5(2)
d_{calc} / g.cm^{-3}	1.161	1.252

Table III - 8. Crystal data of HTAK and ClTAK.

Cohesion of molecules in the crystal packing is also ensured by means of π interactions in T shape, generating infinite chains of molecules in [100] direction. The angle between two consecutive aromatic rings involved into the interaction is circa 60°. The distance between two consecutive rings is 3.9Å. π interactions link together the asymmetric units.

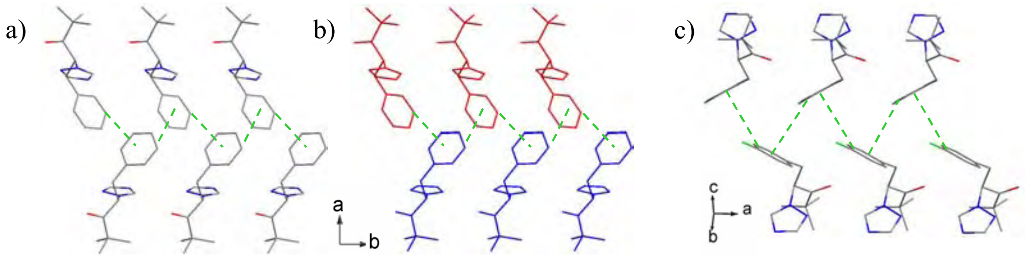

Figure III - 40. π stacking in T shape (dashed green lines). a) HTAK, b) HTAK with colour differentiation of the asymmetric units, c) ClTAK.

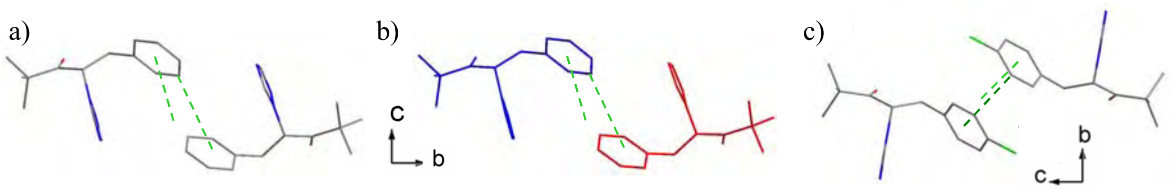

Figure III - 41. The interactions in T-shape generate double chains that are spreading along the [100] direction. a) HTAK, b) HTAK with colour differentiation of the asymmetric units, c) ClTAK.

However, the chains are not identical: the triazol moieties are at the endo position for HTAK whereas they are at the exo position for ClTAK.

Projections along *a* axes give another proof of the similarity existing between the crystal structures of HTAK and ClTAK; the chains are stacked along *b* direction (*c* for ClTAK). Along *c* (*b* for ClTAK), these slices are shifted by ½$\vec{c}$ vector (or ½$\vec{b}$ vector).

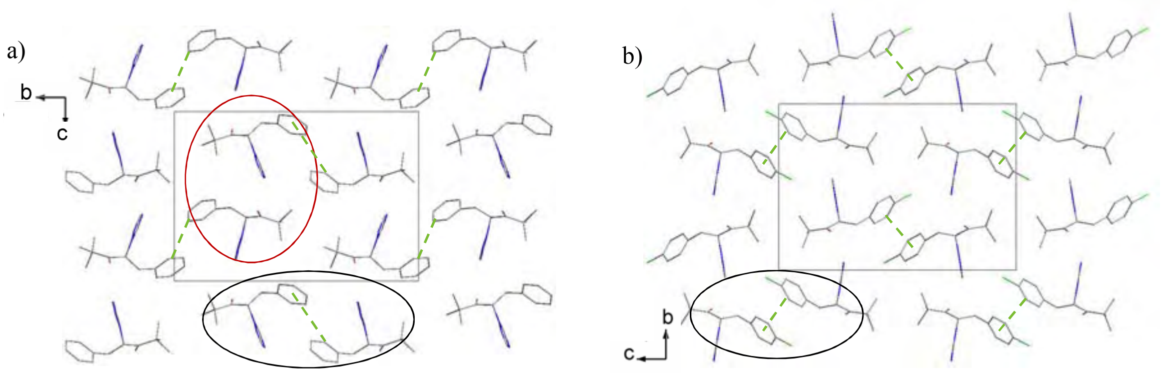

Figure III - 42. Projections along *a* axis a) HTAK, one asymmetric unit is circled in red and one chain is circled in black, b) ClTAK, one chain is circled in black.

Projection along *c* axis of HTAK is also similar to the projection along *b* axis of ClTAK; infinite chains of molecules are clearly visible on these pictures.

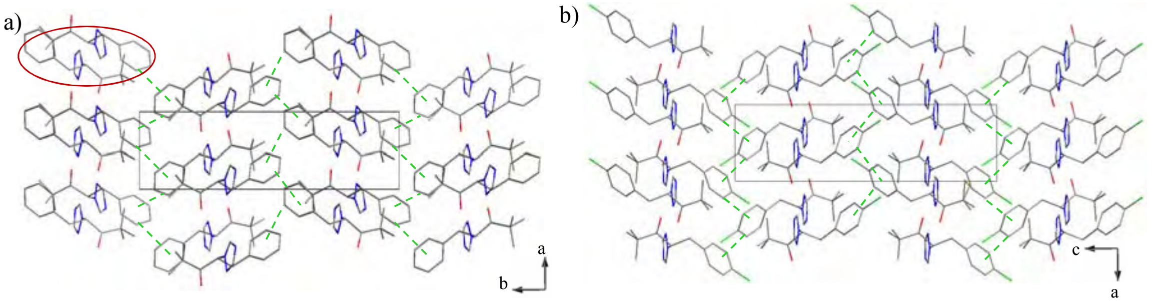

Figure III - 43. Projections along a) *c* axis for HTAK, one asymmetric unit is circled in red and b) *b* axis for ClTAK.

c. Comparision between the crystal packings of 2F-4ClTAK and MeTAK

The crystal structure of another TAK derivative, the 2F-4ClTAK (Figure III - 44), was described in the literature.[173] This compound also crystallised in the $P2_12_12_1$ space group with very close cell parameters (Table III - 9). The comparison will be made between MeTAK and 2F-4ClTAK.

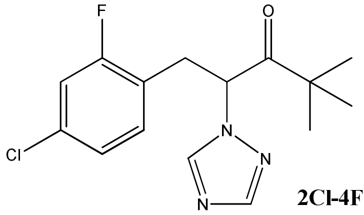
2Cl-4FTAK

Figure III - 44. Chemical structure of 2F-4ClTAK.

	MeTAK	2F-4ClTAK[173]
Chemical Formula	$C_{16}H_{21}N_3O$	$C_{15}H_{17}ClFN_3O$
Molecular Weight / g.mol^{-1}	271.36	309.77
Crystal System	Orthorhombic	Orthorhombic
Space group	$P2_12_12_1$	$P2_12_12_1$
Z , Z' (asymmetric units per unit cell)	4, 1	4, 1
a / *Å*	5.808(1)	5.777(3)
b / *Å*	13.641(1)	13.699(6)
c / *Å*	19.789(1)	19.813(8)
V / *Å*^{3}	1567.9(2)	1567.9(1)

Table III - 9. Crystal data of MeTAK and 2Cl-4FTAK.

The superimposition of these two structures reveals that they both exhibit the same packing: the aromatic rings are interacting with their adjacent equivalents along *b* axis, and by means of π interactions in T shape (Figure III - 45), generate infinite chains of molecules in [100] direction.

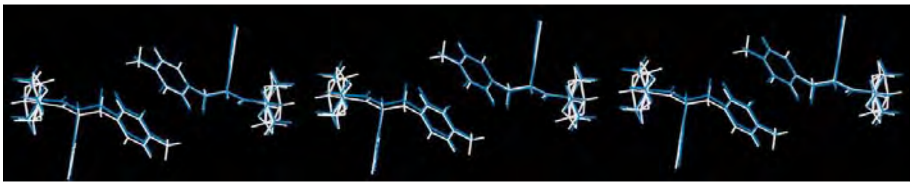

Figure III - 45. Superimposition of a slice, 2F-4ClTAK in blue and MeTAK in white.

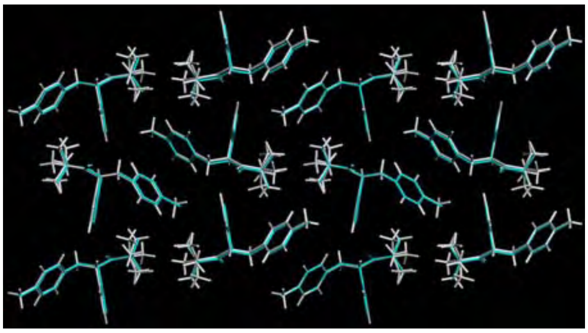

Figure III - 46. Superimposition of projections along *a* axis. 2F-4ClTAK in blue and MeTAK in white.

No disorder was described for the tertbutyl group. However, as it was the case for the first resolution of the structure of ClTAK, it is possible that Branch and Nowell missed the disorder, the quality of the single crystal being maybe not sufficient.

7. Conclusion

The resolution of structures has confirmed what have been predicted from comparisons between XRPD patterns: ClTAK, MeTAK and BrTAK crystallise in the same crystal packing, the non centrosymmetric space group $P2_12_12_1$, with a dynamic disorder of the tertbutyl group. A fourth compound, the 2F-4ClTAK, also exhibits the same structure. The substitution of the aromatic ring of this series of molecules seems to have some degrees of freedom. These compounds behave as if a kind of pocket exists around the aromatic ring in which we can change substituents without changing the crystal packing.

However, the size of this pocket seems to be limited: if the substituent is too large, as it is probably the case for the tBuTAK, another packing becomes more stable.

In the case of HTAK (i.e. without substituent on the aromatic ring) the crystal packing is different, $P2_1$, but it shows extensive similarities with the $P2_12_12_1$ structures. No disorder of the terbutyl group was detected but the two molecules of the asymmetric unit differ mainly by the position of the tertbutyl group, mimicking a 50/50 disorder.

We can also imagine that acid or basic subtituents, or substituents with a strong electronic effect (CF_3, NO_2, OMe…), can prevent the formation of this kind of structure.

It should be interesting to study the crystallisation of other compounds within this series to find the limit of this pocket.

V - Viedma ripening on TAK derivatives

1. Deracemisation of 1-(4-chlorophenyl)-4,4-dimethyl-2-(1H-1,2,4-triazol-1-yl)pentan-3-one ClTAK

Even if the resolution of this compound was already described, the access to the pure enantiomer from the racemic suspension had never been studied. Therefore, the deracemisation of ClTAK was studied at constant temperature to evidence that ClTAK exhibited the same Viedma ripening than the other compounds described in the literature (i.e. an autocatalytic deviation from the 50-50 mixture).

a. Experimental conditions

The experimental conditions described here were applied to all TAK derivatives, except for the solvent. The ratio of methanol and water had to be adjusted for each compound in order to keep similar masses of TAKs in the liquid and in the solid phase. The composition of the solvent was chosen according to the solubility data (Table III - 1) and is given in weight fraction.

It should be noted that the enantiomeric excess of the starting material was checked before its partial dissolution. Therefore, any small imbalance would be increased by the dissolution of the racemic mixture. The first point of each experiment should not be taken in account for the shape of kinetics. Furthermore, all the points are connected together by a line but this line does not represent the real kinetic of the deracemisation.

A suspension of ClTAK was prepared by adding 1g of ClTAK and 5g of glass beads (Ø2mm) into 5g of an 80/20 methanol/water mixture at 25°C. As the solubility of ClTAK at 25°C is 5.5%, 0.29g of ClTAK was dissolved and 0.71g of ClTAK remained as solid phase in the suspension. Sodium hydroxide (0.1g) was added then the suspension was vigorously stirred by using a cross magnetic stirrer.

All along the experiment, samples were taken with a plastic pipette, immediately filtered, washed with a large amount of water to remove all traces of sodium hydroxide then dried overnight at 40°C.

The evolution of the enantiomeric excess was monitored by chiral HPLC. The column was a Chiralcel OD and the eluent was a 95/5 heptane/ethanol mixture at 1.5mL/min. The retentions times of the two enantiomers were at circa 8.3 and 10 minutes (Figure III - 47).

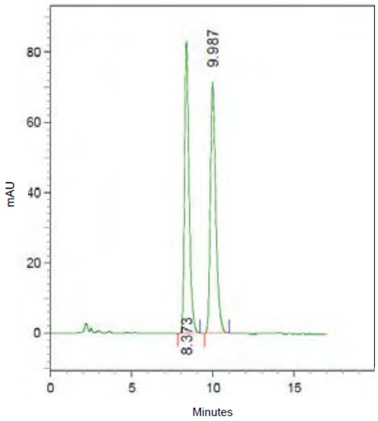

Figure III - 47. Chromatogram of the racemic ClTAK.

b. Results

The results of the first experiment are summarized in Figure III - 48. These graphics show that around five days were necessary to complete the deracemisation of ClTAK in these conditions. Furthermore, ClTAK seems to have exactly the same behaviour than the other compounds described in the literature: the enantiomeric excess exponentially evolves toward the high values (Figure III - 48). The curve ln(e.e.)=f(t) is linear and the corresponding exponential trend line perfectly matches with the experimental points. However, the number of experimental values was not sufficient to have a good accuracy. Therefore, other experiments were carried out, with more sampling, to confirm the exponential evolution of the enantiomeric excess.

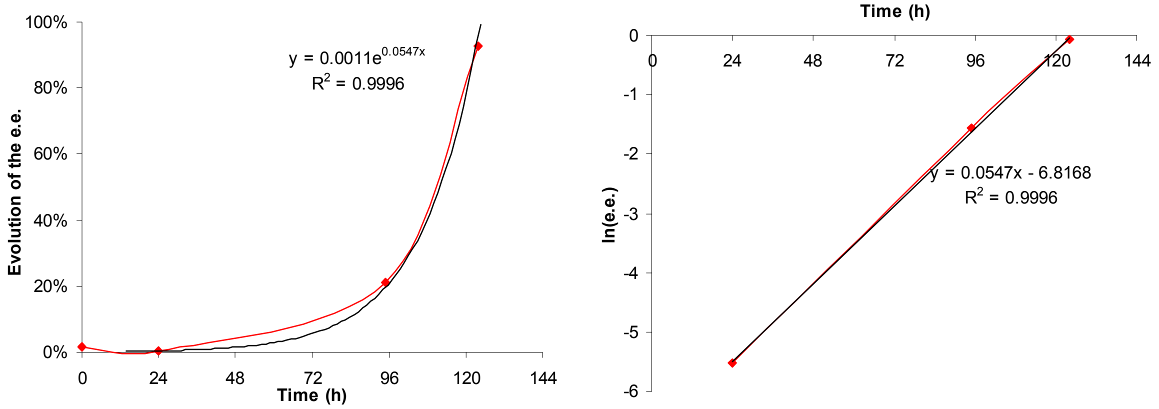

Figure III - 48. Evolution of the enantiomeric excess versus time (left) and ln(e.e.) versus time (right). In black, the exponential trend line (left) and the corresponding linear trend line (right). Red lines are given as a guide to the eyes.

The achievement of the deracemisation points out the absence of impact of epitaxy. Indeed, in classical preferential crystallisation, epitaxial growth is a limiting factor, the counter enantiomer can grow from crystals of the seeded enantiomer. But it is not the case for deracemisation. Kaptein *et al.* previously described that the epitaxial growth does not disturb the deracemisation process, and it is also the case for ClTAK (Black *et al.* previously described the epitaxial crystallisation).[171]

Figure III - 49 shows another experiment, carried out in the same conditions than the first one, but with more sampling. When the e.e. of the solid is below 80%, the evolution of the e.e. is definitively exponential, as evidenced the representation of ln(e.e.) as a function of time. This experiment also highlighted the existence of a slowdown of the kinetics when the e.e. approached 100%. This phenomenon can easily be explained by i) the decreasing of the amount of the minor enantiomer to transform and ii) the increasing of the amount of the major enantiomer that increased its kinetics of racemisation. As the exponential kinetics, the slowdown was also described in the literature.[128]

But, this experiment highlighted a new phenomenon: the exponential evolution of the enantiomeric excess did not start as the same time as the stirring. After 50h, the enantiomeric excess was almost racemic, as if a threshold must be reached to make the process “irreversible”.

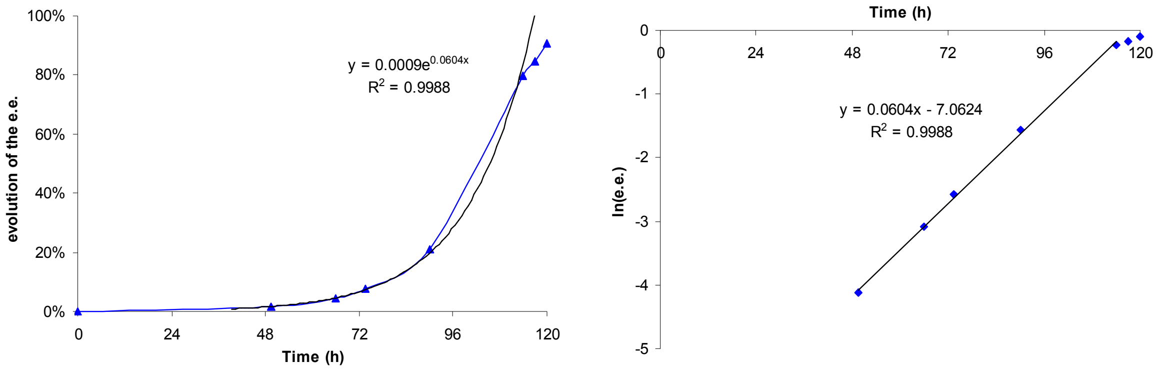

Figure III - 49. Evolution of the enantiomeric excess versus time (left) and ln(e.e.) versus time (right). In black, the exponential trend line (left) and the corresponding linear trend line (right). Blue line is given as a guide to the eyes.

In order to know if this latent period (i.e. the delay in the evolution of the enantiomeric excess) was due to an experimental problem (e.g. stirring) or due to the deracemisation process itself, another experiment was carried out and many samples were taken for 100h. The results are shown below.

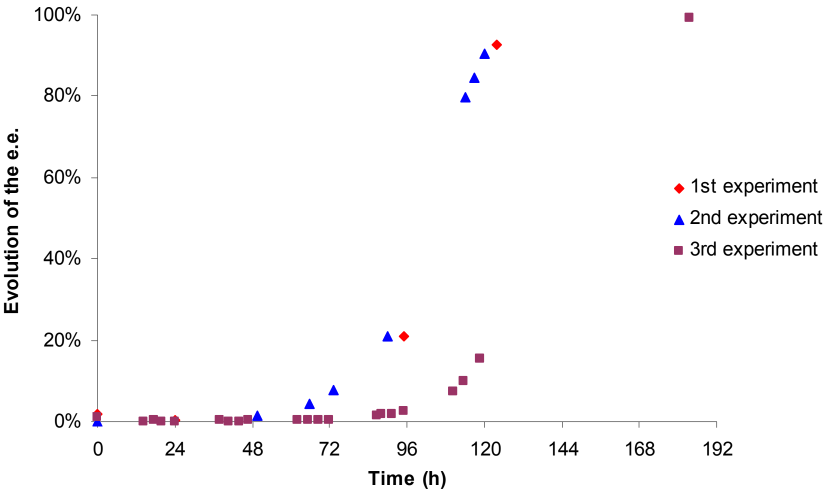

Figure III - 50. Comparison of the evolution of the enantiomeric excess for three experiments carried out in the same experimental conditions.

By looking at the evolution of the e.e., it is clear that the deracemisation process did not start as the same time as the stirring. The first and the second experiment were quite similar whereas the time to complete the deracemisation was much longer in the case of the third experiment; for the first 3 days, the enantiomeric excess stayed very close to 0%. Though, nothing was changed during all the experiments: the number of glass beads as well as the stirring rate and the temperature were kept constant.

It is known that without unbalanced initial e.e. or CDS,[128] the final chirality obtained after a deracemisation process is randomly distributed between the (+) and the (-) enantiomers. The "irreversible" evolution seems to have a certain threshold, below which the enantiomeric excess can go back toward the racemic composition. Contrary, once this threshold is overcome, the enantiomeric excess quickly evolves toward 100%.

Unfortunately, this threshold was difficult to estimate precisely. A first error is inherent in the HPLC method; the accuracy of the result is generally estimated at ±0.2%. The second error comes from the sample; around 0.5mg of TAK was dissolved in 1mL of eluent. As the compounds crystallise as conglomerates, it is possible that this 0.5mg was not representative of the whole sample.

2. Deracemisation of 4,4-dimethyl-1-phenyl-2-(1H-1,2,4-triazol-1-yl) pentan-3-one HTAK

a. Experimental conditions

The experimental conditions were similar as the ones used for ClTAK: 1g of HTAK for 5g of solvent (a mixture of 47% of methanol and 53% of water) and 5g of glass beads (Ø2mm) with 0.10g of NaOH at 25°C. Samples were prepared in the same way and the same chiral column was used. However, the eluent had to be changed: a 98/2 heptane/ethanol mixture was used. The retentions times of the two enantiomers were at circa 23 and 25.7 minutes.

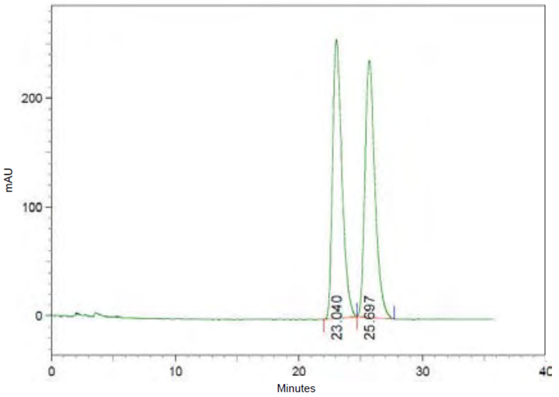

Figure III - 51. Chromatogram of the racemic HTAK.

b. Results

A first experiment was carried out to determine if the deracemisation was possible and therefore if the compound crystallised as a conglomerate or not (at this stage, the structure of HTAK was not resolved yet.) After twenty days, the enantiomeric excess of the solid was checked by chiral HPLC: only one peak was detected. The conversion of the racemic mixture toward the pure enantiomer was thus also possible with HTAK.

An additional experiment was carried out to monitor the kinetics of this deracemisation. The evolution of the enantiomeric excess is shown in Figure III - 52: the kinetics of deracemisation was exponential with a slow down when the e.e. is close to 100%. Moreover, the e.e. stayed close to 0% for the first three days; the latent seems to be a recurrent phenomenon.

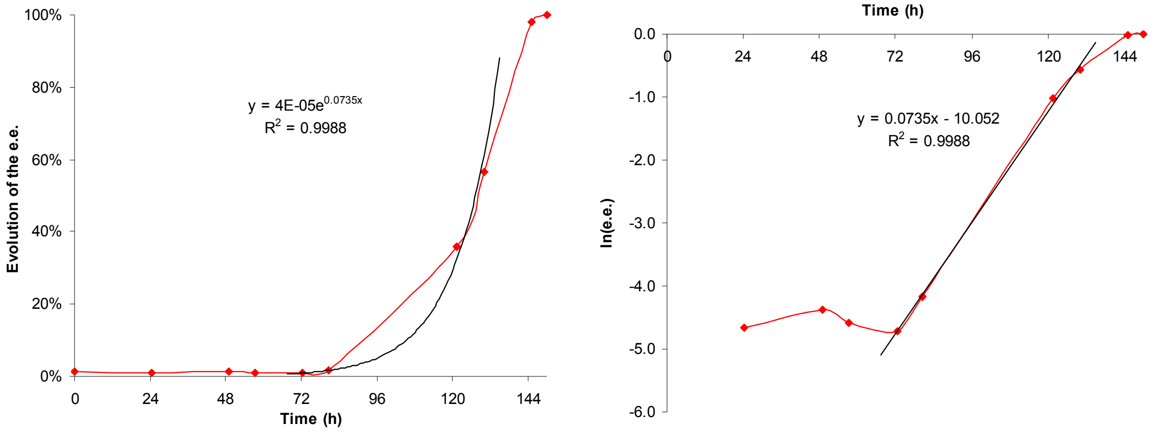

Figure III - 52. Evolution of the e.e. for the deracemisation of HTAK. In black, the exponential trend line (left) and the corresponding linear trend line (right). Red lines are given as a guide to the eyes.

3. Deracemisation of 4,4-dimethyl-1-(p-toluyl)-2-(1H-1,2,4-triazol-1-yl) pentan-3-one MeTAK

a. Experimental conditions

The experimental conditions were similar as the ones used for ClTAK: 1g of MeTAK for 5g of solvent (a mixture of 65% of methanol and 35% of water) and 5g of glass beads with 0.10g of NaOH at 25°C. Samples were prepared in the same way and the same chiral column was used as ClTAK. The retentions of time the two enantiomers are at circa 7.4 and 8.9 minutes, with a return to base line in-between (Figure III - 53).

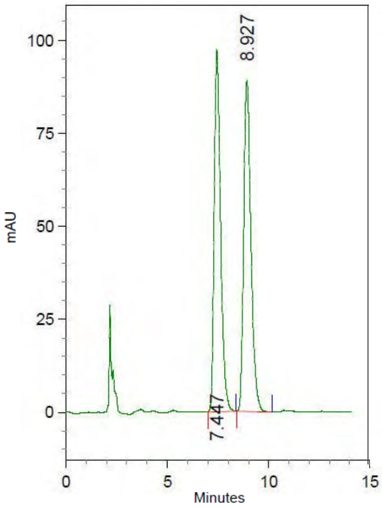

Figure III - 53. Chromatogram of racemic MeTAK.

b. Results

For MeTAK, the resolution of the structure was made before the deracemisation experiments so we knew that MeTAK crystallises as a conglomerate and so that the deracemisation should work. A first experiment was carried out to confirm this and, after 5 days, the enantiomeric excess was around 99%.

An additional experiment was carried out to monitor the evolution of the enantiomeric excess (Figure III - 54). The convertion was also exponential with a slow down when the e.e. reached high values.

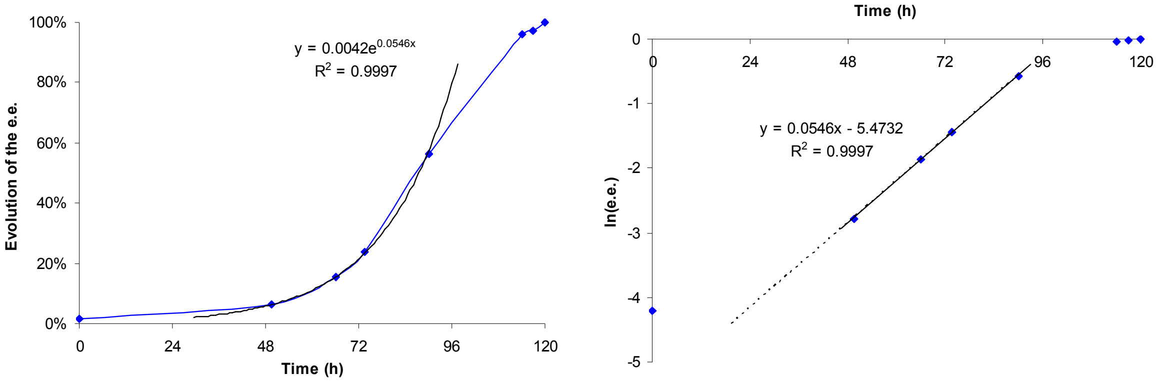

Figure III - 54. Evolution of the enantiomeric excess versus time (left) and ln(e.e.) over time (right). In black, the exponential trend line (left) and the corresponding linear trend line (right). Blue line is given as a guide to the eyes.

To compare kinetics of deracemisations of all TAK derivatives, we tried to keep the solubility constant for all the TAK derivatives. However, the solubility of MeTAK in the solvent used above (65/35 w/w methanol/water mixture) was 6.0% whereas the solubility of ClTAK for the deracemisation experiments (80/20 methanol water mixture) was 5.5%. So, the influence of the solubility of MeTAK was also studied. Two experiments were carried out in parallel, with the same experimental conditions (temperature, stirring rate…) except for the solvent: a 65/35 methanol/water mixture and a 60/40 methanol/water mixture were used.

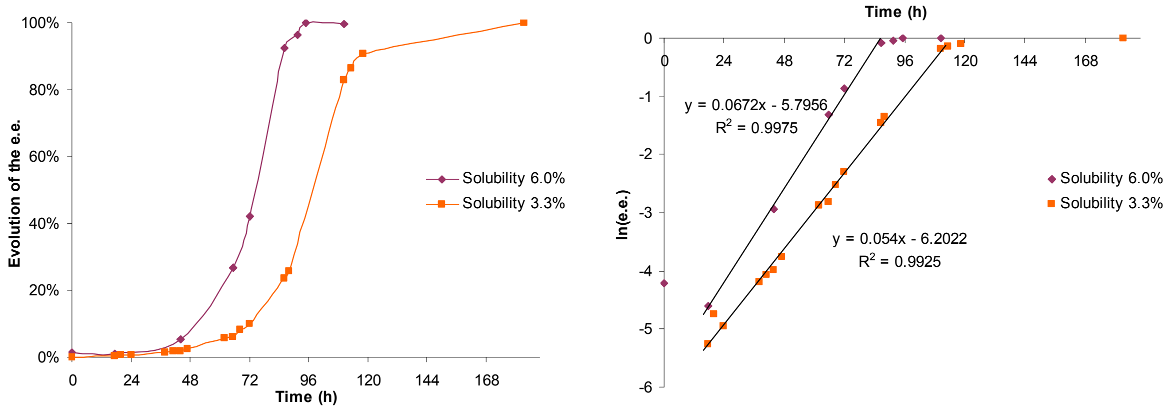

Figure III - 55. Influence of the solubilty of MeTAK on the kinetics of deracemisation depending on the solvent: 65/35 methanol/water mixture (purple) and 60/40 methanol water mixture (orange). Lines are **given as a guide to the eyes.**

As expected, a modification of the solubility did not influence the shape of the kinetics: both enantiomeric excess evolved exponentially toward 100%. But these experiments highlighted two facts: i) it was clear that the deracemisation did not start as the same time as the mechanical treatment, ii) the solubility had an influence on the deracemisation duration, probably because the amount of solid in suspension was higher when the solubility was lower (the same initial mass of MeTAK was used in both cases), iii) the solubility seemed to have an influence on the end of the process; the evolution of the enantiomeric excess seemed to slow down earlier when the solubility is lower.

However, the durations of these two deracemisations were not so different; experiments with 6.0% solubility can be used for the comparison with the other TAK derivatives.

4. Deracemisation of 1-(4-bromophenyl)-4,4-dimethyl-2-(1H-1,2,4-triazol-1-yl)pentan-3-one BrTAK

a. Experimental conditions

The experimental conditions were the similar as the ones used for ClTAK: 1g of BrTAK for 5g of solvent (a mixture of 90% of methanol and 10% of water) and 5g of glass beads (Ø2mm) with 0.10g of NaOH at 25°C. Samples were prepared in the same way and the same chiral column was used than for ClTAK. The retentions of time the two enantiomers are circa 8.3 and 10.4 minutes with a clear return to base line in-between (Figure III - 56).

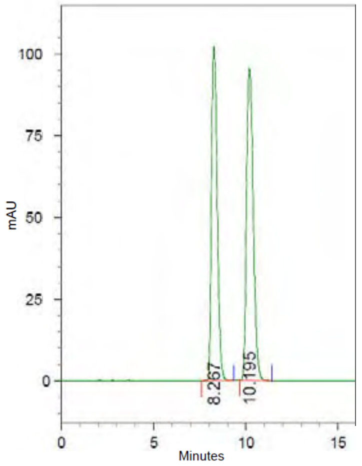

Figure III - 56. Chromatogram of racemic BrTAK.

b. Results

The first experiment carried out with BrTAK aimed at knowing if it crystallises as a stable conglomerate or not (at this stage, the structure of BrTAK was not resolved yet). The results of this first experiment are detailed below:

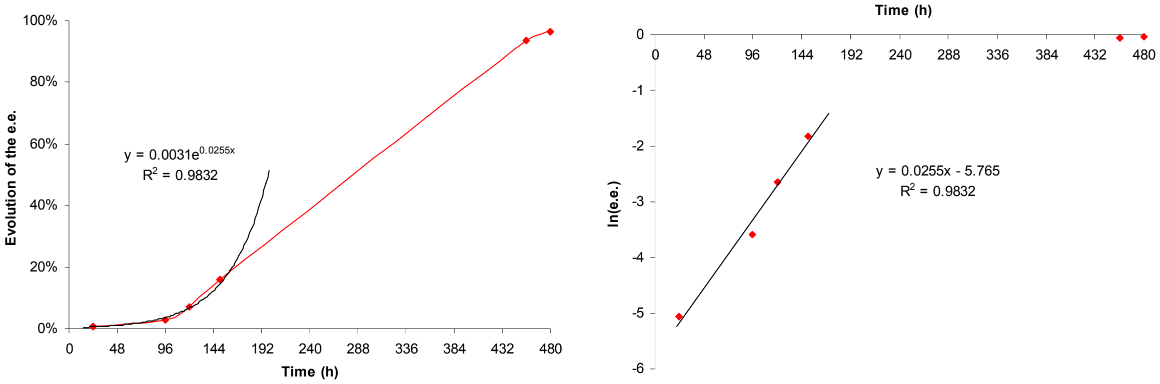

Figure III - 57. Evolution of the enantiomeric excess versus time (left) and ln(e.e.) over time (right). In black, the exponential trend line (left) and the corresponding linear trend line (right). Red line is given as a guide to the eyes.

This experiment had shown that the deracemisation was possible and therefore confirmed that BrTAK crystallised as a conglomerate. This preliminary result suggested that the deracemisation could take more time than for the other TAK derivatives. Therefore, another experiment was carried out, with more sampling (Figure III - 58).

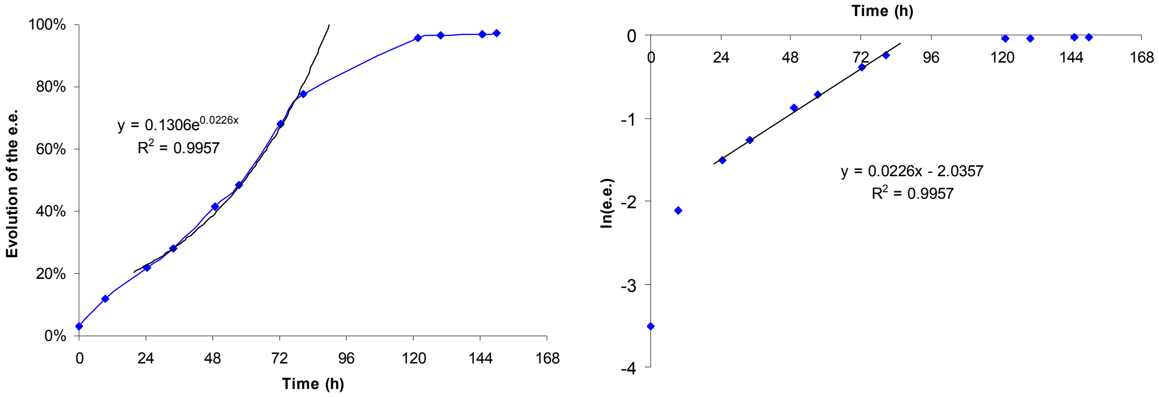

Figure III - 58. Evolution of the enantiomeric excess versus time (left) and ln(e.e.) over time (right). In black, the exponential trend line (left) and the corresponding linear trend line (right). Blue line is given as a guide to the eye.

Even if the shape of the kinetics was less visible than for the other compounds, the evolution of the enantiomeric excess was also exponential.

The process seemed to be slower than for the other TAK derivatives. This point will be discussed in the following paragraph where the kinetics of the deracemisation of the four TAKs will be compared.

5. Comparison between kinetics

The deracemisation of the four TAK derivatives, ClTAK, HTAK, MeTAK and BrTAK, were carried out with success. In all cases, the evolution of the enantiomeric excess was exponential, with a slow down when the e.e. approached 100%. To make easier the comparison between the kinetics, the origins of the deracemisation were shifted: the latent periods before the “irreversible” evolutions of the enantiomeric excess were removed (Figure III - 59).

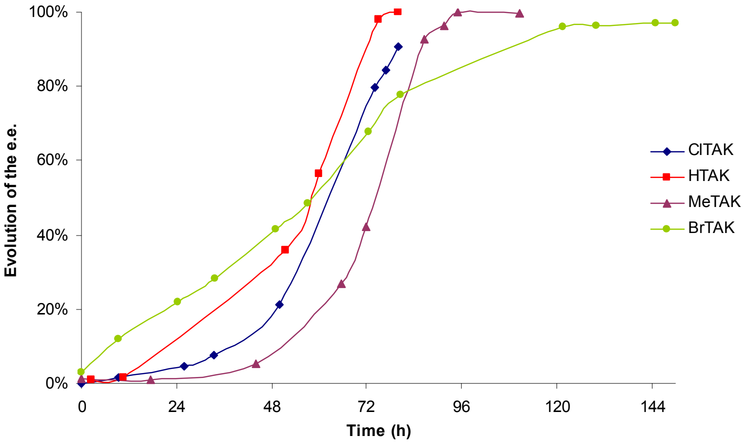

Figure III - 59. Comparison between the kinetics of deracemisation of ClTAK, HTAK, MeTAK and BrTAK. Lines are given as a guide to the eyes. The origins of the deracemisations were shifted to remove the latent period.

The shape of the evolution of the enantiomeric excess against time was very similar for ClTAK, HTAK and MeTAK; around three days were necessary to complete the total symmetry breaking and the autocatalytic shape of the curve was obvious. For BrTAK, more than five days were necessary to reach 100% e.e. and the autocatalytic shape of the kinetics was less visible. This behaviour iss also visible when the curves ln(e.e.) versus time are compared (Figure III - 60).

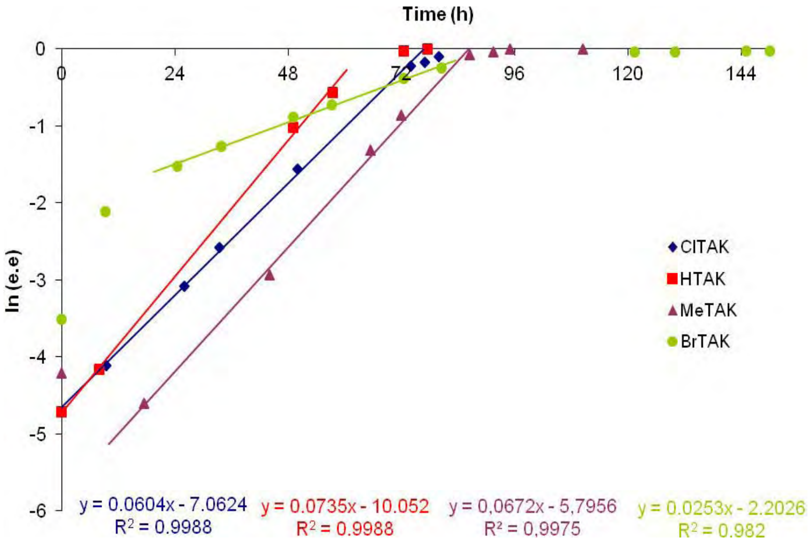

Figure III - 60. Comparison between the evolution of ln(e.e.) versus time for ClTAK, HTAK, MeTAK and BrTAK. Lines are given as a guide to the eyes.

The kinetics of deracemisation of ClTAK was a little bit slower than the deracemisations of MeTAK and HTAK. The difference with MeTAK can be explained by a difference of solubility. Indeed, it has been demonstrated that the solubility affects the kinetics of deracemisation (see paragraph V-3.b) and, in spite of the modifications of the solvent system, the solubilities of ClTAK and MeTAK derivatives were not absolutely identical (5.5% and 6.0% respectively). HTAK crystallised in a different crystal packing that can explain the differences observed between ClTAK and HTAK.

Nevertheless, neither the difference of solubility nor the crystal packing can explain the slowest evolution of the enantiomeric excess of BrTAK.

VI - Evolution of the crystal size distribution

One of the key steps of the mechanism of the deracemisation process seems to be the reduction of the size of crystals, increasing the transfer of matter.[128]

However, a very recent study, conducted by Hein *et al.*, described a new aspect of the deracemisation: "*a transient growth in crystal size*".[178] By monitoring the crystal size during deracemisation experiments, they noticed that "*a broadening of the distribution commenced at the onset of the evolution of the solid-phase CEE* (crystal enantiomeric excess) [...] *and endured through the ermergence of homochirality*".

In order to confirm these observations, the evolution of the CSD was monitored by scanning electron microscopy (SEM) for the four TAK derivatives. Crystal size distribution measurement by LASER diffraction could not be applied because the TAK derivatives are soluble in the solvent usually used for this analysis (n-heptane). Therefore water must be used but the dispersion of particles is not sufficient to perform accurate analyses. Moreover the harvested mass of each sample was not sufficient to perform this analysis.

1. 1-(4-chlorophenyl)-4,4-dimethyl-2-(1H-1,2,4-triazol-1-yl)pentan-3-one ClTAK

a. Starting material

First, the CSD of the starting material and the shape of crystals were observed by SEM (Figure III - 61). Initial powder of ClTAK was made of rod crystals with a scattered CSD; the lengths of particles were between 1µm and 200µm. The edges were clearly visible.

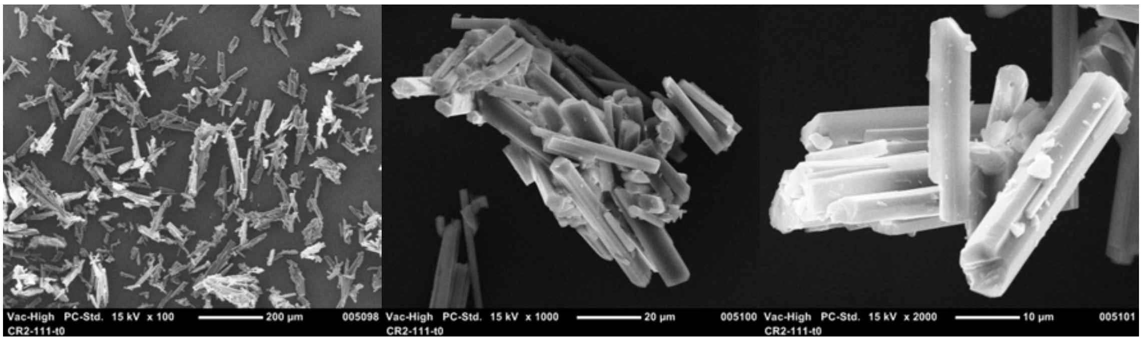
Vac-High PC-Std. 15 kV x 100 200 µm 005098
CR2-111-t0
Vac-High PC-Std. 15 kV x 1000 20 µm 005100
CR2-111-t0
Vac-High PC-Std. 15 kV x 2000 10 µm 005101
CR2-111-t0

Figure III - 61. SEM pictures of the starting material of ClTAK.

---

[178] J. E. Hein, B. H. Cao, C. Viedma, R. M. Kellogg, D. G. Blackmond; *J. Am. Chem. Soc.*, **2012**, 134, 12629-12636.

b. Evolution of the CSD

The evolution of the CSD was monitored by SEM; six samples were chosen depending on their e.e. and on the time of sampling:

- Two samples with e.e. ≈ 0%, during the latent period.
- Three samples during the increasing of the e.e. (exponential part).
- One sample when the deracemisation was complete.

These six samples are indicated by arrows on Figure III - 62.

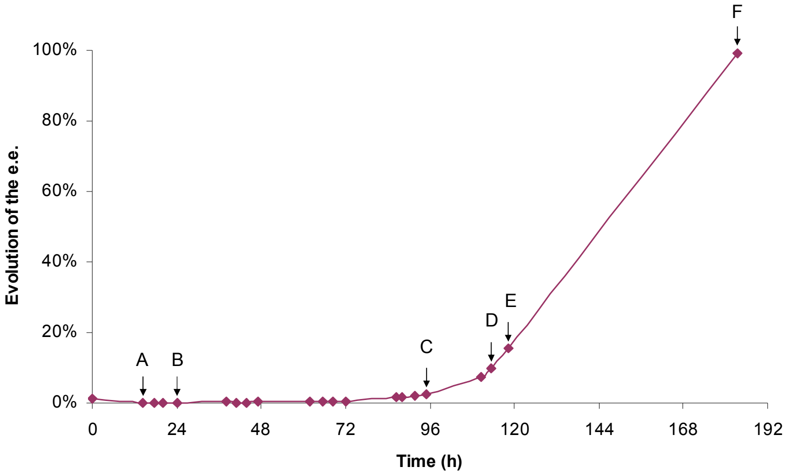

Figure III - 62. Evolution of the enantiomeric excess versus time during deracemisation with glass beads. Arrows indicate time of sampling for SEM pictures shown in Figure III - 63 and Figure III - 64. Line is given as a guide to the eyes.

SEM pictures of these six samples, at two different magnifications (x1000 and x5000, respectively Figure III - 63 and Figure III - 64) are presented below.

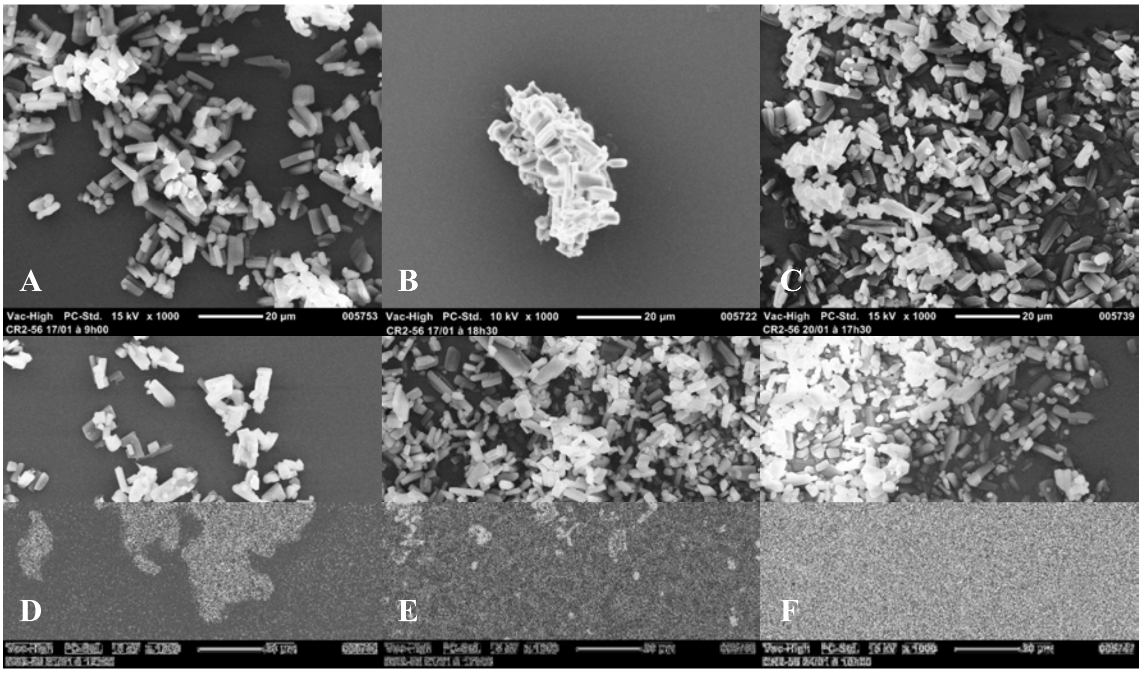
A
Vac-High PC-Std. 15 kV x 1000 20 µm 005753
CR2-56 17/01 à 9h00
B
Vac-High PC-Std. 10 kV x 1000 20 µm 005722
CR2-56 17/01 à 18h30
C
Vac-High PC-Std. 15 kV x 1000 20 µm 005739
CR2-56 20/01 à 17h30
D
E
F

Figure III - 63. SEM pictures of samples during deracemisation of ClTAK with glass beads. Labels A-F correspond to arrows indicated on Figure III - 62. Magnification x1000.

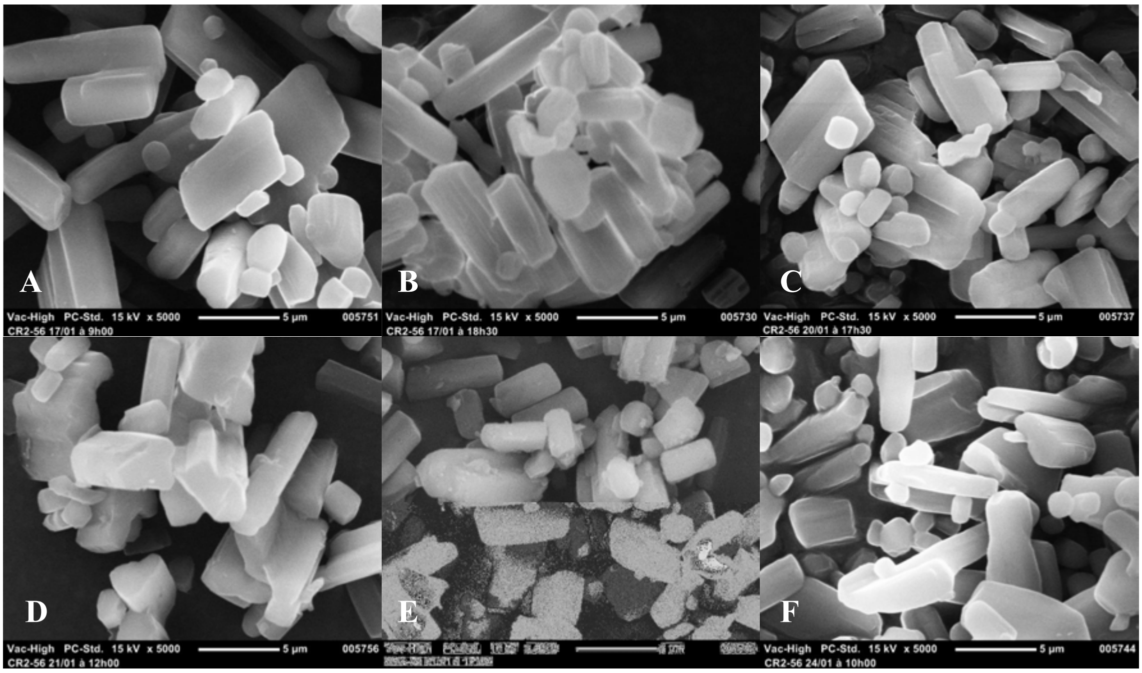
A
B
C
D
E
F
Vac-High PC-Std. 15 kV x 5000 5 μm 005751
CR2-56 17/01 à 9h00
Vac-High PC-Std. 15 kV x 5000 5 μm 005730
CR2-56 17/01 à 18h30
Vac-High PC-Std. 15 kV x 5000 5 μm 005737
CR2-56 20/01 à 17h30
Vac-High PC-Std. 15 kV x 5000 5 μm 005756
CR2-56 21/01 à 12h00
Vac-High PC-Std. 15 kV x 5000 5 μm 005744
CR2-56 24/01 à 10h00

Figure III - 64. SEM pictures of samples during deracemisation of ClTAK with glass beads. Labels A-F correspond to arrows indicated on Figure III - 62. Magnification x5000.

The shape of particles was different compare to the starting material. Crystal length was much shorter (between 1 and 10μm) but the width was quite similar. Edges were almost not visible; they were eroded because of the attrition ensured by glass beads.

The amount of small crystals was not negligible and was in line with the currently accepted mechanism. We can indeed easily imagine their dissolution to the benefit of the growth of the larger ones and the exchange of matter between the two enantiomers.

Another interesting point shown by these pictures is that the CSD was roughly the same from the first sample to the last one, that is to say during: the latent period, the increasing e.e. period and at the final state. The steady state of the size of particles seems to be quickly reached and be independent of the enantiomeric excess. We can thus conclude:

- The grinding ensured by glass beads is definitely efficient all along the experiment and therefore, the latent period is not due to an experimental problem. The reason for the existence of this latent period must involve another phenomenon (for example, a stochastic variation of the e.e.).

- The evolution of the e.e. is not due to a specific size of particles. The CSD depends on the abrasive power produced by glass beads and not on the enantiomeric excess of the solid phase, contrary to that C. Viedma, R. M. Kellogg and D. G. Blackmond described.[178]

2. Evolution of the CSD for the other TAK derivatives

The aim of the following parts is to determine if the behaviour of the other TAK derivatives is the same as for ClTAK. The evolution of the CSD is studied from SEM pictures then the size of particles is compared to know if the nature of the compound has an influence.

For the three TAK derivatives, SEM pictures of three samples were taken:

- One sample with e.e. ≈ 0%.
- One sample during the increasing of the e.e.
- One sample when the deracemisation was complete.

The times of sampling are indicated by arrows on the corresponding representation of the evolution of the enantiomeric excess versus time:

a. 4,4-dimethyl-1-phenyl-2-(1H-1,2,4-triazol-1-yl)pentan-3-one HTAK

As for ClTAK, the initial powder of HTAK was made of rod shaped crystals with a scattered CSD; the length of particles was between 5µm and 200µm.

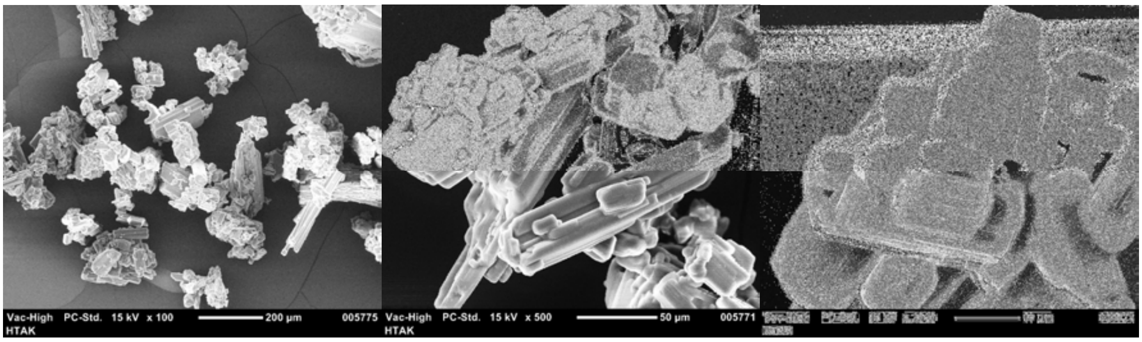

Figure III - 65. SEM pictures of the initial powder of HTAK.

The crystal size distribution of three samples was observed by SEM.

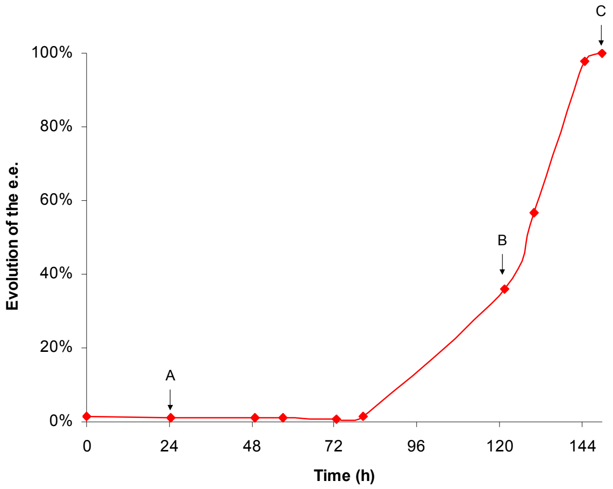

Figure III - 66. Evolution of the enantiomeric excess versus time for HTAK. Arrows indicate time of sampling for SEM pictures. Line is given as a guide to the eyes.

We can observe that the CSD was much narrower than the starting material (with a significant amount of small particles) and crystals were more elongated. Moreover, no edges were visible. As for ClTAK, the steady state of particles size was quickly reached and then no evolution was observed; it was also independent of the enantiomeric excess.

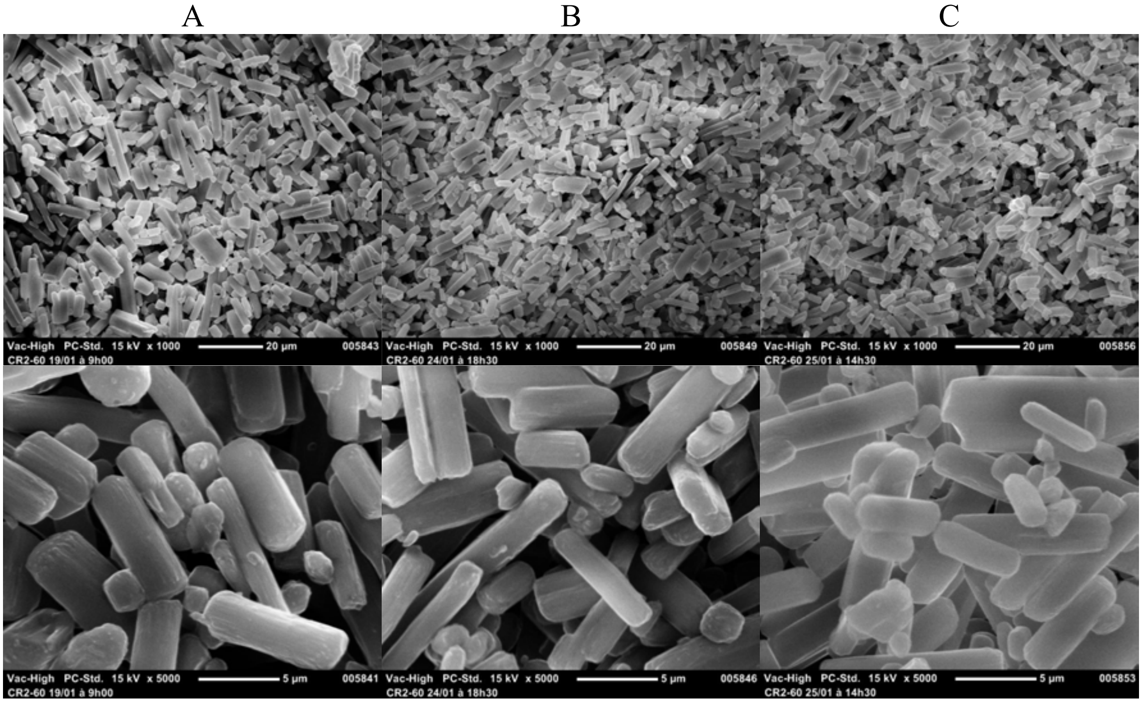
A
B
C
Vac-High PC-Std. 15 kV x 1000 20 µm 005843 CR2-60 19/01 à 9h00
Vac-High PC-Std. 15 kV x 1000 20 µm 005849 CR2-60 24/01 à 18h30
Vac-High PC-Std. 15 kV x 1000 20 µm 005856 CR2-60 25/01 à 14h30
Vac-High PC-Std. 15 kV x 5000 5 µm 005841 CR2-60 19/01 à 9h00
Vac-High PC-Std. 15 kV x 5000 5 µm 005846 CR2-60 24/01 à 18h30
Vac-High PC-Std. 15 kV x 5000 5 µm 005853 CR2-60 25/01 à 14h30

Figure III - 67. SEM pictures of samples during deracemisation of HTAK with glass beads. Labels A-C correspond to arrows indicated on Figure III - 66. Magnification x 1000 and x5000.

b. 4,4-dimethyl-1-(p-toluyl)-2-(1H-1,2,4-triazol-1-yl)pentan-3-one MeTAK

The initial powder of MeTAK was made up by ill-defined particles, with a scattered CSD; rod crystals with a length higher than 200µm, or particles with diameter between 1µm and 200µm (Figure III - 68). The edges were not clearly visible on all particles.

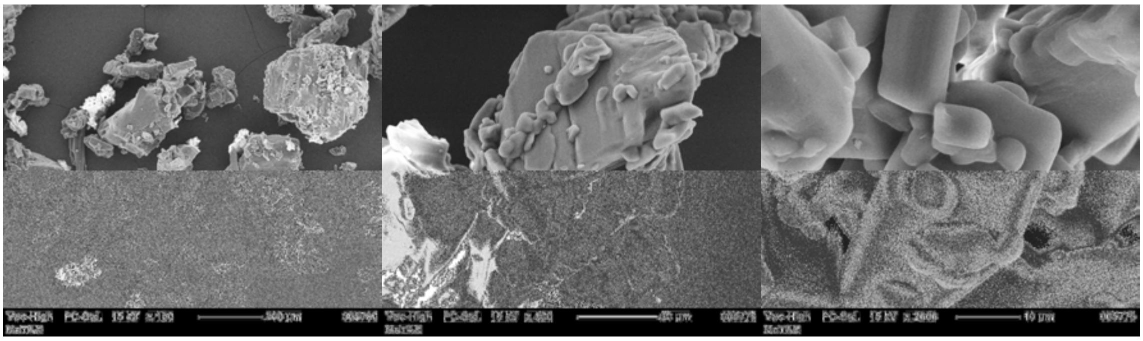

Figure III - 68. SEM pictures of the initial powder of MeTAK.

The crystal size distribution of three samples was observed by SEM.

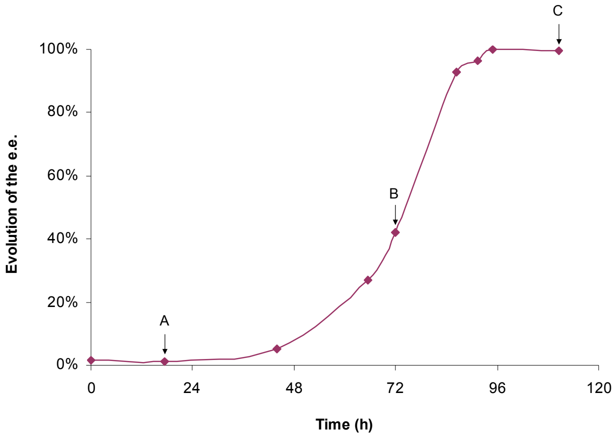

Figure III - 69. Evolution of the enantiomeric excess versus time. Arrows indicate time of sampling for SEM pictures. Line is given as a guide to the eyes.

The shape of crystals was homogeneous, with a narrow CSD (particles between 1 and 10µm, Figure III - 70). A lot of small particles were present and edges were not visible (some particles look like ball). In this case, the steady state of size particles seemed also to be quickly reached.

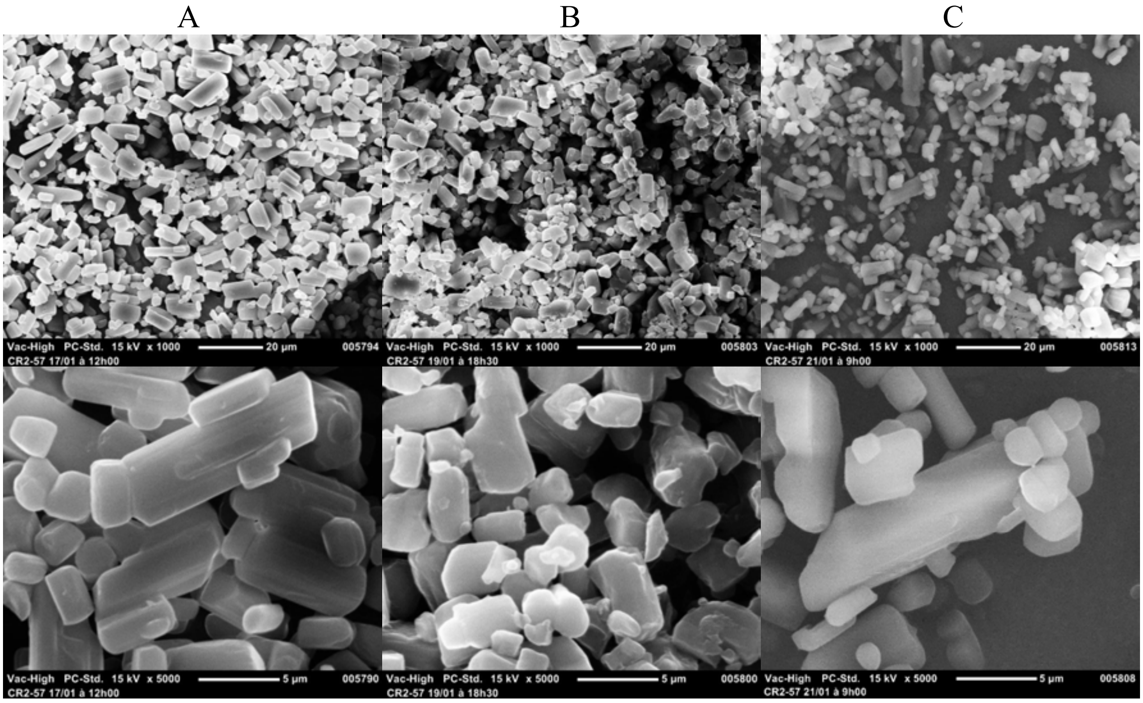
A
B
C
Vac-High PC-Std. 15 kV x 1000 20 µm 005794
CR2-57 17/01 à 12h00
Vac-High PC-Std. 15 kV x 1000 20 µm 005803
CR2-57 19/01 à 18h30
Vac-High PC-Std. 15 kV x 1000 20 µm 005813
CR2-57 21/01 à 9h00
Vac-High PC-Std. 15 kV x 5000 5 µm 005790
CR2-57 17/01 à 12h00
Vac-High PC-Std. 15 kV x 5000 5 µm 005800
CR2-57 19/01 à 18h30
Vac-High PC-Std. 15 kV x 5000 5 µm 005808
CR2-57 21/01 à 9h00

Figure III - 70. SEM pictures of samples during deracemisation of MeTAK with glass beads. Labels A-C correspond to arrows indicated on Figure III - 69Figure III - 66. Magnification x1000 and x5000.

c.1-(4-bromophenyl)-4,4-dimethyl-2-(1H-1,2,4-triazol-1-yl)pentan-3-one BrTAK

The initial powder of BrTAK was made of ill particles, with a scattered CSD; needles, rod crystals with a length higher than 500µm, or 1µm particles (Figure III - 71). The edges were clearly visible.

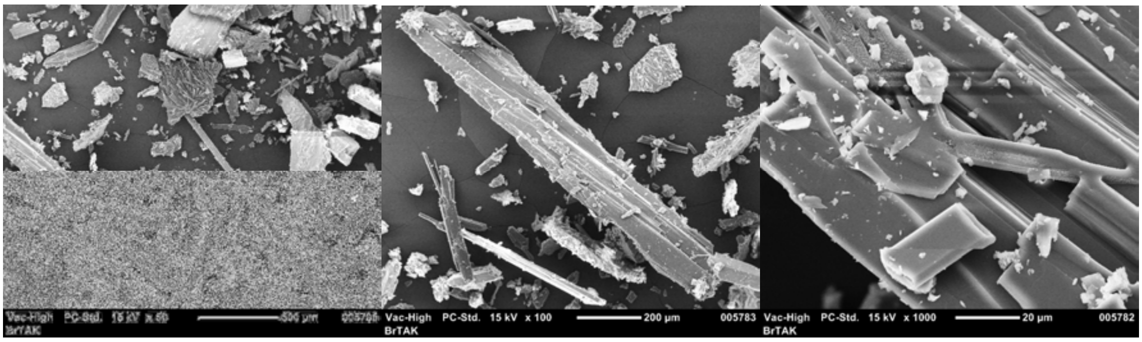
Vac-High PC-Std. 15 kV x 100
200 µm
005783
BrTAK
Vac-High PC-Std. 15 kV x 1000
20 µm
005782
BrTAK

Figure III - 71. SEM pictures of the initial powder of BrTAK.

The crystal size distribution of three samples was observed by SEM. The shape of crystals was homogeneous, with a narrow CSD (particles between 1 and 5µm, Figure III - 73). A lot of small particles were present and edges were not visible. The steady state of the size of the particles was quickly reached.

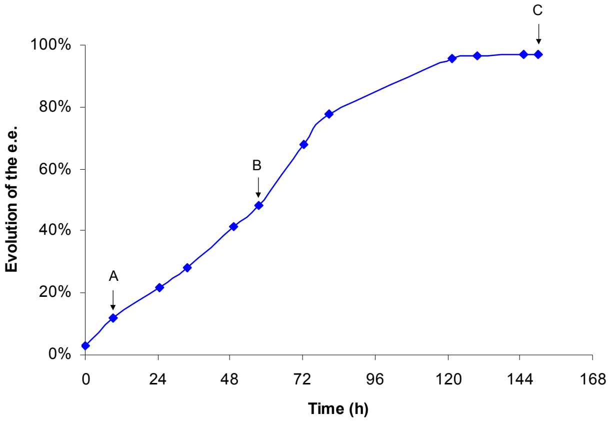

Figure III - 72. Evolution of the enantiomeric excess versus time. Arrows indicate time of sampling for SEM pictures. Line is given as a guide to the eyes.

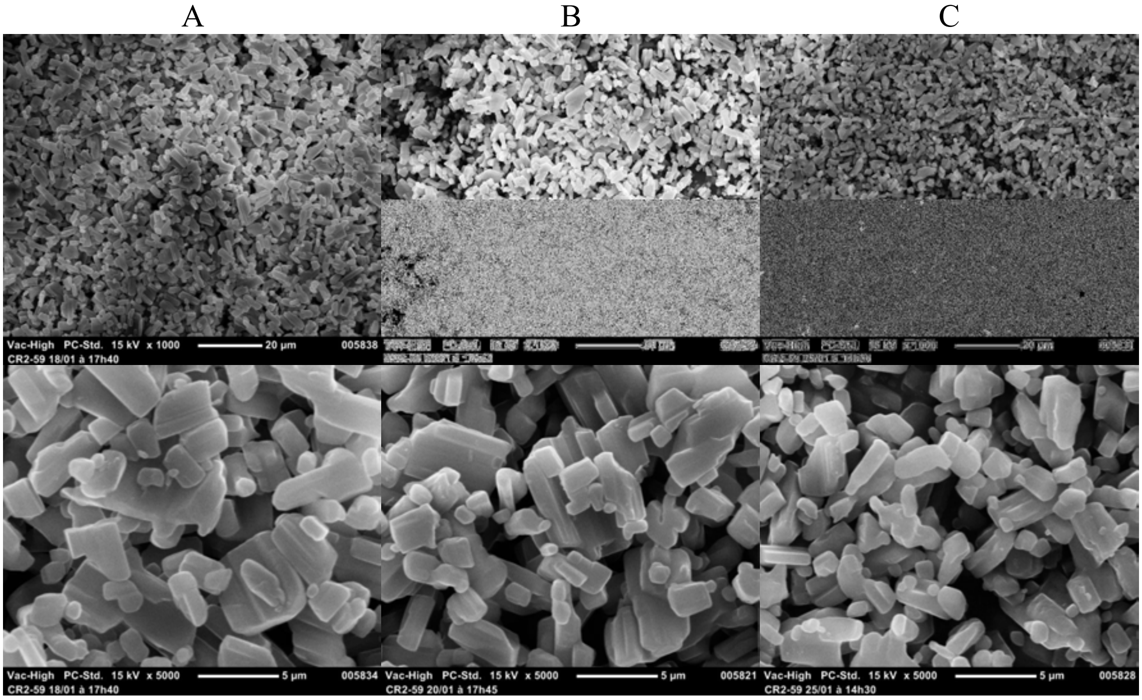
A
B
C
Vac-High PC-Std. 15 kV x 1000
20 µm
005838
CR2-59 18/01 à 17h40
Vac-High PC-Std. 15 kV x 5000
5 µm
005834
CR2-59 18/01 à 17h40
Vac-High PC-Std. 15 kV x 5000
5 µm
005821
CR2-59 20/01 à 17h45
Vac-High PC-Std. 15 kV x 5000
5 µm
005828
CR2-59 25/01 à 14h30

Figure III - 73. SEM pictures of samples during deracemisation of BrTAK with glass beads. Labels A-C correspond to arrows indicated on Figure III - 72. Magnification x1000 and x5000.

3. Comparisons between the sizes of particles

In this paragraph, the particles sizes of the four TAK derivatives were compared to understand why the behaviour of BrTAK was slower than the three others. The study focused on samples with an enantiomeric excess at circa 100% (Figure III - 74).

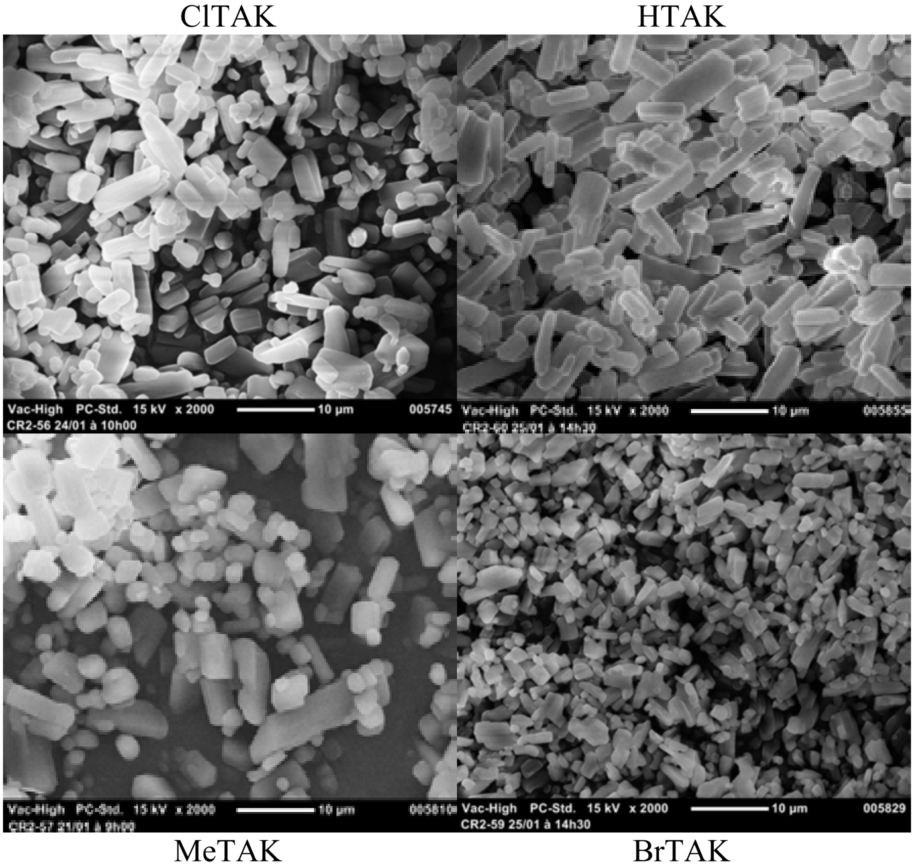
ClTAK
HTAK
MeTAK
BrTAK

Vac-High PC-Std. 15 kV x 2000 10 µm 005745
CR2-56 24/01 à 10h00
Vac-High PC-Std. 15 kV x 2000 10 µm 00585
CR2-60 25/01 à 14h30
Vac-High PC-Std. 15 kV x 2000 10 µm 005810
CR2-57 21/01 à 9h00
Vac-High PC-Std. 15 kV x 2000 10 µm 005829
CR2-59 25/01 à 14h30

Figure III - 74. SEM pictures of samples with a high e.e. of ClTAK, HTAK, MeTAK, BrTAK. Magnification x2000.

A first interesting point was that there was a good correlation between the CSD and the deracemisation kinetics for ClTAK, MeTAK and HTAK (relatively close CSDs and similar kinetics).

The deracemisation duration was longer for BrTAK than for the other TAK derivatives. As all the experimental parameters were identical (same mass of crystals in suspension, same mass concentration, same mass of sodium hydroxide, isomorphous crystal lattices for MeTAK, ClTAK and BrTAK, same set-up, same attrition energy...), larger particles were expected for BrTAK. But SEM pictures shew the opposite: particles of BrTAK were much smaller than particles of ClTAK, HTAK and MeTAK, that was in contradiction with the currently accepted mechanism. BrTAK behaves as if the transfert of matter was inhibited, limiting the growth of particles and slowing down the evolution of the enantiomeric excess.

But no evidence was found to confirm this theory; the slow evolution of the enantiomeric excess of BrTAK remains an open question.

VII – Deracemisation by using ultrasounds

Very recently, a few experiments using ultrasounds instead of glass beads were carried out to perform the deracemisation of sodium chlorate $NaClO_3$. Song *et al.* Provoked the crystallisation of $NaClO_3$ from a supersaturated solution by applying ultrasounds, both with and without seeding.[179,180] In both cases the final enantiomeric excess was close to 100% and without seeding, the final chirality was stochastic, as for glass beads. Following their first study, P. Cintas attributed the effect of the ultrasounds on the deracemisation to their ability to promote the formation of secondary nuclei and/or to increase the mechanical effects,[181] two processes known to be very important in the mechanism of the deracemisation.

Up to now, several experiments combining ultrasounds and glass beads were performed by the Dutch consortium to complete deracemisation of amino acid derivatives but ultrasounds have never been used alone in these cases.[95,100,104,126] Moreover, even if an increase of the kinetics was noticed, the role of the ultrasounds has never been specifically studied.

In order to study the effect of ultrasounds without any glass beads, experiments of deracemisation of ClTAK were carried out.

1. Deracemisation in an ultrasonic bath

Preliminary experiments in a simple ultrasonic bath showed that ultrasounds were indeed able to perform deracemisation of ClTAK without the help of glass beads (Figure III - 75). In the first experiment (solid curve), the vial was just put down inside the US bath and naturally went in a corner, whereas in the second experiment (dotted curve), the vial was fixed in the middle of the bath. In both cases the enantiomeric excess was over 40% after 6h.

---

[179] Y. Song, W. Chen, X. Chen; *Cryst. Growth Des.,* **2008**, 8(5), 1448-1450.

[180] Y. Song, W. Chen, X. Chen; *Cryst. Growth Des.*, **2012**, 12(1), 8-11.

[181] P. Cintas; *Cryst. Growth Des.,* **2008**, 8(8), 2626-2627.

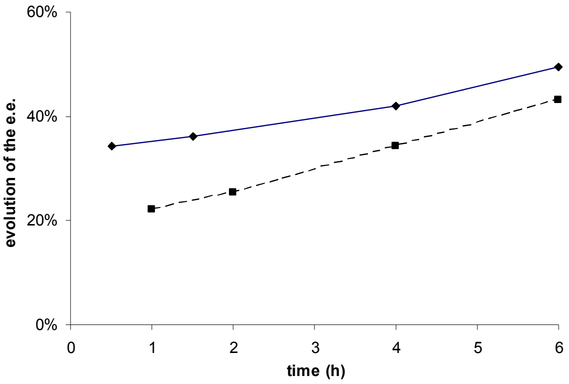

Figure III - 75. . Evolution of the enantiomeric excess during the ultrasonic treatment in an ultrasonic bath. ♦ "free" vial, ■ fixed vial.

However, in the first case, the evolution of the enantiomeric excess was slowest whereas the initial e.e. was higher. That is in contradiction with the exponential evolution of the e.e. (the experimental parameters, such as temperature and initial crystal size distribution, were kept constant). This difference can maybe be explain by the non homogeneity of ultrasounds in the entire bath as the appearance of the surface of water shows; the vial in the middle get more power than the vial in the corner of the bath. The amount of ultrasounds seemed to have a significant effect on the kinetics of the deracemisation.

Moreover, another encountered problem was the difficulty to control the temperature inside the suspension because of the overheating provokes by ultrasounds.

2. Deracemisation in controlled conditions: use of an ultrasonic probe

a. Experimental results

To perform deracemisations in controlled conditions (power and temperature), a different set-up was used; an ultrasonic probe was immerged into a suspension of ClTAK in a double-walled thermostated reactor (Figure III - 76). The generator connected to the probe was able to deliver different powers of ultrasounds and the temperature of the system was monitored by a temperature probe. A magnetic stirrer was added in order to ensure a good homogeneity of the suspension inside the reactor. Indeed, with low powers, ultrasounds were not sufficient to homogenize the system. As stirring was also able to provoke deracemisations, the same stirring rate (750rpm) was used for all the experiments to make possible the comparison between the results.

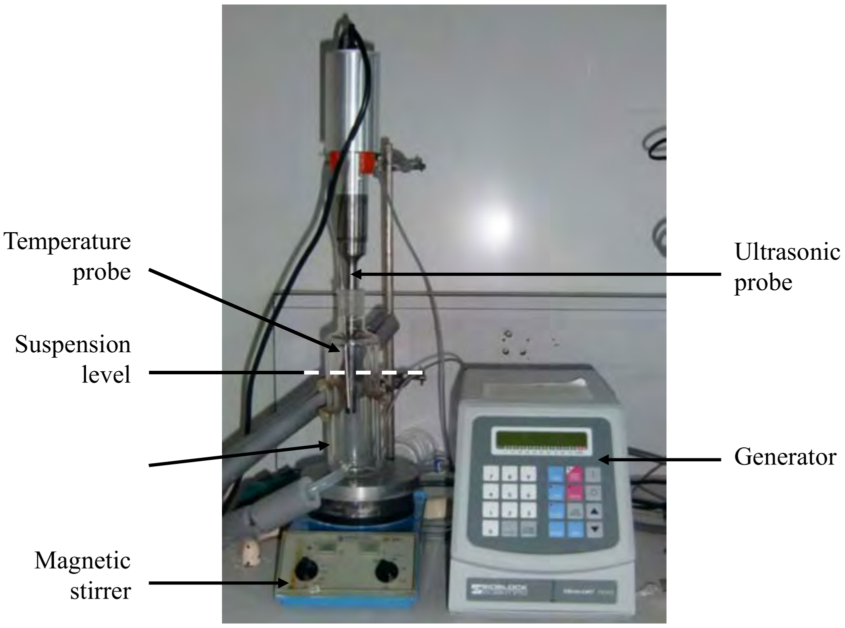

Figure III - 76. The ultrasonic probe immerged into the suspension of ClTAK.

The evolution of the enantiomeric excess was monitored by chiral HPLC for four different powers (50kJ.h^{-1}, 130kJ.h^{-1}, 170kJ.h^{-1} and 325kJ.h^{-1}). The results are shown on Figure III - 77. In the four cases, the enantiomeric excess evolved autocatalytically towards the high values up to a final e.e. close to 100%. Moreover, we can observe that the necessary time to complete deracemization depends on the power delivered by the ultrasonic probe: the higher the power, the faster the kinetics.

It should be noted that almost two months were necessary to complete the deracemisation without ultrasonic radiation in the same conditions (*i.e.* stirring rate at 750rpm, 25°C), which proved that the effect of the stirring itself can be neglected.

Moreover, the maximum continuous irradiation which can be programmable by the generator was 10h. In consequences, the generator was turn off all the evening and the system had to be “frozen” to not modify the size of the crystals and the enantiomeric excess. The temperature of the thermostat was therefore adjusted to 25°C and the stirring was stopped.

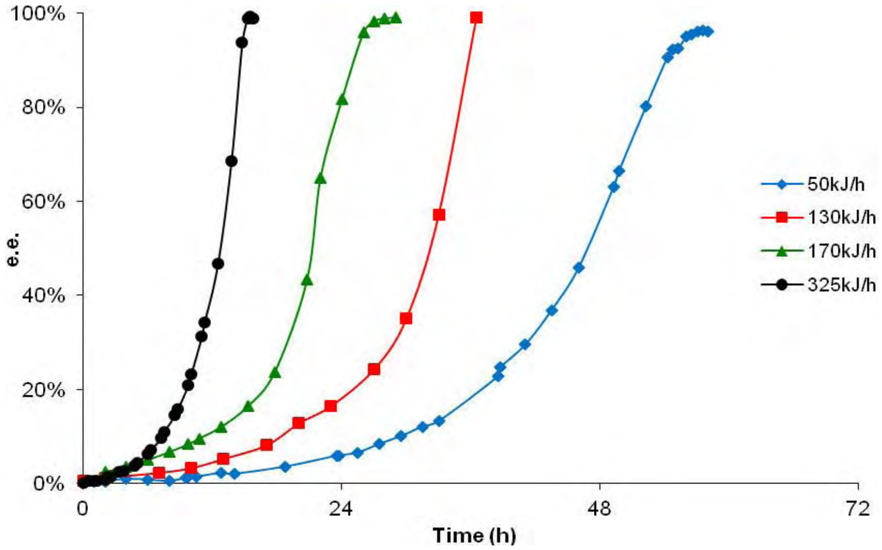

Figure III - 77. Evolution of the enantiomeric excess during deracemisation by using ultrasounds with four different powers. Lines are given as a guide to the eyes.

The study of the size of the particles by SEM revealed that the higher the power (and so the faster the kinetics), the smaller the crystals (Figure III - 78).

This result combined to the exponential evolution of the enantiomeric excess seemed to give the proof that the mechanism of the deracemisation is the same for glass beads as for ultrasonic waves. Therefore these two kinds of deracemisation were compared.

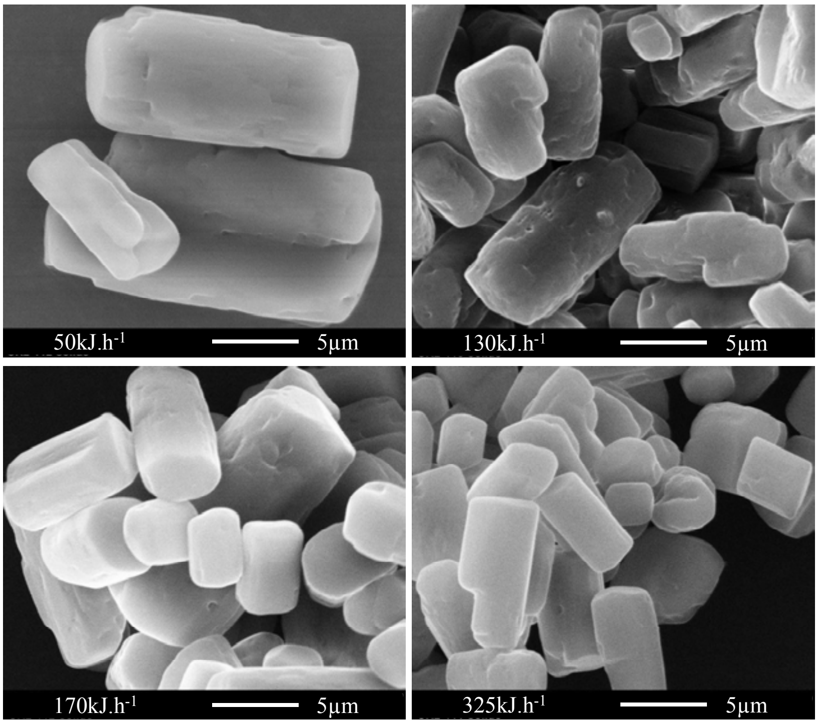

Figure III - 78. SEM pictures of final particles for the four different powers of ultrasounds. Magnification x5000.

b. Comparison between glass beads and ultrasounds: a different mechanism?

First, kinetics of the evolution of the enantiomeric excess were compared. As illustrated on Figure III - 79, the reaction durations were shorter using ultrasonic irradiations, even at the lowest power.

It should be noted that the two kinds of experiments were not performed at the same scale: when attrition was ensured by glass beads, 1g of ClTAK was used whereas 20g were deracemised with ultrasounds. Indeed, because of the size of the ultrasonic probe (≈10x200mm), it was difficult to perform the experiment on a smaller scale than 20g of substrate. As for glass beads, the necessary amount of beads was too large (100g) and make very difficult the stirring of the suspension. Moreover, the workup of the reaction was not easy; the product and the glass beads must be separated. However, to make possible the comparison between the two processes, the substrate/base/solvent proportions and the temperature were kept constant.

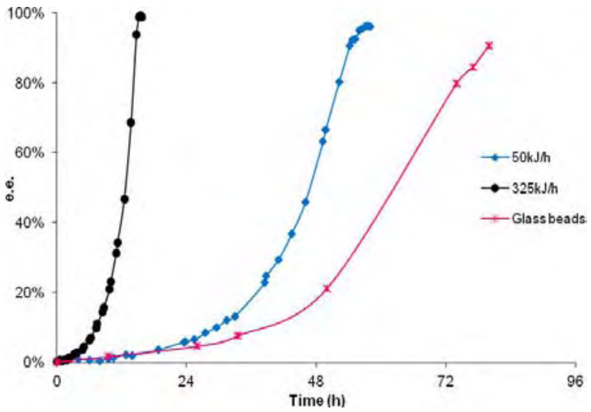

Figure III - 79. Comparison of the evolution of the enantiomeric excess by using glass beads and with two different powers of ultrasounds. The origin of the deracemisation by using glass beads was shifted (the latent period was removed). Lines are given as a guide to the eyes.

This difference of the kinetics can be explained by the energy provided in the system; ultrasonic irradiation is a very energetic technique, as the overheating of the suspension showed. Moreover, ultrasounds are known to produce a high number of clusters. As reincorporation of clusters seems to be one of the key steps of the deracemisation process, it was not surprising that deracemisations under ultrasounds proceeded faster than deracemisations induced by glass beads. Pedro Cintas also pointed out in his publication[181] that cavitations produced by the ultrasonic waves can create a strong mechanical effect. Inside a cavitational bubble, the pressure and the temperature can reach very high values (over 5000K and 1000 bar). When bubbles collapsed, a high energy is released in the system, inducing shear forces, shock waves and high speed liquid jets, responsible for pitting, erosion and abrasion. Thus, ultrasounds seemed to have a similar effect than glass beads, faster kinetics due to the high energy and/or their higher rate of attrition and/or to the high number of clusters.

So, if the mechanism is the same for the two processes, the crystals obtained after ultrasonic treatment should be smaller than those obtained using glass beads. Surprisingly, it is not that can be observed on the SEM pictures (Figure III - 80).

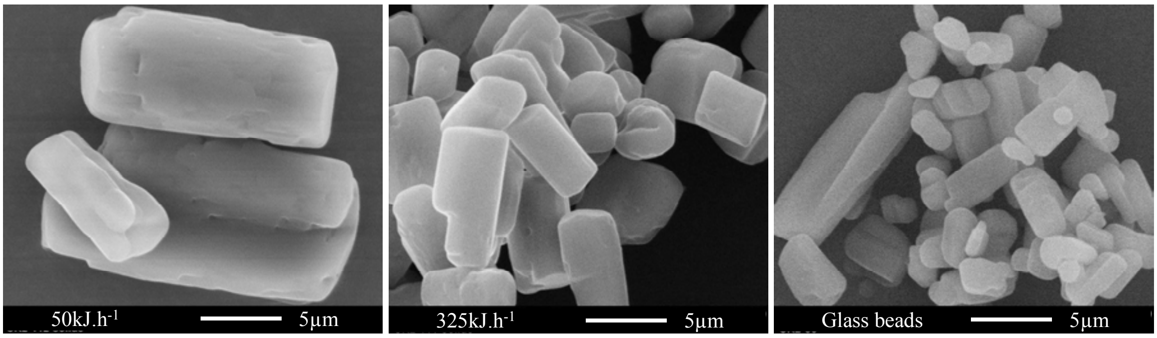

Figure III - 80. SEM pictures of final particles of ClTAK obtained after attrition ensured by ultrasounds or glass beads. Magnification x5000.

The enantiomeric excess evolved faster with ultrasounds than with glass beads but crystals were larger, that was in contradiction with the current mechanism. The high mechanical effect produced by ultrasonic waves cannot explain why this process was so efficient.

Moreover, by looking at the evolution of the crystal size distribution during an ultrasonic treatment (Figure III - 81), another difference appeared. The CSD did not evolve significantly after 14h (e.e. = 2%), as with glass beads, but all the particles have the same size; the CSD was narrow and only few small crystals are present.

So it was difficult to understand how the Ostwald ripening can occur and how it can be responsible of the so fast kinetics if only few small crystals were present in suspension.

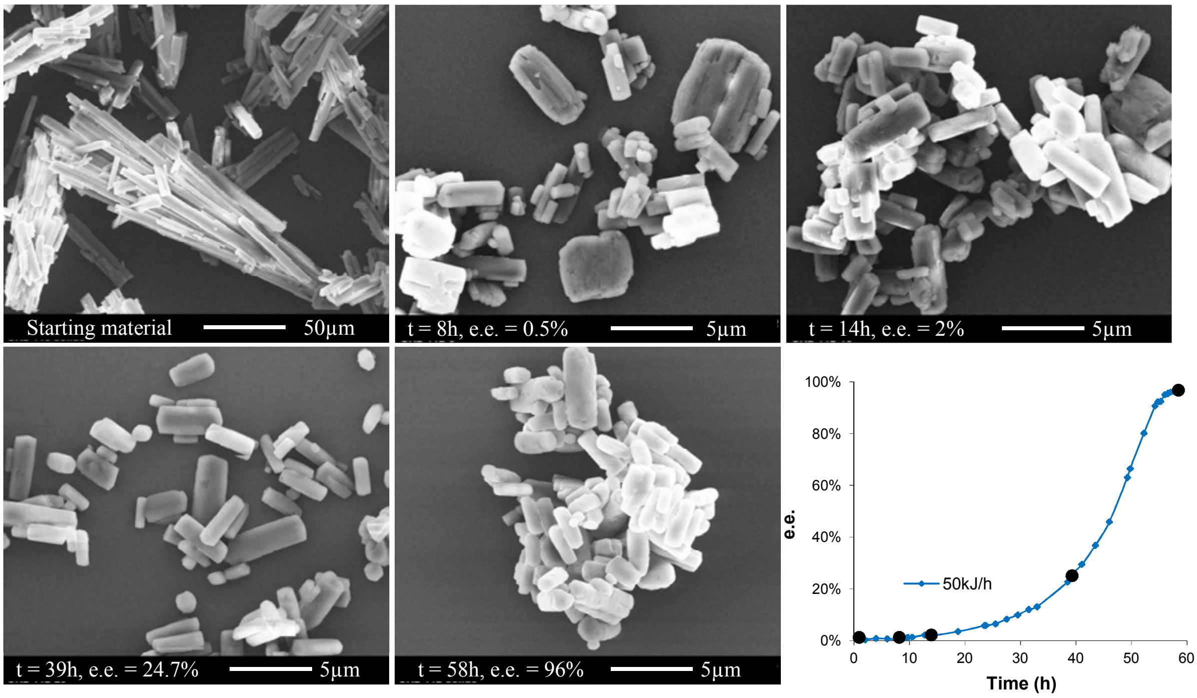

Figure III - 81. SEM pictures of the evolution of the CSD during deracemisation using the slowest power of ultrasounds (50kJ.h-1, corresponding to the blue curve on the Figure III - 79).

A different aspect of the surfaces of the crystals can also be observed: after an ultrasonic treatment, surfaces are quite rough, as if small "flakes" were blown off from the mother crystal (Figure III - 78 and Figure III - 80) whereas after attrition ensured by glass beads, the particles were eroded, with smooth surfaces (Figure III - 80). These flakes can be quickly dissolved, increasing the dissolution/recrystallisation rate and therefore increasing the kinetics of the process.

3. Conclusion

This study allowed to shed some light to the deracemisation mechanism:

- The role of the mechanical effects and of the Ostwald ripening was confirmed (the higher the power of the ultrasonic irradiation, the smaller the particles and the faster the kinetics). But, they are not sufficient to explain how the process proceeds: for the same compound, particles obtaining by deracemisation using ultrasounds are larger than particles particles obtaining by deracemisation using glass beads and the evolution of the enantiomeric excess is faster.

- The important role of clusters was confirmed: a high number of clusters are produced by ultrasounds, speeding up the transfert of matter (clusters can be dissolved or recaptured by docking on the surfaces of crystal of the same handedness).

- The local overheating produced when the cavitational bubbles collapsed lead to the creation of a local supersaturation. This surpersaturation combined with the “instantaneous” racemisation of the compound make possible a significant entrainment effect. As the thermal effect induced by the ultrasonic waves is much higher than the one due to glass beads, the entrainment is also promoted, leading to a faster evolution of the enantiomeric excess. This effect can also explain the difference between the sizes of particles obtained by using ultrasounds or by using glass beads.

VIII – Conclusion

In this chapter, we first demonstrated that several TAK derivatives exhibit the same crystal structure. A kind of pocket seems to exist around the aromatic ring in which the substituents can be changed without modifying the crystal packing: ClTAK, MeTAK, BrTAK and 4Cl-2FTAK crystallise in the $P2_12_12_1$ space group with Z’=1 and with disorder. Limited modulations in the crystal structure are even possible without destroying the full chiral discrimination as exemplified by HTAK ($P2_1$, Z’=2, without disorder). tBuTAK is an example of the limitation of this pocket.

The fairly high degrees of freedom of the pocket (additional experiments are necessary to study its limits) can increase the number of deracemisable chiral intermediates.

The successful deracemisation experiments with glass beads as well as with ultrasounds improved the understanding of the mechanism:

- A random delay to the “irreversible” evolution of the enantiomeric excess exists at the beginning of the process if there is no initial imbalance between the two enantiomers. A threshold needs to be overcome prior making the transformation “irreversible”. This emphasises the stochastic behaviour of the deracemisation.
- The crystal size distribution is dependent on the mechanical energy given to the system, but not on the enantiomeric excess of the solid phase, both with glass beads and with ultrasounds. This observation does not confirm the general charactec of the”*transient growth*” described by Hein *et al.*[178]
- The Ostwald ripening and the mechanical effect are necessary to ensure the total symmetry breaking but they are not sufficient to explain how the evolution proceeds.
- The importance of the reincorporation of clusters was confirmed.

- The role of the entrainment effect was highlighted and might explain, at least partially, the different kinetics observed when using glass beads or ultrasounds.

In addition, a recent study, conjointly made with the Flood's research group in Thailand, gave the proof that total symmetry breaking can be achieved by thermal cycling only (successive heating and cooling cycles) without any mechanical attrition.[182] These results gave another proof of the importance of the entrainment effect.

Nevertheless, the case of BrTAK messes up: even if its deracemisation was carried out in similar conditions as ClTAK, MeTAK (quasi identical crystal lattices, very similar mass concentrations in the saturated solutions, same mass of solid in the suspensions, same temperature, same set-up, same attrition energy injected in the systems...), kinetics are slower and particles are smaller. The current accepted mechanism cannot explain this behaviour, showing that more investigations are needed for a full elucidation of deracemisation.

---

[182] K. Suwannasang , A. E. Flood, C. Rougeot, G. Coquerel; *Oral presentation at CGOM10*, June **2012**, Limerick, Ireland.

Chapter 4: Synthesis of pure enantiomer of Prasugrel by deracemisation

CONFIDENTIAL

I - Introduction

SYNCOM is a chemical company founded in 1988 and based in Groningen, in the north of the Netherlands. Syncom is a global leader in supplying pharmaceutical (such as Pfizer) and biotech (Phillips) industries with custom synthesis solutions.
My work in Syncom was to design a synthesis of pure enantiomer of Prasugrel, a platelet aggregation inhibitor, by deracemisation.

Prasugrel is a α-amino acid derivative with a chiral centre located in the α position. Numerous methods were described in the literature to have access to pure enantiomer of α-amino acid derivatives. Crystallisation methods, and particularly the Pasteurian resolution, are often used and were described in Chapter 1. A quick view of organic synthesis methods was also described. In this Chapter, additional examples will be given on the enzymatic dynamic kinetic resolution (here after enzymatic DKR), an efficient method frequently used to obtain enantiomerically pure amino acid derivatives.

CONFIDENTIAL

1. Enzymatic dynamic kinetic resolution of amino acid derivatives

Numerous DKR were carried out by using an enzyme to selectively convert only one enantiomer. As natural substrates of enzymes are generally proteins, enzymes are particularly efficient to selectively transform amino acids derivatives. Therefore, a lot of examples of enzymatic dynamic kinetic resolution were described in the literature. In this paragraph, a brief overview of these methods is depicted.

Tessaro *et al.* proposed the synthesis of pure enantiomer of *N*-Boc-amino acid amides from *R*,*S*-*N*-boc-amino acid thioethyl esters (Figure IV - 1).[183] Alcalase® (an endoprotease from *Bacillus licheniformis*) transformed only the *S* enantiomer. In the experimental conditions, the chemical aminolysis that may limit the success of the DKR is not efficient and therefore does not disturb the resolution; final yields are circa 80% after purification with an enantiomeric excess >98%.

---

[183] D. Tessaro, L. Cerioli, S. Servi, F. Viani, P. D'Arrigo; *Adv. Synth. Catal.*, **2011**, 353, 2333-2338.

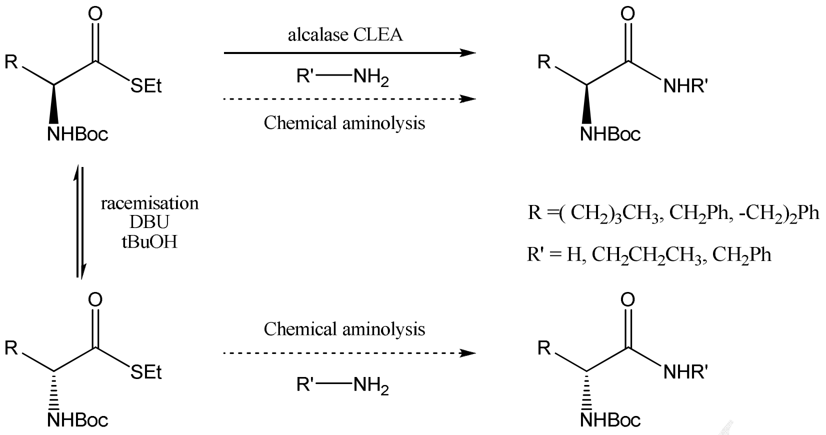

$R = (CH_2)_3CH_3, CH_2Ph, -CH_2)_2Ph$

$R' = H, CH_2CH_2CH_3, CH_2Ph$

Figure IV - 1. DKR of N-Boc-amino acid thioesters.

Another use of the Alcalase® was described by Schichl *et al.* to obtain pure *L* enantiomer of free amino acids from the corresponding ester derivative (Figure IV - 2).[184] The racemisation was ensured by a catalytic amount of 3,5-dinitrosalicylaldehyde. The purpose for the synthesis of pure natural amino acid was limited because they were easily available but the obtaining of enantiomerically pure non natural amino acids was an important issue for the pharmaceutical industry.

Entry	Substrate	*t* [d]	Yield [%]	*ee* [%]
1	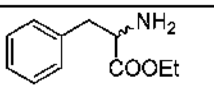	1	95	99 (L)
2	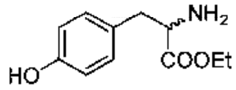	1	87[b]	97 (L)
3	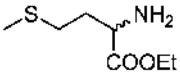	2	96	89 (L)
4	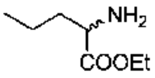	4	98	64 (L)
5	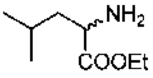	3	99	97 (L)

Figure IV - 2. DKR of α-amino acid ethyl esters with Alcalase® in acetonitrile/water (1:1) at 35 °C with 3,5-dinitrosalicylaldehyde as racemising agent. [b] Reaction was continued for an additional 1 d to give 94% yield and 95%*ee*.

Enzymatic DKR can also be performed by combining the selectivity of an enzyme with the racemisation by using metal catalysts.[185] In the case presented below (Figure IV - 3), the

CONFIDENTIAL

---

[184] D. A. Schichl, S. Enthaler, W. Holla, T. Riermeier, U. Kragl, M. Beller; *Eur. J. Org. Chem.*, **2008**, 20, 3506-3512.

[185] Y. Kim, J. Park,M.-J. Kim; *Chem. Cat.Chem.*, **2011**, 3, 271-277.

enzyme is the Candida antarctica lipase B (CALB) and the racemising catalyst is palladium trapped in aluminium oxyhydroxide Pd/AlO(OH).

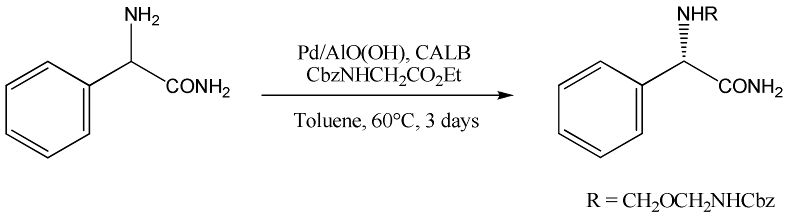

R = CH_2OCH_2NHCbz
y = 92%, e.e. = 97%

Figure IV - 3. DKR of phenylglycine amide catalysed by Pb/AlO(OH).

Because only *L*-amino acids are natural, most of enzymes selectively transform derivatives having the same configuration. The access to enantiomerically pure *D*-amino acids derivatives is therefore more difficult. However, some examples of enzymes which are able to selectively convert *D*-amino acids derivatives exist. In the case presented here (Figure IV - 4), the racemisation is ensured by an enzyme, the ACL racemase (α-amino-ε-caprolactam racemase, from *Achromobacter obae*), and the final configuration of the free amino acid depends on the enzyme used for the conversion; the *D*-aminopeptidase (from *Ochrobactrum anthropi* C1-38) or the *L*-amino acid amidase (from *Brevundimonas diminuta* TPU 5720).[186] *D* and *L*-amino acids are obtained with yields > 99% and with enantiomeric excesses >99%.

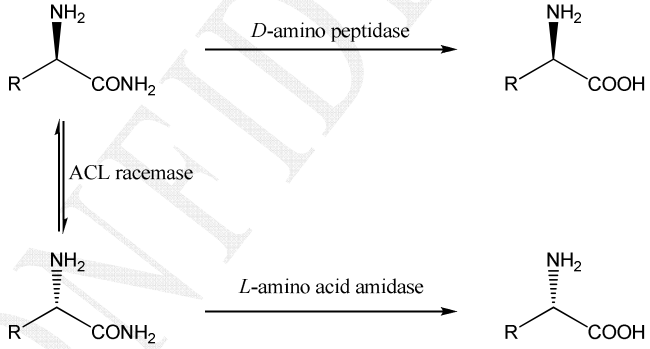

Figure IV - 4. DKR of amino acid amides.

The enzymatic dynamic kinetic resolution is an efficient method to have access to pure enantiomers of free amino acids and amino acids derivatives. Even if the productivity is limited by the optimal conditions to use the enzymes (water is often necessary and the temperature may generally be maintained around 30-35°C), amino acids derivatives are generally compatible with these conditions.

CONFIDENTIAL

---

[186] K. Yasukawa, R. Hasemi, Y. Asano; *Adv. Synth. Catal.*, **2011**, 353(13), 2328-2332.

2. Clopidogrel and Prasugrel

Clopidogrel (**23**, Figure IV - 5), commercially available under the name Plavix, is a platelet aggregation inhibitor used for treatment of ischemic strokes, heart attacks, atherosclerosis and also for the prevention of thrombosis after placement of intracoronary artery stents. Its market was reported to be US$9.3 billons in 2010[187] (US$7.3 billions in 2007[188])

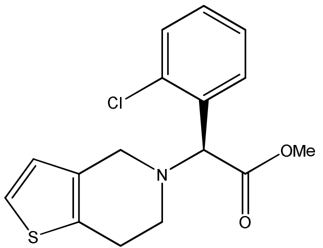

23

Figure IV - 5. Chemical structure of *S*-Clopidogrel.

Prasugrel (**24**, Effient, Figure IV - 6) is the next generation of Clopidogrel, approved for the use in Europe on February 2009[189] and in the USA by the FDA on July 2009. It has approximately 10 times greater potency than Clopidogrel (measures were made by ex vivo inhibition of platelet aggregation and in vivo inhibition in animal models).[190]

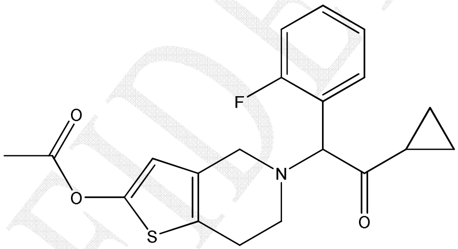

24

Figure IV - 6. Chemical structure of Prasugrel.

Prasugrel and Clopidogrel are prodrugs, members of the thienopyridine class of ADP receptor inhibitors. These compounds are known to reduce the aggregation of platelets by irreversibly binding to $P2Y_{12}$ receptors. For Clopidogrel the first step of the metabolism is a cytochrome P450-dependent oxidative step to generate the active metabolite. For Prasugrel the active metabolite is **25**. It is stated in the literature[190] that Prasugrel is more efficient than Clopidogrel because only one cytochrome P450 is needed rather than the two for Clopidogrel in order to obtain the active intermediate. We note, however, that the chemical transformation

CONFIDENTIAL

---

[187] Pharmactua, from www.pharmactua.com.
[188] MS Global insights, from www.inshealth.com.
[189] EMEA/117561/2009.
[190] J. A. Jakubowskin C. D. Payne, J. T. Brandt, G. J. Weerakkody, N. A. Farid, D. S. Small, H. Naganuma, G. Y. Li, K. J. Winters; *J. Cardiovasc. Pharmacol.*, **2006**, 47(3), 377-384.

of Prasugrel **24** to active intermediate **25** involves only a hydrolysis followed by ring opening. There is no oxidative step.

These two drugs are commonly used in combination with aspirin.

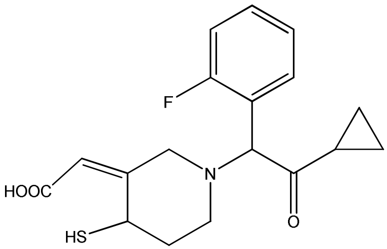

25

Figure IV - 7. Active metabolite of the Prasugrel.

The active enantiomer of Clopidogrel, *S*-Clopidogrel ***S*-23**, was obtained by resolution of the camphorsulfonic acid salt[191] or by resolution of an intermediate with tartaric acid.[192] Three years ago, a new synthesis of the pure enantiomer of Clopidogrel was designed by Syncom BV by attrition-enhanced deracemisation (Figure IV - 8).[100] This new synthesis exhibits two key steps:

- A deracemisation step: a small library of imines (Schiff bases) was synthesized to perform a screening of conglomerate by using various aromatic aldehydes. The compound **26** derived from benzaldehyde was found to be a conglomerate and was used to complete the resolution step by deracemisation in acetonitrile with DBU (1,8-Diazabicyclo[5.4.0]undec-7-ene) as racemising agent. Then the pure enantiomer of the amine **27** was obtained by hydrolysis of the imine ***S*-26**.
- The final step: the enantiopure amine ***S*-28** reacts with a dibromothiophene **29** previously prepared to give *S*-Clopidogrel, with a final enantiomeric excess of >99%.

CONFIDENTIAL

---

[191] US6800759, **2004**.
[192] US2004073057, **2004**.

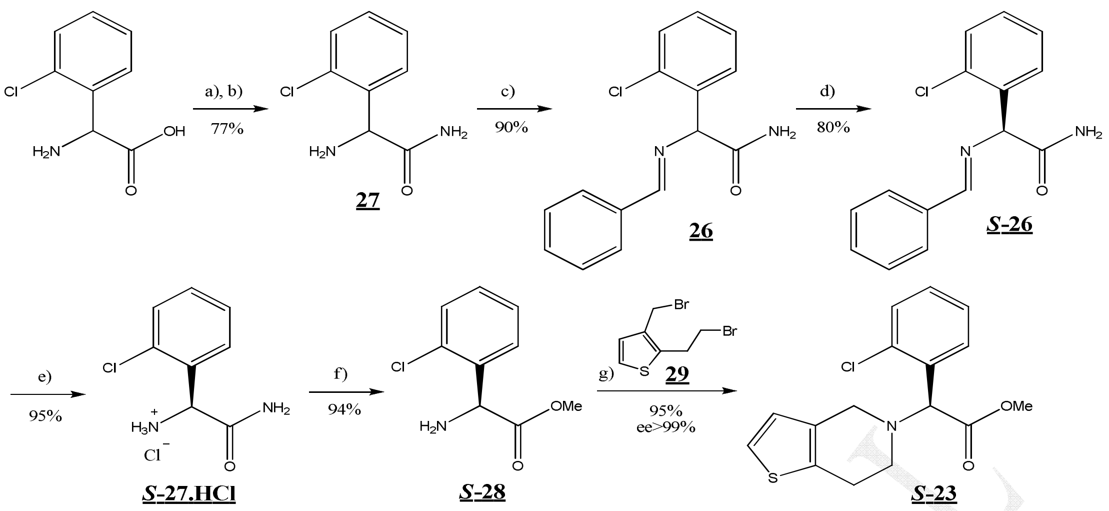
Cl
H2N
OH
O
a), b)
77%
27
NH2
c)
90%
N
26
d)
80%
S-26
e)
95%
H3N
Cl
S-27.HCl
f)
94%
OMe
S-28
Br
g)
S
29
95%
ee>99%
S-23

Figure IV - 8. Synthesis of *S*-Clopidrogrel (*S*-23) developped by Syncom B.V. a) $SOCl_2$, MeOH (95%), b) NH_3 30% in water (81%), c) benzaldehyde, $NaSO_4$, CH_2Cl_2 (90%), d) DBU, glass beads, acetonitrile (80%, e.e. > 99.5%), e) HCl, acetone (95%), f) H_2SO_4, methanol (94%), g) 7, acetonitrile (95%, e.e. > 99%).

CONFIDENTIAL

The synthesis of the racemic Prasugrel was described in a patent in 2009 (Figure IV - 9 and Figure IV - 10).[193] The Grignard reagent, prepared from the 1-(bromoethyl)-2-fluorobenzene **30**, reacted with the cyclopropyl cyanide to give the ketone **31**. A bromination step followed by a substitution led to the formation of **33**. A final acetylation step gave Prasugrel **24**.

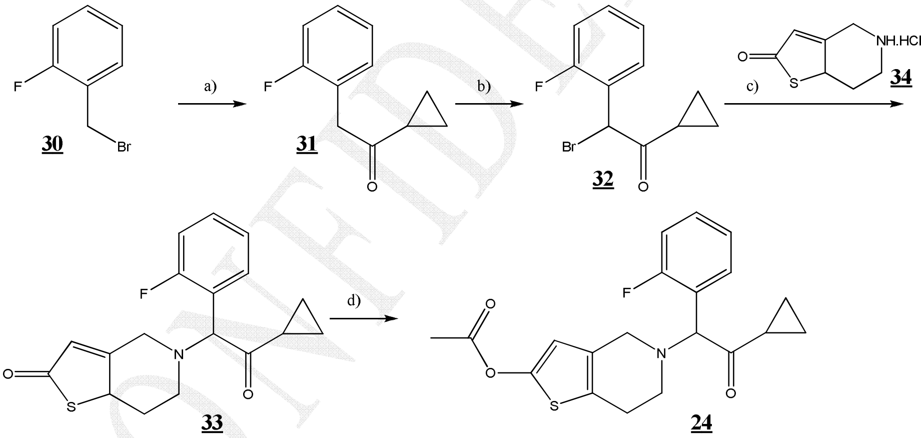
F
Br
30
a)
31
O
b)
32
c)
NH.HCl
S
34
d)
N
33
24

Figure IV - 9. Patented synthesis of Prasugrel. a) Mg, cyclopropyl cyanide, ether, b) Br_2, CCl_4, c) K_2CO_3, DMF, d) Ac_2O, NaH, DMF.

The compound **34** was synthesized by oxidation of the thiophene by the tri-n-butyl borate $(BuO)_3B$ with butyl lithium n-BuLi and H_2O_2 in dry THF. The amine had to be protected by a trityl group.[194]

---

[193] WO2009062044A2

[194] US4740510.

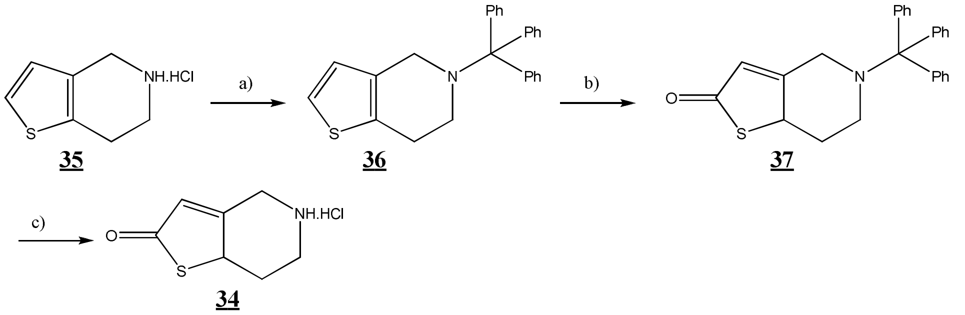

Figure IV - 10. synthesis of 34. a) Trityl chloride, b) n-Buli, $(BuO)_3B$, H_2O_2, THF, c) Formic acid, HCl, diethyl ether.

Up to now, the Prasugrel has been commercially available as the racemic mixture. However, the activity of the two enantiomers is a little bit different and the *S* enantiomer seems to be more active. A workable synthesis of pure *S*-Prasugrel is therefore a potentially important economical issue.

CONFIDENTIAL

II - First synthestic route: synthesis of 2-amino-1-cyclopropyl-2-(2-fluorophenyl)ethanone

The aim of my work in Syncom BV was to design a new synthesis of *S*-Prasugrel with a step of deracemisation, which is an efficient and relatively cheap method to obtain pure enantiomer.

This synthesis is based on the synthetic route of Clopidogrel developed by Syncom B.V., bringing into play the same two key steps:

- The formation of the ring by reaction of the pure enantiomer of the amino ketone **37** with the dibromothiophene derivative **38** (Figure IV - 11).

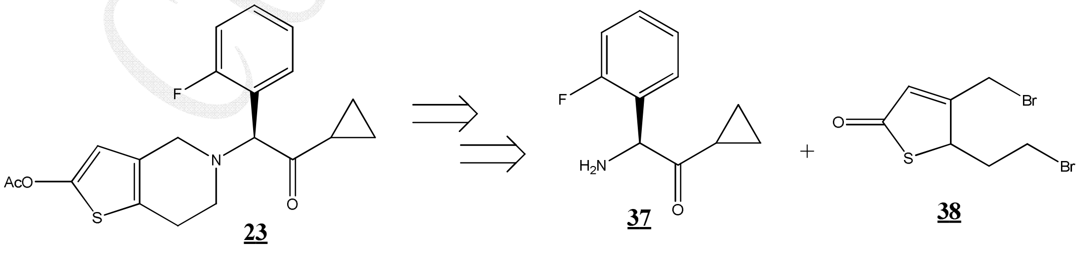

Figure IV - 11. Retrosynthesis of the pure enantiomer of *S*-Prasugrel.

- Deracemisation of the imine **39** by attrition enhanced deracemisation: a screening of substituted benzaldehyde will be performed to find a conglomerate (Figure IV - 12).

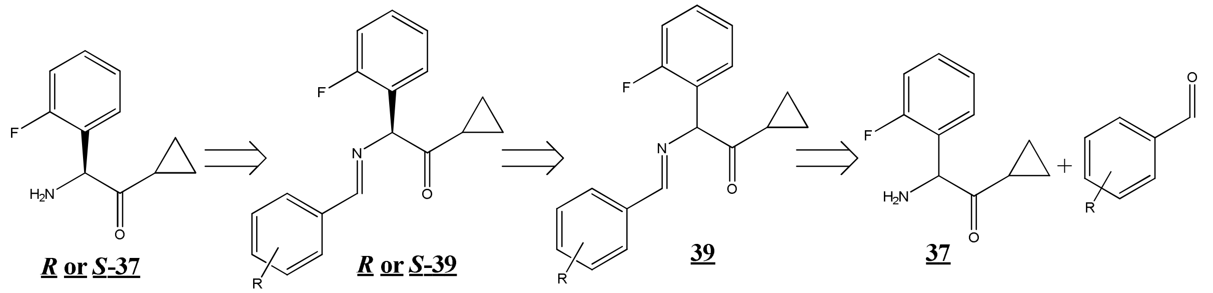

Figure IV - 12. Retrosynthesis of the pure *S*-enantiomer of the intermediate amine 37.

1. Synthesis of 2-amino-1-cyclopropyl-2-(2-fluorophenyl)ethanone

The racemic intermediate 2-amino-1-cyclopropyl-2-(2-fluorophenyl)ethanone **37** can be synthesized from the racemic 2-fluorophenylglycine **40**. The amine group had to be first protected[195] then the Weinreb amide can be formed by a coupling reaction.[196] The cyclopropyl ketone was then obtained by reaction with the corresponding Grignard reagent, the cyclopropyl magnesium bromide.[197] Finally, a deprotection step gave the target amine **37.HCl**.

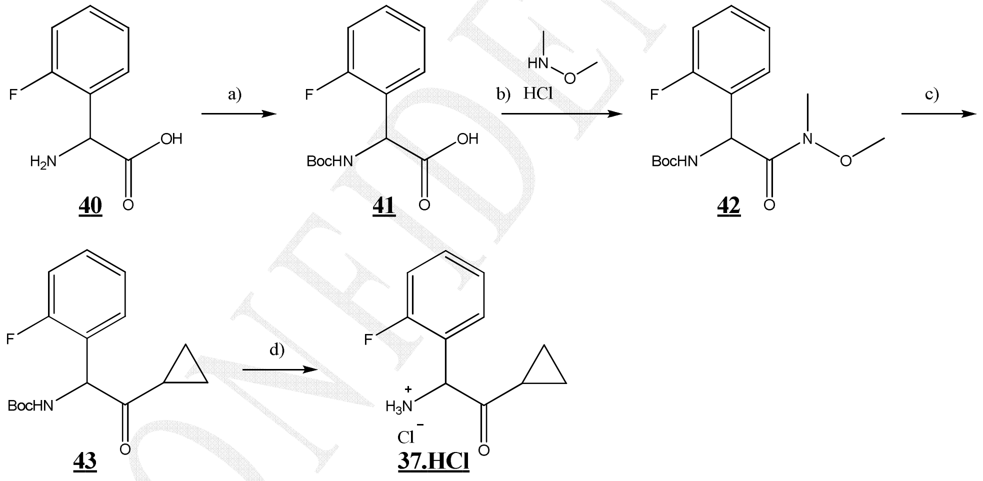

Figure IV - 13. Synthetic route of the racemic 2-amino-1-cyclopropyl-2-(2-fluorophenyl)ethanone hydrochloride. a) Boc$_2$O, NaHCO$_3$, THF, water (quant.), b) CDI, TEA, THF (80%), c) cyclopropylmagnesium bromide, THF (83%), d) HCl, methanol (85%).

The synthesis of the Weinreb amide intermediate was necessary to obtain the desired ketone. In classical Grignard reactions, ketones are more reactive than the starting carbonyl derivatives and, once formed, they are immediately involved in second Grignard reaction to give a tertiary alcohol (Figure IV - 14).

CONFIDENTIAL

---

[195] D. M. Shendage, R. Fro1hlich, G. Haufe; *Org. Lett*, **2004**, 6(21), 3675-3678.

[196] D. E. Levy, F. Lapierre, W. Liang, W. Ye, C. W. Lange, X. Li, D. Grobelny, M. Casabonne, D. Tyrrell, K. Holme, A. Nadzan, R. E. Galardy*; J. Med. Chem.*, **1998**, 41, 199-223.

[197] M. K. Ghorai, A. Kumar, D. P. Tiwari; *J. Org. Chem*., **2010**, 75, 137-151.

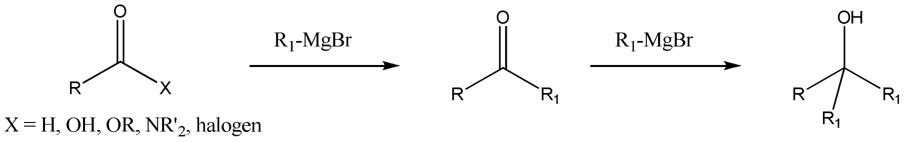
O
R
X
X = H, OH, OR, NR'$_2$, halogen
R$_1$-MgBr
O
R
R$_1$
R$_1$-MgBr
OH
R
R$_1$
R$_1$

Figure IV - 14. Reaction between a carbonyl derivative and a Grignard reagent.

Thanks to the Weinreb amide, the over-addition is avoided by the formation of a stable complex involving the methoxy group as drawn on Figure IV - 15.[198]

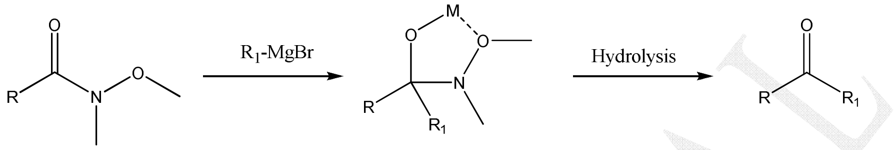
O
R
N
O
R$_1$-MgBr
M
O
O
N
R
R$_1$
Hydrolysis
O
R
R$_1$

Figure IV - 15. Formation of the stable intermediate during the addition of a Grignard reagent on a Weinreb amide.

More recently, reactions using the morpholine instead of the Weinreb amide were described. The morpholine seemed also to be able to stabilise the intermediate complex and so to avoid the formation of the tertiary alcohol. In our case, the same experimental conditions as with the Weinreb amide were applied to synthesize the target amine **44**, with similar yields. As the morpholine was less expensive than the Weinreb amine, the morpholine was used for the synthesis.

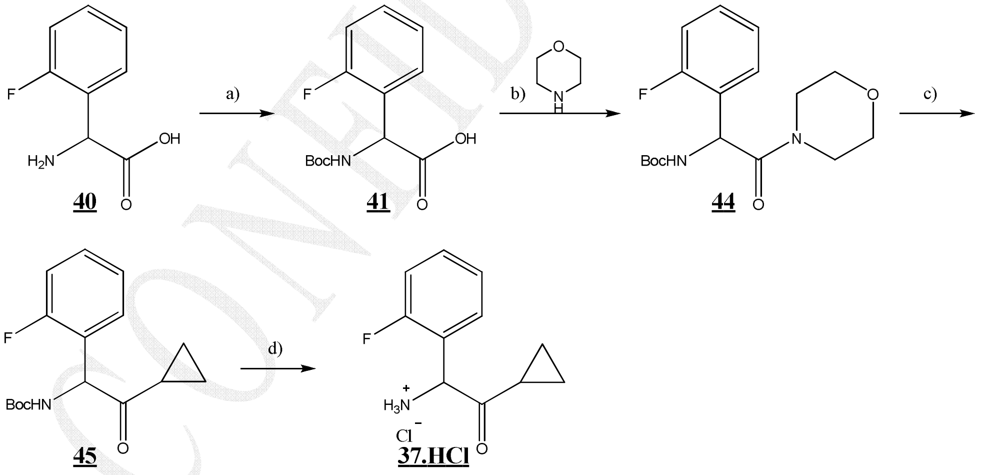
F
H$_2$N
OH
O
40
a)
F
BocHN
OH
O
41
b)
O
N
H
F
BocHN
N
O
O
44
c)
F
BocHN
O
45
d)
F
H$_3$N$^+$
Cl$^-$
O
37.HCl

Figure IV - 16. Modified synthetic route of the racemic 2-amino-1-cyclopropyl-2-(2-fluorophenyl)ethanone hydrochloride. a) Boc$_2$O, NaHCO$_3$, THF, water (quant.), b) CDI, TEA, THF (90%), c) magnesium turnings, cyclopropyl bromide, THF (83%), d) HCl, methanol (90%).

The amino ketone **37** can be reversibly converted to imines by reaction with aldehydes. Compounds derived from an aromatic aldehyde (Schiff bases **39**) can be easily racemised by using an organic base such as DBU. Therefore a screening of conglomerate with various

CONFIDENTIAL

---

[198] S. Nahm, S. M. Weinreb; *Tetrahedron Letters*, **1981**, 22(39), 3815-3818.

substituted benzaldehyde was carried out and the corresponding imines were analysed by SHG.

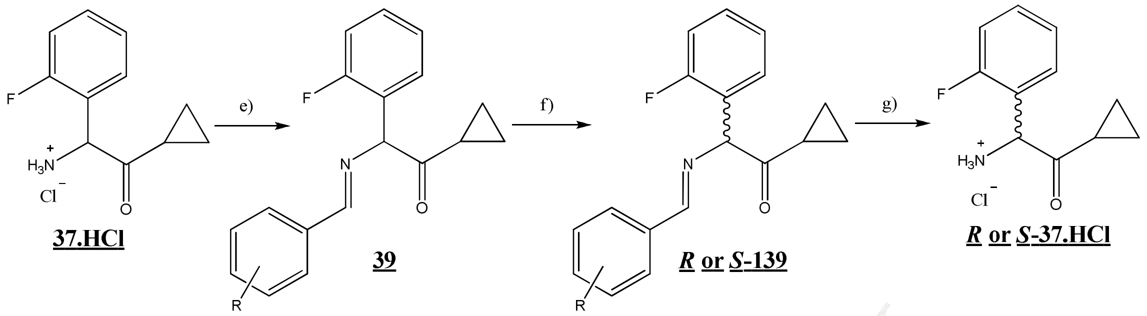

Figure IV - 17. Reversible synthesis of imines into amide with a deracemisation step. a) RCHO, Na_2SO_4, CH_2Cl_2, b) BDU, glass beads, acetonitrile, c) HCl, methanol.

Imines **39** can be synthesized from both the hydrochloride salt **37.HCl** and the free amine **37**. As a base, such as triethylamine (TEA), must be added when the hydrochloride salt is used, leading to an additional purification step, the free amine **37** was prepared. **37** was easily obtained by dissolution of the hydrochloride salt in aqueous NaOH (around 2M). After extraction with an organic solvent and evaporation, a pale yellow solid was obtained. Unfortunately, ^{1}H NRM analysis revealed that the peak corresponding to the hydrogen of the chiral centre is missing (Figure IV - 18).

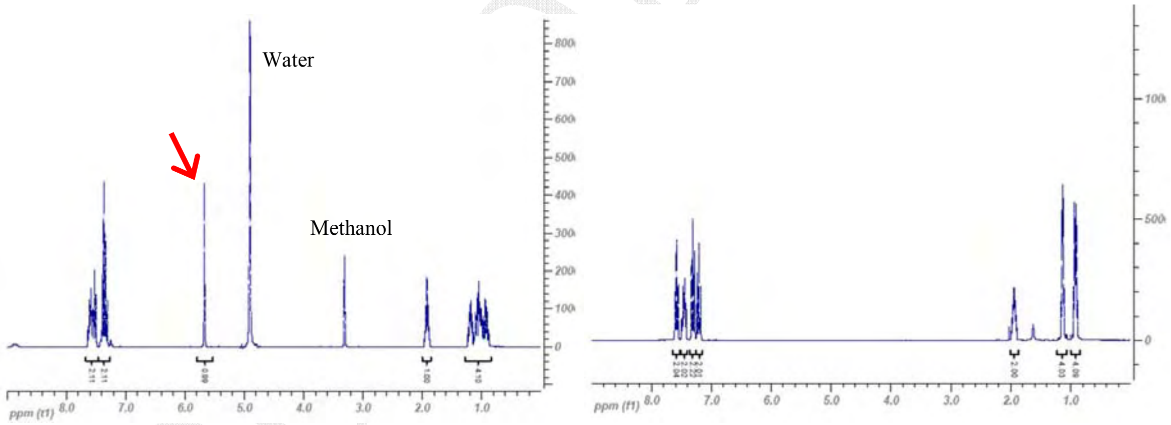

Figure IV - 18. ^{1}H NMR of the hydrochloride amine in methanol-d4 (left), and of the pale yellow solid in $CDCl_3$ (right). Peak corresponding the hydrogen of the chiral centre is indicate by an arrow.

Furthermore, peaks of all the other hydrogens are still present and no supplementary peaks are visible. Therefore we suspected the formation of the dimer (Figure IV - 19), hypothesis supported by the mass spectrometry analysis.

CONFIDENTIAL

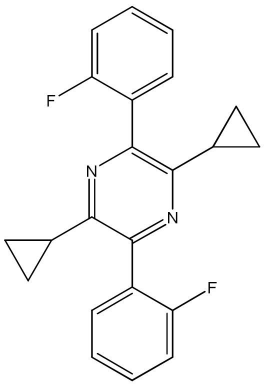

46

Figure IV - 19. Chemical structure of the dimer.

The dimer was recrystallised in acetonitrile, and some large crystals were cropped. Under a microscope, these single crystals exhibited sufficient size and quality for single crystal diffraction (Figure IV - 20).

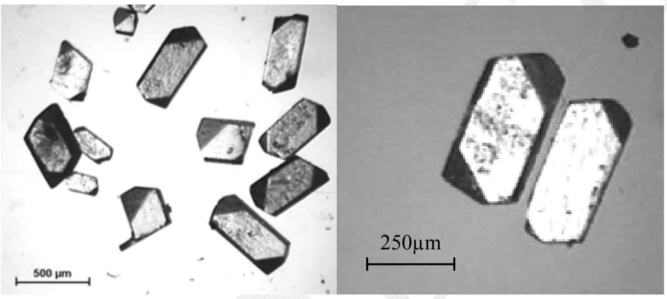

Figure IV - 20. Single crystals of dimer.

The resolution of the structure was performed and confirmed the existence of the dimer. Crystal data are summarized in Table V - 1. The crystal packing presented an uncommon feature: the asymmetric unit was composed of two "half" molecules, that is to say Z'=2x0.5.[199] Each molecule was centred on an inversion centre (located in the centre of the pyrazin ring, Figure IV - 21). On one molecule (Mol-A, Figure IV - 21), the fluorine atom exhibited a partial disorder on the benzene cycle. The statistical occupancy factor (s.o.f.) for this fluorine atom spread over two positions was respectively of 79 % and 21%.

CONFIDENTIAL

---

[199] A. J. C. Wilson; *Acta Cryst A49*, **1993**, 795-806.

	Dimer **46**
Chemical Formula	$C_{22}H_{20}F_2N_2$
Molecular Weight / *g.mol^{-1}*	350.40
Crystal System	Triclinic
Space group	P-1 (n°2)
Z , Z' (asymmetric units per unit cell)	2, 2x0.5
a / *Å*	9.2668(10)
b / *Å*	9.6027(10)
c / *Å*	11.3518(12)
α	65.849(2)°
β	77.487(2)°
γ	86.079(2)°
R factor (with I>2σI)	R1 = 0.0514 R2 = 0.134
V / Å^3	899.61(17)

Table V - 1. Crystal data of the dimer.

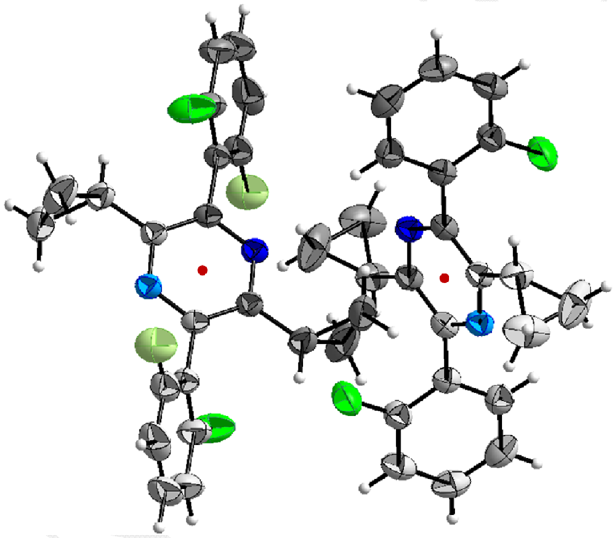

Figure IV - 21. The two fully regenerated molecules of the asymmetric unit (in light grey the part regenerated by the inversion centre - red dot). The molecule to the left exhibits a partial disorder on the fluorine atom which is divided onto two positions with s.o.f. of 79% and 21%.

In fact, the instability of the free amino ketone **37** was not surprising, both the carbonyl group and the free amine being reactive enough to form the diamine **47**. Then the aromatisation occurs, being the transformation irreversible (Figure IV - 22). As the hydrochloride salt was stable, it was used for the screening of conglomerate.

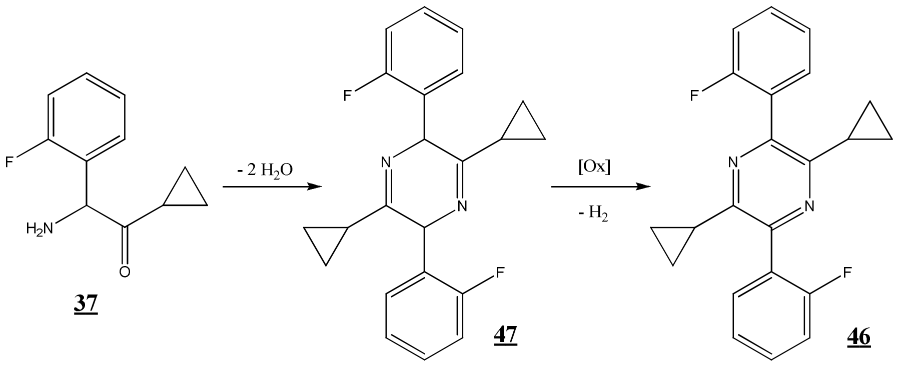

Figure IV - 22. Formation of the dimer.

First, only three different imines were synthesized (**39a-c**, Figure IV - 23). After evaporation of the solvent, mixtures of solid and brown oil were obtained. The ^{1}H NMR analyses revealed that the crude product was a mixture of the desired amine **39**, the unreacted benzaldehyde and the dimer **46** (probably the solid). Moreover, after few hours, imine was totally converted into dimer. Both free amino ketone and imines were not stable; the deracemisation of these compounds was thus impossible.

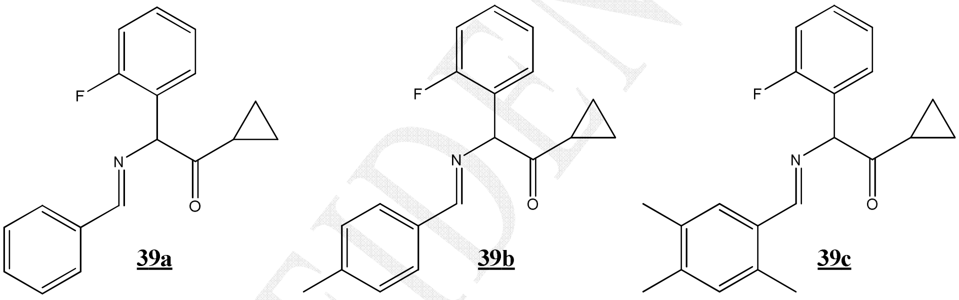

Figure IV - 23. Three cyclopropyl imines.

2. Screening of conglomerate

To avoid the formation of the dimer, a screening of conglomerate was performed by using a compound with a less reactive carbonyl group; the morpholine derivative **48**. The Boc-morpholine derivative was first deprotected then amines were synthesized.

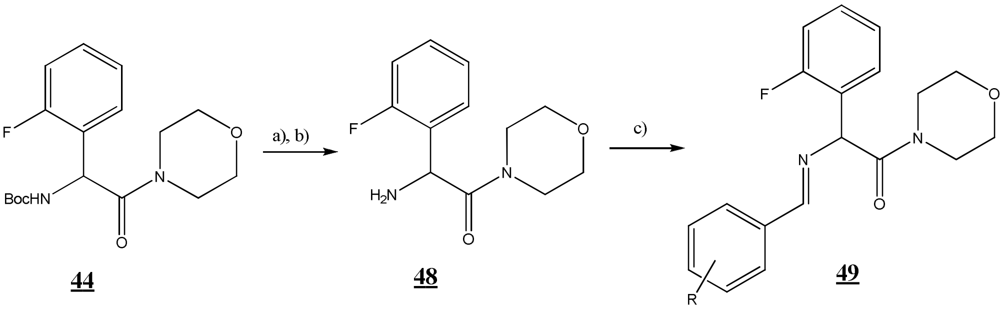

Figure IV - 24. Screening of conglomerate from morpholine derivatives. a) HCl, 1,4-dioxane, 94%, b) NaOH, water, quant., c) substituted benzaldehyde, NaSO$_4$, CH$_2$Cl$_2$.

CONFIDENTIAL

Before performing the screening of conglomerate, the stability of the free amine **48** was tested. The compound was refluxed overnight in acetonitrile then the solvent was evaporated. No signals of dimer or degradations were visible on ^{1}H NMR analyses. The stability of this compound was thus sufficient for the screening. Ten benzaldehydes, with different substituents (nature, number and/or position, Figure IV - 25), were involved in reaction of formation of imines. The choice of these benzaldehydes was arbitrary.

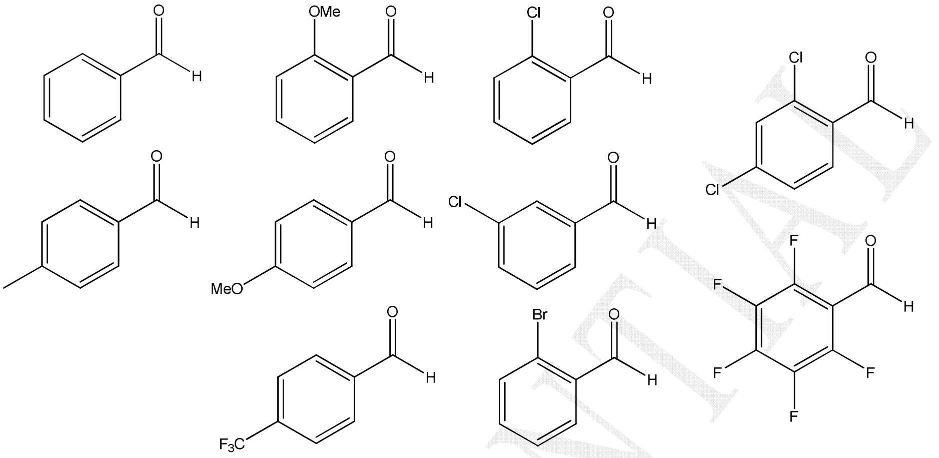

Figure IV - 25. Various benzaldehyde derivatives used for the screening of conglomerate.

Compounds with a good purity were easily obtained after synthesis without purification step and they were stable (no trace of dimer was visible on ^{1}H NMR analyses). Unfortunately, in each case, oil was obtained. Even after one year, samples were still oils. It was thus impossible to perform deracemisation.

Synthesis of imines with the Weinreb amide instead of the morpholine was also carried out (Figure IV - 26). Unfortunately, they also were obtained as oils.

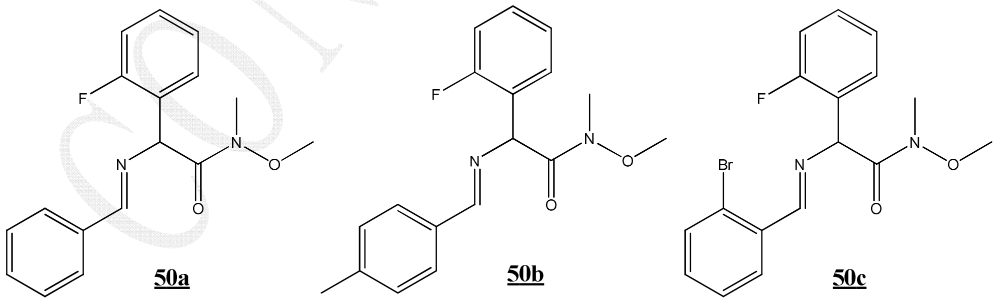

50a **50b** **50c**

Figure IV - 26. Imines synthesised from the Weinreb amide derivative.

CONFIDENTIAL

III - Alternative synthetic route

1. Synthesis of 2-fluorophenylglycinamide

For the synthesis of Clopidogrel, all the amines prepared for the screening of conglomerate were crystalline. These compounds were obtained from the 2-chlorophenylglycinamide **27**. Therefore we decided to modify the synthesis to include the screening of conglomerates from the 2-fluorophenylglycinamide **51**, hoping to have the same crystalline behaviour for the fluorinated imines than for the chlorinated imines.

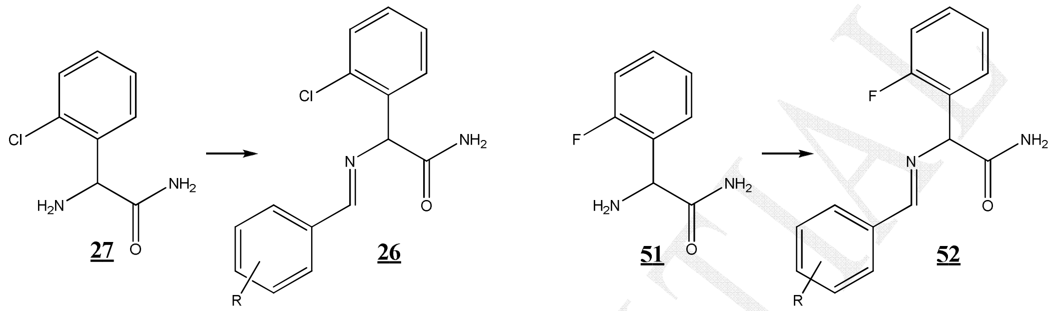

Figure IV - 27. Screening of conglomerates from the 2-chlorophenyglycinamide (left) and of the 2-fluorophenyglycinamide (right).

The same synthetic route was followed to carry out the screening of conglomerate (see Figure IV - 8): the 2-fluorophenylglycine **40** was first converted to the 2-fluorophenylglycinamide **51** then a small library of imines was synthesized by using various substituted benzaldehydes (**52a-j**, Figure IV - 28).

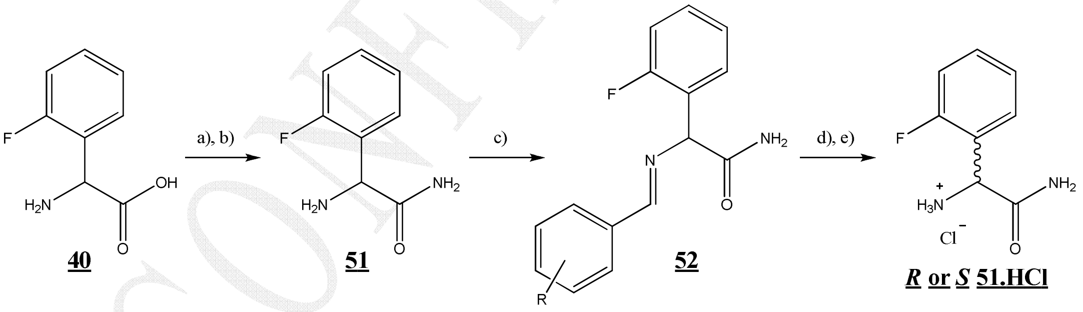

Figure IV - 28. Screening of conglomerate from the 2-fluorophenylglycinamide. a) $SOCl_2$, MeOH (95%), b) NH_3 30% in water (70%), c) substituted benzaldehyde, $NaSO_4$, CH_2Cl_2, d) DBU, glass beads, acetonitrile, e) HCl, acetone.

2. Screening of conglomerates

Ten benzaldehydes with different substituents (nature, number and/or position, Figure IV - 25) were arbitrary chosen then involved in reaction of formation of imines. The results of SHG measurements are summarized in Table V - 2:

CONFIDENTIAL

	52a	**52b**	**52c**	**52d**	**52e**
Aromatic aldehyde	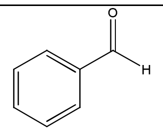	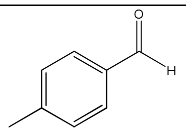	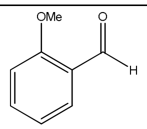	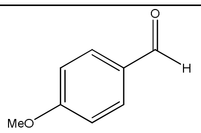	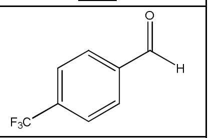
SHG	**positive signal**	negative signal	negative signal	weak positive signal	**positive signal**

	52f	**52g**	**52h**	**52i**	**52j**
Aromatic aldehyde	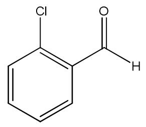	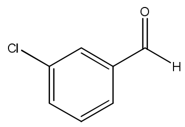	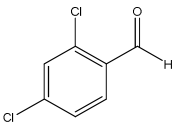	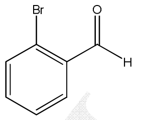	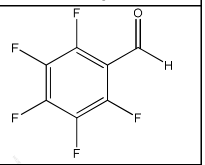
SHG	negative signal	oil	**positive signal**	weak positive signal	negative signal

Table V - 2. SGH measurements of the small library of imines.

Among the ten imines, three exhibited a positive signal in SHG, **52a**, **52e** and **52h**, and could therefore crystallise as conglomerate.

Unfortunately, because a lack of time and product (SHG analyses were performed one week before I went back in France), we had the possibility to try the deracemisation (and so to confirm the crystallisation as a conglomerate) of only one of these three compounds. We decided to work with the benzaldehyde derivative for two reasons:

- Benzaldehyde was cheaper than the 4-(trifluoromethyl)benzaldehyde and the 2,4-dichlorobenzaldehyde.
- The imine **26**, derived from the 2-chlorophenylglycinamide and benzaldehyde crystallised as a conglomerate. As we demonstrated in the previous chapter that it was possible for a series of compounds to exhibit the same crystal packing. We hoped that a same kind of pocket also exists for this series.

After synthesis of the imine **52a**, its deracemisation was tested. The compound **52a** (1g) was dissolved in acetonitrile (5g) at 50°C then BDU (17%) and glass beads (Ø2mm, 2.5g) were added. The reaction mixture was vigorously stirred and the temperature was slowly decreased to 20°C for 5h. The mixture was stirred an additional night at 20°C; the enantiomeric excess of the final solid phase was >99%. The deracemisation has been achieved; **52a** did crystallise as a conglomerate. Furthermore, XRPD patterns of the racemic mixture and of the pure enantiomer were superimposable (Figure IV - 29).

CONFIDENTIAL

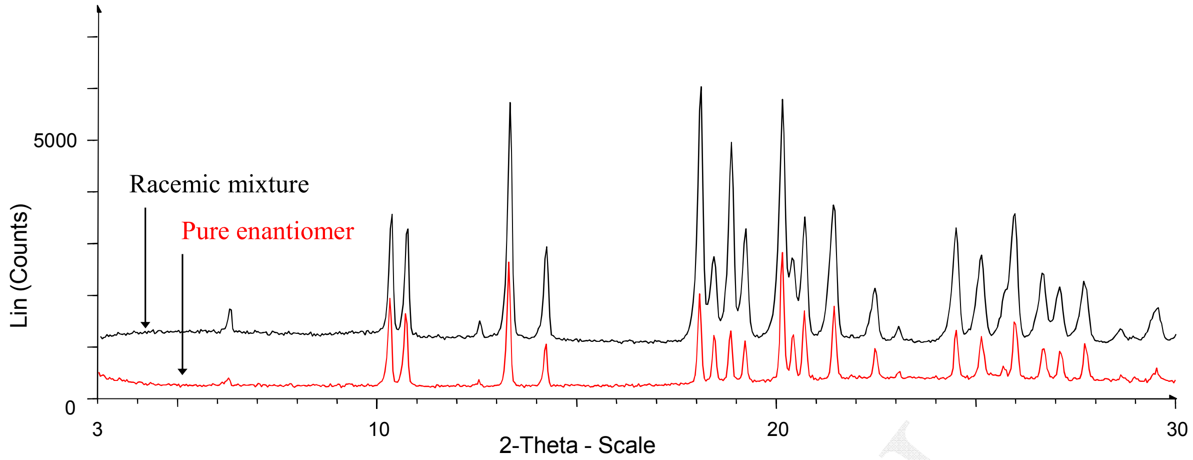

Figure IV - 29. Superimposed XRPD patterns of the racemic (in black) and of the pure enantiomer (in red) of 52a.

However, the yield of the deracemisation was very low since only 138mg (14%) of solid were harvested. This experiment was carried out just to determine if the deracemisation of this imine was possible without optimising the experimental conditions. The solubility was not known, that may explain the low yield. The optimisation of parameters was carried out in Rouen and are described in the following paragraph.

CONFIDENTIAL

IV - Deracemisations

1. Determination of the solubility of the imine

One of the first experiments was the determination of the solubility of the imine **52a** in several solvent, and particularly in acetonitrile, to optimise the parameters of the deracemisation.

a. Solubility in acetonitrile

The solubility of **52a** was determined by using the gravimetric method, at two different temperatures: 25°C (Table V - 3) and 50°C (Table V - 4).

	Mass of saturated solution	Mass of solid	Solubility	Average solubility
1	0.79170g	0.08904g	11.25%	**11.1%**
2	0.87911g	0.09658g	10.99%	
3	0.88336g	0.09824g	11.12%	

Table V - 3. Solubility of 52a in acetonitrile at 25°C.

	Mass of saturated solution	Mass of solid	Solubility	Average solubility
1	0.84660g	0.27906g	32.96%	**32.9%**
2	0.95627g	0.31537g	32.98%	
3	0.95914g	0.31491g	32.83%	

Table V - 4. Solubility of 52a in acetonitrile at 50°C.

29a has a solubility of 11.1% in acetonitrile at 25°C. This value can explain why the yield of the preliminary deracemisation was so low. 1g of **52a** and 5g of acetonitrile were used. At 25°C, and assuming that the DBU did not modify the solubility, 632mg of **52a** was dissolved and so only 368mg were in the solid phase. Therefore the theoretical maximal yield is 36.8% at 25°C and so higher at 20°C, the final temperature of the preliminary experiment. However, the yield was 14%. The solubility alone cannot explain the low yield and the origin of the problem must be finding elsewhere.

b. Solubility in tertbutylmethylether

The tertbutylmethylether (TBME) was used to wash the solid to remove all the DBU. If the solubility of the imine in TBME was not negligible, a part of the solid phase was dissolved, decreasing the yield of the deracemisation. The solubility of **52a** in TBME was thus measured at 25°C.

	Mass of saturated solution	Mass of solid	Solubility	Average solubility
1	0.64165g	0.00041g	0.06%	**0.1%**
2	0.61730g	0.00040g	0.06%	
3	0.70429g	0.00034g	0.05%	

Table V - 5. Solubility of 52a in TBME at 25°C.

The imine was almost insoluble in TBME. TBME was so a good solvent to remove the DBU without dissolving the imine.

c. Solubilities in other solvents

The solubility of imine **52a** was studied at 25°C for four additional solvents: ethyl acetate, ethanol, *n*-heptane and tetrahydrofurane THF (Table V - 6).

Solvent	Solubility
n-Heptane	0.0%
Ethanol	4.7%
Ethyl acetate	5.8%
THF	23.6%

Table V - 6. Solubilities of 52a in different solvents at 25°C.

CONFIDENTIAL

The solubility of **52a** in ethyl acetate and ethanol is around 5%; these values of solubilities are acceptable to perform a deracemisation; the amount of product in solution at the end of the experiment being quite low, but sufficient to ensure the exchange of matter.

The imine is totally insoluble in *n*-heptane which can be therefore used as anti-solvent if necessary. The solubility in THF is too high to perform deracemisation in good conditions; too much product is dissolved in the liquid phase.

CONFIDENTIAL

2. Optimisation of the experimental conditions

In acetonitrile, the solubility is 32.9% at 50°C, that is to say that, for example, that 2.454g of **52a** can be dissolved in 5g of solvent. If the final temperature of the deracemisation is 25°C (solubility = 11.1%), the solid phase is composed of 1.898g of **52a**, giving a theoretical maximal yield of 77%. The next deracemisations were carried out by using these conditions.

2.454g of **52a** were dissolved in 5g of acetonitrile at 52-53°C then the temperature was adjusted to 50°C. Glass beads (5g) and DBU (0.425g) were added then the mixture was cooled down to 25°C in 5h (5°C.h^{-1}) under a vigorous stirring. After 30 additional minutes at 25°C, the solid was filtered, washed with TBME (3x) then dried. 1.059g of solid was harvested, giving a yield of 58%, with an enantiomeric excess over 97%.

The yield increased compare to the first deracemisation but it was always lower than the theoretical yield (77%). 30 minutes at 25°C were maybe not sufficient to reach the equilibrium state; the entire solid had no had time to precipitate.

Two other experiments, A and B, were carried out in parallel, in the same conditions, except for the duration of the stirring at 25°C: the deracemisation A was stirred for one night whereas the deracemisation B was stirred for 3 days at 25°C (Table V - 7).

	52a	DBU	Blass beads	CH_3CN	Cooling rate 50°C → 25°C	Time at 25°C	Yield	e.e.
A	4.908g	0.3eq	10g	10g	5°C.h-1	One night	29%	>96%
B	4.908g	0.3eq	10g	10g	5°C.h-1	3 days	58%	>99.5%

Table V - 7. Experimental conditions of the two deracemisations A and B.

In the two cases, the final enantiomeric excess was very good; the peak of the second enantiomer was not detected in the case B in chiral HPLC. However, the yield of the deracemisation was not improved. It was even twice lower in the case A, experimental conditions (starting material, temperature…) being the same. Moreover, these results contradicted themselves: yields were the same when the mixture was stirred for 30 minutes or for 3 days at 25°C but it was lower when the mixture was stirred for one night. The duration of stirring at 25°C was therefore not a factor affecting the yield but it was necessary to reach an enantiomeric excess of 100%.

Other experiments were carried out from 50°C to 20°C (keeping identical the other experimental conditions) in order to increase the yield. Unfortunately, it was not increased; yields between 20% and 55% were obtained. Moreover, in one case, no solid had precipitated, even after seeding at 20°C then evaporation of a part of the solvent.

Furthermore, it was impossible to isolate the imine from the filtrate. When the solvent was evaporated, oil was obtained: a mixture of imine and DBU. Addition of anti solvent (such as TMBE or n-heptane) to the filtrate or trituration of the oil with solvents did not ensure the crystallisation of the compound.

The imine seemed to be difficult to separate from the DBU. The amount of base was thus decreased; 0.15 equivalent of base was used instead of 0.30 equivalent. Unfortunately, after four days at 20°C, the enantiomeric excess was only 75% with 38% yield and that did not make easier the separation of the imine and the DBU. Furthermore, besides the fact that the yield was not improved, the enantiomeric excess of the solid phase was low. A diminution of the ratio of base was thus not the key factor to increase the productivity of the process.

V - Study and characterisation of the different solid phases of the 2-(benzylideneamino)-2-(2-fluorophenyl)acetamide

For all these experiments, synthesis and deracemisations, the powders were analysed by X ray diffraction. In most cases, **52a** crystallised as a conglomerate. Nevertheless, in two cases, different XRPD patterns were obtained, resulting in the crystallisation of different phases: a monohydrate and an undetermined phase. These different phases were analysed by TGA-DSC and thermal TR-XRPD (temperature resolved X-ray powder diffraction). Moreover, the crystal structures of the conglomerate and of the monohydrate were resolved.

The existence of these two phases could disturb the crystallisation of the pure enantiomer for deracemisations and therefore could explain the low yields.

CONFIDENTIAL

1. Study of the conglomerate

a. Resolution of the structure

No single crystals of the conglomerate were obtained. However, the structure of a similar compound, the 2-(benzylideneamino)-2-(2-chlorophenyl)acetamide **26**, was already described in the literature.[100]

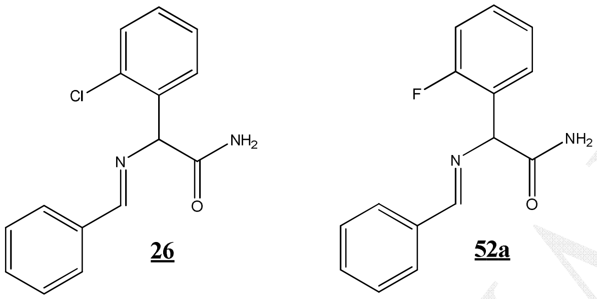

Figure IV - 30. Chemical structures of the 2-(benzylideneamino)-2-(2-chlorophenyl)acetamide 26 and of the 2-(benzylideneamino)-2-(2-fluorophenyl)acetamide 52a.

The crystal data were downloaded on the CSD database (available under the reference code OHODUL) then the chlorine atom was replaced by a fluorine atom in the crystal structure. If these two compounds crystallised in similar crystal packings, the calculated XRPD of the fluorinated compound **52a** resulting of the refinement of the structure parameters were the same than the experimental one. If XRPD were not superimposable, that means that the fluorinated compound **52a** did not crystallise in the same packing that the chlorinated compound **26**. The superimposition of the calculated and the experimental XRPD are shown on Figure IV - 31: they match perfectly. Therefore these two compounds crystallised in the same crystal packing. The cell parameters of **26** and **52a** are summarised in Table V - 8.

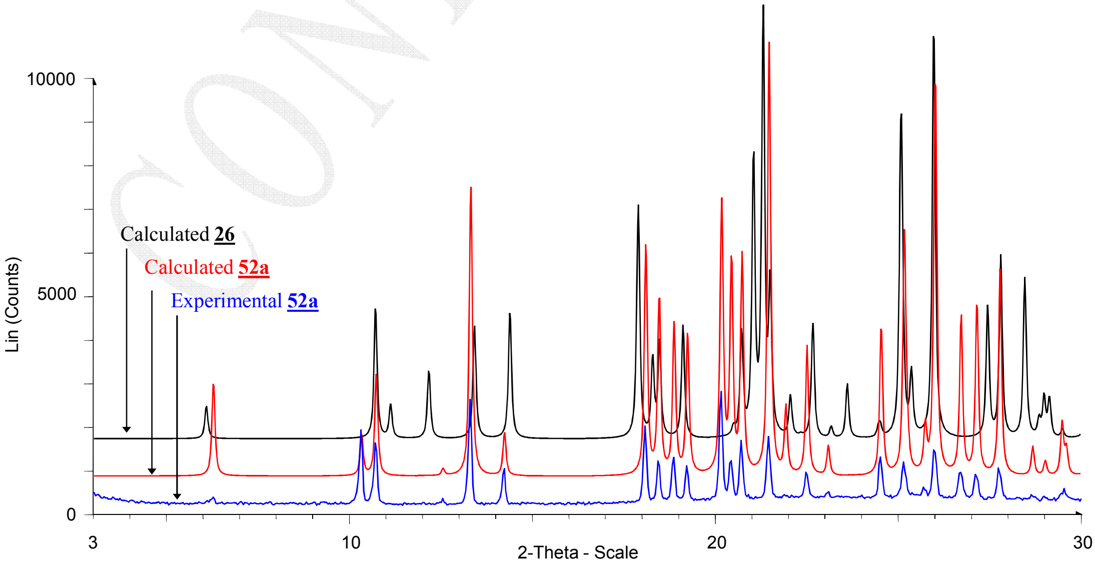

Figure IV - 31. Superimposition of experimental (in blue) and calculated (in red) XRPD patterns of the 2-(benzylideneamino)-2-(2-fluorophenyl)acetamide 52a, and of the calculated XRPD pattern of the 2-(benzylideneamino)-2-(2-chlorophenyl)acetamide 26 (in black).

CONFIDENTIAL

	26	**52a**
Chemical Formula	$C_{15}H_{13}ClN_2O$	$C_{15}H_{13}FN_2O$
Molecular Weight / *g.mol*$^{-1}$	272.73	256.27
Crystal System	Monoclinic	Monoclinic
Space group	$P2_1$	$P2_1$
Z , Z' (asymmetric units per unit cell)	2, 1	2, 1
a / *Å*	8.454(7)	8.814(5)
b / *Å*	5.082(4)	5.105(12)
c / *Å*	14.886(13)	14.509(18)
β / °	102.430(13)	103.821(0)
V / *Å*^{3}	624.559	633.937
d_{calc} / *g.cm*$^{-3}$	1.45	1.34

Table V - 8. Unit cell parameters of 26 (from CSD database) and 52a (obtain from routine XRPD).

The unit cell parameters of the fluorinated imine **52a** are bigger than the cell parameters of the chlorinated imine **26**, that is in contradiction with the relative length of the halogens-carbon bonds; C-F bonds are shorter than C-Cl bonds. The refinement of the structure was limited by the quality of the XRPD pattern, which was sufficient to obtain the crystal lattice but not to obtain the best cell parameters.

The asymmetric unit was built from one molecule of the 2-(benzylideneamino)-2-(2-fluorophenyl)acetamide **52a** (Figure IV - 32).

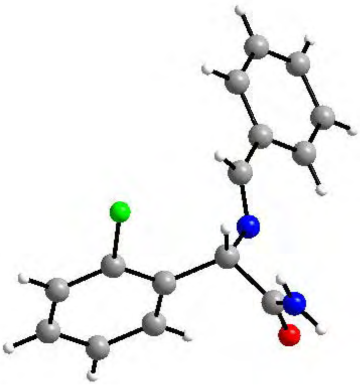

Figure IV - 32. Asymmetric unit of the 2-(benzylideneamino)-2-(2-fluorophenyl)acetamide 52a in the $P2_1$ space group.

The asymmetric units interacted together by means of hydrogen bonds formed with -C=O and $-NH_2$ of amide groups of two different molecules. In one molecule, both C=O and NH_2 group were involved in hydrogen bonds with two different molecules, generating infinite ribbons along *b* axis (Figure IV - 33). The length of the hydrogen bonds was 2.0 Å.

CONFIDENTIAL

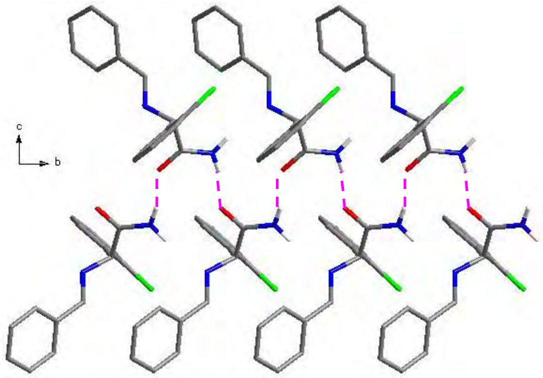

Figure IV - 33. Infinite ribbons along *b* axis generates by means of hydrogen bonds (dashed pink lines).

The cohesion between molecules in these ribbons was reinforced by means of two kinds of π-interactions between two consecutive unsubstituted rings and two consecutive fluorinated rings (Figure IV - 34). The distance between to consecutive cycles was 3.6 Å.

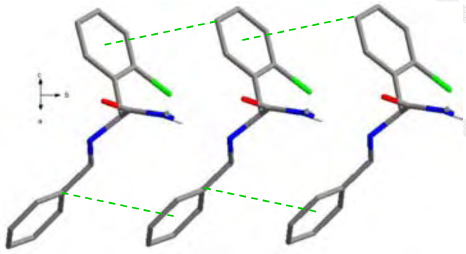

Figure IV - 34. π-interactions between two aromatic rings.

Ribbons were connected between them by means of π-interactions in T-shape (Figure IV - 35). The unsubstituted aromatic rings were interacting in the (001) plan (dashed green lines) whereas the fluorinated aromatics rings were interacting along the *b* axis (dashed blue lines). The distances between two consecutive rings were 3.97 Å and 3.84 Å, respectively and the angles were 78° and 81°, respectively.

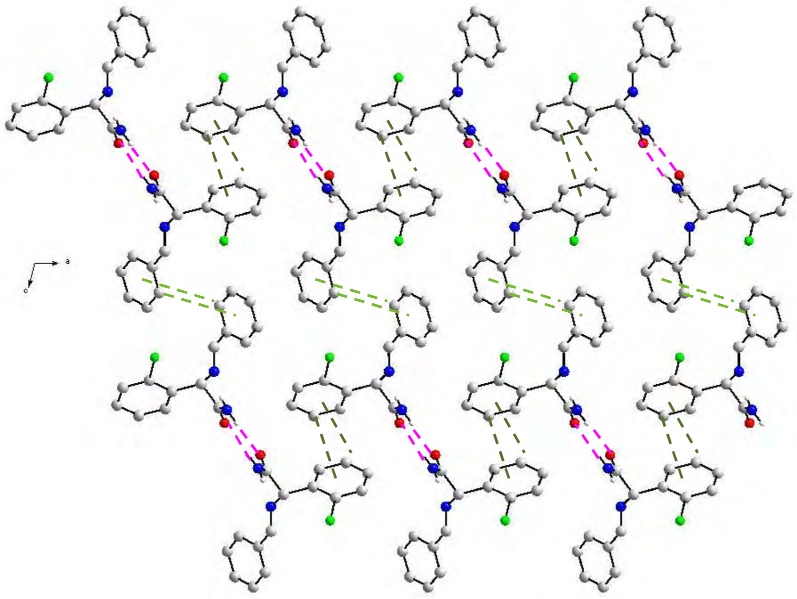

Figure IV - 35. π-interactions between ribbons. One ribbon is encircled in red.

CONFIDENTIAL

b. Thermal analysis

DSC analyses of the pure enantiomer and of the racemic conglomerate were performed (Figure IV - 36). As expected, the melting point of the pure enantiomer (117.5°C) was higher than the melting point of the racemic conglomerate (113.2°C). However, the difference between these two temperatures was lower than usual since only 4.2°C were detected. Both racemic conglomerate and pure enantiomer were stable up to the melt.

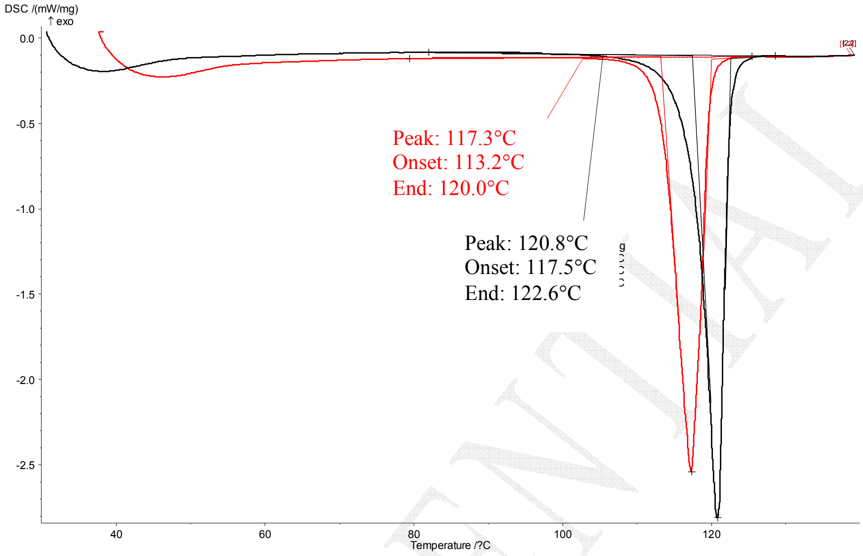

Figure IV - 36. DSC analyses of the racemic conglomerate (in red) and of the pure enantiomer (in black). Heating rate: 5K/min from 30°C to 140°C.

CONFIDENTIAL

2. Study of the unknown phase

a. X Ray diffraction analyses

At the end of one synthesis of the imine, a different XRPD pattern was obtained. The superimposition of XRPD patterns revealed that it was a mixture of phases: the conglomerate and an unknown phase (Figure IV - 37).

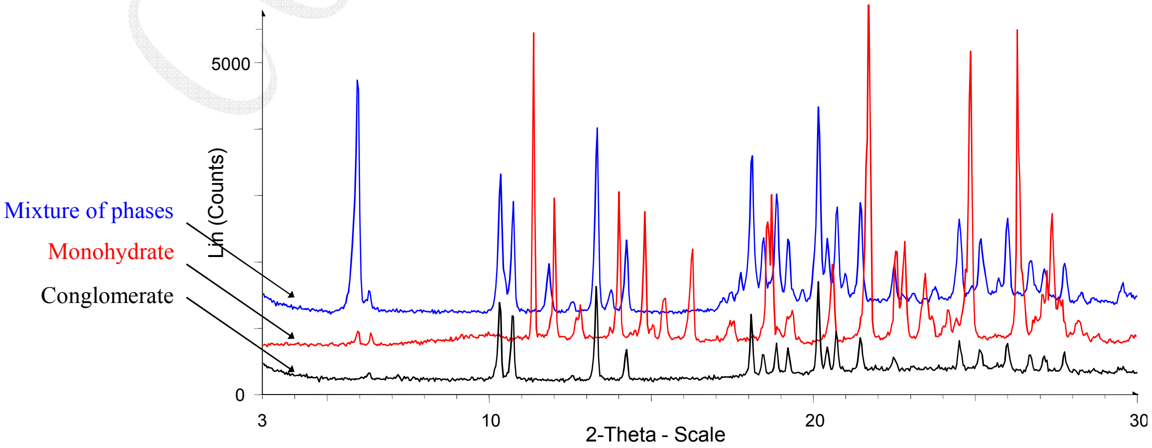

Figure IV - 37. Superimposition of XRPD of the conglomeate (in black), the monohydrate (in red) and of the mixture of conglomerate and of the new phase (in blue).

^{1}H NMR revealed that additional peaks were present in the aromatic zone. The imine was thus not pure. But only ≈5% of impurity(ies) were present so it was difficult to assume that the additional peaks on the XRPD pattern, and most particularly concerning the first large peak, were due to this impurity only.

The stability of this phase was then studied in acetonitrile. A suspension of this powder was stirred in acetonitrile at 25°C. After three days, the powder was analysed: no evolution was visible. Therefore the unknown phase was also stable in acetonitrile and cannot be easily converted into the conglomerate.

As this phase was not pure, it was impossible to have access to structural characteristics and no single crystals were obtained.

b. Thermal analyses

In order to determine the thermal behaviour of this mixture of phases, a DSC analysis was carried out and was compared to the DSC curve of the racemic conglomerate.

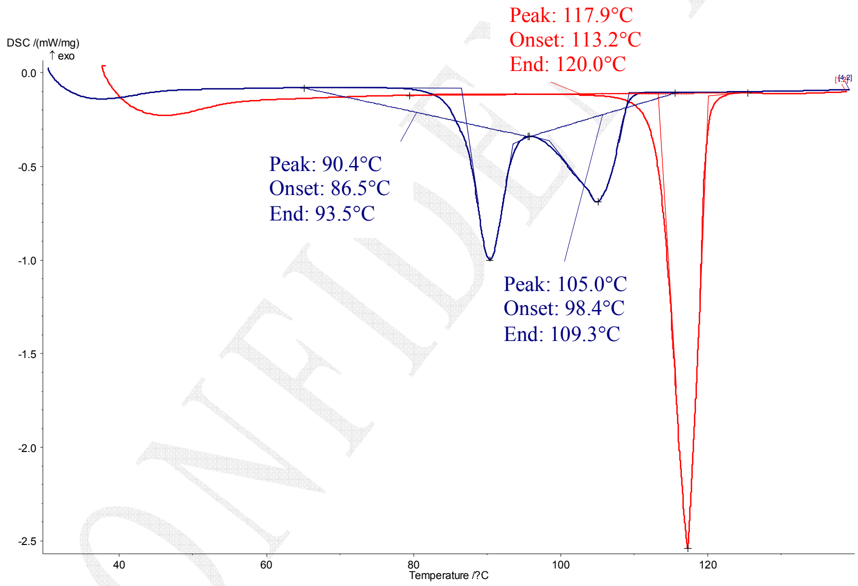

Figure IV - 38. Superimposition of DSC analyses of the racemic conglomerate (in red) and of the mixture of phases (in blue), from 30°C to 140°C (5°C/min).

Two phenomena occurred and something rather surprising appeared: the melting point of the conglomerate was missing while the conglomerate was present in the starting material. In order to better understand what happened during the heating, the evolution of the crystalline structure was monitored by TR-XRPD (Figure IV - 39).

CONFIDENTIAL

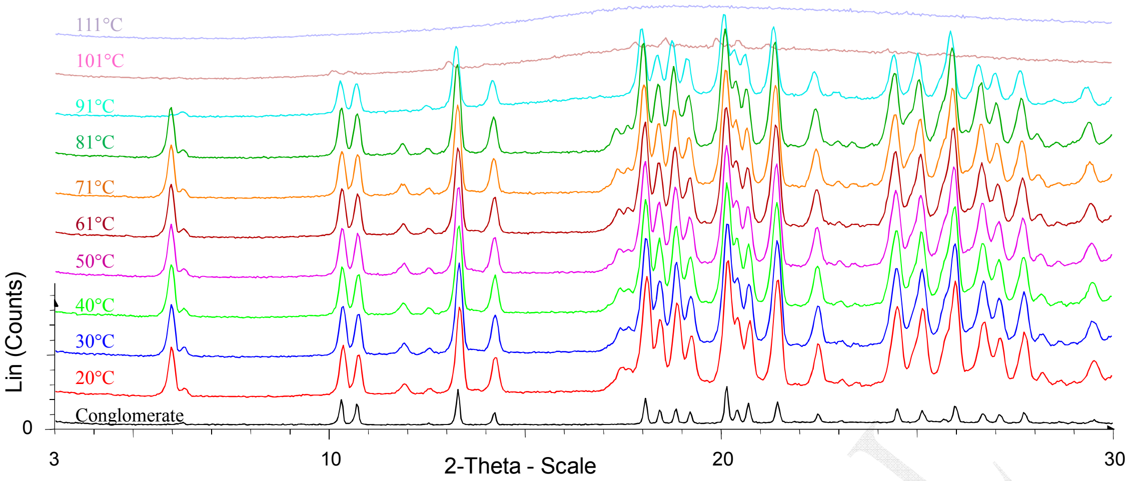

Figure IV - 39. Evolution of the crystalline phase over temperature. Superimposition with the conglomerate (in black). In red, the XRPD pattern of the mixture between the conglomerate and the unknown phase.

Between 81°C and 91°C, a first phenomenon occurred. The unknown phase disappeared but seemed not to be converted into the conglomerate phase; the base line of the diffractogramme became less well defined, most probably due to the melting of the unknown phase. The melting of the conglomerate occurred between 91° and 101°C.

These two phenomena and their corresponding temperatures were in accordance with the DSC analysis of the mixture of phases; the second endothermique peak on the DSC curve was therefore due to the melt of the conglomerate. However it was different than the melting point of the pure racemic conglomerate (Figure IV - 36); the chemical impurity may sufficiently disturb the behaviour of the conglomerate to decrease its melting point.

3. Study of the monohydrate

a. Resolution of the structure

The imine **52a** used for the solubility was recovered in a large beaker by using acetonitrile. The solvent was then evaporated under room conditions and single crystals appeared (Figure IV - 40).

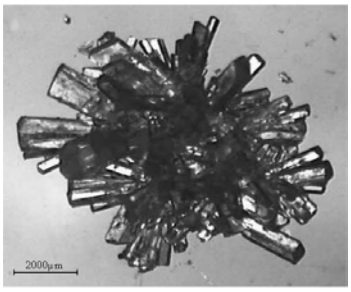

Figure IV - 40. Crystals appears in the beaker.

CONFIDENTIAL

Few of them were kept for the resolution of the structure, the rest was milled. X ray diffraction analyses on the powder highlighted the existence of a new phase which did not match with the conglomerate, as expected (Figure IV - 41).

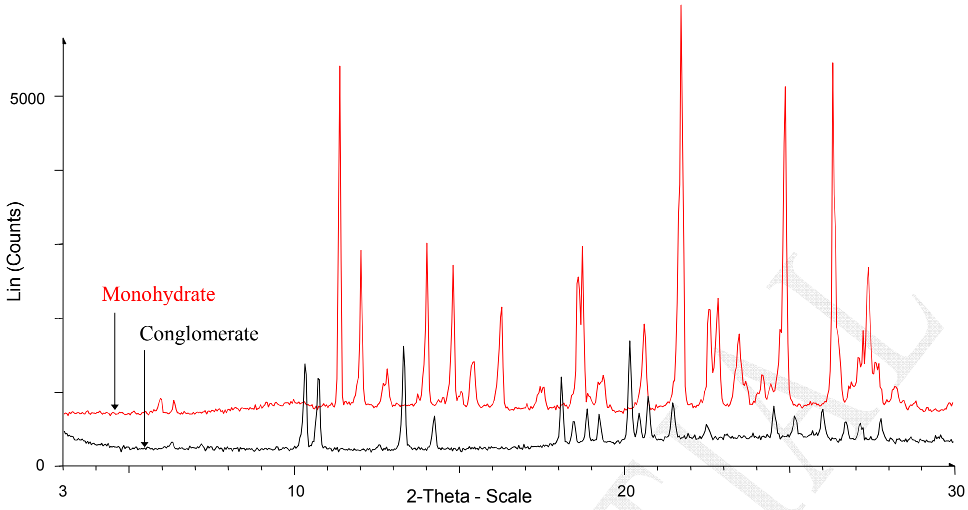

Figure IV - 41. XRPD patterns of conglomerate (in black) and of the monohydrate (in red).

The resolution of the structure from single crystals revealed that this phase corresponds to the crystallisation of the monohydrate of the imine **52a**. The asymmetric unit was made of one molecule of imine and one molecule of water (Figure IV - 42).

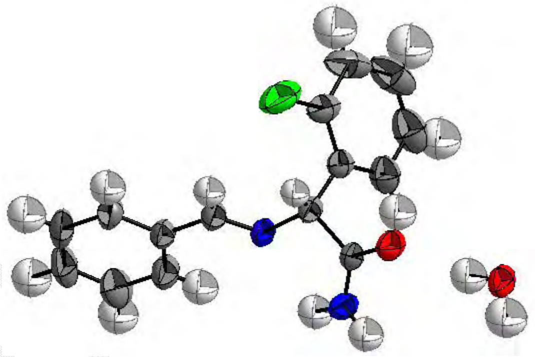

Figure IV - 42. Asymmetric unit of the monohydrate.

The crystal data are given in Table V - 9. The monohydrated form crystallised in $P2_1/c$ space group, a centrosymmetric space group. Therefore the monohydrated form did not crystallise as a conglomerate.

CONFIDENTIAL

	52a.H_2O
Chemical Formula	$C_{15}H_{15}FN_2O_2$
Molecular Weight / *g.mol^{-1}*	274.29
Crystal System	Monoclinic
Space group	*P*2_1/c
Z , Z' (asymmetric units per unit cell)	4, 1
a / *Å*	13.9829(14)
b / *Å*	6.6374(7)
c / *Å*	15.8034(15)
β / °	100.202(2)
V / *Å^3*	1443.5(3)
R factor (with I>2σI)	R1 = 0.0659 wR2 = 0.1907
d_{calc} / *g.cm^{-3}*	1.262

Table V - 9. Crystal data of the monohydrate form.

Imines were connected between them through hydrogen bonds with H_2O: homochiral ribbons were generated by the 2_1 screw axis parallel to the *b* axis (Figure IV - 43). One imine was interacting with three molecules of water, and one molecule of water formed hydrogen bonds with three different molecules of imine. The length of hydrogen bonds was circa 2 Å.

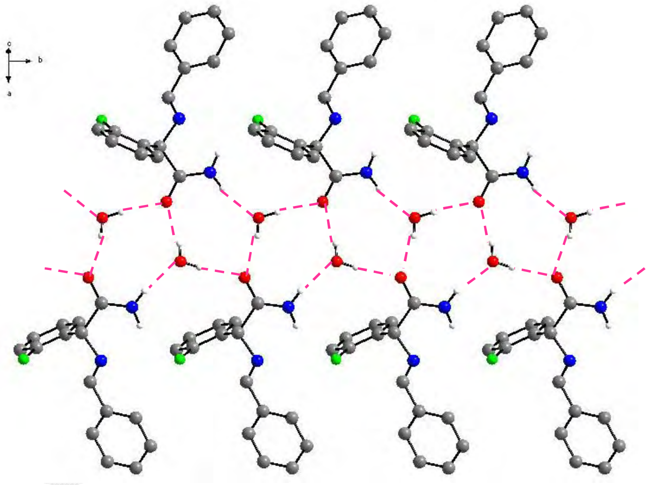

Figure IV - 43. Infinite homochiral ribbons along *b* axis generates by means of hydrogens bonds with water (dashed pink lines).

Homochiral ribbons were connected between them by means of π-interactions (dashed green lines) and π-interactions in T-shape (dashed blue lines). Heterochiral dimers were formed by these two kinds of π-interactions (Figure IV - 44).

CONFIDENTIAL

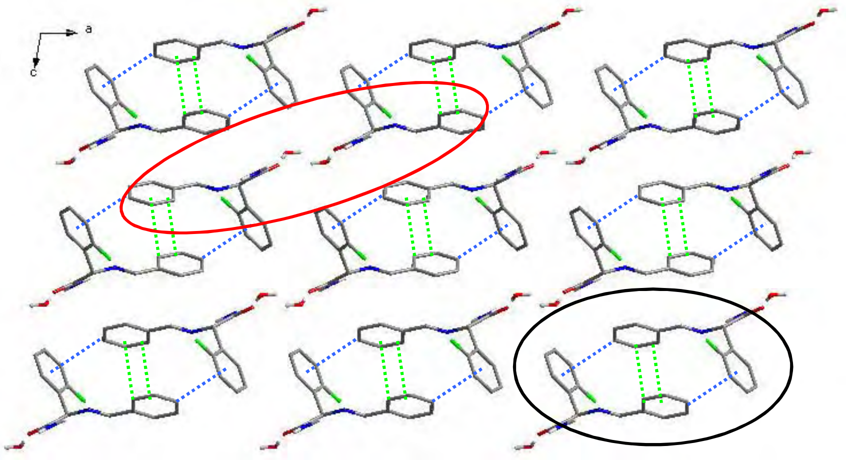

Figure IV - 44. Interactions between homochiral ribbons by means of π-interactions. One homochiral ribbon is circled in red and one heterochiral dimer is circled in black.

The infinite ribbons, connected together by means of π-interactions, were creating heterochiral slices parallel to the (102) plane of the crystal lattice (Figure IV - 45).

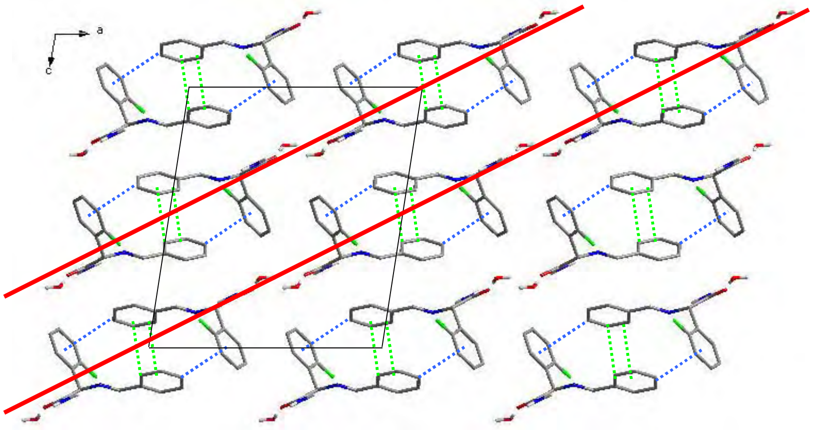

Figure IV - 45. Heterochiral slices creating by hydrogen bonds and π-interactions.

b. Relative stability in solution

The stability of the monohydrate was studied in acetonitrile, the solvent of the deracemisation. A suspension of monohydrate was stirred in acetonitrile at 25°C. After three days, the powder was analysed: the monohydrate was totally converted into the conglomerate. Therefore the monohydrate was not stable in the conditions of the deracemisation and mustn't be the reason why the yields are so low.

CONFIDENTIAL

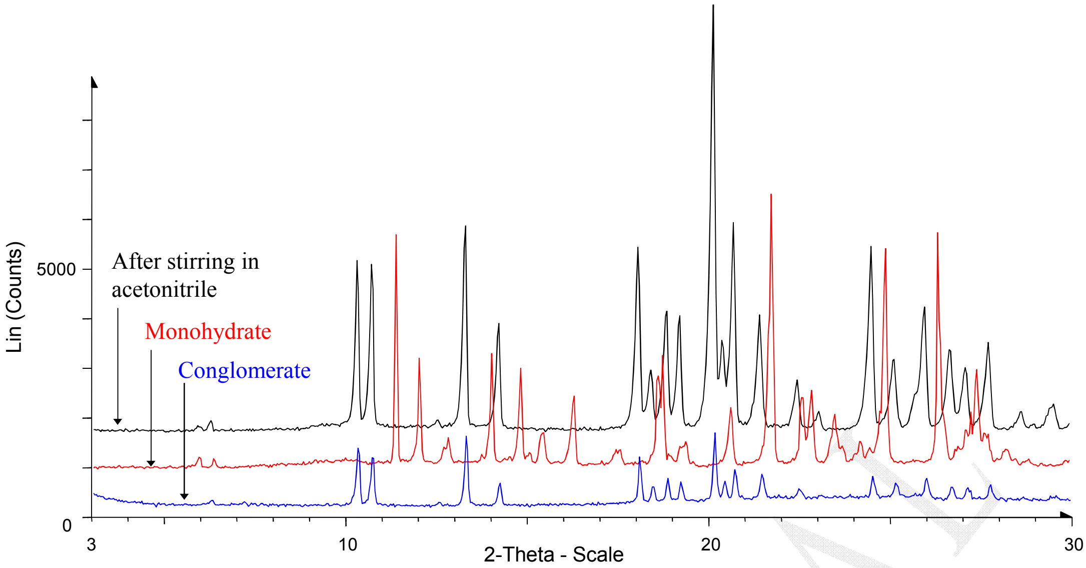

Figure IV - 46. Superimposition of the XRPD patterns of the conglomerate (in blue) and of the monohydrate before (in red) and after (in black) the stirring in acetonitrile.

c. Thermal analyses

The TGA-DSC of the monohydrate was carried out. The mass of the sample decreased during the analysis, corresponding to the departure of water molecules. However, the mass loss was only 5.7% whereas the theoretical mass loss was 6.5%. The monohydrate was most probably not pure which may explain a part of the number of phenomena that occurred during the analysis.

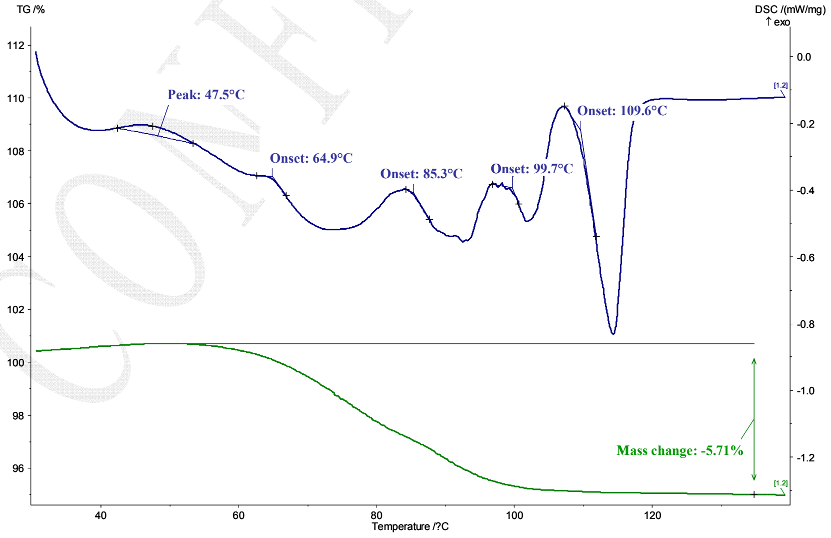

Figure IV - 47. TGA-DSC analysis of the monohydrate from 30°C to 140°C (5°C/min).

To better understand what happened during the heating, the evolution of the crystalline structure was followed by X ray diffraction. The results are drawn on Figure IV - 48

CONFIDENTIAL

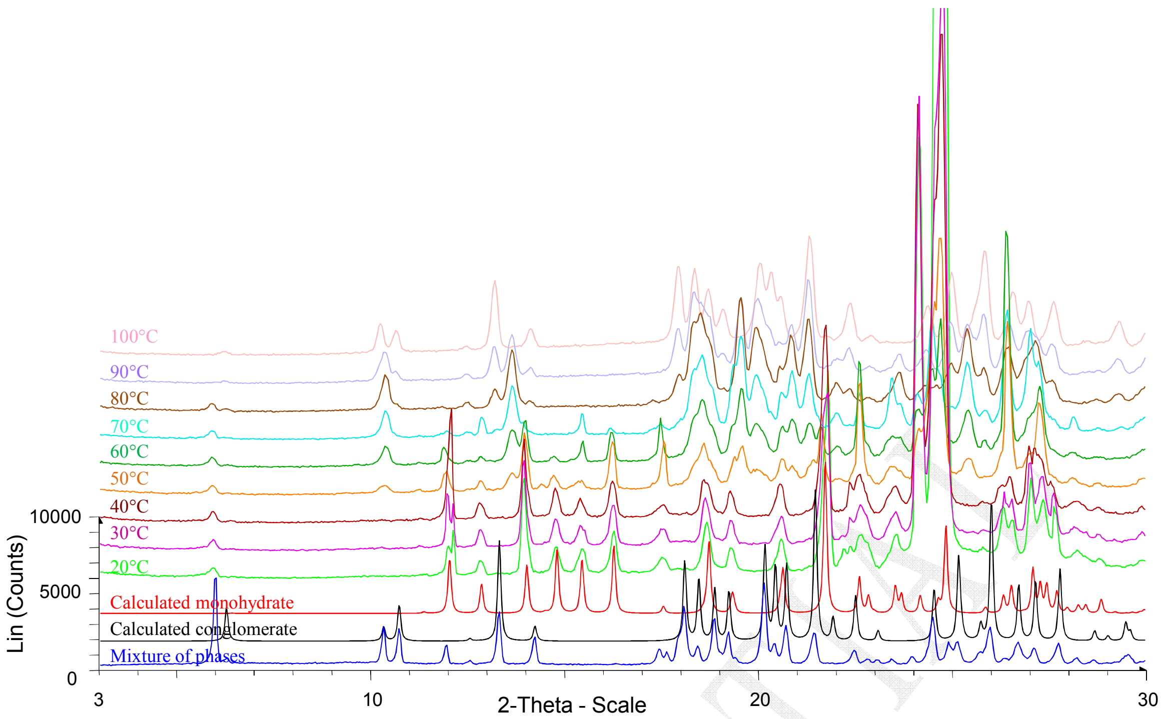

Figure IV - 48. Evolution of the crystalline phase over temperature. Superimposition with calculated XRPD patterns of the monohydrate (in red) and of the conglomerate (in black). In blue, the XRPD pattern of the mixture between the conglomerate and the unknown phase.

First, we can notice that the starting monohydrate phase was not pure since additional peaks are visible compared to the calculated XRPD. Several phenomena on the DSC curve were therefore not only due to the thermal behaviour of the monohydrate phase. The main impurity was clearly detected by a peak at circa 6θ; one peak disappeared when another one (corresponding to the conglomerate) appeared. This peak may correspond to the unknown phase. However, as the characteristics of this phase remained undetermined, it was difficult to conclude.

Secondly, all the starting material, that is to say the monohydrate and the impurity, was converted into the conglomerate at 80°C. Therefore the conglomerate can be considered as the stable form at high temperature.

The DSC analyses of the monohydrate and of the racemic conglomerate were compared (Figure IV - 49): as the monohydrate was converted into the conglomerate, the last phenomenon should correspond to the melt of the racemic conglomerate (113.2°C). Unfortunately, it was not the case since the last phenomenon occurred at 109.5°C. This difference may be explained by the presence of impurities not detected on XRPD patterns.

CONFIDENTIAL

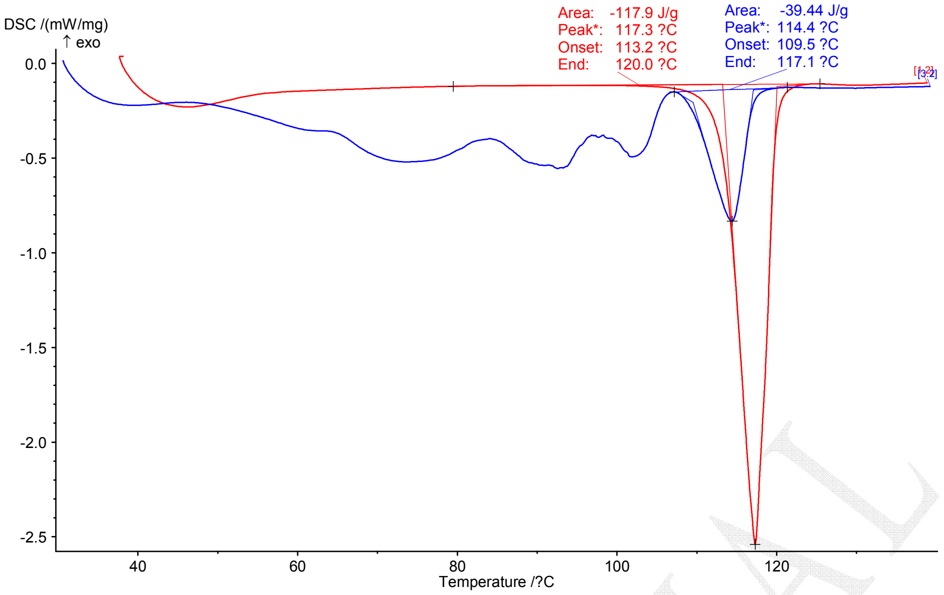

Figure IV - 49. Superimposition of DSC analyses of the racemic conglomerate (in red) and of the monohydrate (in blue), from 30°C to 140°C (5°C/min).

4. Comparisons between structures

TR-XRPD of the monohydrate has shown that the monohydrate was converted into the conglomerate at circa 80°C. Therefore, structures of these two phases were compared to understand how the conversion can occur; if filiations exist between the two structures or if it is a total destructive/reconstructive mechanism.

By comparing the projections along the *b* axis, high similarities were observed: ribbons along the *b* directions were generated by a 2_1 screw axis and molecules were connected by means of hydrogen bonds (Figure IV - 50).

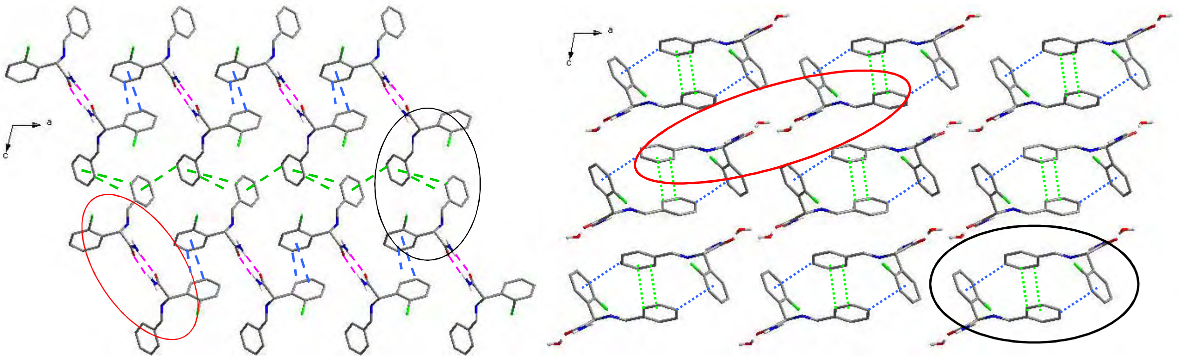

Figure IV - 50. Projections along *b* axes of the conglomerate (left) and of the monohydrate (right). One ribbon is encircled in red and one "dimer" is encircled in black.

No dimer existed in the structure of the conglomerate but the relative position of the aromatic rings shew similarities with the structure of the monohydrate: π interactions between the two

CONFIDENTIAL

unsubstituted rings also existed. We can imagine that the departure of water molecules move closer the molecules of imine to form hydrogen bonds between the amide groups, breaking the dimers. However, such mechanism cannot lead to the crystallisation of a conglomerate since the two enantiomers are present inside the crystal structure.

The case of this imine is very similar to another one previously studied in the laboratory. In 2011, Amharar *et al.* described the dehydration mechanism of a hydantoin derivative, the 5-methyl-5-(4'-ethylphenyl)hydantoin.[200] This compound crystallises as an anhydrous conglomerate (called C-18H) and a monohydrate racemic compound (HR-18H). A third phase, an anhydrous racemic compound (AR-18H) also exists. The three structures exhibit homochiral molecular ribbons generated by hydrogen bond networks (Figure IV - 51).

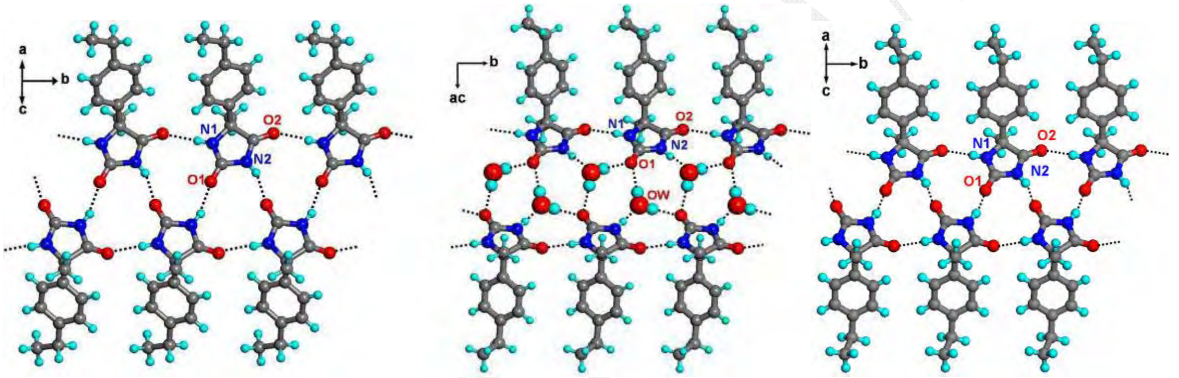

Figure IV - 51. Hydrogen bond networks and resulting molecular ribbons in the crystal structures of the anhydrous conglomerate (left) and the monohydrate racemic compound (middle) and of the anhydrous racemic compound (right).[200]

The authors studied the relative stability of these three phases. HR-18H can be reversibly converted to AR-18H, but the both transformation toward C-18H is irreversible (Figure IV - 52).

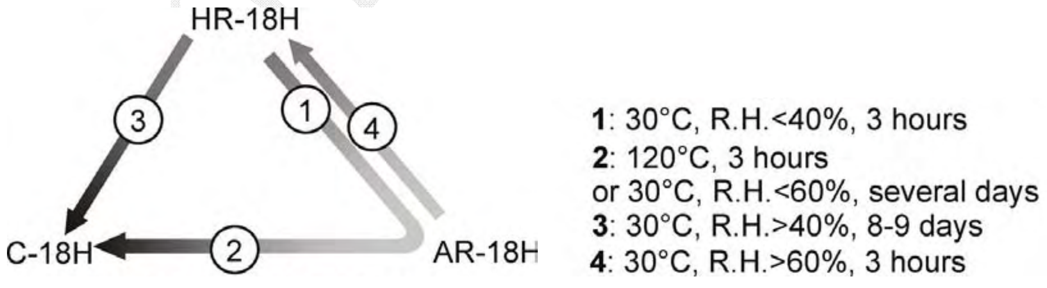
HR-18H
3
1
4
C-18H
2
AR-18H
1: 30°C, R.H.<40%, 3 hours
2: 120°C, 3 hours
or 30°C, R.H.<60%, several days
3: 30°C, R.H.>40%, 8-9 days
4: 30°C, R.H.>60%, 3 hours

Figure IV - 52. Experimental conditions required for solid-solid transformations between HR-18H, AR-18H and C-18H.[200]

To explain the reversible transformation from HR-18H to AR-18H, Amharar *et al.* proposed a zip-mechanism; a nondestructive and cooperative mechanism as illustrated on Figure IV - 53.

---

[200] Y. Amharar, S. Petit, M. Sanselme, Y. Cartigny, M.-N. Petit, G. Coquerel; *Cryst. Growth Des.*, **2011**, 11(6), 1453-2462.

The departure of water along the *b* axis enable the two parts of the ribbon initially hydrated to join them to form a new anhydrous ribbon, inducing a persistence of the main structural features of the crystal lattice.

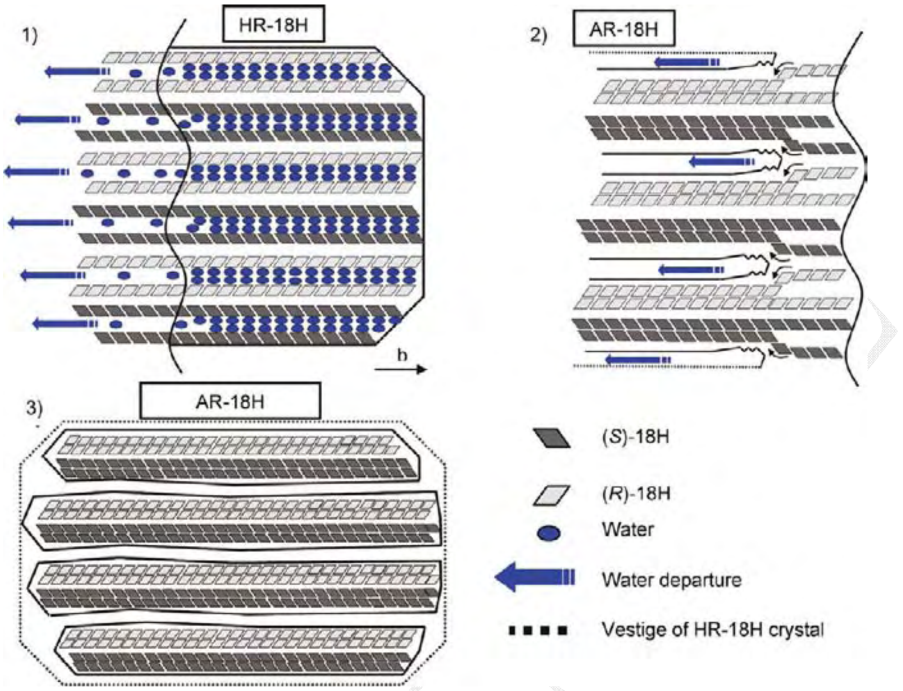
1)
HR-18H
b
2)
AR-18H
3)
AR-18H
(*S*)-18H
(*R*)-18H
Water
Water departure
Vestige of HR-18H crystal

Figure IV - 53. Schematic representation of the probable dehydration mechanism from HR-18H to AR-18H through a zip-mechanism.

One the other hand, a destructive/reconstructive mechanism was proposed to explain the transformation of HR-18H into C-18H, in which water molecules acts as plasticizer (Figure IV - 54). "*The progressive departure of water produces a highly defective crystal packing of 18H that can be assimilated to an amorphous phase, and the presence of residual water in this intermediate zone could facilitate the crystallisation of the conglomerate.*"

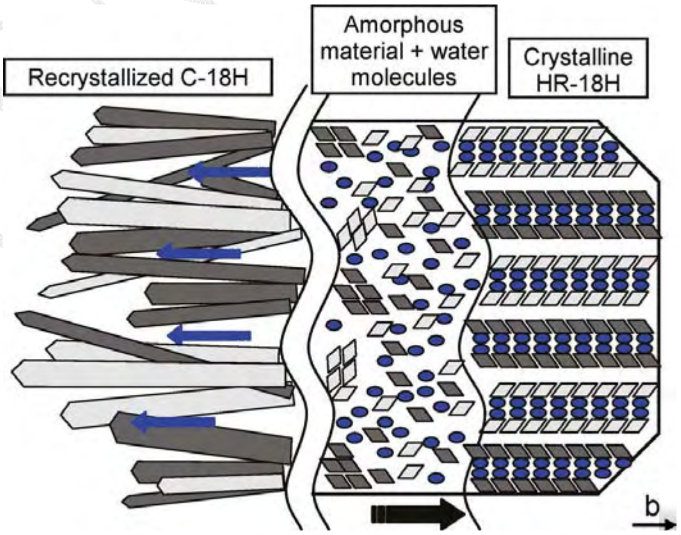
Recrystallized C-18H
Amorphous material + water molecules
Crystalline HR-18H
b

Figure IV - 54. Schematic representation of the hypothetical mechanism for the transformation between HR-18H and C-18H. The bold arrow indicates the direction of propagation of the interface.[200]

These mechanisms could explain the solid-solid transition observed by TR-XRPD analyses, the similarities between the imine **52a** and the 18H being significant:

- Existence of three phases including an anhydrous conglomerate and monohydrate racemic compound.
- The conglomerate is the stable phase.
- Formation of homochiral molecular ribbons generated by hydrogen bond networks.

However, additional experiments, such as DVS analysis and study of the relative stability of the three phases of **52a** must be carried out to conclude. The determination of the structure of the unknown phase could also give relevant information.

VI - Conclusion

The synthesis of Prasugrel as pure enantiomer was found more difficult than anticipated, mainly because the instability of the amino ketone **37** leading to the formation of the stable dimer **46** and because of the formation of oils (**48a-j** and **48a-c**).

The deracemisation by attrition of the imine **52a** has been achieved; the final enantiomeric excess was very good (>95%) but the yield was poor (between 20% and 55%). A screening of organic base could be carried out to find better experimental conditions, but the main issue is most probably the existence of the undetermined phase which is also stable in acetonitrile. The determination of the stability domains of the conglomerate and of the undetermined phase in acetonitrile, and the building of the ternary phase diagram could be a good way to improve the experimental conditions of the deracemisation.

Two other imines, **52e** and **52h**, gave a positive signal in SHG. If these two compounds effectively crystallise as conglomerate, they could be a good alternative to by-pass the existence of several competitive solid phases of **52a** and to increase the productivity of the deracemisation step.

CONFIDENTIAL

CONFIDENTIAL

General Conclusion

This work was dedicated to chirality, and how crystallisation can be an efficient tool for the discrimination and the production of pure enantiomers of active pharmaceutical ingredients.

A small library of β-cyclodextrins with an acidic or basic hook was synthesized with success. The selectivity of the syntheses was satisfactory but the purification was quite difficult, probably due to the ability to the cyclodextrins to form inclusion complexes. Analyses highlighted that a large range of hydrates exists for these cyclodextrins derivatives that can explain the difficulty to obtain well crystalline phases as well as suitable single crystals. The study of inclusion complexes by using the monosubstituted β-cyclodextrins has only just started and no chiral discrimination was yet observed even if the formation of inclusion complexes was confirmed. The optimisation of experimental conditions, and particularly the determination of the host/guest/solvents phase diagrams, may rationalise the chiral discrimination.

The second part of the thesis was devoted to the enantioamplification by means simultaneous: i) Crystallisation of a stable conglomerate. ii) Fast racemisation in solution and iii) Breakage/dissolution/recrystallisation of particles in suspension undergoing a flux of energy (glass beads or ultrasounds or temperature cycling).

Unfortunately, it is currently impossible to predict if a racemic mixture crystallises as a conglomerate or not, but it appears that limited modifications of the substituents of a compound which crystallises as a stable conglomerate can lead to a series of conglomerate forming systems. If they are not isostructural, they, at least, show extensive structural similarities in their crystal packings. Compounds of a such series behave as if a pocket exists, in which substituents can be modulated without impairing the full chiral discrimination of the crystal packing.

The study of the evolution of the crystal size distribution during the deracemisation process with glass beads or with ultrasounds led to spot the following features:

- A random delay in the “irreversible” evolution of the enantiomeric excess exists at the beginning of the process (if there is no initial enantiomeric excess and if the crystal size distribution of the two enantiomers is identical). This emphasises the stochastic character of the deracemisation.
- The crystal size distribution is dependent on the mechanical energy transfered to the system but not on the enantiomeric excess of the solid phase.

- The fast kinetics induced by ultrasounds are consistent with the important role of the formation and recapture of the clusters, i.e. a high number of clusters are produced by ultrasounds and they can be immediately dissolved or be recaptured by docking on the surfaces of crystals with the same handedness, therefore speeding up the transfer of matter.

- The effect of the supersaturation induced by the local heating due to ultrasounds, and more, by the temperature cycles, cannot be neglected. The resulting entrainment effect must be taken in account to explain how the deracemisation process works and is particularly consistent with its autocatalytic character.

In order to achieve the total symmetry breaking, the use of ultrasounds instead of glass beads makes easier the process (the kinetics are faster, the size of reactor is reduced and the work up is easier) and the final size of the particles can be chosen. Those features are important for an industrial application.

Résumé en français

Introduction Générale

Même si la chiralité et ses conséquences sur les êtres vivants sont connues depuis de nombreuses années, les industries pharmaceutiques n'ont commencé à s'intéresser aux différents effets des deux enantiomères d'un composé actif que depuis la fin des années 80. L'accès aux énantiomères purs est alors devenu un enjeu scientifique et économique considérable. C'est dans ce cadre que l'Union européenne a lancé en 2008 un programme appelé IntEnant, rassemblant les différentes compétences de plusieurs laboratoires européens. Le laboratoire SPCMIB de l'Université de Toulouse et le laboratoire SMS de l'Université de Rouen, dans lesquels j'ai effectué ma thèse, étaient tous deux membres de ce programme. Leurs principales compétences, respectivement la synthèse organique et la purification par cristallisation, ont ainsi été combinées afin d'apporter une nouvelle contribution à l'accès d'énantiomères purs.

Les voies d'obtention d'énantiomères purs les plus utilisées et les plus productives sont les dédoublements de mélanges racémiques par cristallisation, telles que le dédoublement pasteurien. Afin d'élargir le champ d'action de ce type de purification, de nouveaux sélecteurs chiraux, basés sur des cyclodextrines monosubstituées, ont été synthétisés. Un motif acide ou basique a été greffé sur les cyclodextrines afin d'augmenter la discrimination entre les deux énantiomères. L'étude de la formation de complexes d'inclusion a été initiée.

Une autre méthode d'obtention d'énantiomères purs, appelée déracémisation ou rupture totale de symétrie, a récemment été décrite. Cette méthode est très prometteuse car elle permet d'obtenir l'énantiomère désiré avec un rendement de 100% en une seule étape. Malheureusement, les limitations inhérentes à ce procédé sont importantes et seuls les composés cristallisant comme des conglomérats (environ 5% des composés) et facilement racémisables dans les mêmes conditions peuvent être utilisés.

La cristallisation sous forme de conglomérat est actuellement imprévisible. Cependant, certaines familles de composés organiques ont une grande tendance à cristalliser de cette façon. Dans ce manuscrit, deux nouvelles familles de molécules ayant un tel comportement seront présentées.

De plus, le mécanisme rendant possible la transformation progressive d'une suspension racémique en une suspension d'énantiomère pur, n'a toujours pas été totalement élucidée. Le troisième chapitre de cette thèse y apportera quelques éclaircissements, notamment grâce à la mise au point et à l'étude de la déracémisation par les ultrasons.

I - La chiralité et la séparation d'énantiomères

1. Généralités

Le mot "chiral" a été introduit pour la première fois par Lord Kelvin, en 1884: "*J'appelle chiral toute figure géométrique ou tout ensemble de points qui n'est pas superposable à son image dans un miroir. Je parle alors de chiralité.* "[201]

Une molécule et son image dans un miroir sont appelées "énantiomères" et sont dites "chirales" lorsqu'elles ne sont pas superposables. Dans le cas contraire, elles sont dites "achirales".

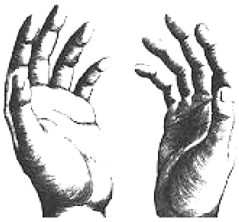

Figure 1. La main droite et la main gauche sont images l'une de l'autre dans un miroir mais ne sont pas superposables ; elles sont donc chirales.

Comme deux énantiomères sont images l'un de l'autre dans un miroir, ils possèdent les mêmes propriétés physiques (température de fusion, solubilité…) et les même réactivités envers des molécules achirales. Par contre, ils peuvent posséder des réactivités différentes vis à vis d'autres molécules chirales.

Le corps humain est composé de nombreuses molécules chirales (protéines, ADN...). Deux énantiomères pourront donc avoir un comportement différent. Par exemple leurs odeurs pourront être différentes.

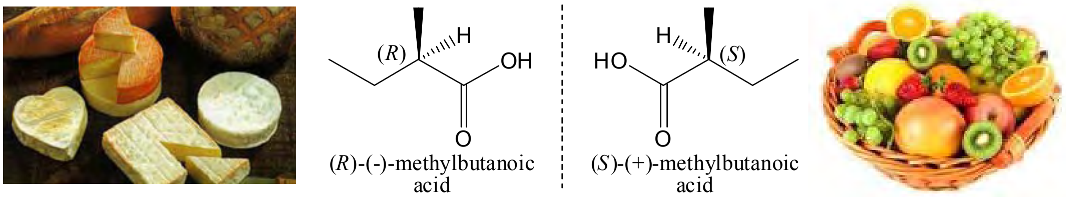

(*R*)-(-)-methylbutanoic acid

(*S*)-(+)-methylbutanoic acid

Figure 2. Les différentes odeurs des deux énantiomères de l'acide 2-methylbutanoïque.[202]

Ce comportement est aussi valable pour les composés pharmaceutiques et l'administration d'un mélange racémique peut avoir des conséquences graves. Un cas tristement célèbre est celui de la thalidomide.[203] Ce médicament a été la cause de nombreuses malformations graves de foetus dans les années 1950 et 1960, l'un des énantiomères étant tératogène.

---

[201] Lord Kelvin; *Baltimore Lectures on Molecular Dynamics and the Wave Theory of Light* **1884**.

[202] M. H. Boelens, H. Boelens, L. J. van Gemert, P. & F., **1993**, 18(6), 1-15.

[203] B. K. Patel, A. J. Hutt; *Chirality in Drug Design and Development* **2004,** Chap. 5, I. K. Reddy, R. Mehvar, Eds, New-York, Marcel Dekker Inc.

Les médicaments énantiomériquement purs sont principalement obtenus par :

- Synthèse à partir du pool chiral (45%).
- Synthèse énantiosélective (9%).
- dédoublement d'un mélange racémique : cristallisation, chromatographie... (46%)

2. La déracémisation

La déracémisation, aussi appelée rupture totale de symétrie, est une méthode d'obtention d'énantiomères purs récemment developpée. Elle permet la transformation progressive d'un mélange racémique en énantiomère pur désiré, en une seule étape, avec un rendement de 100%. C'est donc une technique de dédoublement très puissante. Malheureusement, les limitations inhérentes à cette méthode sont importantes car trois conditions doivent être respectées :

- le composé doit cristalliser sous forme de conglomérat,
- le composé doit être facilement racémisable en solution,
- ces deux conditions doivent être compatibles dans les mêmes conditions opératoires.

Dans un conglomérat, les deux énantiomères cristallisent séparément, rendant possible la discrimination totale à l'état solide. Malheureusement, ce type de cristallisation représente moins de 10% des cas et il est souvent difficile à combiner avec une racémisation en solution.

a. La découverte de la déracémisation

La première observation de rupture totale de symétrie a été faite par Kipping et Pope en 1898 en étudiant la cristallisation de $NaClO_3$.[204,205] Ce composé inorganique, bien qu'achiral, cristallise dans le groupe d'espace chiral $P2_13$, donnant deux types de cristaux chiraux. Si la cristallisation du $NaClO_3$ par évaporation du solvant à partir d'une solution saturée donne bien un mélange racémique de cristaux, la cristallisation à partir de germes énantiopurs conduit majoritairement à la formation de cristaux de ce même énantiomère, avec un excès de plus de 90%. Un siècle plus tard, Kondepudi *et al.* confirmèrent ces observations et mirent en évidence l'importance de l'agitation : avec et sans ensemencement, un seul type de cristaux étaient obtenus après évaporation du solvant. Ils expliquèrent ce phénomène par *"la théorie du cristal mère"* c'est à dire par la propagation de la chiralité de premier nucleus.

---

[204] F. S. Kipping, W. J. Pope; *J. Chem. Soc. Trans.*, **1898**, 73, 606-617.

[205] D. K. Kondepudi, R. J. Kaufman, N. Singh; *Science*, **1990**, 250, 975-976.

b. Le mûrissement de Viedma

En 2004,[206] puis en 2005,[207] Viedma remit en cause cette théorie en réalisant tout d'abord la déracémisation du $NaClO_3$ à partir d'une solution hautement sursaturée (apparition de nucléation primaire catastrophique) puis à partir d'une suspension racémique. Il effectua cette dernière en présence de billes de verre, augmentant considérablement la vitesse du procédé. Depuis, le nombre de publications concernant la déracémisation a fortement augmenté, aussi bien pour la compréhension du mécanisme que pour l'obtention d'énantiomères purs de composés organiques intrinsèquement chiraux.

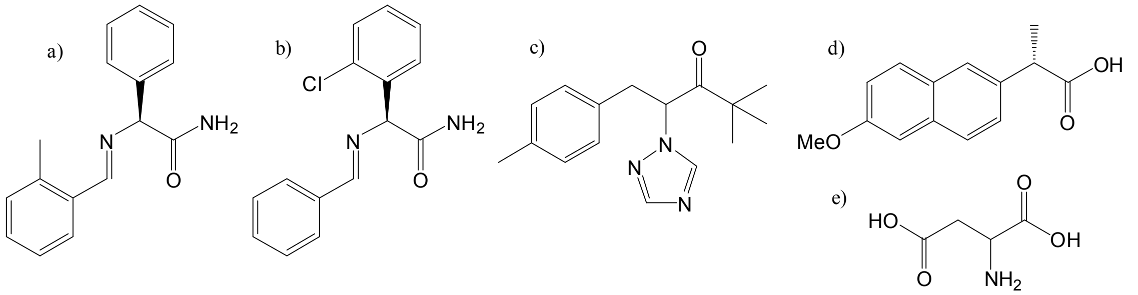

Figure 3. Différents composés organiques déracémisables. a) *N*-(2-methyl-benzylidene)-phenylglycine amide[208], b) *N*-(benzylidene)-2-chlorophenylglycine-amide[209], c) ClTAK[210], d) Naproxène[211], e) Acide aspartique[212].

Dans certains cas,[209,210] le mûrissement de Viedma a été combiné avec une rampe de refroidissement, augmentant encore plus la productivité du procédé.

3. Mécanisme

a. L'expérience de Cairns-Smith

Cairns-Smith décrivit une expérience (Figure 4) utilisant des balles de deux couleurs différentes permettant d'expliquer comment un énantiomère pur (i.e. une seule couleur de balles) pouvait être obtenu à partir d'un mélange racémique (i.e. un mélange comportant le même nombre de balles des deux couleurs). Cependant cette expérience ne reflète pas la réalité du mécanisme de déracémisation puisque les balles n'ont pas la possibilité de changer de couleur (i.e. d'être racémisées). Elle permet toutefois d'illustrer comment un déséquilibre peut être créé à partir d'un mélange racémique.

---

[206] C. Viedma; *J. Crystal Growth*, **2004**, 261, 118-121.

[207] C. Viedma; *Phys.Rev. Lett.*, **2005**, 94, 065504.

[208] W. L. Noorduin, T. Izumi, A. Millemaggi, M. Leeman, H. Meekes, W. J. P. Van Enckevort, R. M. Kellogg, B. Kaptein, E. Vlieg, D. G. Blackmond; *J. Am. Chem. Soc.*, **2008**, 130, 1158-1159.

[209] M. W. van der Meijden, M. Leeman, E. Gelens, W. L. Noorduin, H. Meekes, W. J. P. van Enckevort, B. Kaptein, E. Vlieg, R. M. Kellogg; *Org. Process. Res. Dev.*, **2009**, 13, 1195-1198.

[210] G. Levilain, C. Rougeot, F. Guillen, J.-C. Plaquevent, G. Coquerel; *Tetrahedron: Asymmetry*, **2009**, 20, 2769-2771.

[211] W. L. Noorduin, B. Kaptein, H. Meekes, W. J. P. Van Enckevort, R. M. Kellogg, E. Vlieg; Angew. *Chem. Int. Ed.,* **2009**, 48, 4581-4583.

[212] C. Viedma, J. E. Ortiz, T. De Torres, T.Izumi, D. G. Blackmond; *J. Am. Chem. Soc.*, **2008**, 130, 15274-15275.

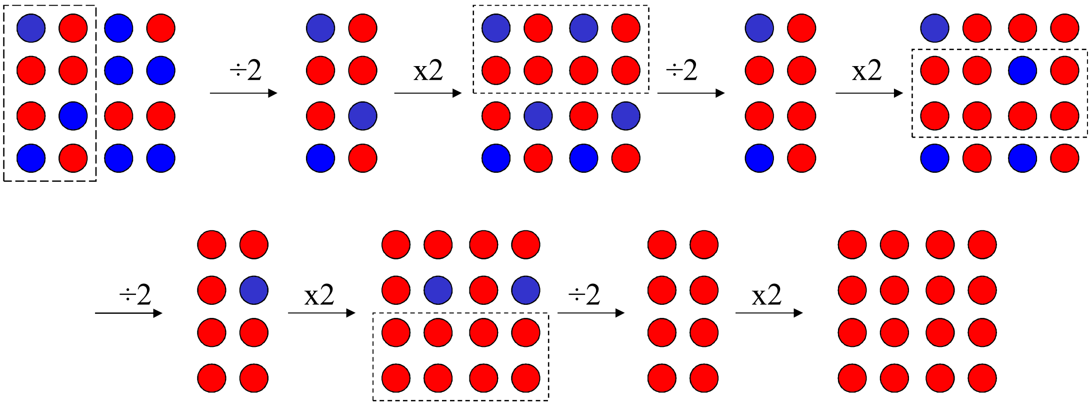

Figure 4. L'expérience de Cairns-Smith: à partir de 100 balles (50 rouges et 50 bleus), la moitié des balles est aléatoirement enlevée à chaque étape puis la moitié restante est multipliée par deux. Après plusieurs étapes, une seule couleur de balles est présente, correspondant à un excès énantiomérique de 100%.

b. Le mûrissement d'Ostwald

De nombreuses études menées sur le mécanisme de la déracémisation ont conduit les scientifiques à déclarer le mûrissement d'Ostwald comme l'un procédé clé de la déracémisation. Grâce à ce phénomène, les petits cristaux se dissolvent spontanément au profit de la croissance des plus gros.[213] Le cas présenté sur la Figure 5 illustre bien ce phénomène,[214] mais montre aussi que, dans le cas particulier du $NaClO_3$, l'état final correspond à une seule des deux phases chirales possibles, comme dans le cas de la déracémisation.

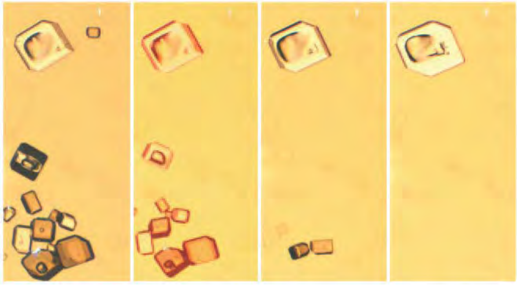

Figure 5. Images au microscope à lumière polarisée du procédé de mûrissement d'Ostwald de cristaux de $NaClO_3$.

Le mûrissement d'Ostwald est un procédé très lent, dépendant largement de la taille des particules : plus les particules sont grosses, plus elles sont lentes à se dissoudre. Mais l'attrition provoquée par l'action des billes de verre permet de fortement diminuer la taille des particules et donc d'accélérer le phénomène du mûrissement d'Ostwald.

---

[213] W. Ostwald; Lehrbuch der Allgemeinen Chemie, Vol. 2, Part 1; Leipzig, Germany, **1896**.

[214] W. L. Noorduin, E. Vlieg, R. M. Kellogg, B. Kaptein; *Angew. Chem. Int. Ed.*, **2009**, 48, 9600-9606.

De nombreuses études et simulations ont été publiées afin d'expliquer comment le mûrissement d'Ostwald pouvait, à partir d'un très faible déséquilibre énantiomérique, conduire à l'obtention d'une phase solide énantiomériquement pure.[215,216]

c. Modèle basé sur la réincorporation de clusters

D'autres scientifiques, ont suggéré que le procédé clé de la déracémisation était la réincorporation de clusters chiraux. En 2004, Uwaha publia une étude dans laquelle il modélisa l'évolution de l'excès énantiomérique par une simple réaction-type d'échange de matière entre les différents constituants de la suspension.[217] Les résultats de cette modélisation montrèrent que la réincorporation de clusters était nécessaire mais aussi que le murissemment d'Ostwald avait un rôle insignifiant en présence d'attrition.

Ce modèle a été soutenu par d'autres publications,[218] dont celle de McBride et Tully,[219] ainsi que celle de Saito et Hyuga[220] qui adaptèrent le modèle aux composés chiraux.

d. Discussion

D'autres études ont été effectuées, comparant ces deux hypothèses, certaines confirmant le rôle des clusters,[221,222] d'autres confirmant le rôle le rôle du mûrissement d'Ostwald.[223]

Cependant, en 2010, un groupe de scientifiques hollandais, en association avec McBride et Tully proposèrent un mécanisme combinant ces deux procédés.[224] Ils donnèrent la preuve de la production de clusters grâce à l'action des billes de verre et conclurent que quatre phénomènes étaient nécessaires à l'évolution de l'excès énantiomérique : i) la racémisation en solution, ii) le mûrissement d'Ostwald, iii) la réincorporation de clusters et iv) l'attrition.

Depuis, d'autres groupes ont modélisé avec succès le procédé de déracémisation en tenant compte à la fois la réincorporation de cluster et du mûrissement d'Ostwald.[225,226]

Cependant, malgré tous les efforts faits pour comprendre le mécanisme responsable de l'évolution spontanée de l'excès énantiomérique lors du procédé de déracémisation, toutes les

---

[215] J. H. E. Cartwright, O. Piro, I. Tuval; *Phys. Rev. Lett.*, **2007**, 165501

[216] W. L. Noorduin, H. Meekes, A. A. C. Bode, W. J. P. Van Enckevort, B. Kaptein, R. M. Kellogg, E. Vielg; *Cryst. Growth. Des.*, **2008**, 8(5), 1675-1681.

[217] M. Uwaha; *J. Phys. Soc. Jpn*, **2004**, 73(10), 2601-2603.

[218] J. Crusats, S. Vientemillas-Verdaguer, J. M. Ribó*; Chem. Eur. J.*, **2006**, 12, 7776-7781.

[219] J. M. McBride, J. C. Tully; *Nature*, **2008**, 452, 161-162.

[220] Y. Saito, H. Hyuga; *J. Phys. Soc. Jpn*, **2004,** 73, 33-35.

[221] M. Uwaha; *J. Phys. Soc. Jpn*, **2008**, 77, 083802.

[222] Y. Saito, H. Hyuga; *J. Phys. Soc. Jpn*, **2005**, 74, 535-537.

[223] T. Izumi, D. G. Blackmond; *Chem. Eur. J.*, **2009**, 15, 3065-3068.

[224] W. L. Noordiun, W. J. P. Van Enckevort, H. Meekes, B. Kaptein, R. M. Kellogg, J. C. Tully, J. M. McBride, E. Vlieg; *Angew. Chem. Int. Ed.*, **2010**, 49(45), 8435-8438.

[225] P. J. Skrdla; *Cryst. Growth Des.*, **2011**, 11, 1957-1965.

[226] M. Iggland, M. Mazzotti; *Cryst. Growth Des.*, **2011**, 11, 4611-4622.

incertitudes n'ont pas été levées et, comme le souligne Viedma, un paradoxe reste à expliquer : "*la force motrice de l'évolution de l'homochiralité de la phase solide est la racémisation en solution - un procédé qui traditionnellement érode la discrimination chirale*."

II - Synthèse de β-cyclodextrines monofonctionnalisées

1. Introduction

Les cyclodextrines sont des molécules cages chirales[227,228] largement utilisées en chromatographie, pour la préparation de phases stationnaires chirales. Cependant leur capacité de discrimination chirale n'est généralement pas suffisante pour assurer la séparation d'énantiomères à l'état solide et seulement quelques exemples d'obtention énantiomères purs par formation de complexes hôte/invité ont été décrits dans la littérature.[229,230,231]

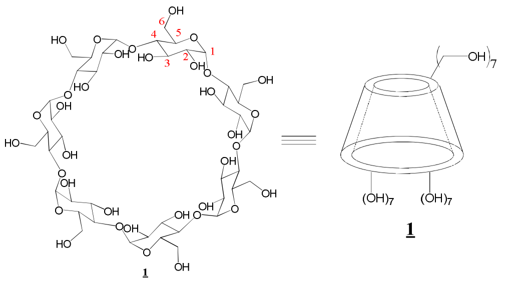

Figure 6. Structure de la β-cyclodextrine à gauche, et sa représentation schématique à droite.

Afin d'augmenter les différences d'inclusion, et donc les chances de discrimination entre les deux énantiomères, il nous est apparu nécessaire de synthétiser de nouvelles cyclodextrines possédant un motif acide ou basique. Ces motifs pourraient permettre de modifier la façon dont la molécule invitée est incluse dans la cavité de la cyclodextrine et ainsi d'augmenter la discrimination entre les deux énantiomères.

2. Synthèse de β-cyclodextrines monosubstituées

Différentes β-cyclodextrines monosubstituées ont donc été synthétisées à partir de la β-cyclodextrine monotosylée β-CDOTs. Celle-ci a été obtenue avec un rendement satisfaisant (40%) et une très bonne pureté à partir de la β-cyclodextrine native et du tosylate

---

[227] A. Villiers ; *Comptes Rendus Hebdomadaires des Séances de l'Académie des Sciences*, **1891**, 112, 536-538.
[228] K. Freudenberg, G. Blomquist, L. Ewald, K. Soff; *Ber. Dtsch. Chem. Ges.* **1936**, *69*, 1258-1266.
[229] A. Grandeury, S. Tisse, G. Gouhier, V. Peulon, S. Petit, G. Coquerel *Chem. Eng. Technol.* **2003**, 26, 354-358.
[230] A. Grandeury, S. Petit, G. Gouhier , V. Agasse, G. Coquerel; *Tetrahedron: Asymm.* **2003**, 14, 2143-2152.
[231] Y. Amharar, A. Grandeury, M. Sanselme, S. Petit, G. Coquerel; *J. Phys. Chem.*, **2012**, 116(20), 6027-6040.

d'imidazole.[232] La substitution en position 6 a été confirmée par des analyses RMN à deux dimensions.

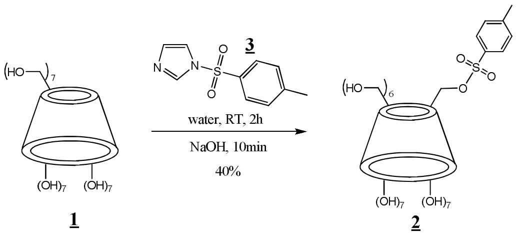

Figure 7. Synthèse de la β-cyclodextrine monotosylée β-CDOTs.

La plupart des autres β-cyclodextrines monosubstituées ont été obtenues par substitutions nucléophiles à partir de la β-CDOTs. Les cyclodextrines **5** et **6b** ont été synthétisées à partir de la β-CDN$_3$ **4**, respectivement, par réduction et par réaction de cycloaddition de Huisgen. Les cyclodextrines **14** et **15** ont quant à elles été obtenues par alkylation des amines correspondantes, en utilisant l'acide chloroacétique.

Tableau 1. Récapitulatif des différentes cyclodextrines synthétisées.

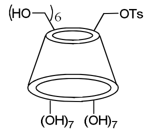	**2** β-CDOTs	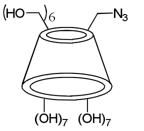	**4** β-CDN$_3$
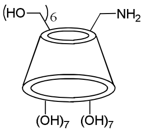	**5** β-CDNH$_2$	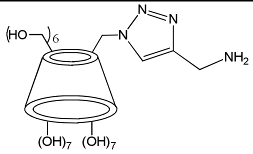	**6b**
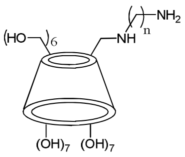	**7** β-CDNH(CH$_2$)$_2$NH$_2$	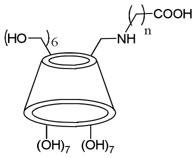	**12a** β-CDNHCH$_2$COOH
	8 β-CDNH(CH$_2$)$_3$NH$_2$		**12b** β-CDNH(CH$_2$)$_2$COOH
	9 β-CDNH(CH$_2$)$_6$NH$_2$		**12c** β-CDNH(CH$_2$)$_3$COOH
	10 β-CDNH(CH$_2$)$_8$NH$_2$		**12d** β-CDNH(CH$_2$)$_4$COOH
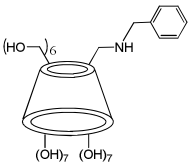	**11** β-CD benzylamine	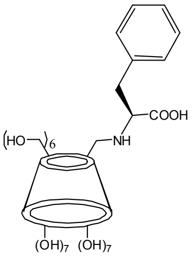	**13** *L*-phenyl glycine β-CD
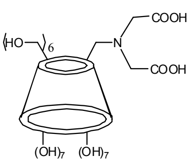	**14**	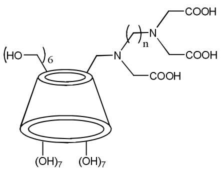	**15a**
			15b
			15c

---

[232] H.-S. Byun, N. Zhong, R. Bittman; *Org. Synth.*, **2000**, 77, 225-227.

3. Etude de la cristallisation des β-cyclodextrines monosubstituées et des complexes d'inclusion

a. Cristallisation des β-cyclodextrines monosubstituées : influence de l'eau

Après synthèse, les cyclodextrines ne sont pas très cristallines, comme le montre la Figure 8Figure 1.

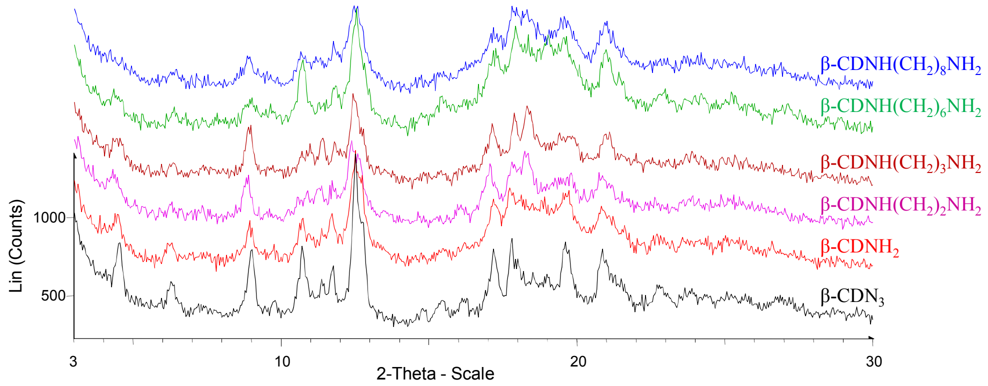

Figure 8. Superposition des diffractogrammes des rayons X sur poudres de différentes cyclodextrines.

Cependant, certaines ont pu être cristallisées dans l'eau (Figure 9). Toutefois, les cristaux se sont révélés instables une fois séparés de la solution saturée : ils sont rapidement devenus blanc, traduisant la cristallisation d'une phase efflorescente.

Des analyses DVS (dynamic vapor sorption, Figure 10) ont montré que le taux d'hydratation des cyclodextrines dépendait largement du taux d'humidité, et qu'aucun hydrate stoechiométrique n'existait.

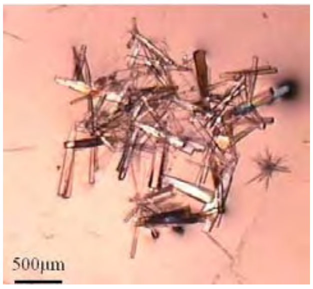

Figure 9. Cristaux de β-CDNH$_2$ dans l'eau.

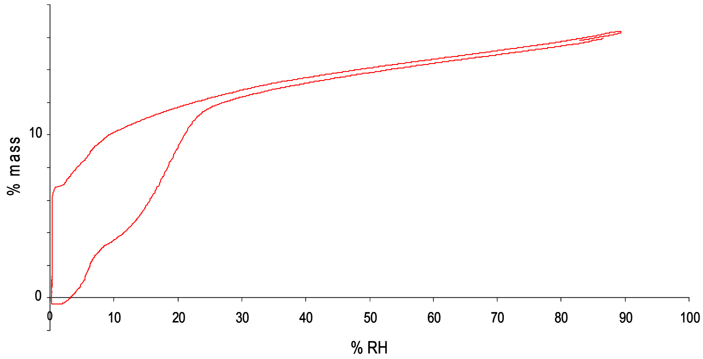

Figure 10. Analyse DVS de la β-CDNH$_2$.

b. Etude du complexe β-CDNH$_2$/ibuprofène

Le complexe β-CDNH$_2$/ibuprofène a été étudié. La β-CDNH$_2$ a été dissoute dans l'eau puis 2 équivalents d'ibuprofène ont été ajoutés. L'ibuprofène n'étant pas soluble dans l'eau, il va se complexer avec la cavité hydrophobe de la cyclodextrine, et ainsi passer en phase aqueuse. La formation d'un complexe de stoechiométrie 1/1 a été mise en évidence par RMN, malheureusement, aucune discrimination chirale n'a pu être obtenue dans ces conditions.

Des essais d'obtention de monocristaux ont été effectués afin de déterminer si une discrimination chirale était possible à l'état solide. Malheureusement, aucun cristal de qualité suffisante n'a été obtenu ; ceux présentés sur la Figure 11 se sont révélés polycristallins.

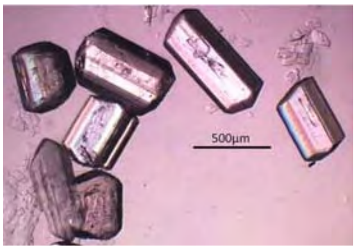

Figure 11. Cristaux du complexe β-CDNH2/ibuprofène 1/1 dans l'eau.

4. Conclusion

Une petite librairie de cyclodextrines monosubstituées a été synthétisée avec succès et avec une assez bonne pureté. Les analyses DVS ont montré que le taux d'hydratation des cyclodextrines dépendait grandement du taux d'humidité, ce qui pourrait expliquer la difficulté d'obtention de phases solides bien cristallisées.

De premières expériences ont montré qu'il était possible de former des complexes d'inclusion avec ces cyclodextrines. Toutefois, aucune discrimination chirale n'a pu être observée pour le moment.

III - Déracémisation d'une famille de conglomérats

1. Introduction

Ce chapitre est consacré à l'étude d'une famille de composés dérivés du 1-(4-chlorophényl)-4,4-diméthyl-2-(1H-1,2,4-triazol-1-yl)pentan-3-one, ClTAK. Ce composé, un précurseur du Placobutrazol,[233] un inhibiteur de croissance des plantes, cristallise sous forme de conglomérat et est facilement racémisable en solution dans les mêmes conditions ;[234] il peut donc être déracémisé.[210]

Dans la littérature, un composé très similaire a été décrit : le 2H-4ClTAK, isomorphe à ClTAK. Afin de déterminer si le fait que ces deux composés cristallisent de façon identique soit une propriété de cette famille ou une coïncidence, quatre autres dérivés ont été synthétisés : BrTAK, MeTAK, HTAK et tBuTAK.

---

[233] US4243405A1.

[234] S. N. Black, L. J. Williams, R. J. Davey, F. Moffat, R. V. H. Jones, D. M. McEwan, D. E. Sadler; Tetrahedron, **1989**, 45(9), 2677-2682.

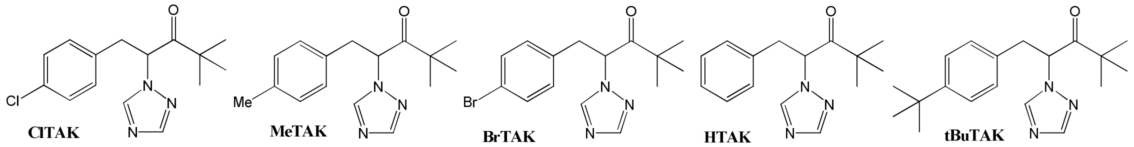

Figure 12. Structures des composés dérivés du ClTAK synthétisés au laboratoire.

2. Etude structurale

D'après la superposition des diffractogrammes sur poudre de ces cinq composés, ClTAK, MeTAK et BrTAK, semblent isomorphes (Figure 13). L'étude de tBuTAK à, quant à elle, été rapidement abandonnée : le composé forme des démixtions avec de nombreux solvants et les analyses SHG (second harmonic generation) ont montré qu'il cristallise dans un groupe d'espace centrosymétrique, et donc qu'il ne forme pas de conglomérat.

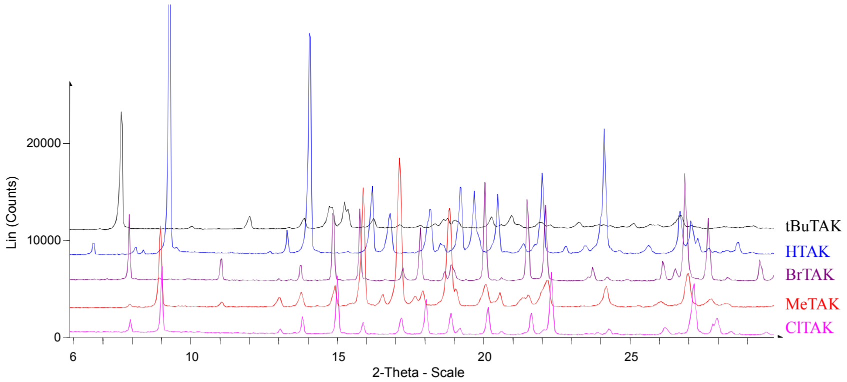

Figure 13. Superposition de DRXP des dérivés du TAK.

La résolution structurale de ClTAK, MeTAK, BrTAK et HTAK a confirmé les résultats obtenus par diffractions de rayons X sur poudre : ClTAK, MeTAK et BrTAK sont isomorphes. Cependant, elle a aussi pu montrer que, même si HTAK cristallise dans un groupe d'espace différent ($P2_1$ au lieu de $P2_12_12_1$), sa structure présente de grandes similitudes avec celle des trois autres composés, notamment au niveau des paramètres de mailles.

Tableau 2. Paramètres de maille de ClTAK, MeTAK, BrTAK et HTAK.

	ClTAK	MeTAK	BrTAK	HTAK
Système cristallin	Orthorhombique	Orthorhombique	Orthorhombique	Monoclinique
Groupe d'espace	$P2_12_12_1$	$P2_12_12_1$	$P2_12_12_1$	$P2_1$
Z , Z' (unités asymétrique par maille)	4, 1	4, 1	4, 1	4, 2
a / Å	5.8076(5)	5.808(1)	5.7875(5)	5.747(1)
b / Å	13.553(1)	13.641(1)	13.629(1)	19.183(1)
c / Å	19.661(2)	19.789(1)	19.882(2)	13.437(1)
β	-	-	-	96.561(1)
V / $Å^3$	1547.5(2)	1567.9(2)	1568.3(2)	1471.8(2)

d_{calc} / g.cm^{-3}	1.252	1.150	1.424	1.161

Dans le cas de ClTAK, MeTAK et BrTAK, l'unité asymétrique est composée d'une seule molécule présentant un désordre au niveau du groupement *tert*-butyl, alors que l'unité asymétrique de HTAK est composée de deux molécules ne présentant aucun désordre. Cependant, la superposition de ces deux molécules montre qu'elles ne diffèrent quasiment que par la position du *tert*-butyl, mimant ainsi un désordre de 50/50.

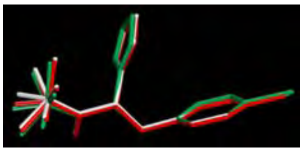

Figure 14. Superposition des unités asymétriques de ClTAK (en blanc), MeTAK (en rouge) et BrTAK (en vert).

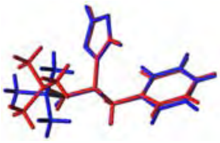

Figure 16. Superposition des deux molécules de l'unité asymétrique de HTAK.

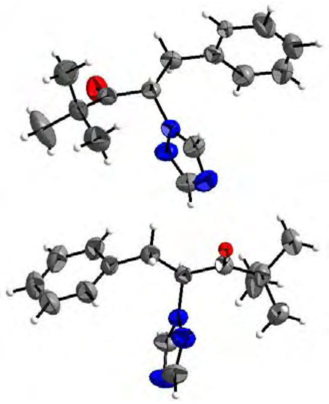

Figure 15. Unité asymétrique de HTAK.

La Figure 17 montre les projections des quatre structures selon l'axe *a*, il est ainsi facile de voir que ClTAK, MeTAK et BrTAK sont isomorphes. Pour ces trois composés, des chaînes sont formées selon *a*, les molécules étant reliées entre elles par des liaisons π en forme de T, les groupements triazoles étant rejetés vers l'extérieur. Dans le cas de HTAK, des chaînes similaires sont formées, mais les groupements triazoles sont dirigés vers l'intérieur de la chaîne.

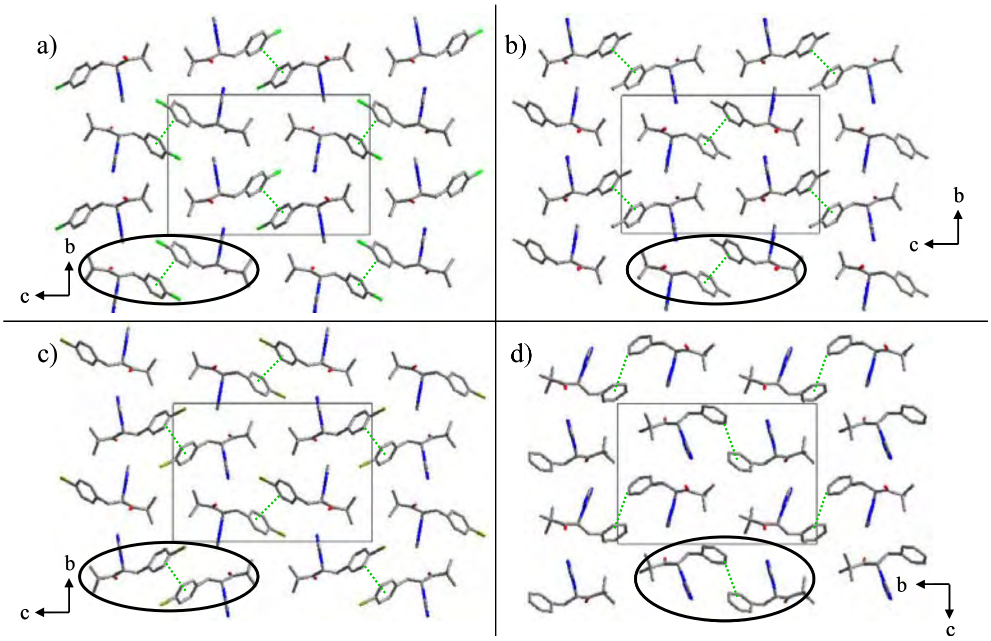

Figure 17. Projections selon l'axe a. a) ClTAK, b) MeTAK, c) BrTAK et d) HTAK. Une chaîne est entourée en noir et les liaisons π en forme de T sont représentées en pointillés verts.

3. Le mûrissement de Viedma

Les déracémisations de ClTAK, MeTAK, BrTAK et HTAK ont été étudiées. Toutes les expériences ont été menées dans des conditions les plus similaires possibles :

- TAK : 1 g
- Billes de verre (diamètre 2 mm) : 5 g
- Solvant (MeOH/eau): 5 g
- Agitateur magnétique en forme de croix
- Température : 25°C
- Vitesse d'agitation : 1000 rpm
- NaOH : 0.1 g

Afin de garder des solubilités similaires pour tous les composés, les proportions de méthanol et d'eau ont du être modulées (Tableau 3).

Tableau 3. Solubilités des dérivés du TAK dans les mélanges de solvants utilisés lors des déracémisations.

	ClTAK	MeTAK	HTAK	BrTAK
MeOH/eau (m/m)	80/20	65/35	47/53	90/10
Solubilité	5.5%	6.0%	4.7%	5.2%

a. ClTAK

Plusieurs expériences de déracémisations de ClTAK ont été effectuées. Des échantillons ont été régulièrement prélevés et analysés par HPLC chirale. Les résultats obtenus pour trois expériences sont présentés sur la Figure 18.

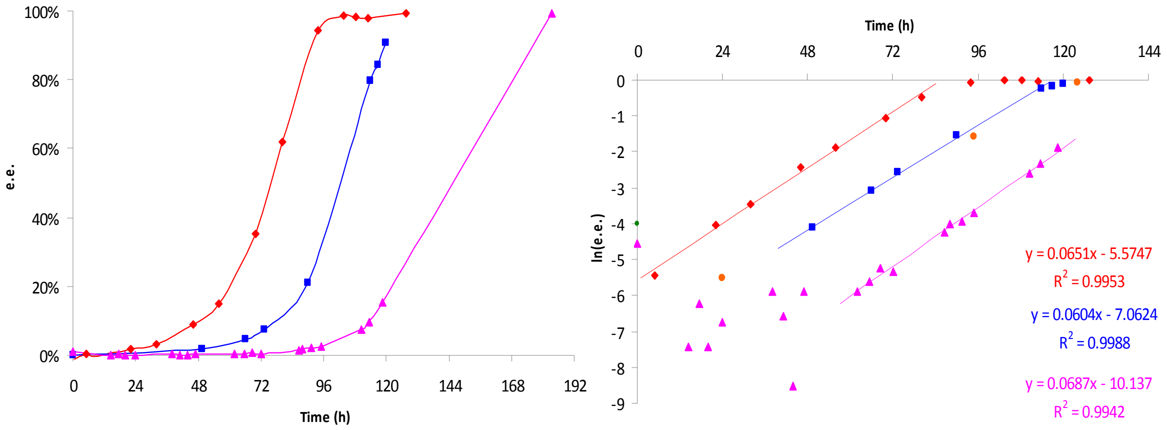

Figure 18. Comparaison de 3 déracémisations de ClTAK conduites dans les mêmes conditions opératoires. A gauche: évolution de l'excès énantiomérique en fonction du temps. A droite: évolution de ln(e.e.) en fonction du temps.

Dans chaque cas, l'évolution de l'excès énantiomérique est exponentielle, comme le prouve la représentation de ln(e.e.) en fonction du temps. Cependant, on peut remarquer que les trois expériences ne démarrent pas au même moment, même si leurs cinétiques sont identiques. Ce phénomène est clairement visible sur la courbe rose : durant les 2-3 premiers jours, l'excès énantiomérique n'évolue pas.

Afin de déterminer si ce retard à l'évolution de l'e.e. n'est pas dû à un problème expérimental, par exemple une mauvaise efficacité des billes de verre, différents échantillons ont été analysés par microscopie électronique à balayage (MEB). Cependant, comme le montre les photos (Figure 19), l'attrition a bien été efficace tout au long de l'expérience, et ne peut donc pas expliquer pourquoi la déracémisation n'a pas démarré à t = 0. De plus, on peut observer que la taille des particules ne dépend pas de l'e.e.

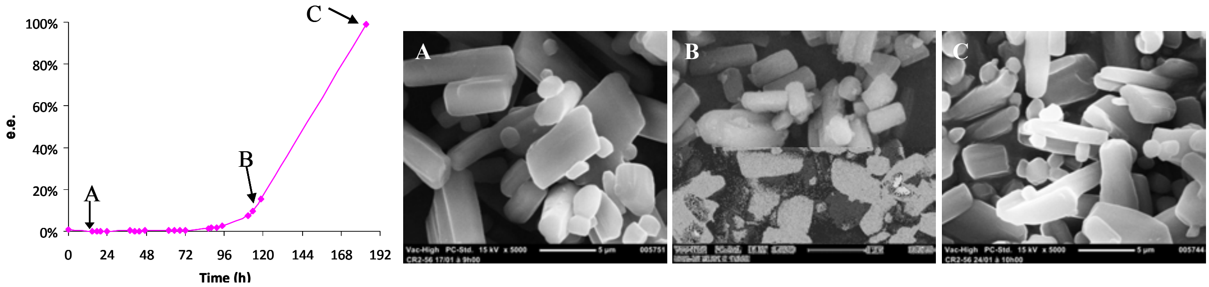

Figure 19. Photos prises au MEB de trois échantillons lors d'une expérience de déracémisation de ClTAK.

b. ClTAK, MeTAK, BrTAK et HTAK

Les cinétiques de déracémisation de quatre dérivés sont comparées. Là encore, on peut observer des retards à l'évolution de l'e.e., et les cinétiques de ClTAK, MeTAK et HTAK sont très similaires. Cependant, le comportement de BrTAK est différent : bien que les conditions expérimentales soient comparables à celles des autres expériences, la vitesse est beaucoup plus lente.

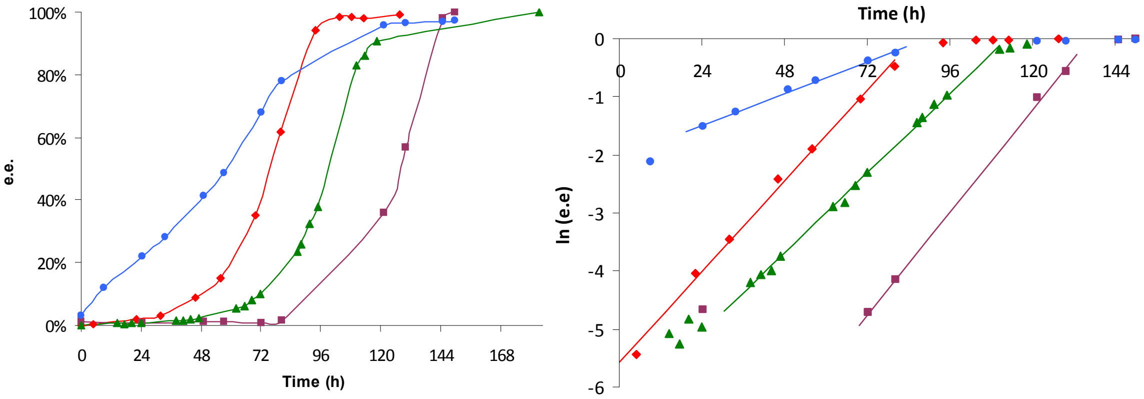

Figure 20. Comparaison des cinétiques d'évolution de l'excès énantiomérique des quatres TAK. ClTAK en rouge, MeTAK en vert, BrTAK en bleu et HTAK en violet.

De plus, comme le montre la Figure 21, les particules de BrTAK sont plus petites que celles des autres TAK, ce qui est en désaccord avec le mécanisme préalablement décrit. Aucune condition expérimentale ne peut expliquer cette différence. BrTAK semble se comporter comme si les échanges de matière entre les particules étaient inhibés, les empêchant ainsi de croître et donc ralentissant l'évolution de l'e.e.

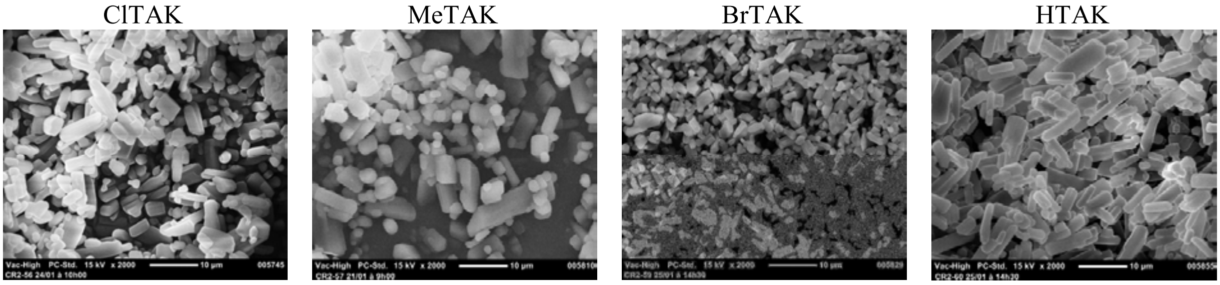

Figure 21. Photos prises au MEB des particules à la fin des déracémisations.

5. Déracémisation par les ultrasons

Les ultrasons sont connus pour réduire la taille des particules, produire un nombre élevé de clusters ainsi qu'augmenter les effets mécaniques grâce à l'implosion des bulles de cavitations qui induisent des forces de cisaillement et des jets de liquides à très grande vitesse. Les ultrasons pourraient donc être utilisés pour remplacer l'action des billes de verre.[235]

En 2008, Song *et al.*[236,237] cristallisèrent le $NaClO_3$ sous ultrasons, et obtinrent un excès énantiomérique proche de 100%. Mais jusqu'à présent, et mis à part les expériences de Song *et al.*, les ultrasons n'ont jamais été utilisés seuls pour déracémiser des molécules organiques. Ils ont en effet souvent été utilisés en combinaison avec les billes de verre, mais, même si une augmentation de la vitesse de déracémisation avait été remarquée, leurs effets n'ont jamais été étudiés. La déracémisation de ClTAK par les ultrasons a donc été effectuée (Figure 22).

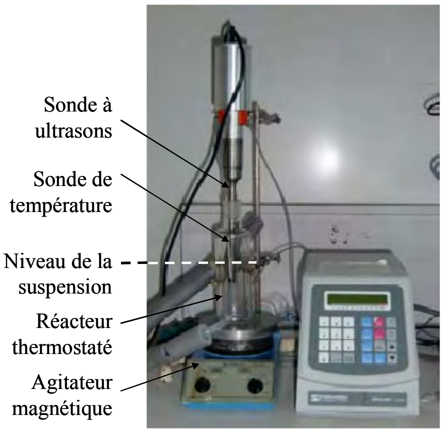

Figure 22. Montage de déracémisation par ultrasons

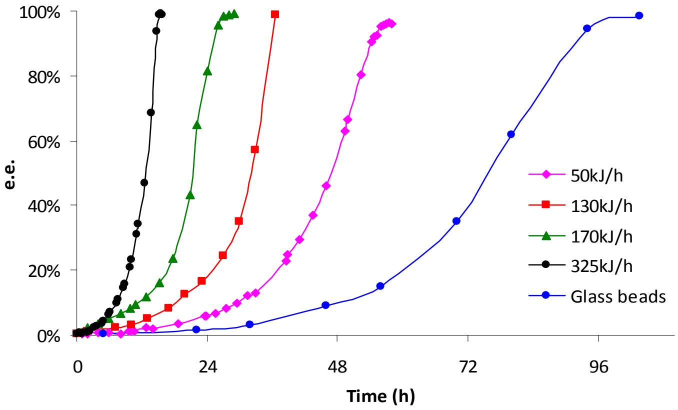

Figure 23. Comparaison de l'évolution de l'e.e. pour quatre différentes puissances d'ultrasons avec les billes de verre.

---

[235] P. Cintas; Cryst. Growth Des., **2008**, 8(8), 2626-2627.
[236] Y. Song, W. Chen, X. Chen; Cryst. Growth Des., **2008**, 8(5), 1448-1450.
[237] Y. Song, W. Chen, X. Chen; Cryst. Growth Des., **2012**, 12, 8-11.

Sur la Figure 23, plusieurs points sont à noter :

- L'évolution de l'e.e. est exponentielle,
- Plus la puissance des ultrasons augmente, plus l'évolution de l'e.e. est rapide. L'analyse de la taille des particules montre que les particules sont aussi de plus en plus petites, ce qui est en accord avec le mécanisme précédemment décrit,
- La déracémisation par ultrasons est plus efficace que la déracémisation utilisant les billes de verre.

Cependant, la comparaison des tailles des particules entre ces deux méthodes montre que les particules sont plus grosses lors des déracémisations par ultrasons, ce qui est en contradiction avec le mécanisme précédemment décrit. Les effets mécaniques induits par les ultrasons et le mûrissement d'Ostwald ne peuvent donc pas expliquer pourquoi les ultrasons sont si efficaces ; d'autres phénomènes doivent être à l'origine de cette rapide évolution.

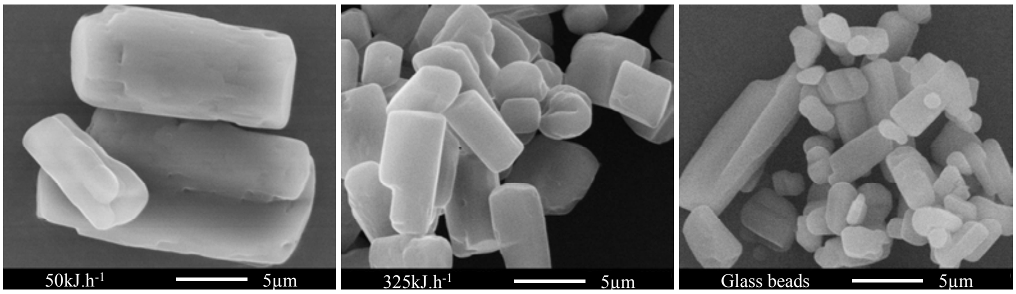

Figure 24. Comparaison de taille des particules après déracémisations par les ultrasons à 50 kJ.h-1 (à gauche) et à 325 kJ.h-1 (au milieu) et par des billes de verre (à droite).

6. Mécanisme

L'étude de la déracémisation des dérivés du TAK par les ultrasons a permis de préciser le mécanisme mis en jeu lors de la déracémisation :

- La réduction de la taille des particules par effet mécanique est responsable d'une accélération de l'évolution de l'e.e. puisque pour un même composé et un même mode opératoire, de plus petites particules sont liées à une évolution plus rapide.
- L'importance de la réincorporation des clusters : les ultrasons sont décrits dans la littérature pour produire un très grand nombre de clusters, qui pourraient être responsables d'une accélération de l'évolution de l'e.e. en favorisant les échanges de matière.
- L'entraînement pourrait aussi expliquer pourquoi la déracémisation par ultrasons est si efficace et pourquoi les particules sont plus grosses. En effet, les ultrasons sont responsables d'un échauffement du système (le réacteur doit être réfrigéré pour maintenir la température du système à 25°C.) Localement, les particules vont donc se dissoudre du fait de la hausse de

température. Une sursaturation va donc se créer lorsque la température redescendra à 25°C, rendant alors possible le phénomène d'entraînement et donc la croissance des particules. D'autres expériences permettent de confirmer l'effet de l'entraînement sur la déracémisation, comme par exemple celles combinant le mûrissement de Viedma avec une rampe de refroidissement.[209,210] Mais l'exemple le plus flagrant est celui permettant la déracémisation en utilisant seulement des cycles de température.[238]

- La taille des particules est indépendante de l'excès énantiomérique, contrairement à ce que a été très récemment décrit par Hein *et al.* ;[239] ils observèrent une "croissance transitoire" des particules au cours de la déracémisation.

IV - Synthèse de l'énantiomère pur du Prasugrel

Le Prasugrel (Effient) est un antiagrégant plaquettaire.[240] Il représente la nouvelle génération d'un médicament très largement utilisé, le Clopidogrel (Plavix), donc le marché était estimé à 9.3 milliards de dollars en 2010. [241] La mise au point d'une voie de synthèse économique de l'énantiomère pur du Prasugrel est un enjeu important pour l'industrie pharmaceutique. Il nous est donc apparu judicieux d'obtenir ce composé en introduisant une étape de déracémisation au cours de la synthèse.

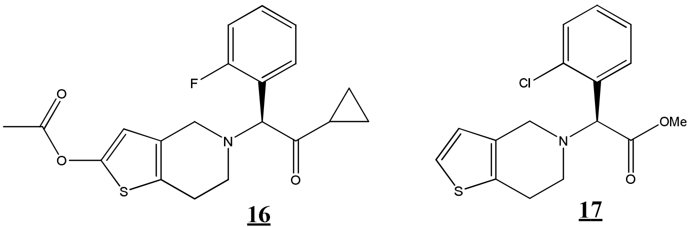

16 17

Figure 25. Structures du *S*-Prasugrel et du *S*-Clopidogrel

---

[238] K. Suwannasang , A. E. Flood, C. Rougeot, G. Coquerel; *Oral presentation at CGOM10*, June **2012**, Limerick, Ireland.

[239] J. E. Hein, B. H. Cao, C. Viedma, R. M. Kellogg, D. G. Blackmond; *J. Am. Chem. Soc.*, **2012**, 134, 12629-12636.

[240] EMEA/117561/2009.

[241] Pharmactua, from www.pharmactua.com.

1. Synthèse de la 2-amino-1-cyclopropyl-2-(2-fluorophényl)éthanone

a. Rétrosynthèse

La première voie de synthèse imaginée est décrite ci-dessus :

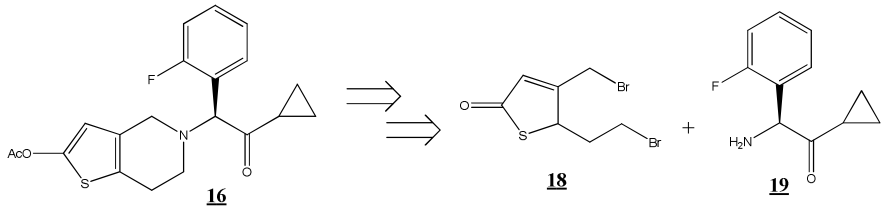
F
AcO
S
N
O
16
O
S
Br
Br
18
+
F
H2N
O
19

Figure 26. Rétrosynthèse de l'énantiomère *S* du Prasugrel.

Le Prasugrel pourrait être obtenu par cyclisation du composé dibromé **18** sur l'amine **19**. L'énantiomère pur de l'amine **19** pourrait être obtenu par déracémisation de la base de Schiff correspondante. Une recherche de conglomérats pourra être effectuée en modulant les substitutants du cycle aromatique apportés par le benzaldéhyde.

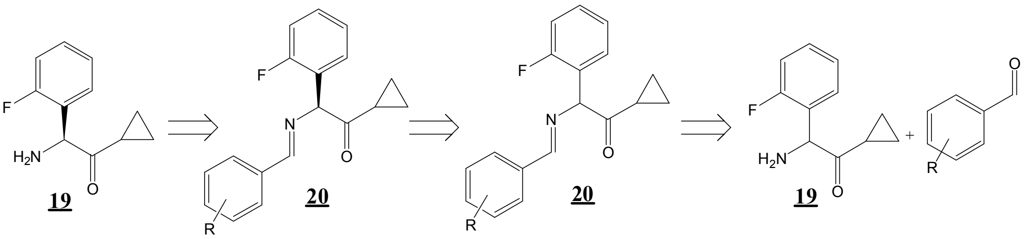
F
H2N
O
19
F
N
O
R
20
F
N
O
R
20
F
H2N
O
19
+
O
R

Figure 27. Rétrosynthèse de l'énantiomère pur de l'amine 19.

Le composé dibromé **18** pourrait, être synthétisé à partir du thiophène éthanol, en trois étapes.

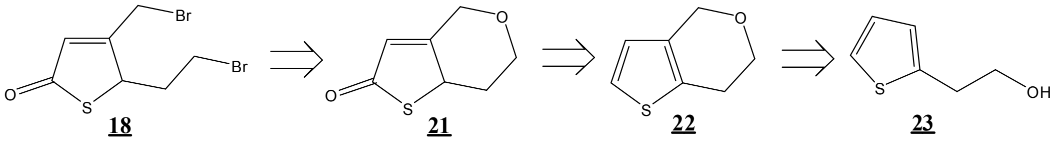
Br
Br
O
S
18
O
O
S
21
O
S
22
S
OH
23

Figure 28. Rétrosynthèse du composé dibromé 18.

b. Synthèse

L'amine **19** a été synthétisée en 4 étapes à partir de la (2-fluorophényl)glycine **24**. L'amine primaire de la (2-fluorophényl)glycine est tout d'abord protégée par un groupement Boc, puis une réaction de couplage est effectuée avec la morpholine. Le groupement cyclopropyle est ensuite introduit grâce à une réaction de Grignard puis une réaction de déprotection conduit au produit attendu sous forme de sel.

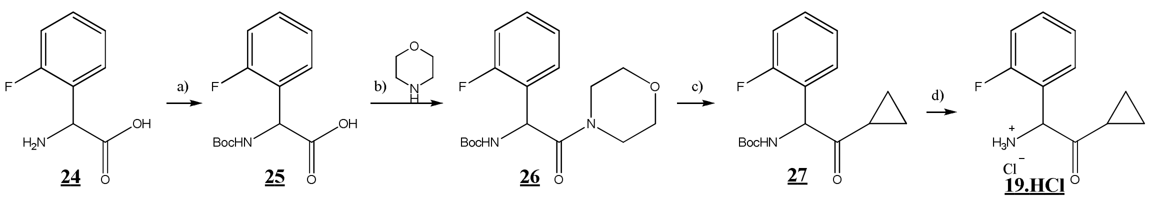
F
H2N
OH
O
24
a)
F
BocHN
OH
O
25
b)
O
N
H
F
BocHN
N
O
O
26
c)
F
BocHN
O
27
d)
F
H3N+
Cl−
O
19.HCl

Figure 29. Synthèse du mélange racémique de la 2-amino-1-cyclopropyl-2-(2-fluorophényl)éthanone hydrochloride. a) Boc_2O, $NaHCO_3$, THF, eau (quant.), b) CDI, TEA, THF (90%), c) copeaux de magnésium, bromure de cyclopropyle, THF (83%), d) HCl, méthanol (90%).

L'amine **19** n'est pas stable sous la forme libre : deux molécules vont réagir ensemble pour former la pyrazine **28**. La structure de ce composé a été confirmée par RMN du proton, spectrométrie de masse et résolution de structure cristalline sur monocristal.

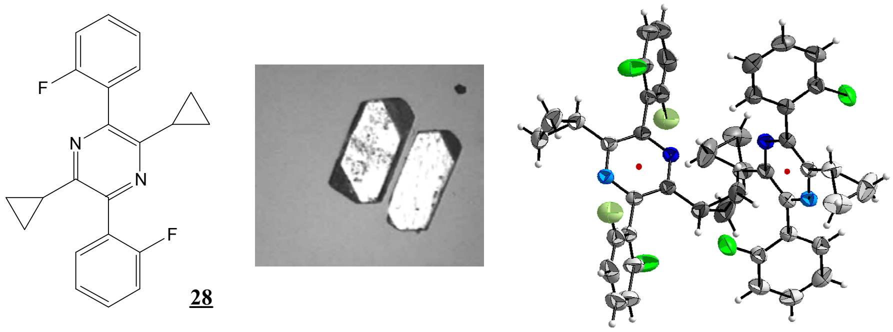

Figure 30. A gauche: structure, au milieu: monocristaux, à droite: résolution structurale de la pyrazine 28.

Cependant l'amine est stable sous forme de sel. La recherche de conglomérats peut donc être effectuée à partir de **19.HCl**. Malheureusement, même si les bases de Schiff ont pu être formées, leurs stabilités n'étaient pas suffisantes pour espérer pouvoir faire une déracémisation, la pyrazine **28** se formant rapidement dans chaque cas.

Afin d'empêcher la formation de ce dimère, une recherche de conglomérats a été effectuée à partir d'un composé possédant un groupement carbonyle moins réactif : le composé **30**. Cette fois, toutes les bases de Schiff obtenues se sont montrées stables. Malheureusement, elles ont aussi toutes étaient obtenues sous forme d'huile et étaient donc impossibles à déracémiser.

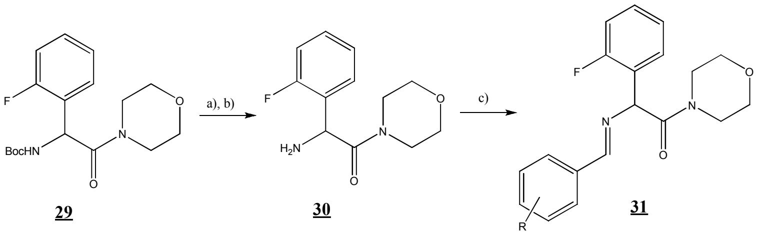

Figure 31. Recherche de conglomérats. a) HCl, 1,4-dioxane (94%), b) NaOH, eau (quant.), c) benzaldéhyde substitué, $NaSO_4$, CH_2Cl_2.

1. Synthèse de la (2-fluorophényl)glycinamide

a. Synthèse

La recherche de conglomérats s'étant révélée infructueuse à partir de la 2-amino-1-cyclopropyl-2-(2-fluorophényl)éthanone **19**, une nouvelle voie de synthèse à été envisagée mettant en jeu la (2-fluorophényl)glycinamide **32**. Celle-ci peut être facilement obtenue en deux étapes à partir de la (2-fluorophényl)glycine.

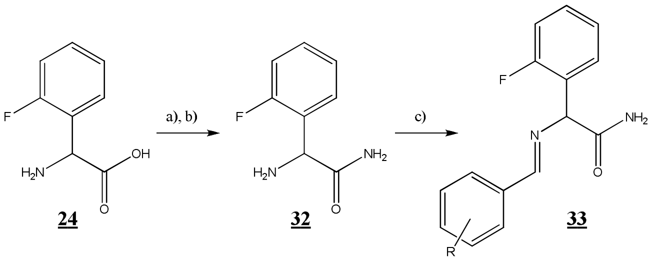

Figure IV - 55. Criblage de conglomérats à partir de la (2-fluorophényl)glycinamide. a) $SOCl_2$, MeOH (95%), b) NH_3 30% dans l'eau (70%), c) benzaldéhyde substitué, $NaSO_4$, CH_2Cl_2.

b. Recherche de conglomérats

Une recherche de conglomérats à ensuite pu être effectuée à partir de la (2-fluorophényl)glycinamide et de dix benzaldéhydes différemment substitués. Neuf des dix composés se sont révélés cristallins et trois d'entre eux ont donnés un signal positif en SHG.

Tableau 4. Résultats de l'analyse SHG des dix bases de Schiff synthétisées à partir de la (2-fluorophenyl)glycinamide.

	33a	**33b**	**33c**	**33d**	**33e**
Aldéhyde aromatique	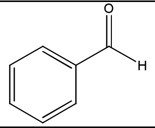	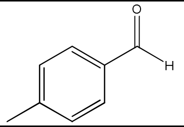	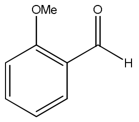	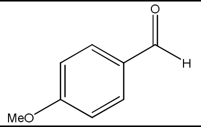	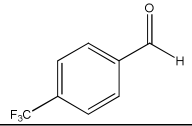
SHG	**Signal positif**	-	-	Faible signal positif	**Signal positif**

	33f	**33g**	**33h**	**33i**	**33j**
Aldéhyde aromatique	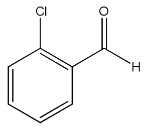	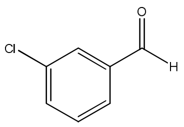	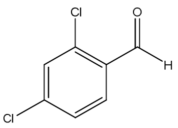	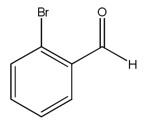	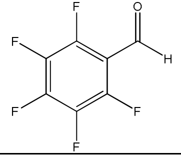
SHG	-	huile	**Signal positif**	Faible signal positif	-

Le composé dérivé du benzaldéhyde, **33a**, a alors été synthétisé, le benzaldéhyde étant le plus économique et très peu toxique.

2. Déracémisation

Une première déracémisation de **33a** a été effectuée et un résultat encourageant a été obtenu puisqu'un excès de 99.1% a été obtenu. Cependant, le rendement n'était que de 14%.

Toutefois, les conditions expérimentales n'avaient pas été optimisées, et notamment, la solubilité de la base de Schiff **33a** dans le solvant de déracémisation était inconnue.

Des essais d'optimisation des conditions expérimentales ont donc été effectués, en adaptant la quantité de solvant à la quantité de produit à déracémiser, en modulant la quantité de solvant ou le programme de refroidissement. Malheureusement, le meilleur rendement obtenu n'a été que de 58% (avec un excès énantiomérique supérieur à 99.5%), un résultat très décevant pour une déracémisation.

D’autres optimisations de conditions expérimentales pourraient être envisagées, notamment un changement d’agent racémisant, jusqu’alors le DBU (1,8-diazabicyclo[5.4.0]undec-ène) ou un changement de solvant (acétonitrile). La déracémisation des deux autres bases de Schiff ayant données un résultat positif en SHG pourraient aussi envisagée.

Conclusion générale

Le travail décrit dans cette thèse est dédié à la chiralité, et plus particulièrement à l’obtention d’énantiomères purs de composés actifs par cristallisation.

Dans un premier temps, une petite librairie de β-cyclodextrines monofonctionnalisées a été synthétisée afin de servir d’agent de résolution par formation de complexes d’inclusion. Même si la formation de complexes a été mise en évidence, aucune discrimination chirale n’a pour l’instant été observée. L’importance du taux d’humidité sur la cristallisation des cyclodextrines a été observée et pourrait expliquer la difficulté d’obtention de phases bien cristallisées et de monocristaux.

La seconde partie de cette thèse est dédiée à l’étude d’un phénomène d’énantioamplification autocatalytique, la déracémisation, mettant en jeu : i) une cristallisation sous forme de conglomérat, ii) une racémisation rapide en solution, iii) une dissolution/recristallisation des particules due à une diminution de leur taille par l’action d’un flux d’énergie (broyage, ultrasons, cycles de température)

Malheureusement, il est, pour l’instant, impossible de prédire si un produit va cristalliser sous forme de conglomérat ou non. Cependant, dans cette étude, deux nouvelles familles de composés ayant une grande tendance à cristalliser sous forme de conglomérats ont été décrites. Des modifications limitées des subtituants ne modifiaient pas (ou très peu) l’empilement cristallin.

L'étude de l'évolution de la distribution de la taille des cristaux au cours du processus de déracemisation en utilisant des billes de verre ou des ultrasons a conduit à repérer les caractéristiques mécanistiques suivantes:

- Un retard à l’évolution spontanée de l’excès énantiomérique peut avoir lieu (à condition qu’aucun déséquilibre ne soit préalablement établi entre les deux énantiomères), confirmant le caractère aléatoire du mécanisme responsable de la déracémisation.
- La distribution de taille des particules dépend de l’énergie mécanique donnée au système mais pas de l’excès énantiomérique de la phase solide.
- L’évolution rapide de l’excès énantiomérique en utilisant les ultrasons est cohérente avec la formation et la recapture de clusters, les nombreux clusters produits par les ultrasons favorisant l’échange de matière entre les particules.
- L’effet d’entraînement produit par l’échauffement du système dû aux ultrasons peut expliquer pourquoi les particules sont plus grosses qu’avec les billes de verre et serait cohérent avec le caractère autocatalytique de la déracémisation.

Experimental Part

I - Generality

All reagents and solvents were purchased from Fisher Scientific, Alfa Aesar, Sigma Aldrich and VWR and were used without further purification.

The NMR spectra were recorded on a Bruker spectrospin 300 Instrument (300MHz and 75MHz for ^{1}H and ^{13}C, respectively) and were calibrated with the solvent ($CDCl_3$: 7.26ppm for ^{1}H NMR and 77.00 for ^{13}C NMR, MeOD: 3.31ppm for ^{1}H NMR and 49.05 for ^{13}C NMR and DMSO-d6: 2.50ppm for ^{1}H NMR and 39.43 for ^{13}C NMR). NMR spectra were analyzed by using the software MestRec.

The mass spectroscopy analyses were carried out by electrospray ionisation by using a Thermo Fisher Scientific LCQ Advantage Max and the Qual Browser software. The chemical ionisations (NH_3) were carried out on a Thermo Fisher Scientific DSQ.

Elementary analyses were performed on a Thermo Scientific Flash 2000 CHNS Series Organic Elemental Analyzers.

Chiral HPLC were carried out by a chiralcel OD connected to a HPLC Finnigan SURVEYOR - LC Pump Plus. The apparatus was controlled by the ChromQuest® software.

The X ray powder diffractograms were recorded on a Diffractometers Siemens D5005 and Siemens D5000 with θ/θ configuration or on a Bruker D8 Advance with a $-\theta/-\theta$ configuration, by using a Cupper anti cathode. The Eva® Software was used for the processing data.

The resolution of structure was carried out by using a Bruker SMART APEX diffractometer with a CCD area detector. The cell parameters and the orientation matrix of the crystal were preliminary determined by using SMART Software. Data integration and global cell refinement were performed with SAINT Software. Intensities were corrected for Lorentz, polarisation, decay and absorption effects (SAINT and SADABS Softwares) and reduced to FO2. The program package WinGX3 was used for space group determination, structure solution and refinement.

DSC and TGA-DSC analyses were recorded respectively on DSC 204 F1 Phoenix NETZSCH® and on TGA-DSC NETZSCH® STA 449C. Measurements are performed in an open aluminum crucible under helium, with a heating rate between 5 and 10K.h^{-1} and the Netzsch–TA Proteus® Software were used for the processing data.

The melting points were determined on a Kofler bench Fisher Scientific®, calibrated with standard compounds.

The DVS analyses were carried out by using a DVS-1 type and a DVS Advantage plus type, Surface Measurement System. The partial vapour pressure is controlled by continuous gas flow containing pure nitrogen and solvent vapour in adequate proportions.

II - Synthesis of monosubstituted β-cyclodextrins for chiral separation

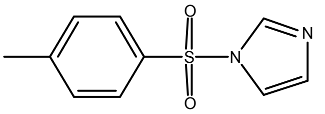

3

3 1-(*p*-toluenesulfonyl)imidazole

Imidazole (65g, 950mmol) was dissolved in CH_2Cl_2 (250mL). The solution was cooled at 0°C then tosyl chloride (80g, 420mmol), dissolved in CH_2Cl_2 (250mL), was added dropwise to the solution over a period of 1h30. The reaction mixture was stirred for 2h at room temperature (RT) then the solution was filtered through a pad of silica gel, which was washed with a 1/1 mixture of ethyl acetate/petroleum ether (500mL). The solvents were evaporated then the solid was dissolved in ethyl acetate (100mL) and petroleum ether (500mL) was added. The solid was filtered, washed with petroleum ether then dried to give 78,6g (353mmol, 84%) of **3** as a white solid. **^{1}H NMR (300MHz, $CDCl_3$):** δ (ppm) = 2.44 (s, 3H), 7.08 (m, 1H), 7.28-7.29 (t, J=1.38Hz, 1H), 7.34-7.37 (d, J=8.6Hz, 2H), 7.81-7.84 (d, J=8.4Hz, 2H), 8.01 (s, 1H). **^{13}C NMR ^{13}C (75MHz, $CDCl_3$):** δ (ppm) = 21.50, 117.26, 121.26, 127.14, 130.24, 131.17, 134.65, 146.17. **Chemical Ionisation MS$^+$ (calc. for $C_{10}H_{10}N_2O_2S$ 222.05):** m/z=223.0 $[M+H]^+$. **Melting point:** 77°C.

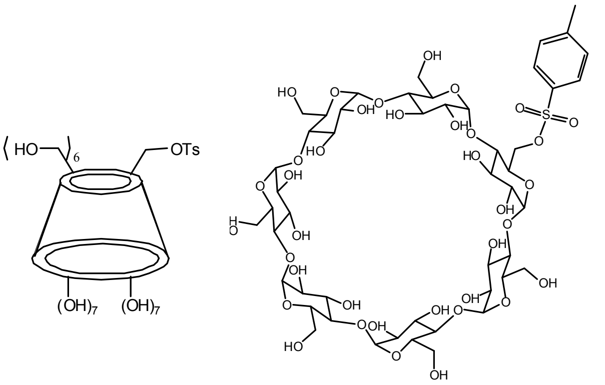

2

2 6-O-*p*-toluenesulfonyl-β-cyclodextrin β-CDOTs

Native β-cyclodextrin hydrate (≈14% H_2O by weight, 40g, 30,3mmol) was suspended in water (900mL) then the mixture was stirred at 60°C until complete dissolution of the β-CD. After cooling at RT, 1-(*p*-toluenesulfonyl)imidazole (31.3g, 141.4mmol) was added. The reaction mixture was stirred 2h at room temperature then NaOH (18g, 450mmol) in water (50mL) was added over 20 minutes. After 10 minutes at RT, the reaction mixture was filtered. NH_4Cl (48,4g, 900mmol) was added to the filtrate then the mixture was stirred for 2h at RT. The solid was filtered, washed with cold water (2x100mL) then with acetone (200mL), and dried under vacuum to give 22.03g (17.1mmol, 56%) of β-CDOTs **2** as a white powder. **^{1}H**

NMR (300MHz, DMSO-d_6): δ (ppm) = 2.40 (s, 3H), 3.22-3.64 (overlap with HDO, m, 40H), 4.16-4.21 (m, 1H, C**H**$_2$OTs), 4.31 (m, 1H, C**H**$_2$OTs) 4.35-4.51 (m, 6H, CH$_2$O**H**), 4.77-4.84 (m, 7H, **H$_1$**), 5.64-5.83 (m, 14H, O**H$_1$** et O**H$_2$**), 7.42-7.44 (d, J=8.1Hz, 2H), 7.74-7.76 (d, J=8.1Hz, 2H). **^{13}C NMR ^{13}C (300MHz, DMSO-d_6):** δ (ppm) = 21.24 (**C**H$_3$), 59.27-60.03 (6x**C**H$_2$OH), 69.77 (**C**H$_2$OTs), 72.06-73.09 (21x**C**H), 80.75-81.67x**C**H), 101.27-102.24 (7x**C$_1$**H), 127.59 (2x**C$_{Ar}$**H), 129.91 (2x**C$_{Ar}$**H), 132.66 (**C$_{Ar}$**), 144.85 (**C$_{Ar}$**). **MS ESI$^+$ (calc. for $C_{49}H_{76}O_{37}S$ 1288.4):** m/z = 1311.2 [M+Na]$^+$.

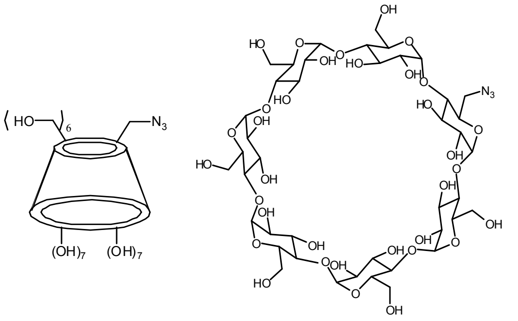

4

4 6-deoxy-6-azido-β-cyclodextrin β-CDN$_3$

β-CDOTs **2** (5g, 3.88mmol) was dissolved in dried DMF (35mL) then sodium azide (0.3g, 4.65mmol) was added. The reaction mixture was stirred at 105°C for 1h. After cooling at room temperature, acetone (200mL) was added then the solid was filtered and washed with acetone (3x50mL). The product was suspended in methanol (50mL) and the mixture was stirred overnight at room temperature. The product was filtered, washed with methanol (10mL) and acetone (2x10mL) then dried under vacuum to give 3.21g (2.75mmol, 71%) of β-CDN$_3$ **4** as a white powder. **^{1}H NMR (300MHz, DMSO-d_6):** δ (ppm) = 3.26-3.43 (m, 18H augmenté par HDO), 3.55-3.70 (m, 27H), 4.45-4.56 (m, 6H, 6xCH$_2$O**H**), 4.81-4.88 (m, 7H, **H$_1$**), 5.63-5.75 (m, 14H, O**H$_1$** et O**H$_2$**) (DMSO = 2.51). **MS ESI$^+$ (calc. for $C_{42}H_{69}N_3O_{34}$ 1159,38) :** 1182.3 [M+Na]$^+$.

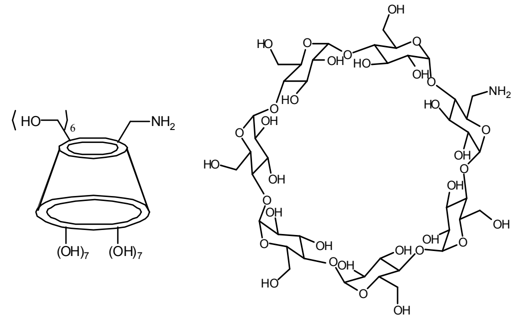

5

5 6-deoxy-6-amino-β-cyclodextrin β-CDNH$_2$

β-CDN$_3$ **4** (8.32g, 7.17mmol) was dissolved in DMF (41mL) then triphenylphosphine (2.07g, 7.89mmol) was added. The reaction mixture was stirred 4h at RT then water (2.58mL, 143mmol) was added and the reaction mixture was stirred at reflux for 30 minutes. After cooling at RT, the product was precipitated in acetone (400mL) then quickly filtered. The solid was washed with acetone (3x75mL) then dried under vacuum. The crude product was suspended in methanol (30mL) and the mixture was stirred overnight at RT. The product was filtered, washed with methanol (10mL) and acetone (2x10mL) then dried under vacuum to give 6.90g (6.09mmol, 85%) of β-CDNH$_2$ **5** as a white powder. **^{1}H NMR (300MHz - D$_2$O):** δ (ppm) = 2.71-2.78 (m, 1H), 2.96-3.01 (m, 1H), 3.33-3.40 (m, 1H), 3.49-3.57 (m, 14H), 3.7779-3.90 (m, 28H), 4.98 (s, 7H). **MS ESI$^+$ (calc. for $C_{42}H_{71}NO_{34}$ 1133,39):** 1134.7 [M+H]$^+$, 1156.8 [M+Na]$^+$.

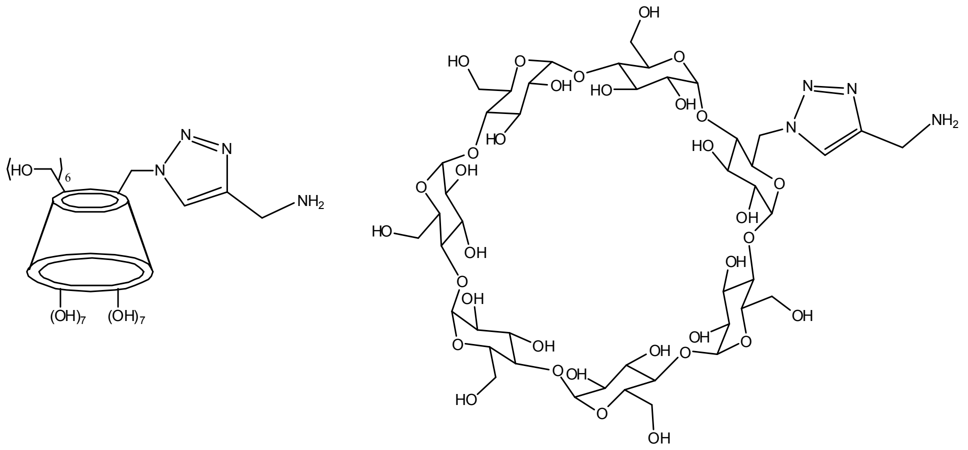

6b

6b 6-deoxy-(4-(aminomethyl)-1,2,3-triazole)-β-cyclodextrin

β-CDN$_3$ **4** (10.0g, 8.6mmol) was dissolved in DMF (75mL) then CuSO4 (1.51g, 9.5mmol) and propargyl amine (1.18g, 12.9mmol) were added. The sodium ascorbate (5.12g, 25.9mmol) was dissolved in water (15mL) then was added dropwise. The reaction mixture was stirred 20h at room temperature then the solvents were evaporated. The residue was dissolved in water (125mL) then HCl 1N (30mL) was added. The mixture was stirred overnight at RT then half of the solvent was evaporated. The product was then precipitated in acetone, filtered, washed with acetone (3x) then dried under vacuum to give 9.68g (7.91mmol, 92%) of **6b** as a white powder. **^{1}H NMR (300MHz - D$_2$O):** δ (ppm) =2.76-2.82 (m, 1H), 3.00-3.04 (m, 1H), 3.29-3.59 (m, 14H), 3.60-3.90 (m, 21H), 4.04-4.10 (m, 1H), 4.21 (s, 1H), 4.62-4.70 (m, overlap with H$_2$O), 4.87-4.93 (m, 6H), 5.04-5.05 (m, 1H), 8.05 (s, 1H). **MS ESI$^+$ (calc. for $C_{45}H_{74}N_4O_{34}$ 1214.42):** 1215.6 [M+H]$^+$, 1237.6 [M+Na]$^+$.

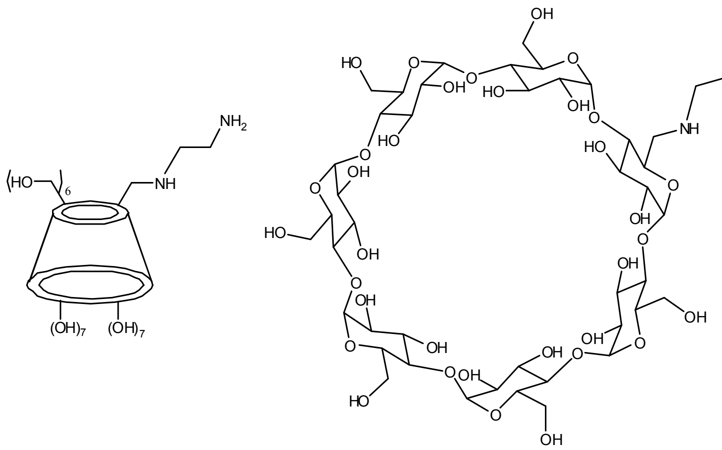
OH
NH$_2$
HO
O
O
OH
HO
OH
O
NH$_2$
(HO)$_6$
NH
HO
O
NH
OH
HO
O
HO
OH
O
OH
O
OH
OH
OH
(OH)$_7$
(OH)$_7$
O
OH
OH
O
HO
OH
O
O
OH
HO
O
OH

7

7 6-deoxy-(2-aminoethylamino)-β-cyclodextrin β-CDNH$(CH_2)_2NH_2$

β-CDOTs **2** (5.0g, 3.9mmol) was dissolved in ethylenediamine (195mmol, 13.0mL) then the reaction mixture was stirred 4h at 75°C. After cooling at room temperature, the product was precipitated in acetone (250mL) then filtered. The solid was washed with acetone (3x50mL) then dried under vacuum. The powder was suspended in methanol then the mixture was stirred overnight at room temperature. The solid was filtered then dried under vacuum to give 3.77g (3.2mmol, 82%) of **7** as a white solid. **^{1}H NMR (300MHz - D_2O):** δ (ppm) = 2.49-2.67 (m, 8H), 2.87-2.91 (m, 3H), 3.23-3.29 (t, 2H), 3.37-3.748 (m, 59H), 4.89 (m, 7H). **^{13}C NMR (D_2O - 75MHz):** δ (ppm) = 39.70, 49.23, 50.47, 57.38, 60.21, 71.4-72.01, 73.13, 81.02-81.15, 83.64, 101.64-101.89. **MS ESI$^+$ (calc. for $C_{44}H_{76}N_2O_{34}$ 1176.43):** 1177.8 $[M+H]^+$, 1199.8 $[M+Na]^+$.

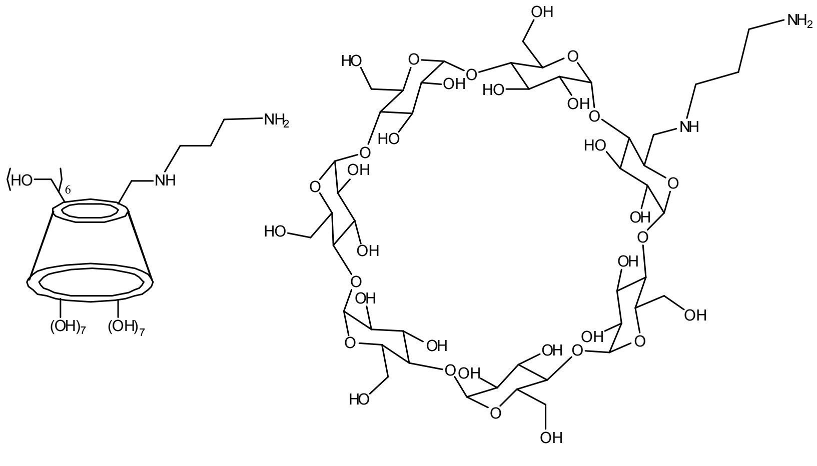
OH
NH$_2$
HO
O
O
OH
HO
OH
O
NH$_2$
NH
HO
(HO)$_6$
NH
O
OH
HO
O
HO
OH
O
OH
O
OH
OH
OH
(OH)$_7$
(OH)$_7$
O
OH
OH
O
HO
OH
O
O
OH
HO
O
OH

8

8 6-deoxy-(3-aminopropylamino)-β-cyclodextrin β-CDNH$(CH_2)_3NH_2$

β-CDOTs **2** (5.0g, 3.9mmol) was dissolved in diaminopropane (195mmol, 16.2mL) then the reaction mixture was stirred 4h at 75°C. After cooling at room temperature, the product was precipitated in acetone (250mL) then filtered. The solid was washed with acetone (3x50mL) then dried under vacuum. The powder was suspended in methanol then the mixture was stirred overnight at room temperature. The solid was filtered then dried under vacuum to give 4.27g (3.6mmol, 93%) of **8** as a white solid.

^{1}H NMR(300MHz - D_2O): δ (ppm) = 1.93-2.10 (m, 2H), 3.00-3.05 (t, 2H), 3.09-3.14 (m, 2H), 3.26-3.33 (m, 1H), 3.41-3.62 (m, 13H), 3.60-3.93 (m, 21H), 4.06-4.13 (m, 1H), 4.98-5.044 (m, 6H). **^{13}C NMR (75MHz - D_2O):** δ (ppm) = 23.54, 36.57, 45.26, 48.38, 60.34-60.69, 67.44, 71.72-72.39, 72.84-73.11, 80.40-83.14, 101.07-101.80. **MS ES$^+$ (calc. for $C_{45}H_{78}N_2O_{34}$ 1190.4):** m/z = 1191.4 [M+H]$^+$, 1213.4 [M+Na]$^+$.

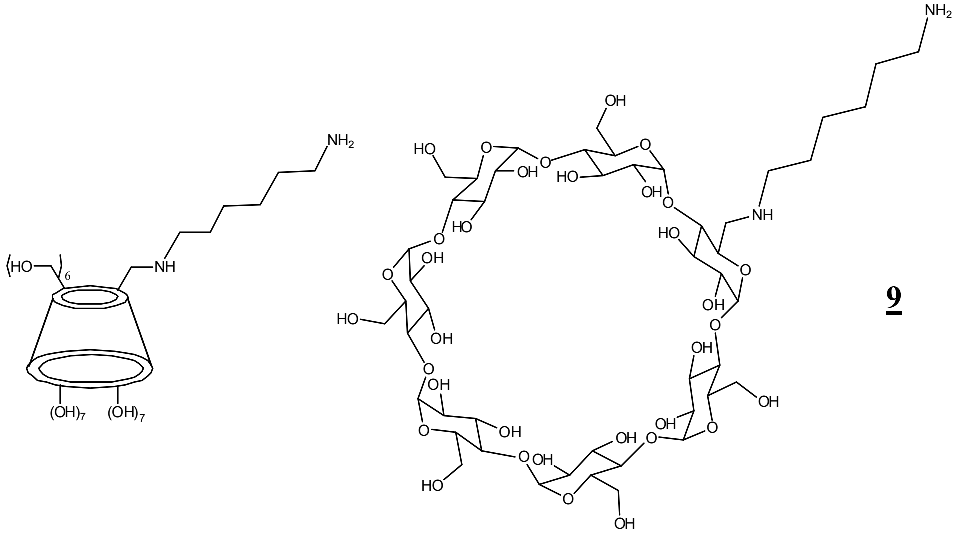

9

9 6-ddeoxy-(6-aminohexylamino)-β-cyclodextrin β-CDNH$(CH_2)_6NH_2$

β-CDOTs **2** (10.0g, 7.8mmol) was dissolved in NMP (150mL) then diaminohexane (3.60g, 31mmol) was added. The reaction mixture was stirred overnight at 75°C. After cooling at room temperature, the product was precipitated in acetone (500mL) then filtered. The solid was washed with acetone (3x100mL) then dried under vacuum. The powder was suspended in methanol then the mixture was stirred overnight at room temperature. The solid was filtered then dried under vacuum to give 9.60g (7.8mmol, 100%) of **9** as a white solid. **^{1}H NMR (300MHz - D_2O):** δ (ppm) = 1.03-1.32 (m, 14H), 1.99-2.07 (m, 2H), 2.49 (m, 7H+DMSO), 2.86 (m, 3), 3.32-3.99 (m, 60H), 4.81 (m, 7H). **^{13}C NMR (75MHz - D_2O):** δ (ppm) = 18.69, 26.63, 27.01, 29.57, 32.25, 41.18, 49.50, 50.80, 56.56, 60.28, 72.43-72.60, 73.39, 81.87, 102.33. **MS ESI$^+$ (calc. for $C_{48}H_{84}N_2O_{34}$ 1232.49):** 1233.7 [M+H]$^+$, 1255.8 [M+Na]$^+$.

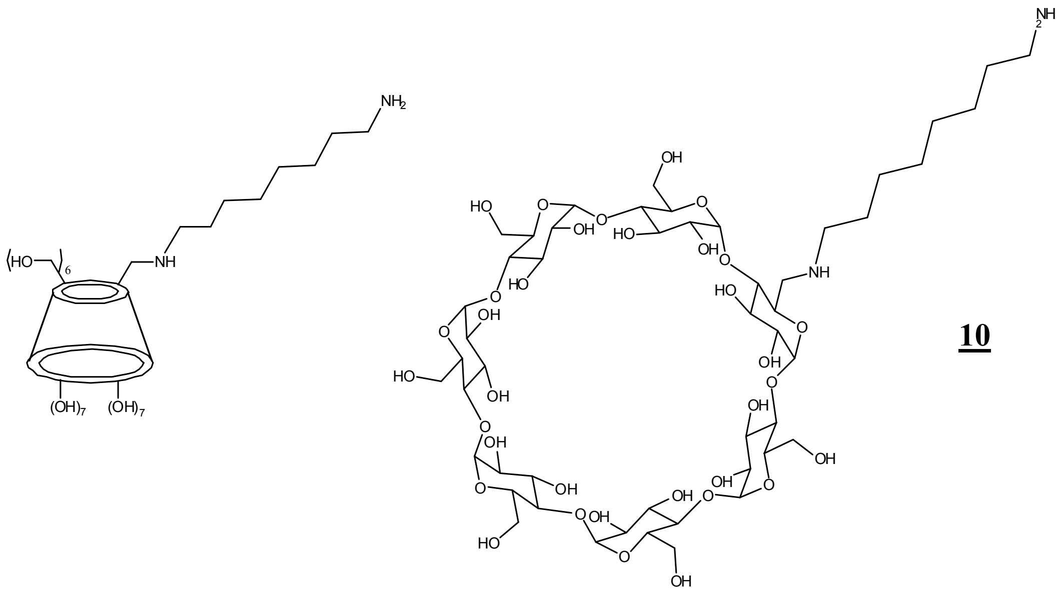

10

10 6-deoxy-(8-aminooctylamino)-β-cyclodextrin β-$CDNH(CH_2)_8NH_2$

β-CDOTs **2** (10.0g, 7.8mmol) was dissolved in NMP (150mL) then diaminohexane (4.48g, 31mmol) was added. The reaction mixture was stirred overnight at 75°C. After cooling at room temperature, the product was precipitated in acetone (500mL) then filtered. The solid was washed with acetone (3x100mL) then dried under vacuum. The powder was suspended in methanol then the mixture was stirred overnight at room temperature. The solid was filtered then dried under vacuum to give 9.47g (7.5mmol, 97%) of **10** as a white solid. **^{1}H NMR (300MHz - DMSO-d6) :** δ (ppm) = 1.50-1.51 (m, 2H), 2.28-2.31 (m, 2H), 2.46-2.48 (m, 2H), 2.64-2.69 (m, 2H), 2.75-2.80 (m, 2H), 2.94-2.98 (m, 2H), 3.28-3.31 (m, 2H), 3.45-3.80 (m, 49H), 4.7 (m, overlap with H_2O) 4.94-5.00 (m, 7H). **MS ESI$^+$ (calc. for $C_{48}H_{84}N_2O_{34}$ 1260.50):** 1261.8 $[M+H]^+$, 1283.7 $[M+Na]^+$.

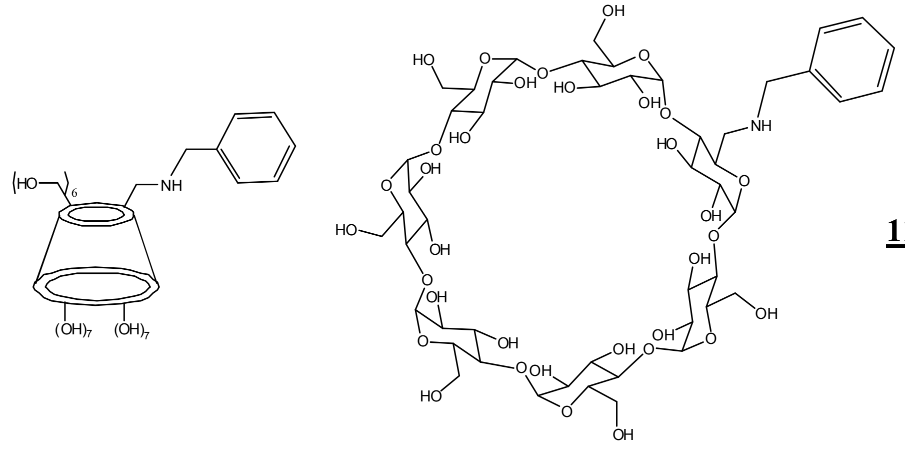

11

11 6-deoxy-(benzylamino)-β-cyclodextrin β-$CDNHCH_2Ph$

β-CDOTs **2** (5.0g, 3.9mmol) was dissolved in benzylamine (195mmol, 21.3mL) then the reaction mixture was stirred 4h at 75°C. After cooling at room temperature, the product was precipitated in acetone (250mL) then filtered. The solid was washed with acetone (3x50mL) then dried under vacuum to give **4.96g** (quant.) of **11** as a white solid. **^{1}H NMR (300MHz - DMSO-d6) :** δ (ppm) = 2.68-2.77 (m, 1H), 2.88-2.94 (m, 1H), 3.12-3.25 (m, 2H), 3.40-3.79 (m, 42H), 4.91 (s, 7H), 7.23-7.32 (m, 5H). **MS ESI$^+$ (calc. for $C_{48}H_{84}N_2O_{34}$ 1260.50):** 1224.20 [M+H]$^+$, 1246.33 [M+Na]$^+$.

General synthesis of amino acid derivatives:

β-CDOTs **2** (5g, 3.9mmol) was dissolved in water (75mL) then triethyl amine (10.81mL, 78mmol) and the corresponding amino acid (39mmol) were successively added. The reaction mixture was stirred overnight at 70°C. After cooling at room temperature, the product was precipitated in acetone (500mL). The solid was filtered, washed with acetone (3x100mL) then dried under vacuum.

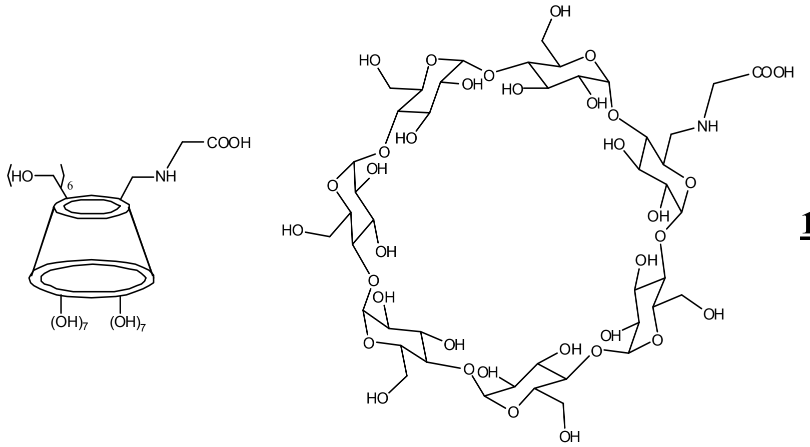

12a

12a 6-carboxymethylamino-6-deoxy-*β*-cyclodextrin

From 5.0g (3.9mmol) of β-CDOTs **2**, 7.51g (y>100% because of glycine) of crude product was collected. **^{1}H NMR (300MHz - D_2O):** δ (ppm) = 3.39-3.52 (m, 26H overlap with glycine), 3.73-3.85 (m, 21H), 4.69 (m, 67H overlap with H_2O), 4.92 (s, 7H). **MS ESI$^-$ (calc. for $C_{44}H_{73}NO_{36}$ 1191.39):** 1190.6 [M-H]$^-$.

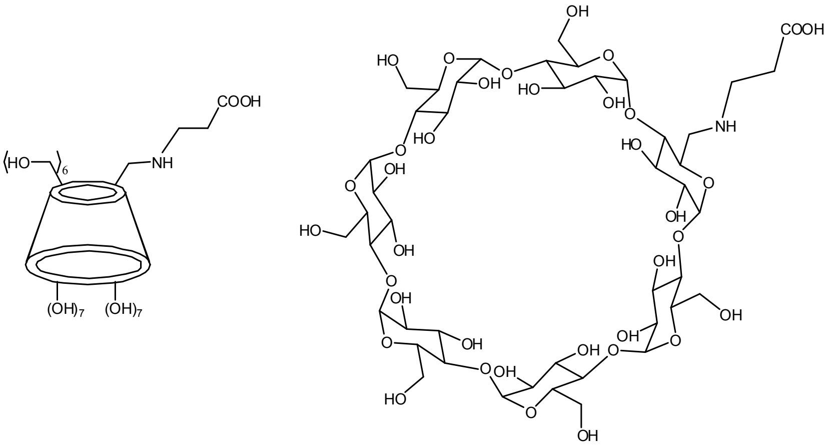

12b

12b 6-(2-carboxyethylamino)-6-deoxy-*β*-cyclodextrin

From 5.0g (3.9mmol) of β-CDOTs **2**, 8.19g (y>100% because of presence of β-alanine) of crude product was collected. **^{1}H NMR (300MHz - D_2O):** δ (ppm) = 2.412-2.46 (t, J=6.67Hz, 2H), 3.04-3.09 (t, J=6.67Hz, 2H), 3.45-3.57 (m, 21H), 3.74-3.89 (m, 28H), 4.96-4.97 (m, 7H), 4.70 (m, overlap with H_2O. **MS ESI$^-$ (calc. for $C_{45}H_{75}NO_{36}$ 1205.41):** 1204.7 [M-H]$^-$.

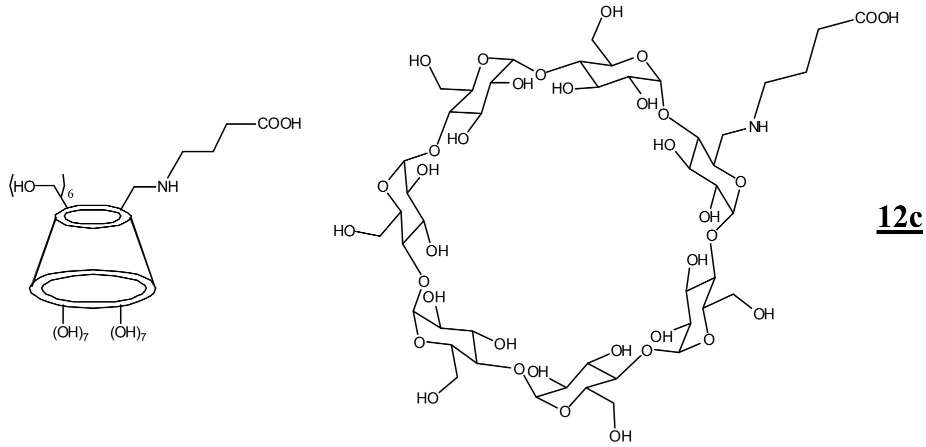

12c

12c 6-(3-carboxypropylamino)-6-deoxy-*β*-cyclodextrin

From 5.5g (4.27mmol) of β-CDOTs **2**, 9.45g (y>100% because of presence of aminobutyric acid) of crude product was collected. **^{1}H NMR (300MHz - D_2O):** δ (ppm) = 1.80-1.88 (m, 2H), 2.15-2.27 (m, 2H), 3.04-3.06 (m, 2H), 3.23-3.30 (m, 1H), 3.43-3.64 (m, 14H), 3.73-3.72 (m, 28H), 4.71 (m, overlap with H_2O), 4.99-5.07 (m, 7H). **MS ESI$^-$ (calc. for $C_{46}H_{75}NO_{36}$ 1219.42):** 1218.8 [M-H]$^-$.

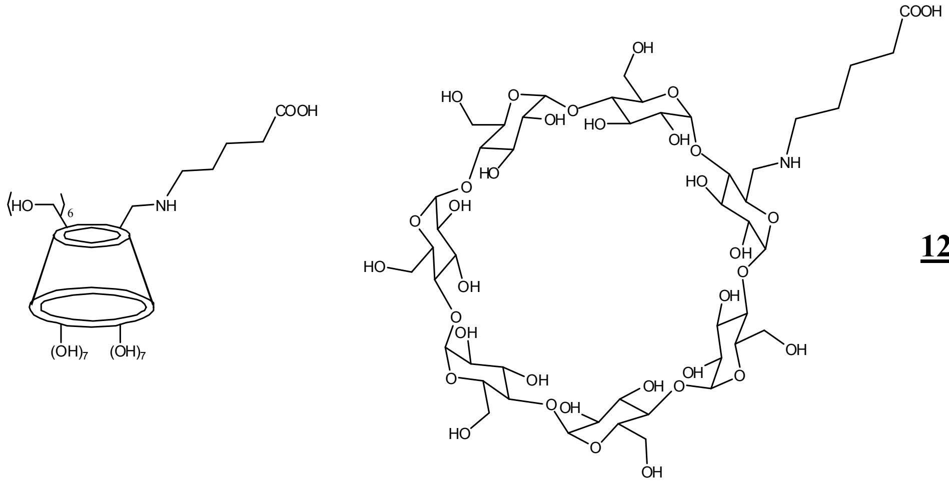

12d

12d 6-(4-carboxybutylamino)-6-deoxy-*β*-cyclodextrin

From 8.44g (6.55mmol) of β-CDOTs **2**, 8.12g (y≈100%, presence of aminovaleric acid) of crude product were collected. **^{1}H NMR (300MHz - D_2O):** δ (ppm) = 1.48-1.50 (m, 4H), 2.05-2.10 (m, 2H), 2.83-2.87 (m, 2H), 3.40-3.52 (m, 14H), 3.69-3.84 (m, 28H), 4.70 (m, overlap with H_2O), 4.92-4.92 (m, 7H). **MS ESI$^-$ (calc. for $C_{47}H_{79}NO_{36}$ 1233.44):** 1232.7 [M-H]$^-$.

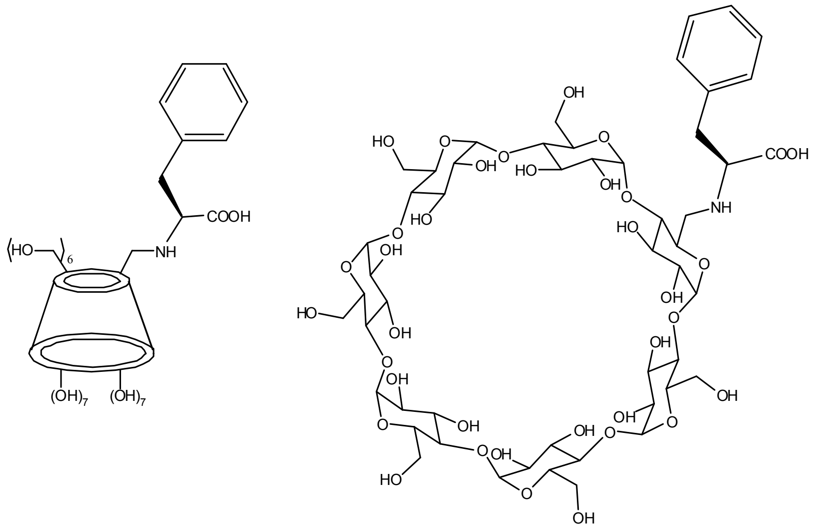

14

14 6-(1-benzyl-1-carboxymethylamino)-6-deoxy-*β*-cyclodextrin

From 5.0g (3.9mmol) of β-CDOTs **2**, 6.72g (y>100%) of crude product were collected.

^{1}H NMR (300MHz - D_2O): δ (ppm) = 1.24 (m, 1H), 1.55-1.56 (m, 2H), 2.80-2.89 (m, 2H), 3.09-3.68 (m, 42H), 4.83-4.84 (m, overlap with H_2O), 5.66-5.77 (m, 7H), 7.21-7.29 (m, 5H).

MS ESI$^+$ (calc. for $C_{51}H_{79}NO_{36}$ 1281.44): 1282.1 $[M+H]^+$, 1304.3 $[M+Na]^+$.

General synthesis of polyacid monosubstituted β-CD:

0.6mmol of cyclodextrins was dissolved in water (5mL) then the solution was cooled to 0°C. Chloroacetic acid (5mmol) and NaOH (5mmol) each dissolved in water (2mL) then both solutions were combined and cooled at 0°C and added to the solution of cyclodextrin. pH was adjusted to 10-11 using a solution of NaOH in water (1M) then the reaction mixture was stirred at 80°C for 24h. pH was regularly adjusted to 10-11 with the solution of NaOH. After cooling to room temperature, the product was precipitated in absolute ethanol. The solid was filtered, washed with absolute ethanol (5mL) then dried under vacuum.

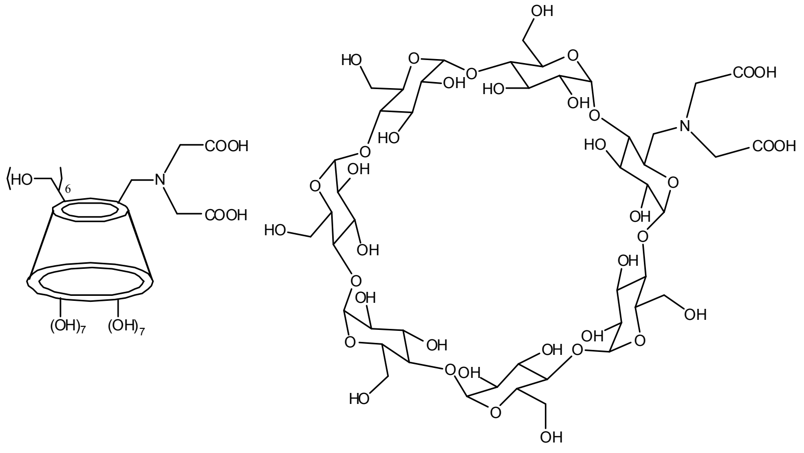

15

15 6-[bis(carboxylatomethyl)amino]-6-deoxy-β-cyclodextrin

From 0.60mmol (0.68g) of β-CDNH$_2$ **5**, 0.58g (0.46, 77%) of a white solid was collected. **^{1}H NMR (300MHz - D$_2$O):** δ (ppm) =2.72 (m, 1H), 3.00-3.05 (m, 1H), 3.18 (s, 2H), 3.42-3.51 (m, 14H), 3.72-3.85 (m, 28H), 4.87-4.99 (m, 7H) . **MS ESI$^-$ (calc. for $C_{46}H_{75}NO_{38}$ 1249.4):** 1248.9 [M-H]$^-$.

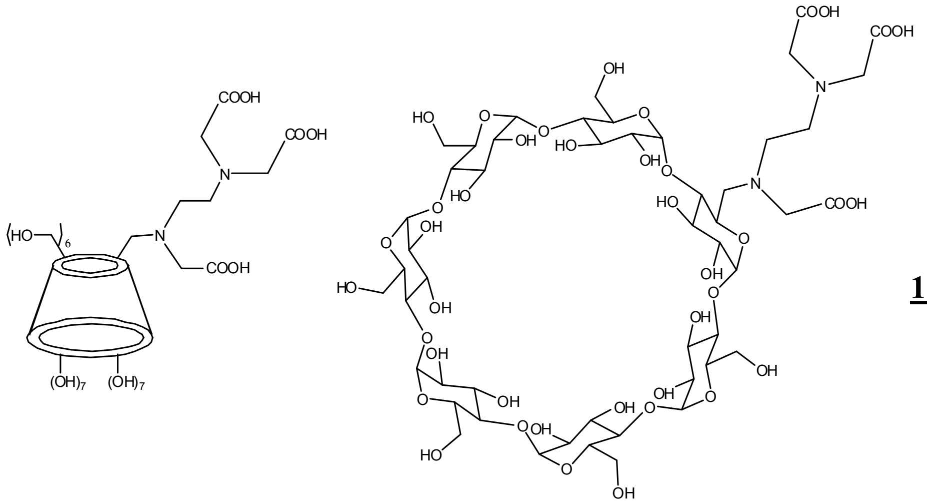

16a

16a 6-[tris(carboxylatomethyl)(2-aminoethyl)amino]-6-deoxy-β-cyclodextrin

From 3.20mmol (3.77g) of β-CDNH(CH$_2$)$_2$NH$_2$ **7**, 3.66g (2.71mmol, 85%) of a white solid were collected. **^{1}H NMR (300MHz - D$_2$O):** δ (ppm) = 2.49-3.23 (m, 1H), 3.43-3.51 (m, 14H), 3.73-3.81 (m, 8H), 3.92 (s, 7H). **MS ESI$^-$ (calc. for $C_{50}H_{82}N_2O_{40}$ 1350.44):** 1349.6 [M-H]$^-$.

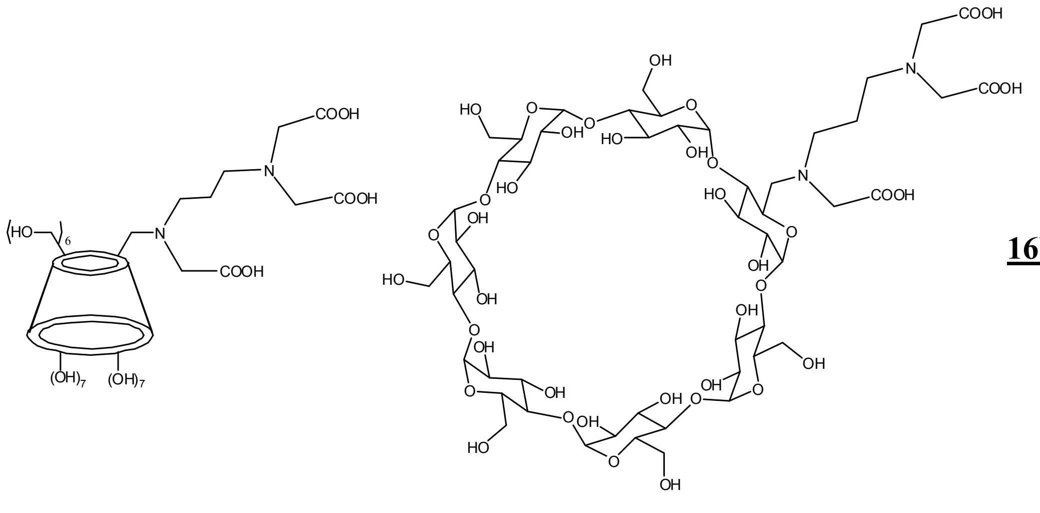

16b

16b 6-[tris(carboxylatomethyl)(3-aminopropyl)amino]-6-deoxy-β-cyclodextrin

From 0.6mmol (0.71g) of β-CDNH(CH$_2$)$_3$NH$_2$ **8**, 0.95g (r>100%) of crude product was collected. **^{1}H NMR (300MHz - D$_2$O):** δ (ppm) =3.24-3.33 (m, 6H), 3.34-3.54 (m, 14H), 3.60-3.88 (m, 28H), 4.05 (s, 1H), 4.13-4.23 (m, 1H), 4.26 (s, 1H), 4.38-4.50 (m, 2H), 4.92-5.06 (m, 7H). **MS ESI$^-$ (calc. for $C_{51}H_{84}N_2O_{40}$ 1364.46):** 1363.9 [M-H]$^-$.

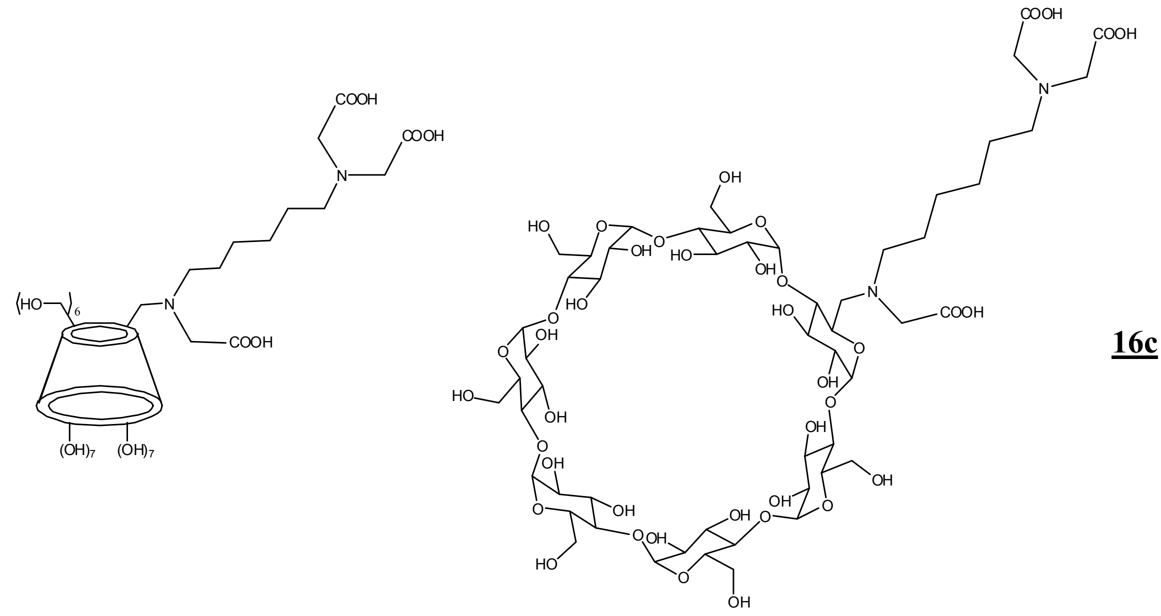

16c

16c 6-[tris(carboxylatomethyl)(6-aminohexyl)amino]-6-deoxyβ-cyclodextrin

From 3.49g (2.8mmol) of β-CDNH$(CH_2)_6NH_2$ **9**, 3.52g (2.49mmol, 89%) of a white solid was collected. **^{1}H NMR (300MHz - D_2O):** δ (ppm) = 1.18-1.53 (m, 8H), 2.47-2.78 (m, 3H), 2.91-3.22 (m, 6H), 3.45-3.52 (m, 14H), 3.63-3.95 (m, 21H), 4.83-5.05-m, 7H). **MS ESI$^-$ (calc. for $C_{54}H_{90}N_2O_{40}$ 1406.51):** 1406.1 $[M-H]^-$, 702.8 $[M-2H]^{2-}$.

Native β-cyclodextrin/ImTs inclusion complex

10g (8.8mmol) of native β-cyclodextrin was suspended in water (400mL) then ImTs 3 (1.96g, 8.8mmol) was added. The suspension was stirred for 24h at RT then the solid was filtered, washed with acetone (3x) then dried overnight at 40°C to give 7.7g (5.6mmol, 64%) of complex as a white solid. **^{1}H NMR (300MHz - DMSO-d6):** δ (ppm) = 3.40 (s, 3H), 3.27-3.38 (m, 40H overlap with H2O), 3.54-3.70 (m, 21H), 4.45-4.49 (m, 7H), 4.82-4.83 (m, 7H), 5.68-5.75 (m, 14H), 7.12 (s, 1H), 7.49-7.51 (d, J=8.35Hz, 2H), 7.74 (s, 1H), 7.96-7.99 (d, J=8.38Hz, 2H), 8.36 (s, 1H).

β-CDNH$_2$/ibuprofen inclusion complex

0.585g (0.5mmol) of β-CDNH$_2$ was dissolved in water (50mL) then ibuprofen (0.206g, 1mmol) was added. The reaction mixture was stirred for 10 minutes at RT then was filtered. The aqueous layer was concentrated then the solid was dried overnight at 40°C to give 0.607 g (0.44mmol, 88%) of inclusion complex as a white solid**. ^{1}H NMR (300MHz - D_2O):** δ (ppm) =0.78-0.80 (d, J=6.57Hz, 6H), 1.22-1.25 (d, J=6.24Hz, 3H), 1.70-1.79 (m, 1H), 2.27-2.39 (d, 6.43Hz, 2H), 3.18-3.23 (m, 1H), 3.28-3.35 (m, 1H), 3.41-3.80 (m, 40H), 4.91-4.92 (m, 7H), 6.93-6.95 (d, J=7.77Hz, 2H), 7.07-7.09 (d, 7.55Hz, 2H).

III - Stochastic chiral symmetry breaking of a conglomerate forming system; study of a series of triazoyl ketone

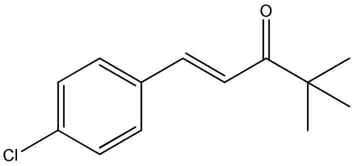

20-Cl

20-Cl (*E*)-1-(4-chlorophenyl)-4,4-dimethylpent-1-en-3-one

NaOH (8g, 200mmol) was dissolved in water (14mL) then ethanol (30mL) was added. The reaction mixture was placed in an ice-bath then a solution of 4-chlorobenzaldehyde (28.11g, 200mmol) and pinacolone (20.03g, 200mmol) in ethanol (40mL) was added dropwise. The ice-bath was removed and the reaction mixture was vigorously stirred at room temperature for 4h then filtered. The solid was washed with water (3x75mL) then dried under vacuum. 36.18g (81%) of **20-Cl** was obtained as a pale yellow solid. **^{1}H NMR (300MHz, $CDCl_3$):** δ (ppm) = 1.21 (s, 9H), 7.06-7.11 (d, J=15.6Hz), 7.31-7.35 (m, 2H), 7.46-7.50 (m, 2H), 7.58-7.63 (d, J=15.6Hz). **^{13}C NMR (75MHz, $CDCl_3$):** δ (ppm) = 26.19, 43.19, 121.08, 129.02, 129.36, 133.35, 136.92, 141.37, 203.86 **Chemical ionisation MS$^+$ (calc. for $C_{13}H_{15}ClO$ 222.71):** m/z = 223.0 $[M+H]^+$, 225.0 $[M+H+2]^+$, 240.0 $[M+NH_4]^+$, 242.1 $[M+NH_4+2]^+$. **Melting point:** 85°C.

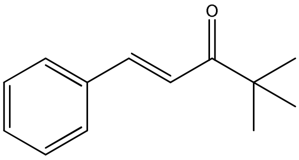

20-H

20-H (*E*)-4,4-dimethyl-1-phenylpent-1-en-3-one

20-H was prepared following the same procedure as **20-Cl** from benzaldehyde (5.31g, 50mmol). As **20-H** is a liquid, the work-up was modified as follow: water (100mL) was added to the reaction mixture and the product was extracted by diethyl ether (3x50mL). The combined organic layers were dried with $MgSO_4$ then the solvent was evaporated and the product was dried under vacuum to give 8.64g (92%) of a colourless liquid. **^{1}H NMR (300MHz, $CDCl_3$):** δ (ppm) = 1.23 (s, 9H), 7.10-7.16 (d, J=15.6Hz, 1H), 7.38-7.40 (m, 3H), 7.56-7.59 (m, 2H), 7.66-7.71 (d, J=15.6Hz, 1H) **^{13}C NMR (75MHz, $CDCl_3$):** δ (ppm) = 26.09, 43.00, 120.484, 128.06, 128.68, 129.98, 134.69, 142.69, 203.86 **Chemical ionisation MS$^+$ (calc. for $C_{13}H_{16}O$ 188.12):** m/z = 189.0 $[M+H]^+$, 206.1 $[M+NH_4]^+$

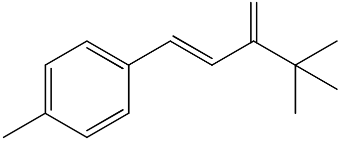

20-Me

20-Me (*E*)-1-(*p*-toluyl)-4,4-dimethylpent-1-en-3-one

20-Me was prepared following the same procedure as **20-Cl** from *p*-tolualdehyde (20.03g, 200mmol) to give 30.1g (75%) of a pale yellow solid. **^{1}H NMR (300MHz, CDCl$_3$):** δ (ppm) = 1.23 (s, 9H), 2.38 (s, 3H), 7.06-7.11 (d, J=15.60Hz, 1H), 7.18-7.21 (d, J=8.0Hz, 2H), 7.46-7.49 (d, J=8.01Hz, 2), 7.63-7.67 (d, J=15.60Hz, 1H). **^{13}C NMR (75MHz, CDCl$_3$):** δ (ppm) = 21.46, 26.35, 43.18, 119.71, 128.26, 129.55, 132.17, 140.59, 142.90, 204.31. **ESI-MS$^+$ (calc. for $C_{14}H_{18}O$ 202.14):** m/z = 203.1 [M+H]$^+$. **Melting point:** 83°C.

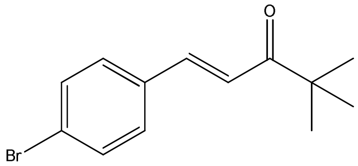

20-Br

20-Br (*E*)-1-(4-bromophenyl)-4,4-dimethylpent-1-en-3-one

20-Br was prepared following the same procedure as **20-Cl** from 4-bromobenzaldehyde (37.00g, 200mmol) to give 41.04g (75%) of a pale yellow solid. **^{1}H NMR (300MHz, CDCl$_3$):** δ (ppm) = 1.22 (s, 9H), 7.07-7.12 (d, J=15.6Hz, 1H), 7.41-7.44 (d, J=8.6Hz, 2H), 7.50-7.52 (d, J=8.6Hz, 2), 7.57-7.62 (d, J=15.6Hz, 1H) **^{13}C NMR (75MHz, CDCl$_3$):** δ (ppm) = 26.23, 43.26, 121.21, 124.33, 129.62, 132.04, 133.81, 141.51, 203.98. **ESI-MS$^+$ (calc. for $C_{13}H_{15}BrO$ 266.03):** m/z = 266.94 [M+H]$^+$, 268.87 [M+H+2]$^+$. **Melting point:** 92°C.

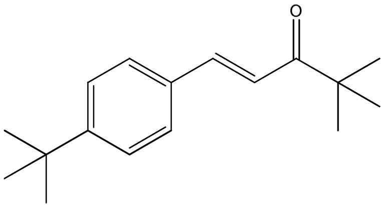

20-tBu

20-tBu (*E*)-1-(4-tertbuthylphenyl)-4,4-dimethylpent-1-en-3-one

20-tBu was prepared following the same procedure as **20-Cl** from 4-tert-butylbenzaldehyde (23.36g, 144mmol). As **20-tBu** is a liquid, the work-up was modified as follow: water (100mL) was added to the reaction mixture and the product was extracted by ethyl acetate (3x50mL). The combined organic layers were washed with water (3x), dried with $MgSO_4$ then the solvent was evaporated. The product was dried under vacuum to give 33.40g (95%) of a pale yellow liquid. **^{1}H NMR (300MHz, CDCl$_3$):** δ (ppm) = 1.23 (s, 9H), 1.33 (s, 9H), 7.07-7.12 (d, J=15.6Hz, 1H), 7.39-7.42 (d, J=8.4Hz, 2H), 7.50-7.53 (d, J=8.4Hz, 2H), 7.65-7.70 (d, J=15.5Hz, 1H). **^{13}C NMR (75MHz, CDCl$_3$):** δ (ppm) = 26.34, 31.15, 34.87, 43.20, 119.93, 125.81, 128.11, 132.15, 142.78, 153.75, 204.37. **ESI-MS$^+$ (calc. for $C_{17}H_{24}O$ 244.18):** m/z = 244.24 [M+H]$^+$.

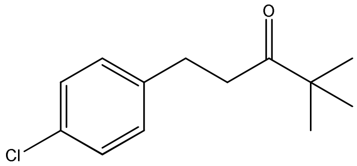

21-Cl

21-Cl 1-(4-chlorophenyl)-4,4-dimethylpentan-3-one

3g of Raney Nickel, 50% slurry in water were placed in a round bottom flask and were washed with ethanol (3x10mL) then with ethyl acetate (3x10mL). A solution of **20-Cl** (10.67g, 47mmol) in ethyl acetate (75mL) was added to the nickel. The reaction mixture was stirred under vacuum for 5 minutes then flushed with hydrogen gaz and stirred at room temperature overnight under hydrogen atmosphere using a rubber balloon. The conversion of the reaction was controlled by NMR. After complete conversion of the starting material, the solution was filtered through a pad of celite. The filtrate was evaporated and the product was dried under vacuum to give 10.32g (46mmol, 96%) of **21-Cl** as a colourless liquid. **^{1}H NMR (300MHz, CDCl$_3$):** δ (ppm) = 1.14 (s, 9H), 2.78-2.83 (m, 2H), 2.86-2.912 (m, 2H), 7.13-7.18 (m, 2H), 7.25-7.30 (m, 2H) **^{13}C NMR (75MHz, CDCl$_3$):** δ (ppm) = 26.26, 29.31, 38.16, 44.02, 128.46, 129.76, 131.70, 140.00, 214.53. **ESI-MS$^+$ (calc. for C$_{13}$H$_{17}$ClO 224.10):** m/z = 225.13 [M+H]$^+$, 227.18 [M+H+2]$^+$.

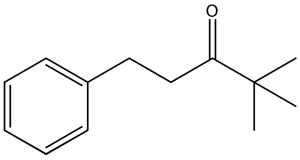

21-H

21-H 4,4-dimethyl-1-phenylpentan-3-one

21-H was prepared following the same procedure as **21-Cl** from 10,23g (54mmol) of **20-H** to give 10.07g (53mmol, 97%) of as a colorless liquid. **^{1}H NMR (300MHz, CDCl$_3$):** δ (ppm) = 1.11 (s, 9H), 2.77-2.83 (m, 2H), 2.86-2.91 (m, 2H), 7.16-7.21 (m, 3H), 7.30-7.31 (m, 2H). **^{13}C NMR (75MHz, CDCl$_3$):** δ (ppm) = 26.16, 29.95, 38.33, 43.91, 125.85, 128.34, 141.42, 142.76, 214,76. **Chemical ionisation MS$^+$ (calc. for C$_{13}$H$_{18}$O 190.28):** m/z = 208.1 [M+NH$_4$]$^+$.

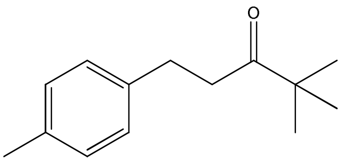

21-Me

21-Me 4,4-dimethyl-1-(p-tolyl)pentan-3-one

21-Me was prepared following the same procedure as **21-Cl** from 30.1g (149mmol) of **20-Me** to give 26.0g (127mmol, 86%) of a colourless liquid. For a complete conversion of the starting material, the rubber balloon was refilled with Hydrogen and the reaction mixture was

stirred another night at room temperature. **^{1}H NMR (300MHz, $CDCl_3$):** δ (ppm) = 1.12 (s, 9H), 2.32 (s, 3H), 2.75-2.88 (m, 4H), 7.09-7.11 (m, 4H). **^{13}C NMR (75MHz, $CDCl_3$):** δ (ppm) = 20.87, 26.21, 29.55, 38.52, 60.24, 128.13, 128.98, 135.30, 138.37, 214.82. **ESI-MS$^+$ (calc. for $C_{14}H_{20}O$ 204.15):** m/z = 205.07 $[M+H]^+$.

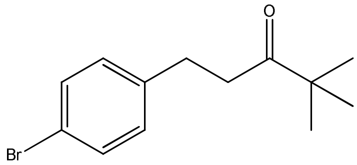

21-Br

21-Br 1-(4-bromophenyl)-4,4-dimethylpentan-3-one

16.6g (154mmol) of **20-Br** were hydrogenated. However the hydrolyse of the Br-Ar bond was significant and, after refilling the rubber balloon six times and changing the catalyst twice, the conversion stopped around 50%. 10.55g of crude product was obtained. It was composed of 4 molecules: **21-Br** (≈35%, 16mmol), unreacted **20-Br** (≈35%, 16mmol) and the corresponding non-brominated products **20-H** (≈15%, 7mmol) and **21-H** (≈15%, 7mmol). Relative proportions of products were determined by NMR. The crude product was used in the following step without purification. **^{1}H NMR (300MHz, $CDCl_3$):** δ (ppm) = 1.09 (s, 9H), 2.73-2.87 (m, 4H). Peaks of aromatic hydrogens are superimposed with those of the by-products. **^{13}C NMR (75MHz, $CDCl_3$):** δ (ppm) = 25.88, 29.69, 37.98, 43.53, 129.83, 130.97, 133.42, 140.15, 213,73. **ESI-MS$^+$ (calc. for $C_{13}H_{17}BrO$ 268.05):** m/z = 269.07 $[M+H]^+$, 271.10 $[M+H+2]^+$, 290.96 $[M+Na]^+$, 293.02 $[M+Na+2]^+$.

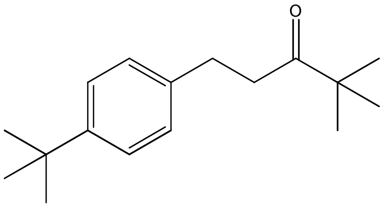

21-tBu

21-tBu 1-(4-tert-butylphenyl)-4,4-dimethylpentan-3-one

21-tBu was prepared following the same procedure as **21-Cl** from 35.7g (146mmol) of **20-tBu** to give 26.0g (146mmol, quant.) of a pale yellow solid. For a complete conversion of the starting material, the rubber balloon was refilled twice with hydrogen and the reaction mixture was stirred two other nights at room temperature. **^{1}H NMR (300MHz, $CDCl_3$):** δ (ppm) = 1.15 (s, 9H), 1.34 (s, 9H), 2.79-2.91 (m, 4H), 7.15-7.18 (d, J=8.3 Hz, 2H), 7.33-7.36 (d, J=8.3Hz, 2H). **^{13}C NMR (75MHz, $CDCl_3$):** δ (ppm) = 26.32, 29.50, 31.35, 34.31, 38.48, 44.04, 125.27, 127.95, 138.41, 148.77, 215.12. **ESI-MS$^+$ (calc. for $C_{17}H_{26}O$ 246.20):** m/z = 246.92 $[M+H]^+$.

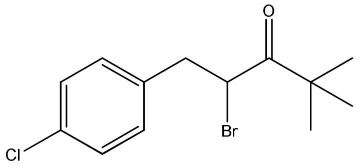

22-Cl

22-Cl 2-bromo-1-(4-chlorophenyl)-4,4-dimethylpentan-3-one

21-Cl (13.46g, 59.89mmol) was dissolved in glacial acetic acid (120mL) then tetrabutyl ammonium tribromide (31.80g, 65.88mmol) was added. The reaction mixture was stirred at room temperature for 5h then water (350mL) was added. The combined organic and aqueous phases were transferred in a separating funnel then the product was extracted with ethyl acetate (4x150mL). Organics layers were combined, then washed with water (2x150mL) and with a sodium hydroxide aqueous solution (around 2,5.10^{-1}mol.L^{-1}) until all acetic acid was removed. The organic layer was dried with $MgSO_4$, the solvent was evaporated and the product was dried under vacuum to give 17.52g (57.7mmol, 96%) of **22-Cl** as a white solid. **^{1}H NMR (300MHz, $CDCl_3$):** δ (ppm) = 1.01 (s, 9H), 3.12-3.18 (dd, J=5.7Hz, J=13.5Hz, 1H), 3.40-3.48 (dd, J=9.3Hz, J=13.2Hz, 1H), 4.68-4.73 (dd, J=5.7Hz, J=9.3Hz, 1H), 7.07-7.12 (d, J=8.6Hz, 2H), 7.23-7.28 (d, J=8.6Hz, 2H). **^{13}C NMR (75MHz, $CDCl_3$):** δ (ppm) = 26.27, 39.90, 43.67, 44.08, 128.75, 130.96, 133.12, 135.71, 208.32. **ESI-MS$^+$ (calc. for $C_{13}H_{16}BrClO$ 302.01):** m/z = 325.07 $[M+Na]^+$, 327.07 $[M+Na+2]^+$, 329.07 $[M+Na+4]^+$.

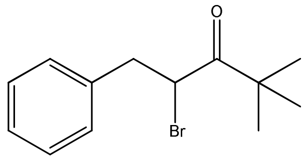

22-H

22-H 2-bromo-4,4-dimethyl-1-phenylpentan-3-one

22-H was prepared following the same procedure as **22-Cl** from 10.00g (53mmol) of **21-H** to give 13.66g (51mmol, 97%) of a white solid. **^{1}H NMR (300MHz, $CDCl_3$):** δ (ppm) = 0.98 (s, 9H), 3.16-3.22 (dd, J=5.6Hz, J=13.3Hz, 1H), 3.43-3.51 (dd, J=9.7Hz, J=13.3Hz, 1H), 4.73-4.78 (dd, J=5.6Hz, J=9.7Hz, 1H), 7.14-7.17 (m, 2H), 7.22-7.31 (m, 3H). **^{13}C NMR (75MHz, $CDCl_3$):** δ (ppm) = 26.18, 40.73, 44.09, 44.32, 127.19, 128.60, 129.63, 137.24, 208.60. **ESI-MS$^+$ (calc. for $C_{13}H_{16}BrO$ 268.05):** m/z = 291.12 $[M+Na]^+$, 293.12 $[M+Na+2]^+$.

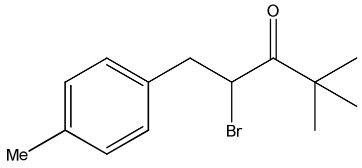

22-Me

22-Me 2-bromo-4,4-dimethyl-1-(p-tolyl)pentan-3-one

22-Me was prepared following the same procedure as **22-Cl** from 26.0g (127mmol) of **21-Me** to give 32.5g (115.6mmol, 91%) of a white solid. **^{1}H NMR (300MHz, $CDCl_3$):** δ (ppm) =

0.99 (s, 9H), 2.30 (s, 3H), 3.11-3.18 (dd, J=5.6Hz, J=13.4Hz, 1H), 3.39-3.52 (m, 2H), 4.71-4.76 (dd, J=5.7Hz, J=9.5Hz, 1H), 7.02-7.11 (m, 4H) ($CDCl_3$ = 7.26ppm). **^{13}C NMR (75MHz, $CDCl_3$):** δ (ppm) = 21.03, 26.22, 33.53, 40.28, 44.27, 129.22, 129.45, 134.12, 136.75, 208.59. **ESI-MS$^+$ (calc. for $C_{13}H_{19}BrO$ 282.06):** m/z = 283.10 $[M+H]^+$, 285.03 $[M+H+2]^+$.

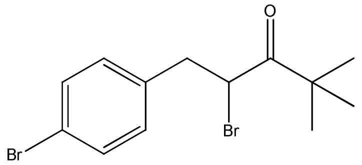

22-Br

22-Br 2-bromo-1-(4-bromophenyl)-4,4-dimethylpentan-3-one

22-Br was prepared following the same procedure as **22-Cl** from 10.55g of the crude product containing **21-Br** by using 1.4 equivalent of TBA.Br_3 (instead of 1.1 equivalent). 16.2g of crude product, containing **22-Br**, were obtained. The crude product was used in the following step without purification. **^{1}H NMR (300MHz, $CDCl_3$):** δ (ppm) = 1.01, 3.10-3.16 (dd, J=5.7Hz, J=13.5Hz, 1H), 3.38-3.46 (dd, J=9.5Hz, J=13.6Hz, 1H), 4.68-4.73 (dd, J=5.7Hz, J=9.5Hz, 1H), 7.02-7.05 (d, J=8.3Hz, 2H), 7.38-7.43 (d, J=8.4Hz, 2H). **ESI-MS$^+$ (calc. for $C_{13}H_{16}Br_2O$ 345.96):** m/z = 348.24 $[M+H+2]^+$.

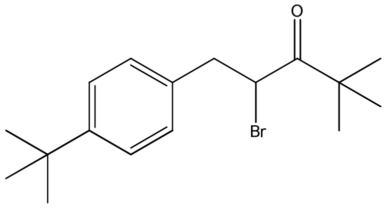

22-tBu

22-tBu 2-bromo-1-(4-tert-butylphenyl)-4,4-dimethylpentan-3-one

22-tBu was prepared following the same procedure than **22-Cl** from 38.00g (154mmol) of **21-tBu** to give 50.1g (154mmol, quant.) of a white solid. **^{1}H NMR (300MHz, $CDCl_3$):** δ (ppm) = 0.97 (s, 9H), 1.28 (s, 9H), 3.13-3.20 (dd, J=5.7Hz, J=13.4Hz, 1H), 3.39-3.47 (dd, J=9.6Hz, J=13.4Hz, 1H), 4.72-4.77 (dd, J=5.7Hz, J=10.2Hz, 1H), 7.04-7.10 (d, J=8.2Hz, 2H), 7.28-7.30 (d, J=8.3Hz, 2H). **^{13}C NMR (75MHz, $CDCl_3$):** δ (ppm) = 26.09, 31.27, 34.41, 40.18, 44.24, 44.33, 125.42, 129.25, 134.10, 150.19, 208.72. **ESI-MS$^+$ (calc. for $C_{17}H_{25}BrO$ 324.11):** m/z = 324.89 $[M+H]^+$, 326.82 $[M+H+2]^+$.

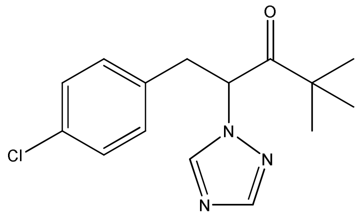

17-Cl

17-Cl 1-(4-chlorophenyl)-4,4-dimethyl-2-(1,2,4-triazol-1-yl)pentan-3-one

22-Cl (24.7g, 81mmol) was dissolved in acetone (170mL) then 1,2,4-1*H*-triazole (5.62g, 81mmol) and K_2CO_3 (22.5g, 163mmol) were added. The reaction mixture was stirred at 45°C for 4h. After cooling to room temperature, the solution was filtered. The solid was washed with acetone (3x100mL). The filtrate was evaporated; a pale orange solid was obtained. It was washed with diisopropyl ether (3x50mL) then with a small amount of methanol (2x10mL) and dried. The filtrate was evaporated and the solid obtained was washed as previously described. The two solids were combined to give 19.7g (67mmol, 83%) of **17-Cl** as a white solid. **^{1}H NMR (300MHz, $CDCl_3$):** δ (ppm) = 0.97 (s, 9H), 3.12-3.19 (dd, J=7.8Hz, J=13.7Hz, 1H), 3.25-3.32 (dd, J=7.5Hz, J=13.7Hz), 5.61-5.66 (t, 1H), 6.93-6.95 (d, J=8.4Hz, 2H), 7.15-7.18 (d, J=8.4Hz, 2H), 7.82 (s, 1H), 8.17 (s, 1H). **^{13}C NMR (75MHz, $CDCl_3$):** δ (ppm) = 25.35, 38.35, 44.68, 62.33, 128.96, 130.33, 133.22, 133.51, 142.15, 151.19, 208.67. **ESI-MS$^+$ (calc. for $C_{15}H_{18}ClN_3O$ 291.11):** m/z = 292.25 $[M+H]^+$, 294.19 $[M+H+2]^+$, 314.13 $[M+Na]^+$, 316.13 $[M+Na+2]^+$. **Elementary analysis (calc. for $C_{15}H_{18}ClN_3O$: %C=61.75, %H=6.22, %N=14.40):** %C=61.73, %H=6.24, %N=14.47%. **Melting point (by DSC):** 120.9°C.

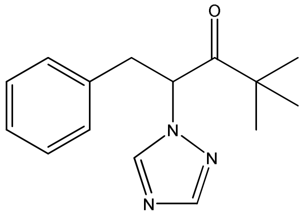

17-H

17-H 4,4-dimethyl-1-phenyl-2-(1,2,4-triazol-1-yl)pentan-3-one

17-H was prepared following the same procedure as **17-Cl** from 13.66g (51mmol) of **22-H** to give 9.24g (36mmol, 71%) of a white solid. **^{1}H NMR (300MHz, $CDCl_3$):** δ (ppm) = 1.03 (s, 9H), 3.21-3.29 (dd, J=7.7Hz, J=13.6Hz, 1H), 3.36-3.43 (dd, J=6.6Hz, J=13.6Hz, 1H), 5.72-5.77 (t, J=7.7Hz, 1H), 7.07-7.10 (m, 2H), 7.24-7.31 (m, 3H+$CHCl_3$), 7.90 (s, 1H), 8.28 (m, 1H). **^{13}C NMR (75MHz, $CDCl_3$):** δ (ppm) = 25.38, 39.17, 44.73, 62.68, 127.36, 128.74, 129.05, 135.01, 142.18, 151.08. **ESI-MS$^+$ (calc. for $C_{15}H_{19}N_3O$ 257.15):** m/z = 258.23 $[M+H]^+$, 280.25 $[M+Na]^+$, 537.05 $[2M+Na]^+$. **Elementary analysis (calc. for $C_{15}H_{19}N_3O$: %C=70.01, %H=7.44, %N=16.33):** %C=69.94, %H=7.42, %N=16.27. **Melting point (by DSC):** 71.0°C.

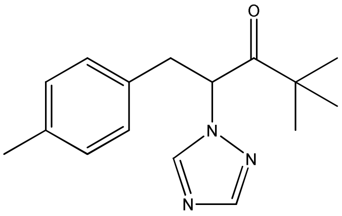

17-Me

17-Me 4,4-dimethyl-1-(p-tolyl)-2-(1,2,4-triazol-1-yl)pentan-3-one

17-Me was prepared following the same procedure as **17-Cl** from 23.10g (81.6mmol) of **22-Me** to give 17.00g (63mmol, 77%) of a white solid. **^{1}H NMR (300MHz, $CDCl_3$):** δ (ppm) = 0.99 (s, 9H), 2.26 (s, 3H), 3.12-3.19 (dd, 2H, J=7.9Hz, J=13.7Hz), 3.27-3.46 (dd, 2H, J=7.5Hz, J=13.7Hz), 5.65-5.70 (t, 1H, J=7.7Hz), 6.90-6.93 (d, 2H, J=8.0Hz), 7.02-7.04 (d, 2H, J=7.9Hz), 7.83 (s, 1H), 8.20 (s, 1H) ($CDCl_3$ = 7.26ppm). **^{13}C NMR (75MHz, $CDCl_3$):** δ (ppm) = 20.96, 25.46, 38.80, 44.74, 62.82, 128.90, 129.42, 131.89, 137.02, 142.24, 151.09, 209.28. **ESI-MS$^+$ (calc. for $C_{16}H_{21}N_3O$ 271.17):** m/z = 272.27 $[M+H]^+$, 294.27 $[M+Na]^+$, 565.13 $[2M+Na]^+$. **Elementary analysis (calc. for $C_{16}H_{21}N_3O$: %C=70.82, %H=7.80, %N=15.49):** %C=70.21, %H=7.77, %N=17.07. **Melting point (by DSC):** 96.2°C.

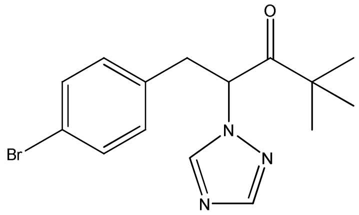

17-Br

17-Br 1-(4-bromophenyl)-4,4-dimethyl-2-(1,2,4-triazol-1-yl)pentan-3-one

17-Br was prepared following the same procedure as **17-Cl** from 16.2g of crude material containing **22-Br** to give 2.8g (8.3mmol) of **17-Br** as a white solid. The work-up was modified as follow: after filtration, the mixture was recrystallized in diisopropyl ether then the solid was stirred in methanol (15mL) for 1h, then filtered and dried under vacuum. **^{1}H NMR (300MHz, $CDCl_3$):** δ (ppm) = 1.01 (s, 9H), 3.14-3.21 (dd, J=7.7Hz, J=13.7Hz, 1H), 3.27-3.34 (dd, J=7.5Hz, J=13.7Hz, 1H), 5.64-5.69 (t, 7.7Hz, 1H), 6.91-6.45 (d, J=8.4Hz, 1H), 7.36-7.39 (d, J= 7.4Hz, 1H), 7.86 (s, 2H), 8.20 (s, 1H). **^{13}C NMR (75MHz, $CDCl_3$):** δ (ppm) = 25.30, 38.30, 44.62, 62.17, 121.21, 130.63, 131.70, 133.98, 142.14, 151.44, 208.57. **ESI-MS$^+$ (calc. for $C_{15}H_{18}BrN_3O$ 335.06):** m/z = 336.20 $[M+H]^+$, 338.13 $[M+H+2]^+$, 358.13 $[M+Na]^+$, 360.07 $[M+Na+2]^+$. **Elementary analysis (calc. for $C_{15}H_{18}BrN_3O$: %C=53.58, %H=5.40, %N=12.50):** %C=53.47, %H=5.74, %N=12.58. **Melting point (by DSC):** 139.3°C.

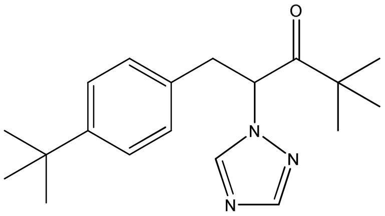

17-tBu

17-tBu 1-(4-tert-butylphenyl)-4,4-dimethyl-2-(1,2,4-triazol-1-yl)pentan-3-one

17-tBu was prepared following the same procedure as **17-Cl** from 50.00g (154mmol) of **22-tBu.** This compound is difficult to crystallize and can not be purified as **17-Cl**. Around a half of the crude product (30.00g) was purified by chromatography on silicagel with petroleum ether/ethyl acetate from 9/1 to 7/3 as eluent. 18.5g of pure **17-tBu** were obtained as a pale yellow solid. **^{1}H NMR (300MHz, CDCl$_3$):** δ (ppm) = 1.00 (s, 9H), 1.26 (s, 9H), 3.17-3.24 (dd, J=7.9Hz, J=13.8Hz, 1H), 3.29-3.36 (dd, J=7.5Hz, J=13.7Hz, 1H), 5.69-5.73 (t, 7.7Hz, 1H), 6.97-6.99 (d, J=8.2Hz, 1H), 7.25-7.28 (d, J=8.2Hz, 1H), 7.87 (s, 2H), 8.24 (s, 1H). **^{13}C NMR (75MHz, CDCl$_3$):** δ (ppm) = 25.39, 31.21, 34.39, 38.62, 44.77, 62.74, 125.67, 128.72, 131.88, 142.26, 150.44, 151.06, 209.34. **ESI-MS$^+$ (calc. for $C_{19}H_{27}N_3O$ 313.22):** m/z = 314.31 [M+H]$^+$, 336.20 [M+Na]$^+$. **Elementary analysis (calc. for $C_{19}H_{27}N_3O$: %C=72.81, %H=8.68, %N=13.41):** %C=72.75, %H=8.67, %N=13.77. **Melting point (by DSC):** 47.4°C.

IV - Synthesis of pure enantiomer of Prasugrel by deracemisation

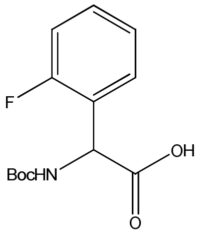

41

41 Boc-2-fluorophenylglycine, 2-(tert-butoxycarbonylamino)-2-(2-fluorophenyl)acetic acid
10g (59.1mmol) of 2-fluorophenylglycine **40** were dissolved in a 1/1 THF/water mixture (350mL) then $NaHCO_3$ (14.9g, 177.0mmol) was added. The reaction mixture was cooled down to 0°C then Boc_2O (15.5g, 71.0mmol) was added. The reaction mixture was stirred for 30 minutes at 0°C then overnight at RT. The product was extracted with Et_2O (2x250mL) then the combined organic layers were washed with brine (250mL). The first aqueous layer was acidified with half saturated aqueous citric acid then the product was extracted with CH_2Cl_2 (3x120mL). The combined organic layers were washed with brine (100mL). Both organic layers were combined, dried ($MgSO_4$) then the solvent was evaporated to give 16.31g (quant.) of **41** as a pale yellow powder. **^{1}H NMR (300MHz, methanol-d4):** δ (ppm) = 1.44 (s, 9H), 5.51, 7.08-7.19 (m, 2H), 7.31-7.42 (m, 2H). **^{13}C NMR (75MHz, methanol-d4):** δ (ppm) = 28.71, 52.86, 80.92, 116.41-116.70 (d, J=22.0Hz), 125.53-125.58 (d, J=3.5Hz), 126.28-126.47 (d, J=14.4Hz), 130.34-130.37 (d, J=2.9Hz), 131.16-131.27 (d, J=8.3Hz), 157.49, 160.23-163.50 (d, J=246.8Hz), 173.52. **MS ESI$^-$ (calc. for $C_{13}H_{16}FNO_4$ 269.11)**: 268.08 $[M-H]^-$. **Melting point:** 136°C.

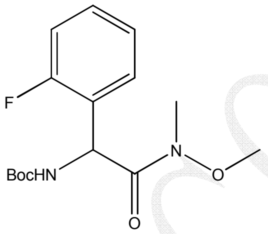

42

42 Tert-butyl 1-(2-fluorophenyl)-2-(methoxy(methyl)amino)-2-oxoethylcarbamate
41 (5g, 18.57mmol) was dissolved in THF (35mL) then carbonyldiimidazole (CDI, 3.01g, 18.57mmol) was added. The reaction mixture was stirred for 2h at RT then N-O-dimethylhydroxylamine hydrochloride (1.81g, 18.57mmol) and triethylamine (TEA, 2.6mL, 18.57mmol) were added. The reaction mixture was stirred overnight at RT then the solvent was evaporated. The residue was dissolved in AcOEt then washed with saturated aqueous $NaHCO_3$ (3x75ml), water (3x75ml) then with brine (1x75mL). The organic layer was dried ($MgSO_4$) then the solvent was evaporated to give 4.83g (15.41mmol, 83%) of **42** as a white

CONFIDENTIAL

powder. **^{1}H NMR (300MHz, CDCl$_3$):** δ (ppm) = 1.34 (s, 9H), 3.09 (s, 3H), 3.41 (s, 3H), 5.76-5.86 (m, 1H), 6.99-7.07 (m, 2H), 7.17-7.29 (m, 2H). **^{13}C NMR (75MHz, CDCl$_3$):** δ (ppm) = 28.23, 49.11, 61.00, 79.76n 115.54-115.83 (d, J=21.9Hz), 124.32-124.36 (d, J=3.4Hz), 125.09-125.29 (d, J=15.4Hz), 128.92-128.96 (d, J=3.9Hz), 129.62-129.73 (d, J=8.2Hz), 154.75, 158.53-161.84 (d, J=249.2Hz), 170.49. **MS ESI+ (calc. for $C_{15}H_{21}FN_2O_4$ 312.15):** 312.90 [M+H]$^+$, 335.05 [M+Na]$^+$. **Melting point:** 136°C.

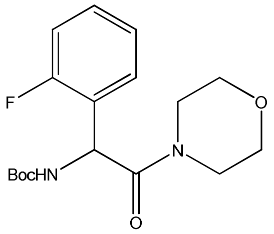

44

44 tert-butyl 1-(2-fluorophenyl)-2-morpholino-2-oxoethylcarbamate

41 (19g, 70.6mmol) was dissolved in THF (140mL) then CDI (11.44g, 70.6mmol) was added. The reaction mixture was stirred for 1h45 at RT then cooled down to 0°C. Morpholine (6.15mL, 70.6mmol) was added dropwise at 0°C then the reaction mixture was stirred overnight at RT. The solvent was evaporated then the residue was dissolved in AcOEt. The organic layer was washed with saturated aqueous NaHCO$_3$ (3x100ml), brine (3x100ml) and water (1x100mL) then dried (MgSO$_4$) and the solvent was evaporated to give 22.65g (67.1mmol, 95%) of 44 as a white powder. **^{1}H NMR (300MHz, CDCl$_3$):** δ (ppm) = 1.32 (s, 9H), 3.08-3.34 (m, 1H), 3.40-3.59 (m, 7H), 5.77-5.79 (d, H), 6.97-7.09 (m, 2H), 7.19-7.32 (m, 2H). **^{13}C NMR (75MHz, CDCl$_3$):** δ (ppm) = 28.09, 42.62, 47.98, 53.26, 65.86, 66.24, 79.61, 115.43-115.72 (d, J=22.0Hz), 124.67-124.71 (d, J=3.7Hz), 124.84, 128.50-128.54 (d, J=3.1Hz), 129.83-129.94 (d, J=8.3Hz), 154.54, 157.70-160.97 (d, J=247.4Hz), 167.97. **MS ESI+ (calc. for $C_{17}H_{23}FN_2O_4$ 312.15):** 338.98 [M+H]$^+$, 361.07 [M+Na]$^+$.

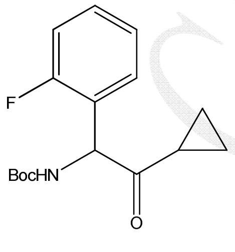

45

45 Tert-butyl 2-cyclopropyl-1-(2-fluorophenyl)-2-oxoethylcarbamate

Magnesium turnings (0.94mg, 38.42mmol) were suspended in dry THF (15ml) at 0°C under nitrogen then few drops of I_2 in THF were added. The bromocyclopropane (7.02mL, 38.42mmol) was dissolved in dry THF (30mL) then 5mL of this solution were added dropwise to the magnesium at 0°C. After the disappearance of the yellow colour, the rest of the solution was added dropwise at 0°C, under nitrogen. The reaction mixture was stirred for

CONFIDENTIAL

2h at 0°C. **42** (3g, 9.60mmol), dissolved in dry THF (25mL), was added dropwise to the bromocyclopropyl magnesium at 0°C. The reaction mixture was stirred for 1h30 at 0°C the overnight at RT. The mixture was quenched with saturated aqueous NH_4Cl at 0°C then the product was extracted with AcOEt (3x50mL). The combined organic layers were washed with brine (1x50mL), dried ($MgSO_4$) then the solvents were evaporated. The crude product was purified on silicagel with n-heptane/AcOEt 9/1 as eluent (Rf = 0.3) to give 2.35g (7.97mmol, 83%) of **45** as pale yellow oil. Exactly the same procedure was used to prepare **45** from the morpholine derivative **44**. **^{1}H NMR (300MHz, $CDCl_3$):** δ (ppm) = 0.71-0.79 (m, 1H), 0.87-0.99 (m, 2H), 1.07-1.14 (m, 1H), 1.39 (s, 9H), 1.84-1.92 (m, 1H), 5.71-5.73 (d, 1H), 7.05-7.17 (m, 2H), 7.26, 7.33 (m, 2H). **^{13}C NMR (75MHz, $CDCl_3$):** δ (ppm) = 11.86, 12.02, 18.31, 28.16, 58.84, 79.71, 115.68-115.97 (d, J=21.5Hz), 124.57-124.61 (d, J=3.5Hz), 125.37, 129.66-129.69 (d, J=2.8Hz), 129.87-120.00 (d, J=8.3Hz), 154.67, 158.92-162.20 (d, J=247.6Hz), 204.77. **MS ESI+ (calc. for $C_{16}H_{20}FNO_3$ 293.14):** 294.09 $[M+H]^+$.

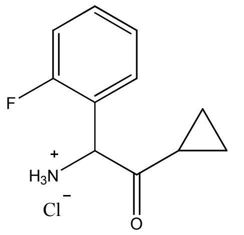

37.HCl

37.HCl 2-amino-1-cyclopropyl-2-(2-fluorophenyl)ethanone hydrochloride

43 (14.15g, 49.43mmol) was dissolved in 1,4-dioxane (125mL) then HCl 4N in 1,4-dioxane (123mL, 494mmol) was added. The reaction mixture was stirred overnight at RT then the solid was filtered, washed with 1,4-dioxane (2x50mL) then dried under vacuum. The filtrate was concentrated. AcOEt was added to the residue and the solid was filtered, washed with AcOEt (2x50mL) then dried under vacuum. The two solids were combined to give 9.50g (41.52mmol, 84%) of **37H.HCl** as a white powder. **^{1}H NMR (300MHz, methanol-d4):** δ (ppm) = 0.88, 1.24 (m, 4H), 1.88-1.95 (m, 1H), 5.67 (s, 1H), 7.31-7.39 (m, 2H), 7.50-7.63 (m, 2H). **^{13}C NMR (75MHz, methanol-d4):** δ (ppm) = 13.07, 13.45, 19.37, 58.38, 117.50-117.78 (d, J=21.3Hz), 120.26-120.45 (d, J=14.3Hz), 126.81-126.85 (d, J=3.6Hz), 132.02-132.05 (d, J=2.5Hz), 133.97-134.08 (d, J=8.5Hz), 160.70-164.00 (d, J=248.7Hz), 203.71. **MS ESI+ (calc. for $C_{11}H_{12}FNO$ 193.09):** 193.09 $[M+H]^+$.

CONFIDENTIAL

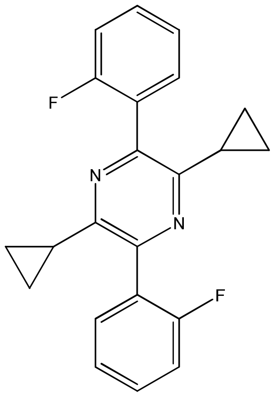

46

46 2,5-dicyclopropyl-3,6-bis(2-fluorophenyl)pyrazine

^{1}H NMR (300MHz, CDCl$_3$): δ (ppm) = 0.88-0.95 (m, 4H), 1.11-1.16 (m, 4H), 1.90-1.99 (m, 2H), 7.18-7.24 (t, 2H), 7.28-7.33 (m, 2H), 7.42-7.50 (m, 2H), 7.55-7.61 (m, 2H). **^{13}C NMR (75MHz, CDCl$_3$):** δ (ppm) = 10.04, 13.37, 13.42, 115.59-115.88 (d, J=21.9Hz), 124.17-124.21 (d, J=3.6Hz), 126.71-126.91 (d, J=15.3Hz), 130.26-130.37 (d, J=8.1Hz), 131.99-132.04 (d, J=3.3Hz), 146.38, 152.00, 158.40-161.70 (d, J = 248.9Hz). **MS ESI+ (calc. for $C_{22}H_{18}F_2N_2$ 348.14):** 349.22 $[M+H]^+$. **Melting point:** 178°C.

CONFIDENTIAL

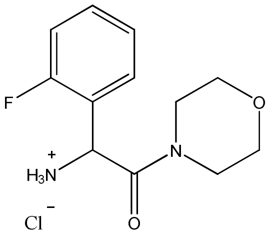

48.HCl

48.HCl 2-amino-2-(2-fluorophenyl)-1-morpholinoethanone hydrochloride

44 (35.5g, 105mmol) was dissolved in 1,4-dioxane (700mL) then HCl 4N in 1,4-dioxane (210mL, 840mmol) was added. The reaction mixture was stirred overnight at RT then the solid was filtered, washed with 1,4-dioxane (3x100mL) then dried under vacuum. The filtrate was concentrated; the solid was filtered then washed with acetone (3x50mL) and dried under vacuum. The two solids were combined to give 24.68g (89.3mmol, 85%) of **48.HCl** as a white powder. **^{1}H NMR (300MHz, methanol-d4):** δ (ppm) = 3.05-3.17 (m, 2H), 3.39-3.70 (m, 6H), 5.75 (s, 1H), 7.30-7.39 (m, 2H), 7.49-7.60 (m, 2H). **^{13}C NMR (75MHz, methanol-d4):** δ (ppm) = 44.15, 46.87, 49.54, 67.00, 67.47, 117.52-117.80 (d, J=21.6Hz), 120.57-120.76 (d, J=14.1Hz), 126.96-127.01 (d, J=3.6Hz), 130.77, 134.06-134.17 (d, J=8.7Hz) 159.87-163.16 (d, J=248.9Hz), 166.40. **MS ESI+ (calc. for $C_{12}H_{15}FN_2O_2$ 238.11):** 239.12 $[M+H]^+$.

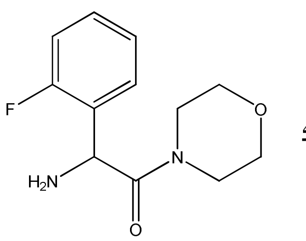

48

48 2-amino-2-(2-fluorophenyl)-1-morpholinoethanone

48.HCl (22.97g, 81.1mmol) was dissolved in water then 150mL of 1N NaOH were added. The reaction mixture was stirred 19 minutes at RT then the product was extracted with CH_2Cl_2 (4x50mL). The combined organic layers were dried (Na_2SO_4) then the solvent was evaporated to give 18.01g (75.6mmol, 93%) of the free amine **48**.

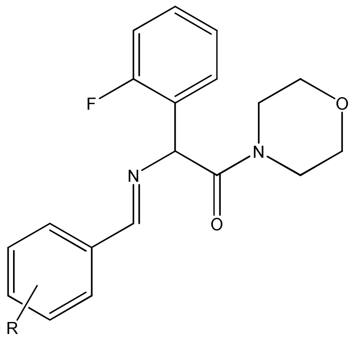

49

49a-j 2-(R-benzylideneamino)-2-(2-fluorophenyl)-1-morpholinoethanone

48 (1g, 4.20mmol), were dissolved in CH_2Cl_2 (10mL) then the corresponding substituted benzaldehyde (4.20mmol) and Na_2SO_4 (1.19g, 8.40mmol) were added. The reaction mixture was stirred overnight at room temperature then the solution was filtered and the solvent was evaporated to give the imines **49a-j** as oils with quantitative yields.

49a: **^{1}H NMR (300MHz, $CDCl_3$):** δ (ppm) = 3.34-3.75 (m, 8H), 5.80 (s, 1H), 7.04-7.18 (m, 2H), 7.23-30 (m, 1H), 7.40-7.51 (m, 4), 7.78-7.81 (d, 2H), 8.35 (s, 1H). **^{13}C NMR (75MHz, $CDCl_3$):** δ (ppm) = 42.70, 46.03, 66.39, 66.65, 68.49, 115.23-115.52 (d, J=21.6Hz), 124.40-124.44 (d, J=3.Hz), 125.09-125.27 (d, J=13.8Hz), 128.48, 128.51, 128.84, 129.01-129.06 (d, J=3.7Hz), 129.44-129.55 (d, J=8.3Hz), 131.17, 134.31, 135.45, 158.20-161.47 (d, J=246.7Hz), 163.89, 168.18. **MS ESI+ (calc. for $C_{19}H_{19}FN_2O_2$ 326.14):** 327.20 $[M+H]^+$.

49b: **^{1}H NMR (300MHz, $CDCl_3$):** δ (ppm) = 2.40 (s, 3H), 3.45-3.80 (m, 8H), 5.80 (s, 1H), 7.05-7.4 (m, 6H), 7.25-7.35 (d, 1H), 7.70 (s, 1H), 9.40 (s, 1H).

49c: **^{1}H NMR (300MHz, $CDCl_3$):** δ (ppm) = 3.40-3.80 (m, 8H), 5.9 (s, 1H), 7.10-7.15 (t, 1H), 7.15-7.25 (t, 1H), 7.25-7.40 (m, 4H), 7.50-7.60 (m, 1H), 8.20 (d, 1H), 8.80 (s, 1H).

49d: **^{1}H NMR (300MHz, $CDCl_3$):** δ (ppm) = 3.40-3.80 (m, 8H), 6.85 (s, 1H), 7.10-7.15 (t, 1H), 7.15-7.20 (t, 1H), 7.30-7.50 (m, 4H), 7.60-7.65 (m, 1H), 7.85 (d, 1H).

CONFIDENTIAL

49e: **^{1}H NMR (300MHz, $CDCl_3$):** δ (ppm) = 3.40-3.80 (m, 8H), 5.90 (s, 1H), 7.10-7.15 (t, 1H), 7.15-7.25 (t, 1H), 7.25-7.40 (m, 3H), 7.45-7.60 (m, 2H), 8.15-8.20 (d, 1H), 8.75 (s, 1H).

49f: **^{1}H NMR (300MHz, $CDCl_3$):** δ (ppm) = 3.40-3.80 (m, 8H), 3.90 (s, 3H), 5.80 (s, 1H), 6.90-7.00 (d, 1H), 7.00-7.20 (m, 4H), 7.25-7.35 (m, 1H), 7.50-7.55 (t, 1H), 7.75-7.80 (d, 1H), 8.30 (s, 1H).

49g: **^{1}H NMR (300MHz, $CDCl_3$):** δ (ppm) = 3.50-3.80 (m, 8H), 3.90 (s, 3H), 5.80 (s, 1H), 6.90-7.20 (m, 4H), 7.25-7.30 (m, 1H), 7.40-7.45 (t, 1H), 7.50-7.55 (t, 1H), 8.05-8.10 (d, 1H), 8.90 (s, 1H).

49h: **^{1}H NMR (300MHz, $CDCl_3$):** δ (ppm) = 3.40-3.80 (m, 8H), 5.90 (s, 1H), 7.10-7.20 (t, 1H), 7.10-7.15 (t, 1H), 7.20-7.30 (m, 1H), 7.45-7.55 (t, 1H), 7.65-7.75 (m, 2H), 7.90-7.95 (m, 2H), 8.40 (s, 1H).

49i: **^{1}H NMR (300MHz, $CDCl_3$):** δ (ppm) = 3.40-3.80 (m, 8H), 6.90 (s, 1H), 7.10-7.15 (t, 1H), 7.20-7.25 (t, 1H), 7.30-7.40 (m, 3H), 7.45-7.55 (t, 1H), 8.10-8.15 (d, 1H), 8.70 (s, 1H).

49j: **^{1}H NMR (300MHz, $CDCl_3$):** δ (ppm) = 3.40-3.80 (m, 8H), 5.90 (s, 1H), 7.10-7.15 (m, 1H), 7.20-7.25 (t, 1H), 7.30-7.40 (m, 1H), 7.40-7.50 (m, 1H), 8.25 (s, 1H).

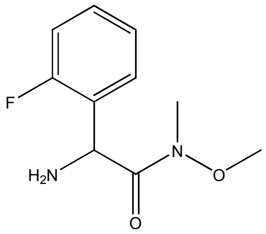

42'

42’ 2-amino-2-(2-fluorophenyl)-N-methoxy-N-methylacetamide

42 (750mg, 2.40mmol) were dissolved in 1,4-dioxane (10mL) then HCl 4N in 1,4-dioxane (4.8mL, 19.21mmol) was added. The reaction mixture was stirred overnight at RT then the solid was filtered, washed with 1,4-dioxane (2x5mL) and with acetone (1x5mL) then dried under vacuum to give 434mg of **42’.HCl**. This product was dissolved in water (10mL) then NaOH 1N in water was added. The reaction mixture was stirred 10 minutes at RT then the free amine was extracted with CH_2Cl_2 (4x10mL). The combined organic layers were dried (Na_2SO_4) then the solvent was evaporated to give 331mg (1.56mmol, 65%) of **42’**.

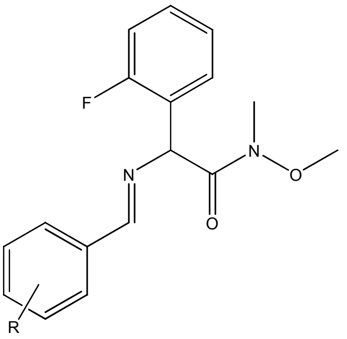

50a-c

CONFIDENTIAL

50a-c 2-(R-benzylideneamino)-2-(2-fluorophenyl)-N-methoxy-N-methylacetamide

41’ (100mg, 0.47mmol), were dissolved in CH_2Cl_2 (1mL) then the corresponding substituted benzaldehyde (0.47mmol) and Na_2SO_4 (134mg, 0.94mmol) were added. The reaction mixture was stirred overnight at room temperature then the solution was filtered and the solvent was evaporated to give the imines **50a-c** as oils with quantitative yields.

50a: **^{1}H NMR (300MHz, $CDCl_3$):** δ (ppm) = 3.15 (s, 3H), 3.65 (s, 3H), 6.10 (s, 1H), 7.05-7.10 (t, 1H), 7.15-7.20 (t, 1H), 7.25-7.30 (m, 2H), 7.35-7.45 (m, 2H), 7.60-7.65 (t, 1H), 8.80-8.85 (m, 2H), 8.35 (s, 1H).

50b: **^{1}H NMR (300MHz, $CDCl_3$):** δ (ppm) = 2.40 (s, 3H), 3.25 (s, 3H), 3.65 (s, 3H), 6.10 (s, 1H), 7.05-7.10 (t, 1H), 7.15-7.35 (m, 4H), 7.60-7.65 (t, 1H), 7.70-7.75 (dd, 2H), 8.30 (s, 1H).

50c: **^{1}H NMR (300MHz, $CDCl_3$):** δ (ppm) = 3.15 (s, 3H), 3.65 (s, 3H), 6.15 (s, 1H), 7.05-7.15 (t, 1H), 7.15-7.25 (t, 1H), 7.15-7.20 (m, 3H), 7.55-7.60 (d, 1H), 7.20-7.30 (m, 1H), 8.15-8.20 (dd, 1H), 8.70 (s, 1H).

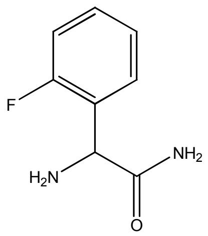

51

51 2-fluorophenylglycinamide

10g (59.12mmol) of 2-fluorophenylglycine were suspended in methanol (60ml) then $SOCl_2$ (5.2mL, 70.94mmol) was added dropwise at 0°C. The reaction mixture was stirred overnight at RT. Additional 1mL of $SOCl_2$ was added. The reaction mixture was stirred 2h at RT then 40-50mL of methanol were evaporated. TBME (400mL) was added to the residue then the solid was filtered, washed with TBME (3x75mL) and dried under vacuum to give 12.58g (57.35mmol, 97%) of the 2-fluorophenylglycine methyl ester hydrochloride as a pale yellow powder. **^{1}H NMR (300MHz, methanol-d4):** δ (ppm) = 3.83 (s, 3H), 5.44 (s, 1H), 7.26-7.35 (m, 2H), 7.48-7.60 (m, 2H).

10.39g (47.3mmol) of the 2-fluorophenylglycine methyl ester hydrochloride were stirred overnight in 33%wt aqueous NH_3 (41.5mL) then the product was extracted with CH_2Cl_2 (15x15mL). The combined organic layers were dried ($MgSO_4$) then the solvent was evaporated to give 5.91g (35.00mmol, 75%) of **51** as a white powder. **^{1}H NMR (300MHz, MeOH-d4):** δ (ppm) = 4.74 (s, 1H), 7.08-7.20 (m, 2H), 7.29-7.37 (m, 1H), 7.43-7.48 (m, 1H). **^{13}C NMR (75MHz, DMSO-d6):** δ (ppm) = 52.75, 114.89-115.18 (d, J=22.0Hz), 124.16-124.21 (d, J=3.4Hz), 128.65-128.73 (d, J=5.9Hz), 128.76-128.79 (d, J=1.2Hz),

CONFIDENTIAL

130.05-130.25 (d, J=14.7Hz), 150.20-161.44 (d, J=244.4Hz), 174.67. **MS ESI+ (calc. for $C_8H_9FN_2O$ 168.07):** 169.07 $[M+H]^+$. **Melting point:** 104°C.

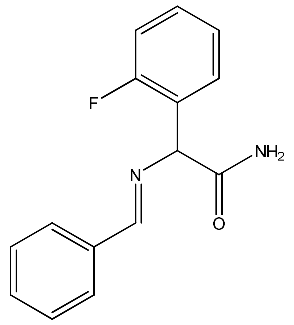

52a

52a 2-(benzylideneamino)-2-(2-fluorophenyl)acetamide

51 (5.5g, 32.7mmol) was dissolved in CH_2Cl_2 then benzaldehyde (3.8g, 36.0mmol) and Na_2SO_4 (8.4g, 58.6mmol) were added. The reaction mixture was stirred overnight at RT then the suspension was filtered and the solvent was evaporated. The solid was washed with TBME (3x10mL) then was dried under vacuum to give 8.03g (31.4mmol, 96%) of **52a** as a white solid. **^{1}H NMR (300MHz, $CDCl_3$):** δ (ppm) = 5.37 (s, 1H), 7.06-7.3 (m, 3H), 7.40-7.48 (m, 4H), 7.76-7.78 (m, 2H), 8.29 (s, 1H). **^{13}C NMR (75MHz, $CDCl_3$):** δ (ppm) = 69.43, 115.56-11585 (d, J=21.9Hz), 124.45-124.50 (d, J=3.5Hz), 125.88, 126.07, 128.41, 128.59, 129.41-129.46 (d, J=3.7Hz), 129.63-129.74 (d, J=8.3Hz), 131.48, 135.22, 158.85-162.13 (d, J=247.5Hz), 163.68, 173.94. **MS ESI+ (calc. for $C_{15}H_{13}FN_2O$ 256.10):** 257.15 $[M+H]^+$. **Elementary analysis (calc. for $C_{15}H_{13}FN_2O$: %C=70.30, %H=5.11, %N=10.93):** %C=70.04, %H=5.12, %N=10.91.

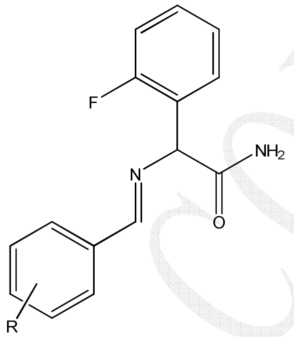

52b-j

52b-j 2-(R-benzylideneamino)-2-(2-fluorophenyl)acetamide

The imines 52b-j were synthesised with quantitative yields following the same protocol as **52a** from 100mg (0.59mmol) of 51.

52b: 1H NMR (300MHz, CDCl3): δ (ppm) = 2.40 (s, 1H), 5.35 (s, 1H), 7.05-7.35 (m, 5H), 7.45-7.50 (t, 1H), 7.65-7.70 (d, 2H), 8.25 (s, 1H).

52c: 1H NMR (300MHz, CDCl3): δ (ppm) = 5.45 (s, 1H), 7.05-7.20 (m, 3H), 7.25-7.40 (m, 3H), 7.45-7.50 (t, 1H), 8.05-8.10 (d, 1H), 8.80 (s, 1H).

CONFIDENTIAL

52d: 1H NMR (300MHz, CDCl3): δ (ppm) = 5.40 (s, 1H), 7.05-7.20 (m, 3H), 7.25-7.50 (m, 3H), 7.55-7.60 (d, 1H), 7.80 (s, 1H), 8.25 (s, 1H).

52e: 1H NMR (300MHz, CDCl3): δ (ppm) = 5.45 (s, 1H), 7.10-7.20 (m, 3H), 7.25-7.40 (m, 2H), 7.45-7.50 (m, 1H), 7.55-7.65 (d, 1H), 8.05-8.10 (d, 1H), 8.70 (s, 1H).

52f: 1H NMR (300MHz, CDCl3): δ (ppm) = 3.85 (s, 3H), 5.35 (s, 1H), 6.90-6.95 (d, 2H), 7.05-7.35 (m, 3H), 7.40-7.45 (t, 1H), 7.70-7.75 (d, 2H), 8.20 (s, 1H).

52g: 1H NMR (300MHz, CDCl3): δ (ppm) = 4.85 (s, 3H), 5.40 (s, 1H), 6.90-7.30 (m, 5H), 7.40-7.55 (m, 2H), 8.00 (d, 1H), 8.80 (s, 1H).

52h: 1H NMR (300MHz, CDCl3): δ (ppm) = 5.40 (s, 1H), 7.05-7.20 (m, 2H), 7.25-7.35 (m, 1H), 7.45-7.50 (t, 1H), 7.70-7.75 (d, 2H), 7.90-7.95 (d, 2H), 8.35 (s, 1H).

52i: 1H NMR (300MHz, CDCl3): δ (ppm) = 5.40 (s, 1H), 7.05-7.20 (m, 3H), 7.30-7.35 (m, 2H), 7.45-7.50 (t, 1H), 8.00-8.05 (d, 1H), 8.65 (s, 1H).

52j: 1H NMR (300MHz, CDCl3): δ (ppm) = 5.40 (s, 1H), 7.10-7.15 (m, 1H), 7.20-7.25 (t, 1H), 7.30-7.40 (m, 1H), 7.40-7.50 (m, 1H), 8.30 (s, 1H).

CONFIDENTIAL

Appendix:
Crystallographic Data

I - ClTAK

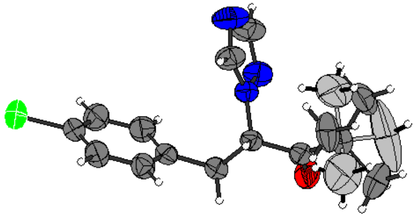

Figure 32. Asymmetric unit of ClTAK, in ellipsoid thermal representation (50% of probability). The two positions of the tBu are represented in grey (sof: 78%) and light grey (sof: 22%).

Table 1 a. Crystal data.

Chemical Formula	$C_{15}H_{18}ClN_3O$
Molecular Weight / *g.mol^{-1}*	291.77
Crystal System	Orthorhombic
Space group	*P*$2_12_12_1$
Z , Z' (asymmetric units per unit cell)	4, 1
a / *Å*	5.8076(5)
b / *Å*	19.661(2)
c / *Å*	13.553(1)
V / *Å^3*	1547.5(2)
dcalc / *g.cm-3*	1.252
R factor (with I>2σI)	R1 = 0.0367 wR2 = 0.0871
R factor (all data)	R1 = 0.0483, wR2 = 0.0938
F(000) / e-	616
Extinction Coefficient	0.017(2)
Absolute structure parameter	-0.06(7)
Absorption coefficient μ (MoKα1) mm-1	0.246
Number of reflections (n) (with FO>4.0σ(FO))	3162 / 2621
Number of refined parameters (p) / restraints	216
Goodness of fit indicator (restrainted GooF)	1.024
Maximum peak in final difference map / e-Å-3	0.123
Maximum hole in final difference map / e-Å-3	-0.135

Table 1 b. Atomic coordinates (x10^4) and equivalent isotropic displacement parameters (Å^2 x 10^3). U(eq) is defined as one third of the trace of the orthogonalized Uij tensor.

	x	y	z	U(eq)
Cl(1)	9584(2)	8044(1)	2056(1)	94(1)
N(1)	13829(2)	4927(1)	1474(1)	44(1)
N(2)	15709(3)	4860(1)	2054(1)	62(1)
N(3)	12449(4)	4766(1)	2950(1)	86(1)
O(1)	17732(2)	4672(1)	-157(1)	68(1)
C(1)	11595(4)	6532(1)	309(1)	54(1)
C(2)	10324(4)	7055(1)	718(2)	59(1)
C(3)	11141(4)	7376(1)	1541(2)	60(1)
C(4)	13192(4)	7188(1)	1955(2)	68(1)
C(5)	14430(4)	6660(1)	1545(1)	62(1)
C(6)	13659(3)	6329(1)	708(1)	47(1)
C(7)	15082(3)	5771(1)	245(1)	50(1)
C(8)	14126(3)	5061(1)	425(1)	41(1)
C(9)	15765(3)	4514(1)	12(1)	47(1)
C(10)	14953(4)	3785(1)	-142(2)	57(1)
C(11)	16125(7)	3520(2)	-1088(3)	88(1)
C(12)	15853(9)	3382(2)	738(3)	87(1)
C(13)	12404(5)	3724(2)	-241(4)	84(2)
C(12A)	*13080(30)*	*3544(7)*	*709(14)*	*119(8)*
C(11A)	*13440(40)*	*3757(9)*	*-1084(14)*	*149(11)*
C(13A)	*16680(40)*	*3266(9)*	*-100(20)*	*210(20)*
C(14)	11926(4)	4869(1)	2021(2)	63(1)
C(15)	14752(5)	4761(1)	2925(2)	80(1)

In italic, the atoms of the *tert*-butyl with a sof of 22%.

Table 1 c. Hydrogen coordinates (x10^4) and equivalent isotropic displacement parameters (Å2 x 10^3). U(eq) is defined as one third of the trace of the orthogonalized Uij tensor.

	x	y	z	U(eq)
H(1)	11039	6312	-250	65
H(2)	8933	7187	437	71
H(4)	13748	7414	2509	82
H(5)	15806	6526	1836	74
H(7A)	16635	5794	506	60
H(7B)	15169	5849	-461	60
H(8)	12631	5020	96	49
H(11A)	15654	3060	-1208	132
H(11B)	17767	3536	-1008	132
H(11C)	15685	3800	-1637	132
H(12A)	15213	3563	1336	130
H(12B)	17502	3414	762	130
H(12C)	15411	2913	671	130
H(13A)	11681	3876	357	126
H(13B)	12002	3258	-361	126
H(13C)	11889	3999	-783	126
H(12D)	*12234*	*3156*	*476*	*178*
H(12E)	*12027*	*3910*	*841*	*178*
H(12F)	*13881*	*3427*	*1304*	*178*
H(11D)	*14280*	*3944*	*-1630*	*223*
H(11E)	*12061*	*4016*	*-980*	*223*
H(11F)	*13044*	*3293*	*-1224*	*223*
H(13D)	*15957*	*2827*	*-125*	*315*
H(13E)	*17521*	*3308*	*509*	*315*
H(13F)	*17714*	*3316*	*-644*	*315*
H(14)	10433	4897	1776	76
H(15)	15629	4692	3490	96

In italic, the atoms of the *tert*-butyl with a sof of 22%.

Table 1 d. Bond lengths (Å).

Cl(1)-C(3)	1.741(2)	C(9)-C(10)	1.523(3)	C(12)-H(12A)	0.96
N(1)-C(14)	1.336(2)	*C(10)-C(13A)*	*1.430(17)*	C(12)-H(12B)	0.96
N(1)-N(2)	1.351(2)	C(10)-C(13)	1.491(4)	C(12)-H(12C)	0.96
N(1)-C(8)	1.456(2)	C(10)-C(12)	1.525(4)	C(13)-H(13A)	0.96
N(2)-C(15)	1.320(3)	C(10)-C(11)	1.542(4)	C(13)-H(13B)	0.96
N(3)-C(14)	1.310(3)	*C(10)-C(11A)*	*1.550(17)*	C(13)-H(13C)	0.96
N(3)-C(15)	1.337(3)	*C(10)-C(12A)*	*1.656(14)*	*C(12A)-H(12D)*	*0.96*
O(1)-C(9)	1.206(2)	C(1)-H(1)	0.93	*C(12A)-H(12E)*	*0.96*
C(1)-C(6)	1.375(3)	C(2)-H(2)	0.93	*C(12A)-H(12F)*	*0.96*
C(1)-C(2)	1.382(3)	C(4)-H(4)	0.93	*C(11A)-H(11D)*	*0.96*
C(2)-C(3)	1.367(3)	C(5)-H(5)	0.93	*C(11A)-H(11E)*	*0.96*
C(3)-C(4)	1.368(3)	C(7)-H(7A)	0.97	*C(11A)-H(11F)*	*0.96*
C(4)-C(5)	1.379(3)	C(7)-H(7B)	0.97	*C(13A)-H(13D)*	*0.9643*
C(5)-C(6)	1.383(3)	C(8)-H(8)	0.98	*C(13A)-H(13E)*	*0.9642*
C(6)-C(7)	1.509(2)	C(11)-H(11A)	0.96	*C(13A)-H(13F)*	*0.9643*
C(7)-C(8)	1.523(2)	C(11)-H(11B)	0.96	C(14)-H(14)	0.93
C(8)-C(9)	1.542(2)	C(11)-H(11C)	0.96	C(15)-H(15)	0.93

In italic, the atoms of the *tert*-butyl with a sof of 22%.

Table 1 e. Angles (°).

C(14)-N(1)-N(2)	109.75(14)	C(12)-C(10)-C(11)	108.9(3)	C(10)-C(11)-H(11B)	109.5
C(14)-N(1)-C(8)	130.95(16)	*C(13A)-C(10)-C(11A)*	*114.0(12)*	C(10)-C(11)-H(11C)	109.5
N(2)-N(1)-C(8)	119.27(14)	*C(13)-C(10)-C(11A)*	*50.2(10)*	C(10)-C(12)-H(12A)	109.5
C(15)-N(2)-N(1)	101.18(18)	*C(9)-C(10)-C(11A)*	*108.8(7)*	C(10)-C(12)-H(12B)	109.5
C(14)-N(3)-C(15)	102.07(19)	*C(12)-C(10)-C(11A)*	*145.0(7)*	C(10)-C(12)-H(12C)	109.5
C(6)-C(1)-C(2)	121.63(19)	*C(11)-C(10)-C(11A)*	*63.5(9)*	C(10)-C(13)-H(13A)	109.5
C(3)-C(2)-C(1)	119.1(2)	*C(13A)-C(10)-C(12A)*	*103.2(13)*	C(10)-C(13)-H(13B)	109.5
C(2)-C(3)-C(4)	120.80(19)	*C(13)-C(10)-C(12A)*	*52.1(8)*	C(10)-C(13)-H(13C)	109.5
C(2)-C(3)-Cl(1)	119.72(18)	C(9)-C(10)-C(12A)	112.2(5)	*C(10)-C(12A)-H(12D)*	*109.5*
C(4)-C(3)-Cl(1)	119.47(16)	*C(12)-C(10)-C(12A)*	*62.1(8)*	*C(10)-C(12A)-H(12E)*	*109.5*
C(3)-C(4)-C(5)	119.47(19)	C(11)-C(10)-C(12A)	140.7(5)	*H(12D)-C(12A)-H(12E)*	*109.5*
C(4)-C(5)-C(6)	121.1(2)	*C(11A)-C(10)-C(12A)*	*101.0(12)*	*C(10)-C(12A)-H(12F)*	*109.4*
C(1)-C(6)-C(5)	117.87(18)	N(3)-C(14)-N(1)	110.7(2)	*H(12D)-C(12A)-H(12F)*	*109.5*
C(1)-C(6)-C(7)	121.69(17)	N(2)-C(15)-N(3)	116.3(2)	*H(12E)-C(12A)-H(12F)*	*109.5*
C(5)-C(6)-C(7)	120.43(18)	C(6)-C(1)-H(1)	119.2	*C(10)-C(11A)-H(11D)*	*109.6*
C(6)-C(7)-C(8)	113.57(15)	C(2)-C(1)-H(1)	119.2	*C(10)-C(11A)-H(11E)*	*109.4*
N(1)-C(8)-C(7)	111.45(13)	C(3)-C(2)-H(2)	120.5	*H(11D)-C(11A)-H(11E)*	*109.5*
N(1)-C(8)-C(9)	107.57(13)	C(1)-C(2)-H(2)	120.5	*C(10)-C(11A)-H(11F)*	*109.4*
C(7)-C(8)-C(9)	110.91(14)	C(3)-C(4)-H(4)	120.3	*H(11D)-C(11A)-H(11F)*	*109.5*
O(1)-C(9)-C(10)	120.67(17)	C(5)-C(4)-H(4)	120.3	*H(11E)-C(11A)-H(11F)*	*109.5*
O(1)-C(9)-C(8)	118.27(16)	C(4)-C(5)-H(5)	119.4	*C(10)-C(13A)-H(13D)*	*110*
C(10)-C(9)-C(8)	121.02(16)	C(6)-C(5)-H(5)	119.4	*C(10)-C(13A)-H(13E)*	*109.8*
C(13A)-C(10)-C(13)	*129.9(8)*	C(6)-C(7)-H(7A)	108.9	*H(13D)-C(13A)-H(13E)*	*109*
C(13A)-C(10)-C(9)	*116.6(8)*	C(8)-C(7)-H(7A)	108.9	*C(10)-C(13A)-H(13F)*	*109.9*
C(13)-C(10)-C(9)	113.27(19)	C(6)-C(7)-H(7B)	108.9	*H(13D)-C(13A)-H(13F)*	*109*
C(13A)-C(10)-C(12)	*49.9(14)*	C(8)-C(7)-H(7B)	108.8	*H(13E)-C(13A)-H(13F)*	*109*
C(13)-C(10)-C(12)	111.7(3)	H(7A)-C(7)-H(7B)	107.7	N(3)-C(14)-H(14)	124.6
C(9)-C(10)-C(12)	106.0(2)	N(1)-C(8)-H(8)	109	N(1)-C(14)-H(14)	124.6
C(13A)-C(10)-C(11)	*59.1(14)*	C(7)-C(8)-H(8)	109	N(2)-C(15)-H(15)	121.9
C(13)-C(10)-C(11)	109.7(3)	C(9)-C(8)-H(8)	109	N(3)-C(15)-H(15)	121.9
C(9)-C(10)-C(11)	107.12(19)	C(10)-C(11)-H(11A)	109.5		

In italic, the atoms of the ter-butyl with a sof of 22%.

Table 1 f. Anisotropic displacement parameters (Å² x 103) The anisotropic displacement factor exponent takes the form: -2 π² [h² a*² U11 + ... + 2 h k a* b* U12].

	U11	U22	U33	U23	U13	U12
Cl(1)	134(1)	65(1)	83(1)	-10(1)	14(1)	33(1)
N(1)	45(1)	47(1)	40(1)	1(1)	-1(1)	-5(1)
N(2)	63(1)	76(1)	48(1)	3(1)	-14(1)	-5(1)
N(3)	98(2)	108(2)	52(1)	8(1)	14(1)	-27(1)
O(1)	55(1)	60(1)	91(1)	-1(1)	22(1)	2(1)
C(1)	61(1)	46(1)	54(1)	-3(1)	-6(1)	-1(1)
C(2)	64(1)	49(1)	64(1)	2(1)	-4(1)	4(1)
C(3)	84(2)	41(1)	57(1)	5(1)	13(1)	6(1)
C(4)	92(2)	57(1)	55(1)	-12(1)	-8(1)	1(1)
C(5)	70(1)	60(1)	56(1)	-1(1)	-10(1)	4(1)
C(6)	57(1)	37(1)	45(1)	5(1)	5(1)	-5(1)
C(7)	56(1)	44(1)	50(1)	6(1)	7(1)	0(1)
C(8)	43(1)	42(1)	37(1)	2(1)	-2(1)	-1(1)
C(9)	49(1)	48(1)	43(1)	2(1)	-1(1)	4(1)
C(10)	57(1)	43(1)	70(1)	-6(1)	-7(1)	7(1)
C(11)	86(3)	86(2)	91(2)	-42(2)	5(2)	4(2)
C(12)	129(4)	43(2)	88(2)	9(2)	-15(2)	4(2)
C(13)	63(2)	45(2)	145(5)	-20(2)	-7(2)	-7(1)
C(12A)	*165(18)*	*68(8)*	*122(14)*	*2(8)*	*30(13)*	*-59(10)*
C(11A)	*240(30)*	*101(12)*	*105(13)*	*-40(10)*	*-50(17)*	*-24(15)*
C(13A)	*142(19)*	*66(10)*	*420(60)*	*-40(20)*	*-160(30)*	*31(10)*
C(14)	60(1)	74(1)	56(1)	2(1)	12(1)	-15(1)
C(15)	105(2)	91(2)	42(1)	8(1)	-15(1)	-21(2)

In italic, the atoms of the *tert*-butyl with a sof of 22%.

Table 1 g. Torsion angles (°)

C(14)-N(1)-N(2)-C(15)	0.3(2)	C(7)-C(8)-C(9)-O(1)	18.2(2)
C(8)-N(1)-N(2)-C(15)	178.73(17)	N(1)-C(8)-C(9)-C(10)	73.75(19)
C(6)-C(1)-C(2)-C(3)	-0.2(3)	C(7)-C(8)-C(9)-C(10)	-164.14(16)
C(1)-C(2)-C(3)-C(4)	0.4(3)	O(1)-C(9)-C(10)-C(13A)	24.5(16)
C(1)-C(2)-C(3)-Cl(1)	179.06(15)	C(8)-C(9)-C(10)-C(13A)	-153.1(16)
C(2)-C(3)-C(4)-C(5)	-1.1(3)	O(1)-C(9)-C(10)-C(13)	-160.0(3)
Cl(1)-C(3)-C(4)-C(5)	-179.73(17)	C(8)-C(9)-C(10)-C(13)	22.4(3)
C(3)-C(4)-C(5)-C(6)	1.5(3)	O(1)-C(9)-C(10)-C(12)	77.2(3)
C(2)-C(1)-C(6)-C(5)	0.7(3)	C(8)-C(9)-C(10)-C(12)	-100.4(2)
C(2)-C(1)-C(6)-C(7)	-178.19(17)	O(1)-C(9)-C(10)-C(11)	-39.0(3)
C(4)-C(5)-C(6)-C(1)	-1.3(3)	C(8)-C(9)-C(10)-C(11)	143.5(2)
C(4)-C(5)-C(6)-C(7)	177.53(19)	O(1)-C(9)-C(10)-C(11A)	-106.1(10)
C(1)-C(6)-C(7)-C(8)	-75.3(2)	C(8)-C(9)-C(10)-C(11A)	76.3(11)
C(5)-C(6)-C(7)-C(8)	105.9(2)	O(1)-C(9)-C(10)-C(12A)	143.1(9)
C(14)-N(1)-C(8)-C(7)	109.1(2)	C(8)-C(9)-C(10)-C(12A)	-34.5(9)
N(2)-N(1)-C(8)-C(7)	-69.0(2)	C(15)-N(3)-C(14)-N(1)	-0.4(3)
C(14)-N(1)-C(8)-C(9)	-129.2(2)	N(2)-N(1)-C(14)-N(3)	0.1(2)

N(2)-N(1)-C(8)-C(9)	52.75(19)	C(8)-N(1)-C(14)-N(3)	-178.12(18)
C(6)-C(7)-C(8)-N(1)	-55.3(2)	N(1)-N(2)-C(15)-N(3)	-0.6(3)
C(6)-C(7)-C(8)-C(9)	-175.10(15)	C(14)-N(3)-C(15)-N(2)	0.7(3)
N(1)-C(8)-C(9)-O(1)	-103.87(18)		

In italic, the atoms of the *tert*-butyl with a sof of 22%.

II - HTAK

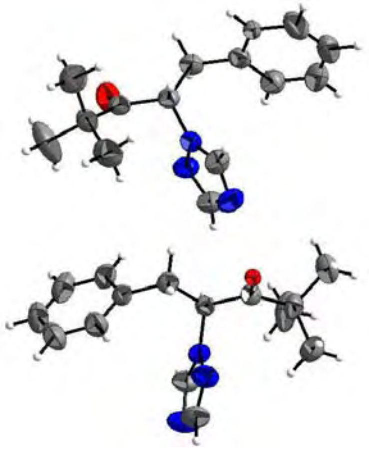

Figure 33. Asymmetric unit of HTAK, in ellipsoid thermal representation (50% of probability).

Table 2 a. Crystal data.

Chemical Formula	$C_{15}H_{19}N_3O$
Molecular Weight / *g.mol^{-1}*	257.33
Crystal System	Monoclinic
Space group	*P*2_1 (n°4)
Z , Z' (asymmetric units per unit cell)	4, 2
a / *Å*	5.747(1)
b / *Å*	19.183(1)
c / *Å*	13.437(1)
β / °	96.561(1)
V / *Å^3*	1471.8(2)
dcalc / *g.cm-3*	1.161
R factor (with I>2σI)	R1 = 0.0623 wR2 = 0.1142
R factor (all data)	R1 = 0.0623 wR2 = 0.1142
F(000) / e-	552
Absolute structure parameter	0.8(12)
Absorption coefficient μ (MoKα1) mm-1	552
Number of reflections (n) (with FO>4.0σ(FO))	5980 / 4664
Number of refined parameters (p) / restraints	349 / 1
Reflection / parameter ratio	
Goodness of fit indicator (restrainted GooF)	1.024
Maximum peak in final difference map / e-Å-3	0.139
Maximum hole in final difference map / e-Å-3	-0.167

Table 2 b. Atomic coordinates (x10^4) and equivalent isotropic displacement parameters (Å^2 x 10^3). U(eq) is defined as one third of the trace of the orthogonalized Uij tensor.

	x	y	z	U(eq)		x	y	z	U(eq)
N(1)	6240(3)	2216(1)	2703(1)	44(1)	N(1A)	8784(3)	1714(1)	7552(1)	44(1)
N(2)	4248(3)	2364(1)	2098(1)	62(1)	N(3A)	7490(4)	1298(1)	6086(2)	71(1)
N(3)	7423(5)	2478(1)	1269(2)	82(1)	N(2A)	10721(3)	1642(1)	7069(1)	57(1)
O(1)	2479(3)	1582(1)	4107(1)	60(1)	O(1A)	12514(3)	2620(1)	8910(1)	74(1)
C(1)	6414(4)	3847(1)	3616(2)	64(1)	C(1A)	6741(4)	713(1)	9797(2)	66(1)
C(2)	7903(6)	4403(1)	3528(2)	81(1)	C(2A)	5362(5)	122(2)	9724(2)	82(1)
C(3)	10058(6)	4417(1)	4075(2)	82(1)	C(3A)	5912(6)	-424(2)	9143(2)	82(1)
C(4)	10741(5)	3880(2)	4703(2)	73(1)	C(4A)	7826(6)	-377(1)	8622(2)	81(1)
C(5)	9249(4)	3319(1)	4789(2)	59(1)	C(5A)	9193(5)	216(1)	8689(2)	66(1)
C(6)	7066(4)	3298(1)	4240(2)	48(1)	C(6A)	8664(4)	773(1)	9276(2)	51(1)
C(7)	5437(4)	2690(1)	4326(2)	51(1)	C(7A)	10087(4)	1432(1)	9316(2)	54(1)
C(8)	6108(3)	2050(1)	3752(1)	40(1)	C(8A)	9006(4)	1979(1)	8580(1)	44(1)
C(9)	4327(3)	1453(1)	3804(1)	43(1)	C(9A)	10461(4)	2653(1)	8612(2)	48(1)
C(10)	4870(3)	717(1)	3459(2)	51(1)	C(10A)	9273(4)	3337(1)	8303(2)	56(1)
C(11)	3896(4)	198(1)	4175(2)	69(1)	C(12A)	11078(5)	3853(2)	8006(3)	111(1)
C(12)	3573(5)	618(2)	2404(2)	77(1)	C(11A)	7269(5)	3256(2)	7443(2)	81(1)
C(13)	7473(4)	584(1)	3473(3)	86(1)	C(13A)	8201(6)	3601(2)	9219(2)	90(1)
C(14)	8071(4)	2296(1)	2201(2)	60(1)	C(14A)	9811(5)	1393(1)	6197(2)	66(1)
C(15)	5083(5)	2512(2)	1255(2)	76(1)	C(15A)	6917(4)	1506(1)	6956(2)	58(1)

Table 2 c. Hydrogen coordinates (x10^4) and equivalent isotropic displacement parameters (Å2 x 10^3). U(eq) is defined as one third of the trace of the orthogonalized Uij tensor.

	x	y	z	U(eq)		x	y	z	U(eq)
H(1)	4944	3845	3247	77	H(1A)	6366	1077	10206	80
H(2)	7439	4768	3095	97	H(2A)	4055	96	10072	99
H(3)	11056	4792	4017	98	H(3A)	4997	-825	9100	99
H(4)	12208	3889	5075	88	H(4A)	8202	-746	8222	97
H(5)	9726	2954	5220	71	H(5A)	10489	241	8335	79
H(7A)	3856	2829	4074	61	H(7A1)	11656	1324	9163	65
H(7B)	5445	2569	5028	61	H(7A2)	10210	1620	9990	65
H(8)	7650	1887	4049	47	H(8A)	7439	2093	8753	53
H(11A)	4235	-269	3979	104	H(12D)	12261	3925	8562	166
H(11B)	2231	258	4148	104	H(12E)	10326	4289	7822	166
H(11C)	4611	281	4845	104	H(12F)	11789	3672	7448	166
H(12A)	4118	957	1959	115	H(11D)	7862	3041	6878	122
H(12B)	1922	678	2427	115	H(11E)	6642	3707	7253	122
H(12C)	3869	158	2167	115	H(11F)	6056	2970	7663	122
H(13A)	8253	693	4125	129	H(13D)	7015	3282	9381	135
H(13B)	8084	874	2981	129	H(13E)	7513	4052	9077	135
H(13C)	7729	103	3323	129	H(13F)	9399	3637	9776	135
H(14)	9618	2231	2473	72	H(14A)	10727	1288	5690	79

H(15)	4111	2635	681	91

H(15A)	5398	1507	7131	70

Table 2 d Bond lengths (Å).

N(1)-C(14)	1.322(3)
N(1)-N(2)	1.356(2)
N(1)-C(8)	1.456(2)
N(2)-C(15)	1.310(3)
N(3)-C(14)	1.312(3)
N(3)-C(15)	1.345(4)
O(1)-C(9)	1.205(2)
C(1)-C(6)	1.371(3)
C(1)-C(2)	1.381(4)
C(2)-C(3)	1.366(4)
C(3)-C(4)	1.360(4)
C(4)-C(5)	1.389(3)
C(5)-C(6)	1.382(3)
C(6)-C(7)	1.508(3)
C(7)-C(8)	1.524(3)
C(8)-C(9)	1.543(3)
C(9)-C(10)	1.531(3)
C(10)-C(13)	1.515(3)
C(10)-C(11)	1.533(3)
C(10)-C(12)	1.536(3)

C(1)-H(1)	0.93
C(2)-H(2)	0.93
C(3)-H(3)	0.93
C(4)-H(4)	0.93
C(5)-H(5)	0.93
C(7)-H(7A)	0.97
C(7)-H(7B)	0.97
C(8)-H(8)	0.98
C(11)-H(11A)	0.96
C(11)-H(11B)	0.96
C(11)-H(11C)	0.96
C(12)-H(12A)	0.96
C(12)-H(12B)	0.96
C(12)-H(12C)	0.96
C(13)-H(13A)	0.96
C(13)-H(13B)	0.96
C(13)-H(13C)	0.96
C(14)-H(14)	0.93
C(15)-H(15)	0.93

N(1A)-C(15A)	1.325(3)
N(1A)-N(2A)	1.358(2)
N(1A)-C(8A)	1.464(2)
N(3A)-C(15A)	1.312(3)
N(3A)-C(14A)	1.337(3)
N(2A)-C(14A)	1.317(3)
O(1A)-C(9A)	1.204(3)
C(1A)-C(6A)	1.379(3)
C(1A)-C(2A)	1.380(4)
C(2A)-C(3A)	1.364(4)
C(3A)-C(4A)	1.373(4)
C(4A)-C(5A)	1.379(4)
C(5A)-C(6A)	1.382(3)
C(6A)-C(7A)	1.503(3)
C(7A)-C(8A)	1.525(3)
C(8A)-C(9A)	1.538(3)
C(9A)-C(10A)	1.515(3)
C(10A)-C(12A)	1.520(3)
C(10A)-C(13A)	1.525(4)
C(10A)-C(11A)	1.543(4)

C(1A)-H(1A)	0.93
C(2A)-H(2A)	0.93
C(3A)-H(3A)	0.93
C(4A)-H(4A)	0.93
C(5A)-H(5A)	0.93
C(7A)-H(7A1)	0.97
C(7A)-H(7A2)	0.97
C(8A)-H(8A)	0.98
C(12A)-H(12D)	0.96
C(12A)-H(12E)	0.96
C(12A)-H(12F)	0.96
C(11A)-H(11D)	0.96
C(11A)-H(11E)	0.96
C(11A)-H(11F)	0.96
C(13A)-H(13D)	0.96
C(13A)-H(13E)	0.96
C(13A)-H(13F)	0.96
C(14A)-H(14A)	0.93
C(15A)-H(15A)	0.93

Table 2 e. Angles (°).

C(14)-N(1)-N(2)	109.66(16)
C(14)-N(1)-C(8)	130.69(17)
N(2)-N(1)-C(8)	119.52(16)
C(15)-N(2)-N(1)	101.31(19)
C(14)-N(3)-C(15)	101.6(2)
C(6)-C(1)-C(2)	121.1(2)
C(3)-C(2)-C(1)	120.1(3)
C(4)-C(3)-C(2)	119.9(3)
C(3)-C(4)-C(5)	120.0(3)
C(6)-C(5)-C(4)	120.7(2)
C(1)-C(6)-C(5)	118.1(2)
C(1)-C(6)-C(7)	120.8(2)
C(5)-C(6)-C(7)	121.1(2)
C(6)-C(7)-C(8)	112.87(16)
N(1)-C(8)-C(7)	110.98(16)
N(1)-C(8)-C(9)	108.36(15)
C(7)-C(8)-C(9)	111.53(15)
O(1)-C(9)-C(10)	120.64(17)
O(1)-C(9)-C(8)	118.59(17)
C(10)-C(9)-C(8)	120.77(15)
C(13)-C(10)-C(9)	112.70(17)
C(13)-C(10)-C(11)	108.3(2)
C(9)-C(10)-C(11)	107.87(17)
C(13)-C(10)-C(12)	111.4(2)
C(9)-C(10)-C(12)	107.38(19)

O(1A)-C(9A)-C(8A)	118.32(19)
C(10A)-C(9A)-C(8A)	119.60(18)
C(9A)-C(10A)-C(12A)	109.6(2)
C(9A)-C(10A)-C(13A)	106.12(19)
C(12A)-C(10A)-C(13A)	110.3(3)
C(9A)-C(10A)-C(11A)	113.1(2)
C(12A)-C(10A)-C(11A)	110.0(2)
C(13A)-C(10A)-C(11A)	107.6(2)
N(2A)-C(14A)-N(3A)	116.0(2)
N(3A)-C(15A)-N(1A)	111.2(2)
C(6)-C(1)-H(1)	119.4
C(2)-C(1)-H(1)	119.4
C(3)-C(2)-H(2)	119.9
C(1)-C(2)-H(2)	119.9
C(4)-C(3)-H(3)	120
C(2)-C(3)-H(3)	120
C(3)-C(4)-H(4)	120
C(5)-C(4)-H(4)	120
C(6)-C(5)-H(5)	119.7
C(4)-C(5)-H(5)	119.7
C(6)-C(7)-H(7A)	109
C(8)-C(7)-H(7A)	109
C(6)-C(7)-H(7B)	109
C(8)-C(7)-H(7B)	109
H(7A)-C(7)-H(7B)	107.8

N(3)-C(14)-H(14)	124.4
N(1)-C(14)-H(14)	124.4
N(2)-C(15)-H(15)	121.9
N(3)-C(15)-H(15)	121.9
C(6A)-C(1A)-H(1A)	119.3
C(2A)-C(1A)-H(1A)	119.3
C(3A)-C(2A)-H(2A)	119.9
C(1A)-C(2A)-H(2A)	119.9
C(2A)-C(3A)-H(3A)	120.2
C(4A)-C(3A)-H(3A)	120.2
C(3A)-C(4A)-H(4A)	119.9
C(5A)-C(4A)-H(4A)	119.9
C(4A)-C(5A)-H(5A)	119.5
C(6A)-C(5A)-H(5A)	119.5
C(6A)-C(7A)-H(7A1)	109.2
C(8A)-C(7A)-H(7A1)	109.2
C(6A)-C(7A)-H(7A2)	109.2
C(8A)-C(7A)-H(7A2)	109.2
H(7A1)-C(7A)-H(7A2)	107.9
N(1A)-C(8A)-H(8A)	108.5
C(7A)-C(8A)-H(8A)	108.5
C(9A)-C(8A)-H(8A)	108.5
C(10A)-C(12A)-H(12D)	109.5
C(10A)-C(12A)-H(12E)	109.5
H(12D)-C(12A)-H(12E)	109.5

C(11)-C(10)-C(12)	109.02(18)
N(3)-C(14)-N(1)	111.2(2)
N(2)-C(15)-N(3)	116.2(2)
C(15A)-N(1A)-N(2A)	109.41(16)
C(15A)-N(1A)-C(8A)	130.69(17)
N(2A)-N(1A)-C(8A)	119.90(16)
C(15A)-N(3A)-C(14A)	102.02(19)
C(14A)-N(2A)-N(1A)	101.40(18)
C(6A)-C(1A)-C(2A)	121.3(2)
C(3A)-C(2A)-C(1A)	120.1(3)
C(2A)-C(3A)-C(4A)	119.6(2)
C(3A)-C(4A)-C(5A)	120.3(3)
C(4A)-C(5A)-C(6A)	120.9(2)
C(1A)-C(6A)-C(5A)	117.8(2)
C(1A)-C(6A)-C(7A)	121.1(2)
C(5A)-C(6A)-C(7A)	121.1(2)
C(6A)-C(7A)-C(8A)	112.12(17)
N(1A)-C(8A)-C(7A)	110.98(16)
N(1A)-C(8A)-C(9A)	107.86(15)
C(7A)-C(8A)-C(9A)	112.39(17)
O(1A)-C(9A)-C(10A)	122.0(2)

N(1)-C(8)-H(8)	108.6
C(7)-C(8)-H(8)	108.6
C(9)-C(8)-H(8)	108.6
C(10)-C(11)-H(11B)	109.5
H(11A)-C(11)-H(11B)	109.5
C(10)-C(11)-H(11C)	109.5
H(11A)-C(11)-H(11C)	109.5
H(11B)-C(11)-H(11C)	109.5
C(10)-C(12)-H(12A)	109.5
C(10)-C(12)-H(12B)	109.5
H(12A)-C(12)-H(12B)	109.5
C(10)-C(12)-H(12C)	109.5
H(12A)-C(12)-H(12C)	109.5
H(12B)-C(12)-H(12C)	109.5
C(10)-C(13)-H(13A)	109.5
C(10)-C(13)-H(13B)	109.5
H(13A)-C(13)-H(13B)	109.5
C(10)-C(13)-H(13C)	109.5
H(13A)-C(13)-H(13C)	109.5
H(13B)-C(13)-H(13C)	109.5
C(10)-C(11)-H(11A)	109.5

C(10A)-C(12A)-H(12F)	109.5
H(12D)-C(12A)-H(12F)	109.5
H(12E)-C(12A)-H(12F)	109.5
C(10A)-C(11A)-H(11D)	109.5
C(10A)-C(11A)-H(11E)	109.5
H(11D)-C(11A)-H(11E)	109.5
C(10A)-C(11A)-H(11F)	109.5
H(11D)-C(11A)-H(11F)	109.5
H(11E)-C(11A)-H(11F)	109.5
C(10A)-C(13A)-H(13D)	109.5
C(10A)-C(13A)-H(13E)	109.5
H(13D)-C(13A)-H(13E)	109.5
C(10A)-C(13A)-H(13F)	109.5
H(13D)-C(13A)-H(13F)	109.5
H(13E)-C(13A)-H(13F)	109.5
N(2A)-C(14A)-H(14A)	122
N(3A)-C(14A)-H(14A)	122
N(3A)-C(15A)-H(15A)	124.4
N(1A)-C(15A)-H(15A)	124.4

Table 2 f. Anisotropic displacement parameters (Å^2 x 103) The anisotropic displacement factor exponent takes the form: -2 π^2 [$h^2 a^{*2}$ U11 + ... + 2 h k a* b* U12].

	U11	U22	U33	U23	U13	U12
N(1)	42(1)	49(1)	40(1)	-1(1)	6(1)	1(1)
N(2)	58(1)	73(1)	54(1)	10(1)	-4(1)	0(1)
N(3)	95(2)	104(2)	51(1)	12(1)	24(1)	0(1)
O(1)	45(1)	57(1)	81(1)	-5(1)	26(1)	-2(1)
C(1)	74(2)	52(1)	67(1)	6(1)	14(1)	2(1)
C(2)	106(2)	52(2)	89(2)	12(1)	34(2)	-6(2)
C(3)	93(2)	51(2)	109(2)	-18(2)	49(2)	-22(1)
C(4)	63(2)	66(2)	92(2)	-29(2)	18(1)	-14(1)
C(5)	68(2)	47(1)	64(1)	-10(1)	13(1)	0(1)
C(6)	59(1)	40(1)	49(1)	-9(1)	20(1)	-3(1)
C(7)	55(1)	49(1)	52(1)	-6(1)	18(1)	-3(1)
C(8)	39(1)	40(1)	40(1)	1(1)	7(1)	0(1)
C(9)	37(1)	47(1)	46(1)	-2(1)	7(1)	-2(1)
C(10)	42(1)	46(1)	68(1)	-12(1)	13(1)	-6(1)
C(11)	71(2)	50(1)	87(2)	7(1)	10(1)	-2(1)
C(12)	99(2)	68(2)	65(2)	-19(1)	16(1)	-15(2)
C(13)	51(1)	54(2)	157(3)	-32(2)	28(2)	-1(1)
C(14)	57(1)	77(2)	51(1)	2(1)	20(1)	2(1)
C(15)	93(2)	82(2)	48(1)	12(1)	-10(1)	-4(2)

	U11	U22	U33	U23	U13	U12
N(1A)	42(1)	45(1)	43(1)	2(1)	5(1)	1(1)
N(3A)	78(2)	76(2)	54(1)	-10(1)	-5(1)	-4(1)
N(2A)	51(1)	72(1)	48(1)	-3(1)	14(1)	-2(1)
O(1A)	63(1)	68(1)	86(1)	11(1)	-15(1)	-14(1)
C(1A)	82(2)	54(1)	67(1)	7(1)	27(1)	2(1)
C(2A)	91(2)	71(2)	90(2)	12(2)	32(2)	-15(2)
C(3A)	106(2)	57(2)	84(2)	9(1)	8(2)	-22(2)
C(4A)	109(2)	55(2)	78(2)	-10(1)	11(2)	-1(2)
C(5A)	75(2)	61(2)	65(2)	-2(1)	18(1)	2(1)
C(6A)	62(1)	49(1)	43(1)	9(1)	5(1)	4(1)
C(7A)	61(1)	56(1)	44(1)	4(1)	3(1)	0(1)
C(8A)	46(1)	47(1)	42(1)	-1(1)	12(1)	2(1)
C(9A)	52(1)	55(1)	40(1)	0(1)	10(1)	-2(1)
C(10A)	64(1)	47(1)	61(1)	5(1)	20(1)	0(1)
C(12A)	86(2)	69(2)	183(4)	51(2)	43(2)	-2(2)
C(11A)	91(2)	68(2)	83(2)	15(1)	6(2)	26(2)
C(13A)	114(2)	72(2)	90(2)	-13(2)	34(2)	10(2)
C(14A)	78(2)	73(2)	50(1)	-4(1)	17(1)	-1(1)
C(15A)	49(1)	64(1)	60(1)	-1(1)	0(1)	-1(1)

Table 2 g. Torsion angles (°).

C(14)-N(1)-N(2)-C(15)	1.0(3)
C(8)-N(1)-N(2)-C(15)	177.23(19)
C(6)-C(1)-C(2)-C(3)	-0.7(4)
C(1)-C(2)-C(3)-C(4)	0.4(4)

O(1)-C(9)-C(10)-C(13)	-158.8(2)
C(8)-C(9)-C(10)-C(13)	22.5(3)
O(1)-C(9)-C(10)-C(11)	-39.3(3)
C(8)-C(9)-C(10)-C(11)	142.03(18)

C(5A)-C(6A)-C(7A)-C(8A)	94.9(2)
C(15A)-N(1A)-C(8A)-C(7A)	105.8(2)
N(2A)-N(1A)-C(8A)-C(7A)	-73.2(2)
C(15A)-N(1A)-C(8A)-C(9A)	-130.7(2)

C(2)-C(3)-C(4)-C(5)	0.0(4)		O(1)-C(9)-C(10)-C(12)	78.1(2)		N(2A)-N(1A)-C(8A)-C(9A)	50.3(2)
C(3)-C(4)-C(5)-C(6)	0.0(3)		C(8)-C(9)-C(10)-C(12)	-100.6(2)		C(6A)-C(7A)-C(8A)-N(1A)	-58.8(2)
C(2)-C(1)-C(6)-C(5)	0.8(3)		C(15)-N(3)-C(14)-N(1)	1.0(3)		C(6A)-C(7A)-C(8A)-C(9A)	-179.65(17)
C(2)-C(1)-C(6)-C(7)	-179.5(2)		N(2)-N(1)-C(14)-N(3)	-1.4(3)		N(1A)-C(8A)-C(9A)-O(1A)	-98.7(2)
C(4)-C(5)-C(6)-C(1)	-0.4(3)		C(8)-N(1)-C(14)-N(3)	-177.0(2)		C(7A)-C(8A)-C(9A)-O(1A)	24.0(3)
C(4)-C(5)-C(6)-C(7)	179.89(19)		N(1)-N(2)-C(15)-N(3)	-0.5(3)		N(1A)-C(8A)-C(9A)-C(10A)	83.2(2)
C(1)-C(6)-C(7)-C(8)	103.0(2)		C(14)-N(3)-C(15)-N(2)	-0.3(3)		C(7A)-C(8A)-C(9A)-C(10A)	-154.12(17)
C(5)-C(6)-C(7)-C(8)	-77.3(2)		C(15A)-N(1A)-N(2A)-C(14A)	0.3(2)		O(1A)-C(9A)-C(10A)-C(12A)	23.9(3)
C(14)-N(1)-C(8)-C(7)	105.9(2)		C(8A)-N(1A)-N(2A)-C(14A)	179.49(18)		C(8A)-C(9A)-C(10A)-C(12A)	-158.1(2)
N(2)-N(1)-C(8)-C(7)	-69.3(2)		C(6A)-C(1A)-C(2A)-C(3A)	1.2(4)		O(1A)-C(9A)-C(10A)-C(13A)	-95.1(3)
C(14)-N(1)-C(8)-C(9)	-131.3(2)		C(1A)-C(2A)-C(3A)-C(4A)	-0.9(5)		C(8A)-C(9A)-C(10A)-C(13A)	82.9(2)
N(2)-N(1)-C(8)-C(9)	53.4(2)		C(2A)-C(3A)-C(4A)-C(5A)	0.4(4)		O(1A)-C(9A)-C(10A)-C(11A)	147.2(2)
C(6)-C(7)-C(8)-N(1)	-55.7(2)		C(3A)-C(4A)-C(5A)-C(6A)	-0.2(4)		C(8A)-C(9A)-C(10A)-C(11A)	-34.8(3)
C(6)-C(7)-C(8)-C(9)	-176.64(17)		C(2A)-C(1A)-C(6A)-C(5A)	-1.1(3)		N(1A)-N(2A)-C(14A)-N(3A)	-0.2(3)
N(1)-C(8)-C(9)-O(1)	-109.35(19)		C(2A)-C(1A)-C(6A)-C(7A)	176.8(2)		C(15A)-N(3A)-C(14A)-N(2A)	0.0(3)
C(7)-C(8)-C(9)-O(1)	13.1(3)		C(4A)-C(5A)-C(6A)-C(1A)	0.6(4)		C(14A)-N(3A)-C(15A)-N(1A)	0.2(3)
N(1)-C(8)-C(9)-C(10)	69.4(2)		C(4A)-C(5A)-C(6A)-C(7A)	-177.3(2)		N(2A)-N(1A)-C(15A)-N(3A)	-0.3(2)
C(7)-C(8)-C(9)-C(10)	-168.19(17)		C(1A)-C(6A)-C(7A)-C(8A)	-82.9(2)		C(8A)-N(1A)-C(15A)-N(3A)	-179.38(18)

III - MeTAK

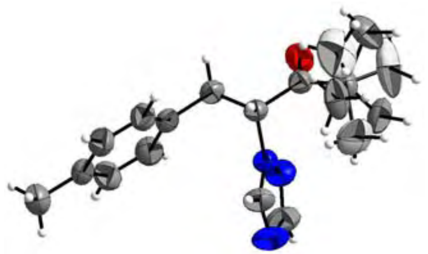

Figure 34. Asymmetric unit of MeTAK, in ellipsoid thermal representation (50% of probability). The two positions of the tertbuthyl are represented in grey (sof: 69%) and light grey (sof: 31%).

Table 3 a. Crystal data.

Chemical Formula	C16 H21 N3 O
Molecular Weight / *g.mol-1*	271.36
Crystal System	Orthorhombic
Space group	P212121
Z , Z' (asymmetric units per unit cell)	4, 1
a / *Å*	5.808(1)
b / *Å*	13.641(1)
c / *Å*	19.789(1)
V / *Å3*	1567.9(2)
dcalc / *g.cm-3*	1.150
R factor (with I>2σI)	R1 = 0.0389 wR2 = 0.1142
R factor (all data)	R1 = 0.0444 wR2 = 0.1210
F(000) / e-	584
Absorption coefficient μ (MoKα1) mm-1	0.074
Number of reflections (n) (with FO>4.0σ(FO))	1880
Number of refined parameters (p) / restraints	216 / 0
Goodness of fit indicator (restrainted GooF)	0.965
Maximum peak in final difference map / e-Å-3	0.128
Maximum hole in final difference map / e-Å-3	-0.108

Table 3 b. Atomic coordinates (x10^4) and equivalent isotropic displacement parameters (Å^2 x 10^3). U(eq) is defined as one third of the trace of the orthogonalized Uij tensor.

	x	y	z	U(eq)			x	y	z	U(eq)
O(1)	5280(3)	7423(1)	2178(1)	76(1)		C(9)	1663(3)	7995(1)	2558(1)	46(1)
N(1)	1344(3)	9041(1)	2414(1)	49(1)		C(10)	3314(3)	7583(1)	2021(1)	52(1)
N(2)	3203(3)	9624(1)	2339(1)	68(1)		C(11)	2492(4)	7400(2)	1293(1)	63(1)
N(3)	-82(5)	10491(2)	2255(1)	91(1)		C(12)	3446(10)	8232(4)	886(2)	89(2)
C(1)	-2889(7)	9509(2)	5438(1)	93(1)		C(13)	3668(9)	6442(4)	1064(3)	94(2)
C(2)	-1491(5)	9073(2)	4873(1)	66(1)		C(14)	-37(6)	7290(5)	1237(2)	85(2)
C(3)	-2201(5)	8248(2)	4533(1)	68(1)		*C(12B)*	*4250(30)*	*7286(19)*	*788(6)*	*159(11)*
C(4)	-915(4)	7858(2)	4014(1)	62(1)		*C(13B)*	*990(50)*	*6472(16)*	*1300(9)*	*181(12)*
C(5)	1148(4)	8275(1)	3817(1)	53(1)		*C(14B)*	*650(30)*	*8231(12)*	*1043(7)*	*131(7)*
C(6)	1852(4)	9110(2)	4152(1)	70(1)		C(15)	-562(4)	9571(2)	2369(1)	68(1)
C(7)	560(5)	9493(2)	4671(1)	75(1)		C(16)	2230(6)	10478(2)	2241(2)	83(1)
C(8)	2616(4)	7832(2)	3266(1)	58(1)						

In italic, the atoms of the *tert*-butyl with a sof of 22%.

Table 3 c. Hydrogen coordinates (x10^4) and equivalent isotropic displacement parameters (Å2 x 10^3). U(eq) is defined as one third of the trace of the orthogonalized Uij tensor

	x	y	z	U(eq)			x	y	z	U(eq)
H(1A)	-4382	9207	5448	139		H(13C)	5303	6498	1125	141
H(1B)	-3057	10201	5366	139		H(14A)	-437	7131	780	128
H(1C)	-2121	9397	5861	139		H(14B)	-770	7893	1364	128
H(3)	-3577	7947	4655	81		H(14C)	-543	6774	1532	128
H(4)	-1444	7301	3792	75		*H(12D)*	*4889*	*6639*	*818*	*239*
H(6)	3216	9416	4026	84		*H(12E)*	*5438*	*7762*	*861*	*239*
H(7)	1083	10052	4892	90		*H(12F)*	*3587*	*7380*	*348*	*239*
H(8A)	2753	7132	3345	69		*H(13D)*	*-429*	*6600*	*1069*	*271*
H(8B)	4148	8112	3291	69		*H(13E)*	*679*	*6287*	*1759*	*271*
H(9)	175	7661	2519	55		*H(13F)*	*1796*	*5949*	*1077*	*271*
H(12A)	5096	8195	882	134		*H(14D)*	*1305*	*8871*	*1101*	*196*
H(12B)	2976	8843	1084	134		*H(14E)*	*-735*	*8181*	*1308*	*196*
H(12C)	2877	8193	432	134		*H(14F)*	*285*	*8129*	*575*	*196*
H(13A)	3336	6327	595	141		H(15)	-2044	9321	2413	82
H(13B)	3097	5905	1329	141		H(16)	3090	11043	2167	100

In italic, the atoms of the *tert*-butyl with a sof of 31%.

Table 3 d. Bond lengths (Å).

O(1)-C(10)	1.203(3)		C(5)-C(6)	1.380(3)
N(1)-C(15)	1.326(3)		C(5)-C(8)	1.510(3)
N(1)-N(2)	1.349(2)		C(6)-C(7)	1.374(3)
N(1)-C(9)	1.467(2)		C(8)-C(9)	1.522(2)

N(2)-C(16)	1.309(3)	C(9)-C(10)	1.538(3)
N(3)-C(15)	1.305(3)	C(10)-C(11)	1.538(3)
N(3)-C(16)	1.343(4)	C(11)-C(12)	1.498(5)
C(1)-C(2)	1.506(3)	C(11)-C(13)	1.543(5)
C(2)-C(3)	1.375(3)	C(11)-C(14)	1.481(4)
C(2)-C(7)	1.381(4)	C(11)-C(12B)	1.435(15)
C(3)-C(4)	1.376(3)	C(11)-C(13B)	1.536(18)
C(4)-C(5)	1.383(3)	C(11)-C(14B)	1.637(14)

Table 3 e. Angles (°).

C(15)-N(1)-N(2)	109.82(16)	C(5)-C(8)-C(9)	*113.60(16)*	C(12)-C(11)-C(10)	105.4(2)
C(15)-N(1)-C(9)	130.51(18)	N(1)-C(9)-C(8)	111.54(15)	C(13B)-C(11)-C(10)	107.5(7)
N(2)-N(1)-C(9)	119.59(15)	N(1)-C(9)-C(10)	107.44(14)	C(12B)-C(11)-C(13)	52.4(10)
C(16)-N(2)-N(1)	101.3(2)	C(8)-C(9)-C(10)	110.85(15)	C(14)-C(11)-C(13)	109.3(3)
C(15)-N(3)-C(16)	101.7(2)	O(1)-C(10)-C(9)	118.62(18)	C(12)-C(11)-C(13)	108.7(4)
C(3)-C(2)-C(7)	117.2(2)	O(1)-C(10)-C(11)	120.50(19)	C(13B)-C(11)-C(13)	63.6(11)
C(3)-C(2)-C(1)	121.7(3)	C(9)-C(10)-C(11)	120.87(17)	C(10)-C(11)-C(13)	105.9(3)
C(7)-C(2)-C(1)	121.1(2)	C(12B)-C(11)-C(14)	129.9(6)	C(12B)-C(11)-C(14B)	109.3(12)
C(2)-C(3)-C(4)	121.2(2)	C(12B)-C(11)-C(12)	56.4(10)	C(14)-C(11)-C(14B)	53.0(7)
C(3)-C(4)-C(5)	121.5(2)	C(14)-C(11)-C(12)	113.8(4)	C(12)-C(11)-C(14B)	63.6(7)
C(6)-C(5)-C(4)	117.4(2)	C(12B)-C(11)-C(13B)	108.6(11)	C(13B)-C(11)-C(14B)	101.7(15)
C(6)-C(5)-C(8)	120.7(2)	C(14)-C(11)-C(13B)	49.8(12)	C(10)-C(11)-C(14B)	111.9(5)
C(4)-C(5)-C(8)	121.92(19)	C(12)-C(11)-C(13B)	147.1(8)	C(13)-C(11)-C(14B)	142.0(5)
C(7)-C(6)-C(5)	120.8(2)	C(12B)-C(11)-C(10)	116.7(6)	N(3)-C(15)-N(1)	111.0(2)
C(6)-C(7)-C(2)	*121.9(2)*	C(14)-C(11)-C(10)	113.2(2)	N(2)-C(16)-N(3)	116.2(2)

In italic, the atoms of the *tert*-butyl with a sof of 31%.

Table 3 f. Anisotropic displacement parameters (Å^2 x 103) The anisotropic displacement factor exponent takes the form: $-2\pi^2 [h^2 a^{*2} U11 + ... + 2 h k a^* b^* U12]$.

	U11	U22	U33	U23	U13	U12
O(1)	60(1)	98(1)	70(1)	-5(1)	0(1)	23(1)
N(1)	51(1)	44(1)	51(1)	1(1)	-5(1)	0(1)
N(2)	68(1)	53(1)	82(1)	2(1)	-4(1)	-14(1)
N(3)	104(2)	57(1)	112(2)	9(1)	-22(2)	18(1)
C(1)	124(2)	89(2)	65(1)	1(1)	23(2)	19(2)
C(2)	90(2)	63(1)	45(1)	6(1)	1(1)	13(1)
C(3)	71(1)	72(1)	61(1)	5(1)	7(1)	-3(1)
C(4)	72(1)	*61(1)*	54(1)	-2(1)	-3(1)	-5(1)
C(5)	62(1)	*53(1)*	44(1)	4(1)	-5(1)	6(1)
C(6)	74(1)	*66(1)*	70(1)	-3(1)	4(1)	-11(1)
C(7)	97(2)	*62(1)*	66(1)	-15(1)	2(1)	-8(1)
C(8)	63(1)	*59(1)*	51(1)	6(1)	-3(1)	12(1)
C(9)	47(1)	*41(1)*	49(1)	0(1)	-1(1)	-1(1)
C(10)	54(1)	*48(1)*	54(1)	1(1)	4(1)	-1(1)
C(11)	63(1)	*76(1)*	50(1)	-9(1)	10(1)	-7(1)
C(12)	121(4)	*98(3)*	49(2)	12(2)	1(2)	-19(3)
C(13)	93(3)	90(3)	99(3)	-42(2)	8(3)	-1(3)
C(14)	62(2)	141(5)	53(2)	-23(3)	-7(2)	-13(2)
C(12B)	*151(13)*	*260(30)*	*62(6)*	*-59(11)*	*15(7)*	*-71(17)*
C(13B)	*280(30)*	*139(15)*	*119(13)*	*-66(11)*	*-10(16)*	*-72(19)*

C(14B)	*188(17)*	*127(12)*	*78(7)*	*-1(7)*	*-64(9)*	*29(12)*
C(15)	64(1)	59(1)	81(2)	5(1)	-10(1)	12(1)
C(16)	104(2)	46(1)	99(2)	7(1)	-11(2)	-10(1)

In italic, the atoms of the *tert*-butyl with a sof of 31%.

Table 3 g. Torsion angles (°).

C(15)-N(1)-N(2)-C(16)	-1.0(2)	C(8)-C(9)-C(10)-O(1)	-18.1(3)
C(9)-N(1)-N(2)-C(16)	-178.1(2)	N(1)-C(9)-C(10)-C(11)	-74.6(2)
C(7)-C(2)-C(3)-C(4)	0.2(3)	C(8)-C(9)-C(10)-C(11)	163.34(18)
C(1)-C(2)-C(3)-C(4)	179.7(2)	O(1)-C(10)-C(11)-C(12B)	-15.7(12)
C(2)-C(3)-C(4)-C(5)	0.4(4)	C(9)-C(10)-C(11)-C(12B)	162.9(12)
C(3)-C(4)-C(5)-C(6)	-1.1(3)	O(1)-C(10)-C(11)-C(14)	159.6(4)
C(3)-C(4)-C(5)-C(8)	177.7(2)	C(9)-C(10)-C(11)-C(14)	-21.9(4)
C(4)-C(5)-C(6)-C(7)	1.2(3)	O(1)-C(10)-C(11)-C(12)	-75.4(3)
C(8)-C(5)-C(6)-C(7)	-177.5(2)	C(9)-C(10)-C(11)-C(12)	103.2(3)
C(5)-C(6)-C(7)-C(2)	-0.7(4)	O(1)-C(10)-C(11)-C(13B)	106.5(13)
C(3)-C(2)-C(7)-C(6)	0.0(4)	C(9)-C(10)-C(11)-C(13B)	-75.0(13)
C(1)-C(2)-C(7)-C(6)	-179.5(2)	O(1)-C(10)-C(11)-C(13)	39.8(4)
C(6)-C(5)-C(8)-C(9)	-106.6(2)	C(9)-C(10)-C(11)-C(13)	-141.7(3)
C(4)-C(5)-C(8)-C(9)	74.7(2)	O(1)-C(10)-C(11)-C(14B)	-142.7(8)
C(15)-N(1)-C(9)-C(8)	-107.0(2)	C(9)-C(10)-C(11)-C(14B)	35.9(8)
N(2)-N(1)-C(9)-C(8)	69.4(2)	C(16)-N(3)-C(15)-N(1)	-0.6(3)
C(15)-N(1)-C(9)-C(10)	131.4(2)	N(2)-N(1)-C(15)-N(3)	1.0(3)
N(2)-N(1)-C(9)-C(10)	-52.3(2)	C(9)-N(1)-C(15)-N(3)	177.7(2)
C(5)-C(8)-C(9)-N(1)	56.8(2)	N(1)-N(2)-C(16)-N(3)	0.7(4)
C(5)-C(8)-C(9)-C(10)	176.43(17)	C(15)-N(3)-C(16)-N(2)	-0.1(4)
N(1)-C(9)-C(10)-O(1)	104.0(2)		

In italic, the atoms of the *tert*-butyl with a sof of 31%.

IV - BrTAK

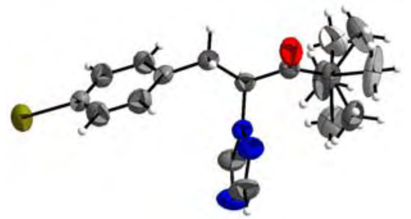

Figure 35. Asymmetric unit of BrTAK, in ellipsoid thermal representation (50% of probability). The two positions of the tertbuthyl are represented in grey (sof: 68%) and light grey (sof: 32%).

Table 4 a. Crystal data.

Chemical Formula	$C15 H18 Br N3 O$
Molecular Weight / *g.mol^{-1}*	336.23
Crystal System	Orthorhombic
Space group	P212121
Z , Z' (asymmetric units per unit cell)	4, 1
a / *Å*	5.7875(5)

b / *Å*	13.629(1)
c / *Å*	19.882(2)
V / *Å*^{3}	1568.3(2)
dcalc / *g.cm-3*	1.424
R factor (with I>2σI)	R1 = 0.0371 wR2 = 0.0848
R factor (all data)	R1 = 0.0544 wR2 = 0.0913
F(000) / e-	688
Absorption coefficient μ (MoKα1) mm-1	2.621
Number of reflections (n) (with FO>4.0σ(FO))	3192 / 2447
Number of refined parameters (p) / restraints	215
Goodness of fit indicator (restrainted GooF)	1.030
Maximum peak in final difference map / e-Å-3	0.405
Maximum hole in final difference map / e-Å-3	-0.161

Table 4 b. Atomic coordinates (x10^4) and equivalent isotropic displacement parameters (Å^2 x 10^3). U(eq) is defined as one third of the trace of the orthogonalized Uij tensor.

	x	y	z	U(eq)
Br(1)	7287(1)	417(1)	590(1)	85(1)
O(1)	15344(4)	2661(2)	-2849(1)	72(1)
N(1)	11433(4)	1041(2)	-2599(1)	44(1)
N(2)	13303(5)	468(2)	-2673(1)	62(1)
N(3)	10045(7)	-422(2)	-2773(2)	85(1)
C(1)	8917(6)	969(2)	-150(1)	57(1)
C(2)	10952(6)	562(2)	-348(2)	66(1)
C(3)	12137(6)	972(2)	-876(2)	61(1)
C(4)	11332(5)	1802(2)	-1205(1)	46(1)
C(5)	9270(5)	2189(2)	-991(2)	54(1)
C(6)	8061(5)	1778(2)	-458(1)	57(1)
C(7)	12709(6)	2259(2)	-1761(1)	51(1)
C(8)	11736(5)	2090(2)	-2464(1)	42(1)
C(9)	13364(5)	2503(2)	-3002(1)	47(1)
C(10)	12528(6)	2689(2)	-3716(1)	57(1)
C(13)	13377(13)	1824(5)	-4132(3)	84(2)
C(11)	9979(10)	2813(7)	-3770(3)	87(3)
C(12)	13701(13)	3653(6)	-3959(4)	100(3)
C(11A)	*10780(30)*	*1849(14)*	*-3999(7)*	*105(7)*
C(13A)	*11140(40)*	*3632(13)*	*-3721(8)*	*116(8)*
C(12A)	*14460(30)*	*2820(20)*	*-4227(7)*	*133(10)*
C(14)	12346(8)	-396(2)	-2774(2)	77(1)
C(15)	9518(6)	512(3)	-2656(2)	63(1)

In italic, the atoms of the *tert*-butyl with a sof of 32%.

Table 4 c. Hydrogen coordinates (x10^4) and equivalent isotropic displacement parameters (Å2 x 10^3). U(eq) is defined as one third of the trace of the orthogonalized Uij tensor.

	x	y	z	U(eq)
H(2)	11534	13	-128	79
H(3)	13513	686	-1017	73
H(5)	8670	2738	-1208	64
H(6)	6679	2056	-313	68
H(7A)	14268	1999	-1745	61
H(7B)	12802	2960	-1682	61
H(8)	10235	2418	-2500	50
H(13A)	13077	1946	-4599	125
H(13B)	12582	1240	-3994	125
H(13C)	15008	1741	-4064	125
H(11A)	9557	2887	-4234	131
H(11B)	9513	3385	-3523	131
H(11C)	9223	2245	-3587	131
H(12A)	15349	3582	-3935	151
H(12B)	13223	4187	-3677	151
H(12C)	13255	3783	-4416	151
H(11D)	*10368*	*1997*	*-4455*	*158*
H(11E)	*9415*	*1832*	*-3726*	*158*
H(11F)	*11535*	*1222*	*-3982*	*158*
H(13D)	*11996*	*4140*	*-3497*	*175*
H(13E)	*9700*	*3530*	*-3491*	*175*
H(13F)	*10839*	*3825*	*-4177*	*175*
H(12D)	*13843*	*3105*	*-4630*	*199*
H(12E)	*15129*	*2194*	*-4329*	*199*
H(12F)	*15622*	*3246*	*-4044*	*199*
H(14)	13228	-958	-2841	92
H(15)	8025	758	-2618	76

In italic, the atoms of the *tert*-butyl with a sof of 32%.

Table 4 d. Bond lengths (Å).

Br(1)-C(1)	1.903(3)	C(9)-C(10)	1.521(4)	C(11)-H(11A)	0.96
O(1)-C(9)	1.205(4)	C(10)-C(11)	1.489(7)	C(11)-H(11B)	0.96
N(1)-C(15)	1.327(4)	C(10)-C(13)	1.521(6)	C(11)-H(11C)	0.96
N(1)-N(2)	1.343(3)	C(10)-C(12)	1.555(7)	C(12)-H(12A)	0.96
N(1)-C(8)	1.464(4)	*C(10)-C(13A)*	*1.516(18)*	C(12)-H(12B)	0.96
N(2)-C(14)	1.317(4)	*C(10)-C(12A)*	*1.520(16)*	C(12)-H(12C)	0.96
N(3)-C(15)	1.329(4)	*C(10)-C(11A)*	*1.627(15)*	*C(11A)-H(11D)*	*0.96*
N(3)-C(14)	1.332(5)	C(2)-H(2)	0.93	*C(11A)-H(11E)*	*0.96*
C(1)-C(6)	1.356(4)	C(3)-H(3)	0.93	*C(11A)-H(11F)*	*0.96*
C(1)-C(2)	1.360(5)	C(5)-H(5)	0.93	*C(13A)-H(13D)*	*0.96*
C(2)-C(3)	1.373(4)	C(6)-H(6)	0.93	*C(13A)-H(13E)*	*0.96*
C(3)-C(4)	1.387(4)	C(7)-H(7A)	0.97	*C(13A)-H(13F)*	*0.96*
C(4)-C(5)	1.373(4)	C(7)-H(7B)	0.97	*C(12A)-H(12D)*	*0.96*
C(4)-C(7)	1.498(4)	C(8)-H(8)	0.98	*C(12A)-H(12E)*	*0.96*
C(5)-C(6)	1.389(4)	C(13)-H(13A)	0.96	*C(12A)-H(12F)*	*0.96*
C(7)-C(8)	1.524(3)	C(13)-H(13B)	0.96	C(14)-H(14)	0.93
C(8)-C(9)	1.532(4)	C(13)-H(13C)	0.96	C(15)-H(15)	0.93

In italic, the atoms of the *tert*-butyl with a sof of 32%.

Table 4 e. Angles (°).

C(15)-N(1)-N(2)	110.3(2)	C(11)-C(10)-C(13)	111.6(5)	C(8)-C(7)-H(7B)	108.6
C(15)-N(1)-C(8)	130.2(3)	*C(13A)-C(10)-C(13)*	*145.6(7)*	H(7A)-C(7)-H(7B)	107.6

N(2)-N(1)-C(8)	119.4(2)
C(14)-N(2)-N(1)	101.4(3)
C(15)-N(3)-C(14)	101.8(3)
C(6)-C(1)-C(2)	121.2(3)
C(6)-C(1)-Br(1)	119.3(3)
C(2)-C(1)-Br(1)	119.5(2)
C(1)-C(2)-C(3)	119.2(3)
C(2)-C(3)-C(4)	121.6(3)
C(5)-C(4)-C(3)	117.4(3)
C(5)-C(4)-C(7)	122.1(3)
C(3)-C(4)-C(7)	120.6(3)
C(4)-C(5)-C(6)	121.3(3)
C(1)-C(6)-C(5)	119.3(3)
C(4)-C(7)-C(8)	114.7(2)
N(1)-C(8)-C(7)	111.1(2)
N(1)-C(8)-C(9)	107.7(2)
C(7)-C(8)-C(9)	110.9(2)
O(1)-C(9)-C(10)	120.5(3)
O(1)-C(9)-C(8)	118.3(3)
C(10)-C(9)-C(8)	121.1(3)
C(11)-C(10)-C(13A)	*51.5(9)*
C(11)-C(10)-C(12A)	*131.8(7)*
C(13A)-C(10)-C(12A)	*106.6(12)*
C(11)-C(10)-C(9)	113.7(3)
C(13A)-C(10)-C(9)	*108.4(6)*
C(12A)-C(10)-C(9)	*114.2(7)*

C(12A)-C(10)-C(13)	*59.4(11)*
C(9)-C(10)-C(13)	105.9(3)
C(11)-C(10)-C(12)	108.4(5)
C(13A)-C(10)-C(12)	*60.9(9)*
C(12A)-C(10)-C(12)	51.1(10)
C(9)-C(10)-C(12)	107.0(4)
C(13)-C(10)-C(12)	110.1(5)
C(11)-C(10)-C(11A)	*55.9(8)*
C(13A)-C(10)-C(11A)	*105.4(11)*
C(12A)-C(10)-C(11A)	*108.0(12)*
C(9)-C(10)-C(11A)	*113.7(6)*
C(13)-C(10)-C(11A)	*57.8(8)*
C(12)-C(10)-C(11A)	*139.3(6)*
N(2)-C(14)-N(3)	116.3(3)
N(1)-C(15)-N(3)	110.1(3)
C(1)-C(2)-H(2)	120.4
C(3)-C(2)-H(2)	120.4
C(2)-C(3)-H(3)	119.2
C(4)-C(3)-H(3)	119.2
C(4)-C(5)-H(5)	119.4
C(6)-C(5)-H(5)	119.4
C(1)-C(6)-H(6)	120.4
C(5)-C(6)-H(6)	120.4
C(4)-C(7)-H(7A)	108.6
C(8)-C(7)-H(7A)	108.6

N(1)-C(8)-H(8)	109
C(7)-C(8)-H(8)	109
C(9)-C(8)-H(8)	109
C(10)-C(13)-H(13A)	109.5
C(10)-C(13)-H(13B)	109.5
C(10)-C(13)-H(13C)	109.5
C(10)-C(11)-H(11A)	109.5
C(10)-C(11)-H(11B)	109.5
C(10)-C(11)-H(11C)	109.5
C(10)-C(12)-H(12A)	109.5
C(10)-C(12)-H(12B)	109.5
C(10)-C(12)-H(12C)	109.5
H(11D)-C(11A)-H(11E)	*109.5*
H(11D)-C(11A)-H(11F)	*109.5*
H(11E)-C(11A)-H(11F)	*109.5*
H(13D)-C(13A)-H(13E)	*109.5*
H(13D)-C(13A)-H(13F)	*109.5*
H(13E)-C(13A)-H(13F)	*109.5*
H(12D)-C(12A)-H(12E)	*109.5*
H(12D)-C(12A)-H(12F)	*109.5*
H(12E)-C(12A)-H(12F)	*109.5*
N(2)-C(14)-H(14)	121.8
N(3)-C(14)-H(14)	121.8
N(1)-C(15)-H(15)	124.9
N(3)-C(15)-H(15)	124.9

In italic, the atoms of the *tert*-butyl with a sof of 32%.

Table 4 f. Anisotropic displacement parameters (Å^2 x 103) The anisotropic displacement factor exponent takes the form: $-2\pi^2 [h^2 a^{*2} U11 + ... + 2 h k a^* b^* U12]$.

	U11	U22	U33	U23	U13	U12
Br(1)	121(1)	75(1)	60(1)	8(1)	26(1)	-10(1)
O(1)	60(2)	97(2)	58(1)	5(1)	1(1)	-23(1)
N(1)	46(1)	44(1)	42(1)	-2(1)	-5(1)	1(1)
N(2)	63(2)	51(2)	71(2)	-2(1)	-6(1)	11(2)
N(3)	98(3)	54(2)	102(2)	-9(2)	-22(2)	-13(2)
C(1)	84(2)	49(2)	37(2)	-4(1)	5(2)	-9(2)
C(2)	83(2)	53(2)	60(2)	13(2)	2(2)	12(2)
C(3)	61(2)	61(2)	61(2)	-3(1)	5(2)	12(2)
C(4)	56(2)	46(2)	37(1)	-8(1)	-5(1)	-6(1)
C(5)	60(2)	51(2)	50(2)	7(1)	-3(2)	7(2)
C(6)	57(2)	61(2)	53(2)	-1(1)	5(1)	2(2)
C(7)	58(2)	52(1)	43(1)	-5(1)	-1(2)	-12(2)
C(8)	44(2)	38(1)	44(1)	-2(1)	-1(1)	3(1)
C(9)	46(2)	47(2)	48(2)	-2(1)	4(1)	0(1)
C(10)	58(2)	68(2)	43(1)	8(1)	8(2)	11(2)
C(13)	107(6)	96(5)	48(3)	-5(3)	8(3)	22(4)
C(11)	62(4)	149(9)	50(3)	27(4)	-3(3)	20(4)
C(12)	89(5)	112(6)	100(6)	56(5)	1(4)	-9(4)
C(11A)	*127(15)*	*124(15)*	*65(8)*	*6(9)*	*-55(9)*	*-23(12)*
C(13A)	*180(20)*	*81(11)*	*91(11)*	*28(9)*	*-9(12)*	*4(12)*
C(12A)	*104(12)*	*260(30)*	*38(7)*	*13(11)*	*20(7)*	*44(17)*
C(14)	93(3)	48(2)	88(2)	-10(2)	-15(2)	16(3)
C(15)	56(2)	59(2)	75(2)	-7(2)	-10(2)	-11(2)

In italic, the atoms of the *tert*-butyl with a sof of 32%.

Table 4 g. Torsion angles (°)

C(15)-N(1)-N(2)-C(14)	0.2(3)
C(8)-N(1)-N(2)-C(14)	179.1(2)
C(6)-C(1)-C(2)-C(3)	-1.0(5)
Br(1)-C(1)-C(2)-C(3)	-179.1(3)
C(1)-C(2)-C(3)-C(4)	1.2(5)
C(2)-C(3)-C(4)-C(5)	-1.4(4)
C(2)-C(3)-C(4)-C(7)	177.4(3)
C(3)-C(4)-C(5)-C(6)	1.3(4)
C(7)-C(4)-C(5)-C(6)	-177.4(3)
C(2)-C(1)-C(6)-C(5)	1.0(5)
Br(1)-C(1)-C(6)-C(5)	179.0(2)
C(4)-C(5)-C(6)-C(1)	-1.1(4)
C(5)-C(4)-C(7)-C(8)	-74.9(3)
C(3)-C(4)-C(7)-C(8)	106.4(3)
C(15)-N(1)-C(8)-C(7)	109.3(3)
N(2)-N(1)-C(8)-C(7)	-69.4(3)
C(15)-N(1)-C(8)-C(9)	-129.0(3)
N(2)-N(1)-C(8)-C(9)	52.3(3)
C(4)-C(7)-C(8)-N(1)	-55.2(3)
C(4)-C(7)-C(8)-C(9)	-174.9(2)
N(1)-C(8)-C(9)-O(1)	-103.1(3)

C(7)-C(8)-C(9)-O(1)	18.6(4)
N(1)-C(8)-C(9)-C(10)	75.6(3)
C(7)-C(8)-C(9)-C(10)	-162.7(2)
O(1)-C(9)-C(10)-C(11)	-159.0(5)
C(8)-C(9)-C(10)-C(11)	22.4(5)
O(1)-C(9)-C(10)-C(13A)	*-103.7(10)*
C(8)-C(9)-C(10)-C(13A)	*77.6(10)*
O(1)-C(9)-C(10)-C(12A)	*15.0(13)*
C(8)-C(9)-C(10)-C(12A)	*-163.7(12)*
O(1)-C(9)-C(10)-C(13)	78.1(5)
C(8)-C(9)-C(10)-C(13)	-100.6(4)
O(1)-C(9)-C(10)-C(12)	-39.4(5)
C(8)-C(9)-C(10)-C(12)	141.9(4)
O(1)-C(9)-C(10)-C(11A)	*139.4(9)*
C(8)-C(9)-C(10)-C(11A)	*-39.2(9)*
N(1)-N(2)-C(14)-N(3)	0.2(4)
C(15)-N(3)-C(14)-N(2)	-0.5(5)
N(2)-N(1)-C(15)-N(3)	-0.5(4)
C(8)-N(1)-C(15)-N(3)	-179.3(3)
C(14)-N(3)-C(15)-N(1)	0.6(4)

In italic, the atoms of the *tert*-butyl with a sof of 32%.

V – Imine monohydrate 52a

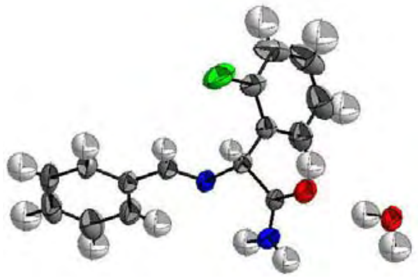

Figure 36. Asymmetric unit of the monohydrate of 52a.

Table 5 a. Crystal data.

Chemical Formula	$C_{15}H_{15}FN_2O_2$
Molecular Weight / *g.mol^{-1}*	274.29
Crystal System	Monoclinic

Space group	$P2_1$/c
Z , Z' (asymmetric units per unit cell)	4, 1
a / Å	13.9829(14)
b / Å	6.6374(7) (1)
c / Å	15.8034 (1)
β / °	100.202(2)
V / Å^3	1443.5(3)
dcalc / *g.cm-3*	1.262
R factor (with I>2σI)	R1 = 0.0659 wR2 = 0.1907
R factor (all data)	R1 = 0.0719 wR2 = 0.1965
F(000) / e-	576
Absorption coefficient μ (MoKα1) mm-1	0.094
Number of reflections (n) (with FO>4.0σ(FO))	11022 / 2960
Number of refined parameters (p) / restraints	189
Goodness of fit indicator (restrainted GooF)	1.093
Maximum peak in final difference map / e-Å-3	0.941
Maximum hole in final difference map / e-Å-3	-0.286

Table 5 b. Atomic coordinates (x10^4) and equivalent isotropic displacement parameters (Å^2 x 10^3). U(eq) is defined as one third of the trace of the orthogonalized Uij tensor.

	x	y	z	U(eq)
OW1	5837(1)	741(3)	7659(2)	72(1)
F(1)	2000(2)	5783(3)	8946(1)	99(1)
O(1)	3926(1)	1637(2)	7779(1)	62(1)
N(1)	1739(1)	826(3)	8637(1)	46(1)
N(2)	3133(1)	-1160(3)	8056(1)	61(1)
C(1)	2748(2)	4953(4)	9471(2)	63(1)
C(2)	3160(3)	6002(5)	10188(2)	94(1)
C(3)	3917(3)	5144(7)	10730(2)	106(1)
C(4)	4238(2)	3261(6)	10558(2)	92(1)
C(5)	3816(2)	2231(5)	9826(2)	68(1)
C(6)	3047(1)	3090(3)	9254(1)	47(1)
C(7)	2545(1)	2064(3)	8447(1)	42(1)
C(8)	890(1)	1512(3)	8424(1)	48(1)
C(9)	23(1)	470(3)	8597(1)	50(1)
C(10)	78(2)	-1392(4)	8997(2)	65(1)
C(11)	-758(2)	-2337(5)	9149(2)	80(1)
C(12)	-1648(2)	-1419(5)	8914(2)	78(1)
C(13)	-1708(2)	421(5)	8524(2)	74(1)
C(14)	-880(2)	1374(4)	8362(2)	62(1)
C(15)	3264(1)	790(3)	8059(1)	44(1)

Table 5 c. Hydrogen coordinates (x10^4) and equivalent isotropic displacement parameters (Å2 x 10^3). U(eq) is defined as one third of the trace of the orthogonalized Uij tensor.

	x	y	z	U(eq)
HW1	5270(20)	810(50)	7702(19)	81(9)
HW2	5920(30)	-460(70)	7500(20)	104(12)
H(2A)	3524	-1941	7848	73
H(2B)	2655	-1662	8262	73
H(2)	2930	7269	10303	113
H(3)	4216	5837	11217	127
H(4)	4745	2670	10938	110
H(5)	4045	961	9714	82
H(7)	2279	3100	8029	50
H(8)	810	2747	8142	58
H(10)	679	-2011	9164	78
H(11)	-718	-3596	9412	96
H(12)	-2208	-2054	9020	94
H(13)	-2311	1038	8366	89
H(14)	-928	2627	8094	75

Table 5 d. Bond lengths (Å).

OW1-HW1	0.81(3)	C(5)-H(5)	0.93
OW1-HW2	0.85(4)	C(6)-C(7)	1.506(3)
F(1)-C(1)	1.333(3)	C(7)-C(15)	1.523(3)
O(1)-C(15)	1.231(2)	C(7)-H(7)	0.98
N(1)-C(8)	1.260(2)	C(8)-C(9)	1.463(3)
N(1)-C(7)	1.468(2)	C(8)-H(8)	0.93
N(2)-C(15)	1.307(3)	C(9)-C(10)	1.384(4)
N(2)-H(2A)	0.86	C(9)-C(14)	1.388(3)
N(2)-H(2B)	0.86	C(10)-C(11)	1.385(3)
C(1)-C(6)	1.368(3)	C(10)-H(10)	0.93
C(1)-C(2)	1.368(4)	C(11)-C(12)	1.377(4)
C(2)-C(3)	1.362(6)	C(11)-H(11)	0.93
C(2)-H(2)	0.93	C(12)-C(13)	1.364(4)
C(3)-C(4)	1.372(6)	C(12)-H(12)	0.93
C(3)-H(3)	0.93	C(13)-C(14)	1.383(4)
C(4)-C(5)	1.382(4)	C(13)-H(13)	0.93
C(4)-H(4)	0.93	C(14)-H(14)	0.93
C(5)-C(6)	1.398(3)		

Table 5 e. Angles (°).

HW1-OW1-HW2	106(3)	C(6)-C(7)-H(7)	108.5
C(8)-N(1)-C(7)	117.65(17)	C(15)-C(7)-H(7)	108.5
C(15)-N(2)-H(2A)	120	N(1)-C(8)-C(9)	123.5(2)
C(15)-N(2)-H(2B)	120	N(1)-C(8)-H(8)	118.3
H(2A)-N(2)-H(2B)	120	C(9)-C(8)-H(8)	118.3
F(1)-C(1)-C(6)	117.3(2)	C(10)-C(9)-C(14)	118.9(2)
F(1)-C(1)-C(2)	118.3(3)	C(10)-C(9)-C(8)	121.75(19)
C(6)-C(1)-C(2)	124.4(3)	C(14)-C(9)-C(8)	119.4(2)
C(3)-C(2)-C(1)	118.3(3)	C(9)-C(10)-C(11)	120.2(2)
C(3)-C(2)-H(2)	120.8	C(9)-C(10)-H(10)	119.9
C(1)-C(2)-H(2)	120.8	C(11)-C(10)-H(10)	119.9
C(2)-C(3)-C(4)	120.1(3)	C(12)-C(11)-C(10)	120.2(3)
C(2)-C(3)-H(3)	119.9	C(12)-C(11)-H(11)	119.9
C(4)-C(3)-H(3)	119.9	C(10)-C(11)-H(11)	119.9
C(3)-C(4)-C(5)	120.7(3)	C(13)-C(12)-C(11)	119.9(2)
C(3)-C(4)-H(4)	119.7	C(13)-C(12)-H(12)	120

C(5)-C(4)-H(4)	119.7
C(4)-C(5)-C(6)	120.3(3)
C(4)-C(5)-H(5)	119.8
C(6)-C(5)-H(5)	119.8
C(1)-C(6)-C(5)	116.2(2)
C(1)-C(6)-C(7)	120.3(2)
C(5)-C(6)-C(7)	123.6(2)
N(1)-C(7)-C(6)	109.86(15)
N(1)-C(7)-C(15)	110.91(16)
C(6)-C(7)-C(15)	110.50(15)
N(1)-C(7)-H(7)	108.5

C(11)-C(12)-H(12)	120
C(12)-C(13)-C(14)	120.4(2)
C(12)-C(13)-H(13)	119.8
C(14)-C(13)-H(13)	119.8
C(13)-C(14)-C(9)	120.3(3)
C(13)-C(14)-H(14)	119.9
C(9)-C(14)-H(14)	119.9
O(1)-C(15)-N(2)	124.36(19)
O(1)-C(15)-C(7)	118.95(18)
N(2)-C(15)-C(7)	116.69(17)

Table 5 f. Anisotropic displacement parameters (Å² x 103) The anisotropic displacement factor exponent takes the form: -2 π² [h² a*² U11 + ... + 2 h k a* b* U12].

	U11	U22	U33	U23	U13	U12
OW1	46(1)	51(1)	125(2)	6(1)	31(1)	-3(1)
F(1)	108(1)	59(1)	136(2)	0(1)	38(1)	27(1)
O(1)	53(1)	57(1)	86(1)	-5(1)	38(1)	-4(1)
N(1)	36(1)	47(1)	58(1)	1(1)	16(1)	2(1)
N(2)	55(1)	45(1)	91(1)	-9(1)	35(1)	0(1)
C(1)	72(2)	47(1)	79(2)	-2(1)	37(1)	-1(1)
C(2)	137(3)	66(2)	96(2)	-31(2)	63(2)	-29(2)
C(3)	135(3)	122(3)	67(2)	-32(2)	37(2)	-59(3)
C(4)	83(2)	129(3)	61(2)	-2(2)	3(1)	-25(2)
C(5)	61(1)	86(2)	57(1)	1(1)	7(1)	-3(1)
C(6)	46(1)	46(1)	54(1)	0(1)	24(1)	-5(1)
C(7)	37(1)	39(1)	53(1)	6(1)	16(1)	4(1)
C(8)	40(1)	50(1)	56(1)	1(1)	10(1)	4(1)
C(9)	37(1)	62(1)	53(1)	-9(1)	12(1)	1(1)
C(10)	46(1)	71(2)	81(2)	5(1)	21(1)	2(1)
C(11)	68(2)	89(2)	89(2)	7(2)	28(1)	-15(2)
C(12)	47(1)	121(3)	71(2)	-11(2)	22(1)	-22(1)
C(13)	35(1)	113(2)	75(2)	-12(2)	9(1)	3(1)
C(14)	40(1)	76(2)	70(1)	-4(1)	7(1)	7(1)
C(15)	38(1)	47(1)	50(1)	-4(1)	14(1)	-1(1)

Table 5 g. Torsion angles (°).

F(1)-C(1)-C(2)-C(3)	179.3(3)
C(6)-C(1)-C(2)-C(3)	-0.3(4)
C(1)-C(2)-C(3)-C(4)	-1.1(5)
C(2)-C(3)-C(4)-C(5)	1.5(5)
C(3)-C(4)-C(5)-C(6)	-0.7(5)
F(1)-C(1)-C(6)-C(5)	-178.5(2)
C(2)-C(1)-C(6)-C(5)	1.1(3)
F(1)-C(1)-C(6)-C(7)	0.6(3)
C(2)-C(1)-C(6)-C(7)	-179.8(2)
C(4)-C(5)-C(6)-C(1)	-0.6(4)
C(4)-C(5)-C(6)-C(7)	-179.6(2)
C(8)-N(1)-C(7)-C(6)	102.5(2)
C(8)-N(1)-C(7)-C(15)	-135.03(19)

C(5)-C(6)-C(7)-C(15)	-34.0(3)
C(7)-N(1)-C(8)-C(9)	-178.12(18)
N(1)-C(8)-C(9)-C(10)	-1.4(3)
N(1)-C(8)-C(9)-C(14)	178.0(2)
C(14)-C(9)-C(10)-C(11)	0.7(4)
C(8)-C(9)-C(10)-C(11)	-179.9(2)
C(9)-C(10)-C(11)-C(12)	-0.8(4)
C(10)-C(11)-C(12)-C(13)	0.4(5)
C(11)-C(12)-C(13)-C(14)	0.1(4)
C(12)-C(13)-C(14)-C(9)	-0.2(4)
C(10)-C(9)-C(14)-C(13)	-0.2(4)
C(8)-C(9)-C(14)-C(13)	-179.6(2)
N(1)-C(7)-C(15)-O(1)	172.32(18)

C(1)-C(6)-C(7)-N(1)	-90.3(2)
C(5)-C(6)-C(7)-N(1)	88.7(2)
C(1)-C(6)-C(7)-C(15)	147.00(19)

C(6)-C(7)-C(15)-O(1)	-65.6(2)
N(1)-C(7)-C(15)-N(2)	-8.2(2)
C(6)-C(7)-C(15)-N(2)	113.8(2)

VI – Dimer 46

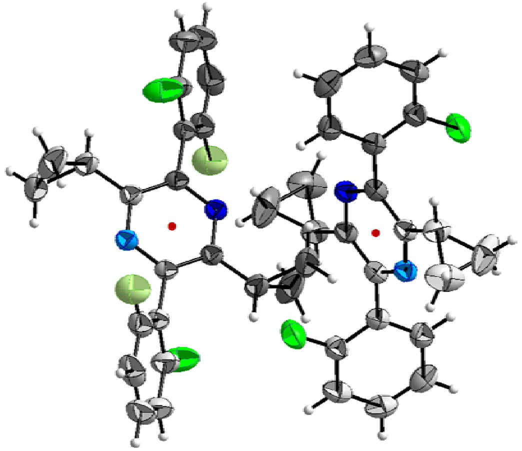

Figure 37. The two fully regenerated molecules of the asymmetric unit (in light grey the part regenerated by the inversion centre - red dot). The molecule to the left exhibits a partial disorder on the fluorine atom which is divided onto two positions with s.o.f. of 79% and 21%.

Table 6 a. Crystal data.

Chemical Formula	$C_{22}H_{18}F_2N_2$
Molecular Weight / *g.mol⁻¹*	348.38
Crystal System	Triclinic
Space group	P-1
Z , Z' (asymmetric units per unit cell)	2, 2x0.5
a / *Å*	9.2668(10)
b / *Å*	9.6027(10)
c / *Å*	11.3518(12)
α / °	65.849(2)
β / °	77.487(2)
γ / °	86.079(2)
V / *Å³*	899.61(17)
dcalc / *g.cm-3*	1.286
R factor (with I>2σI)	R1 = 0.0514, wR2 = 0.1340
R factor (all data)	R1 = 0.0580, wR2 = 0.1394
F(000) / e-	364
Absorption coefficient μ (MoKα1) mm-1	0.09
Number of reflections (n) (with Fo>4.0σ(Fo))	3609 / 3129
Number of refined parameters (p) / restraints	245

Goodness of fit indicator (restrainted GooF)	1.046
Maximum peak in final difference map / e-Å-3	0.280
Maximum hole in final difference map / e-Å-3	-0.215

Table 6 b. Atomic coordinates (x10^4) and equivalent isotropic displacement parameters (Å^2 x 10^3). U(eq) is defined as one third of the trace of the orthogonalized Uij tensor.

	x	y	z	U(eq)
F(1)	10241(1)	6417(1)	2577(1)	71(1)
N(1)	9715(1)	3648(2)	1111(1)	42(1)
C(1)	12186(2)	3049(2)	2597(2)	50(1)
C(2)	12812(2)	2683(2)	3687(2)	63(1)
C(3)	12584(2)	3597(2)	4377(2)	63(1)
C(4)	11733(2)	4863(2)	3999(2)	57(1)
C(5)	11121(2)	5197(2)	2919(2)	47(1)
C(6)	11335(2)	4330(2)	2184(2)	40(1)
C(7)	10638(2)	4716(2)	1023(2)	39(1)
C(8)	9062(2)	3922(2)	99(2)	41(1)
C(9)	7984(2)	2755(2)	256(2)	54(1)
C(10)	7097(3)	1839(3)	1578(2)	88(1)
C(11)	8246(3)	1119(3)	938(3)	96(1)

	x	y	z	U(eq)
F(1A)	5451(2)	-1532(2)	3511(1)	80(1)
F(2A)	1199(6)	-376(8)	1988(6)	73(2)
N(1A)	4055(1)	954(2)	420(1)	39(1)
C(1A)	1829(2)	-829(2)	2862(2)	53(1)
C(2A)	1011(2)	-1237(2)	4140(2)	70(1)
C(3A)	1703(3)	-1772(3)	5182(2)	76(1)
C(4A)	3201(3)	-1888(3)	4965(2)	75(1)
C(5A)	3997(2)	-1468(2)	3701(2)	58(1)
C(6A)	3345(2)	-951(2)	2616(2)	42(1)
C(7A)	4230(2)	-479(2)	1241(1)	37(1)
C(8A)	4821(2)	1461(2)	-827(1)	38(1)
C(9A)	4638(2)	3074(2)	-1691(2)	51(1)
C(10A)	4221(3)	4221(2)	-1110(2)	71(1)
C(11A)	3132(3)	3743(3)	-1636(2)	78(1)

Table 6 c. Hydrogen coordinates (x10^4) and equivalent isotropic displacement parameters (Å2 x 10^3). U(eq) is defined as one third of the trace of the orthogonalized Uij tensor.

	x	y	z	U(eq)
H(1)	12341	2425	2137	60
H(2)	13386	1821	3952	76
H(3)	13011	3353	5105	75
H(4)	11574	5483	4463	69
H(9)	7471	3021	-475	65
H(10A)	7281	2003	2322	105
H(10B)	6076	1600	1640	105
H(11A)	7937	430	604	115
H(11B)	9141	833	1286	115
H(1A)	1344	-467	2160	63
H(2A)	-11	-1145	4285	84
H(3A)	1154	-2056	6037	92
H(4A)	3680	-2250	5671	90
H(5A)	5021	-1535	3566	69
H(9A)	5297	3452	-2563	61
H(10C)	4072	3866	-159	86
H(10D)	4652	5242	-1607	86
H(11C)	2892	4467	-2458	93
H(11D)	2312	3091	-1010	93

Table 6 d. Bond lengths (Å).

F(1)-C(5)	1.350(2)
N(1)-C(8)	1.337(2)
N(1)-C(7)	1.338(2)
C(1)-C(6)	1.382(2)

C(9)-C(11)	1.470(3)
C(9)-C(10)	1.478(3)
C(9)-H(9)	0.98
C(10)-C(11)	1.455(4)

C(4A)-C(5A)	1.370(3)
C(4A)-H(4A)	0.93
C(5A)-C(6A)	1.381(2)
C(5A)-H(5A)	0.93

C(1)-C(2)	1.385(3)
C(1)-H(1)	0.93
C(2)-C(3)	1.376(3)
C(2)-H(2)	0.93
C(3)-C(4)	1.368(3)
C(3)-H(3)	0.93
C(4)-C(5)	1.372(2)
C(4)-H(4)	0.93
C(5)-C(6)	1.379(2)
C(6)-C(7)	1.493(2)
C(7)-C(8)#1	1.394(2)
C(8)-C(7)#1	1.394(2)
C(8)-C(9)	1.483(2)

C(10)-H(10A)	0.97
C(10)-H(10B)	0.97
C(11)-H(11A)	0.97
C(11)-H(11B)	0.97
N(1A)-C(7A)	1.3321(19)
N(1A)-C(8A)	1.3384(19)
C(1A)-C(6A)	1.379(2)
C(1A)-C(2A)	1.389(3)
C(1A)-H(1A)	0.93
C(2A)-C(3A)	1.364(3)
C(2A)-H(2A)	0.93
C(3A)-C(4A)	1.361(3)
C(3A)-H(3A)	0.93

C(6A)-C(7A)	1.494(2)
C(7A)-C(8A)#2	1.398(2)
C(8A)-C(7A)#2	1.398(2)
C(8A)-C(9A)	1.477(2)
C(9A)-C(10A)	1.491(3)
C(9A)-C(11A)	1.495(3)
C(9A)-H(9A)	0.98
C(10A)-C(11A)	1.462(3)
C(10A)-H(10C)	0.97
C(10A)-H(10D)	0.97
C(11A)-H(11C)	0.97
C(11A)-H(11D)	0.97

Table 6 e. Angles (°).

C(8)-N(1)-C(7)	118.40(14)
C(6)-C(1)-C(2)	120.87(17)
C(6)-C(1)-H(1)	119.6
C(2)-C(1)-H(1)	119.6
C(3)-C(2)-C(1)	119.95(18)
C(3)-C(2)-H(2)	120
C(1)-C(2)-H(2)	120
C(4)-C(3)-C(2)	120.41(17)
C(4)-C(3)-H(3)	119.8
C(2)-C(3)-H(3)	119.8
C(3)-C(4)-C(5)	118.49(18)
C(3)-C(4)-H(4)	120.8
C(5)-C(4)-H(4)	120.8
F(1)-C(5)-C(4)	118.27(16)
F(1)-C(5)-C(6)	118.44(14)
C(4)-C(5)-C(6)	123.27(17)
C(5)-C(6)-C(1)	116.99(15)
C(5)-C(6)-C(7)	121.90(15)
C(1)-C(6)-C(7)	121.08(14)
N(1)-C(7)-C(8)#1	121.46(14)
N(1)-C(7)-C(6)	115.54(14)
C(8)#1-C(7)-C(6)	122.98(13)
N(1)-C(8)-C(7)#1	120.13(14)
N(1)-C(8)-C(9)	117.11(14)
C(10)-C(9)-C(8)	119.76(16)

C(7)#1-C(8)-C(9)	122.72(14)
C(11)-C(9)-C(10)	59.12(18)
C(11)-C(9)-C(8)	120.89(17)
C(11)-C(9)-H(9)	115.2
C(10)-C(9)-H(9)	115.2
C(8)-C(9)-H(9)	115.2
C(11)-C(10)-C(9)	60.14(16)
C(2A)-C(1A)-H(1A)	119.4
C(3A)-C(2A)-C(1A)	120.2(2)
C(3A)-C(2A)-H(2A)	119.9
C(1A)-C(2A)-H(2A)	119.9
C(4A)-C(3A)-C(2A)	119.79(18)
C(4A)-C(3A)-H(3A)	120.1
C(2A)-C(3A)-H(3A)	120.1
C(3A)-C(4A)-C(5A)	119.5(2)
C(3A)-C(4A)-H(4A)	120.2
C(5A)-C(4A)-H(4A)	120.2
C(4A)-C(5A)-C(6A)	122.9(2)
C(4A)-C(5A)-H(5A)	118.6
C(6A)-C(5A)-H(5A)	118.6
C(1A)-C(6A)-C(5A)	116.40(16)
C(1A)-C(6A)-C(7A)	121.31(15)
C(5A)-C(6A)-C(7A)	122.23(15)
C(6A)-C(1A)-H(1A)	119.4

N(1A)-C(7A)-C(8A)#2	121.55(13)
N(1A)-C(7A)-C(6A)	115.47(13)
C(8A)#2-C(7A)-C(6A)	122.98(14)
N(1A)-C(8A)-C(7A)#2	119.63(14)
N(1A)-C(8A)-C(9A)	117.07(13)
C(7A)#2-C(8A)-C(9A)	123.29(14)
C(8A)-C(9A)-C(10A)	120.10(16)
C(8A)-C(9A)-C(11A)	119.63(16)
C(10A)-C(9A)-C(11A)	58.59(15)
C(8A)-C(9A)-H(9A)	115.5
C(10A)-C(9A)-H(9A)	115.5
C(11A)-C(9A)-H(9A)	115.5
C(11A)-C(10A)-C(9A)	60.84(14)
C(11A)-C(10A)-H(10C)	117.7
C(9A)-C(10A)-H(10C)	117.7
C(11A)-C(10A)-H(10D)	117.7
C(9A)-C(10A)-H(10D)	117.7
H(10C)-C(10A)-H(10D)	114.8
C(10A)-C(11A)-C(9A)	60.57(14)
C(10A)-C(11A)-H(11C)	117.7
C(9A)-C(11A)-H(11C)	117.7
C(10A)-C(11A)-H(11D)	117.7
C(9A)-C(11A)-H(11D)	117.7
H(11C)-C(11A)-H(11D)	114.8

Table 6 f. Anisotropic displacement parameters (Å² x 103) The anisotropic displacement factor exponent takes the form: -2 π² [h² a*² U11 + ... + 2 h k a* b* U12].

	U11	U22	U33	U23	U13	U12
F(1)	86(1)	75(1)	76(1)	-49(1)	-34(1)	31(1)
N(1)	44(1)	43(1)	39(1)	-18(1)	-8(1)	-4(1)
C(1)	51(1)	46(1)	52(1)	-19(1)	-10(1)	0(1)
C(2)	60(1)	56(1)	65(1)	-13(1)	-22(1)	7(1)
C(3)	65(1)	74(1)	48(1)	-15(1)	-24(1)	-5(1)
C(4)	63(1)	70(1)	47(1)	-30(1)	-14(1)	-5(1)

	U11	U22	U33	U23	U13	U12
F(2A)	43(3)	102(5)	68(4)	-30(3)	-11(3)	8(3)
N(1A)	37(1)	42(1)	36(1)	-15(1)	-3(1)	2(1)
C(1A)	48(1)	52(1)	54(1)	-24(1)	4(1)	-1(1)
C(2A)	58(1)	67(1)	79(2)	-39(1)	25(1)	-10(1)
C(3A)	104(2)	68(1)	44(1)	-26(1)	24(1)	-20(1)
C(4A)	100(2)	78(2)	37(1)	-18(1)	-2(1)	-11(1)

C(5)	48(1)	51(1)	47(1)	-24(1)	-12(1)	3(1)
C(6)	38(1)	44(1)	39(1)	-16(1)	-6(1)	-5(1)
C(7)	38(1)	45(1)	39(1)	-23(1)	-6(1)	0(1)
C(8)	42(1)	44(1)	41(1)	-20(1)	-7(1)	-3(1)
C(9)	64(1)	53(1)	47(1)	-17(1)	-16(1)	-17(1)
C(10)	103(2)	100(2)	59(1)	-28(1)	-4(1)	-56(2)
C(11)	113(2)	45(1)	138(3)	-26(1)	-67(2)	-8(1)
F(1A)	59(1)	116(2)	52(1)	-18(1)	-22(1)	4(1)
C(5A)	66(1)	62(1)	37(1)	-15(1)	-5(1)	-4(1)
C(6A)	45(1)	39(1)	37(1)	-16(1)	1(1)	-2(1)
C(7A)	33(1)	42(1)	34(1)	-14(1)	-4(1)	-1(1)
C(8A)	34(1)	40(1)	36(1)	-14(1)	-4(1)	1(1)
C(9A)	53(1)	45(1)	41(1)	-10(1)	2(1)	6(1)
C(10A)	88(2)	43(1)	70(1)	-20(1)	2(1)	5(1)
C(11A)	65(1)	60(1)	84(2)	-10(1)	-15(1)	23(1)

Table 6 g. Torsion angles (°).

C(6)-C(1)-C(2)-C(3)	0.3(3)
C(1)-C(2)-C(3)-C(4)	0.4(3)
C(2)-C(3)-C(4)-C(5)	-0.1(3)
C(3)-C(4)-C(5)-F(1)	177.77(17)
C(3)-C(4)-C(5)-C(6)	-0.9(3)
F(1)-C(5)-C(6)-C(1)	-177.13(15)
C(4)-C(5)-C(6)-C(1)	1.5(3)
F(1)-C(5)-C(6)-C(7)	0.7(2)
C(4)-C(5)-C(6)-C(7)	179.35(16)
C(2)-C(1)-C(6)-C(5)	-1.2(3)
C(2)-C(1)-C(6)-C(7)	-179.04(16)
C(8)-N(1)-C(7)-C(8)#1	-0.9(3)
C(8)-N(1)-C(7)-C(6)	-179.64(13)
C(5)-C(6)-C(7)-N(1)	-119.16(17)
C(1)-C(6)-C(7)-N(1)	58.6(2)
C(5)-C(6)-C(7)-C(8)#1	62.1(2)
C(1)-C(6)-C(7)-C(8)#1	-120.12(18)
C(7)-N(1)-C(8)-C(7)#1	0.9(2)
C(7)-N(1)-C(8)-C(9)	-176.79(15)
N(1)-C(8)-C(9)-C(11)	-38.2(3)
C(7)#1-C(8)-C(9)-C(11)	144.2(2)
N(1)-C(8)-C(9)-C(10)	31.5(3)
C(7)#1-C(8)-C(9)-C(10)	-146.1(2)
C(8)-C(9)-C(10)-C(11)	-110.3(2)
C(8)-C(9)-C(11)-C(10)	108.4(2)
C(6A)-C(1A)-C(2A)-C(3A)	-0.1(3)
C(1A)-C(2A)-C(3A)-C(4A)	0.8(3)
C(2A)-C(3A)-C(4A)-C(5A)	-0.1(4)
C(3A)-C(4A)-C(5A)-C(6A)	-1.3(3)
C(2A)-C(1A)-C(6A)-C(5A)	-1.2(3)
C(2A)-C(1A)-C(6A)-C(7A)	-178.55(16)
C(4A)-C(5A)-C(6A)-C(1A)	1.9(3)
C(4A)-C(5A)-C(6A)-C(7A)	179.23(19)
C(8A)-N(1A)-C(7A)-C(8A)#2	-0.8(2)
C(8A)-N(1A)-C(7A)-C(6A)	179.50(13)
C(1A)-C(6A)-C(7A)-N(1A)	56.0(2)
C(5A)-C(6A)-C(7A)-N(1A)	-121.25(18)
C(1A)-C(6A)-C(7A)-C(8A)#2	-123.74(18)
C(5A)-C(6A)-C(7A)-C(8A)#2	59.0(2)
C(7A)-N(1A)-C(8A)-C(7A)#2	0.8(2)
C(7A)-N(1A)-C(8A)-C(9A)	-177.73(14)
N(1A)-C(8A)-C(9A)-C(10A)	26.8(2)
C(7A)#2-C(8A)-C(9A)-C(10A)	-151.60(18)
N(1A)-C(8A)-C(9A)-C(11A)	-41.9(2)
C(7A)#2-C(8A)-C(9A)-C(11A)	139.70(19)
C(8A)-C(9A)-C(10A)-C(11A)	-108.4(2)
C(8A)-C(9A)-C(11A)-C(10A)	109.2(2)

Bibliography

Bibliography

[1] Lord Kelvin; *Baltimore Lectures on Molecular Dynamics and the Wave Theory of Light* **1884**.

[2] A. Collet, J. Crassous, J. P. Dutasta, L. Guy; *Molécules chirales : stéréochimie et propriétés*, EDP Sciences, CNRS editions: Les Ulis; Paris, **2006**.

[3] R. J. Hauy; *Traité de minèralogie: Paris*, **1801**.

[4] J. B. Biot; *Bull. Soc. Philomatique,* **1815**, 190-192.

[5] J. L. Gay-Lussac; *Schweigger's journal,* **1828**, *48*, 381.

[6] J. B. Biot; *Annal. Chim.Phys. I,I,* **1838**, 69, 22.

[7] L. Pasteur; *C. R. Acad. Sci. Paris,* **1848**, *26*, 535-538.

[8] L. Pasteur; *C. R. Acad. Sci. Paris,* **1849**, *28*, 477-478.

[9] L. Pasteur ; *Annal. Chim.Phys.,* **1848**, *24*, 442-459.

[10] D. Gernez; *C. R. Acad. Sci. Paris,,* **1866**, 63, 843.

[11] J.H. van't Hoff; *Bul.l Soc. Chim. Fr.,* **1875**, 23, 295.

[12] J. A. Le Bel; *Bul.l Soc. Chim. Fr.,* **1874**, 22, 337.

[13] R. S. Cahn, C. Ingold, V. Prelog; *Angew. Chem. Int. Ed. Engl.,* **1966**, 5, 385-415.

[14] L. Friedman, J.G. Miller; *Science*, **1971**, 172, 1044-1046.

[15] D. Wang, K. Ando, K. Morita,K. Kubota, A. Kobayashi; *Biosci. Biotechnol. Biochem.* **1994**, 58 (11), 2050-2053.

[16] M. H. Boelens, H. Boelens, L. J. van Gemert, *P. & F.*, **1993**, 18(6), 1-15.

[17] L. Friedman, J.G. Miller; *Science*, **1971,** 172, 1044-1046.

[18] C. Bommer, E. Werle, I. Walter-Sack, C. Keller, F. Gehlen, C. Wanner, M. Nauck, W. März, H. Wieland, J. Bommer; *J. Am. Chem. Nephrol.*, **2005**, 16, 2789-2795.

[19] B. K. Patel, A. J. Hutt; *Chirality in Drug Design and Development* **2004,** Chap. 5, I. K. Reddy, R. Mehvar, Eds, New-York, Marcel Dekker Inc.

[20] E. J. Ariens ; *Eur. J. Clin. Pharmacol.,* **1984**, 26, 663-668.

[21] H. Caner, E. Groner, L. Levy; *Discovery Drug Today*, **2004**, 9(3), 105-110.

[22] R. L. Scott; *J. Chem. Soc., Faraday Trans. 2,* **1977**, 73, 356-360.

[23] G. Coquerel; *Enantiomer*, **2000**, 5, 481-498.

[24] R.A. Sheldon; *Chirotechnology : industrial synthesis of optically active compounds*; Marcel Dekker: New York, **1993**.

[25] R. Tamura, D. Fujimoto, Z. Lepp, K. Misaki, H. Miura, H. Takahashi, T. Ushio, T. Nakai, K. Hirotsu*; J. Am. Chem. Soc.*, **2002,** 124(44), 13139-13153.

[26] B. Chion, J. Lajzerowicz, D. Bordeaux, A. Collet, J. Jacques; *J. Phys. Chem.,* **1978**, 82, 2682-2688.

[27] S. K. Kurtz, T. T. Perry; *J. Appl. Phys.,* **1968**, 39, 3798-3813.

[28] A. Galland, V. Dupray, B. Berton, S. Morin-Grognet, M. Sanselme, H. Atmani, G. Coquerel; *Cryst. Growth Des.,* **2009**, 9, 2713-2718.

[29] H.-J. Federsel; *Org. Proc. Res. Dev.*, **2012**, 16, 260-261.

[30] IntEnant website: http://www.intenant.eu/

[31] A. N. Collins, G. N. Sheldrake, J. Crosby; *Chirality in industry: the commercial manufacture and applications of optically active compounds*; Wiley: Chichester, **1992**.

[32] E. J. Corey, S. Shibata, R. K. Baksi; *J. Org. Chem.*, **1988**, 53, 2861-2863.

[33] H. E. Ensley, C. A. Parnell, E. J. Corey; *J. Org. Chem.*, **1978**, 43, 1610-1612.

[34] H. Takaya, K. Mashima, K. Koyano, M. Yagi, H. Kumobayashi, T. Taketomi, S. Akutagawa, R. Noyori; *J. Org. Chem.*, **1986**, 51, 629-635.

[35] T.E. Beesley, R. P. W. Scott; *Chiral chromatography*; J. Wiley: Chichester, England; New York, **1998**.

[36] G. Subramanian; *Chiral Separation Techniques: A Pratical Approach*, Wiley-VCH ed., **2006**

[37] A. Abate, E. Brenna, A. Constantini, C. Fuganti, F. G. Gatti, L. Malpezzi, S. Serra; *J. Org. Chem.*, **2006**, 71, 5228-5240.

[38] S. E. Schaus, B. D. Brandes, J. F. Larrow, M. Tokunaga, K. B. Hansen, A. E. Gould, M. E. Furrow, E. N. Jacobsen; *J. Am. Chem. Soc.*, **2002**, 1307-1315.

[39] R. S. Ward; *Tetrahedron: Asymmetry*, **1995**, 6, 1475-1490.

[40] K. Leijondahl, L. Borén, R. Braun, J.-E. Bäckvall; *J. Org. Chem.*, **2009**, 75, 1988-1993.

[41] J. Jacques, A. Collet, S. H. Wilen; *Enantiomers, racemates, and resolutions* **1981**, New York, Wiley.

[42] G. Levilain, G. Coquerel; *Crystengcomm*, **2010**, 12(7), 1983-1992.

[43] M. E. Jungfleisch; *J. Pharm. Chim.* **1882**, 5, 346-357.

[44] A. Werner; *Chem. Ber.* **1914**, 47, 2171-2182.

[45] R. Duschinsky; *Chem. Ind.* **1934**, 53, 10-20.

[46] G. Amiard; *Experientia* **1959**, 15, 1-7.

[47] R. M. Secor; *Chem. Rev.* **1963**, 63, 297-309.

[48] A. Collet, M. J. Brienne, J. Jacques; *Chem. Rev.,* **1980**, 80, 215-230.

[49] WO9508522 **1995**.

[50] WO2011/07330.

[51] US4417070 **1983**.

[52] S. N. Black, L. J. Williams, R. J. Davey, F. Moffat, R. V. H. Jones, D. M. McEwan, D. E. Sadler; T*etrahedron*, **1989**, 45, 2677-2682.

[53] L. Courvoisier, E. Ndzié, M. N. Petit, U. Hedtmann, U. Sprengard,, G. Coquerel; *Chem. Lett.,* **2001**, 30, 364-365.

[54] L. Courvoisier, L. Mignot, M.N. Petit, G. Coquerel; *Org. Process Res. Dev.,* **2003**, 7, 1007-1016.

[55] W. Schlenk; *Analyst* **1952**, 77, 870; Justus Liebigs; *Ann. Chem.*, **1973**, 1145; 1156; 1179; 1195.

[56] R. Arad-Yellin, B. S. Green, M. Knossow, G. Tsoucaris; *Inclusion Compounds III,* **1984**, Academic Press, London, chap. 9, 278-284.

[57] H. M. Powell; *Nature,* **1952**, 170, 155-155.

[58] F. Toda; *Aust. J. Chem.,* **2001**, 54, 573-582.

[59] Z. Urbanczyk-Lipkowska, F. Toda; *Separations and reactions in organic supramolecular chemistry,* **2004**, J. Wiley & Sons: New York, Chapter 1.

[60] F. Toda; *Enantiomer Separation: Fundamental and Practical Methods,* **2004**, Kluwer Academic Publisher: Dordrecht, Chapter 1, 1-47.

[61] F. Toda, A. Sato, L. R. Nassimbeni, M. L. Niven; *J. Chem. Soc. Perkin Trans. 2,* **1991**, 1971-1975.

[62] K. Hatano, T. Takeda, R. Saito; *J. Chem. Soc., Perkin Trans. 2*, **1994**, 579-584.

[63] B. Szczepanska, M. Gdaniec, U. Rychlewska; *J. Incl. Phen. Mol. Recogn. Chem.*, **1995**, *22*, 211-219.

[64] K. Nemak, M. Acs, Z. M. Jaszay, D. Kozma, E. Fogassy; *Tetrahedron,* **1996**, 52(5), 1637-1642.

[65] O. Bortolini, G. Fantin, M. Fogagnolo; *Chirality*, **2005**, 17, 121-130.

[66] V. Bertolasi, O. Bortolini, M. Fogagnolo, G. Fantin, P. Pedrini; *Tetrahedron: Asymm*etry, **2001**, 12, 1479–1483.

[67] L. R. Sousa, G. D. Y. Sogah , D. H. Hofmann, D. J. Cram; *J. Am. Chem. Soc.*, **1978**, 100, 4569-4576.

[68] H. Nagata, H. Nishi, M. Kamigauchi, T. Ishida; *Chem. Pharm. Bull.,* **2006,** 54(4), 452-457.

[69] W. A. Freeman, W. L. Mock, N. Y. Shin ; *J. Am. Chem. Soc.*, **1981**, 103, 7367-7368.

[70] D. Whang, J. Heo, J. H. Park, K. Kim; *Angew. Chem. Int. Ed.,* **1998**, 37(1-2), 78-80.

[71] V. M. Rekharsky, H. Yamamura, C. Inoue, M. Kawai, I. Osaka, R. Arakawa, K. Shiba, A. Sato, Y. Ho Ko, N. Selvapalam, K. Kim, Y. Inoue; *J. Am. Chem. Soc.,* **2006***,* 128, 14871-14880.

[72] Z. Asfari, V. Böhmer, J. Harrowfield, J. Vicens; *Calixarenes*, **2001**, Kluwer Academic Publishers: Dordrecht, Holland.

[73] U. Darbost, M.-N. Rager, S. Petit, I. Jabin, O. Reinaud; *J. Am. Chem. Soc.,* **2005***,* 127, 8517-8525.

[4] L. Mutihac, J. H. Lee, J. S. Kim, J. Vicens; *Chem. Soc. Rev*., **2011**, 40, 2777-2796.

[75] E. Weber, J. Ahrendt, A, Lohner, P. J. Reddy, K. K. Chacko; *J. Incl. Phenom*., **1993**, 15, 231-245.

[76] J. L. Atwood, S. J. Dalgarno, M. J. Hardie, C. L. Raston; *Chem. Commun*., **2005**, 337-339.

[77] P. R. Martinez-Alanis, I. Castillo; *Tetrahedron Lett*., **2005**, 46, 8845-8848.

[78] W. Saenger; *Angew. Chem., Int. Ed. Eng.*, **1980**, 19, 344-362.

[79] A. Grandeury, E. Condamine, L. Hilfert, G. Gouhier, S. Petit, G. Coquerel; *J. Phys. Chem. B*, **2007**, 111, [7017-7026.

[80] Y. Amharar, A. Grandeury, M. Sanselme, S. Petit, G. Coquerel; *J. Phys. Chem.*, **2012**, 116(20), 6027-6040.

[81] C. Viedma; *Phys. Rev. Lett.*, **2005**, 94, 065504.

[82] F. C. Frank; *Biochem. Biophys. Acta*, **1953**, 11, 459-463.

[83] R. E. Pincock, K. R. Wilson; *J. Am. Chem. Soc.*, **1971**, 93(5), 1291-1292.

[84] F. S. Kipping, W. J. Pope; *J. Chem. Soc. Trans.*, **1898**, 73, 606-617.

[85] D. K. Kondepudi, R. J. Kaufman, N. Singh; *Science*, **1990**, 250, 975-976.

[86] D.K. Kondepudi, K. L. Bullock, J. A. Digits, J. K. Hall, J. M. Miller; *J. Am. Chem. Soc.*, **1993**, 115, 10211-10216.

[87] D. K. Kondepudi, K. L. Bullock, J. A. Digits, P. D. Yarborough; *J. Am. Chem. Soc.*, **1995**, 117, 401-404.

[88] B. Martin, A. Tharrington, X.-I. Wu; *Phys. Rev. Lett.*, **1996**, 77(13), 2826-2829.

[89] D. K. Kondepudi, J. Laudadio, K. Asakura; *J. Am. Chem. Soc.*, **1999**, 121, 1448-1451.

[90] C. Viedma; *J. Crystal Growth*, **2004**, 261, 118-121.

[91] J. Crusats, S. Vientemillas-Verdaguer, J. M. Ribó*; Chem. Eur. J.*, **2006**, 12, 7776-7781.

[92] D. G. Blackmond; *Chem. Eur. J.*, **2007**, 13, 3291-3295.

[93] R. M. Kellogg, B. Kaptein, T. R. Vries; *Top. Curr. Chem.,* **2007**, 269, 159-197.

[94] W. L. Noorduin, T. Izumi, A. Millemaggi, M. Leeman, H. Meekes, W. J. P. Van Enckevort, R. M. Kellogg, B. Kaptein, E. Vlieg, D. G. Blackmond; *J. Am. Chem. Soc.*, **2008**, 130, 1158-1159.

[95] W. L. Noorduin, H. Meekes, W. J. P. van Enckevort, A. Millemaggi, M. Leeman, B. Kaptein,R. M. Kellogg, E. Vlieg; *Angew. Chem. Int. Ed.*, **2008**, 47, 6445-6447.

[96] P. S. M. Cheung, L. A. Cuccia; *Chem. Commun.*, **2009**, 1337- 1338.

[97] W. L. Noorduin, P. van der Asdonk, H. Meekes, W. J. P. van Enckevort, B. Kaptein, M. Leeman, R. M. Kellogg, E. Vlieg, *Angew. Chem. Int. Ed.*, **2009**, 48(18), 3278-3280.

[98] M. Leeman, J. M. De Gooier, K. Boer, K. Zwaagstra, B. Kaptein, R. M. Kellogg; *Tetrahedron: Asymmetry,* **2010**, 21, 1191-1193

[99] B. Kaptein, W. L. Noorduin, H. Meekes, W. J. P. van Enckevort, R. M. Kellogg, E. Vlieg; *Angew. Chem. Int. Ed.*, **2008**, 47(38), 7226-7229.

[100] M. W. van der Meijden, M. Leeman, E. Gelens, W. L. Noorduin, H. Meekes, W. J. P. van Enckevort, B. Kaptein, E. Vlieg, R. M. Kellogg; *Org. Process. Res. Dev.*, **2009**, 13, 1195-1198.

[101] a) U.S. Patent 6,800,759, **2004**, b) U.S. Patent 6,737,411, **2004**. c) U.S. Patent 4,847,265, **1989** d) U.S. Patent 6,074,242, **2006**.

[102] L. Wang, J. Shen, Y. Tang, Y. Chen, W. Wang, Z. Cai, Z. Du; *Org. Process Res. Dev.,* **2007**, 11, 487-489.

[103] a) U.S. Patent 2004073057, **2004**, b) WO2006003671, **2006**, c) U.S. Patent 2007225320, **2007**.

[104] W. L. Noorduin, B. Kaptein, H. Meekes, W. J. P. Van Enckevort, R. M. Kellogg, E. Vlieg; Angew. *Chem. Int. Ed.,* **2009**, 48, 4581-4583.

[105] C. Viedma, J. E. Ortiz, T. De Torres, T.Izumi, D. G. Blackmond; *J. Am. Chem. Soc.*, **2008**, 130, 15274-15275.

[106] R. Yoshihoka; *Top. Curr. Chem.*, **2007**, 269, 83-132.

[107] S. B. Tsogoeva, S. Wei, M. Freund, M. Mauksch; *Angew. Chem. Int Ed.*, **2009**, 48(3), 590-594.

[108] G. Levilain, C. Rougeot, F. Guillen, J.-C. Plaquevent, G. Coquerel; *Tetrahedron: Asymmetry*, **2009**, 20, 2769-2771.

[109] M. Leeman, W. L. Noorduin, A. Millemaggi, E. Vlieg, H. Meekes, W. J. P. van Enckevort, B. Kaptein, R. M. Kellogg; *CrystEngComm,* **2010**, 12 (7), 2051-2053.

[110] W. L. McCabe, J. C. Smith; *Unit operations of chemical engineering;* McGraw-Hill Book Co.: New York, **1956**

[111] D. K. Kondepudi, C. Sabanayagam; *Chem. Phy. Lett.*, **1994**, 217, 364-368.

[112] F. W. Ostwald; *Z. Phys. Chem.*, **1897**, 22, 289-330

[113] F. W. Ostwald; *Z. Phys. Chem.*, **1900**, 34, 495-503

[114] W. Ostwald; *Lehrbuch der Allgemeinen Chemie*, Vol. 2, Part 1; Leipzig, Germany, **1896**.

[115] W. L. Noorduin, E. Vlieg, R. M. Kellogg, B. Kaptein; *Angew. Chem. Int. Ed.*, **2009**, 48, 9600-9606.

[116] A. G. Cairns-Smith; *Chemistry in Britain,* **1986**, 22, 559-561.

[117] J. H. E. Cartwright, O. Piro, I. Tuval; *Phys. Rev. Lett.*, **2007**, 165501

[118] W. L. Noorduin, H. Meekes, A. A. C. Bode, W. J. P. Van Enckevort, B. Kaptein, R. M. Kellogg, E. Vielg; *Cryst. Growth Des.*, **2008**, 8(5), 1675-1681.

[119] M. Uwaha; *J. Phys. Soc. Jpn*, **2004**, 73(10), 2601-2603.

[120] J. M. McBride, J. C. Tully; *Nature*, **2008**, 452, 161-162.

[121] Y. Saito, H. Hyuga; *J. Phys. Soc. Jpn*, **2004,** 73, 33-35.

[122] M. Uwaha; *J. Phys. Soc. Jpn*, **2008**, 77, 083802.

[123] Y. Saito, H. Hyuga; *J. Phys. Soc. Jpn*, **2005**, 74, 535-537.

[124] T. Izumi, D. G. Blackmond; *Chem. Eur. J.*, **2009**, 15, 3065-3068.

[125] J. Crusats, S. Veintemillas-Verdaguer, J. M. Ribo; *Chem. Eur. J.*, **2007**, 13, 10303-10305.

[126] W. L. Noordiun, W. J. P. Van Enckevort, H. Meekes, B. Kaptein, R. M. Kellogg, J. C. Tully, J. M. McBride, E. Vlieg; *Angew. Chem. Int. Ed.*, **2010**, 49(45), 8435-8438.

[127] P. J. Skrdla; *Cryst. Growth Des.*, **2011**, 11, 1957-1965.

[128] M. Iggland, M. Mazzotti; *Cryst. Growth Des.*, **2011**, 11, 4611-4622.

[129] A. Villiers ; *Comptes Rendus Hebdomadaires des Séances de l'Académie des Sciences*, **1891**, 112, 536-538.

[130] J. Szejtli ; *Chem. Rev.*, **1998**, 98(5), 1743-1754.

[131] F. Z. Schardinger; *Unters. Nahr. u. Genussm.* **1903**, 6, 865-880.

[132] H. Pringsheim, *A Comprehensive Survey Of Starch Chemistry*, Ed. Chemical CatalogueCo, R. Walton, New York, **1928**.

[133] H. Pringsheim, *Chemistry of the Saccharides*, McGraw-Hill, New York, **1932**.

[134] P. Karrer,C. Nageli; *Helv. Chim. Acta* **1921**, 4, 169-173.

[135] A. Miekeley; *Ber. Dtsch. Chem. Ges.* **1932**, 65, 69.

[136] K. Freudenberg, G. Blomquist, L. Ewald, K. Soff; *Ber. Dtsch. Chem. Ges.* **1936**, *69*, 1258-1266.

[137] A. R. Khan, P. Forgo, K. J. Stine, V. T. D'Souza; *Chem. Rev.*, **1998**, 98, 1977-1996.a

[138] A. Ueno, R. Breslow; *Tetrahedron Lett.*, **1982**, 23, 3451-3454.

[139] D. Rong, V. T. D'Souza, *Tetrahedron Lett.*, **1990**, 31, 4275-4278.

[140] E. V. van Dienst, B. H. M. Snellink, I. Von Piekartz, M. H. B. Gansey, F. Venema, M. C. Feiters, R. J. M. Nolte, J. F. J. Engbersen, D. N. Reinhoudt, *J. Org. Chem.*, **1995**, 60, 6537-6545.

[141] K. Fujita, S. Nagamura, T. Imoto, T. Tahara, T. Koga; *J. Am. Chem. Soc.*, **1985**, 107, 3233-3235.

[142] K. Fujita, T. Tahara, Y. Egashira, T. Imoto, T. Koga; *Tetrahedron Lett.*, **1992**, 33, 5385-5388.

[143] M. Kojima, F. Toda, K. Hattori*; J. Chem. Soc., Perkin Trans 1*, **1981**, 1647-1651.

[144] T. Ikeda, R. Kojin, C. J. Yoon, H. Ikeda, M. Iijima, F. Toda; *J. Inclusion Phenom. Mol. Recognit. Chem.*, **1987**, 5, 93-98.

[145] K. Fujita, Y. Egashira, T. Imoto, T. Fujoka, K. Mihashi, K. Tahara, T. Koga, *Chem. Lett.*, **1989**, 429-432.

[146] A. M. Mortellaro, A. W. Czarnik; *Bioorg. Med. Chem. Lett.*, **1992**, 2, 1635-1638.

[147] D.-Q. Yuan, K. Ohta, K. Fujita; *J. Chem. Soc., Chem. Commun.*, **1996**, 821-822.

[148] A.R. Hedges; *Chem. Rev.*, **1998**, 98(5), 2035-2044.

[149] K. Higashi, Y. Tozuka, K. Moribe, K. Yamamoto; *J. Pharm. Sci.*, **2010**, 4192-4200.

[150] H.-J. Schneider, F. Hacket, V. Rüdiger; *Chem. Rev.*, **1998**, 1755-1785.

[151] W. Tang, S.-C. Ng; *J. Spe. Sci.,* **2008**, 31, 3246-3256.

[152] K. Harata *Bull. Chem. Soc. Jpn* **1982**, 55, 1367.

[153] K. Uekama, F. Hirayama, T. Imai, M. Otagiri, K. Harata *Chem. Pharm. Bull.* **1984**, 33, 1662.

[154] J. A. Hamilton, L. Chen *J. Am. Chem. Soc.* **1988**, 110, 4379 et 5833.

[155] B. S. Jursic, P. K. Patel; *Tetrahedron*, **2005**, 61, 919-926.

[156] C.-J. Núñez-Agüero, C.-M. Escobar-Llanos, D. Díaz, C. Jaime, R. Garduño-Juárez, *Tetrahedron*, **2006**, 62, 4162-4172.

[157] M. Rekharsky, Y. Inoue; *J. Am. Chem. Soc.*, **2000**, 122, 4418-4435.

[158] A. Grandeury, S. Tisse, G. Gouhier, V. Peulon, S. Petit, G. Coquerel *Chem. Eng. Technol.* **2003**, 26, 354-358.

[159] A. Grandeury, S. Petit, G. Gouhier , V. Agasse, G. Coquerel; *Tetrahedron: Asymmetry,* **2003**, 14, 2143-2152.

[160] N. Zhong, H.-S. Byun, R. Bittman; *Tetrahedron Lett.*, **1998**, 39, 2919-2920.

[161] H.-S. Byun, N. Zhong, R. Bittman; *Org. Synth.*, **2000**, 77, 225-227.

[162] L. Jicsinszky, R. Iványi; *Carbohyd. Polym.*, **2001**, 45, 139-145.

[163] I. W. Muderawan, T. T. Ong, T. C. Lee, D. J. Young, C. B. Chinga, S. C. Ng; *Tetrahedron Lett.*, **2005**, 46, 7905-7907.

[164] Z., Y. Jina, T. Lianga, Y. Liua, Q. Xua, X. Lianga, A. Lei; *J. Chromatogr. A*, **2009**, 1216, 257-263.

[165] M. Mourer, F. Hapiot, S. Tilloy, E. Monflier, S. Menuel; *Eur. J. Org. Chem.*, **2008**, 5723-5730.

[166] Y.-Y. Liu, X.-D. Fan, L. Gao; *Macromol. Biosci.*, **2003**, 3, 715-719.

[167] J. S. Lock, B L. May, P. Clements, J. Tsanaktsidis, C. J. Easton, S. F. Lincoln; *J. Chem. Soc., Perkin Trans. 1*, **2001**, 3361–3364

[168] J. A. Faiz, N. Spencer, Z. Pikramenou; *Org. Biomol. Chem.*, **2005**, 3, 4239-4245.

[169] D.-T. Pham, P. Clements, C. J. Easton, S. F. Lincoln, *Tetrahedron: Asymmetry*, **2008**, 19, 167-175.

[170] D. Mentzafos, A. Terzis, A. W. Coleman, C. de Rango; *Carbohydr. Res.*, **1996**, 282, 125-135.

[171] S. N. Black, L. J. Williams, R. J. Davey, F. Moffat, R. V. H. Jones, D. M. McEwan, D. E. Sadler; *Tetrahedron,* **1989**, 45(9), 2677-2682.

[172] US4243405A1.

[173] S. K. Branch, I. W. Nowell; *Acta Cryst.,* **1986**, *C42*, 440-442.

[174] S. Kajigaeshi, T. Kakinami, T. Okamoto, S. Fujisaki; *Bull. Chem. Soc. Jpn.*, **1987**, 60, 1159-1160.

[175] J.-P. Li, Y.-X. Zhang, Y. Ji; *J. Chin. Chem. Soc.*, **2008**, 55(2), 390-393.

[176] S. N. Black, L. J. Williams, R. J. Davey, F. Moffat, D. M. McEwan, D. E. Sadler, R. Docherty, D. J. Williams; *J. Phys. Chem.*, **1990**, 3223-3226.

[177] C. Gervais, S. Beilles, P. Cardinael, S. Petit, G. Coquerel; *J. Phys. Chem. B*, **2002**, 106 (3), 646-652.

[178] J. E. Hein, B. H. Cao, C. Viedma, R. M. Kellogg, D. G. Blackmond; *J. Am. Chem. Soc.*, **2012**, 134, 12629-12636.

[179] Y. Song, W. Chen, X. Chen; *Cryst. Growth Des.,* **2008**, 8(5), 1448-1450.

[180] Y. Song, W. Chen, X. Chen; *Cryst. Growth Des.,* **2012**, 12(1), 8-11.

[181] P. Cintas; *Cryst. Growth Des.,* **2008**, 8(8), 2626-2627.

[182] K. Suwannasang , A. E. Flood, C. Rougeot, G. Coquerel; *Oral presentation at CGOM10*, June **2012**, Limerick, Ireland.

[183] D. Tessaro, L. Cerioli, S. Servi, F. Viani, P. D'Arrigo; *Adv. Synth. Catal.*, **2011**, 353, 2333-2338.

[184] D. A. Schichl, S. Enthaler, W. Holla, T. Riermeier, U. Kragl, M. Beller; *Eur. J. Org. Chem.*, **2008**, 20, 3506-3512.

[18] Y. Kim, J. Park,M.-J. Kim; *Chem. Cat.Chem.*, **2011**, 3, 271-277.

[186] K. Yasukawa, R. Hasemi, Y. Asano; *Adv. Synth. Catal.*, **2011**, 353(13), 2328-2332.

[187] Pharmactua, from www.pharmactua.com.

[188] MS Global insights, from www.inshealth.com.

[189] EMEA/117561/2009.

[190] J. A. Jakubowskin C. D. Payne, J. T. Brandt, G. J. Weerakkody, N. A. Farid, D. S. Small, H. Naganuma, G. Y. Li, K. J. Winters; *J. Cardiovasc. Pharmacol.*, 2006, 47(3), 377-384.

[191] US6800759, **2004**.

[192] US2004073057, **2004**.

[193] WO2009062044A2.

[194] US4740510.

[195] D. M. Shendage, R. Fro1hlich, G. Haufe, *Org. Lett*, **2004**, 6(21), 3675-3678.

[196] D. E. Levy, F. Lapierre, W. Liang, W. Ye, C. W. Lange, X. Li, D. Grobelny, M. Casabonne, D. Tyrrell, K. Holme, A. Nadzan, R. E. Galardy; *J. Med. Chem.*, **1998**, 41, 199-223.

[197] M. K. Ghorai, A. Kumar, D. P. Tiwari; *J. Org. Chem.*, **2010**, 75, 137-151.

[198] S. Nahm, S. M. Weinreb; *Tetrahedron Letters*, **1981**, 22(39), 3815-3818.

[199] A. J. C. Wilson; *Acta Cryst A49*, **1993**, 795-806.

[200] Y. Amharar, S. Petit, M. Sanselme, Y. Cartigny, M.-N. Petit, G. Coquerel; *Cryst. Growth Des.*, **2011**, 11(6), 1453-2462.

Abstract

The purification of enantiomers by crystallisation is widely used in industry, but cannot be applied to all compounds. The improvement and optimization of existing techniques is therefore a major issue for scientists.

Thus, the synthesis of new chiral selectors has been proposed. A small library of monosubstituted β-cyclodextrins was synthesized to enhance the host-guest interactions. No chiral discrimination was visible so far and the existence of a large range of hydrates was highlighted. Structural studies and the determination of the host/guest/solvents phase diagrams may rationalise the chiral discrimination.

A second method to access to pure enantiomers was studied: the deracemisation. It quantitatively transforms a racemic suspension into pure enantiomer by action of glass beads. Unfortunately, this process is limited to chiral components easily racemisable in solution and crystallising as conglomerates. The crystallisation of conglomerates is uncommon and unpredictable. But, some families of compounds exhibit a high tendency to crystallise as conglomerates. Two new families were studied and it appeared that limited modifications of substituents do not disturb too much the crystal packing so that the full chiral discrimination in the solid state is preserved.

It has also been shown that ultrasounds can replace the action of the glass beads, making the process more efficient. In addition, studies carried out on the 1-(4-X-phenyl)-4,4-dimethyl-2-(1H-1,2,4-triazol-1-yl)pentan-3-one (X = Cl, Me, Br and H) allowed to shed light on the deracemisation mechanism.

An additional study allowed to apply the deracemization process to the synthesis of enantiomerically pure active pharmaceutical compounds.

Résumé

La purification d'énantiomères par cristallisation est largement utilisée en industrie, mais ne peut pas être appliquée à tous les composés. L'amélioration et l'optimisation de techniques déjà existantes est un donc enjeu considérable pour les scientifiques.

Ainsi, la synthèse de nouveaux sélecteurs chiraux a été proposée. Une petite librairie de β-cyclodextrines monosubstituées a été synthétisée, afin de consolider les interactions hote-invité. Aucune discrimination chirale n'a pu être mise en évidence et l'existence d'une large gamme d'hydrates a été observée. Les études structurales et la détermination des diagrammes de phases hôte/invité/solvant pourraient rationnaliser la discrimination chirale.

Un second procédé d'obtention d'énantiomères purs a été étudié : la déracemisation, permettant de transformer quantitativement une suspension racémique en énantiomère pur par action de billes de verre. Malheureusement, ce procédé est limité aux composés chiraux facilement racémisables en solution et cristallisant comme des conglomérats. Or la cristallisation de conglomérats est peu fréquente et surtout imprévisible. Cependant, certaines familles de composés ont une tendance prononcée à former des conglomérats. Deux nouvelles familles ont été étudiées et il est apparu que la modification modérée des substituents ne modifiait pas trop l'empilement cristallin, de telle sorte que la discrimination totale a l'état solide est préservée.

Il a aussi été prouvé que les ultrasons pouvaient remplacer l'action des billes de verre, rendant le procédé plus performant. De plus, les études menées sur les 1-(4-Xphenyl)-4,4-dimethyl-2-(1H-1,2,4-triazol-1-yl)pentan-3-one (X = Cl, Me, Br, et H) ont permis d'éclaircir le mécanisme de déracémisation.

Une seconde étude à permis d'appliquer le procédé de déracémisation à la synthèse de l'énantiomère pur de composés pharmaceutiquement actifs.